MARINE N_2 FIXATION: RECENT DISCOVERIES AND FUTURE CHALLENGES

EDITED BY: Angela Landolfi, Beatriz Mouriño-Carballido and Sophie Rabouille

PUBLISHED IN: Frontiers in Marine Science and Frontiers in Microbiology

frontiers Research Topics

frontiers

ISSN 1664-8714
ISBN 978-2-88966-689-8
DOI 10.3389/978-2-88966-689-8

About Frontiers

Frontiers is more than just an open-access publisher of scholarly articles: it is a pioneering approach to the world of academia, radically improving the way scholarly research is managed. The grand vision of Frontiers is a world where all people have an equal opportunity to seek, share and generate knowledge. Frontiers provides immediate and permanent online open access to all its publications, but this alone is not enough to realize our grand goals.

Frontiers Journal Series

The Frontiers Journal Series is a multi-tier and interdisciplinary set of open-access, online journals, promising a paradigm shift from the current review, selection and dissemination processes in academic publishing. All Frontiers journals are driven by researchers for researchers; therefore, they constitute a service to the scholarly community. At the same time, the Frontiers Journal Series operates on a revolutionary invention, the tiered publishing system, initially addressing specific communities of scholars, and gradually climbing up to broader public understanding, thus serving the interests of the lay society, too.

Dedication to Quality

Each Frontiers article is a landmark of the highest quality, thanks to genuinely collaborative interactions between authors and review editors, who include some of the world's best academicians. Research must be certified by peers before entering a stream of knowledge that may eventually reach the public - and shape society; therefore, Frontiers only applies the most rigorous and unbiased reviews.
Frontiers revolutionizes research publishing by freely delivering the most outstanding research, evaluated with no bias from both the academic and social point of view. By applying the most advanced information technologies, Frontiers is catapulting scholarly publishing into a new generation.

What are Frontiers Research Topics?

Frontiers Research Topics are very popular trademarks of the Frontiers Journals Series: they are collections of at least ten articles, all centered on a particular subject. With their unique mix of varied contributions from Original Research to Review Articles, Frontiers Research Topics unify the most influential researchers, the latest key findings and historical advances in a hot research area! Find out more on how to host your own Frontiers Research Topic or contribute to one as an author by contacting the Frontiers Editorial Office: frontiersin.org/about/contact

MARINE N_2 FIXATION: RECENT DISCOVERIES AND FUTURE CHALLENGES

Topic Editors:
Angela Landolfi, CNR, ISMAR, via Fosso del Cavaliere 100, 00133, Italy
Beatriz Mouriño-Carballido, University of Vigo, Spain
Sophie Rabouille, UMR7621 Laboratoire d'océanographie microbienne (LOMIC), France

Citation: Landolfi, A., Mouriño-Carballido, B., Rabouille, S., eds. (2021). Marine N_2 Fixation: Recent Discoveries and Future Challenges. Lausanne: Frontiers Media SA. doi: 10.3389/978-2-88966-689-8

Table of Contents

frontiers in Marine Science

EDITORIAL
published: 04 March 2021
doi: 10.3389/fmars.2021.664195

Editorial: Marine N_2 Fixation: Recent Discoveries and Future Challenges

Angela Landolfi[1,2]*, *Sophie Rabouille*[3] *and Beatriz Mouriño-Carballido*[4]

[1] GEOMAR Helmholtz Centre for Ocean Research, Marine Biogeochemistry, Kiel, Germany, [2] National Research Council CNR, Institute of Marine Sciences ISMAR, Rome, Italy, [3] Sorbonne Université, CNRS, LOMIC, Banyuls-sur-mer, France, [4] Departamento de Ecoloxía e Bioloxía Animal, Universidade de Vigo, Campus as Lagoas-Marcosende, Pontevedra, Spain

Keywords: N_2 fixation, marine N inventory, environmental controls, aphotic N_2 fixation, diversity, modeling

Editorial on the Research Topic

Marine N_2 Fixation: Recent Discoveries and Future Challenges

Marine N_2 fixation is one of the most critical processes in the ocean, controlling the bioavailability of nitrogen (N), an essential building block for the maintenance of biological activity (Falkowski, 1997). Technological advances in the field of genomics (Zehr et al., 1998) unveiled the existence of a wide variety of both N_2 fixers and N_2 fixation strategies, challenging our knowledge of the factors controlling this important process. Temperature, N deficiency, as well as iron (Fe) and phosphorus availability have been traditionally thought to be the main factors controlling diazotrophs's distribution. These factors now appear insufficient to describe the variety of physiologies associated with the diversity of N_2 fixers, and to explain the wider range of marine habitats occupied by these unique organisms (Zehr and Capone, 2020). At the same time, methodological limitations associated with the N_2 fixation rate measurement (Mohr et al., 2010) have cast some doubt on the robustness of historical data, further increasing the uncertainty of global N_2 fixation rates (Großkopf, 2012). These findings imply that we still have much to learn about the factors that control the magnitude and temporal and spatial variability of this important process, and its role in regulating ocean biogeochemistry. This Research Topic stems from two international workshops on the "Environmental Controls of Marine N_2 Fixation" aiming to connect the scientific community working on N_2 fixation. It gathers contributions from different expertise focusing on novel aspects of the physiology, ecology and biogeochemical role of diazotrophs, spanning from cellular to global scales with the aim of contributing to a more coherent understanding of the triggers and function of N_2 fixation in the marine environment.

Current independent estimates of global marine N_2 fixation from direct measurements, geochemical fingerprints on oceanic nutrient content and model simulations reviewed by Landolfi et al. in this Research Topic, range from about 100–200 $TgNy^{-1}$. Large uncertainties still remain from the lack of a comprehensive understanding of the environmental controls and ecological interactions of marine N_2 fixers. The application of molecular techniques allowed the detection of *nifH* genes in regions that extend far beyond the geographical domain of N_2 fixation originally associated to warm tropical oligotrophic waters. Using molecular fingerprinting Fernandez-Mendez et al. report on the detection of *nifH* genes in the Arctic Ocean, and the existence of a large genetic diversity that appears distinct from surrounding oceanic regions. This wider distribution is further supported by year-round measurable N_2 fixation rates in N-rich temperate waters of the upwelling system of the Iberian peninsula, that appear populated by genetically diverse diazotrophs as reported by the study of Moreira-Coello et al., challenging the traditional low-N paradigm. Oceanic environments are populated by diverse N_2 fixing organisms, including non-cyanobacterial diazotrophs. Albeit expressing low fixation rates non-cyanobacterial diazotrophs thrive both in photic and aphotic regions as reviewed by Moisander et al., potentially

Edited and reviewed by:
Lasse Riemann,
University of Copenhagen, Denmark

***Correspondence:**
Angela Landolfi
angela.landolfi@cnr.it

Specialty section:
This article was submitted to Aquatic Microbiology, a section of the journal Frontiers in Marine Science

Received: *04 February 2021*
Accepted: *11 February 2021*
Published: *04 March 2021*

Citation:
Landolfi A, Rabouille S and Mouriño-Carballido B (2021) Editorial: Marine N_2 Fixation: Recent Discoveries and Future Challenges. Front. Mar. Sci. 8:664195. doi: 10.3389/fmars.2021.664195

making a large contribution to global rates of N_2 fixation. In their perspectives Benavides, Bonnet et al. speculate that extrapolating the sparse low aphotic N_2 fixation rates for the whole mesopelagic NO_3-rich zone, would lead to a significant increase of the oceanic N inputs, largely compensating for the N loss via denitrification, and call for the consolidation of these extrapolations with future aphotic N_2 fixation rate measurement studies.

Several contributions address the control of diazotroph's biogeography by resource availability. While desert dust is considered a primary source of iron (Fe) to the ocean, its low solubility (<12%, Jickells et al., 2005) prompts phytoplankton adaptive strategies to access this micronutrient in bioavailable forms. In controlled laboratory experiments, Polyviou et al. report on the substrate specific physiological and transcriptomic responses of *Trichodesmium* for Fe acquisition from complex matrices. Direct vicinity between cell and dust particles may enhance Fe bioavailability to *Trichodesmium*, suggesting that modes of Fe-supply may be important for the niche determination of this important diazotroph. Benavides, Martias et al. discuss the role of dissolved organic matter as a possible complementary source of energy and nutrients for both cyanobacterial and non-cyanobacterial diazotrophs.

Gradoville et al. used high-throughput 16S rRNA and *nifH* gene sequencing and metagenomics to describe the microbiome associated with *Trichodesmium* colonies in the North Pacific subtropical gyre. They find that colony morphology appears to be tied to different epibiont communities, uncovering the links between physiological characteristics and ecological functions. The fate and mortality pathways of diazotrophs and their effect on biogeochemistry is just starting to be explored. In this collection, Kuznecova et al. provide new insight on the role of virus-host interaction. They investigate how viral infections affect the growth, N_2 fixation ability and gene expression of a bloom-forming heterocytous cyanobacterium *Aphanizomenon flos-aquae*.

Accurate rate measurements are key for assessing the global significance of N_2 fixation. In a combination of dedicated laboratory experiments and a literature meta-analysis Wannike et al. constrain the errors associated with the $^{15}N_2$ methods, that may lead to underestimate N_2 fixation rates measurements. They find that the errors associated with the lack of equilibration of $^{15}N_2$ are highly dependent on incubation time and experimental conditions. By comparing the retentive characteristics of filters for N_2 fixation rates measurements, in different settings from coastal waters to the Baltic Sea and Pacific Ocean, Bombar et al. warn on the potential underestimation of N_2 fixation by the use of borosilicate glass fiber filters (GF/F, Whatman) with a nominal pore size of 0.7 μm that are inadequate to capture small cells. Caputo et al. conducted a comparative analysis of two symbiotic N_2-fixing cyanobacteria, the diazotrophs-diatoms associations (DDA) and diazotroph-prymnesiophyte known as UCYN-A, both providing fixed forms of N to the host. They warn on the pre-filtration step during qPCR *nifH* surveys that lead to systematic underestimation of large and chain-forming DDAs.

In summary, the contributions included in this Research Topic focused on novel aspects of the physiology and ecology of marine diazotrophs, addressing methodological limits and current gaps in our knowledge that make future predictions a challenge. These papers contribute toward a more comprehensive understanding of the controls of this key process, which is core for improving future predictions of marine N_2 fixers under a fast-evolving climate.

AUTHOR CONTRIBUTIONS

All authors listed have made a direct and intellectual contribution to the work, and approved it for publication.

ACKNOWLEDGMENTS

Papers featured in this Special Issue have been leveraged from two workshops on the Environmental Controls of Marine N_2 Fixation: Present Knowledge and Future Challenges that brought together a multidisciplinary group of marine N_2 fixation experts, from genomics to global biogeochemistry, to consolidate current knowledge and define key uncertainties in current understanding of marine N_2 fixation. We acknowledge the funding support from the Deutsche Forschungsgemeinschaft (DFG) project SFB754 and Euromarine 2015 Workshop grant.

REFERENCES

Falkowski, P. G. (1997). Evolution of the nitrogen cycle and its influence on the biological sequestration of CO_2 in the ocean. *Nature* 387, 272–275. doi: 10.1038/387272a0

Großkopf, T. (2012). Direct and indirect costs of dinitrogen fixation in Crocosphaera watsonii WH8501 and possible implications for the nitrogen cycle. *Front. Microbiol.* 3:236. doi: 10.3389/fmicb.2012.00236

Jickells, T. D., An, Z. S., Andersen, K. K., Baker, A. R., Bergametti, G., Brooks, N., et al. (2005). Global iron connections between desert dust, ocean biogeochemistry, and climate. *Science* 308, 67–71. doi: 10.1126/science.1105959

Mohr, W., Großkopf, T., Wallace, D. W. R., and LaRoche, J. (2010). Methodological underestimation of oceanic nitrogen fixation rates. *PLoS ONE* 5:e12583. doi: 10.1371/journal.pone.0012583

Zehr, J. P., and Capone, D. G. (2020). Changing perspectives in marine nitrogen fixation. *Science* 368:eaay9514. doi: 10.1126/science.aay9514

Zehr, J. P., Mellon, M. T., and Zani, S. (1998). New nitrogen-fixing microorganisms detected in oligotrophic oceans by amplification of nitrogenase (nifH) genes. *Appl. Environ. Microbiol.* 64, 3444–3450. doi: 10.1128/AEM.64.9.3444-3450.1998

Conflict of Interest: The authors declare that the research was conducted in the absence of any commercial or financial relationships that could be construed as a potential conflict of interest.

frontiers in Microbiology

ORIGINAL RESEARCH
published: 23 November 2016
doi: 10.3389/fmicb.2016.01884

Diazotroph Diversity in the Sea Ice, Melt Ponds, and Surface Waters of the Eurasian Basin of the Central Arctic Ocean

Mar Fernández-Méndez[1,2], Kendra A. Turk-Kubo[3], Pier L. Buttigieg[1], Josephine Z. Rapp[1,2], Thomas Krumpen[4], Jonathan P. Zehr[3] and Antje Boetius[1,2]*

[1] HGF-MPG Group for Deep Sea Ecology and Technology, Alfred Wegener Institute Helmholtz Centre for Polar and Marine Research, Bremerhaven, Germany, [2] HGF-MPG Group for Deep Sea Ecology and Technology, Max Planck Institute for Marine Microbiology, Bremen, Germany, [3] Department of Ocean Sciences, University of California at Santa Cruz, Santa Cruz, CA, USA, [4] Sea Ice Physics Section, Climate Sciences Department, Alfred Wegener Institute Helmholtz Centre for Polar and Marine Research, Bremerhaven, Germany

OPEN ACCESS

Edited by:
Angela Landolfi, GEOMAR Helmholtz Centre for Ocean Research Kiel, Germany

Reviewed by:
James T. Hollibaugh, University of Georgia, USA
Mikkel Bentzon-Tilia, Technical University of Denmark, Denmark
Isabelle C. Biegala, Institut de Recherche pour le Développement (IRD), France

***Correspondence:**
Mar Fernández-Méndez
mar.fdez.mendez@gmail.com

Specialty section:
This article was submitted to Aquatic Microbiology, a section of the journal Frontiers in Microbiology

Received: *29 June 2016*
Accepted: *09 November 2016*
Published: *23 November 2016*

Citation:
Fernández-Méndez M, Turk-Kubo KA, Buttigieg PL, Rapp JZ, Krumpen T, Zehr JP and Boetius A (2016) Diazotroph Diversity in the Sea Ice, Melt Ponds, and Surface Waters of the Eurasian Basin of the Central Arctic Ocean. Front. Microbiol. 7:1884. doi: 10.3389/fmicb.2016.01884

The Eurasian basin of the Central Arctic Ocean is nitrogen limited, but little is known about the presence and role of nitrogen-fixing bacteria. Recent studies have indicated the occurrence of diazotrophs in Arctic coastal waters potentially of riverine origin. Here, we investigated the presence of diazotrophs in ice and surface waters of the Central Arctic Ocean in the summer of 2012. We identified diverse communities of putative diazotrophs through targeted analysis of the *nifH* gene, which encodes the iron protein of the nitrogenase enzyme. We amplified 529 *nifH* sequences from 26 samples of Arctic melt ponds, sea ice and surface waters. These sequences resolved into 43 clusters at 92% amino acid sequence identity, most of which were non-cyanobacterial phylotypes from sea ice and water samples. One cyanobacterial phylotype related to *Nodularia* sp. was retrieved from sea ice, suggesting that this important functional group is rare in the Central Arctic Ocean. The diazotrophic community in sea-ice environments appear distinct from other cold-adapted diazotrophic communities, such as those present in the coastal Canadian Arctic, the Arctic tundra and glacial Antarctic lakes. Molecular fingerprinting of *nifH* and the intergenic spacer region of the rRNA operon revealed differences between the communities from river-influenced Laptev Sea waters and those from ice-related environments pointing toward a marine origin for sea-ice diazotrophs. Our results provide the first record of diazotrophs in the Central Arctic and suggest that microbial nitrogen fixation may occur north of 77°N. To assess the significance of nitrogen fixation for the nitrogen budget of the Arctic Ocean and to identify the active nitrogen fixers, further biogeochemical and molecular biological studies are needed.

Keywords: nitrogen fixation, *nifH*, Arctic, non-cyanobacterial diazotrophs, sea ice, bacterial diversity

INTRODUCTION

Arctic marine ecosystems are rapidly changing due to climate change (Wassmann et al., 2011). In summer 2012, Arctic sea ice extent declined to its minimum ever recorded (Parkinson and Comiso, 2013), following the general trend in Arctic sea-ice cover decline (Stroeve et al., 2012). This led to vast areas of water being exposed to higher light intensities, which enhances phytoplankton

primary production (Arrigo and van Dijken, 2015). Primary production in this highly stratified ocean is generally limited by nitrogen, most of which is delivered in the form of nitrate via the inflow of Pacific and Atlantic waters (Codispoti et al., 2013). Riverine input of nitrogen, especially from the Lena river that discharges into the Laptev Sea, may be another important source of nitrate in the Eurasian Basin (Holmes et al., 2011), alongside atmospheric deposition by snowfall (Beine et al., 2003), recycling of organic matter, and nitrogen fixation in ice masses. These different nitrogen sources should be balanced by nitrogen sinks, such as primary production and export, as well as microbial denitrification along the broad continental shelves that surround the Arctic Ocean (Devol et al., 1997; Rysgaard et al., 2004). However, current nutrient budgets indicate an imbalance of Arctic nitrogen supply, demand and export, suggesting that nitrogen fixation may have a key role in closing the budget (Torres-Valdés et al., 2013).

The biological fixation of gaseous dinitrogen (N_2) by diazotrophs is an important source of bioavailable nitrogen in nutrient-limited pelagic ecosystems (LaRoche and Breitbarth, 2005), thereby influencing primary productivity and carbon export to the seafloor (Codispoti et al., 2001; Arrigo, 2005). Nitrogen fixation rates in surface waters of tropical, subtropical and some temperate oceans are primarily driven by diazotrophic cyanobacteria (Langlois et al., 2008; Moisander et al., 2010; Turk-Kubo et al., 2012). Non-cyanobacterial diazotrophs have also been detected in numerous marine, pelagic environments (Falcón et al., 2004; Riemann et al., 2010; Farnelid et al., 2011; Moisander et al., 2014), although their contribution to oceanic nitrogen fixation remains poorly understood (Turk-Kubo et al., 2014). In contrast to temperate and tropical seas, the specific contribution of nitrogen fixation and its key microbial agents in ice-covered seas is not well known (Tremblay et al., 2009; Blais et al., 2012; Luo et al., 2012; Torres-Valdés et al., 2013). This study aims at providing a first survey of the nitrogen-fixing potential of the eastern Central Arctic Ocean.

Several factors are thought to constrain oceanic nitrogen fixation: low temperatures (Brauer et al., 2013), high dissolved oxygen, high N:P ratios, and iron or phosphate limitation (Paerl and Zehr, 2000; Mills and Arrigo, 2010; Riemann et al., 2010; Monteiro et al., 2011). The generally low temperatures and the high dissolved oxygen in Arctic waters (Bates et al., 2014) support the long-held assumption that nitrogen fixation is unlikely in the Arctic Ocean. However, diazotrophs have developed strategies to withstand freezing and high salinity by producing antifreeze proteins (Schmidt et al., 1991), and to avoid oxygen by developing endo-symbiosis, like *Rhizobiales*, which include mainly *Alpha-proteobacteria* and *Beta-proteobacteria* and have been identified also in polar soils and frost flowers (Bordeleau and Prévost, 1994; Bowman et al., 2013). Symbiotic associations between diatoms and diazotrophs have been described in other oceans (Villareal, 1992; Foster et al., 2011). We hypothesize that sea-ice related environment of the Eurasian basin of the Central Arctic Ocean might hold diazotrophs.

Arctic waters often have low N:P ratios (Tremblay et al., 2008), which have been hypothesized to favor diazotrophs (Tyrrell, 1999). They are relatively rich in iron (1–3 nM) from river input (Klunder et al., 2012), which could well support the iron demand of nitrogen fixing enzymes. Nitrogen fixation rates and putative diazotrophs from riverine origin (microorganisms containing at least the *nifH* gene) have been identified close to the Mackenzie River and in the water column of the Canadian Arctic shelves (Farnelid et al., 2011; Blais et al., 2012). Relatively high cyanobacterial *nifH* gene diversity (e.g., *Trichodesmium* and *Cyanothece*) has also been described in the sea ice and waters of the Fram Strait in the Eurasian Basin (Díez et al., 2012). In contrast, to date there is no record of marine diazotroph occurrence in the Central Arctic Ocean north of 76°N. Non-diazotrophic cyanobacteria, such as *Prochlorococcus*, which are very abundant in other oceanic regions (Partensky and Hess, 1999), are rare in polar marine waters (Vincent, 2000; Lovejoy and Potvin, 2010) although they appear in both polar regions (Nadeau et al., 2001). Diazotrophic cyanobacteria, which represent a small percentage of marine cyanobacteria, are also the most common autotrophic diazotroph in other oceans (Moisander et al., 2010; Luo et al., 2012) and on glaciers (Yallop et al., 2012), but their diversity and abundance in the marine environments of the polar regions is still understudied.

In the Arctic Ocean, only a few *nifH* gene surveys have been conducted in the past decade, and they focused on coastal regions. In this study, we investigated *nifH* gene diversity in different Arctic environments, including Arctic sea ice and surface water from under-ice and open water locations. To assess diazotroph diversity and discover specific phylotypes that might be unique for the Arctic marine environment, we chose a targeted analysis of the *nifH* gene, coding for the iron protein of the nitrogenase enzyme. In addition, we used molecular fingerprinting analyses of the intergenic spacer region of the rRNA operon to characterize the complete bacterial community, and to reveal the dissimilarity patterns between different sea-ice related environments. Furthermore, we measured the physical-chemical properties of each environment type and we included data about the origin of the sea ice, measured by its drift trajectory.

These datasets allowed us to assess the distribution and diversity of diazotrophs in melt pond, sea-ice and surface waters of the Central Arctic and to evaluate the genetic nitrogen-fixing potential of the microbial communities. Specifically, we addressed the hypotheses that (1) putative diazotrophs of the Central Arctic occupy a niche in the nitrogen-limited sea ice and waters of the Eurasian Basin, (2) they originate from coastal areas such as the Laptev Sea where the ice is formed and transported with the Transpolar Drift, and (3) the Central Arctic marine sea-ice related diazotrophs are distinct from other cold-adapted diazotrophic communities and those of adjacent oceanic regions.

MATERIALS AND METHODS

Sampling

A total of 53 samples were taken for this investigation during the ARKXXVII/3 cruise to the Central Arctic (77–88°N and 30–133°E) from the 7th of August to the 30th of September, 2012, onboard the German icebreaker R/V POLARSTERN

(Supplementary Table S1). Sea ice, melt ponds and seawater were sampled at 9 ice stations and 13 water stations located in different parts of the central Eurasian Basin. Surface water samples from ice-covered waters ($n = 13$) were differentiated from those from open water from the Laptev Sea region ($n = 6$) for the analysis. Our samples come from a wide range of ice conditions and nutrient regimes (**Figure 1**). Samples of rapidly melting sea ice ($n = 21$) were taken using an ice corer (Kovacs Entreprise, Roseburg, OR, USA) and cut into two sections (top and bottom) prior to being transferred to plastic containers that had been rinsed with ultrapure water and ethanol and melted in the dark at 4°C. Samples of melt pond water ($n = 8$) and algal aggregates ($n = 5$) found in melt ponds were collected using a hand pump (Model 6132-0010, Nalgene, Penfield, NY, USA) and stored in clean Nalgene bottles. Samples of water under the ice ($n = 5$) were collected using a peristaltic pump (Masterflex® E/S™ portable sampler, 115 VAC, Oldham, UK). Surface water (2–5 m depth) samples at all other stations ($n = 13$) were collected with a rosette sampler equipped with Niskin bottles and a Conductivity Temperature Depth (CTD) profiler (Sea-Bird Electronics Inc., Bellevue, WA, USA). In addition, ultrapure water was sampled to check for possible contaminations from the onboard water

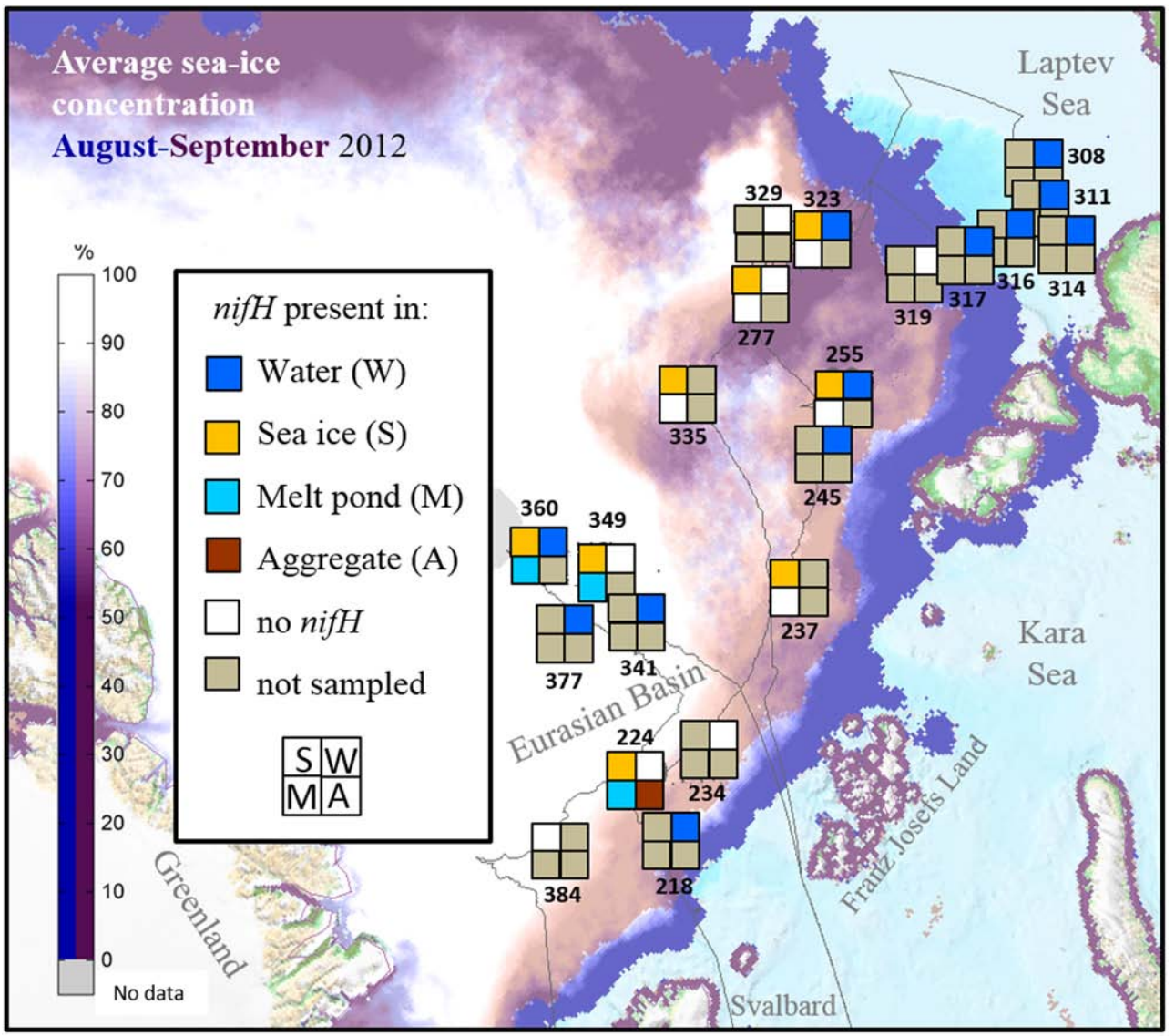

FIGURE 1 | Stations sampled for *nifH* analysis in the Eurasian Basin of the Central Arctic during summer 2012. Station numbers correspond to those in Supplementary Table S1. Each square correspond to one environment. If a particular environment was not samples at one station it appears in gray. If no *nifH* gene could be amplified it is colored in white, and if *niH* genes could be amplified in the color corresponding to each environment (Dark blue = water, Yellow = sea ice, Light Blue = melt pond and Brown = algal aggregates). The thin gray line corresponds to the cruise track. Average sea-ice concentration data source: www.meereisportal.de.

purification system (Milli-Q Gradient A10, Millipore) when using this water to rinse the sampling equipment. Between 0.3 and 2 L volume of each sample were filtered through Sterivex filters of 0.2 μm pore size (Durapore, Milipore, Darmstadt, Germany) using a multichannel peristaltic pump (Model PD 51; Heidolph, Schwabach, Germany). Filters were stored at −80°C until further processing.

Characterization of Central Arctic Environments

Temperature and salinity were measured in sea ice and melt pond water with a hand-held conductivity meter (315i with TetraCon electrode cell, WTW GmbH, Weilheim in Oberbayern, Germany), and in the water column with a CTD profiler. The data is available in the databases of the Data Publisher for Earth and Environmental Science, PANGAEA, doi: 10.1594/PANGAEA.819452 (Rabe et al., 2012). Concentrations of nitrate, phosphate and silicate were measured with a standard photometric method using a Technicon TRAACS 800 continuous flow auto analyzer (Technicon Corporation) as described in Fernández-Méndez et al. (2015). Raw nutrient concentrations and integrated stocks are available in PANGAEA doi: 10.1594/PANGAEA.834081 (Fernández-Méndez et al., 2014a; Bakker, 2014, unpublished).

Data concerning ice thickness and melt pond coverage are stored in PANGAEA, doi: 10.1594/PANGAEA.803221 (Hendricks et al., 2012). The origin of sea ice was determined using ice drift information obtained from satellites. In this study, two different sets of ice drift products were used: The first data set, Polar Pathfinder Sea Ice Motion Vectors (Version 2) obtained from the National Snow and Ice Data Center (NSIDC) was chosen because of its year round availability. We used it to calculate ice drift trajectories during summer months (June–August). The second data set, sea ice motion provided by the Center for Satellite Exploitation and Research (CERSAT) at the Institut Francais de Recherche pour l'Exploitation de la Mer (IFREMER), shows a good performance on the Siberian shelf (Krumpen et al., 2013) and was therefore used to complement the calculation of ice drift trajectories between September and May. To determine drift trajectories and source areas of sampled sea ice a specific ice area is tracked backward until: (a) the ice reaches a position next to a coastline, (b) the ice concentration at a specific location reaches a threshold value of (>15%) when ice parcels are considered lost, or (c) the tracking time exceeds 4 years. A more detailed method description is provided in Krumpen et al. (2016).

nifH Gene Molecular Analysis

Total community DNA was extracted using the DNeasy Plant Mini Kit (QIAGEN, Valencia, CA, USA) and the QIAcube extraction instrument following the manufacturer's instructions (Bombar et al., 2013). To amplify the *nifH* gene, a nested polymerase chain reaction (PCR) employing a high number of amplification cycles ($n = 50$) with two sets of degenerate primers was used since it is a high-sensitivity method (Zehr and Turner, 2001). The four degenerate primers used, *nifH*1-*nifH*4, cover >94% of available *nifH* sequences, allowing our approach to access a high percentage of the known diazotroph diversity (Gaby and Buckley, 2012) at the limited availability of sample volume in this study. PCR amplifications were performed in a MyCycler Thermal Cycler (BioRad, Berkeley, CA, USA). The first PCR amplification of *nifH* in each sample was performed with 2 μl of DNA template in 24 μl of PCR reaction containing 4 mM $MgCl_2$, 0.4 mM dNTPs, 10X Buffer, 1.25 U (0.2 μl) Platinum TaqDNA Polymerase (Invitrogen) and 0.5 μM of the forward *nifH*3 primer (5′-ATR TTR TTN GCN GCR TA-3′) and reverse *nifH*4 primer (5′-TTY TAY GGN AAR GGN GG-3′) (Zehr and Turner, 2001). Amplifications proceeded with 25 cycles of 3 min at 95°C, 30 s of denaturation at 95°C, 30 s of annealing at 55°C and 45 s of elongation at 72°C. The second amplification procedure was performed as described above, save the use of 1 μl of the PCR product from the first amplification process as the template and the forward *nifH*1 primer (5′-TGY GAY CCN AAR GCN GA-3′) and reverse *nifH* primer (5′-ADN GCC ATC ATY TCN CC-3′) (Zehr and Turner, 2001). In addition, the annealing temperature was increased to 57°C. In both steps, negative controls were performed using milliQ water in place of the DNA template.

A 15 μl aliquot of the PCR products from the second amplification was used for electrophoresis separation (1,4% low-melt agarose gel). The DNA band of the appropriate size (360 bp) was extracted with a gel extractor (X-tracta gel extractor, USA Scientific, Ocala, FL, USA). The gel was purified with a QIAquick Gel Extraction Kit (Qiagen) and the DNA cloned with a TOPO® TA Cloning® Kit for Sequencing with One Shot® TOP10 Chemically Competent *E. coli* (Invitrogen) following the manufacturer's guidelines. Dependent on outcomes of the cloning process, plasmids from between 12 and 48 clones per sample were purified using the Millipore Montage Plasmid $Miniprep_{96}$KitsMiniprep kit (Millipore, Darmstadt, Germany) and the inserts were sequenced using the Sanger method (Sanger et al., 1977) at the University of California, Berkeley.

Nucleic acid sequence data were trimmed and quality checked using the Sequencher® sequence analysis software (Gene Codes Corporation, Ann Arbor, MI, USA). Quality-controlled sequences were imported into the software program ARB (Ludwig et al., 2004), translated to amino acid sequences and imported into a publically available, curated GenBank database containing all *nifH* sequences submitted to the nr database that have been validated to be *nifH* based on analysis (Heller et al., 2014; April 2014 release). Amino acid sequences were aligned using the program HMMER which contains a Hidden Markov Model from the protein family database PFAM (Finn et al., 2010). Subsequently, the nucleotide sequences were re-aligned according to the aligned amino acid sequences using ARB. To confirm that the sequences were *nifH* gene, the alignments were visually checked for conserved regions. Our 572 confirmed *nifH* sequences included one sequence from the PCR blank and 28 sequences from the ultrapure water used to rinse the plastic containers where the samples were stored. These sequences clustered at >94% amino acid sequence identity with 15 sequences from our environmental samples, so these were considered putative contaminants and removed from further analyses. We also checked if any of the retrieved sequences were closely related to other sequences reported as

contaminants on other studies. The 45 contaminant amino acid sequences reported in the April 2014 *nifH* database (Farnelid et al., 2009, 2013) were all less than 90% similar to our sequences retrieved from the environment. Despite these checks, one cannot exclude the possibility that some of the sequences reported might be contaminants. From the 529 confirmed environmental *nifH* sequences, a total of 43 clusters with ≥92% amino acid sequence identity were identified using the CD-HIT program suite (Huang et al., 2010). Each cluster was represented by one representative sequence. A maximum likelihood tree of partial *nifH* sequences was built in RAxML version 8.1 (Stamatakis, 2014). This tree included the 43 representative sequences (92% amino acid similarity using the matrix BLOSUM62) of our *nifH* Arctic sequences and their closest cultivated relatives. We used the RAxML function *auto prot* to determine the most appropriate protein substitution model. Following the function's recommendation, we used the LG matrix substitution model to determine relatedness (represented by branch length) and a custom mask for the *nifH* amplicon region (Mask Makyyy in the ARB publicly available database). The stability of the RAxML phylogenetic reconstruction was assessed by bootstrapping 1000 times with RAxML's *-b* function. The tree and its associated metadata were visualized using ITOL (Letunik and Bork, 2007). The phylogenetic affiliation of each *nifH* cluster, defined by CD-HIT, was determined based on the phylogenetic affiliation of the closest cultivated relative, which have been assigned according to the convention suggested by Zehr et al. (2003) and provided in the curated *nifH* database (Heller et al., 2014).

For the comparison of different regions, sequences from nine independent studies, including the present one, were selected from studies submitted to the GenBank database prior to April 2014. All available Arctic sequences from different environments were selected, as well as all Antarctic sequences, which were exclusively from lake microbial mats. In addition, sequences from one study in the North Atlantic (constrained to surface water samples as in our study) and one in the subtropical Atlantic (water samples collected at 8 m depth) were selected for further comparison outside of the polar regions. In total, 1523 sequences were chosen to characterize the diazotroph community structure from: the Central Arctic (this study) (n = 572), the coastal Canadian Arctic (Blais et al., 2012) (n = 21), the coastal Eurasian Basin (Díez et al., 2012) (n = 69), the Arctic tundra soil (Izquierdo and Nüsslein, 2006) (n = 24), the Antarctic ice shelf microbial mats in lakes (Olson et al., 1998; Jungblut and Neilan, 2010) (n = 15+43), the subtropical Atlantic Ocean (Langlois et al., 2005) (n = 175), and the North Atlantic Ocean (Turk et al., 2011) (n = 604). All studies except Díez et al., 2012 used the same primers as used in this study. Nucleotide sequences from these studies were clustered using CD-HIT EST (Li and Godzik, 2006) at 97% nucleotide similarity (Turk-Kubo et al., 2014). From the 243 representative sequences (of 1523 initial sequences), 86 originated from *nifH* genes present in the Central Arctic, 19 from the Canadian Arctic, 20 from the Eurasian Basin, 16 from the Arctic tundra, 25 from the Antarctic microbial mats, 51 from the North Atlantic, and 26 from the subtropical Atlantic. The representative sequences at 97% nt identity retrieved from the Central Arctic sea-ice related environments as well as the ultrapure water blanks were submitted to GenBank and assigned accession numbers KT354077-KT354180. Only five of the CD-HIT clusters represented sequences from both the North Atlantic and the subtropical Atlantic and one CD HIT cluster represented sequences from the Eurasian Basin and the Subtropical Atlantic. All other CD-HIT clusters represented sequences exclusively from one oceanic region. A maximum likelihood tree of these 243 representative sequences was built using RAxML v8.1. The best performing model was the WAG matrix substitution model. The stability of the RAxML tree was assessed by bootstrapping 1000 times with RAxML's *-b* function. The tree and its associated metadata were visualized using ITOL (Letunik and Bork, 2007).

Intergenic Spacer 16SrRNA Molecular Analysis

The bacterial community structure was investigated targeting the Intergenic Spacer (ITS) region of the 16SrRNA by Automated Ribosomal Intergenic Spacer Analysis (ARISA) (Fisher and Triplett, 1999) in the 26 samples where *nifH* could be amplified. ARISA was chosen as a rapid and effective method to analyze bacterial community structure across this large dataset. Results of this method were previously shown to be coherent with diversity patterns retrieved using next generation sequencing approaches (e.g., Gobet et al., 2014). Each ARISA PCR contained 2.5 μl of 10x reaction buffer S (PEQLAB Biotechnologie GmbH, Erlangen, Germany), 1 μl of 25 mM $MgCl_2$ (PEQLAB Biotechnologie GmbH, Erlangen, Germany), 0.625 μl of a 10 mM dNTP mix (PEQLAB Biotechnologie GmbH, Erlangen, Germany), 0.75 μl of 3 mg ml^{-1} bovine serum albumin (Sigma-Aldrich Chemie Gmbh; Munich, Germany), 0.25 μl of 40 μM universal forward primer ITSF (5′-GTCGTAACAAGGTAGCCGTA-3′) (Biomers.net, Ulm, Germany), labeled with 6-carboxyfluorescein (FAM), 0.25 μl of 40 μM ITSReub reverse primer (5′-GCCAAGGCATCCACC-3′) (Biomers.net, Ulm, Germany), 0.25 μl of 5 units μl^{-1} Taq polymerase (PEQLAB Biotechnologie GmbH, Erlangen, Germany) and approximately 10 ng environmental DNA as determined by spectrophotometry (Infinite® M200 NanoQuant, Tecan Group Ltd., Switzerland). PCR water was added to each reaction mix to a final volume of 25 μl. All reactions were conducted in triplicate. PCR conditions were set to 3 min at 94°C, 30 cycles of first 94°C for 45 s, 55°C for 45 s, and 72°C for 90 s followed. Final extension time was 5 min at 72°C.

PCR performance was examined using gel electrophoresis and the length of successfully amplified and purified ITS fragments was analyzed via capillary electrophoresis on an ABI Prism 3130 XL – Genetic Analyzer (Applied Biosystems, Carlsbad, CA, USA). Signals were evaluated using the GeneMapper Software v3.7 (Applied Biosystems, Carlsbad, CA, USA) and subsequent generation of operational taxonomic units (OTUs) was done with custom R scripts[1] as previously described (Ramette, 2009).

Statistical Analysis and Ordination

All statistical tests were performed in R version 3.1.1 (R Core Team, 2015). Differences in diazotroph community structure –

[1]http://www.ecology-research.com

based on the presence or absence of *nifH*-derived operational taxonomic units – were expressed using the Jaccard dissimilarity measure, which was computed as $2B/(1+B)$, where B is the Bray–Curtis dissimilarity measure:

$$B = \frac{\sum_{i-1}^{S}(x_{ij} - x_{ik})}{\sum_{i-1}^{S}(x_{ij} + x_{ik})}$$

and visualized by non-metric multidimensional scaling (NMDS) using the metaMDS routine of the "vegan 2.3" package (Oksanen et al., 2013). Differences in the total bacterial community structure – represented through variations in the internal transcribed spacer region (ITS) fingerprint – were similarly visualized, but calculated using the Bray–Curtis dissimilarity measure (Legendre and Legendre, 1998). Guided by the Shepherd stress of our NMDS results, we chose to ordinate ranked dissimilarities from both analyses in two-dimensional space. In each plot, dissimilarity between samples is approximated by the distances between the points representing them. Stress values reflect the degree of correspondence between the distances between points in the NMDS plot and values in the original dissimilarity matrix. An analysis of similarity (ANOSIM) was used to evaluate how strongly our representations of bacterial community structure differed between *a priori* defined groups. The groups defined were: Laptev Sea ($n = 4$), Surface Waters ($n = 6$), Melt Ponds ($n = 3$), Ice Bottom ($n = 3$), Ice Top ($n = 8$), Brown ice ($n = 1$), and Aggregate ($n = 1$). Groups with one sample only were excluded from the analysis. First, we performed an omnibus test followed by a pairwise ANOSIM as *post hoc* testing. Individual p-values were Bonferroni-corrected. A Mantel test was performed using the mantel routine of the "vegan 2.3" package to compare the two dissimilarity matrices (*nifH* and ARISA).

To complement our dissimilarity-based methods, which may confound location and spread (Warton et al., 2012), redundancy analysis (RDA) using type I scaling was used to estimate the degree of linear association between variation in the diazotroph community and temperature, salinity, nitrate, phosphate and silicate. These environmental variables were standardized by z-scoring prior to use in RDA. The response data was Hellinger transformed to standardize it (Legendre and Gallagher, 2001), using the *decostand* function of the "vegan 2.3" package. The significance of the RDA analysis was calculated using ANOVA and the residuals were plotted in a histogram (Supplementary Figure S3).

To compare the diazotroph community of the Central Arctic Ocean described in this study to the diazotroph community from Arctic adjacent oceanic regions (Canadian and Eurasian Arctic shelves), other polar environments (Antarctic lake microbial mats and Arctic tundra soil), and other oceanic regions (North and Subtropical Atlantic), we performed phylogenetic distance analysis (Unifrac) (Lozupone et al., 2006) on the maximum likelihood phylogenetic tree containing only representative sequences from those environments (CD-HIT clustering at a 97% nucleotide similarity threshold). To calculate dissimilarities based on phylogenetic distances between the diazotrophic communities we used the package "phyloseq" in R (McMurdie and Holmes, 2013). Principal coordinate analysis (PCoA) was used to ordinate Unifrac distances using the functions *cmdscale()* and *ordiplot()* in the R package "vegan 2.3." An automatic correction for negative eigenvalues was used. Rarefaction curves were computed across Hill numbers (Chao et al., 2014) using the iNEXT package (Hsieh et al., 2016), both for 92% amino acid similarity representative sequences in the different sea-ice related environments of the Central Arctic, as well as for the 97% nucleotide identity representative sequences in the different oceanic regions. Hill number 0 refers to species richness, 1 to the number of 'typical' species in the community (exponential of Shannon entropy), and 2 to the number of very abundant species in a community (inverse Simpson).

RESULTS

Characterization of Arctic Diazotroph Communities Based on *nifH* sequences

During our study in summer 2012, *nifH* gene fragments were amplified from 26 of the 53 samples collected in different Arctic environments: sea ice, melt ponds and surface water column (**Figure 1**). A total of 529 sequences were retrieved, 40% of them from the upper part of the sea ice and only 5% from melt ponds (**Table 1**; Supplementary Table S1). These sequences were clustered into 43 clusters at 92% amino acid similarity and were distributed across all four main *nifH* clusters I–IV as defined by Zehr et al. (2003), including both cyanobacterial and non-cyanobacterial phylotypes (**Figures 2** and **3**). Central Arctic sequences affiliated with Cluster I contained mainly *Proteobacteria* (1G and 1K), *Firmicutes* (1E), *Cyanobacteria* (1B) and several uncultivated microorganisms. Cluster II contained *Proteobacteria* (2C), *Firmicutes* (2A), and members of the Archaea (2B). Cluster III contained putative anaerobes including sulfate reducing genera of the *Deltaproteobacteria*, and genera such as *Clostridium*. Cluster IV contained *nifH* paralogs that are thought to function in metabolic processes other than nitrogen fixation (e.g., Young, 2005; Staples et al., 2007).

TABLE 1 | Number of samples screened for *nifH* gene amplification and confirmed *nifH* gene sequences retrieved.

Environment	Total Samples	Samples with *nifH*	Sequences retrieved
Melt ponds	8	3	24
Ice top	8	8	211
Ice bottom	13	4	91
Water under the ice	13	6	120
Surface open waters Laptev Sea	6	4	40
Algal aggregates	5	1	43
Total	53	26	529

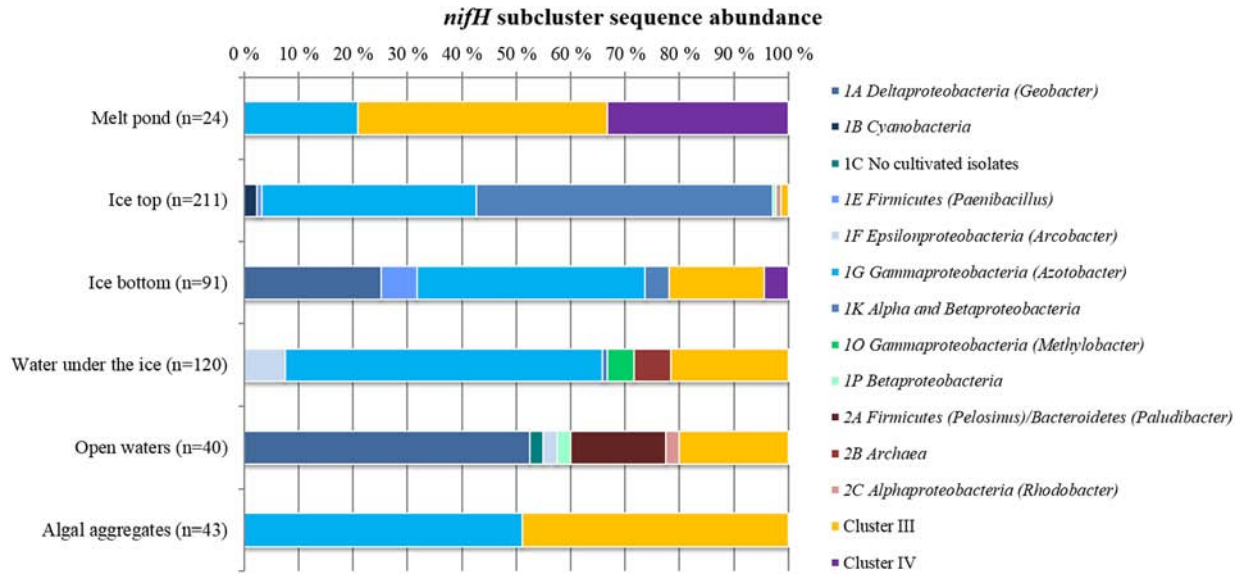

FIGURE 2 | Relative abundances of different *nifH* subclusters in Central Arctic environments. The number of sequences retrieved from each environment is shown in parenthesis. Open waters correspond to the region close to the Laptev Sea.

The vast majority of sequences retrieved across the different environments of the Central Arctic Ocean belonged to non-cyanobacterial diazotrophs of Cluster I (**Figure 2**). In this cluster, 53% of the sequences belonged to the subcluster 1G that contains sequences from genera such as *Azotobacter*, *Brenneria*, *Teredinibacter*, and *Pseudomonas*. Subcluster 1K comprised 29% of the sequences, containing both *Alpha-* and *Beta-proteobacteria* such as *Bradyrhizobium* and *Azospirillum* sp. From subcluster 1B, which contains exclusively cyanobacterial diazotrophs, only five sequences were amplified from the upper layer of the sea ice (top 50 cm of a snow-free core) at ice station 224 (Subcluster 1B, Representative sequence N_224IT_002 in **Figure 3**). These sequences were all closely related (≥92% amino acid sequence similarity) to *Nodularia*. Cluster III sequences accounted for up to 20% of the sequences retrieved by clone libraries from all samples together (**Figure 2**). Only 12 sequences corresponding to *nifH* paralogs (Cluster IV) were retrieved from sea-ice and melt pond samples, but they were not closely related to any cultivated organism (**Figure 3**). Since they do not provide any insight into nitrogen fixation capabilities of the Arctic microbial community, we will not develop them further.

Presence of *nifH* Genes in the Central Arctic and Link to Temperature and Nutrients

Two of the main environmental factors that might affect the presence of diazotrophs, temperature and nutrient concentrations, were quite variable in the environments and stations sampled. Seawater temperatures ranged from −1.7°C below the ice and up to 3°C in open waters of the Laptev Sea shelf (Supplementary Figure S1). Sea-ice temperatures were between −0.2 and −1.8°C and melt pond temperatures between −0.7 and 0.3°C. Nitrogen fixation genes from putative diazotrophs were amplified from samples along the entire temperature range sampled (**Figure 1**).

Regarding nutrients, nitrate concentrations in summer 2012 were very similar in sea ice and melt ponds ranging between 0.2 and 1.5 μM, while being more variable in surface waters ranging between 0.02 and 6.4 μM (with highest concentrations at stations 218 and 245). Phosphate, the most relevant nutrient for diazotrophs, was more variable in sea ice (0.02–1.95 μM) reaching its highest concentrations at ice station 224. Melt ponds had in general very low phosphate concentrations (0.04–0.2 μM) while in surface waters the concentrations were higher (0.15–0.49 μM). As indicated by the N:P molar ratio, during summer in the Central Arctic, two nutrient regimes were identified in the euphotic zone of the water column (Supplementary Figure S2A). All N:P molar ratios in surface waters were below Redfield (<16:1) indicating general nitrogen limitation. The Atlantic-influenced ice margin in the Nansen Basin and the Laptev Sea had N:P ratios around 10, while the more Central Arctic waters in the Amundsen Basin had N:P ratios below 5. In sea ice, nutrient concentrations were in general lower than in the water column and the integrated N:P ratios were more variable. N:P ratios at stations 335 and 349 were close to Redfield, while the rest ranged between 5 and 11 (Supplementary Figure S2B). In melt ponds the N:P ratio ranged between 1 and 16. The genes responsible for nitrogen fixation could be amplified in all environments regardless of their N:P ratio at the time of sampling.

Our RDA suggests that our current set of explanatory variables are only able to account for just over half (∼57%) of the variation in our *nifH* subcluster data (**Figure 4**). Salinity and silicate increasing concentrations showed strong positive covariation, while phosphate concentrations showed a negative covariation with the other variables (**Figure 4**). Nitrate concentrations and

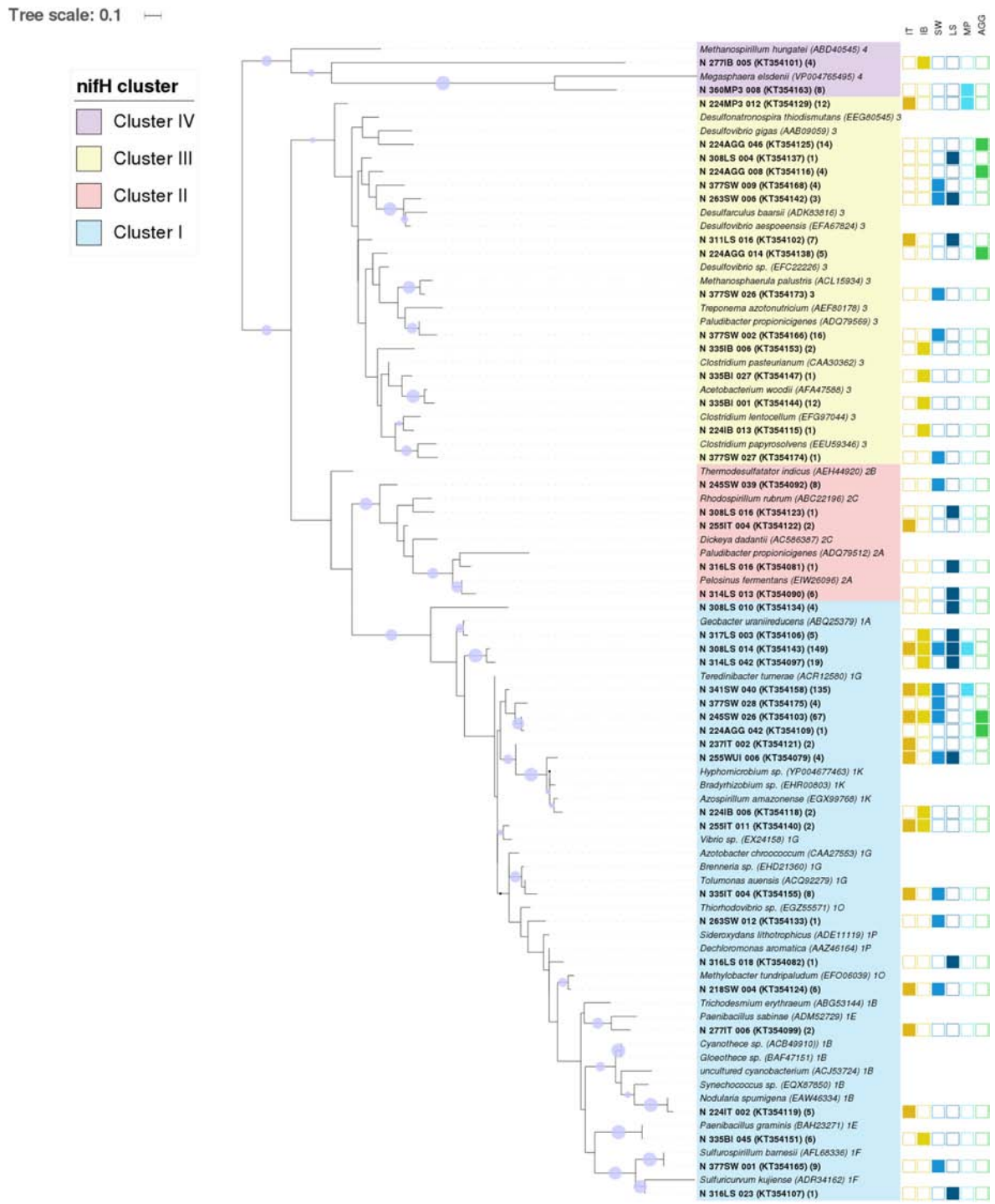

FIGURE 3 | Central Arctic *nifH* gene diversity in summer 2012. Maximum likelihood phylogenetic tree of *nifH* partial amino acid sequences (104 positions) containing representative sequences from the Central Arctic (bold) and their closest cultivated relatives (italics). The Central Arctic *nifH* amino acid sequences were clustered using CD-HIT at 92% amino acid similarity to determine representative sequences. The origin of our Central Arctic representative sequences is indicated in the name. The number of sequences represented by each CD-HIT subcluster are indicated in brackets. The station number is followed by the environment from which it originates: Ice Top (IT), Ice Bottom (IB), Brown Ice (BI), Melt Pond (MP), Algal aggregate (AGG), Water under the ice (WUI), Surface water (SW), and Laptev Sea (LS). The *nifH* subcluster assignment for each cultivated diazotroph is indicated after the name. Branch lengths were determined using the LG protein substitution model as recommended by RAxML Version 8. The percentage of calculated trees in which sequences clustered together in the bootstrap test (1000 replicates) is shown next to the branch as a purple circle when greater than 50% (smallest circle corresponds to 50% and greater to 100%). GenBank accession numbers for the 43 representative sequences are in parenthesis after the sequence name.

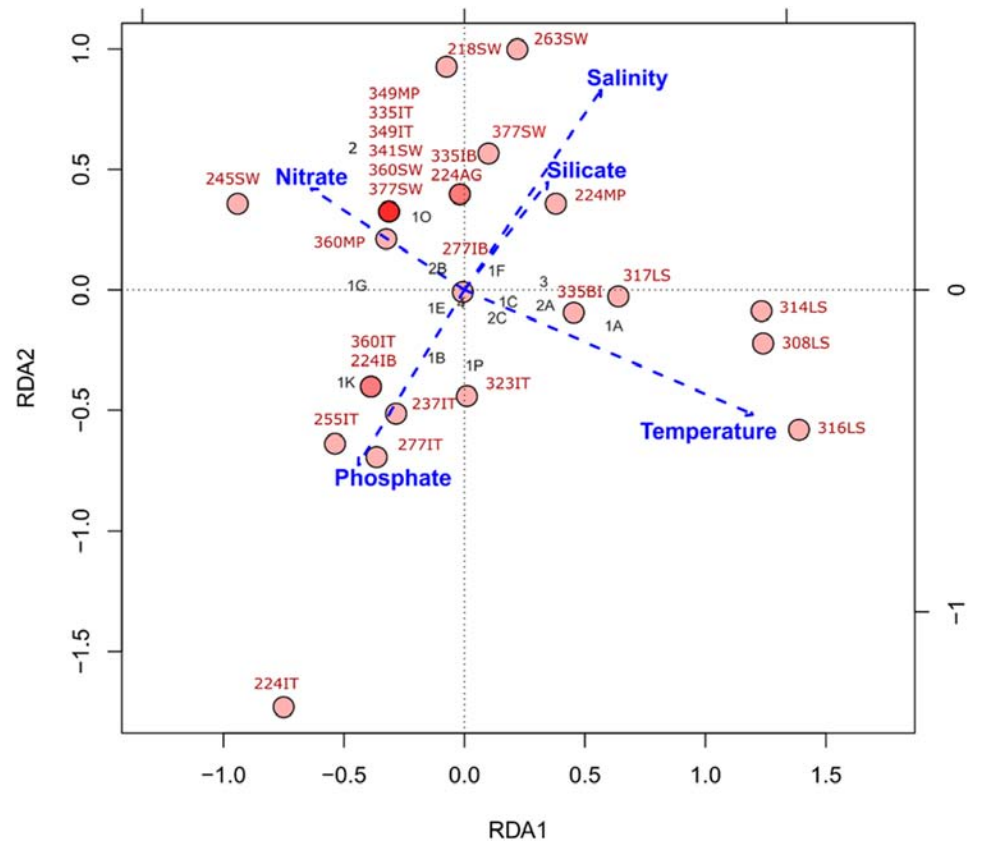

FIGURE 4 | Redundancy analysis (RDA) of *nifH* subcluster presence absence in Central Arctic samples and environmental variables. Environmental variables: temperature, salinity, nitrate, phosphate and silicate were standardized by *z*-scoring prior to RDA. The red circles represent the different samples and the intensity of the color indicates if there is one (light red) or many (dark red) samples at that coordinate in the plot. Sample names in red correspond to those in Supplementary Table S1. The black labels correspond to the different subclusters of *nifH* (Cluster number 1, 2, 3, or 4; and the subcluster letter A-K). The explanatory variables constrained ∼57% of the variance in the *nifH* subclusters across samples. The significance of this type I scaling was 0.001 and the residuals were mostly distributed around zero (Supplementary Figure S3).

temperature showed strong negative covariation. In general, *nifH* genes are found across a wide range of temperature and nutrient values, but with changing community structure. For example, Laptev Sea samples, containing sequences from subclusters 1A (*Deltaproteobacteria*) and 2A (*Firmicutes and Bacteroidetes*), were more associated with increased temperatures and decreased nitrate concentrations relative to the other samples analyzed (**Figure 4**). The presence of cyanobacterial *nifH* genes at the upper layer of the ice at station 224 (labeled as 224IT in **Figure 4**), is associated with the high phosphate concentrations.

Diazotroph and Total Microbial Community Diversity Patterns in Different Environments in the Central Arctic

Comparing the distribution of the *nifH* subclusters across the Central Arctic environments sampled, we observed differences between the Laptev Sea open waters and the sea-ice related environments. According to the dissimilarities between the *nifH* subclusters present in each sample, we detected a cluster of Laptev Sea samples that was distinctly separate from samples from sea ice environments (**Figure 5A**) (ANOSIM $R = 0.46$; *Post hoc* test $p = 0.003$). The rarefaction curve for each environment (Supplementary Figure S4A) shows that the Laptev Sea is under sampled, but the abundant types that we captured (represented in the panels for Hill numbers 1 and 2) were very different from the others. In addition, the 16S rRNA analysis also shows that the total bacterial community of the Laptev Sea is different from the sea-ice related environments (**Figure 5B**). However, in this case, the Laptev Sea clusters together with the other surface water samples, which is not the case for the diazotrophic community. The ice top environment and the Laptev Sea open water communities (ANOSIM $R = 0.90$; $p = 0.014$) showed moderate differences, as well as the ice top and the ice-covered surface waters (ANOSIM $R = 0.94$; $p = 0.005$).

Sea ice and Laptev Sea open waters had the largest number of unique representative sequences. These two environments had four *nifH* subclusters in common (1A, 1K, 1P, and 2C) (**Figure 2**). Most of the recovered *nifH* sequences in the top half of the ice belonged to subclusters 1G and 1K, which contain *Gamma-* and *Alphaproteobacteria*, respectively. We detected the greatest

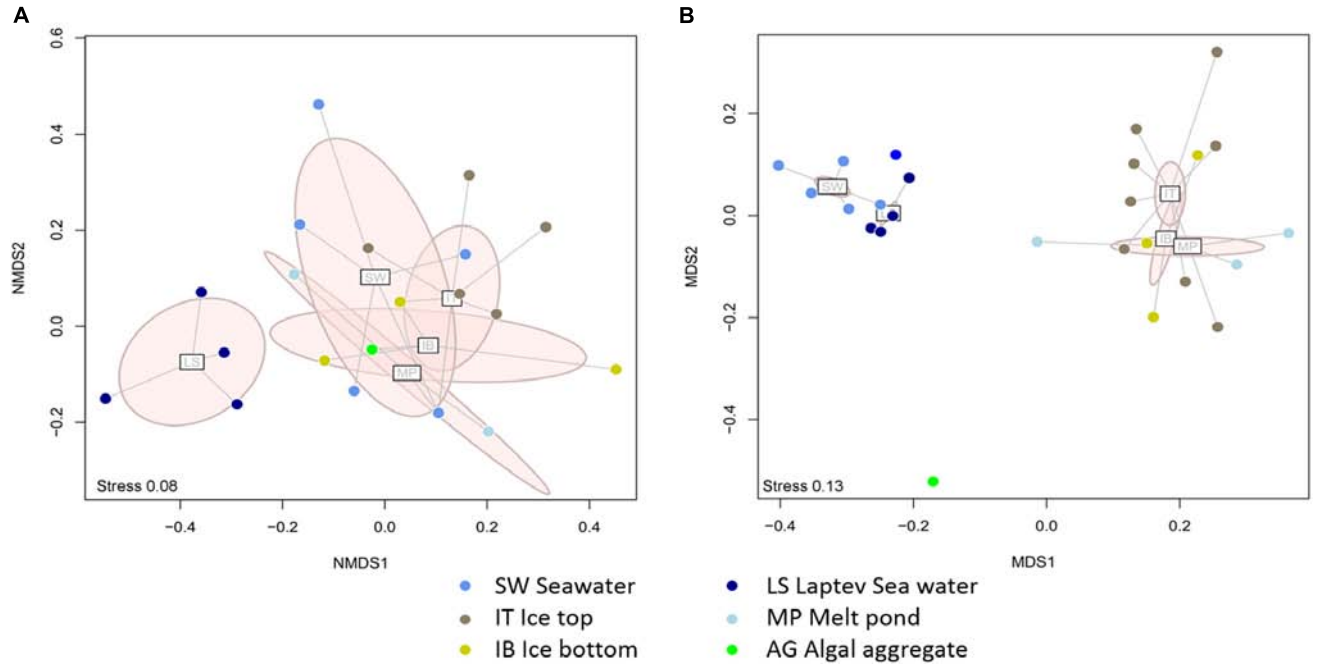

FIGURE 5 | Dissimilarities between the diazotrophic communities (A) and the entire bacterial communities **(B)** of different Central Arctic environments. Laptev Sea (LS) samples are in dark blue, Ice Top (IT) in brown, Ice bottom (IB) in yellow, Surface waters (SW) in blue, Melt Ponds (MP) in light blue, and ice algal aggregate in green. Points within each group are connected to their group centroid with a spider diagram. The light pink ellipses show 95% dispersion of each group. **(A)** Two dimensional NMDS ordination plot of Jaccard dissimilarities based on the presence absence of *nifH* subclusters in each sample. The stress of the plot is 0.08. An ANOSIM *post hoc* test showed that the Laptev Sea samples are significantly different from the sea-ice environment samples ($R = 0.46$, $p = 0.003$). Individual p values were Bonferroni corrected. **(B)** Two dimensional NMDS ordination plot of Bray-Curtis dissimilarities based on the relative abundances of ARISA OTUs. The stress of the plot is 0.13. An ANOSIM *post hoc* test showed strong dissimilarities between the Surface Water and the Ice Top samples ($R = 0.94$, $p = 0.005$) as well as the Laptev Sea and Ice Top samples ($R = 0.90$, $p = 0.014$). Individual *p*-values were Bonferroni corrected.

number of unique representative sequences in samples acquired from the lower portion of the ice, which contained sequences affiliated with subcluster 1A (*Deltaproteobacteria*) and Cluster III (**Figure 2**). Melt ponds, formed on top of the ice, only shared 1G subcluster sequences with the upper part of the ice, and additionally contained sequences from Cluster III (**Figure 2**). We detected sequences from subcluster 1G and from Cluster III – also found in our melt pond samples – in our samples of algal aggregates. These aggregates were primarily composed of algal species associated with sea ice. However, at a higher phylogenetic resolution, sequences in Cluster III differed between both environments (**Figure 3**).

More than half of the *nifH* sequences retrieved from water collected below the ice clustered together with sequences from the bottom part of the ice, an anticipated result because these two environments are in constant connection. However, the rest of the sequences detected in our water samples belonged to subclusters not detected in ice or melt pond samples: 1F (*Epsilonproteobacteria*), 1O (*Gammaproteobacteria*) and 2B (*Archaea*). The 1F subcluster also appeared in the open water samples from the Laptev Sea region (latitudes 77–79°N). The major subclusters present in our Laptev Sea open water samples were 1A and 2A. Subcluster 1A contains non-sulfate reducing *Deltaproteobacteria* such as *Geobacter* sp. and subcluster 2A contains fermenting bacteria from the genus *Pelosinus* and *Paludibacter*. *Deltaproteobacteria* from Cluster III composed around 20% of the sequences from open waters (**Figure 2**).

Comparison of Central Arctic Diazotrophic Communities across Adjacent Polar Environments and Oceanic Regions

The diazotrophic community of the Central Arctic is highly dissimilar to all other regions and environments we compared it to as unweighted unifrac distances were the highest (0.85–0.78), when the other regions were between (0.75–0.58) (Supplementary Table S2). At 97% nucleotide identity almost no sequences from different oceanic regions clustered together (**Figure 6**). Only five phylotypes were shared between the North Atlantic and the Subtropical Atlantic (**Figure 6**). The *nifH* diversity in sea ice, melt ponds and surface waters of the Central Arctic is different from the coastal Canadian Arctic marine diazotrophic community (Mackenzie river, Baffin bay) (**Figure 7**). Furthermore, it also differs from the sea ice, snow and water column communities from the coastal Eurasian Arctic (close to Svalbard) (**Figure 7**). The rarefaction curves show that the diversity in regions from which we acquired a greater number of sequences (i.e., the Central Arctic, the North Atlantic and the Subtropical Atlantic) appears to have been

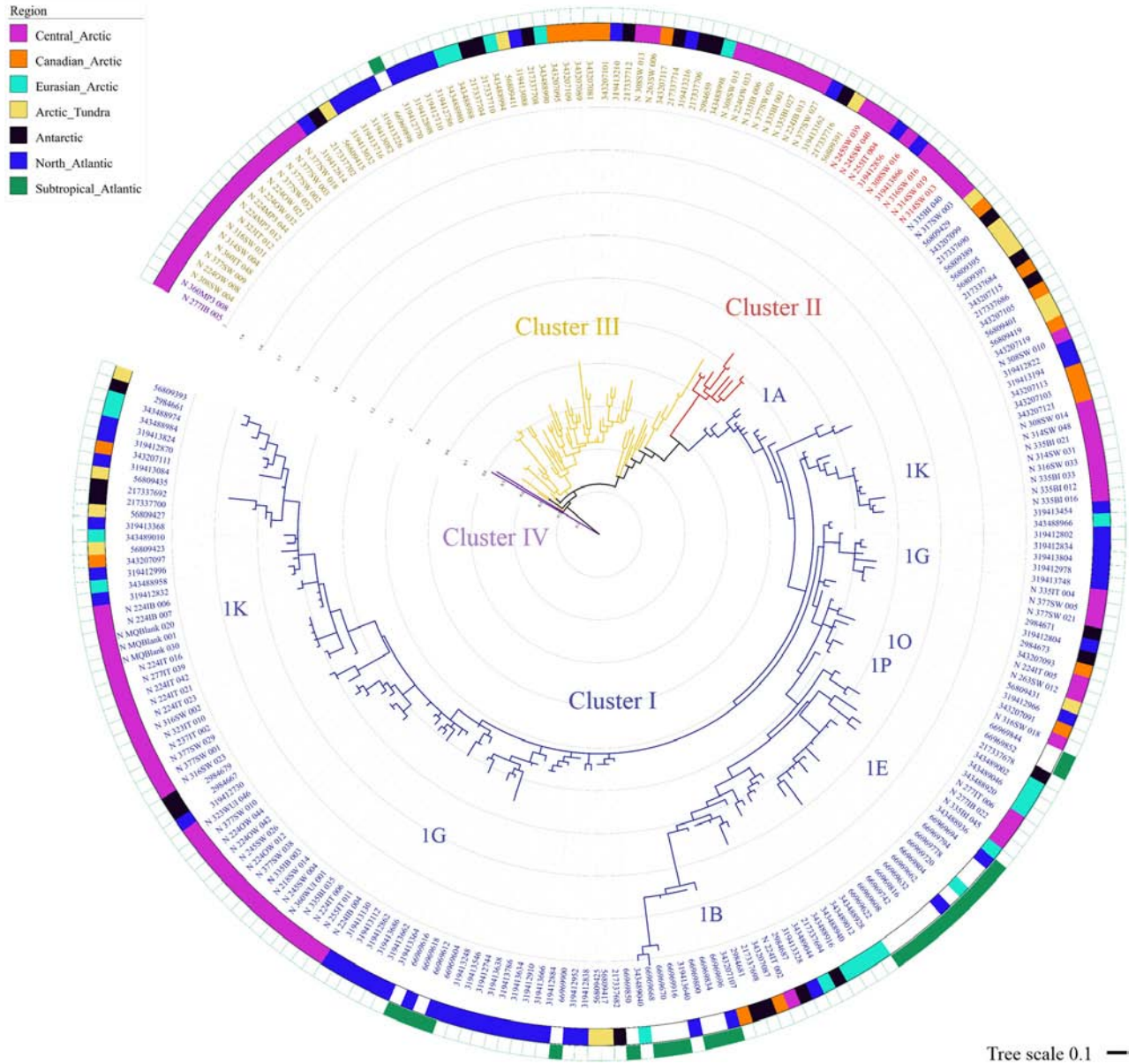

FIGURE 6 | Maximum likelihood phylogenetic tree of *nifH* partial amino acid sequences including sequences from the Central Arctic (this study), as well as other oceanic regions and similar cold environments. Maximum likelihood tree of the 243 representative sequences clustered using CD-HIT EST (Li and Godzik, 2006) at 97% nucleotide similarity (Turk-Kubo et al., 2014) built using RAxML V8.1. The best performing model was the WAG matrix substitution model and we performed 1000 bootstraps. The tree and its associated metadata were visualized using iTOL (Letunik and Bork, 2007). The colored strips indicates the origin of the sequences represented by each representative sequence shown in the tree. From the 243 representative sequences, 86 contained sequences exclusively from the Central Arctic (pink), 19 from the Canadian Arctic (Blais et al., 2012) (orange), 20 from the coastal Eurasian Basin (Díez et al., 2012) (light blue), 16 from the Arctic tundra (Izquierdo and Nüsslein, 2006) (yellow), from the Antarctic ice shelf (Olson et al., 1998; Jungblut and Neilan, 2010) (black), 51 from the North Atlantic (Turk et al., 2011) (dark blue), and 26 from the subtropical Atlantic (Langlois et al., 2005) (green). Note that the North Atlantic and the Subtropical Atlantic shared five representative sequences and the Eurasian Basin and the Subtropical Atlantic share one. The four clusters of *nifH* classification are marked in blue (Cluster I), red (Cluster II), yellow (Cluster III) and purple (Cluster IV). Cluster I subclusters (1A, 1B, 1K, 1G, etc) are indicated close to their node.

reasonably well sampled (Supplementary Figure S4B). However, the other oceanic regions are still in the rapid accumulation phase of their respective curves and deeper sequencing is likely to strongly affect their diversity profiles (Supplementary Figure S4B). We therefore place more interpretive weight on dissimilarities between our well-sampled regions (marked in the dissimilarities Supplementary Table S2), while noting that dissimilarities bearing on the Arctic tundra, Canadian Arctic, Eurasian Basin and Antarctic might be subject to change when the sampling effort is increased.

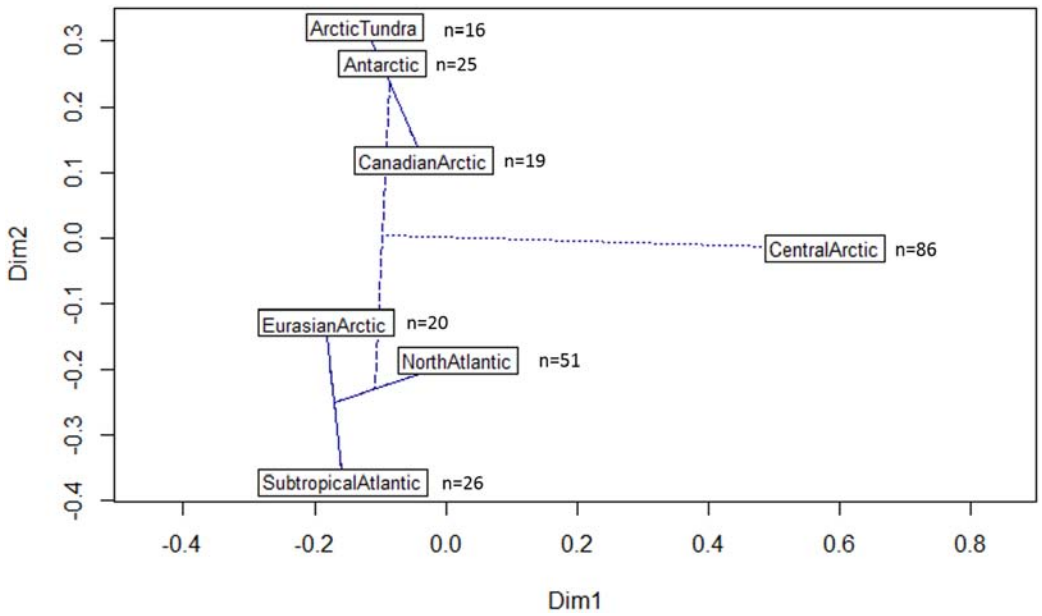

FIGURE 7 | Dissimilarities between different oceanic regions based on their *nifH* phylogenetic signature. Plot of the first two principal coordinate axes of the Principal coordinates analysis (PCoA) derived from the Unifrac distances between different oceanic regions included in the maximum likelihood tree (**Figure 6**). The further away the samples are, the more dissimilar they are in terms of *nifH* phylogenetic signature. An automatic correction for negative eigenvalues was used. A cluster dendrogram is superimposed. The lines indicate the strength of the dissimilarity. Oceanic regions connected with a solid line have a dissimilarity less than 0.69 (Supplementary Table S2). The dashed line indicates a dissimilarity of 0.76 and the doted line between the Central Arctic and the subtropical Atlantic indicates the maximum dissimilarity of 0.85 (Supplementary Table S2). The number of representative sequences (97% nucleotide identity) from each oceanic region included in the analysis is indicated next to the region's name.

DISCUSSION

Distribution of Diazotrophs in the Central Arctic Ocean

Confirming our first hypothesis, we found putative diazotrophs in the nitrogen-limited sea ice and waters of the Central Arctic Ocean (77–89°N). Most of the *nifH* sequences retrieved were non-cyanobacterial diazotrophs, mainly distributed between Cluster I and III as the bacterial phylotypes described in the marine Arctic studies by Farnelid et al. (2011), Blais et al. (2012), and Díez et al. (2012). All prominent nitrogen-fixing taxa at the subclade level present in other oceans were also present in the Central Arctic Ocean. However, most of the *nifH* genes amplified in the Central Arctic belonged to non-cyanobacterial diazotrophs, while cyanobacteria were under-represented. Previous Arctic diazotroph diversity studies also retrieved only a few cyanobacterial phylotypes. *Cyanothece* sp. and *Trichodesmium* sp., were found in the coastal Eurasian Basin in early May (Díez et al., 2012) and *Nostocales* sp., was found in the Beaufort Sea in July–August (Blais et al., 2012). The fact that we recovered only a single cyanobacterial phylotype in late summer, *Nodularia* sp., a cyanobacterial genus that contributes to nitrogen fixation in the Baltic Sea (Bostrom et al., 2007)., is consistent with the results of Farnelid et al. (2011), who observed that their Arctic station sampled in July (in Baffin Bay) only yielded non-cyanobacterial diazotrophs from Cluster III. This implies that cyanobacterial diazotrophs may not thrive in Central Arctic waters late in the productive season, far away from the coast line where there is riverine influence. However, *nifH* clone-library based approaches need to be interpreted with caution due to possible primer bias toward certain non-cyanobacterial diazotrophs (Turk et al., 2011; Turk-Kubo et al., 2015). Furthermore, the use of cyanobacteria-selective primers by Díez et al. (2012) might explain the high cyanobacterial diazotroph diversity reported in their study, compared to others.

The non-cyanobacterial diazotrophic community inhabiting the water column in the Central Arctic Ocean was dominated by Cluster I sequences: mainly *Alphaproteobacteria* (subcluster 1K) and *Deltaproteobacteria* (subcluster 1G) (**Figure 2**). While *Alpha-* and *Gammaproteobacteria* dominated non-cyanobacterial diazotrophic assemblages in the Atlantic and Pacific Oceans (Falcón et al., 2004; Langlois et al., 2005) and were present in lower abundances in the water column above the Canadian Arctic shelves (Blais et al., 2012). Sequences related to anaerobic bacteria (Cluster III) made up to 20% of under ice and open water communities in the Central Arctic (**Figure 2**). Cluster III sequences were once thought to be rare in brackish or marine surface waters (Moisander et al., 2007), but they are increasingly being recovered from ocean waters (Langlois et al., 2008; Turk-Kubo et al., 2014) including the Canadian Arctic shelf region (Farnelid et al., 2011).

Among the sea-ice related environments studied, floating aggregates are conglomerations of sea ice diatoms sticking together in a mucous matrix that can have an anoxic interior

and, therefore, have the potential to provide an environment for anaerobic processes such as denitrification and nitrogen fixation (Fernández-Méndez et al., 2014b; Lehto et al., 2014). Therefore, it is important to study *nifH* diversity in this environment. It is difficult to infer phylogeny from Cluster III sequences; however, some of our sequences were closely related to cultivated *Deltaproteobacteria* (**Figure 3**). For example, nine sequences retrieved from the floating algal aggregate (AGG) were related (88% aa similarity) to the genus *Desulfovibrio,* a common genus in marine coastal sediments and anoxic zones (Herbert, 1999). These aggregates form in late summer below melting sea-ice (Assmy et al., 2013; Fernández-Méndez et al., 2014b) and are not connected with coastal areas at the time of formation. This could indicate that their anaerobic bacterial community does not originate from coastal sediments.

Impact of Temperature and Nutrient Concentrations on Arctic Diazotrophs

The low temperatures and wide range of salinities present in sea ice environments shape their bacterial communities, leading to class-level differences between sea ice and water column communities (Boetius et al., 2015). To further test our first hypothesis regarding the presence of diazotrophs in the Central Arctic, we explored if the distribution and diversity of cyanobacterial and non-cyanobacterial diazotrophs was restricted by low temperatures or a specific nutrient ratio. During our cruise in August–September 2012, which covered a temperature gradient ranging from −1.7 to 3°C, nitrogen fixation genes from putative non-cyanobacterial diazotrophs were consistently amplified. This indicates that temperature limitation did not exclude non-cyanobacterial diazotrophs, an observation in agreement with previous studies (Farnelid et al., 2011; Blais et al., 2012; Díez et al., 2012). Non-cyanobacterial diazotrophs are known to thrive at low water temperatures (Riemann et al., 2010) and have been reported to be relevant for nitrogen fixation in other warmer oligotrophic oceans (Bombar et al., 2013; Moisander et al., 2014) and in the Baltic Sea (Farnelid et al., 2013). Increasing temperature seems to be linked to the structure of diazotroph community composition in the Laptev Sea samples (**Figure 4**) and could imply that a shift in surface water temperatures in the Arctic Ocean may have corresponding consequences on the regional diazotroph community. For example, non-cyanobacterial *nifH* subclusters 1A (*Geobacter*) and 2A (*Pelosinus* and *Paludibacter*) seem to be linked to increased temperatures (**Figure 4**). However, we are aware of the instability of our RDA solution due to the low number of sequences in our dataset and it is possible that deeper and more even sequencing will reveal somewhat different relationships.

The temperature ranges and optima of nitrogenase activities are only known for a few nitrogen-fixing cyanobacteria, such as *Trichodesmium* (Breitbarth et al., 2006) and *Cyanothece* (Brauer et al., 2013), which grow better at warm temperatures. Putative nitrogen-fixing cyanobacteria were only amplified in one sample in the Central Arctic Ocean (upper part of the ice at −0.2°C), supporting previous hypotheses that this group of nitrogen-fixers has not realized a niche in ice-covered polar open oceans (Murphy and Haugen, 1985; Koh et al., 2012b). However, other nitrogen-fixing cyanobacteria have been detected in snow (Harding et al., 2011; Boetius et al., 2015), glacial environments (Yallop et al., 2012; Vonnahme et al., 2015), hydrothermal vents (Mehta et al., 2003), and in other cold environments, such as Antarctic lakes (Olson et al., 1998) and sea ice (Koh et al., 2012a). Therefore, it remains unclear why they have not populated nitrogen-limited marine Arctic waters. The absence of cyanobacterial sequences in most of our samples might be due to undersampling (Supplementary Figure S4A), or to the primer bias of the primers we used toward non-cyanobacterial phylotypes (Turk-Kubo et al., 2015). However, the fact that cyanobacteria are rare in waters of the Arctic Ocean close to the ice (Lovejoy et al., 2002; Sherr et al., 2003) supports our findings.

Besides temperature, nutrient availability also plays a role in the occurrence of diazotrophs. The N:P ratios in surface waters of the Eurasian Basin range between 11 and 16 (Sakshaug et al., 2004). However, in summer the ratio can drop to 2–10, particularly in the Central Arctic north of 80°N (Supplementary Figure S2A), where nitrate availability limits algal growth (Fernández-Méndez et al., 2015). Silicate, which can also be limiting for diatom growth at the end of the productive season, showed no direct impact on *nifH* diversity. The *nifH* profile of the sample where we found cyanobacterial diazotrophs was associated with high phosphate concentrations supporting the low N:P hypothesis for autotrophic diazotrophs. In Central Arctic sea ice the occurrence of nitrogen-fixing cyanobacteria, such as *Nodularia* sp., seems to be driven by phosphate concentrations. However, as discussed previously this is a preliminary conclusion based on the very scarce data available at the moment.

We could retrieve *nifH* genes mostly of non-cyanobacterial putative diazotrophs from environments with a wide range of physical and chemical conditions, including summer sea ice with high N:P molar ratio (>16) and low salinities (0.5–3.6), and surface seawaters with low temperatures (−1.7°C) and higher salinity (33). Further research is required to determine whether any of the putative diazotrophs detected in this study are actively transcribing the *nif* operon and fixing nitrogen in the water, sea ice, and melt ponds of the Eurasian Basin.

The Origin of Marine Diazotrophs in the Central Arctic

Our second hypothesis was that putative diazotrophs in Central Arctic sea ice would come from the coastal areas influenced by rivers, such as the Lena River. The Lena River is a source of organic matter and iron that could provide favorable conditions for nitrogen fixation in the Laptev Sea (Lara et al., 1998). Our results, however, show a distinct entire bacterial community and diazotrophic subcommunity in the Laptev Sea region, close to the Lena Delta, when compared to that present in sea ice communities (**Figure 5**).

The ice floes sampled at the end of the productive season were formed during freeze-up or in polynyas located along the fast ice edge in the Laptev and Kara seas (Supplementary Figure S5). This, together with winds that might transport dust and microorganisms offshore (Harding et al., 2011), might explain the high relative abundance of *nifH* sequences related

to *Bradyrhizobium* sp. (*Alphaproteobacteria* 1K subcluster). *Bradyrhizobium* sp. is a symbiotic soil bacterium present in the nodules of leguminous plants (Hennecke, 1990), that can also fix nitrogen as free-living bacteria (Dreyfus et al., 1988), and is likely to be transported by rivers or wind. Indeed it has also been found in surface waters of the Mediterranean Sea (Le Moal et al., 2011). Some sea ice sequences clustered with the endospore-forming *Paenibacillus* (subcluster 1E) that has also been found in high Arctic soils (Jordan et al., 1978). In both environments, polar soils and sea ice, high salinities can be reached in pore fluids (Tedrow, 1966; Ewert and Deming, 2014), favoring halotolerant diazotrophs. Therefore, halotolerant diazotrophs can be expected. However, the riverine adapted freshwater diazotrophic bacteria are unlikely to thrive in the marine environment partially due to its high salinity (Fernandes et al., 1993). Subcluster 1F, which was present in both waters under the ice and those of the Laptev Sea, includes diazotrophs from the genus *Arcobacter* which is known to occur in roots of salt marsh plants, but also in sulfidic environments such as cold seeps and hydrothermal vents (Mehta et al., 2003). The dispersal of this genus from the soil of Arctic coastal areas to the Central Arctic is possible although other mechanisms might occur.

Overall, our assays of microbial communities based on the 16S rRNA gene and the *nifH* gene showed little support for the notion of the riverine origins of Central Arctic diazotrophs: the most abundant types in the bacterial and diazotrophic communities of the Laptev Sea water were notably dissimilar to those of Central Arctic sea ice and those present in the water under the ice. Sequences retrieved from brown ice (due to a high a concentration of phaeopigments from diatoms and possibly some sediments) are an exception: these clustered with sequences from the Laptev Sea waters. The subcluster represented by sequence 317LS_003 from the Laptev Sea in **Figure 3** includes sequences from sample 335BI (brown ice from station 335). Hence, a coastal (land or riverine) origin of the putative diazotrophs and other microbes in the Central Arctic is possible, but our data indicates that it is not likely the main process for diazotroph dispersal in the Eurasian Basin.

The Distinct Diazotroph Community of the Central Arctic Ocean

To assess potential causes of dissimilarity on the basis of the limited data set available, we grouped all available sequences from the Central Arctic, coming from different environments, and compared them to sequences from other oceanic regions and polar environments such as microbial mats in Antarctic lakes or Arctic tundra soils (**Figure 6**). This comparison assumes that the variability between the different environmental types in one region has a smaller effect than the variability between regions in the phylogenetic signal of *nifH* caused by the environment type.

The Eurasian Arctic communities were more similar to the North Atlantic and Subtropical Atlantic communities than to the Canadian Arctic (**Figure 7**). This is to be expected since these oceanic regions are tightly connected through the Fram Strait. The Arctic tundra soil communities were similar to communities isolated from Antarctic lake microbial mats at the *nifH* subcluster level. These Antarctic microbial mats were described as submerged in sediments of a meltwater pond in the McMurdo ice shelf (Jungblut and Neilan, 2010), or embedded in the permanent ice cover of Lake Bonney in the Antarctic McMurdo Dry Valley in summer (Olson et al., 1998). This indicates that soil-related communities have higher similarity to one another than to marine environments with similar temperature conditions. However, the dissimilarities between the Arctic tundra, the Antarctic and the Canadian Arctic must be interpreted with caution since the *nifH* diversity in these regions is under sampled (Supplementary Figure S4B).

Despite the limitations of this preliminary comparative study due to limited data, the Central Arctic diazotrophic community appears to have a different phylogenetic composition from adjacent regions and similar cold environments (**Figure 7**). Furthermore, our *nifH* gene analysis and the ITS region analysis (**Figures 5A,B**) indicate that Central Arctic sea ice environments harbor a microbial community distinct from that of the water column. We also noted that the marine diazotrophic communities in the Arctic were distinct from the terrestrial diazotrophic communities of the Arctic tundra (Izquierdo and Nüsslein, 2006) and the Antarctic ice shelf (Olson et al., 1998; Jungblut and Neilan, 2010). This bacterial Central Arctic endemism seems to be also reflected in the eukaryotic composition after the polar night when no phototrophs are dominating (Bachy et al., 2011). The diazotrophic communities of the Eurasian Arctic north of Svalbard (Díez et al., 2012), the North Atlantic (Turk et al., 2011) and the Subtropical Atlantic (Langlois et al., 2005) appeared similar to one another. This similarity is probably due to the presence of shared phylotypes (5 CD-HIT clusters 97% nucleotide identity contained sequences from the North Atlantic and the Subtropical Atlantic) and of cyanobacterial diazotrophs in these regions (**Figure 6**). One should note that Diez et al. (2012) used slightly different primers from all other studies and this might be partially responsible for the dissimilarities between the Eurasian Basin and the other regions. As more *nifH* sequences from different Arctic environments and regions will be added to the *nifH* database, more robust conclusions can be drawn from comparisons of diazotrophic community composition among different environments. For example, although cyanobacteria have been found thriving on glaciers and snow (Harding et al., 2011; Yallop et al., 2012) no analyses of *nifH* diversity were performed during these studies. Nevertheless, our initial comparisons, which included all currently available diazotroph sequences in the Arctic, strongly suggest that the Central Arctic Ocean harbors a community of putative diazotrophic microorganisms, which is distinct to those present in other oceanic regions and similarly cold environments.

CONCLUSION AND OUTLOOK

This study reveals the potential for nitrogen fixation far away from the coastal shelves in the Central Arctic, where diazotrophs were previously not detected. Nitrogen availability in the euphotic zone constrains the potential increase of

primary production especially in the central oligotrophic basins (Tremblay et al., 2015). Hence it is relevant to better understand the role of nitrogen fixers. Most of the *nifH* sequences retrieved belonged to putative non-cyanobacterial diazotrophs from Clusters I and III while diazotrophic cyanobacteria were rare. The origin of the sea-ice diazotrophic community in the Central Arctic seems to be marine and not riverine, since we found significant differences between the river-influenced Laptev Sea communities, and the sea-ice related diazotrophic communities. Assuming that the upper limit of nitrogen fixation estimated by Blais et al. (2012) in the Canadian Arctic (up to 0.14 nmol N L^{-1} d^{-1} transformed to carbon using a C:N ratio of 7.3: 0.6 mg C m^{-2} d^{-1}) would also take place in the Central Arctic, the nitrogen fixed by the diazotrophs could sustain ∼7% of the new primary production in the region (9.4 ± 3.6 g C m^{-2} $year^{-1}$, Fernández-Méndez et al., 2015). However, the presence and diversity of diazotrophs does not imply high nitrogen fixation rates (Moisander et al., 2007). With current trends of warming in Arctic waters (Polyakov et al., 2010; IPCC, 2013), higher marine nitrogen fixation rates can be expected in summer ice-free waters (Blais et al., 2012). However, the real contribution of these diazotrophs to nitrogen fixation still needs to be assessed before any further conclusions can be drawn regarding their role in the ecosystem and relevance for Arctic primary production.

AUTHOR CONTRIBUTIONS

MF-M and AB collected the samples. MF-M, KT-K, and JR performed the laboratory molecular analysis and the phylogenetic bioinformatic analysis. MF-M, JR, and PB performed the statistical analysis. TK provided the sea ice physics background information and the ice drift analysis. AB and JZ designed the study, organized the analysis and contributed to the discussion of the results. MF-M prepared the manuscript with contributions from all-coauthors.

FUNDING

This study was supported by the Alfred-Wegener-Institut Helmholtz-Zentrum für Polar- und Meeresforschung and the Max Planck Society, as well as the ERC Advanced Grant Abyss (no.294757) to AB. PB's work on this project is supported through the Micro B3 project, funded by the European Union's Seventh Framework Programme (Joint Call OCEAN.2011-2: marine microbial diversity – new insights into marine ecosystems functioning and its biotechnological potential) under the grant agreement no 287589.

ACKNOWLEDGMENTS

We thank the captain and crew of the RV Polarstern for their support during the ARK XXVII/3 expedition. We are particularly thankful to Anique Stecher, Christiane Uhlig, Ben Lange, Heidi L. Sørensen, Ilka Peeken, and Hauke Flores for their help during the sampling. The technical help of Mary Hogan and Brandon Carter at UCSC is greatly appreciated. We also thank Antonio Fernández-Guerra and the bioinformatics group at the Max Planck Institute for their support and advice.

SUPPLEMENTARY MATERIAL

The Supplementary Material for this article can be found online at: http://journal.frontiersin.org/article/10.3389/fmicb.2016.01884/full#supplementary-material

REFERENCES

Arrigo, K. R. (2005). Marine microorganisms and global nutrient cycles. *Nature* 437, 349–356. doi: 10.1038/nature04158

Arrigo, K. R., and van Dijken, G. L. (2015). Continued increases in Arctic Ocean primary production. *Prog. Oceanogr.* 136, 60–70. doi: 10.1016/j.pocean.2015.05.002

Assmy, P., Ehn, J. K., Fernández-Méndez, M., Hop, H., Katlein, C., Sundfjord, A., et al. (2013). Floating ice-algal aggregates below melting arctic sea ice. *PLoS ONE* 8:e76599. doi: 10.1371/journal.pone.0076599

Bachy, C., López-García, P., Vereshchaka, A., and Moreira, D. (2011). Diversity and vertical distribution of microbial eukaryotes in the snow, sea ice and seawater near the north pole at the end of the polar night. *Front. Microbiol.* 2:106. doi: 10.3389/fmicb.2011.00106

Bates, N. R., Garley, R., Frey, K. E., Shake, K. L., and Mathis, J. T. (2014). Sea-ice melt CO2-carbonate chemistry in the western Arctic Ocean: meltwater contributions to air-sea CO_2 gas exchange, mixed layer properties and rates of net community production under sea ice. *Biogeosci. Dis.* 11, 1097–1145. doi: 10.5194/bgd-11-1097-2014

Beine, H. J., Domine, F., Ianniello, A., Nardino, M., Allegrini, I., Teinilä, K., et al. (2003). Fluxes of nitrates between snow surfaces and the atmosphere in the European high Arctic. *Atmos. Chem. Phys.* 3, 335–346. doi: 10.5194/acp-3-335-2003

Blais, M., Tremblay, J. -É., Jungblut, A. D., Gagnon, J., Martin, J., Thaler, M., et al. (2012). Nitrogen fixation and identification of potential diazotrophs in the Canadian Arctic. *Glob. Biogeochem. Cycles* 26:GB3022. doi: 10.1029/2011GB004096

Boetius, A., Anesio, A. M., Deming, J. W., Mikucki, J., and Rapp, J. Z. (2015). Microbial ecology of the cryosphere: sea ice and glacial habitats. *Nat. Rev. Microbiol.* 13, 677–690. doi: 10.1038/nrmicro3522

Bombar, D., Turk-Kubo, K. A., Robidart, J., Carter, B. J., and Zehr, J. P. (2013). Non-cyanobacterial *nifH* phylotypes in the North Pacific Subtropical Gyre detected by flow-cytometry cell sorting. *Environ. Microbiol. Rep.* 5, 705–715. doi: 10.1111/1758-2229.12070

Bordeleau, L. M., and Prévost, D. (1994). "Nodulation and nitrogen fixation in extreme environments," in *Symbiotic Nitrogen Fixation*, eds P. H. Graham, M. J. Sadowsky, and C. P. Vance (Dordrecht: Springer), 115–125. doi: 10.1007/978-94-011-1088-4_13

Bostrom, K. H., Riemann, L., Zweifel, U. L., and Hagstrom, A. (2007). *Nodularia* sp. *nifH* gene transcripts in the Baltic Sea proper. *J. Plankton Res.* 29, 391–399. doi: 10.1093/plankt/fbm019

Bowman, J. S., Larose, C., Vogel, T. M., and Deming, J. W. (2013). Selective occurrence of Rhizobiales in frost flowers on the surface of young sea ice near Barrow, Alaska and distribution in the polar marine rare biosphere. *Environ. Microbiol. Rep.* 5, 575–582. doi: 10.1111/1758-2229.12047

Brauer, V. S., Stomp, M., Rosso, C., Van Beusekom, S. A. M., Emmerich, B., Stal, L. J., et al. (2013). Low temperature delays timing and enhances the cost of nitrogen fixation in the unicellular cyanobacterium Cyanothece. *ISME J.* 7, 2105–2115. doi: 10.1038/ismej.2013.103

Breitbarth, E., Oschlies, A., and LaRoche, J. (2006). Physiological constraints on the global distribution of Trichodesmium-effect of temperature on diazotrophy. *Biogeosci. Dis.* 3, 779–801. doi: 10.5194/bgd-3-779-2006

Chao, A., Gotelli, N. J., Hsieh, T. C., Sander, E. L., Ma, K. H., Colwell, R. K., et al. (2014). Rarefaction and extrapolation with Hill numbers: a framework for sampling and estimation in species diversity studies. *Ecol. Monogr.* 84, 45–67. doi: 10.1890/13-0133.1

Codispoti, L. A., Brandes, J. A., Christensen, J. P., Devol, A. H., Naqvi, S. W. A., Paerl, H. W., et al. (2001). The oceanic fixed nitrogen and nitrous oxide budgets: moving targets as we enter the anthropocene? *Sci. Mar.* 65, 85–105. doi: 10.3989/scimar.2001.65s285

Codispoti, L. A. A., Kelly, V., Thessen, A., Matrai, P., Suttles, S., Hill, V., et al. (2013). Synthesis of primary production in the Arctic Ocean: III. Nitrate and phosphate based estimates of net community production. *Prog. Oceanogr.* 110, 126–150. doi: 10.1016/j.pocean.2012.11.006

Devol, A., Codispoti, L. A., and Christensen, J. (1997). Summer and winter denitrification rates in western Arctic Shelf sediments. *Cont. Shelf Res.* 17, 1029–1050. doi: 10.1016/S0278-4343(97)00003-4

Díez, B., Bergman, B., Pedrós-Alió, C., Antó, M., and Snoeijs, P. (2012). High cyanobacterial *nifH* gene diversity in Arctic seawater and sea ice brine. *Environ. Microbiol. Rep.* 4, 360–366. doi: 10.1111/j.1758-2229.2012.00343.x

Dreyfus, B., Garcia, J. L., and Gillis, M. (1988). Characterization of *Azorhizobium caulinodans* gen. nov., sp. nov., a stem-nodulating nitrogen-fixing bacterium isolated from *Sesbania rostrata*. *Int. J. Syst. Bacteriol.* 38, 89–98. doi: 10.1099/00207713-38-1-89

Ewert, M., and Deming, J. W. (2014). Bacterial responses to fluctuations and extremes in temperature and brine salinity at the surface of Arctic winter sea ice. *FEMS Microbiol. Ecol.* 89, 476–489. doi: 10.1111/1574-6941.12363

Falcón, L. I., Carpenter, E. J., Cipriano, F., Bergman, B., and Capone, D. G. (2004). N2 fixation by unicellular bacterioplankton from the Atlantic and Pacific Oceans: Phylogeny and in situ rates. *Appl. Environ. Microbiol.* 70, 765–770. doi: 10.1128/AEM.70.2.765

Farnelid, H., Andersson, A. F., Bertilsson, S., Al-Soud, W. A., Hansen, L. H., Sørensen, S., et al. (2011). Nitrogenase gene amplicons from global marine surface waters are dominated by genes of non-cyanobacteria. *PLoS ONE* 6:e19223. doi: 10.1371/journal.pone.0019223

Farnelid, H., Bentzon-Tilia, M., Andersson, A. F., Bertilsson, S., Jost, G., Labrenz, M., et al. (2013). Active nitrogen-fixing heterotrophic bacteria at and below the chemocline of the central Baltic Sea. *ISME J.* 7, 1413–1423. doi: 10.1038/ismej.2013.26

Farnelid, H., Oberg, T., and Riemann, L. (2009). Identity and dynamics of putative N2 -fixing picoplankton in the Baltic Sea proper suggest complex patterns of regulation. *Environ. Microbiol. Rep.* 1, 145–154. doi: 10.1111/j.1758-2229.2009.00021.x

Fernandes, T. A., Iyer, V., and Apte, S. K. (1993). Differential responses of nitrogen-fixing cyanobacteria to salinity and osmotic stresses. *Appl. Environ. Microbiol.* 59, 899–904.

Fernández-Méndez, M., Katlein, C., Rabe, B., Nicolaus, M., Peeken, I., Bakker, K., et al. (2015). Photosynthetic production in the central Arctic Ocean during the record sea-ice minimum in 2012. *Biogeosciences* 12, 3525–3549. doi: 10.5194/bg-12-3525-2015

Fernández-Méndez, M., Peeken, I., and Boetius, A. (2014a). *Integrated Nutrients Concentrations Calculated for CTD Water Samples During POLARSTERN Cruise ARK-XXVII/3 (IceArc) in 2012*. Colaba Mumbai: PANGAEA. doi: 10.1594/PANGAEA.834296

Fernández-Méndez, M., Wenzhöfer, F., Peeken, I., Sørensen, H. L., Glud, R. N., and Boetius, A. (2014b). Composition, buoyancy regulation and fate of ice algal aggregates in the Central Arctic Ocean. *PLoS ONE* 9:e107452. doi: 10.1371/journal.pone.0107452

Finn, R., Mistry, J., Tate, J., Coggill, P., Heger, A., and Je, P. (2010). The Pfam protein families database. *Nucleic Acids Res.* 38, D211–D222. doi: 10.1093/nar/gkp985

Fisher, M. M., and Triplett, E. W. (1999). Automated approach for ribosomal intergenic spacer analysis of microbial diversity and its application to freshwater bacterial communities. *Appl. Environ. Microbiol.* 65, 4630–4636.

Foster, R. A., Kuypers, M. M. M., Vagner, T., Paerl, R. W., Musat, N., and Zehr, J. P. (2011). Nitrogen fixation and transfer in open ocean diatom-cyanobacterial symbioses. *ISME J.* 5, 1484–1493. doi: 10.1038/ismej.2011.26

Gaby, J. C., and Buckley, D. H. (2012). A comprehensive evaluation of PCR primers to amplify the *nifH* gene of nitrogenase. *PLoS ONE* 7:e42149. doi: 10.1371/journal.pone.0042149

Gobet, A., Boetius, A., and Ramette, A. (2014). Ecological coherence of diversity patterns derived from classical fingerprinting and Next Generation Sequencing techniques. *Environ. Microbiol.* 16, 2672–2681. doi: 10.1111/1462-2920.12308

Harding, T., Jungblut, A. D., Lovejoy, C., and Vincent, W. F. (2011). Microbes in high arctic snow and implications for the cold biosphere. *Appl. Environ. Microbiol.* 77, 3234–3243. doi: 10.1128/AEM.02611-10

Heller, P., Tripp, H. J., Turk-Kubo, K., and Zehr, J. P. (2014). ARBitrator: a software pipeline for on-demand retrieval of auto-curated *nifH* sequences from GenBank. *Bioinformatics* 30, 2883–2890. doi: 10.1093/bioinformatics/btu417

Hendricks, S., Nicolaus, M., and Schwegmann, S. (2012). *Sea Ice Conditions During POLARSTERN Cruise ARK-XXVII/3 (IceArc) in 2012*. Bremerhaven: Alfred Wegener Institute for Polar and Marine Research.

Hennecke, H. (1990). Nitrogen fixation genes involved in the Bradyrhizobium japonicum- soybean symbiosis. *FEBS* 268, 422–426. doi: 10.1016/0014-5793(90)81297-2

Herbert, R. A. (1999). Nitrogen cycling in coastal marine ecosystems. *FEMS Microbiol. Rev.* 23, 563–590. doi: 10.1111/j.1574-6976.1999.tb00414.x

Holmes, R. M., Mcclelland, J. W., Peterson, B. J., Tank, S. E., Bulygina, E., Eglinton, T. I., et al. (2011). Seasonal and annual fluxes of nutrients and organic matter from large rivers to the Arctic Ocean and surrounding seas. *Estuaries Coasts* 35, 369–382. doi: 10.1007/s12237-011-9386-6

Hsieh, T. C., Ma, K. H., and Chao, A. (2016). *iNEXT: iNterpolation and EXTrapolation for Species Diversity. R package*. Available at: http://chao.stat.nthu.edu.tw/blog/software-download

Huang, Y., Niu, B., Gao, Y., Fu, L., and Li, W. (2010). CD-HIT Suite: a web server for clustering and comparing biological sequences. *Bioinformatics* 26, 680–682. doi: 10.1093/bioinformatics/btq003

IPCC (2013). *Climate Change 2013: The Physical Science Basis. Contribution of working group I to the Fifth Assessment Report of the IPCC*. Geneva: IPCC

Izquierdo, J. A., and Nüsslein, K. (2006). Distribution of extensive *nifH* gene diversity across physical soil microenvironments. *Microb. Ecol* 51, 441–452. doi: 10.1007/s00248-006-9044-x

Jordan, D. C., McNicol, P. J., and Marshall, M. R. (1978). Biological nitrogen fixation in the terrestrial environment of a high Arctic ecosystem (Truelove Lowland, Devon Island, N.W.T.). *Can. J. Microbiol.* 24, 643–649. doi: 10.1139/m78-108

Jungblut, A. D., and Neilan, B. A. (2010). *NifH* gene diversity and expression in a microbial mat community on the McMurdo Ice Shelf, Antarctica. *Antarct. Sci.* 22, 117–122. doi: 10.1017/S0954102009990514

Klunder, M. B., Bauch, D., Laan, P., de Baar, H. J. W., van Heuven, S., Ober, S., et al. (2012). Dissolved iron in the Arctic shelf seas and surface waters of the central Arctic Ocean: Impact of Arctic river water and ice-melt. *J. Geophys. Res.* 117:C01027. doi: 10.1029/2011JC007133

Koh, E. Y., Cowie, R. O. M., Simpson, A. M., O'Toole, R., and Ryan, K. G. (2012a). The origin of cyanobacteria in Antarctic sea ice: marine or freshwater? *Environ. Microbiol. Rep.* 4, 479–483. doi: 10.1111/j.1758-2229.2012.00346.x

Koh, E. Y., Martin, A. R., McMinn, A., and Ryan, K. G. (2012b). Recent advances and future perspectives in microbial phototrophy in antarctic sea ice. *Biology (Basel).* 1, 542–556. doi: 10.3390/biology1030542

Krumpen, T., Gerdes, R., Haas, C., Hendricks, S., Herber, A., Selyuzhenok, V., et al. (2016). Recent summer sea ice thickness surveys in th Fram Strait and associated volume fluxes. *Cryosph. Discuss.* 9, 5171–5202. doi: 10.5194/tcd-9-5171-2015

Krumpen, T., Janout, M., Hodges, K. I., Gerdes, R., Girard-Ardhuin, F., Hölemann, J. A., et al. (2013). Variability and trends in laptev sea ice outflow between 1992–2011. *Cryosphere* 7, 349–363. doi: 10.5194/tc-7-349-2013

Langlois, R. J., Hümmer, D., and LaRoche, J. (2008). Abundances and distributions of the dominant *nifH* phylotypes in the Northern Atlantic Ocean. *Appl. Environ. Microbiol.* 74, 1922–1931. doi: 10.1128/AEM.01720-07

Langlois, R. J., LaRoche, J., and Raab, P. A. (2005). Diazotrophic diversity and distribution in the tropical and subtropical Atlantic Ocean. *Appl. Environ. Microbiol.* 71, 7910–7919. doi: 10.1128/AEM.71.12.7910

Lara, R. J. R. J., Rachold, V., Kattner, G., Hubberten, H. W., Guggenberger, G., Skoog, A., et al. (1998). Dissolved organic matter and nutrients in the lena

river, siberian arctic: characteristics and distribution. *Mar. Chem.* 59, 301–309. doi: 10.1016/S0304-4203(97)00076-5

LaRoche, J., and Breitbarth, E. (2005). Importance of the diazotrophs as a source of new nitrogen in the ocean. *J. Sea Res.* 53, 67–91. doi: 10.1016/j.seares.2004.05.005

Le Moal, M., Collin, H., and Biegala, I. C. (2011). Intriguing diversity among diazotrophic picoplankton along a Mediterranean transect : a dominance of rhizobia. *Biogeosciences* 8, 827–840. doi: 10.5194/bg-8-827-2011

Legendre, P., and Gallagher, E. (2001). Ecologically meaningful transformations for ordination of species data. *Oecologia* 129, 271–280. doi: 10.1007/s004420100716

Legendre, P., and Legendre, L. (1998). *Numerical Ecology*. 2nd Englis. Amsterdam: Elsevier Science BV.

Lehto, N., Glud, R., Nordi, G., Zang, H., and Davison, W. (2014). Anoxic microniches in marine sediments induced by aggregate settlement: Biogeochemical dynamics and implications. *Biogeochemistry* 119, 307–327.

Letunik, I., and Bork, P. (2007). Interactive Tree Of Life (iTOL): an online tool for phylogenetic tree display and annotation. *Bioinformatics* 23, 127–128. doi: 10.1093/bioinformatics/btl529

Li, W., and Godzik, A. (2006). Cd-hit: a fast program for clustering and comparing large sets of protein or nucleotide sequences. *Bioinformatics* 22, 1658–1659. doi: 10.1093/bioinformatics/btl158

Lovejoy, C., Legendre, L., Martineau, M.-J., Bacle, J., and von Quillfeldt, C. H. (2002). Distribution of phytoplankton and other protists in the North Water. *Deep Sea Res. Part II* 49, 5027–5047. doi: 10.1016/S0967-0645(02)00176-5

Lovejoy, C., and Potvin, M. (2010). Microbial eukaryotic distribution in a dynamic Beaufort Sea and the Arctic Ocean. *J. Plankton Res.* 33, 431–444. doi: 10.1093/plankt/fbq124

Lozupone, C., Hamady, M., and Knight, R. (2006). UniFrac–an online tool for comparing microbial community diversity in a phylogenetic context. *BMC Bioinformatics* 7:371. doi: 10.1186/1471-2105-7-371

Ludwig, W., Strunk, O., Westram, R., Richter, L., Meier, H., Yadhukumar, et al. (2004). ARB: a software environment for sequence data. *Nucleic Acids Res.* 32, 1363–1371. doi: 10.1093/nar/gkh293

Luo, Y.-W. Y.-W., Doney, S. C., Anderson, L. A., Benavides, M., Berman-Frank, I., Bode, A., et al. (2012). Database of diazotrophs in global ocean: abundance, biomass and nitrogen fixation rates. *Earth Syst. Sci. Data* 4, 47–73. doi: 10.5194/essd-4-47-2012

McMurdie, P. J., and Holmes, S. (2013). phyloseq: an R package for reproducible interactive analysis and graphics of microbiome census data. *PLoS ONE* 8:e61217. doi: 10.1371/journal.pone.0061217

Mehta, M. P., Butterfield, D. A., and Baross, J. A. (2003). Phylogenetic diversity of Nitrogenase (*nifH*) genes in deep-sea and hydrothermal vent environments of the Juan de Fuca Ridge. *Appl. Environ. Microbiol.* 69:960. doi: 10.1128/AEM.69.2.960

Mills, M. M., and Arrigo, K. R. (2010). Magnitude of oceanic nitrogen fixation influenced by the nutrient uptake ratio of phytoplankton. *Nat. Geosci.* 3, 412–416. doi: 10.1038/ngeo856

Moisander, P. H., Beinart, R. A., Hewson, I., White, A. E., Johnson, K. S., Carlson, C. A., et al. (2010). Unicellular cyanobacterial distributions broaden the oceanic N2 fixation domain. *Science* 327, 1512–1514. doi: 10.1126/science.1185468

Moisander, P. H., Morrison, A. E., Ward, B. B., Jenkins, B. D., and Zehr, J. P. (2007). Spatial-temporal variability in diazotroph assemblages in Chesapeake Bay using an oligonucleotide *nifH* microarray. *Environ. Microbiol.* 9, 1823–1835. doi: 10.1111/j.1462-2920.2007.01304.x

Moisander, P. H., Serros, T., Paerl, R. W., Beinart, R. A., and Zehr, J. P. (2014). Gammaproteobacterial diazotrophs and *nifH* gene expression in surface waters of the South Pacific Ocean. *ISME J.* 8, 1962–1973. doi: 10.1038/ismej.2014.49

Monteiro, F. M., Dutkiewicz, S., and Follows, M. J. (2011). Biogeographical controls on the marine nitrogen fixers. *Glob. Biogeochem. Cycles* 25:GB2003. doi: 10.1029/2010GB003902

Murphy, L., and Haugen, E. (1985). The distribution and abundance of phototrophic ultraplankton in the North Atlantic. *Limnol. Oceanogr.* 30, 47–58. doi: 10.4319/lo.1985.30.1.0047

Nadeau, T. L., Milbrandt, E. C., and Castenholz, R. W. (2001). Evolutionary relationships of cultivated antarctic oscillatorians (cyanobacteria). *J. Phycol.* 37, 650–654. doi: 10.1046/j.1529-8817.2001.037004650.x

Oksanen, J., Blanchet, F., Guillaume Kindt, R., Legendre, P., Minchin, P. R., O'Hara, R. B., et al. (2013). *Vegan: Community Ecology Package. R package version 2.0-10*. Available at: http://cran.r-project.org/package=vegan

Olson, J. B., Steppe, T. F. T., Litaker, R. W. R., and Paerl, H. W. (1998). N2-fixing microbial consortia associated with the ice cover of Lake Bonney, Antarctica. *Microb. Ecol.* 36, 231–238. doi: 10.1007/s002489900110

Paerl, H. W., and Zehr, J. P. (2000). "Marine nitrogen fixation," in *Microbial Ecology of the Oceans*, ed. D. L. Kirchman (New York, NY: Wiley-Liss), 387–426.

Parkinson, C. L., and Comiso, J. C. (2013). On the 2012 record low Arctic sea ice cover: Combined impact of preconditioning and an August storm. *Geophys. Res. Lett.* 40, 1356–1361. doi: 10.1002/grl.50349

Partensky, F., and Hess, W. R. (1999). Prochlorococcus, a marine photosynthetic prokaryote of global significance. *Microbiol. Mol. Biol. Rev.* 63, 106–127.

Polyakov, I., Timokhov, L., Alexeev, V., Bacon, S., Dmitrenko, I., Fortier, L., et al. (2010). Arctic Ocean warming contributes to reduced polar ice cap. *J. Phys. Oceanogr.* 40, 2743–2756. doi: 10.1175/2010JPO4339.1

R Core Team (2015). *R: A language and Environment for Statistical Computing*. Available at: http://www.r-project.org/

Rabe, B., Wisotzki, A., Rettig, S., Somavilla Cabrillo, R., and Sander, H. (2012). *Physical Oceanography Measured on Water Bottle Samples During POLARSTERN Cruise ARK-XXVII/3*. Bremerhaven: Alfred Wegener Institute for Polar and Marine Research.

Ramette, A. (2009). Quantitative community fingerprinting methods for estimating the abundance of operational taxonomic units in natural microbial communities. *Appl. Environ. Microbiol.* 75, 2495–2505. doi: 10.1128/AEM.02409-08

Riemann, L., Farnelid, H., and Steward, G. (2010). Nitrogenase genes in non-cyanobacterial plankton: prevalence, diversity and regulation in marine waters. *Aquat. Microb. Ecol.* 61, 235–247. doi: 10.3354/ame01431

Rysgaard, S., Glud, R. N., Risgaard-Petersen, N., and Dalsgaard, T. (2004). Denitrification and anammox activity in Arctic marine sediments. *Limnol. Oceanogr.* 49, 1493–1502. doi: 10.4319/lo.2004.49.5.1493

Sakshaug, E., Stein, R., and Macdonald, R. W. (2004). "Primary and secondary production in the Arctic Seas," in *The Organic Carbon Cycle in the Arctic Ocean*, eds R. Stein and R. W. Macdonald (Berlin: Springer), 57–82.

Sanger, F., Nicklen, S., and Coulson, A. R. (1977). DNA sequencing with chain-terminating inhibitors. *Proc. Natl. Acad. Sci. U.S.A.* 74, 5463–5467.

Schmidt, S., Moskall, W., De Mora, S. J., Howard-Williams, C., and Vincent, W. F. (1991). Limnological properties of Antarctic ponds during winter freezing. *Antarct. Sci.* 3, 379–388. doi: 10.1017/S0954102091000482

Sherr, E. B., Sherr, B. F., Wheeler, P. A., and Thompson, K. (2003). Temporal and spatial variation in stocks of autotrophic and heterotrophic microbes in the upper water column of the central Arctic Ocean. *Deep Sea Res. Part I Oceanogr. Res. Pap.* 50, 557–571. doi: 10.1016/S0967-0637(03)00031-1

Stamatakis, A. (2014). RAxML Version 8: a tool for Phylogenetic analysis and post-analysis of large phylogenies. *Bioinformatics* 30, 1312–1313. doi: 10.1093/bioinformatics/btu033

Staples, C. R., Lahiri, S., Raymond, J., Von Herbulis, L., Mukhophadhyay, B., and Blankenship, R. E. (2007). Expression and association of group IV nitrogenase *NifD* and *NifH* homologs in the non-nitrogen-fixing archaeon *Methanocaldococcus jannaschii*. *J. Bacteriol.* 189, 7392–7398. doi: 10.1128/JB.00876-07

Stroeve, J. C., Kattsov, V., Barrett, A., Serreze, M., Pavlova, T., Holland, M., et al. (2012). Trends in Arctic sea ice extent from CMIP5, CMIP3 and observations. *Geophys. Res. Lett.* 39, L16502. doi: 10.1029/2012GL052676

Tedrow, J. C. F. (1966). Polar desert soils. *Soil Sci. Soc. Am. J.* 30, 381. doi: 10.2136/sssaj1966.03615995003000030024x

Torres-Valdés, S., Tsubouchi, T., Bacon, S., Naveira-Garabato, A. C., Sanders, R., McLaughlin, F. A., et al. (2013). Export of nutrients from the Arctic Ocean. *J. Geophys. Res. Ocean* 118, 1625–1644. doi: 10.1002/jgrc.20063

Tremblay, G., Belzile, C., Gosselin, M., Poulin, M., and Roy, S. (2009). Late summer phytoplankton distribution along a 3500 km transect in Canadian Arctic waters: strong numerical dominance by picoeukaryotes. *Aquat. Microb. Ecol.* 54, 55–70. doi: 10.3354/ame01257

Tremblay, J.-É., Anderson, L. G., Matrai, P., Coupel, P., Bélanger, S., Michel, C., et al. (2015). Global and regional drivers of nutrient supply, primary production and CO_2 drawdown in the changing Arctic Ocean. *Prog. Oceanogr.* 139, 171–196. doi: 10.1016/j.pocean.2015.08.009

Tremblay, J. -É., Simpson, K., Martin, J., Miller, L., Gratton, Y., Barber, D., et al. (2008). Vertical stability and the annual dynamics of nutrients and chlorophyll fluorescence in the coastal, southeast Beaufort Sea. *J. Geophys. Res.* 113:C07S90. doi: 10.1029/2007JC004547

Turk, K. A., Rees, A. P., Zehr, J. P., Pereira, N., Swift, P., Shelley, R., et al. (2011). Nitrogen fixation and nitrogenase (*nifH*) expression in tropical waters of the eastern North Atlantic. *ISME J.* 5, 1201–1212. doi: 10.1038/ismej.2010.205

Turk-Kubo, K. A., Achilles, K. M., Serros, T. R. C., Ochiai, M., Montoya, J. P., and Zehr, J. P. (2012). Nitrogenase (*nifH*) gene expression in diazotrophic cyanobacteria in the Tropical North Atlantic in response to nutrient amendments. *Front. Microbiol.* 3:386. doi: 10.3389/fmicb.2012.00386

Turk-Kubo, K. A., Frank, I. E., Hogan, M. E., Desnues, A., Bonnet, S., and Zehr, J. P. (2015). Diazotroph community succession during the VAHINE mesocosm experiment (New Caledonia lagoon). *Biogeosciences* 12, 7435–7452. doi: 10.5194/bg-12-7435-2015

Turk-Kubo, K. A., Karamchandani, M., Capone, D. G., and Zehr, J. P. (2014). The paradox of marine heterotrophic nitrogen fixation: abundances of heterotrophic diazotrophs do not account for nitrogen fixation rates in the Eastern Tropical South Pacific. *Environ. Microbiol.* 16, 3095–3114. doi: 10.1111/1462-2920.12346

Tyrrell, T. (1999). The relative influences of nitrogen and phosphorus on oceanic primary production. *Nature* 400, 525–531. doi: 10.1038/22941

Villareal, T. A. (1992). "Marine nitrogen-fixing diatom-cyanobacteria symbiosis," in *Marine Pelagic Cyanobacteria: Trichodesmium and other Diazotrophs*, eds E. J. Carpenter, D. G. Capone, and J. G. Rueter (Dordrecht: Springer), 163–175. doi: 10.1007/978-94-015-7977-3_10

Vincent, W. F. (2000). "Cyanobacterial dominance in the polar regions," in *The Ecology of Cyanobacteria*, eds A. Whitton and M. Potts (Amsterdam: Kluwer Academic Publishers), 321–340.

Vonnahme, T. R., Devetter, M., Žárský, J. D., Šabacká, M., and Elster, J. (2015). Controls on microalgal community structures in cryoconite holes upon high Arctic glaciers, Svalbard. *Biogeosci. Discuss.* 12, 11751–11795. doi: 10.5194/bgd-12-11751-2015

Warton, D. I., Wright, S. T., and Wang, Y. (2012). Distance-based multivariate analyses confound location and dispersion effects. *Methods Ecol. Evol.* 3, 89–101. doi: 10.1111/j.2041-210X.2011.00127.x

Wassmann, P., Duarte, C. M., Agustí, S., and Sejr, M. K. (2011). Footprints of climate change in the Arctic marine ecosystem. *Glob. Chang. Biol.* 17, 1235–1249. doi: 10.1111/j.1365-2486.2010.02311.x

Yallop, M. L., Anesio, A. M., Perkins, R. G., Cook, J., Telling, J., Fagan, D., et al. (2012). Photophysiology and albedo-changing potential of the ice algal community on the surface of the Greenland ice sheet. *ISME J.* 6, 2302–2313. doi: 10.1038/ismej.2012.107

Young, J. P. W. (2005). "The phylogeny and evolution of nitrogenases," in *Genomes and Genomics of Nitrogen Fixing Organisms*, eds R. Palacios and W. E. Newton (Dordrecht: Springer), 221–241. doi: 10.1007/1-4020-3054-1_14

Zehr, J. P., Jenkins, B. D., Short, S. M., and Steward, G. F. (2003). Nitrogenase gene diversity and microbial community structure : a cross-system comparison. *Environ. Microbiol.* 5, 539–554. doi: 10.1046/j.1462-2920.2003.00451.x

Zehr, J. P., and Turner, P. J. (2001). "Nitrogen fixation: Nitrogenase genes and gene expression," in *Methods in Microbiology*, ed. J. H. Paul (San Francisco, CA: Elsevier), 271–286.

Conflict of Interest Statement: The authors declare that the research was conducted in the absence of any commercial or financial relationships that could be construed as a potential conflict of interest.

frontiers in Microbiology

ORIGINAL RESEARCH
published: 06 July 2017
doi: 10.3389/fmicb.2017.01122

Microbiome of *Trichodesmium* Colonies from the North Pacific Subtropical Gyre

Mary R. Gradoville[1]†, Byron C. Crump[1], Ricardo M. Letelier[1], Matthew J. Church[2] and Angelicque E. White[1]*

[1] College of Earth, Ocean and Atmospheric Sciences, Oregon State University, Corvallis, OR, United States, [2] Flathead Lake Biological Station, University of Montana, MT, United States

Filamentous diazotrophic Cyanobacteria of the genus *Trichodesmium*, often found in colonial form, provide an important source of new nitrogen to tropical and subtropical marine ecosystems. Colonies are composed of several clades of *Trichodesmium* in association with a diverse community of bacterial and eukaryotic epibionts. We used high-throughput 16S rRNA and *nifH* gene sequencing, carbon (C) and dinitrogen (N_2) fixation assays, and metagenomics to describe the diversity and functional potential of the microbiome associated with *Trichodesmium* colonies collected from the North Pacific Subtropical Gyre (NPSG). The 16S rRNA and *nifH* gene sequences from hand-picked colonies were predominantly (>99%) from *Trichodesmium* Clade I (i.e., *T. thiebautii*), which is phylogenetically and ecologically distinct from the Clade III IMS101 isolate used in most laboratory studies. The bacterial epibiont communities were dominated by Bacteroidetes, Alphaproteobacteria, and Gammaproteobacteria, including several taxa with a known preference for surface attachment, and were relatively depleted in the unicellular Cyanobacteria and small photoheterotrophic bacteria that dominate NPSG surface waters. Sequencing the *nifH* gene (encoding a subcomponent of the nitrogenase enzyme) identified non-*Trichodesmium* diazotrophs that clustered predominantly among the Cluster III *nifH* sequence-types that includes putative anaerobic diazotrophs. *Trichodesmium* colonies may represent an important habitat for these Cluster III diazotrophs, which were relatively rare in the surrounding seawater. Sequence analyses of *nifH* gene transcripts revealed several cyanobacterial groups, including heterocystous *Richelia*, associated with the colonies. Both the 16S rRNA and *nifH* datasets indicated strong differences between *Trichodesmium* epibionts and picoplankton in the surrounding seawater, and also between the epibionts inhabiting *Trichodesmium* puff and tuft colony morphologies. Metagenomic and 16S rRNA gene sequence analyses suggested that lineages typically associated with a copiotrophic lifestyle comprised a large fraction of colony-associated epibionts, in contrast to the streamlined genomes typical of bacterioplankton in these oligotrophic waters. Additionally, epibiont metagenomes were enriched in specific genes involved in phosphate and iron acquisition and denitrification pathways relative to surface seawater metagenomes. We propose that the unique microbial consortium inhabiting colonies has a significant impact on the biogeochemical functioning of *Trichodesmium* colonies in pelagic environments.

Keywords: *Trichodesmium*, marine microbiome, *nifH* diversity, heterotrophic marine diazotrophs, metagenomics, 16S rRNA, nitrogen fixation

OPEN ACCESS

Edited by:
Sophie Rabouille, Centre National de la Recherche Scientifique (CNRS), France

Reviewed by:
Eric A. Webb, University of Southern California, United States
Alyson E. Santoro, University of California, Santa Barbara, United States

****Correspondence:***
Mary R. Gradoville
mgradoville@ucsc.edu

†Present Address:
Mary R. Gradoville, Ocean Sciences Department, University of Santa Cruz, Santa Cruz, CA, United States

Specialty section:
This article was submitted to Aquatic Microbiology, a section of the journal Frontiers in Microbiology

Received: *29 December 2016*
Accepted: *01 June 2017*
Published: *06 July 2017*

Citation:
Gradoville MR, Crump BC, Letelier RM, Church MJ and White AE (2017) Microbiome of Trichodesmium Colonies from the North Pacific Subtropical Gyre. Front. Microbiol. 8:1122. doi: 10.3389/fmicb.2017.01122

INTRODUCTION

The filamentous, dinitrogen (N_2)-fixing (diazotrophic) cyanobacterium *Trichodesmium* provides a major source of bioavailable nitrogen (N) to the oligotrophic subtropical and tropical oceans (Karl et al., 2002; Capone et al., 2005). *Trichodesmium* abundances and N_2 fixation rates have been integral components of global N_2 fixation estimates and models (e.g., Coles et al., 2004; Mahaffey et al., 2005); thus, an accurate understanding of the physiology and ecology of this genus is crucial. Most *Trichodesmium* laboratory studies have used a single isolate, *T. erythraeum* strain IMS101, grown in culture with minimal heterotrophic bacteria. In contrast, natural *Trichodesmium* populations are composed of species from four known phylogenetically distinct clades (Hynes et al., 2012), which can vary in physiological traits, such as carbon (C) affinity and phosphonate biosynthesis (Dyhrman et al., 2009; Hutchins et al., 2013). Furthermore, in nature they are commonly found associated with attached microorganisms (Borstad and Borstad, 1977). The diversity of this complex community likely affects the overall functioning of colonies (Gradoville et al., 2014), yet few studies have examined the ecology of *Trichodesmium* species and associated epibionts (although see Hmelo et al., 2012; Rouco et al., 2016).

Trichodesmium cells exist as free filaments or aggregate colonies (Letelier and Karl, 1996) with varying morphologies, namely spherical "puffs" and fusiform "tufts." These colonies have been reported to maintain an active and diverse assemblage of attached organisms, including bacteria, eukaryotic phytoplankton, protozoa, fungi, and copepods (Borstad and Borstad, 1977; Sheridan et al., 2002). *Trichodesmium* colonies constitute a favorable environment for associated epibionts by providing buoyancy (Walsby, 1992), elevated concentrations of dissolved organic N (Capone et al., 1994), and a substrate for attachment (O'Neil, 1998). Recent studies using 16S rRNA gene sequencing have shown that *Trichodesmium*-associated bacterial epibionts include surface-associated taxa (Hmelo et al., 2012) and that selective processes appear to drive epibiont community structure (Rouco et al., 2016).

Less is known about how associated microorganisms affect the functioning of the *Trichodesmium* holobiont. *Trichodesmium* colonies appear to be hotspots for microbial activity: hydrolytic enzyme activities are elevated within colonies (Stihl et al., 2001; Sheridan et al., 2002) and a metatranscriptome from *Trichodesmium* bloom material recovered more transcripts from associated organisms than from *Trichodesmium* cells (Hewson et al., 2009). Microbial processes carried out by associated microorganisms have the potential to influence rates of N_2 or C fixation. For instance, quorum sensing by associated bacteria can increase alkaline phosphatase activity within colonies (Van Mooy et al., 2011), which could stimulate *Trichodesmium* dissolved organic phosphorus utilization, thereby increasing N_2 fixation rates when phosphate is limiting. Likewise, specific epibiont bacteria may secrete siderophores, chelating iron which could subsequently become bioavailable to *Trichodesmium* after photodegradation (Roe et al., 2012). Associated microorganisms may also directly contribute to the fixation of C and/or N_2. Phototrophs including filamentous Cyanobacteria (Siddiqui et al., 1992) and diatoms (Borstad and Borstad, 1977) have historically been observed within *Trichodesmium* colonies. More recently, heterocystous cyanobacterial diazotrophs have been observed within *Trichodesmium* colonies (Momper et al., 2015) and *nifH* genes (encoding a subcomponent of the nitrogenase enzyme) phylogenetically clustering among facultative anaerobes and aerobic heterotrophic bacteria have been retrieved from *Trichodesmium* colonies (Gradoville et al., 2014). The degree to which these associated diazotrophs contribute to bulk colony N_2 fixation rates is unknown.

Here, we examine the microbiome associated with *Trichodesmium* colonies collected from the North Pacific Subtropical Gyre (NPSG). We used a combined approach of high-throughput 16S rRNA and *nifH* gene sequencing, metagenomics, and ^{13}C and $^{15}N_2$ fixation assays to survey the diversity of the *Trichodesmium* holobiont, test for the presence and activity of non-*Trichodesmium* colony-associated diazotrophs, and explore the functional potential of the colonies. We compare the colony-associated microbiome to the microbial community structure and metagenomic composition of surrounding seawater, revealing diverse and unique microbial structure and functional potential associated with *Trichodesmium* colonies.

METHODS

Sample Collection

Samples were collected in March 2014 aboard the R/V *Kilo Moana* at Stn. ALOHA (A Long-term Oligotrophic Habitat Assessment; 22.45°N, 158°W), an open-ocean field site ∼100 km north of Oahu (**Table 1**). *Trichodesmium* colonies were collected using a 202 μm plankton net which was hand-towed at $<2\,km\,h^{-1}$ through near-surface waters (<10 m depth) for 10–15 min. Once recovered, colonies were isolated using an inoculating loop and rinsed twice with 0.2 μm-filtered surface seawater prior to all analyses. Colonies were sorted into morphological classes of spherical "puffs" (further divided into "radial puffs" and "non-radial puffs" on 23 Mar), fusiform "tufts," and "mixed" morphologies (**Figure 1**), and either filtered for subsequent extraction of DNA and RNA or used for C and N_2 fixation measurements. Additionally, bulk seawater from 25 m depth was collected for comparison with *Trichodesmium* colony DNA. Seawater samples were collected using sampling bottles attached to a CTD (conductivity, temperature, depth) rosette, and subsampled into 4 L acid-washed, MilliQ-rinsed polycarbonate bottles prior to filtration.

Carbon and Nitrogen Fixation Rates

Carbon (C) and dinitrogen (N_2) fixation rates were measured using the ^{13}C method of Legendre and Gosselin (1997) and a modification of the $^{15}N_2$ uptake method of Montoya et al. (1996) to avoid delayed bubble dissolution (Mohr et al., 2010; Wilson et al., 2012). $^{15}N_2$ was added to incubations via $^{15}N_2$-enriched seawater, which was prepared onshore ∼1 week prior to departure using Stn. ALOHA surface seawater according to the methods of Wilson et al. (2012). Briefly, seawater was 0.2

TABLE 1 | Summary and environmental conditions for sampling dates during a March 2014 cruise at Stn. ALOHA.

Date	SST (°C)	Chl (μg L^{-1})	Morphologies used	Measurements	C fixation rate (nmol C μmol C^{-1} h^{-1})	N_2 fixation rate (nmol N μmol C^{-1} h^{-1})
12 Mar	24.2	0.16	25 m seawater only	DNA	ND	ND
13 Mar	24.2	0.15	Puff, tuft	DNA	ND	ND
14 Mar	24.1	0.16	Puff, tuft	DNA, RNA, rates	Puff: 7.9 (1.2) Tuft: 7.2 (0.6)	Puff: 0.02 (0.003) Tuft: 0.01 (0.004)
18 Mar	23.8	0.25	25 m seawater only	DNA	ND	ND
20 Mar	23.8	0.22	Mixed	DNA, rates	9.1 (1.8)	0.09 (0.05)
21 Mar	23.8	0.21	Puff, tuft	DNA, RNA	ND	ND
22 Mar	23.8	0.20	Mixed	DNA, RNA, rates	10.1 (1.9)	0.14 (0.08)
23 Mar	23.8	0.18	Mixed	Rates	9.7 (1.5)	0.17 (0.05)
23 Mar	23.9	0.11	R puff, NR puff, tuft	DNA, microscopy	ND	ND

*All samples were collected pre-dawn, with the exception of 23 Mar 2014, when samples were collected mid-afternoon. Sea surface temperature (SST) and surface chlorophyll fluorescence (Chl) were measured at 25 m depth using conductivity-temperature-depth sensors. Rates represent averages of duplicate incubation bottles, with standard deviations in parentheses. R denotes radial; NR denotes non-radial (see **Figure 1**); ND indicates not determined.*

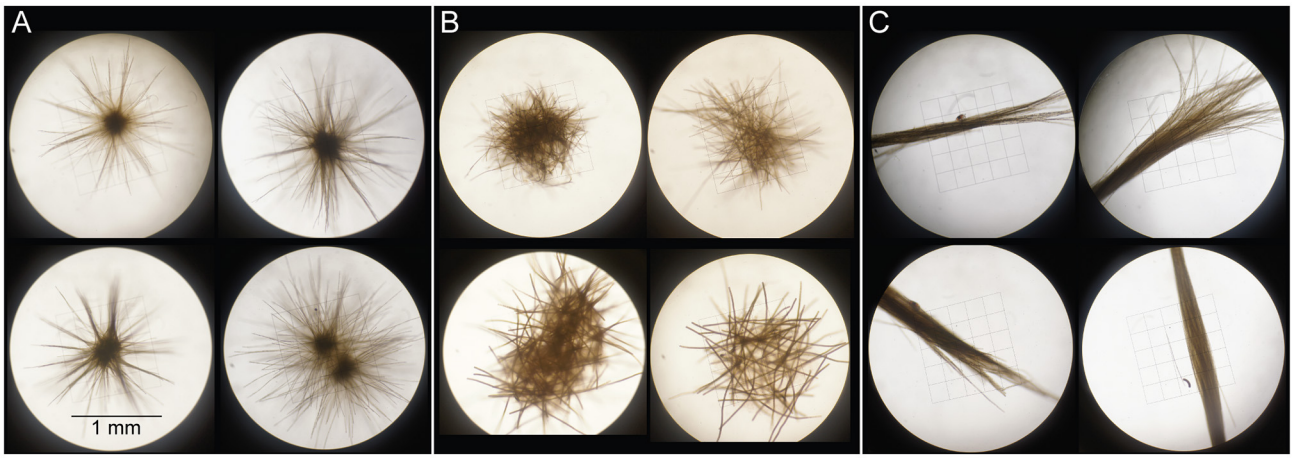

FIGURE 1 | Examples of *Trichodesmium* colonies sorted into the morphological classes "radial puffs" **(A)**, "non-radial puffs" **(B)**, and "tufts" **(C)** on 23 Mar 2014. On all other collection days, "puffs" designate mixtures of morphotypes **(A,B)**, "tufts" designate morphotype **(C)**, and "mixed" designates mixtures of all morphotypes.

μm-filtered and degassed, then dispensed into gas-tight 3 L PTFE bags (Welch Fluorocarbon); 12.9 mL^{-L} $^{15}N_2$ gas (Cambridge Isotopes, 99%) was injected into the bag, which was manually agitated to facilitate dissolution. This $^{15}N_2$-enriched seawater was dispensed into glass serum bottles, which were capped, crimped, and stored at 4°C until use. The $^{15}N_2$ content of enriched seawater was validated via Membrane Inlet Mass Spectrometry according to the methods of Böttjer et al. (2017).

For the incubations, 20–30 colonies were transferred into 37 mL glass serum bottles filled with 0.2 μm-filtered surface seawater. Samples were spiked with 4 mL $^{15}N_2$-enriched seawater and 0.5 mL of 48 mmol L^{-1} ^{13}C bicarbonate stock, and bottles were topped off with filtered seawater, capped with Viton septa and aluminum caps, and crimp-sealed. Samples were incubated from dawn to dusk (~12 h) in flow-through deckboard incubators with blue acrylic shading used to simulate ~60% of the sea-surface irradiance. Incubations were terminated by gentle filtration onto 25 mm diameter pre-combusted glass fiber filters (Whatman GF/F). Additionally, 20–30 colonies were preserved for duplicate δ^{15}N natural abundance (time-zero samples) after each net tow. Filters were flash-frozen and shipped to Oregon State University, where they were dried at 60°C overnight and packed into tin and silver capsules. Isotopic composition and masses of particulate N and C were measured with an isotope ratio mass spectrometer at Oregon State University. Fixation rates were calculated according to Montoya et al. (1996) and normalized to particulate C concentrations; thus, N_2 fixation rates are expressed as nmol N μmol C^{-1} d^{-1} rather than nmol N_2 L^{-1} d^{-1}.

Nucleic Acid Extraction, Amplification, and Sequencing

For samples used for subsequent extraction of DNA and RNA, 20–30 *Trichodesmium* colonies were transferred into filtered seawater and gently filtered onto 25 mm diameter, 0.2 μm polyethersulfone Supor filters (Pall Corporation). Samples for subsequent extraction of planktonic DNA from 25 m seawater were filtered onto 0.2 μm Supor filters using a peristaltic pump.

Filters were placed into empty microcentrifuge tubes (DNA) or microcentrifuge tubes containing 0.5 mL RNAlater (RNA), flash-frozen, transported in liquid N_2 to Oregon State University, and stored at −80°C until analysis. DNA was extracted using the DNeasy Plant MiniKit (Qiagen), with a modified protocol to include a freeze-fracture step and Proteinase K treatment. RNA was extracted using the RNeasy MiniKit (Qiagen) according to manufacturer instructions, with additional steps for cell disruption through flash-freezing and bead-beating filters in mixtures of 500 μL RLT buffer, 5 μL β-mercaptoethanol, and 200 μL of mixed 0.1 mm and 0.5 mm glass beads (Biospec products). Possible carry-forward DNA contamination was minimized from RNA extracts by using the Turbo DNA-free kit (Ambion), and extracts were quantified using a Qubit RNA HS Assay kit (Invitrogen). Complimentary DNA (cDNA) was synthesized using the SuperScript III First-Strand kit (Invitrogen) according to the manufacturer's instructions, using the nifH3 gene-specific primer (Zani et al., 2000). DNA and cDNA were quantified with the Quant-iT PicoGreen dsDNA Assay Kit (Invitrogen) using a MicroMax 384 plate reading fluorometer, and extracts were stored at −20 or −80°C.

The polymerase chain reaction (PCR) was used to amplify a portion of the 16S rRNA gene, targeting the entire prokaryotic community (DNA samples only), and the *nifH* gene, targeting diazotrophs (for both DNA and cDNA). All PCR reactions were performed using a Veriti (Applied Biosystems) or DNAEngine (BioRad) thermocycler and 10 or 20 μL reaction volumes. 16S rRNA PCR consisted of 1X HotMasterMix (5 PRIME), 1 μL DNA extract, and 5 pmol 515f (GTGCCAGCMGCCGCGGTAA) and 806r (GGACTACHVGGGTWTCTAAT) primers (Caporaso et al., 2010) which were modified to include Illumina adapters and dual-index barcodes as described by Kozich et al. (2013). Thermal cycling conditions for 16S rRNA gene amplifications were: 94°C for 3 min, followed by 30 cycles of 94°C for 45 s, 50°C for 60 s, and 72°C for 90 s, with a final 72°C extension for 10 min.

The *nifH* gene was amplified using nested degenerate *nifH* primers (Zehr and McReynolds, 1989; Zani et al., 2000). The first round contained 1X PCR buffer, 0.1U Platinum High Fidelity *Taq* polymerase (Invitrogen), 200 μmol L^{-1} dNTPs, 3% BSA, 4 mmol L^{-1} Mg^{2+}, 1 μL DNA or cDNA, and 1 μmol L^{-1} nifH1 and nifH2 primers (Simon et al., 2014). Reaction conditions were: 94°C for 7 min, followed by 30 cycles of 94°C for 1 min, 57°C for 1 min, and 72°C for 1 min, and a final 72°C extension for 7 min. The second round of *nifH* PCR used the same components and thermocycling conditions as the first round, except the DNA extract was replaced with 1 μL of the amplified product generated during the first round PCR reaction, and custom primers were used, consisting of gene-specific sites (nifH3 and nifH4), dual-indexed barcodes, Illumina linkers, and a sequencing primer binding region, similar to those described by Kozich et al. (2013; Table S1). PCR negative controls and filter blank samples were included in PCR reactions.

Triplicate PCR reactions were visualized by gel electrophoresis, then pooled and quantified as above. Samples were only sequenced if they had three successful PCR reactions, except for PCR negative controls and filter blanks, which were sequenced despite the absence of visual gel bands after amplification. 16S rRNA and *nifH* gene amplicons were pooled to equimolar concentrations, cleaned using both the UltraClean PCR (MoBio) and AMPure XP Bead cleanup kits, and sequenced at Oregon State University using MiSeq Standard v.3, 2 × 300 bp paired-end sequencing.

Metagenomes were constructed from two *Trichodesmium* puff DNA samples (**Figure 1**). Libraries were constructed using an Illumina Nextera XT library prep kit, and cleaned using the AMPure XP Bead cleanup kits. Samples were sequenced on an Illumina MiSeq using a v.3 MiSeq Reagent Kit and a 2 × 300 bp paired-end protocol. Metagenome library preparation, cleaning, and sequencing were carried out by the Oregon State University Center for Genome Research and Biocomputing Center.

Bioinformatic Analyses

Sequence reads from 16S rRNA gene amplicons, *nifH* gene amplicons, and metagenomes were demultiplexed using the Illumina MiSeq Reporter (MSR) version 2.5.1. For 16S rRNA gene sequences, primers were also removed using MSR. The majority of 16S rRNA gene paired-end reads were merged and screened for quality, retaining sequences between 245 and 254 bp with no ambiguities using mothur (Schloss et al., 2009). For a subset of 16S rRNA gene samples, only forward reads were used for phylogenetic analyses due to the poor quality of reverse reads. The reverse primer was trimmed from forward reads, and reads with ambiguities, homopolymers (>8 bp) or poor quality (average score <25 or any score <20) were removed using mothur. Finally, forward reads with lengths between 245 and 254 bp were retained and combined with the paired-end sequences for subsequent analyses. Singletons were removed, operational taxonomic units (OTUs) were clustered at 97% nucleotide sequence similarity, and a chimera check was performed with the Gold ChimeraSlayer reference database using USearch (Edgar, 2010). After quality control procedures, two of four PCR negative controls, and one of two triplicate-pooled filter blank samples retained a small number of sequences (8, 1496, and 21 sequences, respectively). Taxonomy was assigned in QIIME using the Silva v123 reference database, and sequences classified as chloroplasts, mitochondria, Archaea, Eukaryota, or an unknown domain were removed. Sequences were subsampled to 7,011 sequences per sample, resulting in near-saturation for most rarefaction curves (Figure S1). Negative control and filter blank samples contained less sequences than this cutoff, and were thus excluded from further analyses. Nonmetric multidimensional scaling analyses (NMDS, via Bray-Curtis similarity) and alpha diversity metric calculations were performed using QIIME (Caporaso et al., 2010). This same procedure was performed on reduced datasets containing *Trichodesmium* OTUs only (excluding 25 m seawater samples; rarefied to 2,248 sequences per sample) and containing all non-*Trichodesmium* OTUs (rarefied to 3,128 sequences per sample).

For *nifH* amplicons, though both forward and reverse barcodes were used for demultiplexing, only forward reads were used for phylogenetic analyses due to the poor quality of reverse reads. Reads with ambiguities, poor quality, or homopolymers were discarded. Forward primers were removed, sequences were trimmed to 244 bp, and OTUs were clustered at 97%

nucleotide sequence similarity using USearch with a *de novo* chimera checker (Edgar, 2010). OTUs containing chimeras, frameshifts, and non-*nifH* sequences were removed. The three PCR negative controls contained no *nifH* sequences after these quality control procedures, while two of five filter blank samples contained a small number of sequences (1 and 330 sequences). Sequences were subsampled to 9,651 sequences per sample, saturating most rarefaction curves (Figure S1). Both filter blank samples contained less sequences than this cutoff, and were excluded from further analyses. The *nifH* OTUs were translated and phylogenetically classified into *nifH* gene clusters (Zehr et al., 2003) via BLAST-p similarity to a reference database of *nifH* gene sequences (http://www.jzehrlab.com/#!nifh-database/c1coj). Sequences were termed "undefined" if they had equal amino acid similarity to sequences from multiple *nifH* gene sequence-types. BLASTn searches of the National Center for Biotechnology Information (https://blast.ncbi.nlm.nih.gov) were also performed for select *nifH* and 16S rRNA gene OTUs.

Metagenome sequences were demultiplexed using the Illumina MSR version 2.5.1. All further processing steps were performed for the two *Trichodesmium* colony metagenomes and a metagenome previously constructed from Stn. ALOHA surface seawater DNA (15 m depth, 0.2 μm pore-size filter) on 30 July 2015 (Wilson et al., under review; NCBI BioProject accession PRJNA358725, BioSample S37C001). Raw reads were assembled separately for each sample using MEGAHIT (Li et al., 2015). Assemblies were uploaded to the Joint Genome Institute Genomes Online Database (https://gold.jgi.doe.gov/), where coding sequences (CDS) were predicted and annotated to the Kyoto Encyclopedia of Genes and Genomes (KEGG, Kanehisa and Goto, 2000; Huntemann et al., 2015). Metagenome sequences were processed according to the methods of Nalven (2016). Sequence reads were then trimmed for quality using seqtk (https://github.com/lh3/seqtk) and mapped back to CDS using Bowtie 2 (Langmead and Salzberg, 2012). Counts (one for single reads and two for paired reads mapped), CDS lengths, and alignment lengths were extracted using SAMtools (Li et al., 2009), and counts were normalized to account for length of reads and length of CDS (Wagner et al., 2012). Counts within KEGG ortholog groups (KO) were summed and normalized as counts per million mapped to KO-annotated contigs [Genes Per Million (GPM), Wagner et al., 2012] and as counts per million mapped to KO-annotated contigs of known function (designated GPMK). GPM counts were used to analyze overall taxonomy, while GPMK were used for functional analyses. Counts from each KO were also divided into categories assigned to Cyanobacteria (assumed to be predominantly *Trichodesmium*) and non-Cyanobacteria. Details on the assembly and annotation of each sample are provided in **Table 2**.

All raw sequences are available from NCBI (accession SRP078449). Assemblies and annotation data are available from IMG/M ER (http://img.jgi.doe.gov/mer; Taxon OIDs 3300009572, 3300009536, and 3300010936).

Statistical Analyses

Two-way ANOVA with subsequent Tukey Honest Significant Difference (HSD) *post-hoc* tests were used to test the effect of day and sample type on N_2 fixation rates and alpha diversity metrics. The Welch Two Sample *t*-test was used to test for differences in the relative proportion of puff and tuft sequences in dominant OTUs, using the Bonferroni correction for multiple comparisons. Both ANOVA and *t*-tests were performed using the program R (http://www.r-project.org/). One-way ANOSIM tests were used to test for significant differences in community structure among sample types, using the program PRIMER. Detection limits for N_2 fixation rate measurements were calculated using standard propagation of errors via the observed variability between replicate samples as described by Gradoville et al. (2017) (Table S2).

RESULTS

Carbon and Nitrogen Fixation Rates

Shipboard incubation experiments showed that *Trichodesmium* colonies were actively fixing N_2 and C. Biomass-normalized $^{15}N_2$ fixation rates ranged from 0.24 to 4.16 nmol N μmol

TABLE 2 | Summary of metagenome assembly, annotation, and mapping.

	Trichodesmium non-radial puff colonies	*Trichodesmium* radial puff colonies	Stn. ALOHA surface seawater
Illumina paired-end reads	13,294,194	8,629,462	14,035,332
Contigs assembled	1,771,587	1,341,086	444,296
Weighted-average contig length (N50[a])	315 bp	301 bp	539 bp
Contigs annotated to KO	454,684	290,117	330,104
Contigs annotated (%)	25.7	21.6	74.3
Counts mapped to KO	6,446,495	3,743,920	3,669,469
Counts mapped to KO of known function[b]	3,664,674	2,116,212	2,550,585
Genomes per million genes[b,c]	417 (478)	423 (476)	823
KO of known function (%)	56.8 (57.9)	56.5 (59.6)	69.5

Trichodesmium samples were collected 23 Mar 2014; seawater sample was collected 30 July 2015. Parenthetical values represent only those KO assigned to non-Cyanobacteria.
[a] *N50 values were generated by MEGAHIT.*
[b] *Length-corrected counts.*
[c] *Average GPM from 29 KOs previously identified as single-copy genes (Nayfach and Pollard, 2015, Table S4).*

C^{-1} d^{-1} (**Table 1**); all rates were above detection limits (Table S2). Biomass-normalized ^{13}C fixation rates ranged from 173 to 243 nmol C μmol C^{-1} d^{-1} (**Table 1**). Both $^{15}N_2$ and ^{13}C rates were normalized to C content rather than colony number due to the known variability in the size of *Trichodesmium* colonies (Letelier and Karl, 1996). These ranges are similar to previously reported *Trichodesmium* colony-specific (Lomas et al., 2012) and C-specific (Gradoville et al., 2014) N_2 and C fixation rates. N_2 fixation rates varied by day of sampling (two-way ANOVA, $p < 0.01$) but not by morphology ($p > 0.05$). C fixation rates did not vary by either day or morphology (two-way ANOVA, $p > 0.05$).

Trichodesmium Species Diversity

The *Trichodesmium* species diversity within our samples was assessed via PCR amplification and sequencing of 16S rRNA and *nifH* genes. Sequences from both genes indicate that *Trichodesmium* Clade I (e.g., *T. thiebautii*) dominated our samples, with Clade III (e.g., *T. erythraeum*) representing <1% of *Trichodesmium* sequences (**Figure 2**). The 16S rRNA gene dataset contained 2 OTUs classified as *Trichodesmium*, with the most abundant OTU classified as Clade I (16S OTU 2, 99.5% of *Trichodesmium* 16S rRNA sequences). Likewise, 2 of the 3 *Trichodesmium nifH* gene OTUs (*nifH* OTU 1 and *nifH* OTU 27) were classified as Clade I and together comprised 99.9% of the *Trichodesmium nifH* gene sequences (**Figure 2**). Puff, tuft, and mixed morphology samples from 16S rRNA and *nifH* genes all contained >99% Clade I *Trichodesmium* sequences (Table S3), and the *Trichodesmium* community structure did not vary by morphology (ANOSIM $R = -0.042$, $p = 0.6$; **Figure 3C**). No sequences from the 16S rRNA or *nifH* gene datasets were classified as *Trichodesmium* Clade II or Clade IV.

Microbial Diversity via 16S rRNA Gene Amplicons

The microbial diversity of the *Trichodesmium* microbiome was assessed using high-throughput sequencing of partial 16S rRNA genes from 17 *Trichodesmium* colony samples and 4 surface seawater samples for comparison. *Trichodesmium* sequences represented 24–75% of 16S rRNA amplicons from colony samples; the remaining 25–76% of sequences corresponded to associated bacteria, termed epibionts (though it is possible that a subset of these organisms were endobionts). The most

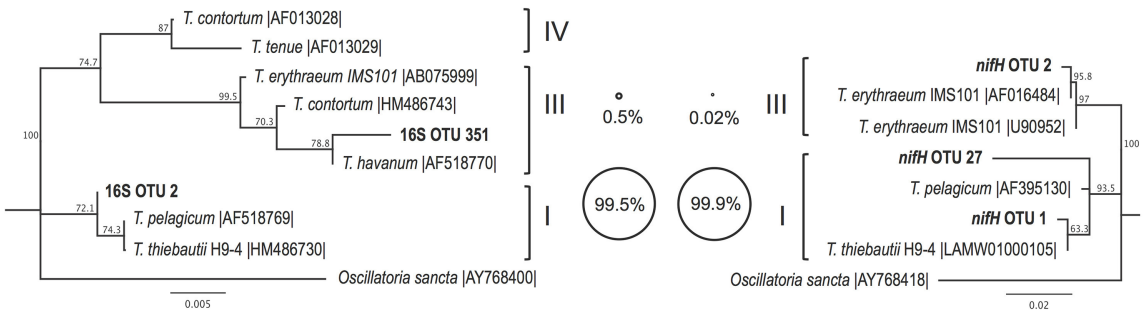

FIGURE 2 | Neighbor joining phylogenetic trees depicting the relationships between *Trichodesmium* OTUs (97% nucleotide similarity) from partial 16S rRNA **(left)** and partial *nifH* **(right)** gene sequences, together with reference sequences from cultivated representatives (accession numbers given). Major *Trichodesmium* clades (Lundgren et al., 2005) are shown in Roman numerals. Bubble plots depict the percentage of *Trichodesmium* DNA sequences from this study which group with each clade, according to partial 16S rRNA **(left)** and partial *nifH* **(right)** amplicon datasets. Bootstrap values (1,000 replicates) of >50% are provided. Scale bars represent nucleotide substitutions per site.

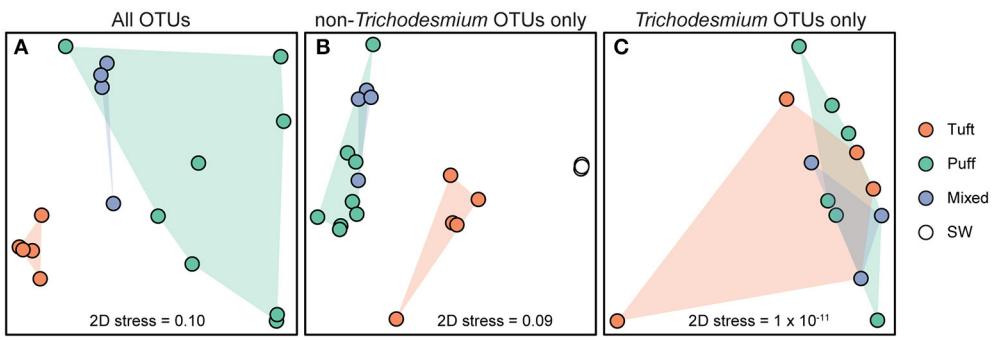

FIGURE 3 | Non-metric multi-dimensional scaling (NMDS) plots derived from the Bray–Curtis dissimilarity matrix of 16S rRNA OTUs from **(A)** all *Trichodesmium* colony sample OTUs (7011 sequences per sample), **(B)** *Trichodesmium* colony and surface seawater samples excluding *Trichodesmium* OTUs (3128 sequences per sample), and **(C)** *Trichodesmium* colony samples excluding non-*Trichodesmium* OTUs (2248 sequences per sample). Each point represents an individual sample. Colors represent sample type [tuft colonies, puff colonies, mixed colonies, and bulk seawater (SW) from 25 m].

abundant epibiotic taxa belonged to Bacteroidetes (Cytophagia, Sphingobacteriales, and Flavobacteriales), Alphaproteobacteria (predominantly Rhodobacteriales, Rhodospirillales, and Rhizobiales), and Gammaproteobacteria (e.g., *Marinicella* sp., *Alteromonas* sp., Oceanospirillales) (**Figure 4**, Figure S2, Table S3). Even at broad phylum- and class-level taxonomic groupings, the *Trichodesmium* epibiont community differed from the bacterial community in the surrounding seawater: all colonies were relatively enriched in Bacteroidetes, and puff and mixed colony samples were enriched in Acidobacteria and Deltaproteobacteria, compared to the surrounding seawater (**Figure 4**). Additionally, some of the most abundant taxa in NPSG near-surface seawater samples, including the Cyanobacteria *Prochlorococcus* sp., and *Synechococcus* sp., the Actinobacteria *Actionomarina* sp., and marine groups AEGEAN-169, SAR11, SAR86, and SAR116, were relatively depleted or absent in *Trichodesmium* colony samples (**Figure 4**, Figure S2). At the 97% identity level, *Trichodesmium* colonies and seawater samples had few dominant epibiont OTUs (OTUs containing >1% non-*Trichodesmium* sequences in samples of either morphology) in common (Figure S2). NMDS analyses provide further evidence that the community structure of the epibionts was distinct from that of the surrounding seawater, and also illustrate greater dissimilarity among *Trichodesmium* samples than among surface seawater samples (ANOSIM $R = 0.852$, $p = 0.001$; **Figure 3B**).

The *Trichodesmium* epibiont community varied with colony morphology. *Trichodesmium* colonies with puff morphology ($n = 8$ samples) contained a smaller fraction of *Trichodesmium* sequences (24–51% *Trichodesmium* 16S rRNA), and thus a larger fraction of epibiont sequences, than tuft morphologies ($n = 5$ samples; 57–75% *Trichodesmium* 16S rRNA) (**Figure 4**). The epibiont communities of puff colonies contained a larger fraction of Bacteroidetes (including Cytophagia and Saprospiraceae) and Deltaproteobacteria (including Desulfuromonadales) than tuft colonies (**Figure 4**,

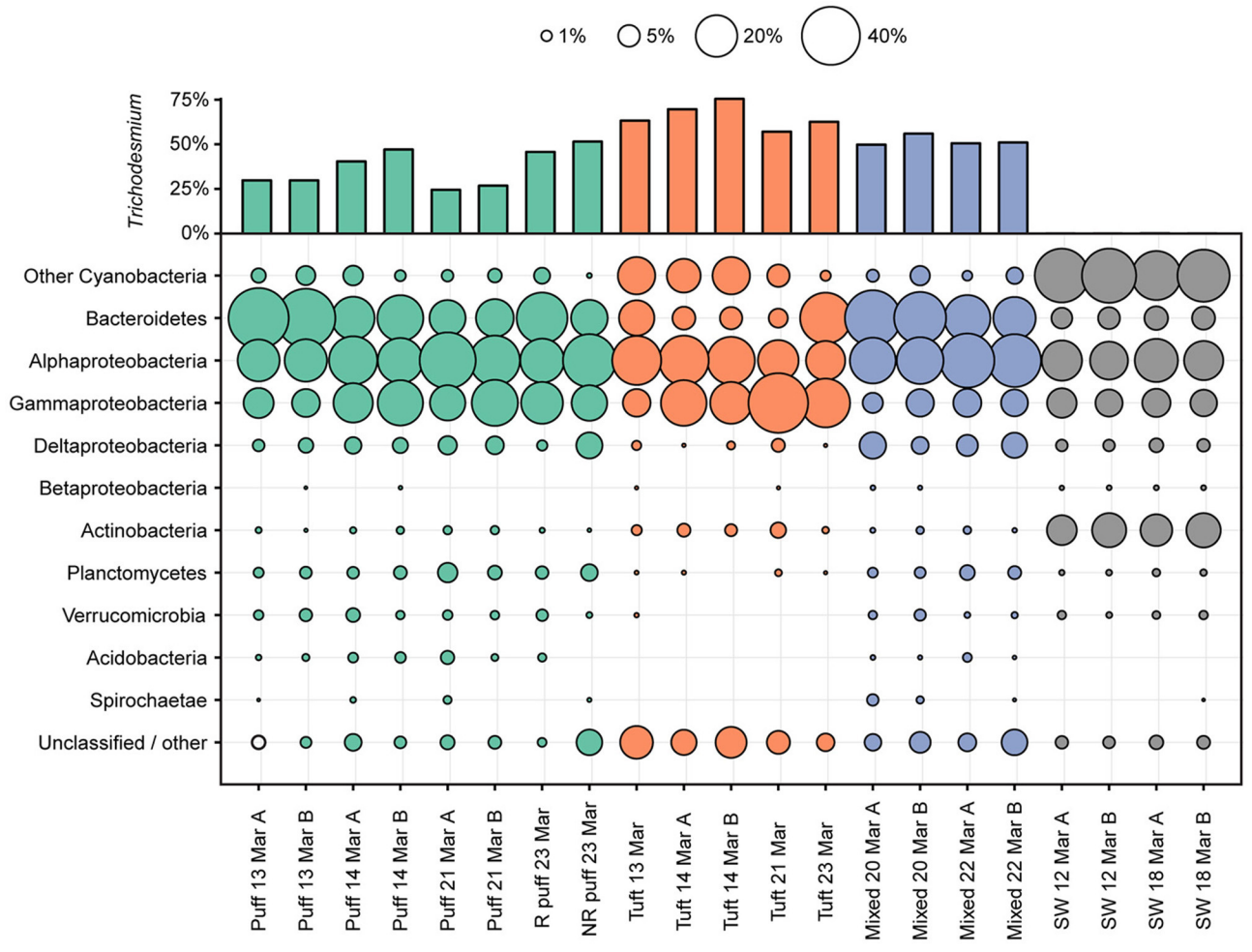

FIGURE 4 | Percentages of partial 16S rRNA gene sequences assigned to bacterial taxa. Percentages of sequences assigned to *Trichodesmium* are displayed in the upper bar plot. The area plot displays the percentages of non-*Trichodesmium* sequences assigned to other bacterial taxa. Color indicates the sample type/morphology [green, red, blue, and gray for puff colonies, tuft colonies, mixed colonies, and bulk 25 m seawater (SW), respectively]. R denotes radial and NR denotes non-radial puff morphologies (see **Figure 1**).

TABLE 3 | Diversity and species richness estimates.

	Sample type	Diversity (Shannon)	Species richness (Chao1)
All OTUs	Puff	4.5 (0.8)	268 (70)
	Tuft	2.5 (0.5)	208 (58)
	Mixed	3.8 (0.2)	263 (15)
	SW	5.1 (0.3)	513 (55)
non-*Trichodesmium* OTUs only	Puff	5.6 (0.6)	250 (66)
	Tuft	4.4 (0.6)	212 (57)
	Mixed	5.8 (0.3)	269 (38)
	SW	5 (0.3)	426 (27)

Estimates are derived from partial 16S rRNA gene sequences using all OTUs (7011 sequences per sample) and OTUs excluding Trichodesmium sequences (3128 sequences per sample). Data are presented as averages within sample type (n = 8 puff, 5 tuft, 4 mixed morphology, and 4 25 m bulk seawater (SW) samples), with standard deviations in parentheses.

Figure S2). Tuft colonies contained a larger fraction of non-*Trichodesmium* Cyanobacteria (predominantly *Limnothrix*) and Gammaproteobacteria (including Alteromonadaceae, Oleiphilaceae, and Piscirickettsiaceae) than puff colonies. There were also differences between puff and tuft colony epibionts at the OTU level: over half of the most abundant *Trichodesmium* OTUs had significantly different relative abundances between the two morphotypes (Figure S2). NMDS analyses demonstrated that the overall epibiont community structure varied by morphology, with puff colonies clustering separately from tuft colonies (**Figure 3**).

Alpha diversity metrics were calculated from 16S rRNA gene OTUs at 97% identity (**Table 3**). Both diversity (Shannon) and species richness (Chao1) varied by sample type (i.e., seawater or morphology) and by day of sampling ($p < 0.05$, two-way ANOVA). Species richness did not vary among *Trichodesmium* morphologies (Tukey HSD $p > 0.05$), but all morphotypes had significantly lower (by a factor of ∼2) species richness than surface seawater samples (Tukey HSD $p \leq 0.001$). Diversity was higher in *Trichodesmium* puff samples and mixed morphology samples than in tuft samples (Tukey HSD $p < 0.001$). *Trichodesmium* samples of all morphotypes had lower diversity than seawater samples (Tukey HSD $p < 0.05$); however, when excluding *Trichodesmium* OTUs, diversity in samples of all *Trichodesmium* morphotypes were not significantly different from seawater (Tukey HSD $p > 0.05$). Thus, the *Trichodesmium* epibiont community had lower species richness, but insignificant differences in evenness, compared to seawater.

Diazotroph Diversity via *nifH* Amplicons

We sequenced partial *nifH* genes and transcripts from *Trichodesmium* colonies, and from surface seawater samples for comparison, to test for the presence and transcriptional activities of non-*Trichodesmium* diazotrophs associated with the colonies. While sequences belonging to *Trichodesmium* dominated the *nifH* dataset, we also recovered non-*Trichodesmium nifH* genes and transcripts (**Figure 5**). In the DNA samples, *Trichodesmium* represented 64–99% of *nifH* sequences, with an average of 7% of sequences corresponding to non-*Trichodesmium* diazotrophs. Most non-*Trichodesmium nifH* DNA sequences were classified as *nifH* Cluster III, a group that includes anaerobic microorganisms, such as *Desulfovibrio* and *Clostridium* (Zehr et al., 2003). Non-*Trichodesmium* groups other than Cluster III represented 1.5% of *nifH* gene sequences, and included previously identified *nifH* groups, such as 1G (presumed Gammaproteobacteria), 1J/1K (presumed Alpha- and Betaproteobacteria), and a very small percentage of sequences belonging to the cyanobacterium UCYN-A. The non-*Trichodesmium* diazotrophs associated with the colonies were distinct from diazotrophic taxa in the surrounding seawater, where *nifH* gene sequences were dominated by UCYN-A and presumed Gammaproteobacteria and contained <0.01% *nifH* Cluster III.

A much smaller fraction of *nifH* transcript sequences belonged to non-*Trichodesmium* diazotrophs (**Figure 5**). Sequences phylogenetically related to the *nifH* Cluster III, 1G, and 1J/1K, which constituted a modest proportion of *nifH* gene sequences, were conspicuously absent from the *nifH* transcript sequences. The small fraction of non-*Trichodesmium nifH* transcripts (0–3.5%) belonged to Cyanobacteria, predominantly cyanobacterium UCYN-A and *Richelia/Calothrix* (with the exception of one sample containing 0.01% 1J/1K, presumed Alpha- and Betaproteobacteria).

The *nifH* DNA and RNA sequences show that *Trichodesmium* puff and tuft colonies harbored different communities of non-*Trichodesmium* diazotrophs (**Figure 5**). Puff colonies harbored a larger fraction of Cluster III (average 9.6% of *nifH* gene sequences) than tuft colonies (average 2.1% of *nifH* DNA sequences), while tuft colonies harbored a larger fraction of 1G (presumed Gammaproteobacteria, average 2.9% of *nifH* gene sequences) than puff colonies (average 0.2% of *nifH* gene sequences). Additionally, *nifH* transcripts from puff and tuft colony morphologies included different phylotypes of heterocystous Cyanobacteria (*Richelia*/*Calothrix*). One puff RNA sample contained transcripts derived from the *Calothrix* SC01/HET-3 group (Foster and Zehr, 2006; Foster et al., 2010). No tuft samples contained *Calothrix* SC01 sequences, but all 4 tuft RNA samples contained transcripts derived from the *Richelia*/HET-1 group (Church et al., 2005b). Neither heterocystous phylotype matched qPCR primer sets developed by Momper et al. (2015) to target the heterocystous cyanobiont hetDA (≥4 mismatches with forward primer for both phylotypes; reverse primer was out of our sequencing region).

Metagenomic Taxonomy and Functional Potential

We sequenced metagenomes from two *Trichodesmium* puff samples collected on 23 Mar 2014 ("radial puff" and "non-radial puff") and assembled and annotated these sequences along with sequences from a publically available Stn. ALOHA surface seawater metagenome collected in July 2015. Colony metagenomes were dominated by bacteria (>99% of total counts), with ∼70% of counts assigned to Cyanobacteria (**Table 4**). Cyanobacteria accounted for an average of 57 and 67%

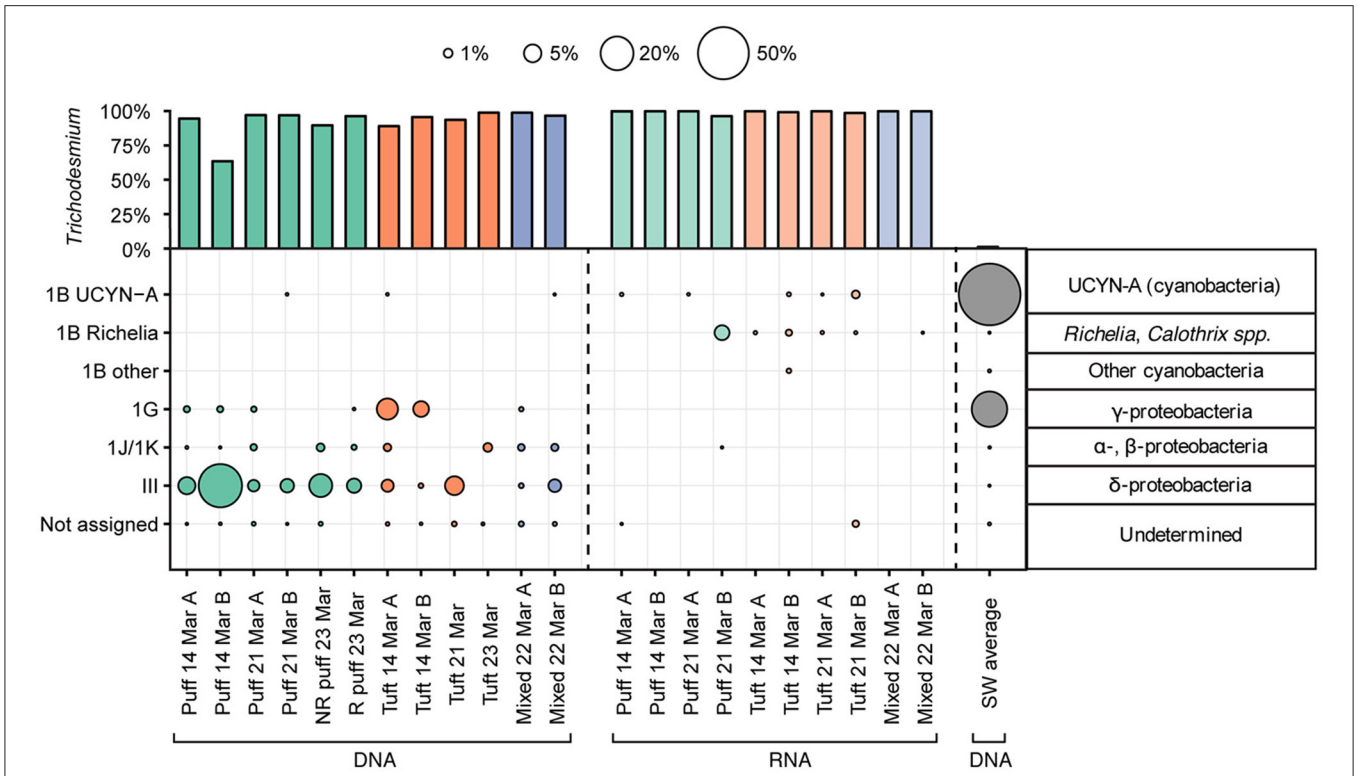

FIGURE 5 | Percentages of *nifH* gene (left, right) and transcript (center) sequences assigned to *nifH* cluster groups. Percentages of *Trichodesmium* sequences are displayed in the upper bar plot; sequences assigned to other taxa are displayed in the lower area plot. Representative taxa from canonical *nifH* clusters (Zehr et al., 2003) are shown to the right. Color indicates the sample type/morphology [green, red, blue, and gray for puff colonies, tuft colonies, mixed colonies, and bulk 25 m seawater (SW), respectively]. R denotes radial and NR denotes non-radial puff morphologies (see **Figure 1**).

of counts from a set of 29 single-copy genes (Table S4) from radial and non-radial puff colonies, respectively. Thus, assuming one copy of each of these genes per genome (Nayfach and Pollard, 2015), equal levels of ploidy among taxa, and that the majority of cyanobacterial counts belong to *Trichodesmium*, both total metagenome and single-copy gene counts produce conservative estimates of ∼1 epibiont cell for every 1–3 *Trichodesmium* cells within colonies. Less than 1% of *Trichodesmium* colony counts were assigned to Eukarya, Archaea, or viruses, compared to 3.6% of surface seawater counts (**Table 4**). Eukaryotes represented 0.5 and 0.3% of non-radial and radial puff colony counts, respectfully, with dominant groups including green algae (Streptophyta and Chlorophyta), chordates, heterotrophic flagellates (Choanoflagellida), arthropods, diatoms, ciliates, and fungi (**Table 4**, Table S5). The relative abundances of bacterial taxa mirrored trends observed in the 16S rRNA gene dataset, with the majority of colony sequences belonging to Cyanobacteria (primarily *Trichodesmium*), Alphaproteobacteria, Bacteroidetes, and Gammaproteobacteria (**Table 4**, **Figure 4**).

Metagenome counts were annotated to KO and normalized to GPM in order to compare the relative abundance of genes and pathways among samples. However, ∼75% of assembled contigs from *Trichodesmium* colonies failed KO annotation,

TABLE 4 | Taxonomic assignments from three metagenome samples.

	Trichodesmium non-radial puff colonies (%)	*Trichodesmium* radial puff colonies (%)	Stn. ALOHA surface seawater (%)
Cyanobacteria	75.9	65.5	31.8
α-proteobacteria	11.1	12.5	41.6
γ-proteobacteria	3.2	5.3	11.2
δ-proteobacteria	1.2	0.9	0.8
β-proteobacteria	0.5	1.1	0.7
Bacteroidetes	4.1	8.6	5.4
Firmicutes	1.1	1.3	1.3
Planctomycetes	0.8	1.9	0.3
Actinobacteria	0.5	0.6	1.0
Verrucomicrobia	0.1	0.5	0.6
Chloroflexi	0.1	0.2	0.1
Eukaryota	0.5	0.3	2.6
Archaea	0.1	0.2	0.5
Viruses	0.1	0.1	0.5
Other bacteria	0.7	1.0	1.6

Values denote percentages of length-corrected reads mapped to annotated assemblies. Trichodesmium and surface seawater metagenomes are derived from samples collected 23 Mar 2014 and 30 July 2015, respectively.

far exceeding the ∼25% of failed contig annotations observed in the surface seawater sample (**Table 2**). Furthermore, of the sequences that were successfully mapped to annotated contigs, *Trichodesmium* samples contained a larger fraction of KO with unknown function than the surface seawater sample (**Table 2**). This resulted in smaller GPM values from *Trichodesmium* metagenomes than the surface seawater metagenome for most KEGG gene categories (Figure S3). Hence, we chose to use a normalization of counts per million mapped to a KO of known function (GPMK) in order to compare the functional potential of *Trichodesmium* colonies and surface seawater.

The gene contents of the *Trichodesmium* colony samples were distinct from those observed in the near-surface seawater. Colonies contained ∼40% fewer single-copy GPM than the seawater samples (both in Cyanobacteria and non-Cyanobacteria fractions, **Table 2**, Table S4), suggesting larger average genome sizes for *Trichodesmium* and epibiont cells. Summing KOs from KEGG gene groups revealed broad functional differences between colonies and surface seawater (**Figure 6**). Seawater samples were relatively enriched in KEGG groups including nucleotide and amino acid metabolism, transcription, translation, and replication and repair, while the colony samples were relatively enriched in energy metabolism, metabolism of terpenoids and polyketides, and cell motility.

Trichodesmium colony and surface seawater metagenomes also differed in the abundances of specific genes and pathways involved in nutrient cycling (**Figure 7**). Colonies were enriched in genes encoding alkaline phosphatase and transporters for phosphate, phosphonates, and Fe(II), but depleted in Fe(III) transporter genes, compared to seawater. There were similar abundances of phosphate starvation response and Fe complex (siderophore) transport genes in colonies and seawater; however, the majority of these genes in the colonies belonged to non-Cyanobacteria (epibionts), which only represented ∼30% of total colony metagenome counts. Thus, phosphate starvation response and Fe complex transport genes were enriched in epibionts compared to the surrounding plankton.

Trichodesmium colonies were also enriched in N cycling genes. Compared to seawater, the colony metagenomes contained higher total N metabolism gene abundances (34 and 46% higher abundances in radial and non-radial puffs, respectively, Table S6), and were strongly enriched in genes involved in N transformation pathways (**Figure 7**). Nitrogenase genes were ∼2,000X more abundant in colonies than seawater, and included a large fraction assigned to non-Cyanobacteria (11 and 20% of nitrogenase genes in radial and non-radial puff colonies, respectively). Assimilatory nitrate reduction genes were present in both colony and seawater samples, but were ∼5X more abundant in colonies, where the majority of genes corresponded to Cyanobacteria. Dissimilatory nitrate reduction and denitrification genes were absent in seawater samples but present in both colony samples; genes in these pathways were nearly exclusively assigned to non-Cyanobacteria (**Figure 7**). Genes involved in nitrification pathways were not observed in colony or seawater metagenomes.

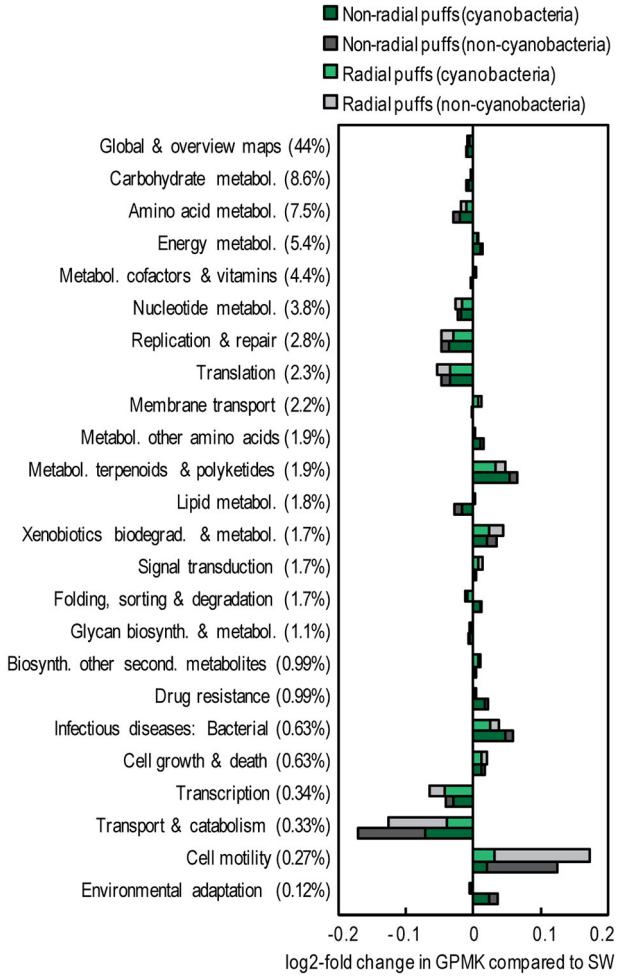

FIGURE 6 | Relative abundance of KEGG gene groups in *Trichodesmium* colony samples (collected 23 Mar 2014) compared to a surface seawater sample from Stn. ALOHA (collected 30 July 2015). The percentages of total counts within each gene group are provided in parentheses. Colors represent sample type and taxonomic assignment. Pathways involved with organ systems, human disease, and/or representing <0.1% of total GPMK were excluded. Pathways displayed represent >97% of total GPMK.

DISCUSSION

Several decades of research have documented the presence of bacterial and eukaryotic epibionts inhabiting *Trichodesmium* colonies (Borstad and Borstad, 1977; Siddiqui et al., 1992; Rouco et al., 2016), but the taxonomic composition and functional potential of these associated communities are not well-understood. Here, we used a variety of molecular tools to probe the diversity of *Trichodesmium* and associated epibionts in colonies from the NPSG. We found that the colonies were dominated by a single clade of *Trichodesmium*, but harbored a diverse community of associated microorganisms. These microbial assemblages were distinct from the surrounding seawater, differed by colony morphology, and included bacteria with a known preference for surface attachment, as well as

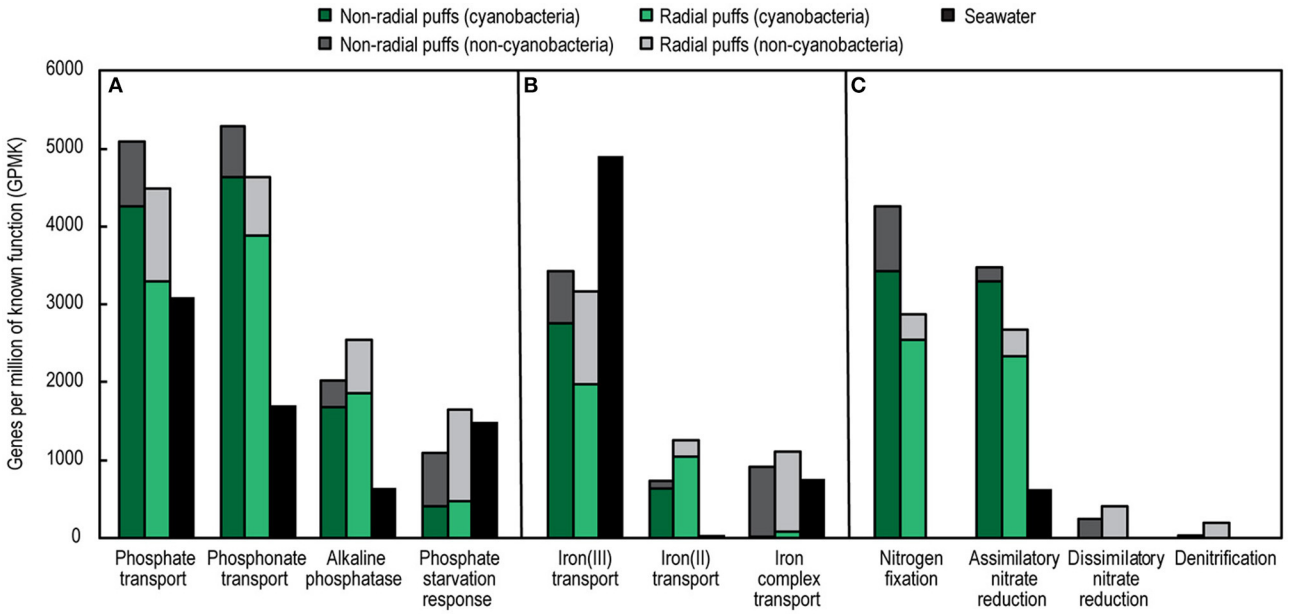

FIGURE 7 | Abundances of select genes and pathways involved in phosphorus **(A)**, iron **(B)**, and nitrogen **(C)** cycling from *Trichodesmium* colony and surface seawater metagenomes. Colors represent sample type and taxonomic assignment. See Table S6 for a list of KO included in each pathway.

putative anaerobic diazotrophs. Colony metagenomes contain genes and pathways not present in *Trichodesmium* genomes, including siderophore transport and denitrification genes, which likely affects the biogeochemical functioning of *Trichodesmium* colonies.

Trichodesmium Species Diversity

The abundance and distribution of *Trichodesmium* have been studied extensively, but most work has focused on *Trichodesmium* at the genus-level, using techniques including microscopy, video plankton recording, and satellite imaging (e.g., Dugdale, 1961; Subramaniam et al., 2001; Davis and McGillicuddy, 2006). In the laboratory, *Trichodesmium* isolates have been phylogenetically classified into four major clades (based on the hetR and ITS genes), with the majority of isolates falling into Clade I (e.g., *T. thiebautii*) and Clade III (e.g., *T. erythraeum*) (Orcutt et al., 2002; Hynes et al., 2012), but the geographical distributions of these clades in field populations has only begun to be investigated. Our finding of Clade I dominance is in agreement with recent surveys in the N. Pacific, N. Atlantic, and S. Pacific (Hmelo et al., 2012; Gradoville et al., 2014; Rouco et al., 2014, 2016), which all observed the majority of *Trichodesmium* sequences belonging to Clade I. However, most physiological studies of *Trichodesmium* use the cultivated Clade III laboratory isolate *T. erythraeum* IMS101. Isolates from Clade I and Clade III appear to respond differently to environmental stimuli; for example, elevating pCO_2 enhances rates of N_2 and C fixation by Clade III isolates IMS101 and GBRTRLI101 but not by the Clade I isolate H9-4 (Hutchins et al., 2007, 2013). While more work is needed to resolve the spatial and temporal variability of *Trichodesmium* species biogeography, current evidence suggests that at a global scale *Trichodesmium* Clade I may be more abundant than Clade III. Hence, modeling studies using the response of isolate IMS101 to predict the pCO_2 response of natural *Trichodesmium* populations should be viewed with caution. In addition, our findings agree with previous reports that colony morphology is not an accurate proxy for *Trichodesmium* clade (Hynes et al., 2012), as both puff and tuft colony samples were composed of >99% Clade I (**Figure 2**).

Diversity of Associated Microbiome

Our samples contained diverse bacterial and eukaryotic taxa associated with *Trichodesmium* colonies. While relative abundances derived from metagenomic and 16S rRNA gene sequences can be biased by taxa-specific genome sizes and copy numbers of genes and genomes (e.g., Sargent et al., 2016), respectively, the large fractions of non-*Trichodesmium* sequences in both datasets suggest that epibionts are numerically abundant within the colonies. Colony metagenome sequences were dominated by bacteria, but we also observed sequences from viruses, Archaea, and many eukaryotic taxa previously observed associated with *Trichodesmium* colonies (Borstad and Borstad, 1977; Sheridan et al., 2002). Bacterial species richness within colonies was ∼10-fold higher than the richness previously assessed for Atlantic colonies using clone libraries (Hmelo et al., 2012), and approximately half of the richness in surrounding seawater, reaffirming that colonies harbor a diverse epibiont community (Sheridan et al., 2002; Rouco et al., 2016).

The taxonomic composition of colony epibionts was distinct from that of the surrounding bacterioplankton. The warm, oligotrophic waters of the NPSG are known to be dominated by the Cyanobacteria *Prochlorococcus* (Campbell et al., 1994)

and photo- and chemoheterotrophs including SAR11 and Rhodobacteraceae (DeLong et al., 2006). Indeed, the most abundant taxa in our near-surface seawater samples were those clustering among *Prochlorococcus*, *Synechococcus*, and the small photoheterotroph Actinomarina (SAR11 represented only 3.2% of seawater sequences, likely due to a known bias in the 16S rRNA gene primer set used, Apprill et al., 2015); however, these taxa were all conspicuously absent from *Trichodesmium* colony samples. The relative absence of typical oligotrophic bacteria with streamlined genomes in colonies could be due to elevated nutrient concentrations favoring copiotrophic taxa (Lauro et al., 2009; Giovannoni et al., 2014), and is consistent with previous observations of large marine particle size classes being enriched with copiotrophic bacterial genes (Allen et al., 2013). Instead, colony epibionts were dominated by Bacteroidetes, Alphaproteobacteria, and Gammaproteobacteria, which is consistent with previous 16S rRNA gene surveys of microbial communities associated with *Trichodesmium* (Hmelo et al., 2012; Rouco et al., 2016). Several dominant epibiont taxa have been previously observed associated with marine particulates, including the Bacteroidetes classes Cytophagia and Flavobacteriia (DeLong et al., 1993; Crump et al., 1999; Bryant et al., 2016), Alteromonadales (Fontanez et al., 2015), and Planctomycetes (DeLong et al., 1993). Though epibiont communities had several abundant taxa in common with the surrounding seawater at the order-level (e.g., Rhodobacterales, Rhodospirillales, and Oceanospirillales), there were few commonalities with surface seawater phylotypes at the 97% OTU-level. The distinct community structure and lower species richness of epibionts compared to surrounding bacterioplankton, and the commonalities between epibiont taxa from our samples and previous *Trichodesmium* studies (Hmelo et al., 2012; Rouco et al., 2016) together suggest that *Trichodesmium* colonies provide a niche favoring select bacterial taxa.

In addition, we observed distinct epibiont communities associated with puff and tuft colonies, in agreement with Rouco et al. (2016), as well as evidence that certain bacterial species may consistently associate with specific morphotypes. Tuft colonies contained a larger fraction of *Trichodesmium* 16S rRNA gene sequences than puff colonies, possibly due to less colonizable surface area in this morphotype, which likely drives the lower diversity values observed for tufts (**Table 3**). This finding contrasts with the microscopic observations of Sheridan et al. (2002), who reported tuft colonies harboring higher bacterial densities than puff colonies. Furthermore, the epibiont composition differed between the two morphologies, both in terms of phyla-level taxonomy (e.g., puffs contained more Bacteroidetes and tufts contained more non-*Trichodesmium* Cyanobacteria, **Figure 4**) and, even more strikingly, in the relative abundance of specific phylotypes (Figure S2). For example, a phylotype clustering among the filamentous Cyanobacteria *Limnothrix* represented 11.7% of non-*Trichodesmium* tuft sequences but only 0.1% of non-*Trichodesmium* puff sequences. Filamentous Cyanobacteria have been observed in close association with *Trichodesmium* filaments from tuft colonies (e.g., Paerl et al., 1989a; Siddiqui et al., 1992; Hewson et al., 2009), and *Limnothrix*-like sequences represented 31% of 16S rRNA gene clone library sequences in tuft (but not puff) colonies from the N. Atlantic (Hmelo et al., 2012). Thus, this *Limnothrix* phylotype may be a common associate of *Trichodesmium* tufts. Likewise, *Microscilla* represented 7.7% of tufts but only 0.01% of non-*Trichodesmium* puff sequences, and this genus has been previously recovered from *Trichodesmium* tufts in the N. Pacific, N. Atlantic, and Caribbean Sea (Janson et al., 1999; Rouco et al., 2016). Puff colonies also contained abundant phylotypes which were relatively absent from tufts, including Alphaproteobacteria and Bacteroidetes phylotypes, the cyanobacterium *Rivularia*, and a *Marinicella* phylotype which shares 100% nucleotide sequence identity to a sequence previously recovered from *Trichodesmium* colonies (accession GU726121). It is remarkable that so many phylotypes had significantly different relative abundances between the two morphotypes (Figure S2), and also that many of the most abundant genera from our samples have also been dominant in previous surveys of *Trichodesmium* epibionts (Hmelo et al., 2012; Rouco et al., 2016). Since the species composition of *Trichodesmium* did not vary by colony morphology, physical (i.e., filament compactness, colonizable surface area) and/or chemical properties of puff and tuft colonies likely drive the observed differences in epibiont community structure.

Colony-Associated Diazotrophs

There have been several reports of cyanobacterial and heterotrophic diazotrophs associated with *Trichodesmium* colonies (Paerl et al., 1989b; Gradoville et al., 2014; Momper et al., 2015), but the community composition and metabolic activity of these organisms have been largely unexplored. Here, we used high-throughput sequencing of partial *nifH* genes and transcripts to explore the diversity of colony-associated diazotrophs. We observed non-*Trichodesmium* *nifH* genes (including genes from putative heterotrophs) in all *Trichodesmium* DNA samples, representing 1–35% of the colony *nifH* sequences (**Figure 5**).

The ecological importance of non-cyanobacterial marine diazotrophs is a current enigma in N_2 fixation research: non-cyanobacterial *nifH* genes have been recovered from numerous marine environments (Bombar et al., 2016), but rates of N_2 fixation in marine environments dominated by non-cyanobacterial diazotrophs are often low or undetectable (e.g., Knapp et al., 2016; Gradoville et al., 2017). Here, we found robust evidence that *Trichodesmium* colonies comprise yet another habitat for these seemingly cosmopolitan organisms. The majority of our non-*Trichodesmium* *nifH* gene sequences phylogenetically grouped among Cluster III *nifH* genes, which includes diverse anaerobic microorganisms (Zehr et al., 2003). The possibility of anaerobic bacteria inhabiting *Trichodesmium* colonies appears plausible since colonies have been reported to contain anoxic microzones (Paerl and Bebout, 1988); indeed, we also found denitrification and Fe(II) transporter genes enriched in colony metagenomes (see *Functional potential within Trichodesmium colonies*). However, *nifH* Cluster III contains diverse lineages (Zehr et al., 2003), and the physiology and ecology of these organisms are not well-understood. In our

study, the three most abundant Cluster III OTUs each share <85% nucleotide identity with any cultured representative in the BLASTn database. One of these OTUs matches a qPCR primer/probe set designed by Church et al. (2005a) to quantify a specific group of Cluster III *nifH* sequence-types in the NPSG, while all three OTUs share >99% nucleotide identity with sequences previously obtained from *Trichodesmium* colonies at Stn. ALOHA (Gradoville et al., 2014). Such results suggest that *Trichodesmium* colonies may selectively harbor members of the Cluster III *nifH* phylotypes, including organisms not currently captured by existing Cluster III qPCR primers and probes (Church et al., 2005a).

It is interesting to note that both Cluster III and the 1J/1K (presumed Alpha- and Betaproteobacteria) group had higher relative abundances in our *Trichodesmium* colony samples than in the surrounding seawater, where *nifH* sequences were dominated by the unicellular cyanobacterium UCYN-A, the Gammaproteobacterial *nifH* group 1G, and other Cyanobacteria including *Trichodesmium* (**Figure 5**). This suggests that *Trichodesmium* colonies may represent a niche for Cluster III and 1J/1K diazotrophs. It is possible that the relative enrichment of these groups in *Trichodesmium* colonies could reflect a preference for marine particulates—for example, Bryant et al. (2016) observed marine plastic particles to be enriched in *nifH* genes—rather than a unique property of the colonies themselves. Marine particles may be favorable environments for heterotrophic diazotrophs (Bombar et al., 2016), especially putative anaerobic Cluster III taxa, which could inhabit anoxic microzones of particles (Benavides et al., 2015). Future research is needed to determine whether *Trichodesmium* colonies represent an important niche for *nifH* Cluster III diazotrophs in the NPSG and other oceanic regions.

Though *Trichodesmium nifH* amplicons included genes belonging to non-Cyanobacteria, the absence of non-cyanobacterial *nifH* transcripts suggests that these taxa were not actively fixing N_2 at the time of sampling (**Figure 5**). However, we did observe non-*Trichodesmium* cyanobacterial *nifH* transcripts, mostly belonging to two OTUs in the heterocystous *Calothrix/Richelia* group. One of the *Calothrix*/*Richelia* OTUs matched primer/probe sets for group HET-1 (Church et al., 2005b), and was present in all tuft RNA samples, while another *Calothrix*/*Richelia* OTU, present in one puff RNA sample, matched primer/probe sets for the SC01/HET-3 group (Foster and Zehr, 2006; Foster et al., 2010). This suggests that there may be morphotype-specific associations between heterocystous Cyanobacteria and *Trichodesmium* other than the cohabitation described by Momper et al. (2015). While *Calothrix*/*Richelia* sequences were absent in the *nifH* DNA dataset (likely due to poor amplification of this group by the *nifH* primers used; Turk-Kubo et al., 2015), we did see evidence of heterocystous Cyanobacteria inhabiting colonies in the 16S rRNA datset (*Rivularia* and a small number of *Richelia* sequences; Figure S2, Table S3). Furthermore, the presence of *Calothrix*/*Richelia nifH* transcripts indicates high cell-specific transcription rates by this group. Our observation of higher *nifH* transcription levels in cyanobacterial diazotrophs than non-cyanobacterial diazotrophs is consistent with previous *nifH* gene expression surveys using bulk seawater from Stn. ALOHA (Church et al., 2005b).

Functional Potential within *Trichodesmium* Colonies

Our metagenomic data suggest that *Trichodesmium* epibionts may benefit from a colony-associated lifestyle and influence nutrient cycling within colonies. Epibionts appeared to possess larger average genome sizes than bulk plankton, suggesting non-streamlined genomes, consistent with the relative absence of oligotrophic taxa (*Prochlorococcus, Actinomarina*, etc.) observed in colonies. Furthermore, epibionts were depleted in genes involved in replication and basic metabolic functioning relative to seawater metagenomes, again consistent with a lack of streamlined genomes (Giovannoni et al., 2014). Instead, colony samples were enriched in genes involved in motility, which could be useful in a colony-associated lifestyle, and in metabolic pathways not present in the seawater metagenome (**Figures 6**, **7**, Table S6). Additionally, a large fraction of *Trichodesmium* colony contigs failed annotation. This could be due to the large fraction of non-coding DNA in the *Trichodesmium* genome (Walworth et al., 2015), but could also arise from a larger fraction of uncultivated microorganisms in the *Trichodesmium* microbiome than in the surrounding seawater. Likewise, colony samples contained a larger fraction of genes with unknown function than seawater samples. Our findings of enrichments in copiotrophic taxa, motility genes, and genes of unknown function within *Trichodesmium* colonies have also been observed in particle-attached marine microbial communities (Simon et al., 2014).

The NPSG is a chronically oligotrophic system, with production rates limited by the availability of N (Karl et al., 1997) and sometimes P (Karl et al., 1995). Since diazotrophs such as *Trichodesmium* circumvent N limitation through N_2 fixation, their growth and N_2 fixation rates are typically limited by the availability of P and/or Fe (as well as light and temperature, Luo et al., 2014). Hence, there is considerable interest in understanding the mechanisms of P and Fe acquisition by *Trichodesmium*. We observed enrichments in alkaline phosphatase, phosphate transport, and phosphonate transport genes in colonies, which agrees with previous demonstrations of efficient organic phosphorus scavenging and utilization by *Trichodesmium* (Dyhrman et al., 2006). Furthermore, colony epibionts contained genes encoding the synthase for acyl homoserine lactoses (Table S6), quorum sensing molecules which have been shown to stimulate alkaline phosphatase activity by *Trichodesmium* cells in culture (Van Mooy et al., 2011). We also found that phosphate starvation response genes were enriched in epibionts, which could reflect P-limitation due to the release of inorganic and organic N compounds by *Trichodesmium* cells (Capone et al., 1994; Mulholland et al., 2004).

The genes involved in Fe transport also differed between colony and seawater metagenomes. Fe(II) transporters were enriched in colony samples, consistent with previous observations of these genes in *Trichodesmium* isolates (Chappell and Webb, 2010), but were nearly absent in the

seawater metagenome. In well-oxygenated seawater, most Fe exists as Fe(III), hence our observation of epibionts enriched in Fe(II) transport genes suggests that low-oxygen microzones within colonies could result in reduction of Fe(III). Additionally, we found low abundances of cyanobacterial siderophore transport genes, reflecting the inability of *Trichodesmium* to use highly chelated Fe sources (Chappell and Webb, 2010), but these genes were enriched in non-cyanobacterial epibionts. Our observations of abundant P and Fe acquisition genes in *Trichodesmium* and epibionts could reflect competition for these resources in the colony community. However, we also found metagenomic evidence for previously described potential mutualisms, as epibionts could facilitate *Trichodesmium* nutrient uptake through quorum sensing (Van Mooy et al., 2011) and siderophore production (Roe et al., 2012).

Finally, we observed the genetic capacity for denitrification within *Trichodesmium* colonies. Both colony samples contained all necessary genes for the denitrification and dissimilatory nitrate reduction pathways, while no genes from either pathway were observed in the seawater sample. Furthermore, 16S OTU 18, comprising 9.9% of non-*Trichodesmium* 16S rRNA gene sequences from tuft colonies, was classified as the denitrifier *Nisaea* sp. These results agree with Wyman et al. (2013), who reported *nosZ* amplicons isolated from *Trichodesmium* colonies in the Arabian Sea. Denitrification within the colonies would be biogeochemically significant, producing a tight spatial coupling between N_2 fixation and denitrification and reducing apparent colony N_2 fixation rates. However, denitrification requires nitrate, and we did not observe any nitrification genes within colonies (Table S6), although it is possible that nitrate could be supplied through diurnal migration to deeper nitrate-rich waters (Walsby, 1978). Furthermore, denitrification is an anaerobic process, and while early reports indicated that colonies could contain anoxic zones (Paerl and Bebout, 1988), more recent work has found no evidence for this (Eichner et al., 2017). Thus, it is possible that the presence of denitrification genes does not indicate active denitrification within colonies, but rather reflects the diverse gene repertoire of copiotrophic epibionts.

CONCLUSIONS

Our multifaceted high-throughput sequencing approach enabled a detailed view of the *Trichodesmium* colony microbiome. While the species composition of *Trichodesmium* was dominated by a single clade and uniform in all of our samples, the community structure of bacterial epibionts differed between puff and tuft colony morphologies, suggesting that differences in biogeochemical rates among colony morphologies may be driven by processes carried out by the associated microbiome. Epibionts appear copiotrophic, with the genetic capacity to influence colony nutrient cycling. Additionally, we found that colonies contained active cyanobacterial diazotrophs and presumed heterotrophic and anaerobic diazotrophs, suggesting that *Trichodesmium* colonies harbor a unique microbial community with the potential to influence rate processes classically attributed to *Trichodesmium* spp.

AUTHOR CONTRIBUTIONS

This study was conceived by MG. Data were collected by MG and analyzed by MG, BC, MC, RL, and AW. MG wrote the first draft of the manuscript. All authors contributed substantial revisions through the drafting process and approved the final submitted manuscript.

ACKNOWLEDGMENTS

Support for this project was provided by the National Science foundation through the Center for Microbial Oceanography: Research and Education (C-MORE; EF0424599) and the Simons Collaboration on Ocean Processes and Ecology (SCOPE award ID 329108). We are grateful to Ed Delong and Frank Aylward for supplying Stn. ALOHA metagenome data.

SUPPLEMENTARY MATERIAL

The Supplementary Material for this article can be found online at: http://journal.frontiersin.org/article/10.3389/fmicb.2017.01122/full#supplementary-material

REFERENCES

Allen, A. E., Allen, L. Z., McCrow, J. P. (2013). Lineage specific gene family enrichment at the microscale in marine systems. *Curr. Opin. Microbiol.* 16, 605–617. doi: 10.1016/j.mib.2013.10.001

Apprill, A., McNally, S., Parsons, R., and Webe, L. (2015). Minor revision to V4 region SSU rRNA 806R gene primer greatly increases detection of SAR11 bacterioplankton. *Aquat. Microb. Ecol.* 75, 129–137. doi: 10.3354/ame01753

Benavides, M., Moisander, P. H., Berthelot, H., Dittmar, T., Grosso, O., and Bonnet, S. (2015). Mesopelagic N_2 fixation related to organic matter composition in the Solomon and Bismarck Seas (Southwest Pacific). *PLoS ONE* 10:e0143775. doi: 10.1371/journal.pone.0143775

Bombar, D., Paerl, R. W., and Riemann, L. (2016). Marine non-cyanobacterial diazotrophs: moving beyond molecular detection. *Trends Microbiol.* 24, 916–927. doi: 10.1016/j.tim.2016.07.002

Borstad, G., and Borstad, L. (1977). "The Oscillatoria erythraea (*Cyanophyta*) community of associates," in *Cooperative Investigations of the Caribbean and Adjacent Regions-II*, ed H. B. Stewart, FAO Fish. Report 200, 51–57.

Böttjer, D., Dore, J. E., Karl, D. M., Letelier, R. M., Mahaffey, C., Wilson, S. T., et al. (2017). Temporal variability of nitrogen fixation and particulate nitrogen export at Station ALOHA. *Limnol. Oceanogr.* 62, 200–216. doi: 10.1002/lno.10386

Bryant, J. A., Clemente, T. M., Viviani, D. A., Fong, A. A., Thomas, K. A., Kemp, P., et al. (2016). Diversity and activity of communities inhabiting plastic debris in the North Pacific Gyre. *mSystems* 1, e00024–e00016. doi: 10.1128/mSystems.00024-16

Campbell, L., Nolla, H., and Vaulot, D. (1994). The importance of *Prochlorococcus* to community structure in the central North Pacific Ocean. *Limnol. Oceanogr.* 39, 954–961. doi: 10.4319/lo.1994.39.4.0954

Capone, D. G., Burns, J. A., Montoya, J. P., Subramaniam, A., Mahaffey, C., Gunderson, T., et al. (2005). Nitrogen fixation by *Trichodesmium* spp.: an

important source of new nitrogen to the tropical and subtropical North Atlantic Ocean. *Glob. Biogeochem. Cycles* 19, GB2024. doi: 10.1029/2004GB002331

Capone, D. G., Ferrier, M. D., and Carpenter, E. J. (1994). Amino acid cycling in colonies of the planktonic marine cyanobacterium *Trichodesmium thiebautii*. *Appl. Env. Microbiol.* 60, 3989–3995.

Caporaso, J. G., Kuczynski, J., Stombaugh, J., Bittinger, K., Bushman, F. D., Costello, E. K., et al. (2010). QIIME allows analysis of high-throughput community sequencing data. *Nat. Methods* 7, 335–336. doi: 10.1038/nmeth.f.303

Chappell, P. D., and Webb, E. A. (2010). A molecular assessment of the iron stress response in the two phylogenetic clades of *Trichodesmium*. *Env. Microbiol.* 12, 13–27. doi: 10.1111/j.1462-2920.2009.02026.x

Church, M. J., Jenkins, B. D., Karl, D. M., and Zehr, J. P. (2005a). Vertical distributions of nitrogen-fixing phylotypes at Stn ALOHA in the oligotrophic North Pacific Ocean. *Aquat. Microb. Ecol.* 38, 3–14. doi: 10.3354/ame038003

Church, M. J., Short, C. M., Jenkins, B. D., Karl, D. M., and Zehr, J. P. (2005b). Temporal patterns of nitrogenase gene (*nifH*) expression in the oligotrophic North Pacific Ocean. *Appl. Env. Microbiol.* 71, 5362–5370. doi: 10.1128/AEM.71.9.5362-5370.2005

Coles, V. J., Hood, R. R., Pascual, M., and Capone, D. G. (2004). Modeling the impact of *Trichodesmium* and nitrogen fixation in the Atlantic Ocean. *J. Geophys. Res.* 109, C06007. doi: 10.1029/2002JC001754

Crump, B. C., Armbrust, E. V., and Baross, J. A. (1999). Phylogenetic analysis of particle-attached and free-living bacterial communities in the Columbia River, its estuary, and the adjacent coastal ocean. *Appl. Env. Microbiol.* 65, 3192–3204.

Davis, C. S., and McGillicuddy, D. J. (2006). Transatlantic abundance of the N_2-fixing colonial cyanobacterium *Trichodesmium*. *Science* 312, 1517–1520. doi: 10.1126/science.1123570

DeLong, E. F., Franks, D. G., and Alldredge, A. L. (1993). Phylogenetic diversity of aggregate-attached vs. free-living marine bacterial assemblages. *Limnol. Oceanogr.* 38, 924–934. doi: 10.4319/lo.1993.38.5.0924

DeLong, E. F., Preston, C. M., Mincer, T., Rich, V., Hallam, S. J., Frigaard, N. U., et al. (2006). Community genomics among stratified microbial assemblages in the ocean's interior. *Science* 311, 496–503. doi: 10.1126/science.1120250

Dugdale, R. (1961). Nitrogen fixation in the Sargasso Sea. *Deep Sea Res. Pt. II* 7, 297–300. doi: 10.1016/0146-6313(61)90051-x

Dyhrman, S., Chappell, P., Haley, S., Moffett, J., Orchard, E., Waterbury, J., et al. (2006). Phosphonate utilization by the globally important marine diazotroph *Trichodesmium*. *Nature* 439, 68–71. doi: 10.1038/nature04203

Dyhrman, S. T., Benitez-Nelson, C. R., Orchard, E. D., Haley, S. T., and Pellechia, P. J. (2009). A microbial source of phosphonates in oligotrophic marine systems. *Nat. Geosci.* 2, 696–699. doi: 10.1038/ngeo639

Edgar, R. C. (2010). Search and clustering orders of magnitude faster than BLAST. *Bioinformatics* 26, 2460–2461. doi: 10.1093/bioinformatics/btq461

Eichner, M. J., Klawonn, I., Wilson, S. T., Littmann, S., Whitehouse, M. J., Church, M. J., et al. (2017). Chemical microenvironments and single-cell carbon and nitrogen uptake in field-collected colonies of *Trichodesmium* under different pCO_2. *ISME J.* 11, 1305–1317. doi: 10.1038/ismej.2017.15

Fontanez, K. M., Eppley, J. M., Samo, T. J., Karl, D. M., and DeLong, E. F. (2015). Microbial community structure and function on sinking particles in the North Pacific Subtropical Gyre. *Front. Microbiol.* 6:469. doi: 10.3389/fmicb.2015.00469

Foster, R. A., Goebel, N. L., and Zehr, J. P. (2010). Isolation of Calothrix rhizosoleniae (*cyanobacteria*) strain SC01 from *Chaetoceros* (*Bacillariophyta*) spp. diatoms of the Subtropical North Pacific ocean. *J. Phycol.* 46, 1028–1037. doi: 10.1111/j.1529-8817.2010.00885.x

Foster, R. A., and Zehr, J. P. (2006). Characterization of diatom–cyanobacteria symbioses on the basis of *nifH, hetR* and 16S rRNA sequences. *Env. Microbiol.* 8, 1913–1925. doi: 10.1111/j.1462-2920.2006.01068.x

Giovannoni, S. J., Cameron Thrash, J., and Temperton, B. (2014). Implications of streamlining theory for microbial ecology. *ISME J.* 8, 1553–1565. doi: 10.1038/ismej.2014.60

Gradoville, M. R., Bombar, D., Crump, B. C., Letelier, R. M., Zehr, J. P., and White, A. E. (2017). Diversity and activity of nitrogen-fixing communities across ocean basin. *Limnol. Oceanogr.* doi: 10.1002/lno.10542. [Epub ahead of print].

Gradoville, M. R., White, A. E., Böttjer, D., Church, M. J., and Letelier, R. M. (2014). Diversity trumps acidification: lack of evidence for carbon dioxide enhancement of *Trichodesmium* community nitrogen or carbon fixation at Station ALOHA. *Limnol. Oceanogr.* 59, 645–659. doi: 10.4319/lo.2014.59.3.0645

Hewson, I., Poretsky, R. S., Dyhrman, S. T., Zielinski, B., White, A. E., Tripp, H. J., et al. (2009). Microbial community gene expression within colonies of the diazotroph, *Trichodesmium*, from the Southwest Pacific Ocean. *ISME J.* 3, 1286–1300. doi: 10.1038/ismej.2009.75

Hmelo, L. R., Van Mooy, B. A. S., and Mincer, T. J. (2012). Characterization of bacterial epibionts on the cyanobacterium *Trichodesmium*. *Aquat. Microb. Ecol.* 67, 1–14. doi: 10.3354/ame01571

Huntemann, M., Ivanova, N. N., Mavromatis, K., Tripp, H. J., Paez-Espino, D., Palaniappan, K., et al. (2015). The standard operating procedure of the DOE-JGI Microbial Genome Annotation Pipeline (MGAP v. 4). *Stand. Genomic Sci.* 10:86. doi: 10.1186/s40793-015-0077-y

Hutchins, D. A., Fu, F.-X., Webb, E. A., Walworth, N., and Tagliabue, A. (2013). Taxon-specific response of marine nitrogen fixers to elevated carbon dioxide concentrations. *Nat. Geosci.* 6, 790–795. doi: 10.1038/ngeo1858

Hutchins, D., Fu, F. X., Zhang, Y., Warner, M., Feng, Y., Portune, K., et al. (2007). CO_2 control of *Trichodesmium* N_2 fixation, photosynthesis, growth rates, and elemental ratios: implications for past, present, and future ocean biogeochemistry. *Limnol. Oceanogr.* 52, 1293–1304. doi: 10.4319/lo.2007.52.4.1293

Hynes, A. M., Webb, E. A., Doney, S. C., and Waterbury, J. B. (2012). Comparison of cultured *Trichodesmium* (Cyanophyceae) with species characterized from the field. *J. Phycol.* 48, 196–210. doi: 10.1111/j.1529-8817.2011.01096.x

Janson, S., Bergman, B., Carpenter, E. J., Giovannoni, S. J., and Vergin, K. (1999). Genetic analysis of natural populations of the marine diazotrophic cyanobacterium *Trichodesmium*. *FEMS Microbiol. Ecol.* 30, 57–65. doi: 10.1111/j.1574-6941.1999.tb00635.x

Kanehisa, M., and Goto, S. (2000). KEGG: Kyoto Encyclopedia of Genes and Genomes. *Nucleic Acids Res.* 28, 27–30. doi: 10.1093/nar/28.1.27

Karl, D., Letelier, R., Hebel, D., Tupas, L., Dore, J., Christian, J., et al. (1995). Ecosystem changes in the North Pacific subtropical gyre attributed to the 1991–92 El Nino. *Nature* 373, 230–234. doi: 10.1038/373230a0

Karl, D., Letelier, R., Tupas, L., Dore, J., Christian, J., and Hebel, D. (1997). The role of nitrogen fixation in biogeochemical cycling in the subtropical North Pacific Ocean. *Nature* 388, 533–538. doi: 10.1038/41474

Karl, D., Michaels, A., Bergman, B., Capone, D., Carpenter, E., Letelier, R., et al. (2002). Dinitrogen fixation in the world's oceans. *Biogeochemistry* 57, 47–98. doi: 10.1023/A:1015798105851

Knapp, A. N., Casciotti, K. L., Berelson, W. M., Prokopenko, M. G., and Capone, D. G. (2016). Low rates of nitrogen fixation in eastern tropical South Pacific surface waters. *Proc. Natl. Acad. Sci. U. S.A.* 113, 4398–4403. doi: 10.1073/pnas.1515641113

Kozich, J. J., Westcott, S. L., Baxter, N. T., Highlander, S. K., and Schloss, P. D. (2013). Development of a dual-index sequencing strategy and curation pipeline for analyzing amplicon sequence data on the MiSeq Illumina sequencing platform. *Appl. Env. Microbiol.* 79, 5112–5120. doi: 10.1128/AEM.01043-13

Langmead, B., and Salzberg, S. L. (2012). Fast gapped-read alignment with Bowtie 2. *Nat. Methods* 9, 357–359. doi: 10.1038/nmeth.1923

Lauro, F. M., McDougald, D., Thomas, T., Williams, T. J., Egan, S., Rice, S., et al. (2009). The genomic basis of trophic strategy in marine bacteria. *Proc. Natl. Acad. Sci. U.S.A.* 106, 15527–15533. doi: 10.1073/pnas.0903507106

Legendre, L., and Gosselin, M. (1997). Estimation of N or C uptake rates by phytoplankton using ^{15}N or ^{13}C: revisiting the usual computation formulae. *J. Plankton Res.* 19, 263–271. doi: 10.1093/plankt/19.2.263

Letelier, R. M., and Karl, D. M. (1996). Role of *Trichodesmium* spp. in the productivity of the subtropical North Pacific Ocean. *Mar. Ecol. Prog. Ser.* 133, 263–273. doi: 10.3354/meps133263

Li, D., Liu, C.-M., Luo, R., Sadakane, K., and Lam, T.-W. (2015). MEGAHIT: an ultra-fast single-node solution for large and complex metagenomics assembly via succinct de Bruijn graph. *Bioinformatics* 31, 1674–1676. doi: 10.1093/bioinformatics/btv033

Li, H., Handsaker, B., Wysoker, A., Fennell, T., Ruan, J., Homer, N., et al. (2009). The sequence alignment/map format and SAMtools. *Bioinformatics* 25, 2078–2079. doi: 10.1093/bioinformatics/btp352

Lomas, M., Hopkinson, B., Losh, J., Ryan, D., Shi, D., Xu, Y., et al. (2012). Effect of ocean acidification on cyanobacteria in the subtropical North Atlantic. *Aquat. Microb. Ecol.* 66, 211–222. doi: 10.3354/ame01576

Lundgren, P., Janson, S., Jonasson, S., Singer, A., and Bergman, B. (2005). Unveiling of novel radiations within *Trichodesmium* cluster by *hetR* gene sequence analysis. *Appl. Env. Microbiol.* 71, 190–196. doi: 10.1128/AEM.71.1.190-196.2005

Luo, Y.-W., Lima, I., Karl, D., Deutsch, C., and Doney, S. (2014). Data-based assessment of environmental controls on global marine nitrogen fixation. *Biogeosciences* 11, 691–708. doi: 10.5194/bg-11-691-2014

Mahaffey, C., Michaels, A. F., and Capone, D. G. (2005). The conundrum of marine N_2 fixation. *Am. J. Sci.* 305, 546–595. doi: 10.2475/ajs.305.6-8.546

Mohr, W., Großkopf, T., Wallace, D. W. R., and LaRoche, J. (2010). Methodological underestimation of oceanic nitrogen fixation rates. *PLoS ONE* 5:e12583. doi: 10.1371/journal.pone.0012583

Momper, L. M., Reese, B. K., Carvalho, G., Lee, P., and Webb, E. A. (2015). A novel cohabitation between two diazotrophic cyanobacteria in the oligotrophic ocean. *ISME J.* 9, 882–893. doi: 10.1038/ismej.2014.186

Montoya, J. P., Voss, M., Kahler, P., and Capone, D. G. (1996). A simple, high-precision, high-sensitivity tracer assay for N_2 fixation. *Appl. Env. Microbiol.* 62, 986–993.

Mulholland, M. R., Bronk, D. A., and Capone, D. G. (2004). Dinitrogen fixation and release of ammonium and dissolved organic nitrogen by *Trichodesmium* IMS101. *Aquat. Microb. Ecol.* 37, 85–94. doi: 10.3354/ame037085

Nalven, S. G. (2016). *Decoding DOM Degradation with Metatranscriptomics: How do Sunlight and Microbial Communities Interact to Degrade Dissolved Organic Matter in Arctic Freshwaters?* Dissertation/Master's Thesis, Corvallis OR: Oregon State University.

Nayfach, S., and Pollard, K. S. (2015). Average genome size estimation improves comparative metagenomics and sheds light on the functional ecology of the human microbiome. *Genome Biol.* 16:51. doi: 10.1186/s13059-015-0611-7

O'Neil, J. M. (1998). The colonial cyanobacterium *Trichodesmium* as a physical and nutritional substrate for the harpacticoid copepod *Macrosetella gracilis*. *J. Plankton Res.* 20, 43–59. doi: 10.1093/plankt/20.1.43

Orcutt, K., Rasmussen, U., Webb, E. A., Waterbury, J. B., Gundersen, K., and Bergman, B. (2002). Characterization of *Trichodesmium* spp. by genetic techniques. *Appl. Env. Microbiol.* 68, 2236–2245. doi: 10.1128/AEM.68.5.2236-2245.2002

Paerl, H. W., and Bebout, B. M. (1988). Direct measurement of O_2-depleted microzones in marine *Oscillatoria*: Relation to N_2 fixation. *Science* 241, 442–445. doi: 10.1126/science.241.4864.442

Paerl, H. W., Bebout, B. M., and Prufert, L. E. (1989a). Bacterial associations with marine Oscillatoria sp. (*Trichodesmium* sp.) populations: Ecological implications. *J. Phycol.* 25, 773–784. doi: 10.1111/j.0022-3646.1989.00773.x

Paerl, H. W., Priscu, J. C., and Brawner, D. L. (1989b). Immunochemical localization of nitrogenase in marine *Trichodesmium* aggregates: relationship to N_2 fixation potential. *Appl. Env. Microbiol.* 55, 2965–2975.

Roe, K. L., Barbeau, K., Mann, E. L., and Haygood, M. G. (2012). Acquisition of iron by *Trichodesmium* and associated bacteria in culture. *Env. Microbiol.* 14, 1681–1695. doi: 10.1111/j.1462-2920.2011.02653.x

Rouco, M., Haley, S. T., and Dyhrman, S. T. (2016). Microbial diversity within the *Trichodesmium* holobiont. *Env. Microbiol.* 18, 5151–5160. doi: 10.1111/1462-2920.13513

Rouco, M., Warren, H. J., McGillicuddy, D. J., Waterbury, J. B., and Dyhrman, S. T. (2014). *Trichodesmium* sp. clade distributions in the western North Atlantic Ocean. *Limnol. Oceanogr.* 59, 1899–1909. doi: 10.4319/lo.2014.59.6.1899

Sargent, E. C., Hitchcock, A., Johansson, S. A., Langlois, R., Moore, C. M., LaRoche, J., et al. (2016). Evidence for polyploidy in the globally important diazotroph *Trichodesmium*. *FEMS Microbiol. Lett.* 362:fnw244. doi: 10.1093/femsle/fnw244

Schloss, P. D., Westcott, S. L., Ryabin, T., Hall, J. R., Hartmann, M., Hollister, E. B., et al. (2009). Introducing mothur: Open-source, platform-independent, community-supported software for describing and comparing microbial communities. *Appl. Environ. Microbiol.* 75, 7537–7541. doi: 10.1128/AEM.01541-09

Sheridan, C., Steinberg, D., and Kling, G. (2002). The microbial and metazoan community associated with colonies of *Trichodesmium* spp.: A quantitative survey. *J. Plankton Res.* 24, 913–922. doi: 10.1093/plankt/24.9.913

Siddiqui, P., Bergman, B., and Carpenter, E. (1992). Filamentous cyanobacterial associates of the marine planktonic cyanobacterium *Trichodesmium*. *Phycologia* 31, 326–337. doi: 10.2216/i0031-8884-31-3-4-326.1

Simon, H. M., Smith, M. W., Herfort, L. (2014). Metagenomic insights into particles and their associated microbiota in a coastal margin ecosystem. *Front. Microbiol.* 5:466. doi: 10.3389/fmicb.2014.00466

Stihl, A., Sommer, U., and Post, A. F. (2001). Alkaline phosphatase activities among populations of the colony-forming diazotrophic cyanobacterium *Trichodesmium* spp. (cyanobacteria) in the Red Sea. *J. Phycol.* 37, 310–317. doi: 10.1046/j.1529-8817.2001.037002310.x

Subramaniam, A., Brown, C. W., Hood, R. R., Carpenter, E. J., and Capone, D. G. (2001). Detecting *Trichodesmium* blooms in SeaWiFS imagery. *Deep Sea Res. Pt. II* 49, 107–121. doi: 10.1016/S0967-0645(01)00096-0

Turk-Kubo, K. A., Frank, I. E., Hogan, M. E., Desnues, A., Bonnet, S., and Zehr, J. P. (2015). Diazotroph community succession during the VAHINE mesocosm experiment (New Caledonia lagoon). *Biogeosciences* 12, 7435–7452. doi: 10.5194/bg-12-7435-2015

Van Mooy, B. A., Hmelo, L. R., Sofen, L. E., Campagna, S. R., May, A. L., Dyhrman, S. T., et al. (2011). Quorum sensing control of phosphorus acquisition in *Trichodesmium* consortia. *ISME J.* 6, 422–429. doi: 10.1038/ismej.2011.115

Wagner, G. P., Kin, K., and Lynch, V. J. (2012). Measurement of mRNA abundance using RNA-seq data: RPKM measure is inconsistent among samples. *Theory Biosci.* 131, 281–285. doi: 10.1007/s12064-012-0162-3

Walsby, A. (1978). The properties and buoyancy-providing role of gas vacuoles in *Trichodesmium* Ehrenberg. *Brit. Phycol. J.* 13, 103–116. doi: 10.1080/00071617800650121

Walsby, A. (1992). "The gas vesicles and buoyancy of Trichodesmium," in *Marine Pelagic Cyanobacteria: Trichodesmium and Other Diazotrophs*, eds E. J. Carpenter, D. G. Capone, and J. G. Rueter (Berlin: Springer), 141–161.

Walworth, N., Pfreundt, U., Nelson, W. C., Mincer, T., Heidelberg, J. F., Fu, F., et al. (2015). *Trichodesmium* genome maintains abundant, widespread noncoding DNA *in situ*, despite oligotrophic lifestyle. *Proc. Natl. Acad. Sci. U.S.A.* 112, 4251–4256. doi: 10.1073/pnas.1422332112

Wilson, S. T., Böttjer, D., Church, M. J., and Karl, D. M. (2012). Comparative assessment of nitrogen fixation methodologies, conducted in the oligotrophic North Pacific Ocean. *Appl. Env. Microbiol.* 78, 6516–6523. doi: 10.1128/AEM.01146-12

Wyman, M., Hodgson, S., and Bird, C. (2013). Denitrifying Alphaproteobacteria from the Arabian Sea that express *nosZ*, the gene encoding nitrous oxide reductase, in oxic and suboxic waters. *Appl. Env. Microbiol.* 79, 2670–2681. doi: 10.1128/AEM.03705-12

Zani, S., Mellon, M. T., Collier, J. L., and Zehr, J. P. (2000). Expression of *nifH* genes in natural microbial assemblages in Lake George, New York, detected by reverse transcriptase PCR. *Appl. Env. Microbiol.* 66, 3119–3124. doi: 10.1128/AEM.66.7.3119-3124.2000

Zehr, J. P., Jenkins, B. D., Short, S. M., and Steward, G. F. (2003). Nitrogenase gene diversity and microbial community structure: a cross-system comparison. *Env. Microbiol.* 5, 539–554. doi: 10.1046/j.1462-2920.2003.00451.x

Zehr, J. P., and McReynolds, L. A. (1989). Use of degenerate oligonucleotides for amplification of the nifH gene from the marine cyanobacterium Trichodesmium thiebautii. *Appl. Environ. Microbiol.* 55, 2522–2526.

Conflict of Interest Statement: The authors declare that the research was conducted in the absence of any commercial or financial relationships that could be construed as a potential conflict of interest.

frontiers in Microbiology

CORRECTION
published: 19 September 2017
doi: 10.3389/fmicb.2017.01780

Corrigendum: Microbiome of *Trichodesmium* Colonies from the North Pacific Subtropical Gyre

Mary R. Gradoville[1†], Byron C. Crump[1], Ricardo M. Letelier[1], Matthew J. Church[2] and Angelicque E. White[1]*

[1] College of Earth, Ocean and Atmospheric Sciences, Oregon State University, Corvallis, OR, United States, [2] Flathead Lake Biological Station, University of Montana, MT, United States

Keywords: *Trichodesmium*, marine microbiome, *nifH* diversity, heterotrophic marine diazotrophs, metagenomics, 16S rRNA, nitrogen fixation

A corrigendum on

Microbiome of *Trichodesmium* Colonies from the North Pacific Subtropical Gyre
by Gradoville, M. R., Crump, B. C., Church, M. J., Letelier, R. M., and White, A. E. (2017). Front. Microbiol. 8:1122. doi: 10.3389/fmicb.2017.01122

In the original article, there were two errors. First, an incorrect NCBI accession number was provided. A correction has been made to Methods, Bioinformatic Analyses, Paragraph 4:

"All raw sequences are available from NCBI (accession SRP095769). Assemblies and annotation data are available from IMG/M ER (http://img.jgi.doe.gov/mer; Taxon OIDs 3300009572, 3300009536, and 3300010936)."

Additionally, in the original article, the two primer sets used for nested *nifH* PCR were listed in the incorrect order and included an incorrect reference. A correction has been made to Methods, Nucleic Acid Extraction, Amplification, and Sequencing, Paragraph 3:

"The *nifH* gene was amplified using nested degenerate *nifH* primers (Zehr and McReynolds, 1989; Zani et al., 2000). The first round contained 1X PCR buffer, 0.1U Platinum High Fidelity Taq polymerase (Invitrogen), 200 μmol L^{-1} dNTPs, 3% BSA, 4 mmol L^{-1} Mg^{2+}, 1 μL DNA or cDNA, and 1 μmol L^{-1} nifH3 and nifH4 primers (Zani et al., 2000). Reaction conditions were: 94°C for 7 min, followed by 30 cycles of 94°C for 1 min, 57°C for 1 min, and 72°C for 1 min, and a final 72°C extension for 7 min. The second round of *nifH* PCR used the same components and thermocycling conditions as the first round, except the DNA extract was replaced with 1 μL of the amplified product generated during the first round PCR reaction, and custom primers were used, consisting of gene-specific sites (nifH1 and nifH2), dual- indexed barcodes, Illumina linkers, and a sequencing primer binding region, similar to those described by Kozich et al. (2013; Table S1). PCR negative controls and filter blank samples were included in PCR reactions."

Finally, there was a mistake in the legend for Supplementary Table 1 as published. This table listed the incorrect *nifH* primer names. The correct legend appears below.

Table S1: Dual-index barcoded, forward and reverse *nifH* primers (5′ -> 3′) used in this study. Sample barcodes are shown in bold. Forward and reverse *nifH* PCR primers are indicated by nifH1 (TGYGAYCCNAARGCNGA) and nifH2 (ADNGCCATCATYTCNCC; note the misprint of this primer in the original manuscript by Zani et al., 2000). NNNN indicate Illumina linker regions: AATGATACGGCGACCACCGAGATCTACAC (forward) and CAAGCAGAAGACGGCATACGAGAT (reverse). Blue text indicates the binding site for sequencing primers, which were designed to optimize melting temperature during sequencing, as described by Kozich et al. (2013).

The authors apologize for these errors and state that they do not change the scientific conclusions of the article in any way.

Edited and reviewed by:
Sophie Rabouille, Centre National de la Recherche Scientifique (CNRS), France

***Correspondence:**
Mary R. Gradoville
mgradoville@ucsc.edu

***Present Address:**
Mary R. Gradoville, Ocean Sciences Department, University of Santa Cruz, Santa Cruz, CA, United States

Specialty section:
This article was submitted to Aquatic Microbiology, a section of the journal Frontiers in Microbiology

Received: *14 August 2017*
Accepted: *01 September 2017*
Published: *19 September 2017*

Citation:
Gradoville MR, Crump BC, Letelier RM, Church MJ and White AE (2017) Corrigendum: Microbiome of Trichodesmium Colonies from the North Pacific Subtropical Gyre. Front. Microbiol. 8:1780. doi: 10.3389/fmicb.2017.01780

REFERENCES

Kozich, J. J., Westcott, S. L., Baxter, N. T., Highlander, S. K., and Schloss, P. D. (2013). Development of a dual-index sequencing strategy and curation pipeline for analyzing amplicon sequence data on the MiSeq Illumina sequencing platform. *Appl. Environ. Microbiol.* 79, 5112–5120. doi: 10.1128/AEM.01043-13

Zani, S., Mellon, M. T., Collier, J. L., and Zehr, J. P. (2000). Expression of *nifH* genes in natural microbial assemblages in Lake George, New York, detected by reverse transcriptase PCR. *Appl. Environ. Microbiol.* 66, 3119–3124. doi: 10.1128/AEM.66.7.3119-3124.2000

Zehr, J. P., and McReynolds, L. A. (1989). Use of degenerate oligonucleotides for amplification of the nifH gene from the marine cyanobacterium *Trichodesmium thiebautii*. *Appl. Environ. Microbiol.* 55, 2522–2526.

Conflict of Interest Statement: The authors declare that the research was conducted in the absence of any commercial or financial relationships that could be construed as a potential conflict of interest.

frontiers in Microbiology

PERSPECTIVE
published: 08 September 2017
doi: 10.3389/fmicb.2017.01736

Chasing after Non-cyanobacterial Nitrogen Fixation in Marine Pelagic Environments

Pia H. Moisander[1], Mar Benavides[2], Sophie Bonnet[3], Ilana Berman-Frank[4], Angelicque E. White[5] and Lasse Riemann[2]*

[1] Department of Biology, University of Massachusetts Dartmouth, North Dartmouth, MA, United States, [2] Marine Biology Section, Department of Biology, University of Copenhagen, Helsingør, Denmark, [3] Centre National de la Recherche Scientifique, IRD, Aix-Marseille Université, Université de Toulon, Marseille, France, [4] Mina and Everard Goodman Faculty of Life Sciences, Bar-Ilan University, Ramat Gan, Israel, [5] College of Earth, Ocean, and Atmospheric Sciences, Oregon State University, Corvallis, OR, United States

Traditionally, cyanobacterial activity in oceanic photic layers was considered responsible for the marine pelagic dinitrogen (N_2) fixation. Other potentially N_2-fixing bacteria and archaea have also been detected in the pelagic water column, however, the activity and importance of these non-cyanobacterial diazotrophs (NCDs) remain poorly constrained. In this perspective we summarize the N_2 fixation rates from recently published studies on photic and aphotic layers that have been attributed to NCD activity via parallel molecular measurements, and discuss the status, challenges, and data gaps in estimating non-cyanobacterial N_2 fixation NCNF in the ocean. Rates attributed to NCNF have generally been near the detection limit thus far (<1 nmol N L^{-1} d^{-1}). Yet, if considering the large volume of the dark ocean, even low rates of NCNF could make a significant contribution to the new nitrogen input to the ocean. The synthesis here shows that *nifH* transcription data for NCDs have been reported in only a few studies where N_2 fixation rates were detected in the absence of diazotrophic cyanobacteria. In addition, high apparent diversity and regional variability in the NCDs complicate investigations of these communities. Future studies should focus on further investigating impacts of environmental drivers including oxygen, dissolved organic matter, and dissolved inorganic nitrogen on NCNF. Describing the ecology of NCDs and accurately measuring NCNF rates, are critical for a future evaluation of the contribution of NCNF to the marine nitrogen budget.

Keywords: bacteria, diazotroph, DOM, mesopelagic, *nifH*, nitrogenase, oxygen minimum zone

OPEN ACCESS

Edited by:
Angela Landolfi, GEOMAR Helmholtz Centre for Ocean Research Kiel (HZ), Germany

Reviewed by:
Natalie Loick-Wilde, Leibniz Institute for Baltic Sea Research (LG), Germany
Mark Moore, University of Southampton, United Kingdom

****Correspondence:***
Pia H. Moisander
pmoisander@umassd.edu

Specialty section:
This article was submitted to Aquatic Microbiology, a section of the journal Frontiers in Microbiology

Received: *17 June 2017*
Accepted: *25 August 2017*
Published: *08 September 2017*

Citation:
Moisander PH, Benavides M, Bonnet S, Berman-Frank I, White AE and Riemann L (2017) Chasing after Non-cyanobacterial Nitrogen Fixation in Marine Pelagic Environments. Front. Microbiol. 8:1736. doi: 10.3389/fmicb.2017.01736

INTRODUCTION

Biological dinitrogen (N_2) fixation produces biologically available nitrogen (N) through reduction of atmospheric N_2 to ammonium (NH_4^+) (Postgate, 1998). In oligotrophic marine environments, N_2 fixation can provide ~50% of the "new" N (Karl et al., 2002; Capone et al., 2005; Berthelot et al., 2017), and probably contributes more in hot spots such as the Western Tropical South Pacific (Bonnet et al., 2017). N_2 fixation (diazotrophy) is catalyzed by the enzyme nitrogenase (Mortenson and Thorneley, 1979; Postgate, 1998). The *nifH* gene that encodes the dinitrogenase reductase is distributed in many phylogenetic groups of bacteria and archaea (Chien and Zinder, 1996), and used to assess the diversity and expression of the enzyme in marine diazotrophs (Zehr et al., 2003).

Cyanobacteria have traditionally been considered the most important diazotrophs in the ocean. The predominantly described taxa include the filamentous, bloom-forming *Trichodesmium*, heterocystous, symbiotic groups (e.g., diatom-diazotroph associations), and the unicellular cyanobacteria UCYN-A (*Candidatus* Atelocyanobacterium thalassa), UCYN-B (*Crocosphaera watsonii*), and UCYN-C (Zehr, 2011). Early molecular studies also reported the presence of non-cyanobacterial diazotrophs (NCDs) (Kirshtein et al., 1991; Zehr et al., 1995, 1998). These findings stimulated recent research on diversity, composition, and ecology of marine NCDs (Bombar et al., 2016), leading to a currently perceived emergence of a new paradigm: non-cyanobacterial N_2 fixation (NCNF). Extensive research on free-living and symbiotic NCDs in soils has provided evidence of the activity, regulation, and the significance of these processes in terrestrial ecosystems (Postgate, 1998; Herridge et al., 2008; Hayat et al., 2010). While the diversity and abundance of marine NCDs indicate that NCNF could potentially have a large impact on the marine N budget, at present, the activity and contribution of marine NCNF to total N_2 fixation remain poorly constrained.

In many oceanic waters, NCD sequences dominate the *nifH* gene pool (Riemann et al., 2010; Farnelid et al., 2011), and detection of transcripts of some of the NCD *nifH* genes suggests that at least some of the NCDs fix N_2 in the oceanic water column and sediments (Bird et al., 2005; Church et al., 2005b; Halm et al., 2012; Brown and Jenkins, 2014; Moisander et al., 2014; Bentzon-Tilia et al., 2015b). However, gene expression cannot be equated with active N_2 fixation rates without evidence of cell-specific activity. Current broadly available methods cannot discern the relative contribution of cyanobacteria and NCDs to measured N_2 fixation rates. The contribution of NCNF could be studied by parallel rate measurements and molecular detection in areas where cyanobacterial diazotrophs are typically not present (such as the oceanic water column below the euphotic layer, i.e., aphotic waters). Here we summarize data from studies where N_2 fixation rates were reported in parallel to molecular characterization of NCDs when cyanobacterial diazotrophs were *not* detected (presence and/or expression of the *nifH* gene; **Table 1**). Presumed NCNF rates ranged from undetectable to 8 and 0.89 nmol N L^{-1} d^{-1} in photic and aphotic studies, respectively (**Table 1**). The goal of this perspective is to synthesize emerging trends and data gaps from these studies and highlight future research directions.

NCNF IN PHOTIC WATERS

Most early studies of oceanic N_2 fixation (Montoya et al., 1996; Karl et al., 2002; Hood et al., 2004; Mahaffey et al., 2005; Mulholland et al., 2006) and diazotroph diversity and activity (Zehr, 2011) focused on photic waters and cyanobacterial diazotrophs. Traditionally, the photic layer has been considered an optimal environment selecting for cyanobacterial N_2 fixation, as abundant light energy (harnessed via photosynthesis) supplies the high energetic demands of the N_2 fixation process, while dissolved inorganic nitrogen (DIN) limits non-diazotrophic autotrophs. Yet, since the first molecular studies (Zehr et al., 1998), *nifH* sequence libraries have revealed diverse NCD phylotypes from surface waters of various oceans and estuaries (Falcon et al., 2004; Church et al., 2005a; Langlois et al., 2005; Hewson et al., 2007; Moisander et al., 2008; Foster et al., 2009; Farnelid et al., 2011; Halm et al., 2012; Bentzon-Tilia et al., 2015b; Messer et al., 2016). Transcripts from a range of NCD groups have been recovered in surface layers (Man-Aharonovich et al., 2007; Halm et al., 2012; Loescher et al., 2014). One of the few consistent NCDs in photic layers is a gamma-proteobacterial cluster of sequences (termed γ-24774A11, Gamma A, or UMB; representatives of the same phylotype). Gamma A shows a wide distribution and expression of the *nifH* gene (Bird et al., 2005; Church et al., 2005b; Moisander et al., 2014; Langlois et al., 2015). This group appears to be broadly distributed across tropical and subtropical surface waters compared with cyanobacterial diazotrophs (Moisander et al., 2014; Bonnet et al., 2015; Langlois et al., 2015). Its presence exclusively in surface layers suggests either reliance on a photosynthetic machinery, rhodopsin, or photosynthesis products from other organisms. Once cultivated or its genome assembled, we can learn more about its autecology. A few other studies have detected N_2 fixation from photic layers in the reported absence of cyanobacterial sequences (Yogev et al., 2011; Blais et al., 2012). However, due to the difficulty of demonstrating the absence of cyanobacterial diazotrophs, it has generally been difficult to prove that NCNF is active in photic layers.

The nitrogenase enzyme may be downregulated or inactivated by NH_4^+ (Zehr et al., 1997). As typically assumed for cyanobacterial diazotrophs (Zehr, 2011), DIN could negatively impact NCDs directly (physiological inhibition) or indirectly (NCDs outcompeted by faster growing non-diazotrophs). However, DIN availability may not always have immediate negative effects on NCDs. For example, Gamma A transcripts and Cluster III diazotrophs (Chien and Zinder, 1996) were found in the presence of micromolar concentrations of DIN in the upper layers of the Arabian Sea (Bird and Wyman, 2013). N_2 fixation rates were also detected in the Benguela Upwelling System in the presence of micromolar nitrate and in the absence of cyanobacterial diazotrophs (Sohm et al., 2011). In other surface waters (Eastern Tropical South Pacific; ETSP), N_2 fixation rates were similarly reported in the absence of cyanobacterial diazotrophs and presence of high DIN (Fernandez et al., 2011; Dekaezemacker et al., 2013; Gradoville et al., 2017). In Indian Ocean surface waters with a shallow nitracline, N_2 fixation rates were reported in parallel with up to 10^4 *nifH* gene copies L^{-1} of Gamma A, while cyanobacterial groups were undetectable (Shiozaki et al., 2014). Collectively these field studies suggests that NCDs may have a low sensitivity to DIN (Knapp, 2012), but recent work with cultivated NCDs suggest that responses to DIN may be strain specific (Bentzon-Tilia et al., 2015a).

PCR amplification biases likely influence our current data and conclusions of studies on NCDs. A recent study using metagenomic data from the TARA Oceans survey reports

TABLE 1 | Compilation of photic and aphotic N_2 fixation rates published with molecular data and associated with non-cyanobacterial diazotrophs in waters reportedly devoid of cyanobacterial diazotrophs.

References	Location	Latitude	Longitude	Average rate or range of rates (nmol N L^{-1} d^{-1})	Depth (m)	Sequencing: Associated non-cyanobacterial phylotype genes and transcripts	qPCR: non-cyanobacterial diazotroph gene and transcript abundance (*nifH* copies L^{-1})
SOUTH AND NORTH PACIFIC OCEAN							
Benavides et al., 2015	Western South Pacific	3–9°S	146–153°E	0.08–0.89	200–1000	Cluster I, III, IV, and *Trichodesmium* nd	0–900 nd
Halm et al., 2012	South Pacific Gyre	20–50°S	180°E–120°W	0.41.5	0–200	Cluster I, III nd	0–7*10^6 0–8*10^4
Fernandez et al., 2011	Eastern Tropical South Pacific	1.5°N–17.8°S	86.9–70.8°W	0.01–3.5	70–400[a]	Cluster I, II, III nd	nd nd
Dekaezemacker et al., 2013	Eastern Tropical South Pacific	10–20°S	100–80°W	0–0.88	15–150	b b	b b
Turk-Kubo et al., 2014	Eastern Tropical South Pacific	10–20°S	100–80°W	b	10–200	Cluster I, III Cluster I	0–420 ~400
Loescher et al., 2014	Eastern Tropical South Pacific	2°N–16°S	85–74°W	0.4	0–350	Cluster I, III, IV nd	0–10^6 0–150
Bonnet et al., 2013	Eastern Tropical South Pacific	10–20°S	100–80°W	0–0.8	200–2,000	Cluster I, III nd	nd nd
Gradoville et al., 2017	Eastern Tropical South Pacific	20.1–26.3°S	104–77°W	0.5–5.1	5 m for N_2 fix, 5–420 m for *nifH*	Cluster I, III nd	1.5 × 10^2 –1.4 × 10^4 nd
Hamersley et al., 2011	Southern California Bight	33.55°N	118.4°W	0.07	500–885	Cluster I, III, IV nd	nd nd
ATLANTIC OCEAN, ARCTIC OCEAN							
Sohm et al., 2011	South Atlantic Gyre and Benguela upwelling system	11–25°S	29°W–15°E	0.06–8	8 m for N_2 fix, 8–110 m for *nifH*	nd nd	nd nd
Blais et al., 2012	Arctic Ocean coastal	69.3–75°N	69–134°W	0.02–4.45	5 m, DCM (30–57)	Cluster I, III nd	nd nd
INDIAN OCEAN							
Shiozaki et al., 2014	Indian Ocean	4°N–20°S	65–70°E	0.18–0.23	0–90	Cluster I nd	10^3 nd

(Continued)

TABLE 1 | Continued

References	Location	Latitude	Longitude	Average rate or range of rates (nmol N L^{-1} d^{-1})	Depth (m)	Sequencing: Associated non-cyanobacterial phylotype genes and transcripts	qPCR: non-cyanobacterial diazotroph gene and transcript abundance (*nifH* copies L^{-1})
Jayakumar et al., 2012	Indian Ocean	13–19°N	64°–66°E	nd	110–175 (OMZ)	Cluster I, III, IV Cluster I, III	nd nd
MEDITERRANEAN SEA, RED SEA, AND BALTIC SEA							
Rahav et al., 2013a	Mediterranean Sea, Red Sea	29°55N–32°57N	34°29E–34°45E	0.01–0.38	150–720	Pseudomonas stutzeri-related nd	nd nd
Rahav et al., 2016	Eastern Mediterranean Sea	32°N	34°E	0.1–0.15	5	nd Cluster I: (Alpha–), and "other"	nd nd
Yogev et al., 2011	Eastern Mediterranean Sea	33.14–34.00°N	25°–33°E	0–0.3	0–160 m	Cluster I, II Cluster I, II	nd nd
Farnelid et al., 2013	Baltic Sea	57.20°N	20.03°E	0.44	200	Cluster I, II, III[d] Cluster I, III	$0–2*10^7$ $0–10^4$

*All rates are based on the $^{15}N_2$ method and no conversions were made to originally reported values. The station location and depth information is specific for locations where **no** cyanobacterial diazotrophs were detected (unless otherwise indicated). Red letters indicate transcripts. Clusters I, II, III, and IV follow Chien and Zinder (1996).*

[a]Depths range from photic to aphotic.

[b]Dekaezemacker et al. (2013) reported rates and Turk-Kubo et al. (2014) reported corresponding molecular data.

[c]nd, data not available/not done.

[d]Nodularia transcripts were detected at abundances below the level of quantification via RT-qPCR and its transcripts were not detected by sequencing.

presence of nitrogenase containing Planctomycetes in oceanic photic waters and suggests they have a substantially greater abundance than the NCDs reported based on past PCR approaches (Delmont et al., 2017).

NCNF IN APHOTIC WATERS AND OXYGEN DEFICIENT ZONES

Several studies have recently reported N_2 fixation rates in the aphotic ocean where active autotrophic cyanobacterial diazotrophy is not expected. Early evidence for aphotic N_2 fixation showed proteobacterial and archaeal diazotrophs and N_2 fixation in hydrothermal vent fluids (Mehta and Baross, 2006). Deep-sea sediment archaea fixing N_2 apparently function in associations with anaerobic methane oxidizers (Dekas et al., 2009, 2014). Proteobacterial *nifH* sequences were reported from the meso- to abyssopelagic water column in different oceans (Hewson et al., 2007; Moisander et al., 2008).

Laboratory studies have shown that nitrogenase activity in cells is reduced under increasing concentrations of oxygen, and the enzyme is irreversibly modified by oxygen *in vitro* (Fay, 1992; Berman-Frank et al., 2008). Thus, oxygen deficient zones (ODZs) that may span photic and aphotic layers could serve as sites of N_2 fixation due to low oxygen, in parallel with N losses from these zones (Deutsch et al., 2007). The first studies reporting planktonic N_2 fixation rates in aphotic waters were ones associated with ODZs in the Eastern Tropical North Pacific Ocean (ETNP) (Hamersley et al., 2011) and ETSP (Fernandez et al., 2011; Dekaezemacker et al., 2013). N_2 fixation rates were reported in mesopelagic waters down to 400 and 800 m, and abyssopelagic waters down to 2,000 m (Fernandez et al., 2011; Bonnet et al., 2013; Loescher et al., 2014). These rates were attributed to various NCD DNA sequences, including Cluster I (Proteobacteria), II and III (Turk-Kubo et al., 2014). N_2 fixation in the presence of NCD *nifH* expression was also reported in the aphotic ODZ of the Baltic Sea (Farnelid et al., 2013), and in the ODZ of the Arabian Sea (Jayakumar et al., 2012). These studies suggest that NCNF may be active in ODZs, however evidence of the relationship between oxygen and NCNF is variable. N_2 fixation in the aphotic Western Tropical South Pacific had a negative correlation with dissolved oxygen (Benavides et al., 2015). However, mesopelagic N_2 fixation rates in the Mediterranean Sea were reported from fully oxygenated waters (Rahav et al., 2013a), or were negatively correlated with apparent oxygen utilization values (i.e., N_2 fixation was higher in more recently ventilated waters; Benavides et al., 2016). Gammaproteobacteria (Cluster I) and Cluster III generally dominated the *nifH* DNA sequences in these studies. In addition, both spatial coupling (Deutsch et al., 2007) and decoupling (Knapp et al., 2016; Bonnet et al., 2017) of N_2 fixation and denitrification has been proposed. Collectively these studies suggest that NCNF is occurring in aphotic waters, and may correlate with oxygen availability, but the mechanisms by which oxygen and possibly other factors regulate NCNF in aphotic waters remain poorly known.

THE POTENTIAL ROLE OF DISSOLVED ORGANIC MATTER (DOM) IN SUPPORTING NCNF

Organic particles may provide a site of low oxygen and a source of DOM that both can benefit specific bacterial attachment (Thiele et al., 2015; Dang and Lovell, 2016). If NCDs are heterotrophic (Riemann et al., 2010), overall DOM availability should play a role in controlling their growth and activity (Kirchman, 1990). Genomic and physiological analyses have confirmed that gamma- and alphaproteobacterial diazotrophs isolated from the Baltic Sea are heterotrophic and contain genes responsible for DOM metabolism (Bentzon-Tilia et al., 2015a). Evidence for DOM influence on NCDs was reported from the South Pacific Gyre (SPG) photic layers (Halm et al., 2012) and in the Mediterranean Sea (Rahav et al., 2016), where DOM originating from primary production was suggested to impact N_2 fixation. Most of the SPG sequences were gammaproteobacterial, but represented different groups from those found in the ETSP (Fernandez et al., 2011; Turk-Kubo et al., 2014). Mesopelagic N_2 fixation rates had a positive correlation with relatively labile DOM (Benavides et al., 2015), and were enhanced upon the addition of sugars, amino acids, or transparent exopolymeric particles (Bonnet et al., 2013; Rahav et al., 2013a; Loescher et al., 2014; Benavides et al., 2015).

In the eastern Mediterranean Sea, N_2 fixation in the photic zone was uncoupled from primary production and correlated significantly and positively with bacterial production (Rahav et al., 2013b). However, even in coastal waters with high dissolved inorganic nutrient loads, organic carbon stimulated light and dark N_2 fixation in a community containing cyanobacterial and NCD *nifH* phylotypes (Rahav et al., 2016). Saharan dust addition (serving potentially as a source of trace elements, nutrients, and/or DOM) enhanced N_2 fixation and both NCD (Gamma A) and cyanobacterial diazotroph abundances in the North Atlantic (Langlois et al., 2012). Gamma A abundances were also enhanced by addition of sugars in the South Pacific (Moisander et al., 2012). Many cyanobacteria, including diazotrophs, take up organic forms of carbon (Hietanen et al., 2002; Church et al., 2004; Moisander et al., 2012; Benavides et al., 2017) thus rates of N_2 fixation in mixed communities, measured after DOM amendments, may reflect responses of both cyanobacterial and NCDs. Whether some marine NCDs also use light as an energy source remains to be demonstrated (Bombar et al., 2016).

CURRENT AND FUTURE CHALLENGES

The data synthesis here shows that while N_2 fixation rates have been reported by several studies in waters dominated by NCD *nifH* sequences (**Table 1**), most studies of NCDs did not measure transcription. The *nifH* DNA sequences often do not appear as transcripts in the same samples, suggesting that some of the organisms are not active (Moisander et al., 2006; Short and Zehr, 2007; Yogev et al., 2011; Halm et al., 2012; Severin et al., 2015), thus it would be misleading to use *nifH* gene (DNA) data as proof for NCNF. Despite the common detection of cyanobacterial and NCD *nifH* in DNA sequence libraries and, at times, in transcripts, only a few studies from surface layers reported the *absence* of cyanobacterial diazotrophs when N_2 fixation rates were detected (**Table 1**). Due to various methodological constraints, proving the absence of low numbers of cyanobacterial cells in a sample is difficult, if not impossible, yet such low abundance may be sufficient to result in detectable N_2 fixation rates. Aphotic waters may be considered a good case study for NCNF, as photoautotrophic N_2 fixation in these waters is conceivably absent. However, the common detection of diazotrophic cyanobacteria in aphotic layers (Hamersley et al., 2011; Farnelid et al., 2013; Benavides et al., 2015), possibly due to either settling material that could be viable upon experimental incubations (Agusti et al., 2015), or caused by contamination during sampling, complicate attributing measured aphotic N_2 fixation rates to NCDs alone. Overall, the measured rates of *in situ* aphotic N_2 fixation are higher than the parallel abundance and transcript numbers of NCDs would potentially support. Moreover, the reported cell-specific rates of NCDs are under debate (Turk-Kubo et al., 2014; Benavides et al., 2015; Bentzon-Tilia et al., 2015a; Gradoville et al., 2017).

Various factors of the $^{15}N_2$ method, such as uncertainties in the ^{15}N-labeling step, influence N_2 fixation rate determination (Mohr et al., 2010; Grosskopf et al., 2012; Wilson et al., 2012). In addition, commercially available $^{15}N_2$ gases are at times contaminated with substrates other than N_2 (Dabundo et al., 2014), which could lead to false positive NCNF rates. An additional source of uncertainty that must be considered when assessing minimum quantifiable N_2 fixation rates is the concentration and isotopic composition of particulate organic N (PON), which at typical concentrations requires large volumes in incubations (usually >4 L) to constrain rates in deep waters. While N_2 fixation rates per volume are most informative for budgetary calculations, rates normalized to PON concentration would provide an additional measure for comparing rates across studies. Further, variability of the natural $\delta^{15}N$ background of PON, changes in the $\delta^{15}N$ of PON that may occur over the incubation period or due to substrate additions, and $\delta^{15}N$ of the N_2 pool, should be considered (Montoya et al., 1996; Gradoville et al., 2017). These sources of uncertainty are not routinely reported and detection limits are infrequently calculated. Taking into account these sources of error, Gradoville et al. (2017) estimated the minimum quantifiable N_2 fixation rate in their study at ~0.4 nmol L^{-1} d^{-1} which is higher than many reported rates of NCNF (**Table 1**).

To our knowledge, direct field measurements of N_2 fixation per cell are currently lacking for marine NCDs; such measurements would be important in assessing their contribution to N_2 fixation rates, along with other efforts to separate signals of NCNF and cyanobacterial N_2 fixation (see also Bombar et al., 2016). High NCD *nifH* diversity renders identification and quantification of biogeochemically significant individual groups challenging. The combination of *in situ* hybridization approaches using halogenated probes together with single-cell mass spectrometry (nanoscale secondary ion mass spectrometry; nanoSIMS) has recently advanced quantification of single-cell N_2 fixation rates in UCYN-A

(Thompson et al., 2012; Krupke et al., 2013). Similar approaches could provide insights into the NCNF in marine environments. Stable isotope probing and isotope microarrays could lead to valuable future insights (Seyler et al., 2014; Arandia-Gorostidi et al., 2017).

In describing the communities, sequencing depth and primer specificity influence what portion of the NCD community is detected. In addition, the detection limit for diazotroph transcripts or genes and the detection limit for N_2 fixation are not necessarily equal. The quantification limit of quantitative PCR is often on the order of 10^2 *nifH* gene copies L^{-1} (and often unreported), which could potentially result in false negatives for cyanobacterial diazotrophs, and subsequently, lead to false positive NCNF rates. Using small water volumes when abundance of cyanobacterial diazotrophs is low would increase the chances of reporting false negatives for these organisms. On the other hand, metabolic rate measurements of microbial samples brought to the surface from aphotic depths may be underestimated (Tamburini et al., 2013), making both rate and transcription analyses of deep communities challenging.

CONCLUSIONS

Our compiled analysis of data illustrates that low N_2 fixation rates were reported from marine environments where NCD abundance was high and cyanobacterial diazotrophs were low or undetected. NCD *nifH* sequences show a wider geographical and depth distribution in pelagic environments overall than their cyanobacterial counterparts. The emerging data suggest that the NCD communities are diverse but only a few groups have been identified that appear in several studies (Farnelid et al., 2011; Turk-Kubo et al., 2014). Studies on NCD *nifH* transcripts in aphotic layers are scarce or missing for many areas of the oceans.

We currently lack a fundamental understanding of the key players and environmental regulation of NCNF in the ocean. Ecophysiological data of the organisms contributing to these rates are still preliminary and incomplete. Moreover, the measured rates in most environments are generally "snapshots" determined during a cruise/sampling foray and have not been examined over seasonal and annual cycles. In addition, several methodological concerns complicate interpretation of N_2 fixation rate data. Modeling the significance of NCNF in marine N_2 fixation remains a challenge due to these various constraints. If these rates are confirmed, however, NCNF could contribute significantly to new N inputs to the ocean. How factors such as temperature, DIN, oxygen, trace elements, and hydrostatic pressure drive the metabolic capacities and adaptations of NCNF are currently only partially revealed. The actual activities and taxon specific roles of marine NCDs remain enigmatic at present, as do their contributions to regional and global N_2 fixation.

AUTHOR CONTRIBUTIONS

PM and LR designed the study, wrote the initial drafts, and compiled the majority of **Table 1**. All authors wrote sections of the manuscript and contributed to **Table 1**.

FUNDING

PM was supported by NSF 1733610, AW was supported by NSF 1732206, and MB and LR were supported by grant 6108-00013 from the Danish Council for Independent Research to LR.

REFERENCES

Agusti, S., Gonzalez-Gordillo, J. I., Vaque, D., Estrada, M., Cerezo, M. I., Salazar, G., et al. (2015). Ubiquitous healthy diatoms in the deep sea confirm deep carbon injection by the biological pump. *Nat. Commun.* 6:7608. doi: 10.1038/ncomms8608

Arandia-Gorostidi, N., Weber, P. K., Alonso-Saez, L., Moran, X. A. G., and Mayali, X. (2017). Elevated temperature increases carbon and nitrogen fluxes between phytoplankton and heterotrophic bacteria through physical attachment. *ISME J.* 11, 641–650. doi: 10.1038/ismej.2016.156

Benavides, M., Berthelot, H., Duhamel, S., Raimbault, P., and Bonnet, S. (2017). Dissolved organic matter uptake by *Trichodesmium* in the Southwest Pacific. *Sci. Rep.* 7:41315. doi: 10.1038/srep41315

Benavides, M., Bonnet, S., Hernandez, N., Martinez-Perez, A. M., Nieto-Cid, M., Alvarez-Salgado, X. A., et al. (2016). Basin-wide N2 fixation in the deep waters of the Mediterranean Sea. *Glob. Biogeochem. Cycles* 30, 952–961. doi: 10.1002/2015gb005326

Benavides, M., Moisander, P. H., Berthelot, H., Dittmar, T., Grosso, O., and Bonnet, S. (2015). Mesopelagic N_2 fixation related to organic matter composition in the Solomon and Bismarck Seas (Southwest Pacific). *PLoS ONE* 10:e0143775. doi: 10.1371/journal.pone.0143775

Bentzon-Tilia, M., Severin, I., Hansen, L. H., and Riemann, L. (2015a). Genomics and ecophysiology of heterotrophic nitrogen-fixing bacteria isolated from estuarine surface water. *MBio* 6:e00929. doi: 10.1128/mBio.00929-15

Bentzon-Tilia, M., Traving, S. J., Mantikci, M., Knudsen-Leerbeck, H., Hansen, J. L., Stiig, M., et al. (2015b). Significant N2 fixation by heterotrophs, photoheterotrophs and heterocystous cyanobacteria in two temperate estuaries. *ISME J.* 9, 273–285. doi: 10.1038/ismej.2014.119

Berman-Frank, I., Chen, Y.-B., Gao, Y., Fennel, K., Follows, M. J., Milligan, A. J., et al. (2008). "Feedbacks between the nitrogen, carbon and oxygen cycles," in *Nitrogen in the Marine Environment, 2nd Edn*, eds D. G. Capone, D. A. Bronk, M. R. Mulholland, and E. J. Carpenter (Burlington, MA: Elsevier, Inc.), 1537–1563.

Berthelot, H., Benavides, M., Moisander, P. H., Grosso, O., and Bonnet, S. (2017). High nitrogen fixation rates in the particulate and dissolved pools in the Western Tropical Pacific (Solomon and Bismarck Seas). *Geophys. Res. Lett.* doi: 10.1002/2017GL073856. [Epub ahead of print].

Bird, C., and Wyman, M. (2013). Transcriptionally active heterotrophic diazotrophs are widespread in the upper water column of the Arabian Sea. *FEMS Microb. Ecol.* 84, 189–200. doi: 10.1111/1574-6941.12049

Bird, C., Martinez, J. M., O'Donnell, A. G., and Wyman, M. (2005). Spatial distribution and transcriptional activity of an uncultured clade of planktonic diazotrophic gamma-proteobacteria in the Arabian Sea. *Appl. Environ. Microbiol.* 71, 2079–2085. doi: 10.1128/AEM.71.4.2079-2085.2005

Blais, M., Tremblay, J.-E., Jungblut, A. D., Gagnon, J., Martin, J., Thaler, M., et al. (2012). Nitrogen fixation and identification of potential diazotrophs in the Canadian Arctic. *Global Biogeochem. Cycles* 26:GB3022. doi: 10.1029/2011GB004096

Bombar, D., Paerl, R. W., and Riemann, L. (2016). Marine non-cyanobacterial diazotrophs: moving beyond molecular detection. *Trends Microbiol.* 24, 916–927. doi: 10.1016/j.tim.2016.07.002

Bonnet, S., Caffin, M., Berthelot, H., and Moutin, T. (2017). Hot spot of N2 fixation in the western tropical South Pacific pleads for a spatial decoupling between

N2 fixation and denitrification. *Proc. Natl. Acad. Sci. U.S.A.* 114, E2800–E2801. doi: 10.1073/pnas.1619514114

Bonnet, S., Dekaezemacker, J., Turk-Kubo, K. A., Moutin, T., Hamersley, R. M., Grosso, O., et al. (2013). Aphotic N_2 fixation in the Eastern Tropical South Pacific Ocean. *PLoS ONE* 8:e81265. doi: 10.1371/journal.pone.0081265

Bonnet, S., Rodier, M., Turk, K., Germineaud, C., Menkes, C., Ganachaud, A., et al. (2015). Contrasted geographical distribution of N2 fixation rates and nifH phylotypes in the Coral and Solomon Seas (South-Western Pacific) during austral winter conditions. *Global Biogeochem. Cycles* 29, 1874–1892. doi: 10.1002/2015GB005117

Brown, S. M., and Jenkins, B. D. (2014). Profiling gene expression to distinguish the likely active diazotrophs from a sea of genetic potential in marine sediments. *Environ. Microbiol.* 16, 3128–3142. doi: 10.1111/1462-2920.12403

Capone, D. G., Burns, J. A., Montoya, J. P., Subramaniam, A., Mahaffey, C., Gunderson, T., et al. (2005). Nitrogen fixation by *Trichodesmium* spp.: an important source of new nitrogen to the tropical and subtropical North Atlantic Ocean. *Global Biogeochem. Cycles* 19:GB2024. doi: 10.1029/2004GB002331

Chien, Y.-T., and Zinder, S. H. (1996). Cloning, functional organization, transcript studies, and phylogenetic analysis of the complete nitrogenase structurel genes (nifHDK2) and associated genes in the archaeon *Methanosarcina barkeri* 227. *J. Bacteriol.* 178, 143–148. doi: 10.1128/jb.178.1.143-148.1996

Church, M. J., Ducklow, H. W., and Karl, D. A. (2004). Light dependence of H-3 leucine incorporation in the oligotrophic North Pacific ocean. *Appl. Environ. Microbiol.* 70, 4079–4087. doi: 10.1128/AEM.70.7.4079-4087.2004

Church, M. J., Jenkins, B. D., Karl, D. M., and Zehr, J. P. (2005a). Vertical distributions of nitrogen-fixing phylotypes at Stn ALOHA in the oligotrophic North Pacific Ocean. *Aquat. Microb. Ecol.* 38, 3–14. doi: 10.3354/ame038003

Church, M. J., Short, C. M., Jenkins, B. D., Karl, D. M., and Zehr, J. P. (2005b). Temporal patterns of nitrogenase gene (*nifH*) expression in the oligotrophic North Pacific Ocean. *Appl. Environ. Microbiol.* 71, 5362–5370. doi: 10.1128/AEM.71.9.5362-5370.2005

Dabundo, R., Lehmann, M. F., Treibergs, L., Tobias, C. R., Altabet, M. A., Moisander, P. H., et al. (2014). The contamination of commercial $^{15}N_2$ gas stocks with ^{15}N-labeled nitrate and ammonium and consequences for nitrogen fixation measurements. *PLoS ONE* 9:e110335. doi: 10.1371/journal.pone.0110335

Dang, H., and Lovell, C. R. (2016). Microbial surface colonization and biofilm development in marine environments. *Microbiol. Mol. Biol. Rev.* 80, 91–138. doi: 10.1128/MMBR.00037-15

Dekaezemacker, J., Bonnet, S., Grosso, O., Moutin, T., Bressac, M., and Capone, D. G. (2013). Evidence of active dinitrogen fixation in surface waters of the eastern tropical South Pacific during El Nino and La Nina events and evaluation of its potential nutrient controls. *Global Biogeochem. Cycles* 27, 768–779. doi: 10.1002/gbc.20063

Dekas, A. E., Chadwick, G. L., Bowles, M. W., Joye, S. B., and Orphan, V. J. (2014). Spatial distribution of nitrogen fixation in methane seep sediment and the role of the ANME archaea. *Environ. Microbiol.* 16, 3012–3029. doi: 10.1111/1462-2920.12247

Dekas, A. E., Poretsky, R. S., and Orphan, V. J. (2009). Deep-sea archaea fix and share nitrogen in methane-consuming microbial consortia. *Science* 326, 422–426. doi: 10.1126/science.1178223

Delmont, T. O., Quince, C., Shaiber, A., Esen, O. C., Lee, S. T. M., Lucker, S., et al. (2017). Nitrogen fixing populations of Planctomycetes and Proteobacteria are abundant in the surface ocean. *BioRxiv*. doi: 10.1101/129791

Deutsch, C., Sarmiento, J. L., Sigman, D. M., Gruber, N., and Dunne, J. P. (2007). Spatial coupling of nitrogen inputs and losses in the ocean. *Nature* 445, 163–167. doi: 10.1038/nature05392

Falcon, L. I., Carpenter, E. J., Cipriano, F., Bergman, B., and Capone, D. G. (2004). N-2 fixation by unicellular bacterioplankton from the Atlantic and Pacific oceans: phylogeny and *in situ* rates. *Appl. Environ. Microbiol.* 70, 765–770. doi: 10.1128/AEM.70.2.765-770.2004

Farnelid, H., Andersson, A. F., Bertilsson, S., Abu Al-Soud, W., Hansen, L. H., Sorensen, S., et al. (2011). Nitrogenase gene amplicons from global marine surface waters are dominated by genes of non-cyanobacteria. *PLoS ONE* 6:e19223. doi: 10.1371/journal.pone.0019223

Farnelid, H., Bentzon-Tilia, M., Andersson, A. F., Bertilsson, S., Jost, G., Labrenz, M., et al. (2013). Active nitrogen-fixing heterotrophic bacteria at and below the chemocline of the central Baltic Sea. *ISME J.* 7, 1413–1423. doi: 10.1038/ismej.2013.26

Fay, P. (1992). Oxygen relations of nitrogen fixation in cyanobacteria *Microbiol. Rev.* 56, 340–373.

Fernandez, C., Farias, L., and Ulloa, O. (2011). Nitrogen fixation in denitrified marine waters. *PLoS ONE* 6:e20539. doi: 10.1371/journal.pone.0020539

Foster, R. A., Paytan, A., and Zehr, J. P. (2009). Seasonality of N-2 fixation and *nifH* gene diversity in the Gulf of Aqaba (Red Sea). *Limnol. Oceanogr.* 54, 219–233. doi: 10.4319/lo.2009.54.1.0219

Gradoville, M. R., Bombar, D., Crump, B., Letelier, R. M., Zehr, J. P., and White, A. E. (2017). Diversity and activity of nitrogen-fixing communities across ocean basins. *Limnol. Oceanogr.* doi: 10.1002/lno.10542. [Epub ahead of print].

Grosskopf, T., Mohr, W., Baustian, T., Schunck, H., Gill, D., Kuypers, M. M. M., et al. (2012). Doubling of marine dinitrogen-fixation rates based on direct measurements. *Nature* 488, 361–364. doi: 10.1038/nature11338

Halm, H., Lam, P., Ferdelman, T. G., Lavik, G., Dittmar, T., LaRoche, J., et al. (2012). Heterotrophic organisms dominate nitrogen fixation in the South Pacific Gyre. *ISME J.* 6, 1238–1249. doi: 10.1038/ismej.2011.182

Hamersley, M. R., Turk, K. A., Leinweber, A., Gruber, N., Zehr, J. P., Gunderson, T., et al. (2011). Nitrogen fixation within the water column associated with two hypoxic basins in the Southern California Bight. *Aquat. Microb. Ecol.* 63, 193–205. doi: 10.3354/ame01494

Hayat, R., Ali, S., Amara, U., Khalid, R., and Ahmed, I. (2010). Soil beneficial bacteria and their role in plant growth promotion: a review. *Ann. Microbiol.* 60, 579–598. doi: 10.1007/s13213-010-0117-1

Herridge, D. F., Peoples, M. B., and Boddey, R. M. (2008). Global inputs of biological nitrogen fixation in agricultural systems. *Plant Soil* 311, 1–18. doi: 10.1007/s11104-008-9668-3

Hewson, I., Moisander, P. H., Achilles, K. M., Carlson, C. A., Jenkins, B. D., Mondragon, E. A., et al. (2007). Characteristics of diazotrophs in surface to abyssopelagic waters of the Sargasso Sea. *Aquat. Microb. Ecol.* 46, 15–30. doi: 10.3354/ame046015

Hietanen, S., Lehtimäki, J. M., Tuominen, L., Sivonen, K., and Kuparinen, J. (2002). *Nodularia* spp. (Cyanobacteria) incorporate leucine but not thymidine: importance for bacterial-production measurements. *Aquat. Microb. Ecol.* 28, 99–104. doi: 10.3354/ame028099

Hood, R. R., Coles, V. J., and Capone, D. G. (2004). Modeling the distribution of *Trichodesmium* and nitrogen fixation in the Atlantic Ocean. *J. Geophys. Res.* 109:C06006. doi: 10.1029/2002JC001753

Jayakumar, A., Al-Rshaidat, M. M. D., Ward, B. B., and Mulholland, M. R. (2012). Diversity, distribution, and expression of diazotroph *nifH* genes in oxygen-deficient waters of the Arabian Sea. *FEMS Microb. Ecol.* 82, 597–606. doi: 10.1111/j.1574-6941.2012.01430.x

Karl, D., Michaels, A., Bergman, B., Capone, D., Carpenter, E., Letelier, R., et al. (2002). Dinitrogen fixation in the world's oceans. *Biogeochemistry* 57–58, 47–98. doi: 10.1023/A:1015798105851

Kirchman, D. L. (1990). Limitation of bacterial growth by dissolved organic matter in the subarctic Pacific. *Mar. Ecol. Prog. Ser.* 62, 47–54. doi: 10.3354/meps062047

Kirshtein, J. D., Paerl, H. W., and Zehr, J. P. (1991). Amplification, cloning, and sequencing of a *nifH* segment from aquatic microorganisms and natural communities. *Appl. Environ. Microbiol.* 57, 2645–2650.

Knapp, A. N. (2012). The sensitivity of marine N-2 fixation to dissolved inorganic nitrogen. *Front. Microbiol.* 3:374. doi: 10.3389/fmicb.2012.00374

Knapp, A. N., Casciotti, K. L., Berelson, W. M., Prokopenko, M. G., and Capone, D. G. (2016). Low rates of nitrogen fixation in eastern tropical South Pacific surface waters. *Proc. Natl. Acad. Sci. U.S.A.* 113, 4398–4403. doi: 10.1073/pnas.1515641113

Krupke, A., Musat, N., LaRoche, J., Mohr, W., Fuchs, B. M., Amann, R. I., et al. (2013). *In situ* identification and N_2 and C fixation rates of uncultivated cyanobacteria populations. *Syst. Appl. Microbiol.* 36, 259–271. doi: 10.1016/j.syapm.2013.02.002

Langlois, R. J., LaRoche, J., and Raab, P. A. (2005). Diazotrophic diversity and distribution in the tropical and subtropical Atlantic ocean. *Appl. Environ. Microbiol.* 71, 7910–7919. doi: 10.1128/AEM.71.12.7910-7919.2005

Langlois, R. J., Mills, M. M., Ridame, C., Croot, P., and LaRoche, J. (2012). Diazotrophic bacteria respond to Saharan dust additions. *Mar. Ecol. Prog. Ser.* 470, 1–14. doi: 10.3354/meps10109

Langlois, R., Grokopf, T., Mills, M., Takeda, S., and LaRoche, J. (2015). Widespread distribution and expression of Gamma A (UMB), an uncultured, diazotrophic, gamma-Proteobacterial *nifH* Phylotype. *PLoS ONE*10:e0128912. doi: 10.1371/journal.pone.0128912

Loescher, C. R., Grosskopf, T., Desai, F. D., Gill, D., Schunck, H., Croot, P. L., et al. (2014). Facets of diazotrophy in the oxygen minimum zone waters off Peru. *ISME J.* 8, 2180–2192. doi: 10.1038/ismej.2014.71

Mahaffey, C., Michaels, A. F., and Capone, D. G. (2005). The conundrum of marine N-2 fixation. *Am. J. Sci.* 305, 546–595. doi: 10.2475/ajs.305.6-8.546

Man-Aharonovich, D., Kress, N., Bar Zeev, E., Berman-Frank, I., and Beja, O. (2007). Molecular ecology of *nifH* genes and transcripts in the eastern Mediterranean Sea. *Environ. Microbiol.* 9, 2354–2363. doi: 10.1111/j.1462-2920.2007.01353.x

Mehta, M. P., and Baross, J. A. (2006). Nitrogen fixation at 92 degrees C by a hydrothermal vent archaeon. *Science* 314, 1783–1786. doi: 10.1126/science.1134772

Messer, L. F., Mahaffey, C., Robinson, C. M., Jeffries, T. C., Baker, K. G., Isaksson, J. B., et al. (2016). High levels of heterogeneity in diazotroph diversity and activity within a putative hotspot for marine nitrogen fixation. *ISME J.* 10, 1499–1513. doi: 10.1038/ismej.2015.205

Mohr, W., Grosskopf, T., Wallace, D. W. R., and LaRoche, J. (2010). Methodological underestimation of oceanic nitrogen fixation rates. *PLoS ONE* 5:e12583. doi: 10.1371/journal.pone.0012583

Moisander, P. H., Beinart, R. A., Voss, M., and Zehr, J. P. (2008). Diversity and abundance of diazotrophic microorganisms in the South China Sea during intermonsoon. *ISME J.* 2, 954–967. doi: 10.1038/ismej.2008.51

Moisander, P. H., Serros, T., Paerl, R. W., Beinart, R. A., and Zehr, J. P. (2014). Gammaproteobacterial diazotrophs and *nifH* gene expression in surface waters of the South Pacific Ocean. *ISME J.* 8, 1962–1973. doi: 10.1038/ismej.2014.49

Moisander, P. H., Shiue, L., Steward, G. F., Jenkins, B. D., Bebout, B. M., and Zehr, J. P. (2006). Application of a *nifH* oligonucleotide microarray for profiling diversity of N-2-fixing microorganisms in marine microbial mats. *Environ. Microbiol.* 8, 1721–1735. doi: 10.1111/j.1462-2920.2006.01108.x

Moisander, P. H., Zhang, R., Boyle, E. A., Hewson, I., Montoya, J. P., and Zehr, J. P. (2012). Analogous nutrient limitations in unicellular diazotrophs and *Prochlorococcus* in the South Pacific Ocean. *ISME J.* 6, 733–744. doi: 10.1038/ismej.2011.152

Montoya, J. P., Voss, M., Kähler, P., and Capone, D. G. (1996). A simple, high-precision, high-sensitivity tracer assay for N_2 fixation. *Appl. Environ. Microbiol.* 62, 986–993.

Mortenson, L. E., and Thorneley, R. N. F. (1979). Structure and function of nitrogenase. *Ann. Rev. Biochem.* 48, 387–418. doi: 10.1146/annurev.bi.48.070179.002131

Mulholland, M. R., Bernhardt, P. W., Heil, C. A., Bronk, D. A., and O'Neil, J. M. (2006). Nitrogen fixation and release of fixed nitrogen by *Trichodesmium* spp. in the Gulf of Mexico. *Limnol. Oceanogr.* 51, 1762–1776. doi: 10.4319/lo.2006.51.4.1762

Postgate, J. (1998). *Nitrogen Fixation, 3rd Edn*. New York, NY: Cambridge University Press.

Rahav, E., Bar-Zeev, E., Ohayon, S., Elifantz, H., Belkin, N., Herut, B., et al. (2013a). Dinitrogen fixation in aphotic oxygenated marine environments. *Front. Microbiol.* 4:227. doi: 10.3389/fmicb.2013.00227

Rahav, E., Giannetto, M. J., and Bar-Zeev, E. (2016). Contribution of mono and polysaccharides to heterotrophic N2 fixation at the eastern Mediterranean coastline. *Sci. Rep.* 6:27858. doi: 10.1038/srep27858

Rahav, E., Herut, B., Stambler, N., Bar-Zeev, E., Mulholland, M. R., and Berman-Frank, I. (2013b). Uncoupling between dinitrogen fixation and primary productivity in the eastern Mediterranean Sea. *J. Geophys. Res.* 118, 195–202. doi: 10.1002/jgrg.20023

Riemann, L., Farnelid, H., and Steward, G. F. (2010). Nitrogenase genes in non-cyanobacterial plankton: prevalence, diversity, and regulation in marine waters. *Aquat. Microb. Ecol.* 61, 235–247. doi: 10.3354/ame01431

Severin, I., Bentzon-Tilia, M., Moisander, P. H., and Riemann, L. (2015). Nitrogenase expression in estuarine bacterioplankton influenced by organic carbon and availability of oxygen. *FEMS Microb. Lett.* 326:fnv105. doi: 10.1093/femsle/fnv105

Seyler, L. M., McGuinness, L. M., and Kerkhof, L. J. (2014). Crenarchaeal heterotrophy in salt marsh sediments. *ISME J.* 8, 1534–1543. doi: 10.1038/ismej.2014.15

Shiozaki, T., Ijichi, M., Kodama, T., Takeda, S., and Furuya, K. (2014). Heterotrophic bacteria as major nitrogen fixers in the euphotic zone of the Indian Ocean. *Global Biogeochem. Cycles* 28, 1096–1110. doi: 10.1002/2014GB004886

Short, S. M., and Zehr, J. P. (2007). Nitrogenase gene expression in the Chesapeake Bay Estuary. *Environ. Microbiol.* 9, 1591–1596. doi: 10.1111/j.1462-2920.2007.01258.x

Sohm, J. A., Hilton, J. A., Noble, A. E., Zehr, J. P., Saito, M. A., and Webb, E. A. (2011). Nitrogen fixation in the South Atlantic Gyre and the Benguela Upwelling System. *Geophys. Res. Lett.* 38:L16608. doi: 10.1029/2011GL048315

Tamburini, C., Boutrif, M., Garel, M., Colwell, R. R., and Deming, J. W. (2013). Prokaryotic responses to hydrostatic pressure in the ocean - a review. *Environ. Microbiol.* 15, 1262–1274. doi: 10.1111/1462-2920.12084

Thiele, S., Fuchs, B. M., Amann, R., and Iversen, M. H. (2015). Colonization in the photic zone and subsequent changes during sinking determine bacterial community composition in marine snow. *Appl. Environ. Microbiol.* 81, 1463–1471. doi: 10.1128/AEM.02570-14

Thompson, A. W., Foster, R. A., Krupke, A., Carter, B. J., Musat, N., Vaulot, D., et al. (2012). Unicellular cyanobacterium symbiotic with a single-celled eukaryotic alga. *Science* 337, 1546–1550. doi: 10.1126/science.1222700

Turk-Kubo, K. A., Karamchandani, M., Capone, D. G., and Zehr, J. P. (2014). The paradox of marine heterotrophic nitrogen fixation: abundances of heterotrophic diazotrophs do not account for nitrogen fixation rates in the Eastern Tropical South Pacific. *Environ. Microbiol.* 16, 3095–3114. doi: 10.1111/1462-2920.12346

Wilson, S. T., Boettjer, D., Church, M. J., and Karl, D. M. (2012). Comparative assessment of nitrogen fixation methodologies, conducted in the oligotrophic North Pacific Ocean. *Appl. Environ. Microbiol.* 78, 6516–6523. doi: 10.1128/AEM.01146-12

Yogev, T., Rahav, E., Bar-Zeev, E., Man-Aharonovich, D., Stambler, N., Kress, N., et al. (2011). Is nitrogen fixation significant in the Levantine Basin, East Mediterranean Sea? *Environ. Microbiol.* 13, 854–871. doi: 10.1111/j.1462-2920.2010.02402.x

Zehr, J. P. (2011). Nitrogen fixation by marine cyanobacteria. *Trends Microbiol.* 19, 162–173. doi: 10.1016/j.tim.2010.12.004

Zehr, J. P., Jenkins, B. D., Short, S. M., and Steward, G. F. (2003). Nitrogenase gene diversity and microbial community structure: a cross-system comparison. *Environ. Microbiol.* 5, 539–554. doi: 10.1046/j.1462-2920.2003.00451.x

Zehr, J. P., Mellon, M. T., and Zani, S. (1998). New nitrogen-fixing microorganisms detected in oligotrophic oceans by amplification of nitrogenase (*nifH*) genes. *Appl. Environ. Microbiol.* 64, 3444–3450.

Zehr, J. P., Mellon, M., Braun, S., Litaker, W., Steppe, T., and Paerl, H. W. (1995). Diversity of heterotrophic nitrogen fixation genes in a marine cyanobacterial mat. *Appl. Environ. Microbiol.* 61, 2527–2532.

Zehr, J. P., Harris, D., Dominic, B., and Salerno, J. (1997). Structural analysis of the *Trichodesmium* nitrogenase iron protein: implications for aerobic nitrogen fixation activity. *FEMS Microb. Lett.* 153, 303–309. doi: 10.1111/j.1574-6968.1997.tb12589.x

Conflict of Interest Statement: The authors declare that the research was conducted in the absence of any commercial or financial relationships that could be construed as a potential conflict of interest.

frontiers in Marine Science

ORIGINAL RESEARCH
published: 22 September 2017
doi: 10.3389/fmars.2017.00303

Biological N_2 Fixation in the Upwelling Region off NW Iberia: Magnitude, Relevance, and Players

Víctor Moreira-Coello[1], Beatriz Mouriño-Carballido[1], Emilio Marañón[1], Ana Fernández-Carrera[1,2], Antonio Bode[3] and Marta M. Varela[3]*

[1] Facultade de Ciencias do Mar, Universidade de Vigo, Vigo, Spain, [2] School of Biology, Georgia Institute of Technology, Atlanta, GA, United States, [3] Instituto Español de Oceanografía, A Coruña, Spain

The classical paradigm about marine N_2 fixation establishes that this process is mainly constrained to nitrogen-poor tropical and subtropical regions, and sustained by the colonial cyanobacterium *Trichodesmium* spp. and diatom-diazotroph symbiosis. However, the application of molecular techniques allowed determining a high phylogenic diversity and wide distribution of marine diazotrophs, which extends the range of ocean environments where biological N_2 fixation may be relevant. Between February 2014 and December 2015, we carried out 10 one-day samplings in the upwelling system off NW Iberia in order to: (1) investigate the seasonal variability in the magnitude of N_2 fixation, (2) determine its biogeochemical role as a mechanism of new nitrogen supply, and (3) quantify the main diazotrophs in the region under contrasting hydrographic regimes. Our results indicate that the magnitude of N_2 fixation in this region was relatively low ($0.001 \pm 0.002 - 0.095 \pm 0.024$ μmol N m^{-3} d^{-1}), comparable to the lower-end of rates described for the subtropical NE Atlantic. Maximum rates were observed at the surface during both upwelling and relaxation conditions. The comparison with nitrate diffusive fluxes revealed the minor role of N_2 fixation (<2%) as a mechanism of new nitrogen supply into the euphotic layer. Small diazotrophs (<10 μm) were responsible for all N_2 fixation activity detected in the region. Quantitative PCR targeting the *nifH* gene revealed the highest abundances of two sublineages of *Candidatus* Atelocyanobacterium thalassa or UCYN-A (UCYN-A1 and UCYN-A2), mainly at surface waters during upwelling and relaxation conditions, and of Gammaproteobacteria γ-24774A11 at deep waters during downwelling. Maximum abundance for the three groups were up to 6.7×10^2, 1.5×10^3, and 2.4×10^4 *nifH* copies L^{-1}, respectively. Our findings demonstrate measurable N_2 fixation activity and presence of diazotrophs throughout the year in a nitrogen-rich temperate region.

Keywords: N_2 fixation, nitrate diffusive flux, *nifH*, UCYN-A, Gammaproteobacteria, NW Iberian upwelling, Atlantic Ocean

OPEN ACCESS

Edited by:
Lasse Riemann, University of Copenhagen, Denmark

Reviewed by:
Hanna Maria Farnelid, Linnaeus University, Sweden
Yao Zhang, Xiamen University, China

****Correspondence:***
Víctor Moreira-Coello
vmoreira@uvigo.es

Specialty section:
This article was submitted to Aquatic Microbiology, a section of the journal Frontiers in Marine Science

Received: *08 July 2017*
Accepted: *04 September 2017*
Published: *22 September 2017*

Citation:
Moreira-Coello V, Mouriño-Carballido B, Marañón E, Fernández-Carrera A, Bode A and Varela MM (2017) Biological N_2 Fixation in the Upwelling Region off NW Iberia: Magnitude, Relevance, and Players. Front. Mar. Sci. 4:303. doi: 10.3389/fmars.2017.00303

INTRODUCTION

Dinitrogen (N_2) is the most abundant form of nitrogen (N) in aquatic and terrestrial ecosystems, however only a limited, but diverse, group of bacteria and archaea (termed diazotrophs) can use this large N reservoir by the energy-costly process of biological N_2 fixation (BNF) (Karl et al., 2002). Diazotrophs possess nitrogenase, the enzyme that catalyzes this process, which reduces

atmospheric N_2 to bioavailable ammonium (NH_4^+). With an estimated global flux of ∼140–177 Tg N $year^{-1}$, BNF is the main mechanism that supplies new N to the ocean, fueling phytoplanktonic photosynthesis and the subsequent export of organic matter into the deep waters through the "biological carbon pump" (Voss et al., 2013). The limited number of studies simultaneously quantifying BNF vs. the transport of nitrate into the euphotic zone through turbulent mixing indicate that BNF can equal or even exceed nitrate diffusion in some regions of the subtropical gyres (Capone et al., 2005; Mouriño-Carballido et al., 2011; Painter et al., 2013; Fernández-Castro et al., 2015). Therefore, BNF is a key process controlling oceanic productivity, the carbon cycle, and climate (Gruber and Galloway, 2008).

Traditionally, it has been considered that marine BNF is mainly restricted to nitrogen-poor tropical and subtropical regions, and sustained by the filamentous cyanobacterium *Trichodesmium* spp. and diatom-diazotroph associations. However, the development and application of molecular techniques allowed to determine an extremely high phylogenic diversity of nitrogenase genes (*nifH*) (Zehr et al., 2000). In addition to *Trichodesmium* and diatom-diazotroph associations, marine diazotrophic groups include unicellular cyanobacteria (UCYN-A, -B, -C) and non-cyanobacterial diazotrophs (heterotrophic bacteria and archaea) (Zehr et al., 2003). Diazotrophic heterotrophic bacteria comprise a wide range of phylogenetic groups, including Firmicutes, Alpha-, Beta-, Gamma-, Delta- and Epsilonproteobacteria (Zehr et al., 2003).

Recently, UCYN-A (or *Candidatus* Atelocyanobacterium thalassa), which lives in obligate symbiosis with a picoeukaryotic prymnesiophyte (Thompson et al., 2012), has been revealed as a key component of the global diazotrophic community, since it shows a wide distribution, and relatively high N_2 fixation rates (Farnelid et al., 2016; Martínez-Pérez et al., 2016). Six different UCYN-A sublineages (UCYN-A1, -A2, -A3, -A4, -A5, -A6) have been defined based on the genetic diversity of the *nifH* sequences available in GenBank (Thompson et al., 2014; Farnelid et al., 2016; Turk-Kubo et al., 2017). The Gammaproteobacteria-affiliated phylotype γ-24774A11 (also named Gamma A or UMB) also exhibits a wide distribution, including contrasting marine environments in the Atlantic, Pacific and Indian Oceans (e.g., Church et al., 2005; Moisander et al., 2008; Langlois et al., 2015; Benavides et al., 2016). Gammaproteobacteria γ-24774A11 is considered one of the most important heterotrophic diazotrophs in the oligotrophic (sub)tropical regions (Moisander et al., 2014).

Although numerous studies have investigated the biogeography and controlling mechanisms of marine BNF in recent years (e.g., Moore et al., 2009; Monteiro et al., 2011; Luo et al., 2014; Fernández-Castro et al., 2016), the limiting factors of this process are still under debate. Due to the high energetic cost of fixing N_2 in comparison to the assimilation of dissolved inorganic nitrogen (DIN) (mainly ammonia and nitrate), DIN-replete environments have been considered as inhibitory for the growth of diazotrophs and BNF activity (Holl and Montoya, 2005). However, the discovery of a large diversity of organisms able to fix N_2, and their wide distribution, indicated that BNF may be more widespread than previously thought (Moisander et al., 2010). Recent studies demonstrate the presence and activity of diazotrophs in DIN-enriched environments such as the eastern tropical North Atlantic (Voss et al., 2004), the western English Channel (Rees et al., 2009), the Mekong River plume in the South China Sea (Grosse et al., 2010), the temperate NE American coast (Mulholland et al., 2012), and mesohaline temperate estuaries between the Baltic Sea and the North Sea (Bentzon-Tilia et al., 2015). Evidences of BNF have also been reported in upwelling systems such as the eastern equatorial Atlantic (Voss et al., 2004; Foster et al., 2009; Subramaniam et al., 2013), the Benguela upwelling system (Sohm et al., 2011; Benavides et al., 2014), and the region off central Chile (Raimbault and Garcia, 2008; Fernández et al., 2015).

The NW Iberian Peninsula is part of the Iberia-Canary upwelling domain, one of the eastern boundary upwelling ecosystems in the global ocean (Arístegui et al., 2009). This area is characterized by the presence of coastal embayments named Rías and the seasonal influence of wind-driven upwelling and downwelling events (Wooster et al., 1976; Fraga, 1981). From April to September, the prevailing northerly winds cause upwelling, and the subsequent rise of cold and nutrient-rich subsurface waters into the coastal euphotic layer. These nutrient inputs, and their amplification due to remineralisation inside the Rías (Bode et al., 1996; Álvarez-Salgado et al., 2002), fuel the high phytoplankton production that supports a rich marine ecosystem and productive fisheries (Fraga, 1981; Varela, 1992). From October to March, the prevailing southerly winds favor downwelling events (Wooster et al., 1976; Fraga, 1981). Knowledge about diazotrophic activity in the NW Iberia region is limited to a single observation carried out in summer 2009, when relatively low BNF rates, mainly attributed to UCYN-A, were reported by Agawin et al. (2014) and Benavides et al. (2011). Here we describe the results of a survey conducted in the outer part of Ría de A Coruña between February 2014 and December 2015, which covered contrasting hydrographic regimes. Our main goals are to: (1) investigate the seasonal variability in the magnitude of BNF, (2) determine its biogeochemical role as a mechanism of new N supply, and (3) quantify the main diazotrophs.

MATERIALS AND METHODS

Sampling and Hydrographic Measurements

Between February 2014 and December 2015, within the framework of the NICANOR (Nitrogen fixation and diffusive fluxes in the NW Iberian Peninsula) project, 10 one-day samplings were carried out on board B/O Lura at station 2 (43.42°N, 8.44°W; depth = 80 m) of the RADIALES time-series project (http://www.seriestemporales-ieo.com) (**Figure 1**). This station is located in the adjacent shelf off Ría de A Coruña (Golfo Ártabro, NW Iberian Peninsula). The samplings were designed to cover the main hydrographic stages in this system over a seasonal cycle, and spanned over a period of 20 months. To simplify the interpretation of the results, we classified the samplings into three conditions: five cruises were characterized by downwelling (February 2014, December 2014, May 2015, November 2015, and December 2015), three by upwelling (May

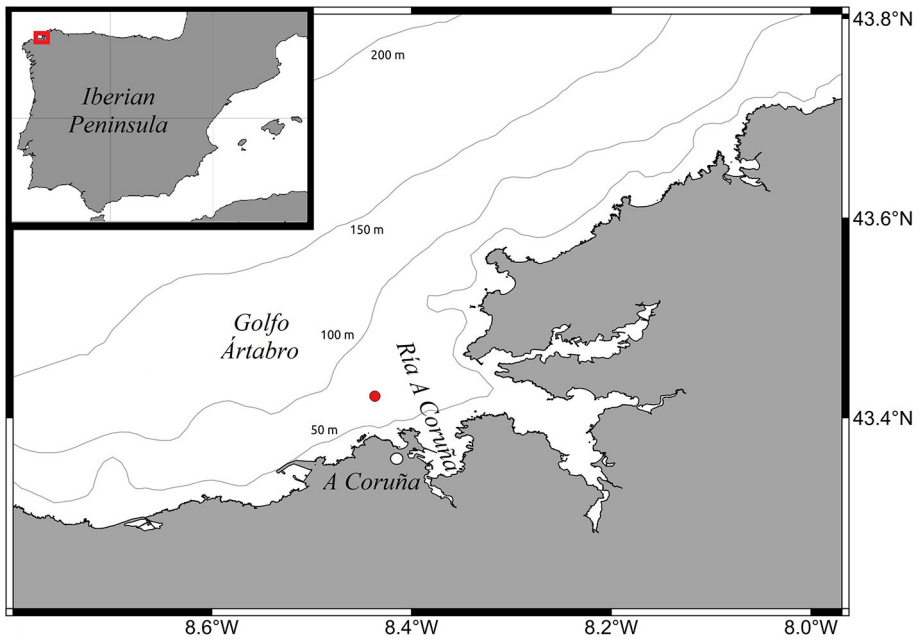

FIGURE 1 | Sampling station (red dot) located at 80 m depth in the adjacent shelf off Ría de A Coruña (Golfo Ártabro, NW Iberian Peninsula). The 50, 100, 150, and 200 m isobaths are indicated.

2014, April 2015, and June 2015), and another two by relaxation, i.e., intermediate conditions between upwelling and downwelling pulses (July 2015, and September 2015). This classification was based on the wind-driven upwelling index and the hydrographic conditions of the water column (see results). The upwelling index (I_W) was estimated by the Ekman transport ($m^3\ s^{-1}\ km^{-1}$) and computed from wind data for the sector Rías Altas (44°N 9°W), near Ría de A Coruña, using the NAVGEM model of Fleet Numerical Meteorology and Oceanography Center (FNMOC) (http://www.indicedeafloramiento.ieo.es), averaged over the 3 days period before each cruise. On each sampling day, profiles of temperature, salinity and fluorescence were obtained with a CTD (Conductivity-Temperature-Depth) probe SBE25plus (SeaBird Electronics) attached to a rosette of Niskin bottles. Water samples were collected for the determination of inorganic nutrients, chlorophyll *a*, primary production, picoplankton composition, biological N_2 fixation, as well as for DNA extraction. In 7 out of the 10 surveys, measurements of dissipation rates of turbulent kinetic energy were conducted using a microstructure turbulence profiler (MSS, Prandke and Stips, 1998).

In order to facilitate the comparison between hydrographic conditions, we provide mean and standard deviation for the variables quantified under the relaxation condition, despite the low number of samplings ($n = 2$). We are aware that a higher number of samplings would be desirable to better characterize averaged physical, chemical and biological fields in this system, where variability happens at short temporal scales of a few days (Casas et al., 1997; Gilcoto et al., 2017).

Inorganic Nutrients, Chlorophyll *a*, and Primary Production

Unfiltered samples for the determination of dissolved inorganic nutrients (NO_3^-, PO_4^{3-}) were collected from 3 to 7 depths in rinsed polyethylene 15-mL tubes and stored frozen at −20°C, until further analysis by standard colorimetric methods on a segmented flow AutoAnalyzer 3 Bran Luebbe (Aminot and Kerouel, 2007). Nutrient analysis were performed at the facilities of the University of Oviedo (Spain). Data for nutrient concentrations were not available for December 2014 and April 2015. In these cases, nitrate concentration was computed from a nitrate-density (σ_t) relationship built by using all samples ($n = 52$) collected during the sampling period. The relationship showed a linear behavior ($NO_3^- = 9.948\sigma_t - 260.850$; $R^2 = 0.930$; $p < 0.05$) for σ_t ranging between 26.1 and 27.1 Kg m^{-3}.

During all samplings except February 2014, when only the total fraction was available, size-fractionated (< and > 10 μm) chlorophyll *a* and primary production were determined at 0, 20, and 40 m. 150-mL samples were filtered onto Whatman GF/F filters for the total fraction, and onto Whatman polycarbonate filters for the >10 μm fraction. Filters for chlorophyll *a* quantification were extracted in 90% acetone at 4°C overnight and measured using the spectrofluorometric method, as described in Bode et al. (2011). Fluorometrically determined chlorophyll *a* concentrations, ranging from 0.1 to 5.8 mg m^{-3}, were used to calibrate the fluorometer attached to the CTD-rosette (Chl $a = 0.533 \times$ fluorescence $- 0.212$; $R^2 = 0.830$, $n = 121$), which was used to plot the chlorophyll *a* distribution in February 2014, December 2014, and December

2015. In May 2014, and from April to November 2015, we used the fluorometer included in the MSS profiler (see below), also calibrated with chlorophyll *a* concentrations ranging from 0.1 to 6.5 mg m^{-3} (Chl $a = 3.520 \times$ fluorescence–5.125; $R^2 = 0.770$, $n = 36$), obtained in the same station during the same sampling period. Size-fractionated primary production was measured by ^{14}C-uptake. Seawater samples were transferred to triplicate 300–mL polycarbonate bottles (Nalgene) (2 light and 1 dark bottles), which were spiked with 2–10 μCi of $NaH^{14}CO_3$ and incubated during 24 h in refrigerated incubators equipped with a system of recirculating water, and covered with neutral density screens to simulate the corresponding in situ irradiance. Sample filtration, filter processing and primary production calculations were conducted as described in detail in Bode et al. (2011).

Flow Cytometric Counting

Samples for the determination of picoplankton abundance and cell properties were taken at 0, 40, and 70 m depth. Picoplankton samples (1.8 ml) were preserved with 1% paraformaldehyde + 0.05% glutaraldehyde (final concentration), flash-frozen in liquid N_2 for 10 min and stored at −80°C until analysis with a FACSCalibur flow cytometer (Becton-Dickinson) equipped with a laser emitting at 488 nm. To estimate the abundance of the different groups (cell mL^{-1}), calibration of the cytometer flow rate was performed before each use. A suspension (approximately 1×10^5 mL^{-1}) of fluorescent latex beads 1 μm in diameter (Molecular Probes, Life Technologies) was added to all the samples as internal standard. Two aliquots from the same sample were used for the study of picophytoplankton (0.6 ml) and heterotrophic bacteria (0.4 ml), analyzed at high (∼mean 58 μL min^{-1}) and low (∼mean 22 μL min^{-1}) flow rate, respectively. Before the analysis, the DNA of heterotrophic bacteria was stained with the nucleic acid fluorochrome SYTO-13 (2.5 μM; Molecular Probes, Life Technologies) in the dark for 10 min.

Autotrophic cells were separated into 2 groups of cyanobacteria (*Synechococcus* and *Prochlorococcus*) and 2 groups of picoeukaryotes (small and large), based on their orange (FL2, 585 nm) and red (FL3, >650 nm) fluorescence and side-scattered light (SSC) (Calvo-Díaz and Morán, 2006). Two groups of heterotrophic bacteria, with high and low nucleic acid content (HNA and LNA, respectively), were distinguished based on their relative green fluorescence (FL1, 530 nm), which was used as a proxy for nucleic acid content.

To estimate biovolume, we used an empirical calibration between SSC and cell diameter, assuming spherical shape for all groups. Finally, picoplankton biomass was computed using the following conversion factors of biovolume to carbon: 350 fg C $μm^{-3}$ for heterotrophic bacteria (Bjørnsen, 1986), 230 fg C $μm^{-3}$ for *Synechococcus*, 240 fg C $μm^{-3}$ for *Prochlorococcus* and 237 fg C $μm^{-3}$ for picoeukaryotes (Worden et al., 2004).

Biological N_2 Fixation

Water samples from 0, 20, 40, and 70 m depth were collected with Niskin bottles to determine size-fractionated (< and >10 μm) N_2 fixation following the $^{15}N_2$-uptake technique (Montoya et al., 1996), with the modifications described in Rees et al. (2009). In February 2014, only surface water (0 m) was sampled. Triplicate 2-L acid-cleaned clear polycarbonate bottles (Nalgene) were filled directly from the Niskin bottle using acid-washed silicone tubing. After carefully removing all air bubbles, bottles were closed with caps provided with silicone septa, through which 3 mL of $^{15}N_2$ (98 atom%, Isotec Stable Isotopes lot TV0533 in February 2014, and Cambridge Isotope Laboratories lots I-16727 and I-19168A in the remaining samplings) were injected with a gas-tight syringe. The pressure across the septum was equilibrated by allowing the excess water to escape through a syringe needle piercing the septum. Incubation bottles were gently shaken by manually inverting them fifty times, and then incubated for 24 h in the same incubators used for primary production measurements. The incubation of seawater from 70 m (collected in the aphotic zone) was performed under complete darkness, by covering the incubation bottles with black duct tape and placing them inside a black opaque plastic bag.

Incubations ended by filtration through 25 mm Whatman GF/F filters to obtain total N_2 fixation rates. N_2 fixation rates of the <10 μm size-fraction were determined by pre-filtering the water sample through 47 mm Whatman polycarbonate filters of 10 μm pore-size, and subsequently collecting onto GF/F filters. Total and pre-filtered 2-L seawater samples from each depth were also filtered at time zero for the determination of natural abundance of N stable isotopes ($\delta^{15}N$). After filtration, filters were dried at 40°C during 24 h and stored at room temperature until pelletization in tin capsules. Measurement of particulate organic nitrogen and carbon (PON and POC) content and ^{15}N atom% were carried out with an elemental analyser combined with a continuous-flow isotope ratio mass-spectrometer (FlashEA112 + Deltaplus, ThermoFinnigan), and using an acetanilide standard as reference. The precision of the analysis, expressed as the standard deviation of the ^{15}N values determined in a series of 10 standards, was 0.15‰. Isotopic analyses were made at the stable isotope facility (SAI) of the University of A Coruña (Spain). Assuming that the minimum acceptable change of δ^{15} N between the initial and the final PON sample is 4‰ (Montoya et al., 1996), and given that the detection limit of the used elemental analyzer is 0.15–0.20 μg N, the detection limit of our method is approximately 0.0005 nmol N L^{-1} d^{-1}. The equations of Weiss (1970) and Montoya et al. (1996) were used to calculate the initial N_2 concentration (assuming equilibrium with atmosphere) and N_2 fixation rates, respectively. The fact that we obtained in several samplings at different depths BNF rates equal to zero, or below the detection limit, allowed us to discard any effect of potential contamination in the commercial $^{15}N_2$ gas stocks (Dabundo et al., 2014).

Average cell-specific N_2 fixation rates by UCYN-A that would be required to explain the observed BNF rates, were calculated based on their qPCR-estimated abundances and the BNF measured, following the assumptions and calculations indicated in Turk-Kubo et al. (2014). Representative cell-specific rates for UCYN-A ranging from 0.02 to 2.6 fmol N $cell^{-1}$ h^{-1} have been directly estimated or modeled by Goebel et al. (2010). Considering these known cell-specific rates, we roughly estimated whether the UCYN-A abundances in our samples could account for the measured bulk BNF rates.

DNA Samples Collection and Extraction

During all samplings except February 2014, when only the sample at 0 m was collected, seawater samples for DNA were collected at 0, 20, 40, and 70 m depth, transferred to acid-cleaned carboys using acid-washed silicone tubes and kept in darkness until further processing in the laboratory. Microbial biomass was collected by filtering 7.5-10 L of seawater through a 0.22 μm Sterivex™ filter unit (Millipore) using a peristaltic pump. The filters were preserved with 1.8 mL of lysis buffer (50 mM Tris-HCl pH 8.3, 40 mM EDTA pH 8.0, 0.75 M sucrose) and stored at −80°C until extraction. DNA was extracted using the PowerWater® DNA Isolation Kit (MO BIO, Laboratories, Inc.), quantified and quality-checked (according to the A_{260}/A_{280} ratio) using a spectrophotometer NanoDrop 2000™ (Thermo Fisher Scientific).

Quantification of *nifH* Gene by qPCR

The abundance of diazotrophs was determined by quantitative polymerase chain reaction (qPCR) using TaqMan primers-probe sets (PrimeTime® qPCR Assays, Integrated DNA Technologies) targeting Gammaproteobacteria-affiliated phylotype γ-24774A11 (Moisander et al., 2008), UCYN-A1 (Church et al., 2005), and UCYN-A2 (Thompson et al., 2014). However, we are aware that the primers-probe set designed for UCYN-A2 does not contain enough mismatches to avoid cross-hybridization with the UCYN-A3 and UCYN-A4 sublineages (Farnelid et al., 2016). The probes were 5′FAM labeled and double-quenched with ZEN™/3′-IBFQ (Integrated DNA Technologies). The reactions were run on a MyiQ2™ Real-Time PCR Detection System (Bio-Rad Laboratories) at the *Instituto Español de Oceanografía* (IEO). Final reaction volume of 20 μL contained 10 μL PrimeTime® Gene Expression Master Mix (IDT), 2 μL DNA template, 2 μL of primers-probe set (0.5 and 0.25 μM final concentrations, respectively), and 6 μL PCR grade water (Sigma-Aldrich). Thermal cycling conditions were 95°C for 3 min, followed by 45 cycles of 95°C for 15 s and 60°C for 1 min. Standards, consisting of nine 10-fold serial dilutions containing the targeted *nifH* fragments (gBlocks® Gene Fragments, IDT), were included with each qPCR run. All samples and standards were run in duplicate. Standard curves were obtained by linear regression of the threshold cycle (Ct) and $\log_{10}$ gene copies per reaction using standards ranging from 10^8 to 10^0 gene copies per reaction. Amplification efficiencies were >90% for all reactions. No-template control sample was run in duplicate in all plates and it did not amplify in any runs. We performed inhibition tests by 2- and 5-folds dilutions of all samples and we concluded that our samples were not inhibited. The limit of detection (LOD) and detected but not quantified (DNQ) limits were 4 *nifH* copies L^{-1} and 41 *nifH* copies L^{-1}, respectively. Abundances below LOD were considered 0 copies L^{-1}, whereas *nifH* copies higher than LOD but less than DNQ were assigned a conservative value of 1 *nifH* copy per liter.

Dissipation Rates of Turbulent Kinetic Energy and Estimates of Nitrate Fluxes through Vertical Diffusion

Measurements of dissipation rates of turbulent kinetic energy were conducted on each cruise during 6–10 vertical casts down to a maximum depth of 70 m. The microstructure turbulence profiler was equipped with 2 velocity microstructure shear sensors (type PNS98), a microstructure temperature sensor (FPO7), a sensor to measure horizontal acceleration of the profiler and a high-precision CTD probe. Fluorometrically determined chlorophyll *a* concentrations were used to calibrate the fluorometer sensor included in the MSS profiler, as previously indicated. The profiler was balanced to have negative buoyancy and a sinking velocity of ∼0.4 to 0.7 m s^{-1}. The frequency of data sampling was 1024 Hz. The sensitivity of the shear sensors was checked after each use. Due to significant turbulence generation close to the ship, only the data below 5 m were considered reliable. Data processing and calculation of dissipation rates of turbulent kinetic energy (ε) was carried out with the commercial software MSSpro as described in detail in Fernández-Castro et al. (2014). The squared Brunt Väisälä frequency (N^2), a proxy for water column stratification, was computed from the CTD profiles according to the equation:

$$N^2 = -\left(\frac{g}{\rho_w}\right)\left(\frac{\partial \rho}{\partial z}\right) \quad (s^{-2}) \tag{1}$$

where g is the acceleration due to gravity (9.8 m s^{-2}), ρ_w is seawater density (1,025 kg m^{-3}), and ∂_ρ/∂_z is the vertical potential density gradient. After averaging ε and N^2 over depth intervals of 1 m length, vertical diffusivity or mixing (Kz) was estimated as:

$$Kz = e\frac{\varepsilon}{N^2} \ (m^2 s^{-1}) \tag{2}$$

where e is the mixing efficiency, here considered as 0.2 (Osborn, 1980).

Vertical diffusive fluxes of nitrate into the euphotic layer were calculated following the Fick's law, from the product of the nitrate gradient, obtained by linearly fitting nitrate concentrations in the 10–40 m depth layer, and the averaged Kz for the same depth interval. For those samplings in which the microstructure profiler was not deployed (February 2014, December 2014, and December 2015), estimates of Kz under similar hydrographic conditions were considered: October 2014 (for February 2014), and November 2015 (for December 2014 and December 2015). In order to quantify the biogeochemical relevance of BNF, we compared it with the supply of nitrate into the euphotic zone through vertical diffusion.

Nitrate Supply through Vertical Advection

A simplified calculation of nitrate supply by vertical advection due to upwelling was computed considering the Golfo Ártabro as a single box divided into two layers (Álvarez-Salgado et al., 2000; Villamaña et al., 2017), the deeper one influenced by upwelled water and the surface layer dominated by the outgoing flow. Assuming that the bottom layer volume is conservative and stationary, the vertical advective flux (Q_Z, m^3 s^{-1}) would be equal to the incoming bottom flux (Q_B, m^3 s^{-1}), computed as the product of the upwelling index (I_W, m^3 s^{-1} km^{-1}) and the length of the mouth of the Golfo Ártabro (ca. 11.5 km). Finally,

the nitrate transport into the euphotic layer by vertical advection was computed as:

$$NO_3^- \ advective\ flux = \frac{Q_Z}{A_{basin}} [NO_3^-]_{70\ m} \quad (3)$$

where A_{basin} is the surface area of the Golfo Ártabro (ca. 400 km^2), Q_Z is the vertical advective flux, and $[NO_3^-]_{70\ m}$ is the nitrate concentration determined at 70 m depth for each cruise in the sampling station.

All the statistical analysis were performed by using SPSS v. 22 for Windows (IBM SPSS Statistics).

RESULTS

Hydrography and Turbulent Mixing

During our survey we encountered the main hydrographic features of a temperate coastal region subjected to seasonal variability and influenced by upwelling pulses, which in this system induce large variability at short temporal scales (Bode et al., 1996; Casas et al., 1997). During downwelling conditions, we sampled winter (February 2014 and December 2014) and autumn (November 2015 and December 2015) mixing, and also a spring transitional period under prevailing predominance of downwelling (May 2015) (**Figure 2**). Autumn mixing was characterized by thermohaline mixing, whereas during winter mixing the slight haline stratification caused mixed layer depth being shallower (**Figure 3**, Table S1). In May 2015, the higher vertical gradient in temperature and salinity at the surface produced that the mixed layer depth was even shallower. However, during downwelling averaged vertical stratification (determined as Brunt Väisälä frequency) between 10 and 40 m was relatively low ($4.4 \pm 7.1 \times 10^{-5}$ s^{-2}), and as a result the mixed layer depth was significantly deeper (50 ± 22 m), than during upwelling and relaxation conditions (**Table 1**, Figure S1). Microstructure turbulence observations, which were only available for May and November 2015, showed relatively low values of averaged vertical (10–40 m) dissipation rates of turbulent kinetic energy (ε) in both cruises ($1.3–2.2 \times 10^{-8}$ m^2 s^{-3}).

Cruises which sampled spring-summer upwelling (May 2014, April 2015, and June 2015) were characterized by shallow mixed layer depths (9 ± 3 m) (**Table 1**, Figure S1). Due to the enhanced values observed in the upper 20 m in May 2014, averaged dissipation rates were slightly higher during this cruise ($4.3 \pm 7.3 \times 10^{-8}$ m^2 s^{-3}) (**Figure 3**, Table S1).

Relaxation conditions included two cruises (July 2015 and September 2015), which sampled the transition between intense upwelling and downwelling events during the summer thermal stratification period (**Figure 2**). Both cruises were characterized by intense vertical stratification ($19.7 \pm 21.9 \times 10^{-5}$ s^{-2}), and shallow mixed layer depths (12 ± 1 m) (**Table 1**, **Figure 3**). As a result of the relatively low vertical stratification and enhanced dissipation rates observed between 25 and 40 m depth layer, averaged vertical diffusivity ($12.0 \pm 33.0 \times 10^{-4}$ m^2 s^{-1}) was higher, although not statistically significant, than during downwelling ($4.5 \pm 7.6 \times 10^{-4}$ m^2 s^{-1}) and upwelling conditions ($1.5 \pm 4.2 \times 10^{-4}$ m^2 s^{-1}).

Nutrients, Chlorophyll *a*, and Primary Production

In downwelling conditions, due to the low stratification and deeper mixed layers, nitrate and phosphate vertical profiles were relatively homogeneous, whereas during upwelling, the input of cold and high-nitrate waters at depth caused significant enhanced nutrient vertical gradients (**Figure 4**). Vertical gradients of nitrate were also higher during relaxation, and the concentrations at depth of both nitrate and phosphate were higher during September 2015, compared to July 2015, due to the intensifying upwelling observed one week before the September 2015 sampling (**Figure 2**). On average, the vertical nitrate gradient between 10 and 40 m depth during upwelling (148 ± 41 μmol m^{-4}) and relaxation (139 ± 2 μmol m^{-4}) was significantly higher than during downwelling (15 ± 13 μmol m^{-4}) (**Table 1**).

Vertical profiles of total chlorophyll *a* and primary production were also homogeneous during downwelling (**Figure 5**). During

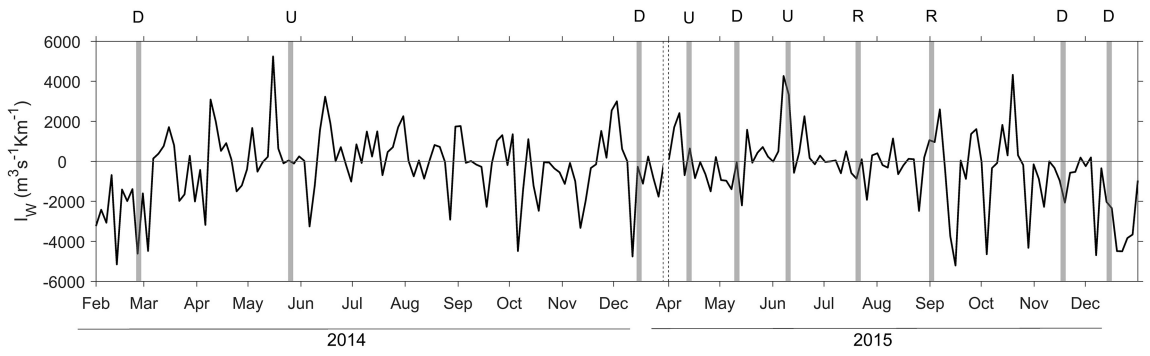

FIGURE 2 | Upwelling index (I_W) computed in the region during the sampling period covering from February 2014 to December 2014, and April 2015 to December 2015. Positive (negative) values correspond to upwelling (downwelling) due to northerly (southerly) winds. The shaded areas indicate the 3 days period before each sampling, and the dashed lines indicate the break between 2014 and 2015. Letters on the top indicate downwelling (D), upwelling (U), and relaxation (R) conditions.

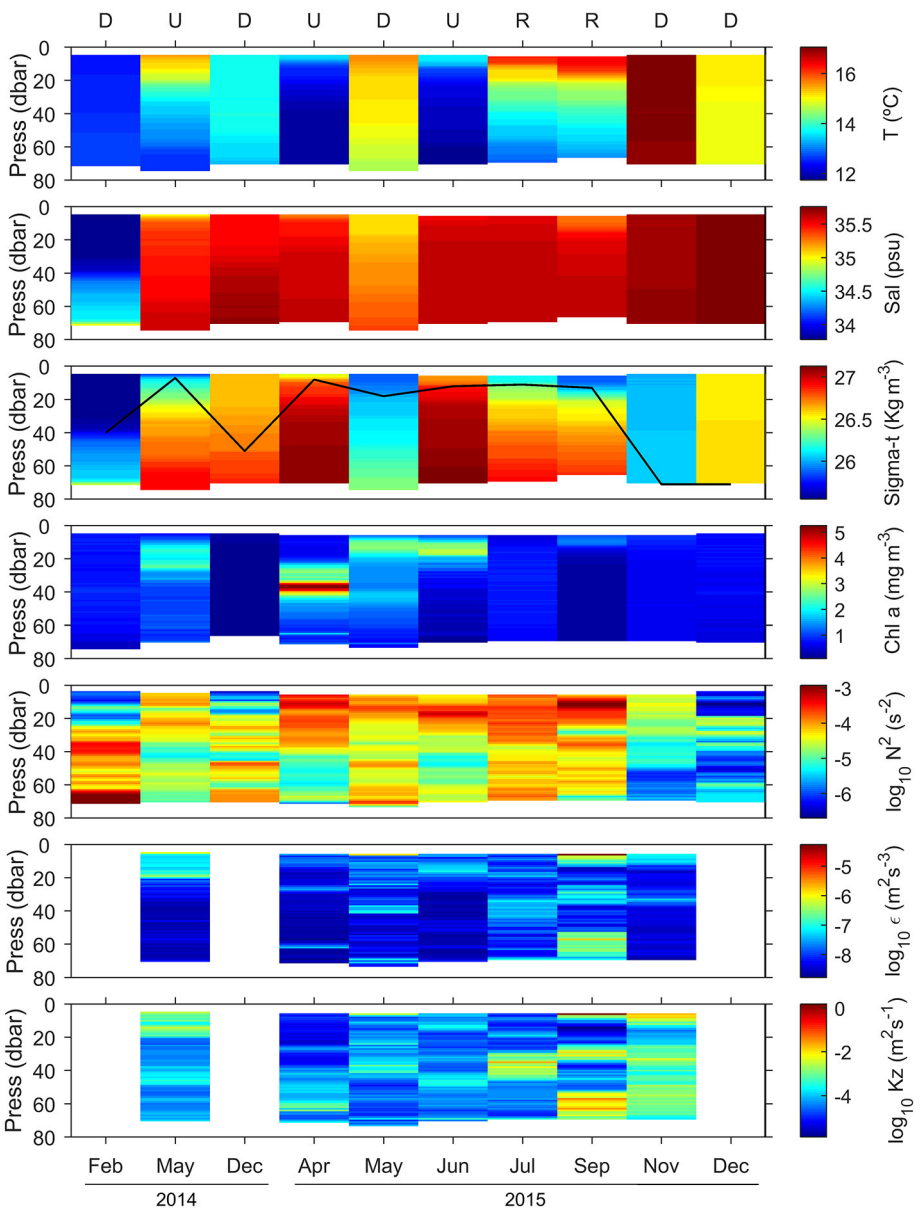

FIGURE 3 | Vertical distribution of temperature (T), salinity (Sal), density (sigma-t), chlorophyll *a* concentration (Chl *a*), squared Brunt Väisälä frequency (N^2), dissipation rates of turbulent kinetic energy (ε), and vertical diffusivity (*Kz*). The black line in the sigma-t panel indicates the mixed layer depth, estimated from an increase in water column density of 0.125 kg m^{-3} relative to surface values. Letters on top panel indicate the hydrographic condition sampled on each cruise (D, downwelling; U, upwelling; and R, relaxation). Chlorophyll *a* concentration was calculated from the calibrated fluorescence sensor included in the CTD-rosette (February 2014, December 2014, and December 2015) and the MSS profiler (May 2014, April-November 2015) (see section Materials and Methods).

these conditions depth-integrated chlorophyll *a* and primary production were, on average, relatively low (31 ± 16 mg m^{-2} and 1,359 ± 1,032 mg C m^{-2} d^{-1}, respectively), and dominated (>80 %) by small (<10 μm) phytoplankton cells (**Table 1**, Figure S1). During upwelling the fertilization effect of deep waters stimulates phytoplankton growth, and increases the contribution of larger cells (>10 μm). Averaged depth-integrated chlorophyll *a* (65 ± 35 mg m^{-2}) and primary production (5,192 ± 538 mg C m^{-2} d^{-1}) were slightly and significantly, respectively, higher than during downwelling and relaxation, and the contribution of larger cells to both chlorophyll *a* and primary production was higher than 60%. During relaxation depth-integrated chlorophyll *a* (20 ± 2 mg m^{-2}) and primary production (1,611 ± 295 mg C m^{-2} d^{-1}) were relatively low. In September 2015, small phytoplankton cells contributed more than 80% to both chlorophyll *a* and primary production, whereas in July 2015 the contribution was lower than 50%.

TABLE 1 | Mean (±SD) values for selected variables determined during the samplings classified as downwelling (D), upwelling (U), and relaxation (R) conditions.

Variable	D ($n = 5$)	U ($n = 3$)	R ($n = 2$)	Kruskal-Wallis p-value	Bonferroni comparisons
Upwelling Index ($m^3\ s^{-1}\ Km^{-1}$)	−1858 ± 1585	1338 ± 1878	472 ± 1176	0.120	
Surface temperature (°C)	14.8 ± 1.8	14.2 ± 1.1	16.3 ± 0.1	0.216	
Surface salinity	35.2 ± 0.8	35.3 ± 0.3	35.4 ± 0.2	0.700	
MLD (m)	50 ± 22	9 ± 3	12 ± 1	0.027*	D > U, R
N^2 (s^{-2}) × 10^{-5}	4.4 ± 7.1	11.7 ± 12.3	19.7 ± 21.9	0.047*	D < R
ε ($m^2\ s^{-3}$) × 10^{-8}	1.8 ± 1.8	2.2 ± 4.6	3.0 ± 3.9	0.738	
Kz ($m^2\ s^{-1}$) × 10^{-4}	4.5 ± 7.6	1.5 ± 4.2	12.0 ± 33.0	0.107	
Surface NO_3^- (μM)	3.9 ± 2.5	1.7 ± 1.8	1.2 ± 1.6	0.295	
(40 m) NO_3^- (μM)	3.3 ± 2.4	6.9 ± 3.0	5.7 ± 2.9	0.354	
Surface PO_4^{3-}(μM)	0.20 ± 0.09	0.20 ± 0.18	0.34 ± 0.01	0.181	
(40 m) PO_4^{3-} (μM)	0.39 ± 0.19	0.28 ± 0.12	0.37 ± 0.27	0.705	
NO_3^- gradient ($\mu mol\ m^{-4}$)	15 ± 13	148 ± 41	139 ± 2	0.032*	D < U, R
NO_3^- diffusive flux ($\mu mol\ m^{-2}\ d^{-1}$)	795 ± 902	2241 ± 3134	14324 ± 3063	0.106	
Surface Chl *a* ($mg\ m^{-3}$)	0.9 ± 0.3	1.6 ± 0.1	0.8 ± 0.5	0.055	
Int Chl *a* ($mg\ m^{-2}$)	31 ± 16	65 ± 35	20 ± 2	0.094	
% Int Chl *a* <10 μm	85 ± 8	34 ± 8	64 ± 25	0.047*	D > U, R
Int PP ($mg\ C\ m^{-2}\ d^{-1}$)	1359 ± 1032	5192 ± 538	1611 ± 295	0.040*	U > D, R
% Int PP <10 μm	81 ± 8	38 ± 3	59 ± 42	0.054	
Surface N_2 fixation ($\mu mol\ N\ m^{-3}\ d^{-1}$)	0.016 ± 0.020	0.068 ± 0.038	0.072 ± 0.008	0.085	
Int N_2 fixation ($\mu mol\ N\ m^{-2}\ d^{-1}$)	0.7 ± 0.6	1.1 ± 0.7	0.8 ± 0.1	0.639	
Contribution BNF (%)	0.15 ± 0.20	0.65 ± 0.82	0.01	0.260	
Surface Gamma (*nifH* copies L^{-1})	2557 ± 4351	305 ± 528	1286 ± 912	0.284	
Int Gamma (*nifH* copies m^{-2} ×10^5)	145 ± 205	13 ± 23	132 ± 124	0.151	
Surface UCYN-A1 (*nifH* copies L^{-1})	33 ± 64	189 ± 31	617 ± 74	0.001**	R > D, U
Int UCYN-A1 (*nifH* cop. m^{-2} ×10^5)	1.4 ± 1.3	1.3 ± 0.2	13.0 ± 0.0	<0.001***	R > D, U
Surface UCYN-A2 (*nifH* copies L^{-1})	137 ± 240	427 ± 562	867 ± 863	0.165	
Int UCYN-A2 (*nifH* cop. m^{-2} ×10^5)	7.3 ± 6.6	9.7 ± 9.8	21.0 ± 15.6	0.386	
S-picoEuk biomass ($mg\ C\ m^{-2}$)	28 ± 12	14 ± 9	10 ± 9	0.129	
S-picoEuk contribution (%)	13 ± 5	6 ± 4	6 ± 4	0.135	
L-picoEuk biomass ($mg\ C\ m^{-2}$)	38 ± 38	34 ± 27	13 ± 11	0.425	
L-picoEuk contribution (%)	14 ± 7	14 ± 13	7 ± 4	0.571	
Synechococcus biomass ($mg\ C\ m^{-2}$)	15 ± 7	4 ± 5	5 ± 6	0.201	
Synechococcus contribution (%)	7 ± 3	1 ± 1	3 ± 3	0.053	
Prochlorococcus biomass ($mg\ C\ m^{-2}$)	7 ± 6	2 ± 0	2 ± 0	0.138	
Prochlorococcus contribution (%)	3 ± 3	1 ± 0	1 ± 0	0.262	
HNA biomass ($mg\ C\ m^{-2}$)	96 ± 38	164 ± 56	99 ± 8	0.152	
HNA contribution (%)	43 ± 6	62 ± 10	62 ± 13	0.032*	D < U
LNA biomass ($mg\ C\ m^{-2}$)	48 ± 23	40 ± 13	36 ± 14	0.834	
LNA contribution (%)	20 ± 3	15 ± 2	21 ± 3	0.131	

MLD corresponds to the mixed layer depth, estimated from an increase in water column density of 0.125 Kg m^{-3} relative to surface values. Squared Brunt Väisälä frequency (N^2), dissipation rates of turbulent kinetic energy (ε), and vertical diffusivity (Kz) correspond to averaged values for the 10–40 m depth interval. The same interval was used to compute vertical NO_3^- gradients and diffusive fluxes. Depth-integrated values (Int) for chlorophyll a, primary production (PP), contribution of <10 μm size-fraction, N_2 fixation rates, Gammaproteobacteria γ-24774A11 (Gamma) and UCYN-A nifH abundances, and biomass of picoplankton groups were calculated down to 40 m. BNF contribution represents the contribution of biological N_2 fixation to the supply of new N (considering N_2 fixation plus nitrate vertical diffusion). The contribution of each group to total picoplankton biomass is also included. A nonparametric one-way ANOVA (Kruskal-Wallis) was performed to test the null hypothesis that independent groups come from distributions with equal medians ($p < 0.05$; **$p < 0.01$; ***$p < 0.001$). The Bonferroni multiple comparison test was applied a posteriori to analyse the differences between every pair of groups (D, U, R). n, Indicates the number of cruises included in each hydrographic condition.*

Picoplankton Community Composition

Flow cytometry data showed that picoplankton biomass was largely dominated by heterotrophic bacteria (HNA and LNA), followed by picoeukaryotes (large and small), and finally cyanobacteria (*Synechococcus* and *Prochlorococcus*) (**Table 1**, Table S1, Figure S2). The averaged contribution of HNA bacteria to total biomass peaked (ca. 60%) during upwelling and relaxation conditions. Consistently with the information provided by size-fractionated chlorophyll *a*, which showed the predominance of small (<10 μm) cells during downwelling

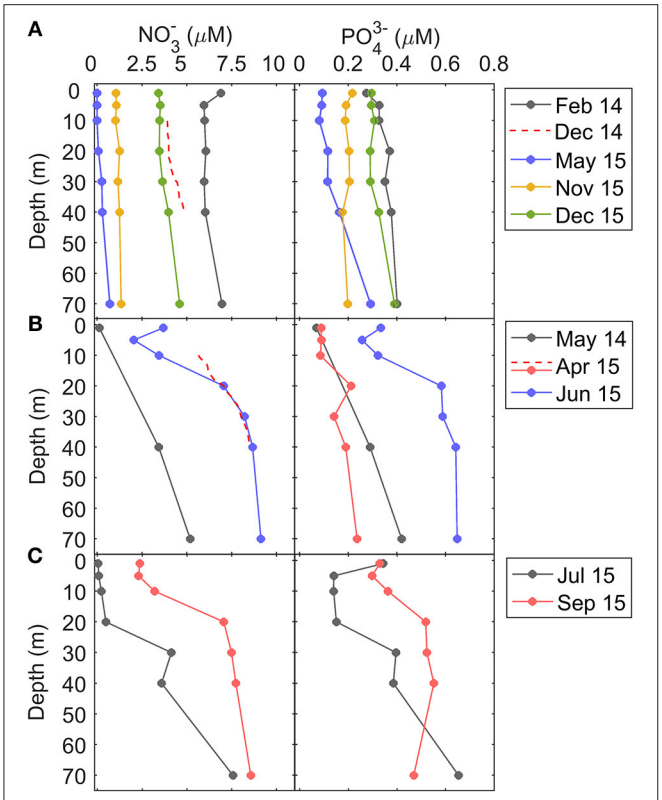

FIGURE 4 | Vertical distribution of nitrate (NO_3^-) and phosphate (PO_4^{3-}) concentration (μM) during **(A)** downwelling, **(B)** upwelling, and **(C)** relaxation conditions. Dashed line in nitrate profiles between 10 and 40 m depth in December 2014 and April 2015 indicate nitrate concentrations computed from the nitrate-density (σ_t) relationship (see section Materials and Methods).

(**Figure 5**), the averaged depth-integrated biomass of total picophytoplankton (i.e., large and small picoeukaryotes plus *Synechococcus* and *Prochlorococcus* cyanobacteria) (88 ± 48 mg C m^{-2}), was during this condition slightly higher than during upwelling (54 ± 23 mg C m^{-2}), and relaxation (31 ± 26 mg C m^{-2}).

The vertical distribution of picoeukaryotic biomass, which potentially would include the UCYN-A diazotroph-prymnesiophyte host (Thompson et al., 2012, 2014), was relatively homogeneous during downwelling, with the exception of May 2015, when the highest biomass (>3 µg C L^{-1}) was observed in the upper 40 m (**Figure 6**). During upwelling conditions, the vertical distribution of picoeukaryotes biomass showed small vertical variability in May 2014, whereas in April and June 2015 enhanced values (>2 µg C L^{-1}) were observed at the surface. During relaxation, small vertical variability was observed in July 2015, whereas in September 2015 enhanced values (>1.5 µg C L^{-1}) also occurred at surface waters.

Magnitude and Biogeochemical Relevance of Biological N_2 Fixation

No significant differences (Kruskal-Wallis, $p > 0.05$) were found between the BNF rates corresponding to the total and small (<10 µm) size-fractions (data not shown), suggesting that small diazotrophs, presumably unicellular, were responsible for all the BNF activity detected in the region. For this reason, only BNF rates corresponding to the total size-fraction are described here. Whereas no significant differences were observed in depth-integrated rates, which ranged from 0.1 ± 0.1 to 1.6 ± 0.5 µmol N m^{-2} d^{-1} (**Table 1**), contrasting vertical patterns were observed during downwelling, upwelling and relaxation conditions (**Figure 6**).

During downwelling, the vertical distribution of BNF was relatively homogeneous, and no significant differences were found between the rates determined at different depths (Kruskal-Wallis, $p > 0.05$) (**Figure 6**). Depth-integrated rates were slightly higher in December 2014 (1.3 ± 0.4 µmol N m^{-2} d^{-1}) and May 2015 (1.0 ± 0.3 µmol N m^{-2} d^{-1}), compared to November 2015 (0.3 ± 0.1 µmol N m^{-2} d^{-1}) and December 2015 (0.1 ± 0.1 µmol N m^{-2} d^{-1}). During both upwelling and relaxation conditions, maximum rates were observed in general at the surface, decreasing between 20 and 40 m and slightly increasing again at 70 m. Depth-integrated rates were higher in April 2015 (1.6 ± 0.5 µmol N m^{-2} d^{-1}, upwelling) and September 2015 (0.8 ± 0.1 µmol N m^{-2} d^{-1}, relaxation) compared to June 2015 (0.6 ± 0.3 µmol N m^{-2} d^{-1}, upwelling). As a result of the hydrographic patterns described, when considering all the samplings together, BNF was negatively correlated with mixed layer depth (Pearson's $r = -0.364$, $p < 0.05$), whereas a positive significant relationship was found with the primary production corresponding to the small (<10 µm) size-fraction (Pearson's $r = 0.573$, $p < 0.01$).

Due to the increased vertical diffusivity and vertical nitrate gradient determined during relaxation conditions, averaged nitrate diffusive fluxes during these samplings were more than six-fold higher (14.3 ± 3.1 mmol m^{-2} d^{-1}), compared to upwelling (2.2 ± 3.1 mmol m^{-2} d^{-1}), and downwelling (0.8 ± 0.9 mmol m^{-2} d^{-1}) conditions (**Table 1**, **Figures 3**, **4**). These numbers were between 2 and 5 orders of magnitude higher than the estimates of depth-integrated BNF (0.1 ± 0.1–1.6 ± 0.5 µmol m^{-2} d^{-1}) carried out during the NICANOR samplings. From a biogeochemical perspective, the comparison between these two processes evidences that the relevance of BNF in this system, which was relatively higher during the upwelling conditions sampled in April 2015, was always <2% (Table S1).

nifH Gene Abundances

Clone library analysis of the nitrogenase gene (*nifH*) recovered from DNA samples obtained during the NICANOR samplings revealed that most of sequenced clones belonged to unicellular cyanobacterial and heterotrophic bacterial diazotrophs (Moreira-Coello et al., in preparation). *nifH* clusters 1G (Gammaproteobacteria), 1B (Cyanobacteria) and 3E (Verrucomicrobia and Deltaproteobacteria) were the most abundant, representing 29, 21, and 22% of total *nifH* clones, respectively. The other clusters represented less than 8% of relative abundances each. Most of clones belonged to *Pseudomonas stutzeri* (1G) (21%), UCYN-A (1B) (21%), *Opitutaceae bacterium* (3E) (9%) and *Desulfovibrio aespoeensis* (3E) (8%), whereas the rest of diazotrophs represented <7%

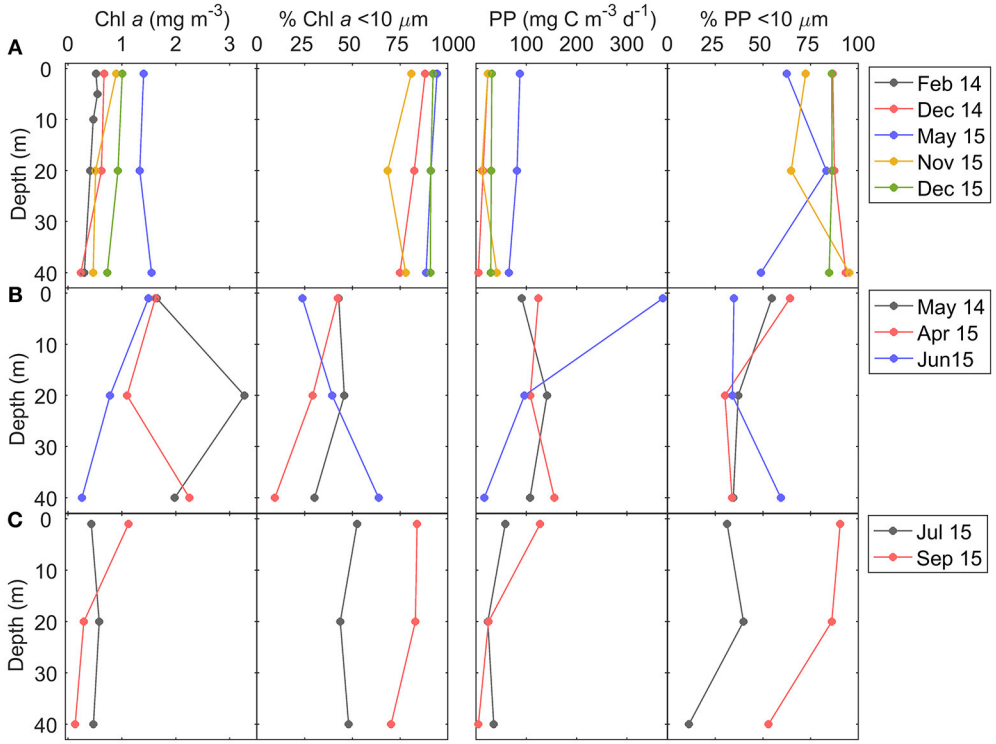

FIGURE 5 | Vertical distribution of total chlorophyll *a* concentration (Chl *a*), contribution of <10 μm size-fraction to total chlorophyll *a* (%), total primary production (PP), and contribution of <10 μm size-fraction to total primary production, during **(A)** downwelling, **(B)** upwelling, and **(C)** relaxation conditions.

each. Considering that the two most abundant groups were UCYN-A and Gammaproteobacteria-affiliated phylotypes (1G), we used the qPCR primers-probe sets available for quantifying UCYN-A sublineages (-A1 and -A2) and Gammaproteobacteria γ-24774A11 phylotype, widely distributed and considered one of the most important heterotrophic diazotrophs (e.g., Moisander et al., 2014; Langlois et al., 2015). The quantification of these diazotrophs allowed examining their relative importance through the year. All the abundances were above the limit of detection, except the abundance of UCYN-A1 determined at the surface in February 2014 (downwelling), and the abundances of Gammaproteobacteria determined at the surface and 40 m depth in May 2014 and April 2015 (upwelling) (**Figure 6**).

The Gammaproteobacteria phylotype was significantly more abundant than UCYN-A1 and UCYN-A2 during downwelling and relaxation (Bonferroni comparisons, $p < 0.05$) (**Table 1**, **Figure 6**). Although not statistically significant, both surface ($3.1 \pm 5.3 \times 10^2$ *nifH* copies L^{-1}) and depth-integrated ($13 \pm 23 \times 10^5$ *nifH* copies m^{-2}) abundances of Gammaproteobacteria were slightly lower during upwelling, as in May 2014 and April 2015 the abundances between 0 and 40 m depth were below LOD or DNQ limits (Table S1, Figure S1). During downwelling and relaxation conditions, Gammaproteobacteria showed vertical variability, reaching maximum abundances at 70 m depth. In November 2015 (downwelling) and September 2015 (relaxation) we found the highest surface (9.0×10^3 and 1.9×10^3 *nifH* copies L^{-1}, respectively) and depth-integrated abundances (380×10^5 and 220×10^5 *nifH* copies m^{-2}, respectively) measured on all cruises.

During relaxation, UCYN-A1 abundance increased at the surface, and both surface ($6.2 \pm 0.7 \times 10^2$ *nifH* copies L^{-1}) and depth-integrated ($13 \pm 0 \times 10^5$ *nifH* copies m^{-2}) abundance were significantly higher than during downwelling (33 ± 64 *nifH* copies L^{-1} and $1.4 \pm 1.3 \times 10^5$ *nifH* copies m^{-2}, respectively) and upwelling conditions ($1.9 \pm 0.3 \times 10^2$ *nifH* copies L^{-1} and $1.3 \pm 0.2 \times 10^5$ *nifH* copies m^{-2}, respectively), when the vertical distribution of this group did not exhibit important vertical variability (**Table 1**, **Figure 6**).

The abundance of UCYN-A2 was higher than UCYN-A1 (Kruskal-Wallis, $p < 0.05$) and showed larger vertical variability (**Figure 6**, Table S1). On average, surface and depth-integrated abundances of UCYN-A2 were slightly higher during relaxation ($8.7 \pm 8.6 \times 10^2$ *nifH* copies L^{-1} and $21 \pm 16 \times 10^5$ *nifH* copies m^{-2}, respectively), compared to upwelling ($4.3 \pm 5.6 \times 10^2$ *nifH* copies L^{-1} and $10 \pm 10 \times 10^5$ *nifH* copies m^{-2}, respectively) and downwelling ($1.4 \pm 2.4 \times 10^2$ *nifH* copies L^{-1} and $7 \pm 7 \times 10^5$ *nifH* copies m^{-2}, respectively) (**Table 1**). During downwelling, higher values occurred at 70 m in November 2015 (6.9×10^2 *nifH* copies L^{-1}), and also at the surface in December 2015 (5.0×10^2 *nifH* copies L^{-1}). During upwelling and relaxation, the maximum abundances were quantified at the surface in June 2015 (1.1×10^3 *nifH* copies L^{-1}) and September 2015 (1.5×10^3 *nifH* copies L^{-1}), respectively.

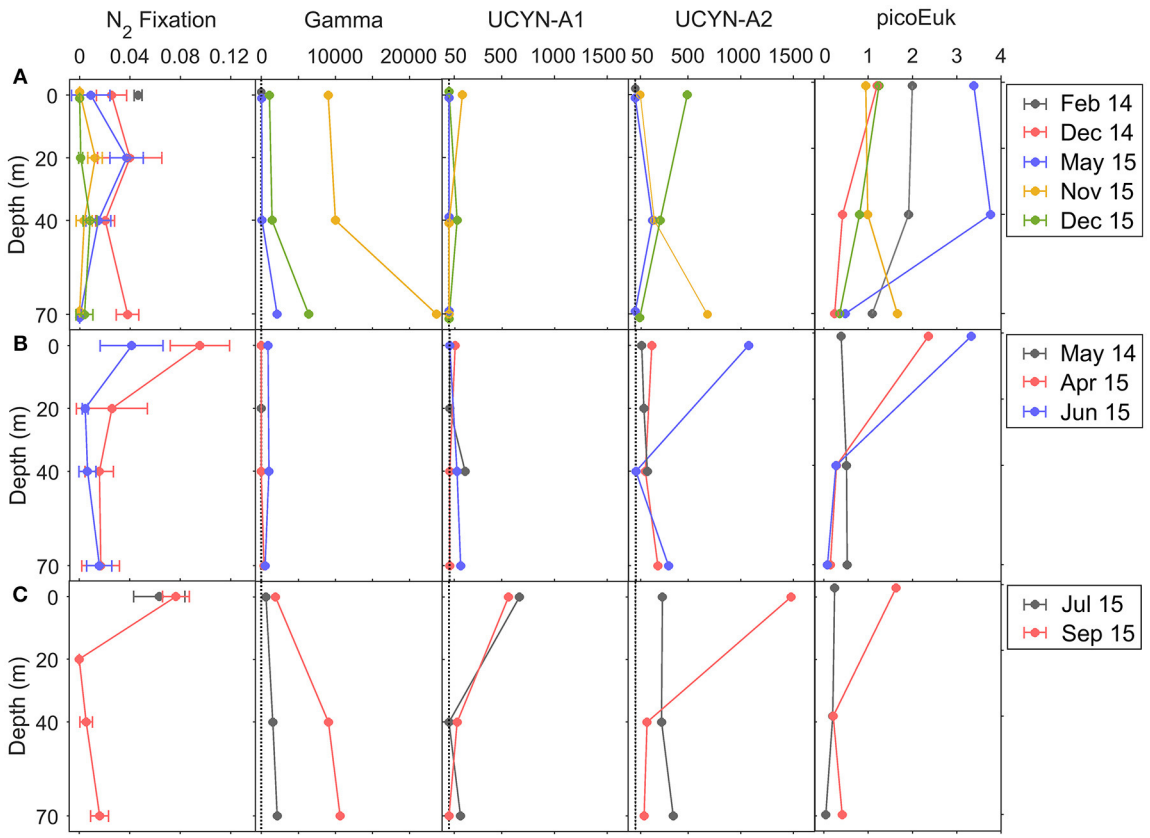

FIGURE 6 | Vertical distribution of BNF rates (μmol N m^{-3} d^{-1}), Gammaproteobacteria γ-24774A11, UCYN-A1, and UCYN-A2 *nifH* copies L^{-1}, and carbon biomass (μg C L^{-1}) of total (small+large) picoeukaryotes during **(A)** downwelling, **(B)** upwelling, and **(C)** relaxation conditions. Error bars in BNF panels represent standard deviation. Abundances below DNQ limit (detected but not quantified, <41 *nifH* copies L^{-1}) were assigned a conservative value of 1 *nifH* copy L^{-1}, which is indicated by a dotted line on the charts.

DISCUSSION

Magnitude and Biogeochemical Relevance of BNF

Our results demonstrate the existence of detectable BNF activity (0.001 ± 0.002–0.095 ± 0.024 μmol N m^{-3} d^{-1}) under contrasting hydrographic regimes in a nitrogen-rich temperate coastal system subjected to upwelling pulses. During downwelling-influenced cruises the vertical pattern of BNF was rather homogeneous, whereas during upwelling and relaxation the BNF rates peaked in the well-lit surface waters, where we measured the highest rates of all cruises. Comparing with other studies using the same technique ($^{15}N_2$-gas tracer method, Montoya et al., 1996) and performed in similar nitrate-rich and temperate areas, our volumetric BNF rates were of similar magnitude to those measured by Benavides et al. (2011) in Cape Silleiro (NW Iberian Peninsula) in summer 2009, but between 1 and 3 orders of magnitude lower than those measured by Mulholland et al. (2012) in the temperate NE American coast during several summer and autumn cruises, and by Rees et al. (2009) in the western English Channel in summer. On a global context, our BNF rates estimated in the outer part of Ría de A Coruña are similar to the lower-end described for the subtropical NE Atlantic (Luo et al., 2012). Although our rates were relatively low, our results contradict the traditional paradigm about marine BNF. This view established that BNF is mainly restricted to the nitrogen-poor, warm (>20°C) (sub)tropical ocean, as high nutrient inputs and the relatively low surface temperatures in temperate coastal systems would not favor N_2 fixation (Howarth et al., 1988; Conley et al., 2009; Stal, 2009). The BNF activity detected in this study is a further evidence that high nitrate concentrations (and high N:P ratios) do not inhibit BNF activity, such as it was also observed in other upwelling regions (e.g., Voss et al., 2004; Sohm et al., 2011; Subramaniam et al., 2013; Benavides et al., 2014). Indeed, recent studies demonstrated that BNF can occur upon exposure to elevated DIN (nitrate and/or ammonium), as long as phosphate is available (Knapp, 2012), and point toward iron as the primary control factor of BNF (Knapp et al., 2016; Bonnet et al., 2017). Thus, the sensitivity of marine BNF to high DIN is not clear. Along with the wide distribution and large diversity of diazotrophs (Zehr et al., 2000; Moisander et al., 2010), our results indicate that restricting BNF measurements exclusively to oligotrophic (sub)tropical regions may result in an underestimation of the global magnitude of this

flux, contributing to the apparent imbalances observed in the marine N budget (Brandes and Devol, 2002; Mahaffey et al., 2005; Codispoti, 2007).

The contribution of BNF to new N supply into the euphotic zone was negligible (<2%) in this system, as it was between 2 and 5 orders of magnitude lower than diffusive fluxes. These numbers represent the first estimate of the contribution of both processes in a coastal upwelling system. Few studies have simultaneously quantified BNF and nitrate diffusion (Mouriño-Carballido et al., 2011; Painter et al., 2013; Fernández-Castro et al., 2015), mainly due to the methodological difficulties to estimate vertical mixing (*Kz*) in the field, which has frequently motivated the use of constant values of *Kz* (Capone et al., 2005), and empirical parameterizations (Planas et al., 1999; Fernández-Castro et al., 2014). Capone et al. (2005) estimated in the tropical North Atlantic that BNF could equal or even exceed nitrate vertical diffusion into the euphotic zone. In the subtropical NE Atlantic, Mouriño-Carballido et al. (2011) reported a contribution of BNF to new nitrogen input of 2 ± 2%, whereas Painter et al. (2013) indicated that BNF represented a significant source of new N, but not as large as the diffusive fluxes. In their study across the (sub)tropical Atlantic, Pacific and Indian oceans, Fernández-Castro et al. (2015) pointed out that, on average and compared to BNF, nitrate diffusion was the main mechanism supplying new N. The magnitude of averaged nitrate diffusion estimated in our study (3.9 ± 5.8 mmol m^{-2} d^{-1}) was slightly higher than the estimations for the subtropical NE Atlantic by Mouriño-Carballido et al. (2011) (0.8 ± 1.3 mmol m^{-2} d^{-1}) and Painter et al. (2013) (0.06 ± 0.02 mmol m^{-2} d^{-1}), and by Fernández-Castro et al. (2015) (0.2 ± 0.2 mmol m^{-2} d^{-1}) in the (sub)tropical Atlantic, Pacific and Indian oceans. The range of diffusive fluxes here reported (0.1–16.5 mmol m^{-2} d^{-1}) was comparable to that obtained in a nearby coastal system (Ría de Vigo, NW Iberia) by Cermeño et al. (2016) (0.8–20.1 mmol m^{-2} d^{-1}) and Villamaña et al. (2017) (9.4–34.6 mmol m^{-2} d^{-1}).

We cannot discard that our N_2 fixation rates may be underestimated (Mohr et al., 2010; Großkopf et al., 2012) due to the use of the $^{15}N_2$-bubble addition technique (Montoya et al., 1996) instead of the modified tracer method with $^{15}N_2$-enriched seawater (Mohr et al., 2010). However, the biogeochemical relevance of BNF in this system would be still very low since other important mechanisms of new N supply, such as advective vertical and horizontal transport, atmospheric deposition or internal waves (Oschlies and Garçon, 1998; Duce et al., 2008; Villamaña et al., 2017), were not taken into account in this study.

In order to get a rough estimation of the fertilization effect of the upwelling, we compared a simplified estimate of nitrate supply through vertical advection (see Materials and Methods) with the input of nitrogen through nitrate vertical diffusion. As expected, nitrate vertical advection was the main mechanism of N supply during upwelling (79 ± 119 mmol m^{-2} d^{-1}) and during relaxation in September 2015 (77 mmol m^{-2} d^{-1}), which was probably influenced by an upwelling pulse happening a few days before the sampling. This nitrogen supply was more than 180-fold higher than nitrate diffusion during upwelling, and up to 6-fold higher in September 2015. Obviously, non-upwelling situations implied higher contribution to new N supply by diffusion. In any case, the consideration of this process would decrease, even more, the contribution of BNF to the new nitrogen supply in this system. Overall, the proportion of gross primary production (GPP) that could be sustained by diazotrophy, calculated by assuming Redfield stoichiometry, would be irrelevant (<0.1%) when compared to the proportion of GPP supported by nitrate (41.9 ± 31.2%) and ammonium (6.8 ± 5.0%) uptake rates, measured in the same region in an earlier study (Bode et al., 2004).

Players

Small diazotrophs (<10 μm), presumably unicellular, were responsible for all BNF activity detected in this region. This is consistent with analysis of the *nifH* clone library, which revealed that most of sequenced clones belonged to unicellular cyanobacterial and heterotrophic diazotrophs (Moreira-Coello et al., in preparation). Most of *nifH* clones belonged to Gammaproteobacteria-affiliated phylotypes of the cluster 1G (29%) and UCYN-A (21%).

The abundance of Gammaproteobacteria γ-24774A11 phylotype (0–2.4 × 10^4 *nifH* copies L^{-1}) was significantly higher than UCYN-A1 and UCYN-A2 during downwelling and relaxation (Bonferroni comparisons, $p < 0.05$). These values were in the medium-high range of global abundances reviewed by Luo et al. (2012), and by Benavides and Voss (2015) specifically from studies performed in the North Atlantic. In fact, heterotrophic diazotrophs abundances higher than 10^4 *nifH* copies L^{-1} have seldom been reported in the marine environment (e.g., Moisander et al., 2008; Halm et al., 2012). The abundance of the heterotrophic Gammaproteobacteria was positively correlated with temperature (Pearson's $r = 0.473$, $p < 0.05$) and mixed layer depth (Pearson's $r = 0.495$, $p < 0.05$), since slightly higher abundances were measured during downwelling conditions, when the water column was warmer, less stratified and probably depleted in bioessential nutrients. These hydrographic features could cause the dominance of Gammaproteobacteria as the primary productivity was low and dominated by small cells, and likely sustained by regenerated nutrients (mainly nitrogen) through bacterial remineralisation of organic matter, such as it was observed previously in this region (Bode et al., 2004, 2011). The production based on bacterial recycling of nutrients may also have occurred in September 2015, when the abundance of Gammaproteobacteria increased significantly, probably fueled by the organic matter produced during the upwelling pulse happening before the sampling (Bode et al., 1996; Casas et al., 1997).

The symbiosis of UCYN-A with picoeukaryotic prymnesiophyte cells also thrives in these nitrogen-rich and relatively cold (<17°C) waters. Similar findings were also reported by Agawin et al. (2014) and Benavides et al. (2011) in the same upwelling region, and by Mulholland et al. (2012) in the N-rich temperate NE American coast. Furthermore, UCYN-A1 and its small uncultured host were detected in the Galician Bank, an open ocean environment relatively close to our region (Cabello et al., 2015). Foster et al. (2009) also found abundant UCYN-A in the nutrient-rich Equatorial Atlantic upwelling area in summer 2007.

The pattern of vertical distribution of picoeukaryotes was consistent with those of UCYN-A. When the abundances of UCYN-A peaked, the biomass of the picophytoplankton also peaked (but not vice versa), except in July 2015, when the consistency was observed in the profile of abundance (data not shown). Indeed, qPCR analysis of picoeukaryotic populations sorted with flow cytometry unequivocally demonstrated that UCYN-A are associated with picoeukaryotes (Thompson et al., 2012, 2014). Furthermore, we did not find a link between UCYN-A abundance and phytoplankton biomass (Chlorophyll *a*), which could be expected on the basis of the symbiotic association of UCYN-A with a photosynthetic prymnesiophyte in regions where picoplankton dominates phytoplankton biomass, such as it was previously observed in the oligotrophic (sub)tropical SW Pacific (Moisander et al., 2010). This decoupling was probably due to the fact that our study was carried out in an upwelling system, where usually most biomass corresponds to large phytoplankton (>10 μm), mainly chain-forming diatoms (Casas et al., 1997; Varela et al., 2001).

The abundance of UCYN-A2 sublineage (1–1.5 × 10^3 *nifH* copies L^{-1}) was on average 3-fold higher than that of UCYN-A1 (0–6.7 × 10^2 *nifH* copies L^{-1}). The higher UCYN-A2 abundance is consistent with recent findings pointing out this sublineage, although globally distributed (Cabello et al., 2015; Martínez-Pérez et al., 2016), mainly inhabit coastal regions, whereas UCYN-A1 dominates in the oligotrophic open ocean (Thompson et al., 2014; Messer et al., 2015; Turk-Kubo et al., 2017). The UCYN-A abundances detected were in the medium-low range of global abundances reported by Luo et al. (2012), Martínez-Pérez et al. (2016), and Benavides and Voss (2015) in the North Atlantic. In the temperate NE American coast, Mulholland et al. (2012) showed that UCYN-A was the most abundant diazotroph, reaching 3.5 × 10^7 *nifH* copies L^{-1}, among the highest abundances ever observed. Several studies performed in the North Atlantic reported that, after *Trichodesmium,* UCYN-A is the most abundant diazotrophic phylotype (Benavides and Voss, 2015; Ratten et al., 2015; Benavides et al., 2016). Even though it extends along a wide latitudinal and longitudinal range, it dominates mainly the eastern basin, where iron inputs by Saharan dust are higher (Benavides et al., 2013), which favors its growth and N_2-fixing activity (Krupke et al., 2015).

Higher abundances of UCYN-A1 and UCYN-A2 occurred at the well-lit surface waters during upwelling and relaxation conditions, suggesting a possible seasonal variability on the growth of the UCYN-A–prymnesiophyte symbiosis, such as it was previously observed in the (sub)tropical SW Pacific (Moisander et al., 2010; Bonnet et al., 2015). These high values coincided with the highest BNF rates, and in fact UCYN-A abundances were positively correlated with BNF rates (Pearson's $r = 0.534$, $p < 0.05$), consistent with the fact that small diazotrophs (<10 μm) were responsible for all BNF activity in this system. This relationship has also been observed in other regions, as the NE American coast (Mulholland et al., 2012), or the tropical SW Pacific (Bonnet et al., 2015). Therefore, UCYN-A–prymnesiophyte associations may be responsible for most BNF activity, or at least a large fraction, in our region, since Gammaproteobacteria abundance and BNF rates were not correlated or consistent. Turk-Kubo et al. (2014) reported that Gammaproteobacteria phylotypes do not contribute significantly to marine BNF, based on their analysis of heterotrophic cell-specific N_2 fixation rates required to explain previously reported BNF rates in different marine environments (e.g., Zehr et al., 2007; Großkopf et al., 2012; Halm et al., 2012; Farnelid et al., 2013). In our study, average cell-specific N_2 fixation rates required to account for BNF rates (see Material and Methods) ranged from 0.8 fmol N $cell^{-1}$ h^{-1} (November 2015, 40 m) to 19.3 fmol N $cell^{-1}$ h^{-1} (April 2015, 0 m). Therefore, in several samples UCYN-A may have been responsible for all the BNF activity, since cell-specific rates estimated for this diazotrophic group range from 0.02 to 2.6 fmol N $cell^{-1}$ h^{-1} (Goebel et al., 2010). However, in some samples the required cell-specific rates are too high to be due solely to the UCYN-A quantified. Thus, BNF rates may result from small contributions from Gammaproteobacteria phylotypes or other diazotrophs that we have not quantified by qPCR.

OUTLOOK

Our study provides a novel assessment of the magnitude and seasonal variability of BNF, its contribution to the budget of new N inputs into the euphotic zone, and the abundance of diazotrophs in a NE Atlantic temperate upwelling region, subjected to contrasting hydrographic regimes. In contrast, most studies focusing on marine BNF have been conducted in the western basin, and in the (sub)tropical North Atlantic. BNF activity and presence of diazotrophs have been demonstrated in a N-rich temperate region, even though their ecological role remains unclear. This will require further spatial–temporal studies in the zone. By calculating the geometric mean of depth-integrated BNF rates estimated during the NICANOR cruises and assuming the surface area of a 3° × 3° grid cell (following Luo et al., 2012), we estimated an averaged new N input in the study area of about 0.4 Gg N $year^{-1}$ from planktonic BNF. In the region of the Canary Current and NW African upwelling, Benavides et al. (2011) estimated an input of 0–20 Gg N $year^{-1}$, whereas Mulholland et al. (2012) estimated an input of 0.5–107 × 10^3 Gg N $year^{-1}$ in the temperate NE American coast (Luo et al., 2012; Benavides and Voss, 2015). Therefore, the current biogeochemical relevance of BNF in our study system is negligible. However, the weakening of the Iberian coastal upwelling in the last decades (Pérez et al., 2010; Pardo et al., 2011), and the enhancement of stratification due to the warming in ocean surface waters might favor an increase of the relative importance of the diazotrophy in the future (Boyd and Doney, 2002; Doney, 2006). In any case, the study of the BNF processes and the responsible organisms in this region shed light on the ecophysiology of the present diazotrophic community. This first report of the presence of UCYN-A and Gammaproteobacteria γ-24774A11 in this region extends the geographic area where these diazotrophs thrive. Moreover, it provides further evidence of the co-occurrence of the UCYN-A sublineages, their wide distribution in the ocean (Farnelid et al., 2016; Martínez-Pérez et al., 2016), as well as their ability to grow in relatively cold waters with high DIN concentrations. Considering the large diversity of marine diazotrophs, and our limited knowledge of their physiology and ecology, sustained observational efforts

throughout the ocean will be required to delimit accurately the magnitude and variability of marine BNF.

AUTHOR CONTRIBUTIONS

BM and EM conceived the overall study. VM, BM, EM, AF, AB, and MV designed the experiments and analyzed the data. VM collected the samples, performed the microstructure turbulence measurements and the molecular analysis. VM and AF performed the N_2 fixation measurements. VM and BM analyzed the microstructure turbulence data. AB performed the chlorophyll *a* and primary production measurements. BM, EM, AB, and MV supplied reagents/materials/analysis tools and equipment. VM wrote the manuscript with contributions from all coauthors.

FUNDING

This work was funded by the NICANOR project (Galician Government, EM2013/021) granted to BM and by the RADIALES project of the *Instituto Español de Oceanografía* (http://www.seriestemporales-ieo.com). VM was supported by a FPU predoctoral fellowship from the Spanish Ministry of Education, Culture and Sports (FPU13/01674).

ACKNOWLEDGMENTS

We thank the crew of the B/O *Lura* for their support during the sampling at sea. We are also very grateful to Paloma Chouciño, Antonio Fuentes, Elisa Guerrero-Feijoo, Carlota Rodríguez, and Ángel F. Lamas for logistic and technical support during the work at sea and in the lab. Special thanks to Fátima Eiroa for the flow cytometry analysis.

SUPPLEMENTARY MATERIAL

The Supplementary Material for this article can be found online at: http://journal.frontiersin.org/article/10.3389/fmars.2017.00303/full#supplementary-material

REFERENCES

Agawin, N. S. R., Benavides, M., Busquets, A., Ferriol, P., Stal, L. J., and Arístegui, J. (2014). Dominance of unicellular cyanobacteria in the diazotrophic community in the Atlantic Ocean. *Limnol. Oceanogr.* 59, 623–637. doi: 10.4319/lo.2014.59.2.0623

Álvarez-Salgado, X. A., Beloso, S., Joint, I., Nogueira, E., Chou, L., Pérez, F. F., et al. (2002). New production of the NW Iberian shelf during the upwelling season over the period 1982-1999. *Deep Res. I* 49, 1725–1739. doi: 10.1016/S0967-0637(02)00094-8

Álvarez-Salgado, X. A., Gago, J., Míguez, B. M., Gilcoto, M., and Pérez, F. F. (2000). Surface waters of the NW Iberian margin: upwelling on the Shelf versus outwelling of upwelled waters from the Rías Baixas. *Estuar. Coast. Shelf Sci.* 51, 821–837. doi: 10.1006/ecss.2000.0714

Aminot, A., and Kerouel, R. (2007). *Dosage Automatique des Nutriments Dans les Eaux Marines: Méthodes en Flux Continu. Méthodes D'analyse en Milieu Marin*. Plouzané: Ifremer.

Arístegui, J., Barton, E. D., Álvarez-Salgado, X. A., Santos, A. M. P., Figueiras, F. G., Kifani, S., et al. (2009). Sub-regional ecosystem variability in the canary current upwelling. *Prog. Oceanogr.* 83, 33–48. doi: 10.1016/j.pocean.2009.07.031

Benavides, M., Agawin, N., Arístegui, J., Ferriol, P., and Stal, L. (2011). Nitrogen fixation by Trichodesmium and small diazotrophs in the subtropical northeast Atlantic. *Aquat. Microb. Ecol.* 65, 43–53. doi: 10.3354/ame01534

Benavides, M., and Voss, M. (2015). Five decades of N_2 fixation research in the North Atlantic Ocean. *Front. Mar. Sci.* 2:40. doi: 10.3389/fmars.2015.00040

Benavides, M., Arístegui, J., Agawin, N. S. R., López Cancio, J., and Hernández-León, S. (2013). Enhancement of nitrogen fixation rates by unicellular diazotrophs vs. Trichodesmium after a dust deposition event in the Canary Islands. *Limnol. Oceanogr.* 58, 267–275. doi: 10.4319/lo.2013.58.1.0267

Benavides, M., Moisander, P. H., Daley, M. C., Bode, A., and Arístegui, J. (2016). Longitudinal variability of diazotroph abundances in the subtropical North Atlantic Ocean. *J. Plankton Res.* 38, 662–672. doi: 10.1093/plankt/fbv121

Benavides, M., Santana-Falcón, Y., Wasmund, N., and Arístegui, J. (2014). Microbial uptake and regeneration of inorganic nitrogen off the coastal Namibian upwelling system. *J. Mar. Syst.* 140, 123–129. doi: 10.1016/j.jmarsys.2014.05.002

Bentzon-Tilia, M., Traving, S. J., Mantikci, M., Knudsen-Leerbeck, H., Hansen, J. L., Markager, S., et al. (2015). Significant N_2 fixation by heterotrophs, photoheterotrophs and heterocystous cyanobacteria in two temperate estuaries. *ISME J.* 9, 273–285. doi: 10.1038/ismej.2014.119

Bjørnsen, P. K. (1986). Automatic determination of Bacterioplankton biomass by image analysis. *Appl. Environ. Microbiol.* 51, 1199–1204.

Bode, A., Anadón, R., Morán, X. A. G., Nogueira, E., Teira, E., and Varela, M. (2011). Decadal variability in chlorophyll and primary production off NW Spain. *Clim. Res.* 48, 293–305. doi: 10.3354/cr00935

Bode, A., Barquero, S., González, N., Alvarez-Ossorio, M. T., and Varela, M. (2004). Contribution of heterotrophic plankton to nitrogen regeneration in the upwelling ecosystem of A Coruña (NW Spain). *J. Plankton Res.* 26, 11–28. doi: 10.1093/plankt/fbh003

Bode, A., Casas, B., Fernández, E., Marañón, E., Serret, P., and Varela, M. (1996). Phytoplankton biomass and production in shelf waters off NW Spain: spatial and seasonal variability in relation to upwelling. *Hydrobiologia* 341, 225–234.

Bonnet, S., Caffin, M., Berthelot, H., and Moutin, T. (2017). Hot spot of N_2 fixation in the western tropical South Pacific pleads for a spatial decoupling between N_2 fixation and denitrification. *Proc. Natl. Acad. Sci.* 114, 2800–2801. doi: 10.1073/pnas.1619514114

Bonnet, S., Rodier, M., Turk-Kubo, K., Germineaud, C., Menkes, C., Ganachaud, A., et al. (2015). Contrasted geographical distribution of N_2 fixation rates and nifH phylotypes in the Coral and Solomon Seas (southwestern Pacific) during austral winter conditions. *Glob. Biogeochem. Cycles* 29, 1874–1892. doi: 10.1002/2015GB005117

Boyd, P. W., and Doney, S. C. (2002). Modelling regional responses by marine pelagic ecosystems to global climate change. *Geophys. Res. Lett.* 29, 53-1–53-4. doi: 10.1029/2001GL014130

Brandes, J. A., and Devol, A. H. (2002). A global marine-fixed nitrogen isotopic budget: Implications for Holocene nitrogen cycling. *Glob. Biogeochem. Cycles* 16, 0–1. doi: 10.1029/2001GB001856

Cabello, A. M., Cornejo-Castillo, F. M., Raho, N., Blasco, D., Vidal, M., Audic, S., et al. (2015). Global distribution and vertical patterns of a prymnesiophyte–cyanobacteria obligate symbiosis. *ISME J.* 10, 693–706. doi: 10.1038/ismej.2015.147

Calvo-Díaz, A., and Morán, X. A. G. (2006). Seasonal dynamics of picoplankton in shelf waters of the southern Bay of Biscay. *Aquat. Microb. Ecol.* 42, 159–174. doi: 10.3354/ame042159

Capone, D. G., Burns, J. A., Montoya, J. P., Subramaniam, A., Mahaffey, C., Gunderson, T., et al. (2005). Nitrogen fixation by *Trichodesmium* spp.: an important source of new nitrogen to the tropical and subtropical North Atlantic Ocean. *Glob. Biogeochem. Cycles* 19, GB2024. doi: 10.1029/2004GB002331

Casas, B., Varela, M., Canle, M., González, N., and Bode, A. (1997). Seasonal variations of nutrients, seston and Phytoplankton, and upwelling

intensity off La Coruña (NW Spain). *Estuar. Coast. Shelf Sci.* 44, 767–778. doi: 10.1006/ecss.1996.0155

Cermeño, P., Chouciño, P., Fernández-Castro, B., Figueiras, F. G., Marañón, E., Marrase, C., et al. (2016). Marine primary productivity is driven by a selection effect. *Front. Mar. Sci.* 3:173. doi: 10.3389/fmars.2016.00173

Church, M. J., Jenkins, B. D., Karl, D. M., and Zehr, J. P. (2005). Vertical distributions of nitrogen-fixing phylotypes at Station ALOHA in the oligotrophic North Pacific Ocean. *Aquat. Microb. Ecol.* 38, 3–14. doi: 10.3354/ame038003

Codispoti, L. A. (2007). An oceanic fixed nitrogen sink exceeding 400 Tg N a^{-1} vs the concept of homeostasis in the fixed-nitrogen inventory. *Biogeosci. Discuss.* 4, 233–253. doi: 10.5194/bg-4-233-2007

Conley, D. J., Paerl, H. W., Howarth, R. W., Boesch, D. F., Seitzinger, S. P., Havens, K. E., et al. (2009). Controlling eutrophication: nitrogen and phosphorus. *Science* 323, 1014–1015. doi: 10.1126/science.1167755

Dabundo, R., Lehmann, M. F., Treibergs, L., Tobias, C. R., Altabet, M. A., Moisander, P. H., et al. (2014). The contamination of commercial $^{15}N_2$ Gas Stocks with ^{15}N–labeled nitrate and ammonium and consequences for nitrogen fixation measurements. *PLoS ONE* 9:e110335. doi: 10.1371/journal.pone.0110335

Doney, S. C. (2006). Oceanography: plankton in a warmer world. *Nature* 444, 695–696. doi: 10.1038/444695a

Duce, R. A, LaRoche, J., Altieri, K., Arrigo, K. R., Baker, A. R., Capone, D. G., et al. (2008). Impacts of atmospheric anthropogenic nitrogen on the open ocean. *Science* 320, 893–897. doi: 10.1126/science.1150369

Farnelid, H., Bentzon-Tilia, M., Andersson, A.F., Bertilsson, S., Jost, G., Labrenz, M., et al. (2013). Active nitrogen-fixing heterotrophic bacteria at and below the chemocline of the central Baltic Sea. *ISME J.* 7, 1413–1423. doi: 10.1038/ismej.2013.26

Farnelid, H., Turk-Kubo, K., Muñoz-Marín, M., and Zehr, J. (2016). New insights into the ecology of the globally significant uncultured nitrogen-fixing symbiont UCYN-A. *Aquat. Microb. Ecol.* 77, 125–138. doi: 10.3354/ame01794

Fernández, C., Lorena González, M., Munoz, C., Molina, V., and Farías, L. (2015). Temporal and spatial variability of biological nitrogen fixation off the upwelling system of central Chile (35–38.5°S). *J. Geophys. Res. Ocean* 120, 3330–3349. doi: 10.1002/2014JC010410

Fernández-Castro, B., Mouriño-Carballido, B., Benítez-Barrios, V. M., Chouciño, P., Fraile-Nuez, E., Graña, R., et al. (2014). Microstructure turbulence and diffusivity parameterization in the tropical and subtropical Atlantic, Pacific and Indian Oceans during the Malaspina 2010 expedition. *Deep Res. I Oceanogr. Res. Pap.* 94, 15–30. doi: 10.1016/j.dsr.2014.08.006

Fernández-Castro, B., Mouriño-Carballido, B., Marañón, E., Chouciño, P., Gago, J., Ramírez, T., et al. (2015). Importance of salt fingering for new nitrogen supply in the oligotrophic ocean. *Nat. Commun.* 6, 1–10. doi: 10.1038/ncomms9002

Fernández-Castro, B., Pahlow, M., Mouriño-Carballido, B., Marañón, E., and Oschlies, A. (2016). Optimality-based Trichodesmium diazotrophy in the North Atlantic subtropical gyre. *J. Plankton Res.* 38, 946–963. doi: 10.1093/plankt/fbw047

Foster, R. A, Subramaniam, A, and Zehr, J. P. (2009). Distribution and activity of diazotrophs in the Eastern Equatorial Atlantic. *Environ. Microbiol.* 11, 741–750. doi: 10.1111/j.1462-2920.2008.01796.x

Fraga, F. (1981). Upwelling off the Galician Coast, northwest Spain. *Coast. Upwelling* 1, 176–182. doi: 10.1029/CO001p0176

Gilcoto, M., Largier, J. L., Barton, E. D., Piedracoba, S.,Torres, R., Graña, R. et al. (2017). Rapid response to coastal upwelling in a semienclosed bay. *Geophys. Res. Lett.* 44, 2388–2397. doi: 10.1002/2016GL072416.

Goebel, N. L., Turk, K. A., Achilles, K. M., Paerl, R., Hewson, I., Morrison, A. E., et al. (2010). Abundance and distribution of major groups of diazotrophic cyanobacteria and their potential contribution to N_2 fixation in the tropical Atlantic Ocean. *Environ. Microbiol.* 12, 3272–3289. doi: 10.1111/j.1462-2920.2010.02303.x

Grosse, J., Bombar, D., Doan, H. N., Nguyen, L. N., and Voss, M. (2010). The Mekong River plume fuels nitrogen fixation and determines phytoplankton species distribution in the South China Sea during low- and high-discharge season. *Limnol. Oceanogr.* 55, 1668–1680. doi: 10.4319/lo.2010.55.4.1668

Großkopf, T., Mohr, W., Baustian, T., Schunck, H., Gill, D., Kuypers, M. M. M., et al. (2012). Doubling of marine dinitrogen-fixation rates based on direct measurements. *Nature* 488, 361–364. doi: 10.1038/nature11338

Gruber, N., and Galloway, J. N. (2008). An Earth-system perspective of the global nitrogen cycle. *Nature* 451, 293–296. doi: 10.1038/nature06592

Halm, H., Lam, P., Ferdelman, T. G., Lavik, G., Dittmar, T., LaRoche, J., et al. (2012). Heterotrophic organisms dominate nitrogen fixation in the South Pacific gyre. *ISME J.* 6, 1238–1249. doi: 10.1038/ismej.2011.182

Holl, C. M., and Montoya, J. P. (2005). Interactions between nitrate uptake and nitrogen fixation in continuous cultures of the marine diazotroph *Trichodesmium* (Cyanobacteria). *J. Phycol.* 41, 1178–1183. doi: 10.1111/j.1529-8817.2005.00146.x

Howarth, R. W., Marino, R., Lane, J., and Cole, J. J. (1988). Nitrogen fixation in freshwater, estuarine, and marine ecosystems. 1. Rates and importance. *Limnol. Oceanogr.* 33, 669–687.

Karl, D., Michaels, A., Bergman, B., Capone, D., Carpenter, E., Letelier, R., et al. (2002). Dinitrogen fixation in the world's oceans. *Biogeochemistry* 57/58, 47–98. doi: 10.1023/A:1015798105851

Knapp, A. N. (2012). The sensitivity of marine N_2 fixation to dissolved inorganic nitrogen. *Front. Microbiol.* 3, 1–14. doi: 10.3389/fmicb.2012.00374

Knapp, A. N., Casciotti, K. L., Berelson, W. M., Prokopenko, M. G., and Capone, D. G. (2016). Low rates of nitrogen fixation in eastern tropical South Pacific surface waters. *Proc. Natl. Acad. Sci. U.S.A.* 113, 4398–4403. doi: 10.1073/pnas.1515641113

Krupke, A., Mohr, W., Laroche, J., Fuchs, B. M., Amann, R. I., and Kuypers, M. M. M. (2015). The effect of nutrients on carbon and nitrogen fixation by the UCYN-A – haptophyte symbiosis. *ISME J.* 9, 1635–1647. doi: 10.1038/ismej.2014.253

Langlois, R., Großkopf, T., Mills, M., Takeda, S., and LaRoche, J. (2015). Widespread distribution and expression of Gamma A (UMB), an uncultured, diazotrophic, γ-proteobacterial *nifH* phylotype. *PLoS ONE* 10, 1–17. doi: 10.1371/journal.pone.0128912

Luo, Y. W., Lima, I. D., Karl, D. M., Deutsch, C. A., and Doney, S. C. (2014). Data-based assessment of environmental controls on global marine nitrogen fixation. *Biogeosciences* 11, 691–708. doi: 10.5194/bg-11-691-2014

Luo, Y. W., Doney, S. C., Anderson, L. A., Benavides, M., Bode, A., Bonnet, S., et al. (2012). Database of diazotrophs in global ocean: abundances, biomass and nitrogen fixation rates. *Earth Syst. Sci. Data Discuss.* 5, 47–106. doi: 10.5194/essdd-5-47-2012

Mahaffey, C., Michaels, A. F., and Capone, D. G. (2005). The conundrum of Marine N_2 fixation. *Am. J. Sci.* 305, 546–595. doi: 10.2475/ajs.305.6-8.546

Martínez-Pérez, C., Mohr, W., Löscher, C. R., Dekaezemacker, J., Littmann, S., Yilmaz, P., et al. (2016). The small unicellular diazotrophic symbiont, UCYN-A, is a key player in the marine nitrogen cycle. *Nat. Microbiol.* 1:16163. doi: 10.1038/nmicrobiol.2016.163

Messer, L. F., Doubell, M., Jeffries, T. C., Brown, M. V., and Seymour, J. R. (2015). Prokaryotic and diazotrophic population dynamics within a large oligotrophic inverse estuary. *Aquat. Microb. Ecol.* 74, 1–15. doi: 10.3354/ame01726

Mohr, W., Großkopf, T., Wallace, D. W. R., and LaRoche, J. (2010). Methodological underestimation of oceanic nitrogen fixation rates. *PLoS ONE* 5, 1–7. doi: 10.1371/journal.pone.0012583

Moisander, P. H., Beinart, R. A, Hewson, I., White, A. E., Johnson, K. S., Carlson, C. A, et al. (2010). Unicellular cyanobacterial distributions broaden the oceanic N_2 fixation domain. *Science* 327, 1512–1514. doi: 10.1126/science.1185468

Moisander, P. H., Beinart, R. A., Voss, M., and Zehr, J. P. (2008). Diversity and abundance of diazotrophic microorganisms in the South China Sea during intermonsoon. *ISME J.* 2, 954–967. doi: 10.1038/ismej.2008.51

Moisander, P. H., Serros, T., Paerl, R. W., Beinart, R. A., and Zehr, J. P. (2014). Gammaproteobacterial diazotrophs and *nifH* gene expression in surface waters of the South Pacific Ocean. *ISME J.* 8, 1962–1973. doi: 10.1038/ismej.2014.49

Monteiro, F. M., Dutkiewicz, S., and Follows, M. J. (2011). Biogeographical controls on the marine nitrogen fixers. *Glob. Biogeochem. Cycles* 25, 1–8. doi: 10.1029/2010GB003902

Montoya, J. P., Voss, M., Kahler, P., and Capone, D. G. (1996). A simple, high-precision, high-sensitivity tracer assay for N_2 fixation. *Appl. Environ. Microbiol.* 62, 986–993.

Moore, C. M., Mills, M. M., Achterberg, E. P., Geider, R. J., LaRoche, J., Lucas, M. I., et al. (2009). Large-scale distribution of Atlantic nitrogen

fixation controlled by iron availability. *Nat. Geosci.* 2, 867–871. doi: 10.1038/ngeo667

Mouriño-Carballido, B., Graña, R., Fernández, A., Bode, A., Varela, M., Domínguez, J. F., et al. (2011). Importance of N_2 fixation vs. nitrate eddy diffusion along a latitudinal transect in the Atlantic Ocean. *Limnol. Oceanogr.* 56, 999–1007. doi: 10.4319/lo.2011.56.3.0999

Mulholland, M. R., Bernhardt, P. W., Blanco-Garcia, J. L., Mannino, A., Hyde, K., Mondragon, E., et al. (2012). Rates of dinitrogen fixation and the abundance of diazotrophs in North American coastal waters between cape hatteras and georges bank. *Limnol. Oceanogr.* 57, 1067–1083. doi: 10.4319/lo.2012.57.4.1067

Osborn, T. R. (1980). Estimates of the local rate of vertical diffusion from dissipation measurements. *J. Phys. Oceanogr.* 10, 83–89.

Oschlies, A., and Garçon, V. (1998). Eddy-induced enhancement of primary production in a model of the North Atlantic Ocean. *Nature* 394, 266–269. doi: 10.1038/28373

Painter, S. C., Patey, M. D., Forryan, A., and Torres-Valdes, S. (2013). Evaluating the balance between vertical diffusive nitrate supply and nitrogen fixation with reference to nitrate uptake in the eastern subtropical North Atlantic Ocean. *J. Geophys. Res. Ocean* 118, 5732–5749. doi: 10.1002/jgrc.20416

Pardo, P. C., Padín, X. A., Gilcoto, M., Farina-Busto, L., and Pérez, F. F. (2011). Evolution of upwelling systems coupled to the long-term variability in sea surface temperature and Ekman transport. *Clim. Res.* 48, 231–246. doi: 10.3354/cr00989

Pérez, F. F., Padín, X. A., Pazos, Y., Gilcoto, M., Cabanas, M., Pardo, P. C., et al. (2010). Plankton response to weakening of the Iberian coastal upwelling. *Glob. Chang. Biol.* 16, 1258–1267. doi: 10.1111/j.1365-2486.2009.02125.x

Planas, D., Agustí, S., Duarte, C. M., Granata, T. C., and Merino, M. (1999). Nitrate uptake and diffusive nitrate supply in the Central Atlantic. *Limnol. Oceanogr.* 44, 116–126. doi: 10.4319/lo.1999.44.1.0116

Prandke, H., and Stips, A. (1998). Test measurements with an operational microstructure-turbulence profiler: detection limit of dissipation rates. *Aquat. Sci.* 60, 191–209. doi: 10.1007/s000270050036

Raimbault, P., and Garcia, N. (2008). Evidence for efficient regenerated production and dinitrogen fixation in nitrogen-deficient waters of the South Pacific Ocean: impact on new and export production estimates. *Biogeosciences* 5, 323–338. doi: 10.5194/bg-5-323-2008

Ratten, J. M., LaRoche, J., Desai, D. K., Shelley, R. U., Landing, W. M., Boyle, E., et al. (2015). Sources of iron and phosphate affect the distribution of diazotrophs in the North Atlantic. *Deep Res. II Top. Stud. Oceanogr.* 116, 332–341. doi: 10.1016/j.dsr2.2014.11.012

Rees, A., Gilbert, J., and Kelly-Gerreyn, B. (2009). Nitrogen fixation in the western english channel (NE Atlantic Ocean). *Mar. Ecol. Prog. Ser.* 374, 7–12. doi: 10.3354/meps07771

Sohm, J. A., Hilton, J. A., Noble, A. E., Zehr, J. P., Saito, M. A., and Webb, E. A. (2011). Nitrogen fixation in the South Atlantic gyre and the benguela upwelling system. *Geophys. Res. Lett.* 38, 1–6. doi: 10.1029/2011GL048315

Stal, L. J. (2009). Is the distribution of nitrogen-fixing cyanobacteria in the oceans related to temperature? *Environ. Microbiol.* 11, 1632–1645. doi: 10.1111/j.1758-2229.2009.00016.x

Subramaniam, A., Mahaffey, C., Johns, W., and Mahowald, N. (2013). Equatorial upwelling enhances nitrogen fixation in the Atlantic Ocean. *Geophys. Res. Lett.* 40, 1766–1771. doi: 10.1002/grl.50250

Thompson, A., Carter, B. J., Turk-Kubo, K., Malfatti, F., Azam, F., and Zehr, J. P. (2014). Genetic diversity of the unicellular nitrogen-fixing cyanobacteria UCYN-A and its prymnesiophyte host. *Environ. Microbiol.* 16, 3238–3249. doi: 10.1111/1462-2920.12490

Thompson, A. W., Foster, R. A., Krupke, A., Carter, B. J., Musat, N., Vaulot, D., et al. (2012). Unicellular cyanobacterium symbiotic with a single-celled Eukaryotic alga. *Science* 337, 1546–1550. doi: 10.1126/science.1222700

Turk-Kubo, K. A., Farnelid, H. M., Shilova, I. N., Henke, B., and Zehr, J. P. (2017). Distinct ecological niches of marine symbiotic N_2-fixing cyanobacterium *Candidatus Atelocyanobacterium thalassa* sublineages. *J. Phycol.* 53, 451–461. doi: 10.1111/jpy.12505

Turk-Kubo, K. A., Karamchandani, M., Capone, D. G., and Zehr, J. P. (2014). The paradox of marine heterotrophic nitrogen fixation: abundances of heterotrophic diazotrophs do not account for nitrogen fixation rates in the Eastern Tropical South Pacific. *Environ. Microbiol.* 16, 3095–3114. doi: 10.1111/1462-2920.12346

Varela, M. (1992). Upwelling and phytoplankton ecology in Galician (NW Spain) rias and shelf waters. *Boletín Inst. Español. Oceanogr.* 8, 57–74.

Varela, M., Prego, R., Belzunce, M. J., and Salas, F. M. (2001). Inshore-offshore differences in seasonal variations of phytoplankton assemblages: the case of a Galician Ria Alta (Ria de A Coruña) and its adjacent shelf (NW of Spain). *Cont. Shelf Res.* 21, 1815–1838. doi: 10.1016/S0278-4343(01)00032-2

Villamaña, M., Mouriño-Carballido, B., Marañón, E., Cermeño, P., Chouciño, P., da Silva, J. C. B., et al. (2017). Role of internal waves on mixing, nutrient supply and phytoplankton community structure during spring and neap tides in the upwelling ecosystem of Ría de Vigo (NW Iberian Peninsula). *Limnol. Oceangr.* 62, 1014–1030. doi: 10.1002/lno.10482

Voss, M., Bange, H. W., Dippner, J. W., Middelburg, J. J., Montoya, J. P., and Ward, B. (2013). The marine nitrogen cycle: recent discoveries, uncertainties and the potential relevance of climate change. *Philos. Trans. R. Soc.* 368:20130121. doi: 10.1098/rstb.2013.0121

Voss, M., Croot, P., Lochte, K., Mills, M., and Peeken, I. (2004). Patterns of nitrogen fixation along 10°N in the tropical Atlantic. *Geophys. Res. Lett.* 31, 1–4. doi: 10.1029/2004GL020127

Weiss, R. F. (1970). The solubility of nitrogen, oxygen and argon in water and seawater. *Deep Sea Res.* 17, 721–735. doi: 10.1016/0011-7471(70)90037-9

Worden, A. Z., Nolan, J. K., and Palenik, B. (2004). Assessing the dynamics and ecology of marine picophytoplankton: the importance of the eukaryotic component. *Limnol. Oceanogr.* 49, 168–179. doi: 10.4319/lo.2004.49.1.0168

Wooster, W. S., Bakun, A., and McClain, D. R. (1976). The seasonal upwelling cycle along the eastern boundary of the North Atlantic. *J. Mar. Res.* 34, 131–146.

Zehr, J. P., Carpenter, E., and Villareal, T. A. (2000). New perspectives on nitrogen-fixing microrganisms in tropical and subtropical oceans. *Trends Microbio.* 8, 68–73. doi: 10.1016/S0966-842X(99)01670-4

Zehr, J., Jenkins, B., Short, S., and Steward, G. (2003). Nitrogenase gene diversity and microbial community structure: a cross-system comparison. *Environ. Microbiol.* 5, 539–554. doi: 10.1046/j.1462-2920.2003.00451.x

Zehr, J.P., Montoya, J.P., Jenkins, B.D., Hewson, I., Mondragon, E., Short, C.M., et al. (2007). Experiments linking nitrogenase gene expression to nitrogen fixation in the North Pacific subtropical gyre. *Limnol. Oceanogr.* 52, 169–183. doi: 10.4319/lo.2007.52.1.0169

Conflict of Interest Statement: The authors declare that the research was conducted in the absence of any commercial or financial relationships that could be construed as a potential conflict of interest.

frontiers in Microbiology

ORIGINAL RESEARCH
published: 17 January 2018
doi: 10.3389/fmicb.2017.02683

Desert Dust as a Source of Iron to the Globally Important Diazotroph *Trichodesmium*

Despo Polyviou[1], Alison J. Baylay[1], Andrew Hitchcock[2], Julie Robidart[3], C. M. Moore[1] and Thomas S. Bibby[1]*

[1] Ocean and Earth Science, University of Southampton, Waterfront Campus, Southampton, United Kingdom, [2] Department of Molecular Biology and Biotechnology, University of Sheffield, Firth Court, Sheffield, United Kingdom, [3] Ocean Technology and Engineering Group, National Oceanography Centre, Southampton, United Kingdom

The marine cyanobacterium *Trichodesmium* sp. accounts for approximately half of the annual 'new' nitrogen introduced to the global ocean but its biogeography and activity is often limited by the availability of iron (Fe). A major source of Fe to the open ocean is Aeolian dust deposition in which Fe is largely comprised of particles with reduced bioavailability over soluble forms of Fe. We report that *Trichodesmium erythraeum IMS101* has improved growth rate and photosynthetic physiology and down-regulates Fe-stress biomarker genes when cells are grown in the direct vicinity of, rather than physically separated from, Saharan dust particles as the sole source of Fe. These findings suggest that availability of non-soluble forms of dust-associated Fe may depend on cell contact. Transcriptomic analysis further reveals unique profiles of gene expression in all tested conditions, implying that *Trichodesmium* has distinct molecular signatures related to acquisition of Fe from different sources. *Trichodesmium* thus appears to be capable of employing specific mechanisms to access Fe from complex sources in oceanic systems, helping to explain its role as a key microbe in global biogeochemical cycles.

Keywords: *Trichodesmium*, iron, dust, nitrogen fixation, cyanobacteria

OPEN ACCESS

Edited by:
Angela Landolfi, GEOMAR Helmholtz Centre for Ocean Research Kiel, Germany

Reviewed by:
Peter Croot, National University of Ireland Galway, Ireland
Yeala Shaked, Hebrew University of Jerusalem, Israel

****Correspondence:***
Despo Polyviou
d.polyviou@noc.soton.ac.uk

Specialty section:
This article was submitted to Aquatic Microbiology, a section of the journal Frontiers in Microbiology

Received: *01 September 2017*
Accepted: *22 December 2017*
Published: *17 January 2018*

Citation:
Polyviou D, Baylay AJ, Hitchcock A, Robidart J, Moore CM and Bibby TS (2018) Desert Dust as a Source of Iron to the Globally Important Diazotroph Trichodesmium. Front. Microbiol. 8:2683. doi: 10.3389/fmicb.2017.02683

INTRODUCTION

Cyanobacterial diazotrophs are responsible for most of the fixed-nitrogen entering marine ecosystems and as such have a major role in regulating oceanic productivity (Mahaffey et al., 2005; Zehr and Bombar, 2015). The availability of iron (Fe) in marine ecosystems heavily regulates the biogeography and activity of such cyanobacteria (Mills et al., 2004; Moore et al., 2009; Chappell et al., 2012; Snow et al., 2015b) due to the absolute requirement of Fe in the catalysts of both photosynthesis and dinitrogen (N_2) fixation (Geider and La Roche, 1994; Sañudo-Wilhelmy et al., 2001; Shi et al., 2007; Richier et al., 2012). The colonial, non-heterocystous cyanobacteria *Trichodesmium* sp. are responsible for almost half of the N_2 fixed in marine systems annually (Capone et al., 1997; Mahaffey et al., 2005). *Trichodesmium's* requirement for Fe is thought to be enhanced relative to single-celled or heterocystous species as it simultaneously requires Fe for both photosynthesis and N_2 fixation (Berman-Frank et al., 2007), processes which are temporally or spatially separated in most N_2 fixing microorganisms (Tuit et al., 2004). *Trichodesmium* may therefore need to be particularly adept at acquiring Fe from the environment.

Desert dust is a major source of Fe to the surface ocean (Jickells et al., 2005). Total Fe supply from dust is dominated by particulate (>0.4 μm) or colloidal (0.02–0.4 μm) rather than readily soluble (<0.02 μm) forms (Aguilar-Islas et al., 2010; Fitzsimmons et al., 2015), although solubility

of Fe from dust can vary further as a function of either dry or wet deposition modes and the time spent interacting with a variety of processes occurring within the oceanic mixed layer (Croot et al., 2004; Baker and Croot, 2010; Schlosser et al., 2014). Comparisons between computations of the total dust inputs and the Fe inventory of the oceans indicate low overall solubility of Fe from dust (<12%) (Jickells and Spokes, 2001). Although soluble Fe is typically considered to be the major source of bioavailable Fe to phytoplankton (Wells, 1989; Schlosser and Croot, 2008; Chester, 2009; Fitzsimmons, 2013) particulate/colloidal forms have been suggested to play a role (Kuma and Matsunaga, 1995) and a growing number of studies have demonstrated that microbes can access Fe from these sources (Nodwell and Price, 2001; Frew et al., 2006; Sugie et al., 2013; van der Merwe et al., 2015), with *Trichodesmium* potentially capable of accessing Fe from both colloidal (Wang and Dei, 2003) and particulate (Rubin et al., 2011) forms.

Cyanobacteria display a number of distinct Fe acquisition pathways including Fe^{3+} and Fe^{2+} transporters, the latter often coupled to biological reduction of Fe^{3+} to Fe^{2+}, alongside production of siderophores which are released from the cell, bind Fe and are subsequently taken up through dedicated transporters (Neilands, 1995; Hopkinson and Barbeau, 2012; Boiteau and Repeta, 2015). Homologs to Fe^{2+} (FeoAB), Fe^{3+} (FutABC) and siderophore (FhuD) transporter components are encoded in the *Trichodesmium* genome; however, the proteins involved in Fe reduction are not well characterized (Chappell and Webb, 2010). Inorganic Fe reduction and uptake is possibly facilitated by reactive oxygen species (ROS) produced intracellularly (Roe and Barbeau, 2014; Hansel et al., 2016) while cell surface processes appear to be involved in observed facilitated dissolution of Fe from dust by *Trichodesmium* (Rubin et al., 2011). These include active trapping and directed transport of particulate Fe into the core of *Trichodesmium* colonies (Rubin et al., 2011). However, the mechanisms and physiological impacts of cell-to-substrate contact for acquisition of Fe from dust are yet to be fully determined.

Using non-axenic *Trichodesmium erythraeum* IMS101 (*Trichodesmium*) cultures, we investigate the Fe uptake strategies involved in accessing Fe from Saharan desert dust within an experimental situation. We evaluate the significance of permitting cell contact for acquiring Fe from dust by physically separating dust from cells using porous membranes. We report both on the physiological and transcriptomic responses of *Trichodesmium* to bound (particulate and colloidal) and free dissolved Fe to understand the factors that enable this key microbe to apparently dominate N_2 fixation within regions of high dust input.

MATERIALS AND METHODS

Culture Conditions and Growth

Trichodesmium erythraeum IMS101 (*Trichodesmium*) was grown on an orbital shaker (150 rpm) under a 12h dark: 12h light cycle (ca. 130 μmol photons m^{-2} s^{-1}) in modified YBC-II medium (Polyviou et al., 2015; Snow et al., 2015a) having a final EDTA concentration of 20 μM (Hong et al., 2017). Experimental cultures at a total volume of 40 ml were initiated from an Fe replete stock culture rinsed with no-added Fe media before inoculation and incubation in triplicate under 4 conditions: (Fe−) with no added Fe, (Fe+) with 400 nM added $FeCl_3$-EDTA as a source of dissolved soluble Fe (sFe), equivalent to a calculated bioavailable inorganic Fe concentration of 1100 pM Fe' (Snow et al., 2015a) and two treatments with 0.25 mg ml^{-1} of Saharan dust, collected between 04°43'N, 28°55'W and 06°56'N, 28°07'W using a mesh system aboard the RSS Shackleton (Murphy, 1985). Dust was added either directly (Dust+) or inside a barrier to the culture created using 8 kDa MWCO dialysis tubing (DT) (BioDesign, Carmel, NY, United States) ([Dust]). For consistency and to confirm that diffusion of sFe through the membrane was possible the $FeCl_3$-EDTA was also released into the Fe+ media through the DT. DT was washed by boiling in 120 mM Na_2HCO_3 and subsequently in 10 mM Na_2EDTA and 10 mM NaOH twice before rinsing three times in milli-Q H_2O. Clean DT, handled with 10% HCl washed plastic tweezers, was included in all experimental treatments except for a no-DT control. The no-DT control was grown under no added Fe conditions (i.e., as per the Fe− treatments) with the physiology of *Trichodesmium* showing no significant differences when compared to the Fe− treatment, suggesting that inclusion of DT did not result in any significant Fe contamination (Supplementary Figure S1). Within a separate control experiment the physiological responses of *Trichodesmium* were monitored to test whether nutrients from dust dissolved preferentially when dust was free in the culture vessels compared to when it was enclosed in DT (Supplementary Figure S2). Within this control experiment, the same series of treatments (i.e., +Fe, −Fe, Dust+ and [Dust]) were incubated abiotically, i.e., without the addition of *Trichodesmium* for a period of 14 days before filtration through a 0.2 μm filter into clean culture flasks and subsequent inoculation of the filtrate (i.e., with the dust particles removed) with equal concentrations of cells.

Trichodesmium growth was monitored by cell counts performed using a Sedgewick Rafter counting chamber and a GX CAM-1.3 camera on an L1000A biological microscope (GT Vision Ltd., Suffolk, United Kingdom). Cell and filament lengths were identified using GX capture (GX 14 Optical, Suffolk, United Kingdom) and ImageJ (Schneider et al., 2012). The concentration of cells was calculated for the duration of the experiment (Supplementary Figure S3) by dividing the total filament length by the average cell length and growth rates calculated using the gradient of the natural logarithm of measurements during exponential growth.

Photosynthetic Physiology

Photosynthetic physiology was monitored using a FASTtracka™ MkII Fast Repetition Rate fluorometer (FRRf) integrated with a FastAct™ Laboratory system (Chelsea Technologies Group Ltd., Surrey, United Kingdom). Measurements were made 2.5 h after the beginning of the photoperiod following dark adaptation of samples for 20 min and consequent exposure to a background irradiance of 29 μmol photons m^{-2} s^{-1} for 2–5 min (Richier et al., 2012). F_v/F_m was used as an estimate of the apparent

PSII photochemical quantum efficiency (Kolber et al., 1998). Data presented is the average of three technical replicate measurements for each of the three biological replicates.

RNA Sequencing

Trichodesmium cultures were filtered onto GF/F filters on day 17 of the experiment and snap frozen in liquid nitrogen. RNA was subsequently extracted using the RNeasy Plant Mini Kit (Qiagen, Manchester, United Kingdom), treated with TURBO DNA-free^{TM} DNase (Life Technologies Ltd., Paisley, United Kingdom) and stored at −80°C. Absence of genomic DNA contamination was confirmed by PCR.

Paired end libraries for Illumina sequencing were prepared using the TruSeq Stranded mRNA Library Prep Kit (Illumina), following the manufacturer's low-throughput protocol. This was modified for use with bacterial RNA samples by replacing the initial poly-A-based mRNA isolation step with ribosomal RNA (rRNA) depletion using a bacterial Ribo-Zero rRNA Removal Kit (Illumina Inc., San Diego, CA, United States). Libraries were pooled and sequenced on an Illumina MiSeq instrument using paired-end sequencing, with a read length of 151 bp.

The raw sequence reads were pre-processed with CutAdapt (v1.8.1, Martin, 2011) to remove TruSeq adapter sequences and low quality bases from the 3′ end of reads, using a quality threshold of 15 and minimum read length of 36 bp. Trimmed reads were mapped against the *Trichodesmium erythraeum* IMS101 reference genome assembly (Ensembl Bacteria database, accession GCA_000014265.1) using TopHat v2.0.14 (Kim et al., 2013), and reads mapping to annotated genes in IMS101 were counted using HTSeq, version 0.6.0, (Anders et al., 2015). The –library-type fr-firststrand and -stranded = reverse options were used in TopHat and HTSeq, respectively, to correctly account for strand-specific read mapping. Libraries were normalized based on the total library size using the median-of-ratios method that is implemented in DESeq2 (Love et al., 2014).

Differential Gene Expression Analysis

Differential gene expression analysis was carried out using the Bioconductor package DESeq2 version 1.8.2 (Love et al., 2014), running on R version 3.2.0. A set of genes with expression significantly affected by growth condition was identified using an ANODEV approach implemented in the DESeq2 package. The fit of read count data against a one-factor negative binomial general linear model, where replicates were grouped by growth condition, was compared (using likelihood ratio testing) to a reduced model where condition information was removed. Pairwise contrasts between conditions were calculated using a Wald test. In both cases, genes with an adjusted P-value of < 0.05 following Benjamini–Hochberg correction for multiple testing were classed as significantly differentially expressed.

The results of the RNA sequencing (RNAseq) analysis were validated via quantitative reverse transcription (RT) Polymerase Chain Reaction (qPCR) using the cytochrome c_{553} gene (*cyt* c_{553}, *Tery_2561*) the iron-stressed-induced protein-A gene (*isiA*, *Tery_1667*) and the Mo-dependent nitrogenase-like-protein gene (nif-like, *Tery_4114*). Patterns of expression from the two methods closely resembled each other and regression analysis indicated a good correlation (R^2 = 99%) (Supplementary Figure S4).

Hierarchical Clustering

To group differentially transcribed genes by transcription profile across treatments, the Pearson product moment correlation coefficient (PPMCC) was calculated for each pair of genes from regularized log (rlog) transformed read count data. Hierarchical clustering was then carried out using the WPGMA method, with 1-PPMCC as the distance metric. Similarly, to cluster samples based on overall transcription profile, pairwise sample distances were calculated using correlation coefficients and hierarchical clustering was carried out using the average linkage method (Minitab 17.3.1, Minitab Inc., Coventry, United Kingdom).

RESULTS

Effects of Desert Dust and Fe' on *Trichodesmium* Physiology

The effect of Saharan desert dust addition on the physiology of non-axenic *Trichodesmium erythraeum IMS101* (hereafter *Trichodesmium*) when in the direct vicinity (Dust+) or separated ([Dust]) from the cells within otherwise low Fe medium was compared to iron deplete (Fe−) and iron replete (Fe+) treatments (as described in Materials and Methods). Growth of *Trichodesmium* was significantly faster under Fe+ (0.31 day^{-1}) and Dust+ (0.28 day^{-1}) compared to Fe− (0.16 day^{-1}) and [Dust] (0.17 day^{-1}) conditions (**Figure 1A** and Supplementary Figure S3) (GLM and Tukey test; $P < 0.05$). Additionally, while photosynthetic efficiency (F_v/F_m) declined rapidly in Fe− and [Dust] treatments from day 6 until the end of the experiment, it was maintained at significantly higher levels in Fe+ and Dust+ treatments (**Figure 1B**). In contrast, although the Fe+ media similarly supported a higher growth rate within the abiotic control experiment, growth rates within media preincubated with dust either inside or outside the DT were statistically indistinguishable from both each other and the −Fe treatment (Supplementary Figure S2).

Transcriptomic Response of *Trichodesmium* to Desert Dust and Fe'

Samples collected on the last day of the main experiment (day 17) were analyzed using RNAseq to ascertain the gene transcription profiles relating to each experimental condition. The *Trichodesmium erythraeum* IMS101 genome is composed of 4451 annotated genes, ∼54% of which are annotated with a Gene Ontology (GO) classification number (GO annotated) (**Figure 2**). The majority of *Trichodesmium* genes (∼98%) were identified (read counts/million > 0) to be transcribed in at least one treatment and 4076 (∼92%) were identified in all four treatments. Of these, 3257 genes had read counts above the statistical threshold required for inclusion in differential gene transcription analysis, as determined by the DESeq2 Bioconductor package (Love et al., 2014). Approximately one third of those genes (1050) were significantly affected by growth condition (adjusted

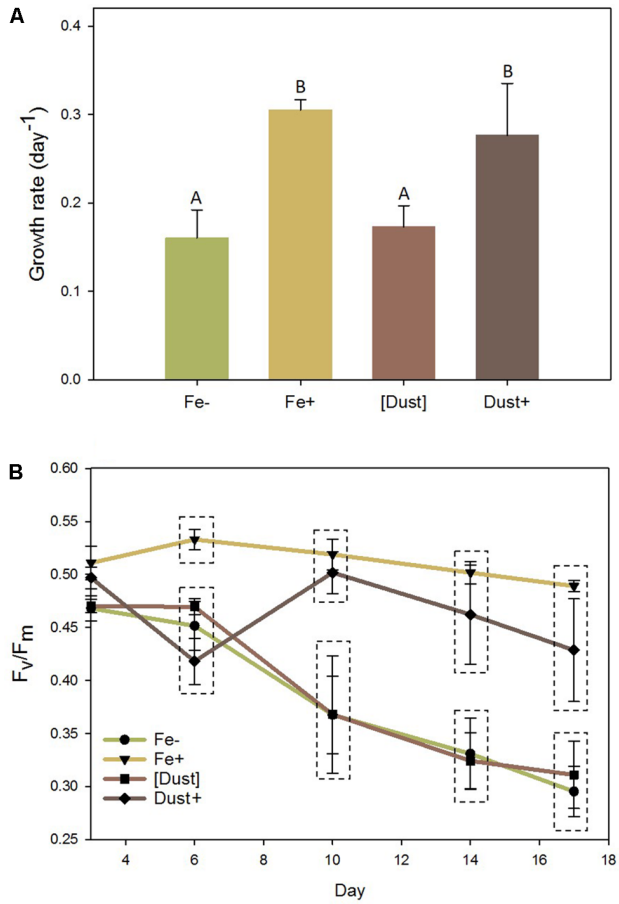

FIGURE 1 | Effects of desert dust and Fe' on *Trichodesmium* physiology. Dust added (Dust+, dark brown), dust separated ([Dust], light brown), Fe' replete (Fe+, yellow) and Fe' deficient (Fe–, green) *Trichodesmium* cultures were monitored over 17 days during which **(A)** growth rates (day^{-1}) and **(B)** photosynthetic efficiency (F_v/F_m) were recorded. Statistically significant differences (GLM and Tukey test; $P < 0.05$) between treatments are indicated with dissimilar letter groups **(A)** or dashed boxes **(B)**. Error bars represent standard deviations of three biological replicates. (GLM and Tukey test, $P < 0.05$).

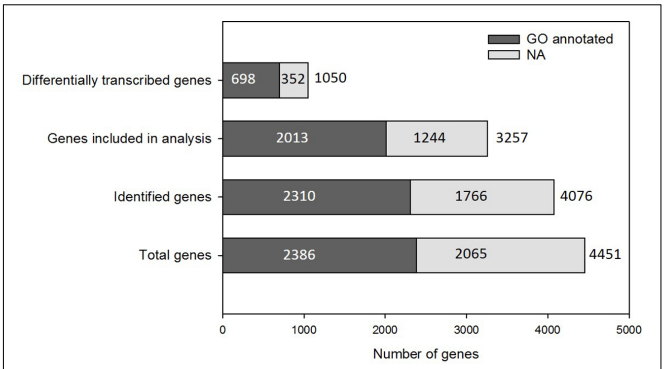

FIGURE 2 | Gene numbers and GO annotation coverage. The majority of *Trichodesmium* genes are identified in at least one condition of the experiment. Genes for which expression is recorded in all treatments above threshold quantities are analyzed to identify differential transcription. A large proportion of the *Trichodesmium* genome is not GO annotated (NA, light gray).

P-value < 0.05 following Benjamini–Hochberg correction for multiple testing, DESeq ANODEV) (**Figure 2**).

The validity of experimental biological replicates was confirmed through hierarchical clustering of gene transcription profiles which revealed closer intra-treatment compared to inter-treatment similarities (**Figure 3**). In addition, two distinct groups of treatments were resolved, highlighting similarities in gene regulation between [Dust] and Fe− treatments (group 1) and between Fe+ and Dust+ treatments (group 2) (**Figure 3A**).

A heat map illustrating all 1050 differentially regulated genes identified in the transcriptomic analysis revealed 10 distinct patterns of gene transcription from the clustering analysis (**Figure 3B** and Supplementary Figure S5) demonstrating significant changes in gene expression across all treatments. The majority of genes (42%) fall in clusters regulated similarly between Fe+ and Dust+ treatments with either increased (Cluster 2, $n = 185$) or reduced (Cluster 10, $n = 259$) transcription relative to Fe− and [Dust] (Supplementary Figure S5). Differential gene regulation in Fe+ compared to Fe−, Dust+ and [Dust] treatments (Supplementary Figure S5) is also observed for a large number of genes (Cluster 4, $n = 109$ and Cluster 6, $n = 135$).

Known Markers of Iron Limitation

The expression of a set of 12 genes (Supplementary Table S1) of known importance during Fe stress conditions and/or previously identified to be differentially expressed (at the transcript or protein level) under variable Fe concentrations was examined in order to access the molecular response to Fe specifically. The genes include the chlorophyll-binding antenna (*isiA*, iron stress induced protein A gene, *Tery_1667*) (Bibby et al., 2001; Shi et al., 2007; Richier et al., 2012; Snow et al., 2015a), the flavodoxin genes (*fld1, Tery_1666*; *fld2, Tery_2559*) which are an Fe free alternative to ferredoxin (LaRoche et al., 1996; Chappell and Webb, 2010), the interchangeable plastocyanin (copper binding) and cytochrome c_{553} (Fe binding) genes (*petE, Tery_2563* and *petJ,Tery_2561*, respectively) (Wood, 1978; Peers and Price, 2006; De la Cerda et al., 2007), genes for the Fe storage proteins bacterioferritin (*bfr, Tery_2787*) and ferritin (*ftn, Tery_4282*) (Keren et al., 2004; Marchetti et al., 2009), the ferric uptake regulators (*fur1, Tery_1958*; *fur2- Tery_3404* and *fur3, Tery_1953*) (González et al., 2012, 2016), the Fe binding nitrogenase NifH subunit (*nifH, Tery_4136*) (Shi et al., 2007; Richier et al., 2012; Snow et al., 2015a) and fructose bisphosphate aldolase class II (*fbaA, Tery_1687*) (Snow et al., 2015a).

Four of these twelve genes, *petJ, petE, fur1* and *fld2*, show significant regulation both in response to direct dust addition (Dust+ compared to [Dust]) and increased availability of dissolved Fe (Fe') (Fe+ compared to Fe−) while a further four genes, *fbaA*, *isiA*, *fur2* and *fld1*, were only significantly regulated through variable Fe' (**Figure 4A**). Genes *bfr*, *ftn, fur3* and *nifH*

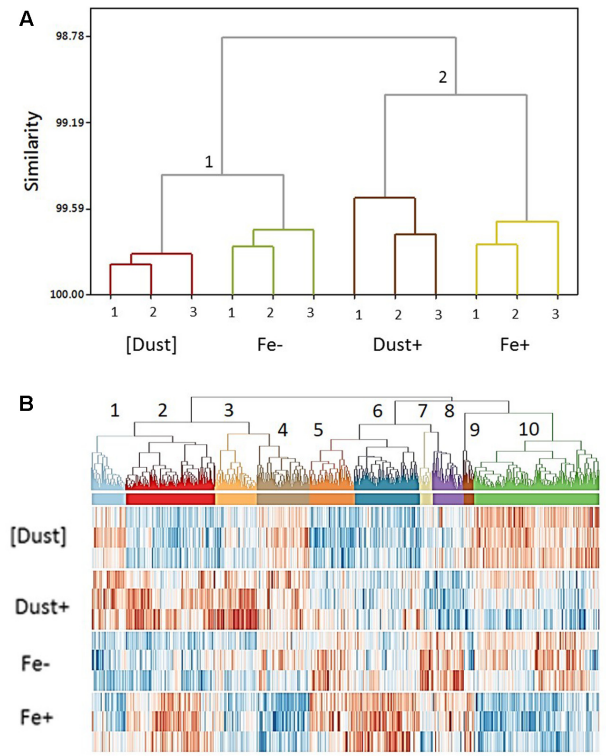

FIGURE 3 | (A) Clustering of gene transcription across treatments and replicates. Replicates of each treatment ([Dust], Fe–, Dust+, Fe+) cluster close together while transcription in (1) [Dust] (light brown) and Fe– (green) cultures groups closer together compared to (2) Dust+ (dark brown) and Fe+ (yellow) cultures. To calculate distances the average linkage method was used. **(B)** Clustering of transcription across all differentially regulated genes. Ten clusters of different transcription profiles across the [Dust], Dust+, Fe–, and Fe+ treatments (computed using the Pearson product moment correlation coefficient between each pair of differentially expressed genes and WPGMA) are detailed in a heat map of transcript level in a dendrogram.

were not found to be differentially regulated by any experimental condition.

Molecular Signatures of Fe Utilization

Analysis of a further set of genes (Supplementary Table S2) was targeted to better understand mechanisms of Fe acquisition under the differing growth conditions. Suggested mechanisms for Fe reduction by cyanobacteria include the transfer of electrons to extracellular Fe^{3+} through the plasma-membrane-located alternative respiratory terminal oxidase (ARTO) (Kranzler et al., 2014) and potentially electrically conductive pili (Lamb et al., 2014). Genes *ctaC* (*Tery_0278*), *ctaD* (*Tery_0277*), and *ctaE* (*Tery_0276*) encoding subunits of ARTO displayed elevated transcription in Fe− compared to Fe+ and [Dust] compared to Dust+ (**Figure 4B**) revealing regulation by Fe' and dust additions within the vicinity of the cells. Interestingly, transcripts of these genes were significantly downregulated in Dust+ compared to all other treatments. The *pilA* (*Tery_2388*) gene encoding the pili protein A was not differentially transcribed as a function of Fe' (Fe+ compared to Fe−) and although transcription was reduced by dust (compared to Fe−), this was only significant when dust was separated from the cells (**Figure 4B**).

Well-characterized cyanobacterial Fe uptake pathways include the FutABC and FeoABC systems for transport of ferric (Fe^{3+}) and ferrous (Fe^{2+}) iron, respectively, across the inner membrane (Kammler et al., 1993; Katoh et al., 2001a,b). The *futA* (*Tery_3377*) gene, annotated as *idiA* (iron-deficiency induced) and encoding the Fe-binding subunit of the Fut Fe^{3+} transporter (Polyviou et al., unpublished), was downregulated in response to increased Fe' (**Figure 4B**). Similarly, the transcript abundance of *feoB* (*Tery_2878*) was reduced in Fe+ cultures compared to the other treatments although the difference was not statistically significant.

Translocation of organically complexed Fe to the periplasm in cyanobacteria happens through TonB dependent transporters (TBDTs) at the outer membrane which seem to require energy transduction by TonB and ExbBD (Larsen et al., 1999; Brinkman and Larsen, 2008; Ollis et al., 2009; Ollis and Postle, 2012; Ollis et al., 2012), although ExbB and ExbD have also been previously linked to inorganic Fe uptake in *Synechocystis* sp. PCC 6803 (Jiang et al., 2015). Transport of organically complexed Fe across the inner membrane employs Fec/FhuD systems (Krewulak and Vogel, 2008; Stevanovic, 2015). The only *Trichodesmium* homolog to *fhu/fec* genes, *fhuD* (*Tery_3943*) (encoding for a periplasmic binding protein homolog), was downregulated by increased Fe' and dust when added to the immediate cellular environment (**Figure 4B**). Homologs of *tonB* (*Tery_1560, Tery_2593*) and *exbBD* (*exbB: Tery_1868, Tery_4448; exbD: Tery_4449*) were not identified to be significantly differentially regulated, although transcription appeared higher in the Fe+ and Fe− treatments compared to the [Dust] and Dust+ treatments (with the exception of *Tery_1868* for which read counts were below the threshold for inclusion in the analysis) (**Figure 4B**).

Members of a previously identified putative siderophore production and uptake pathway, proteins *Tery_3824–3826* (Snow et al., 2015a) were observed to be significantly downregulated under increased Fe' (significant difference for *Tery_3825 and Tery_3826*) (**Figure 4B**). Finally, transcription of the heme oxygenase homolog (*hmox, Tery_0335*), involved in extraction of heme-bound Fe was stimulated by the dust treatments compared to Fe+ and Fe− irrespective of the separation from the cells using the DT (**Figure 4B**). Some indication of increased transcript abundance due to increased Fe' was also observed although this was not statistically significant.

Strongly Differentially Regulated Uncharacterized Genes

One third of the differentially regulated genes in the analysis were not GO annotated. Amongst them was a series of genes encoding for proteins with Haemolysin-Type Calcium Binding (HTCaB)-like domains (Supplementary Table S3) members of which were identified amongst the most differentially regulated genes in this study. Of 10 genes annotated as having a HTCaB-like domain and identified as regulated by some experimental

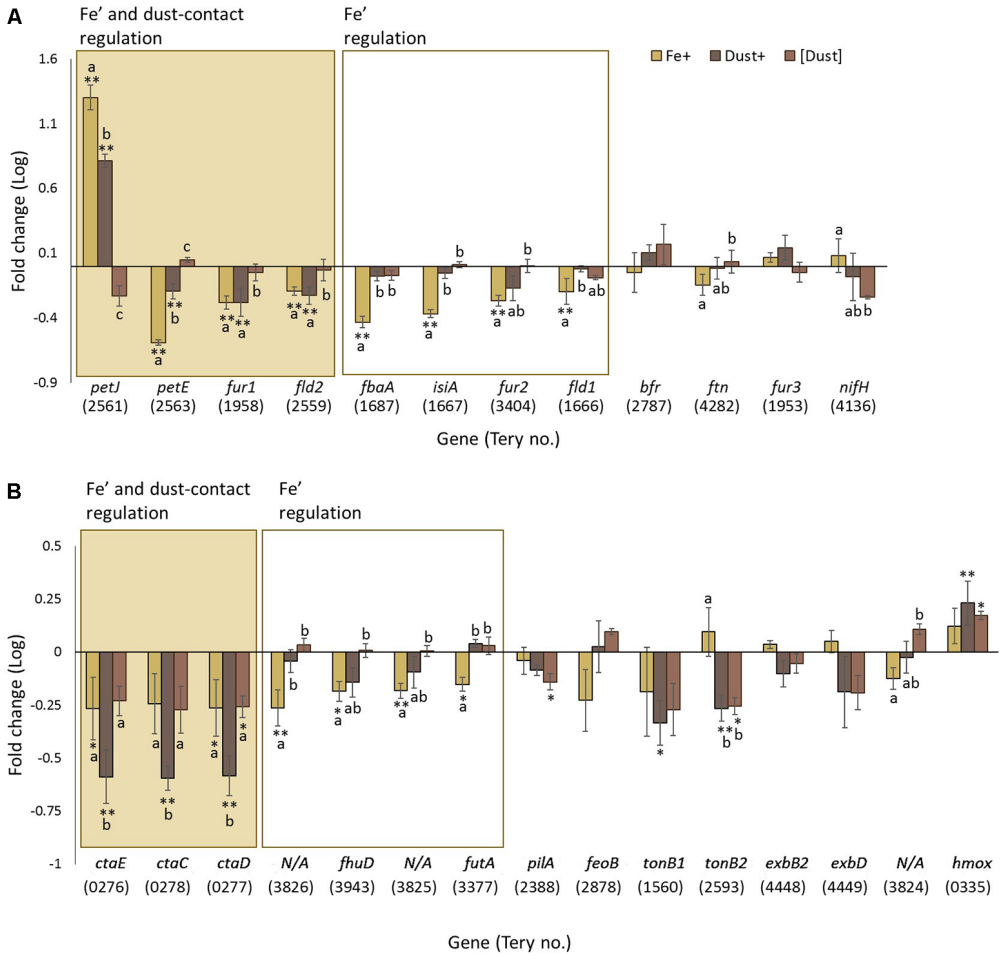

FIGURE 4 | Transcription changes in genes of interest across the experimental treatments. Gene regulation (log fold change) in Fe+ (yellow), Dust+ (dark brown) and [Dust] (light brown) treatments all compared to Fe–, is presented for **(A)** genes expected to be regulated by Fe and **(B)** genes predicted to be involved in Fe utilization. Significantly differentially transcribed genes (Wald test, $P < 0.05$) due to both direct dust additions (Dust+ vs. [Dust]) and Fe' availability (Fe+ vs. Fe–) (shaded box) or replete Fe' only (white box) are plotted in order of highest to lowest fold change. Differences to Fe– are depicted with single (*) or double (**) stars for $P < 0.05$ and $P < 0.01$, respectively. Similarities between treatments Fe+, Dust+ and [Dust] are indicated as identical letter groups (a–c).

condition in our analysis, *Tery_0419, Tery_0424, Tery_2055* and *Tery_1355*, are regulated by Fe' and when contact with dust is permitted and *Tery_3467* and *Tery_2710* by Fe' only (**Figure 5A**). Bioinformatic analysis indicates that HTCaB genes include multiple CHRD domains (identified in chordin) expected to have an immunoglobulin-like β-barrel structure based on some similarity to superoxide dismutases (Hyvönen, 2003). Among these genes, *Tery_3467* which was regulated by Fe' has been previously identified as the zinc binding alkaline phosphatase (APase) gene *phoA* (Orchard et al., 2003).

Also among the uncharacterized genes is a cluster which spans eight genes (*Tery_0843–Tery_0850*) all of which were strongly differentially regulated in response to Fe' availability and dust addition to the direct cellular vicinity (**Figure 5B**) with five (*Tery_0850, Tery_0845, Tery_0846, Tery_0849, Tery_0847*) amongst the top twenty most differentially transcribed genes in the RNAseq analysis. Tery_0848 and Tery_0849 are annotated as cell surface proteins while Tery_0843 is recognized by the UniProtKB Automatic Annotation pipeline as a membrane protein (Supplementary Table S3). In addition, Tery_0844 is predicted to contain an iron-sulfur binding site and Tery_0845 belongs to the heme oxygenase superfamily. The fifth gene in this cluster (*Tery_0847*) encodes for MetE (5-methyltetrahydropteroyltriglutamate-homocysteine S-methyltransferase) which catalyzes the transfer of a methyl group to and from methionine (Supplementary Table S3).

Regulatory DNA

Trichodesmium has a large genome, with abundant non-protein coding regions, and has recently been shown to exploit sophisticated gene regulation (Pfreundt et al., 2014; Pfreundt and Hess, 2015; Walworth et al., 2015), as well as being polyploid (Sargent et al., 2016). The *Trichodesmium* genome harbors 17 group-II introns interrupting a total of 11 genes, 7 of which (*Tery_0428, Tery_4732, Tery_4799, Tery_3633, Tery_2080, Tery_1635, and Tery_0008*) are differentially regulated in one

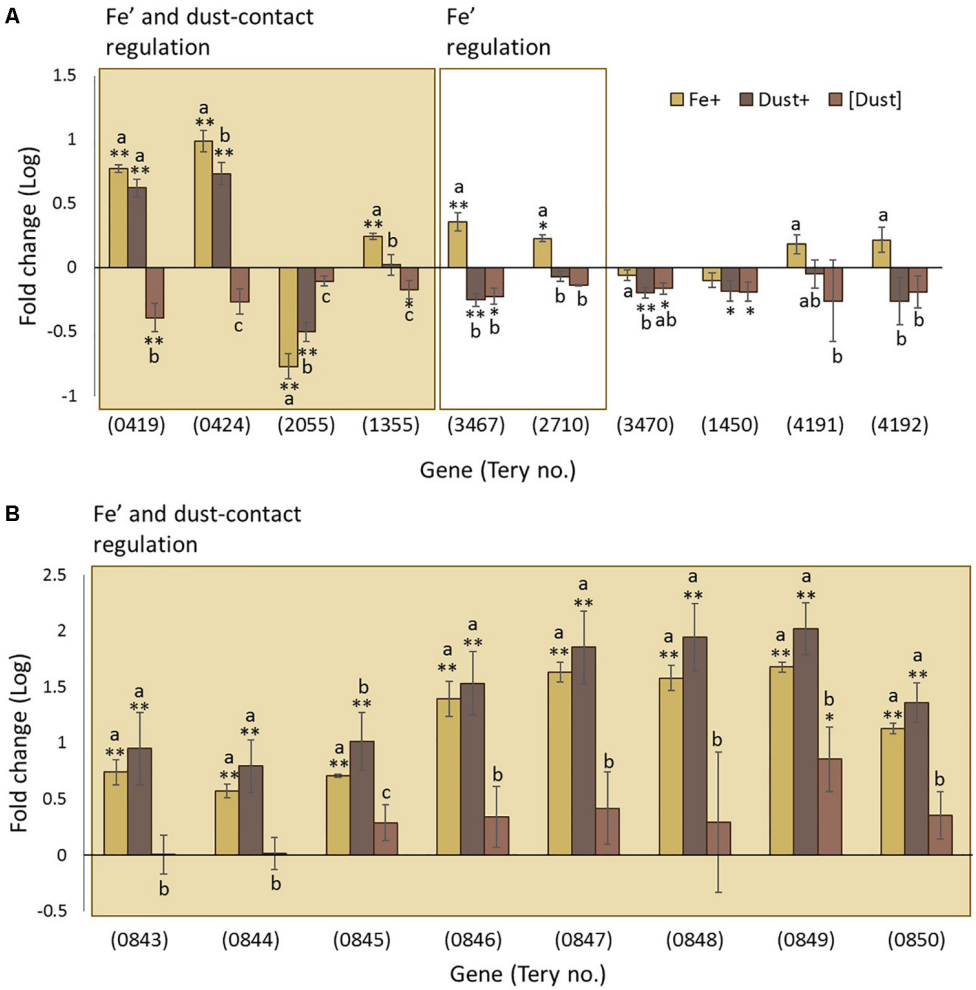

FIGURE 5 | Transcription changes in uncharacterized genes across the experimental treatments. Regulation of **(A)** Haemolysin-Type Calcium Binding (HTCaB)-like genes and **(B)** genes of the *Tery_0843–0850* cluster are shown as log fold change for Fe+ (yellow), Dust+ (dark brown) and [Dust] (light brown) treatments all compared to Fe–. Significantly differentially transcribed genes (Wald test, $P < 0.05$) due to both direct dust additions (Dust+ vs. [Dust]) and Fe' availability (Fe+ vs. Fe–) (shaded box) or replete Fe' only (white box) are plotted in order of highest to lowest fold change **(A)** or order in the genome **(B)**. Differences to the Fe– are depicted with single (*) or double (**) stars for $P < 0.05$ and $P < 0.01$, respectively, while similarities between treatments Fe+, Dust+ and [Dust] are indicated as identical letter groups (a–c).

or more of the experimental treatments (**Figure 6**). Genes *Tery_0428, Tery_4732*, and *Tery_4799* are regulated only when dust is added directly to the cell environment, while *Tery_2080* is expressed more highly in both Dust+ and [Dust] compared to the Fe− and Fe+ treatments. Significant Fe' regulation is only observed for *Tery_3633*.

DISCUSSION

Using cultures of filamentous *Trichodesmium erythraeum* IMS101 we show that these organisms can utilize Saharan desert dust as its sole source of Fe. However, this appeared to only be the case under conditions where direct physical contact was possible, as when dust was separated from the cells using dialysis tubing, both growth rate and photosynthetic efficiency were significantly reduced (**Figure 1**). Moreover, growth rates within media pre-incubated abiotically with dust, irrespective of whether it was constrained within or external to dialysis tubing, were indistinguishable to low Fe cultures and lower than Fe amended cultures (Supplementary Figure S2). In contrast, dust added directly to the growth media with the cells present supported similar growth rates and photosynthetic physiology to cells grown through the addition of dissolved Fe to EDTA buffered media (i.e., increased Fe'), all suggesting that direct contact between cells and dust particles or colloids might be necessary to facilitate Fe-acquisition from dust. Microscopic determination of such contact was not attempted here and therefore whether such contact is transient or if robust, long-term adhesion of particles to filaments occurs cannot be specified. Disentangling the nature of cell-to-particle contact can be challenging but it is perhaps interesting to consider future studies directed

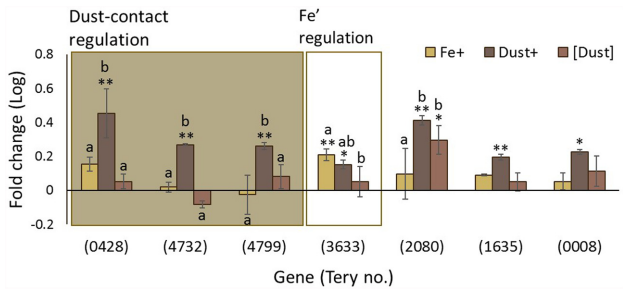

FIGURE 6 | Changes in transcription of genes associated with non-protein coding DNA in *Trichodesmium*. Gene regulation (log fold change) in Fe+ (yellow), Dust+ (dark brown) and [Dust] (light brown) treatments all compared to Fe–. Group II intron host genes (as identified in Pfreundt et al., 2014) are significantly differentially transcribed (Wald test, $P < 0.05$) in response to dust in their immediate environment (Dust+ vs. [Dust]) (shaded box), or Fe' availability (Fe+ vs. Fe–) (white box). Differences to the Fe- treatment are depicted with single (*) or double (**) stars for $P < 0.05$ and $P < 0.01$, respectively, while similarities between treatments Fe+, Dust+ and [Dust] are indicated as identical letter groups (a–c).

towards the identification of cell features which facilitate this interaction.

Cell surface processes occurring in environmentally collected *Trichodesmium* of the puff colony morphology have previously been suggested to enhance dissolution of Fe from dust (Rubin et al., 2011). The efficiency of colonies specifically, as opposed to filaments, for Fe acquisition was suggested to be attributed to specific features of the *Trichodesmium* colonies and the associated microbial consortia (Rubin et al., 2011). Our observations suggest that, in addition, processes which can be undertaken by filamentous *Trichodesmium*, potentially including any associated bacterial consortia, may also be relevant. Although not investigated in this study, microbial communities with some similarity to those found in the natural environment are associated with *Trichodesmium* cultures and can potentially influence the physiological response of *Trichodesmium* to the various conditions relating to the acquisition of Fe and ROS detoxification (Lee et al., 2017).

Potential molecular processes underlining the observed physiological differences between treatments were identified through RNA sequencing analysis on samples acquired at the end of the growth experiment. Such an analysis only provides a snapshot of the molecular response to the experimental conditions which is also likely to change temporally over the course of the experiment. However, clustering of transcription patterns in our experiment indicated that dust added cultures had a similar transcriptomic profile to cells grown replete with Fe', only when contact of the cells with dust was permitted (**Figure 3**). In contrast, when dust was separated from cells, transcription patterns were more similar to that of Fe-deficient cultures. These observations further suggest that filaments can access Fe from dust by employing processes acting at the cell surface, although it should be noted that the pore size of the dialysis tubing, 8 kDa MWCO, will also prevent colloids from passing. Some of the differences between the two dust treatments could thus have resulted from a proportion of any bioavailable Fe released from the dust passing through a colloidal phase before being taken up by *Trichodesmium* and thus we cannot fully differentiate between likely cell surface interaction direct with the particulate dust or smaller colloids which may be derived from it. However, results from the abiotic control experiment (Supplementary Figure S2), argue that 'dissolution' of either soluble or colloidal Fe would appear to be insufficient to augment growth rates within our experimental conditions.

Pertinently, transcriptional patterns caused by Fe' and dust were also distinct between all conditions (**Figure 3B**), suggesting complex transcriptional regulation, likely associated with some combination of the different nature of Fe in the treatments, the overall amounts of available Fe provided in each case, and/or the supply of additional nutrients from dust. Indeed, the differential transcription profiles between the dialysis isolated dust treatment and both the +Fe and −Fe treatments demonstrate that the presence of the former also had an observable biological effect, suggestive of the passage of some soluble constituents other than Fe across the membrane.

An analysis of 12 genes with known Fe regulation patterns was performed to assess the relative Fe status of the cultures (**Figure 4A**). The majority showed the predicted pattern of regulation by differential Fe' availability and 4 were similarly regulated when dust was directly accessible to the cells. Since this was not the case after physical separation of dust from the cells, we suggest that specific cell surface processes are likely to be involved in acquiring Fe from dust. In this case, the improved physiology when dust was within the cell environment can be explained through additional Fe acquisition in this treatment. Some Fe biomarker genes did not show the expected pattern of regulation in dust amended cultures. While this could be due to the cells experiencing different severities of Fe stress when grown with replete Fe' or dust, it may also reflect a specific response to Fe depending on its source and this may impact the interpretation of the transcription of certain Fe stress biomarker genes (Chappell and Webb, 2010; Richier et al., 2012; Snow et al., 2015a; Spungin et al., 2016).

The mechanisms by which *Trichodesmium* transports Fe across the cell membrane can potentially be inferred through homology to other know Fe transporters and omics responses to Fe replete versus deplete conditions (Shi et al., 2007; Chappell et al., 2012; Snow et al., 2015a). Genes such as *futA* and *feoB* encoding members of these transport systems showed the expected downregulation in response to replete Fe', but not due to dust (**Figure 4B**) likely reflecting differences in the response of this organism depending on the source of Fe. The mechanisms by which *Trichodesmium* accesses particulate, or colloidal, Fe and transports Fe across the outer membrane are unknown. The only characterized system in cyanobacteria involves TBDTs powered by the TonB and ExbBD proteins. Homologs to these genes were not regulated by Fe in our study (**Figure 4B**) suggesting they might be

regulated by other factors, or were possibly not required for accessing the types of Fe used in this study (Schauer et al., 2008).

A molecular level understanding of Fe reduction prior to its uptake in cyanobacteria is also lacking. The cell membrane localized ARTO of *Synechocystis* sp. PCC 6803, was recently indicated to use Fe^{3+} as an electron acceptor, reducing it to Fe^{2+} in the periplasmic space prior to its uptake by FeoAB (Kranzler et al., 2014). Downregulation by replete Fe' and direct dust addition to the cells as observed here (**Figure 4B**) for *Trichodesmium* supports possible involvement of the complex, not only in reduction and subsequent acquisition of Fe', but also of Fe provided by dust particles. It is of interest that the largest reduction in expression of subunits of ARTO was observed when cells were in the direct vicinity of dust particles. While this may reflect summative influences of increased Fe availability and the presence of dust, it suggests that filaments may have a dramatically reduced requirement for any ARTO mediated Fe uptake when exposed to dust. As the depleted, oxidized nature of Fe in the marine environment could render ARTO-mediated Fe reduction a limiting step to Fe uptake and consequently to *Trichodesmium* growth, further analysis is required to fully elucidate the importance of this pathway. Finally, a possible siderophore production/utilization pathway (Tery_3823–3826) (Snow et al., 2015a) was also regulated by Fe' availability (**Figure 4B**) but further evidence is required to characterize its involvement in Fe utilization by *Trichodesmium*.

With a large fraction of *Trichodesmium* genes either mis-annotated or annotated as encoding hypothetical proteins of unknown function, it is likely that a wealth of information regarding its physiological adaptations to Fe depletion are yet to be determined. However, based on strong differential transcription, we identify a protein class not previously recognized to be Fe regulated, and a gene cluster encoding proteins with putative extracellular or outer membrane functions. The former includes HTCaB region domain proteins (**Figure 5A**) which, as far as we can ascertain, have not been studied previously in *Trichodesmium*. HTCaB domains occur in tandem repeats in proteins that can form a parallel β roll structure (Baumann et al., 1993; Lilie et al., 2000) and are exported from the cell to function as haemolysins, cyclolysins, leukotoxins and metallopeptidases (Boehm et al., 1990; Duong et al., 1992; Rose et al., 1995). Further they may have adhesive properties (Sánchez-Magraner et al., 2007) and roles in motility (Brahamsha and Haselkorn, 1996; Hoiczyk and Baumeister, 1997; Pitta et al., 1997). These characteristics, alongside the differential regulation observed here (**Figure 5A**) suggest an important function of the proteins in Fe metabolism and a putative role in attachment to particles or mobilization of Fe from the dust. Our data also indicates a cluster of eight consecutive genes (*Tery_0843–Tery_0850*, Supplementary Table S3), which are strongly responsive to direct dust additions and also regulated by Fe' availability. The encoded uncharacterised proteins have features associating them with the cell membranes/surface and possibly the degradation of Fe-containing compounds like heme (**Figure 5B**).

Lastly, transcriptional patterns suggest a significant involvement of non-protein coding DNA in the Fe' and dust response of *Trichodesmium*. The *Trichodesmium* genome has a large non-coding content (40% against the cyanobacterial average of 15%) with the most non-coding DNA transcription start sites (TSS) of currently analyzed bacterial species (Pfreundt et al., 2014; Pfreundt and Hess, 2015). That the non-protein coding fraction of the genome is maintained in the environment (Walworth et al., 2015), leads to the conclusion that regulatory RNA is linked to the organisms' lifestyle, possibly its cohabitation with other microorganisms and the nutrient fluctuations it encounters. In support of this, we observe that group II intron host genes were differentially regulated in response to Fe' and/or dust (**Figure 6**). Based on these results we suggest that *Trichodesmium's* non-coding DNA could be involved in facilitating the regulatory complexity required in a fluctuating environment with ephemeral Fe supplies.

CONCLUSION

We present evidence that cell-to-particle interaction may be a key component of Fe acquisition and the broader ecophysiological functioning of *Trichodesmium*. Cells grown in the direct vicinity of dust displayed unique physiological and molecular characteristics that contrasted with those only having access to soluble species released from the same substrate and from those grown under Fe stress and Fe replete conditions through manipulation of Fe' availability. In addition to providing further evidence that substrate specific responses might influence the bioavailability of Fe to *Trichodesmium in situ*, these results further suggest that variability in substrate might need to be directly considered when using Fe uptake transporters as *in situ* markers of Fe limitation. Indeed, the generated transcriptomic profiles could potentially be used for the identification of specific traits linked to the responses of *Trichodesmium* to differing modes of Fe supply, a stepping stone in better understanding the apparent niche success of this organism within Fe enriched areas of the more generally anemic open oceans.

AUTHOR CONTRIBUTIONS

DP, AH, CM, and TB conceived and planned the experiments. DP carried out the experiments. DP and AB analyzed the data. DP, AB, AH, JR, CM, and TB interpreted the data and wrote the manuscript.

FUNDING

Research presented here was supported by funding by the Graduate School of the National Oceanography Centre Southampton (GSNOCS), NERC, and the A.G. Leventis Foundation.

ACKNOWLEDGMENTS

The authors thank Mark Hopwood (GEOMAR, Kiel, Germany) for constructive discussions that led to the development of this experiment and provision of Saharan dust.

SUPPLEMENTARY MATERIAL

The Supplementary Material for this article can be found online at: https://www.frontiersin.org/articles/10.3389/fmicb.2017.02683/full#supplementary-material

REFERENCES

Aguilar-Islas, A. M., Wu, J., Rember, R., Johansen, A. M., and Shank, L. M. (2010). Dissolution of aerosol-derived iron in seawater: leach solution chemistry, aerosol type, and colloidal iron fraction. *Mar. Chem.* 120, 25–33. doi: 10.1016/j.marchem.2009.01.011

Anders, S., Pyl, P. T., and Huber, W. (2015). HTSeq-A Python framework to work with high-throughput sequencing data. *Bioinformatics* 31, 166–169. doi: 10.1093/bioinformatics/btu638

Baker, A. R., and Croot, P. L. (2010). Atmospheric and marine controls on aerosol iron solubility in seawater. *Mar. Chem.* 120, 4–13. doi: 10.1016/j.marchem.2008.09.003

Baumann, U., Wu, S., Flaherty, K. M., and McKay, D. B. (1993). Three-dimensional structure of the alkaline protease of *Pseudomonas aeruginosa*: a two-domain protein with a calcium binding parallel beta roll motif. *EMBO J.* 12, 3357–3364.

Berman-Frank, I., Quigg, A., Finkel, Z. V., Irwin, A. J., and Haramaty, L. (2007). Nitrogen-fixation strategies and Fe requirements in cyanobacteria. *Limnol. Oceanogr.* 52, 2260–2269. doi: 10.4319/lo.2007.52.5.2260

Bibby, T., Nield, J., and Barber, J. (2001). Iron deficiency induces the formation of an antenna ring around trimeric photosystem I in cyanobacteria. *Nature* 412, 743–745. doi: 10.1038/35089098

Boehm, D. F., Welch, R. A., and Snyder, I. S. (1990). Calcium is required for binding of *Escherichia coli* hemolysin (HlyA) to erythrocyte membranes. *Infect. Immun.* 58, 1951–1958.

Boiteau, R. M., and Repeta, D. J. (2015). An extended siderophore suite from *Synechococcus* sp. PCC 7002 revealed by LC-ICPMS-ESIMS. *Metallomics* 7, 877–884. doi: 10.1039/C5MT00005J

Brahamsha, B., and Haselkorn, R. (1996). An abundant cell-surface polypeptide is required for swimming by the nonflagellated marine cyanobacterium *Synechococcus*. *Microbiology* 93, 6504–6509. doi: 10.1073/pnas.93.13.6504

Brinkman, K. K., and Larsen, R. A. (2008). Interactions of the energy transducer TonB with noncognate energy-harvesting complexes. *J. Bacteriol.* 190, 421–427. doi: 10.1128/JB.01093-07

Capone, D. G., Zehr, J. P., Paerl, H. W., Bergman, B., and Carpenter, E. J. (1997). *Trichodesmium*, a globally significant marine cyanobacterium. *Science* 276, 1221–1229. doi: 10.1126/science.276.5316.1221

Chappell, P. D., Moffett, J. W., Hynes, A. M., and Webb, E. A. (2012). Molecular evidence of iron limitation and availability in the global diazotroph *Trichodesmium*. *ISME J.* 6, 1728–1739. doi: 10.1038/ismej.2012.13

Chappell, P. D., and Webb, E. (2010). A molecular assessment of the iron stress response in the two phylogenetic clades of *Trichodesmium*. *Environ. Microbiol.* 12, 13–27. doi: 10.1111/j.1462-2920.2009.02026.x

Chester, R. (2009). *Marine Geochemistry. Nutrients, Organic Carbon and the Carbon Cycle in Sea Water*, 2nd Edn. Chichester: John Wiley & Sons, Ltd, 212.

Croot, P. L., Streu, P., and Baker, A. R. (2004). Short residence time for iron in surface seawater impacted by atmospheric dry deposition from Saharan dust events. *Geophys. Res. Lett.* 31, L23S08. doi: 10.1029/2004GL020153

De la Cerda, B., Castielli, O., Durán, R. V., Navarro, J. A., Hervás, M., and De la Rosa, M. A. (2007). A proteomic approach to iron and copper homeostasis in cyanobacteria. *Brief. Funct. Genomic Proteomic* 6, 322–329. doi: 10.1093/bfgp/elm030

Duong, F., Lazdunski, A., Carni, B., and Murgier, M. (1992). Sequence of a cluster of genes controlling synthesis and secretion of alkaline protease in *Pseudomonas aeruginosa*: relationships to other secretory pathways. *Gene* 121, 47–54. doi: 10.1016/0378-1119(92)90160-Q

Fitzsimmons, J. N. (2013). *The Marine Biogeochemistry of Dissolved and Colloidal Iron*. Doctoral dissertation, Massachusetts Institute of Technology, Cambridge, MA.

Fitzsimmons, J. N., Carrasco, G. G., Wu, J., Roshan, S., Hatta, M., Measures, C. I., et al. (2015). Partitioning of dissolved iron and iron isotopes into soluble and colloidal phases along the GA03 GEOTRACES North Atlantic Transect. *Deep Sea Res. Part II Top. Stud. Oceanogr.* 116, 130–151. doi: 10.1016/j.dsr2.2014.11.014

Frew, R. D., Hutchins, D. A., Nodder, S., Sanudo-Wilhelmy, S., Tovar-Sanchez, A., Leblanc, K., et al. (2006). Particulate iron dynamics during FeCycle in subantarctic waters southeast of New Zealand. *Global Biogeochem. Cycles* 20:GB1S93. doi: 10.1029/2005GB002558

Geider, R. J., and La Roche, J. (1994). The role of iron in phytoplankton photosynthesis, and the potential for iron-limitation of primary productivity in the sea. *Photosynth. Res.* 39, 275–301. doi: 10.1007/BF00014588

González, A., Bes, M. T., Peleato, M. L., and Fillat, M. F. (2016). Expanding the role of FurA as essential global regulator in cyanobacteria. *PLOS ONE* 11:e0151384. doi: 10.1371/journal.pone.0151384

González, A., Bes, M. T., Valladares, A., Peleato, M. L., and Fillat, M. F. (2012). FurA is the master regulator of iron homeostasis and modulates the expression of tetrapyrrole biosynthesis genes in *Anabaena* sp. PCC 7120. *Environ. Microbiol.* 14, 3175–3187. doi: 10.1111/j.1462-2920.2012.02897.x

Hansel, C. M., Buchwald, C., Diaz, J. M. A., Ossolinski, J. E., Dyhrman, S. T., Van Moo, B. A. S., et al. (2016). Dynamics of extracellular superoxide production by *Trichodesmium* colonies from the Sargasso Sea. *Limnol. Oceanogr.* 61, 1188–1200. doi: 10.1002/lno.10266

Hoiczyk, E., and Baumeister, W. (1997). Oscillin, an extracellular, Ca 2+ -binding glycoprotein essential for the gliding motility of cyanobacteria. *Mol. Microbiol.* 26, 699–708. doi: 10.1046/j.1365-2958.1997.5971972.x

Hong, H., Shen, R., Zhang, F., Wen, Z., Chang, S., Lin, W., et al. (2017). The complex effects of ocean acidification on the prominent N2-fixing cyanobacterium *Trichodesmium*. *Science* 356, 527–531. doi: 10.1126/science.aal2981

Hopkinson, B. M., and Barbeau, K. A. (2012). Iron transporters in marine prokaryotic genomes and metagenomes. *Environ. Microbiol.* 14, 114–128. doi: 10.1111/j.1462-2920.2011.02539.x

Hyvönen, M. (2003). CHRD, a novel domain in the BMP inhibitor chordin, is also found in microbial proteins. *Trends Biochem. Sci.* 28, 470–473. doi: 10.1016/S0968-0004(03)00171-3

Jiang, H.-B., Lou, W.-J., Ke, W.-T., Song, W.-Y., Price, N. M., and Qiu, B.-S. (2015). New insights into iron acquisition by cyanobacteria: an essential role for ExbB-ExbD complex in inorganic iron uptake. *ISME J.* 9, 297–309. doi: 10.1038/ismej.2014.123

Jickells, T. D., An, Z. S., Andersen, K. K., Baker, A. R., Bergametti, G., Brooks, N., et al. (2005). Global iron connections between desert dust, ocean biogeochemistry, and climate. *Science* 308, 67–71. doi: 10.1126/science.1105959

Jickells, T. D., and Spokes, L. J. (2001). "Atmospheric iron inputs to the oceans," in *The Biogeochemistry of Iron in Seawater*, eds D. Hunter and K. A. Turner (Chichester: John Wiley & Sons, Ltd).

Kammler, M., Schön, C., and Hantke, K. (1993). Characterization of the ferrous iron uptake system of *Escherichia coli*. *J. Bacteriol.* 175, 6212–6219. doi: 10.1128/jb.175.19.6212-6219.1993

Katoh, H., Hagino, N., Grossman, A. R., and Ogawa, T. (2001a). Genes essential to iron transport in the cyanobacterium *Synechocystis* sp. strain PCC 6803. *J. Bacteriol.* 183, 2779–2784. doi: 10.1128/JB.183.9.2779

Katoh, H., Hagino, N., and Ogawa, T. (2001b). Iron-binding activity of FutA1 subunit of an ABC-type iron transporter in the cyanobacterium *Synechocystis* sp. strain PCC 6803. *Plant Cell Physiol.* 42, 823–827. doi: 10.1093/pcp/pce106

Keren, N., Aurora, R., and Pakrasi, H. B. (2004). Critical roles of bacterioferritins in iron storage and proliferation of cyanobacteria. *Plant Physiol.* 135, 1666–1673. doi: 10.1104/pp.104.042770

Kim, D., Pertea, G., Trapnell, C., Pimentel, H., Kelley, R., and Salzberg, S. L. (2013). TopHat2: accurate alignment of transcriptomes in the presence of insertions, deletions and gene fusions. *Genome Biol.* 14:R36. doi: 10.1186/gb-2013-14-4-r36

Kolber, Z., Prasil, O., and Falkowski, P. (1998). Measurements of variable chlorophyll fluorescence using fast repetition rate techniques: defining methodology and experimental protocols. *Biochim. Biophys. Acta* 1367, 88–106. doi: 10.1016/S0005-2728(98)00135-2

Kranzler, C., Lis, H., Finkel, O. M., Schmetterer, G., Shaked, Y., and Keren, N. (2014). Coordinated transporter activity shapes high-affinity iron acquisition in cyanobacteria. *ISME J.* 8, 409–417. doi: 10.1038/ismej.2013.161

Krewulak, K. D., and Vogel, H. J. (2008). Structural biology of bacterial iron uptake. *Biochim. Biophys. Acta* 1778, 1781–1804. doi: 10.1016/j.bbamem.2007.07.026

Kuma, K., and Matsunaga, K. (1995). Availability of colloidal ferric oxides to coastal marine phytoplankton. *Mar. Biol.* 122, 1–11. doi: 10.1007/BF00349272

Lamb, J. J., Hill, R. E., Eaton-Rye, J. J., and Hohmann-Marriott, M. F. (2014). Functional role of PilA in iron acquisition in the Cyanobacterium *Synechocystis* sp. PCC 6803. *PLOS ONE* 9:e105761. doi: 10.1371/journal.pone.0105761

LaRoche, J., Boyd, P. W., McKay, R. M. L., and Geider, R. J. (1996). Flavodoxin as an *in situ* marker for iron stress in phytoplankton. *Nature* 382, 802–805. doi: 10.1038/382802a0

Larsen, R. A., Thomas, M. G., and Postle, K. (1999). Protonmotive force, ExbB and ligand-bound FepA drive conformational changes in TonB. *Mol. Microbiol.* 31, 1809–1824. doi: 10.1046/j.1365-2958.1999.01317.x

Lee, M. D., Walworth, N. G., McParland, E. L., Fu, F.-X., Mincer, T. J., Levine, N. M., et al. (2017). The *Trichodesmium* consortium: conserved heterotrophic co-occurrence and genomic signatures of potential interactions. *ISME J.* 11, 1813–1824. doi: 10.1038/ismej.2017.49

Lilie, H., Haehnel, W., Rudolph, R., and Baumann, U. (2000). Folding of a synthetic parallel. *FEBS Lett.* 470, 173–177. doi: 10.1016/S0014-5793(00)01308-9

Love, M. I., Huber, W., and Anders, S. (2014). Moderated estimation of fold change and dispersion for RNA-seq data with DESeq2. *Genome Biol.* 15:550. doi: 10.1186/s13059-014-0550-8

Mahaffey, C., Michaels, A., and Capone, D. (2005). The conundrum of marine N2 fixation. *Am. J. Sci.* 305, 546–595. doi: 10.2475/ajs.305.6-8.546

Marchetti, A., Parker, M. S., Moccia, L. P., Lin, E. O., Arrieta, A. L., Ribalet, F., et al. (2009). Ferritin is used for iron storage in bloom-forming marine pennate diatoms. *Nature* 457, 467–470. doi: 10.1038/nature07539

Martin, M. (2011). Cutadapt removes adapter sequences from high-throughput sequencing reads. *EMBnet J.* 17, 10–12. doi: 10.14806/ej.17.1.200

Mills, M. M., Ridame, C., Davey, M., La Roche, J., and Geider, R. J. (2004). Iron and phosphorus co-limit nitrogen fixation in the eastern tropical North Atlantic. *Nature* 429, 292–294. doi: 10.1038/nature02550

Moore, M. C., Mills, M. M., Achterberg, E. P., Geider, R. J., LaRoche, J., Lucas, M. I., et al. (2009). Large-scale distribution of Atlantic nitrogen fixation controlled by iron availability. *Nat. Geosci.* 2, 867–871. doi: 10.1038/ngeo667

Murphy, K. (1985). *The Trace Metal Chemistry of the Atlantic Aerosol*. Liverpool: University of Liverpool.

Neilands, J. B. (1995). Siderophores: structure and function of microbial iron transport compounds. *J. Biol. Chem.* 270, 26723–26726. doi: 10.1074/jbc.270.45.26723

Nodwell, L. M., and Price, N. M. (2001). Direct use of inorganic colloidal iron by marine mixotrophic phytoplankton. *Limnol. Oceanogr.* 46, 765–777. doi: 10.4319/lo.2001.46.4.0765

Ollis, A. A., Kumar, A., and Postle, K. (2012). The ExbD periplasmic domain contains distinct functional regions for two stages in TonB energization. *J. Bacteriol.* 194, 3069–3077. doi: 10.1128/JB.00015-12

Ollis, A. A., Manning, M., Held, K. G., and Postle, K. (2009). Cytoplasmic membrane protonmotive force energizes periplasmic interactions between ExbD and TonB. *Mol. Microbiol.* 73, 466–481. doi: 10.1111/j.1365-2958.2009.06785.x

Ollis, A. A., and Postle, K. (2012). ExbD mutants define initial stages in TonB energization. *J. Mol. Biol.* 415, 237–247. doi: 10.1016/j.jmb.2011.11.005

Orchard, E., Webb, E., and Dyhrman, S. (2003). Characterization of phosphorus-regulated genes in *Trichodesmium* spp. *Biol. Bull.* 205, 230–231. doi: 10.2307/1543268

Peers, G., and Price, N. M. (2006). Copper-containing plastocyanin used for electron transport by an oceanic diatom. *Nature* 441, 341–344. doi: 10.1038/nature04630

Pfreundt, U., and Hess, W. (2015). Sequential splicing of a group II twintron in the marine cyanobacterium *Trichodesmium*. *Sci. Rep.* 5:16829. doi: 10.1038/srep16829

Pfreundt, U., Kopf, M., Belkin, N., Berman-Frank, I., and Hess, W. R. (2014). The primary transcriptome of the marine diazotroph *Trichodesmium erythraeum* IMS101. *Sci. Rep.* 4:6187. doi: 10.1038/srep06187

Pitta, T. P., Sherwood, E. E., Kobel, A. M., and Berg, H. C. (1997). Calcium is required for swimming by the nonflagellated cyanobacterium *Synechococcus* strain WH8113. *J. Bacteriol.* 179, 2524–2528. doi: 10.1128/jb.179.8.2524-2528.1997

Polyviou, D., Hitchcock, A., Baylay, A. J., Moore, C. M., and Bibby, T. S. (2015). Phosphite utilization by the globally important marine diazotroph *Trichodesmium*. *Environ. Microbiol. Rep.* 7, 824–830. doi: 10.1111/1758-2229.12308

Richier, S., Macey, A. I., Pratt, N. J., Honey, D. J., Moore, C. M., and Bibby, T. S. (2012). Abundances of iron-binding photosynthetic and nitrogen-fixing proteins of *Trichodesmium* both in culture and *in situ* from the North Atlantic. *PLOS ONE* 7:e35571. doi: 10.1371/journal.pone.0035571

Roe, K. L., and Barbeau, K. A. (2014). Uptake mechanisms for inorganic iron and ferric citrate in *Trichodesmium erythraeum* IMS101. *Metallomics* 6, 2042–2051. doi: 10.1039/C4MT00026A

Rose, T., Sebo, P., Bellalou, J., and Ladant, D. (1995). Interaction of Calcium with Bordetella pertussis adenylate cyclase toxin. Characterization of multiple calcium-binding sites and calcium-induced conformational changes. *J. Biol. Chem.* 270, 26370–26376. doi: 10.1074/jbc.270.44.26370

Rubin, M., Berman-Frank, I., and Shaked, Y. (2011). Dust- and mineral-iron utilization by the marine dinitrogen-fixer *Trichodesmium*. *Nat. Geosci.* 4, 529–534. doi: 10.1038/NGEO1181

Sánchez-Magraner, L., Viguera, A. R., García-Pacios, M., Garcillán, M. P., Arrondo, J.-L. R., de la Cruz, F., et al. (2007). The calcium-binding C-terminal domain of *Escherichia coli* alpha-hemolysin is a major determinant in the surface-active properties of the protein. *J. Biol. Chem.* 282, 11827–11835. doi: 10.1074/jbc.M700547200

Sañudo-Wilhelmy, S. A., Kustka, A. B., Gobler, C. J., Hutchins, D. A., Yang, M., Lwiza, K., et al. (2001). Phosphorus limitation of nitrogen fixation by *Trichodesmium* in the central Atlantic Ocean. *Nature* 411, 66–69. doi: 10.1038/35075041

Sargent, E. C., Hitchcock, A., Johansson, S. A., Langlois, R., Moore, C. M., LaRoche, J., et al. (2016). Evidence for polyploidy in the globally important diazotroph Trichodesmium. *FEMS Microbiol. Lett.* 363:fnw244. doi: 10.1093/femsle/fnw244

Schauer, K., Rodionov, D. A., and de Reuse, H. (2008). New substrates for TonB-dependent transport: do we only see the "tip of the iceberg"? *Trends Biochem. Sci.* 33, 330–338. doi: 10.1016/j.tibs.2008.04.012

Schlosser, C., and Croot, P. L. (2008). Application of cross-flow filtration for determining the solubility of iron species in open ocean seawater. *Limnol. Oceanogr.* 6, 630–642. doi: 10.4319/lom.2008.6.630

Schlosser, C., Klar, J. K., Wake, B. D., Snow, J. T., Honey, D. J., Woodward, E. M. S., et al. (2014). Seasonal ITCZ migration dynamically controls the location of the (sub)tropical Atlantic biogeochemical divide. *Proc. Natl. Acad. Sci. U.S.A.* 111, 1438–1442. doi: 10.1073/pnas.1318670111

Schneider, C. A., Rasband, W. S., and Eliceiri, K. W. (2012). NIH Image to ImageJ: 25 years of image analysis. *Nat. Methods* 9, 671–675. doi: 10.1038/nmeth.2089

Shi, T., Sun, Y., and Falkowski, P. G. (2007). Effects of iron limitation on the expression of metabolic genes in the marine cyanobacterium *Trichodesmium erythraeum* IMS101. *Environ. Microbiol.* 9, 2945–2956. doi: 10.1111/j.1462-2920.2007.01406.x

Snow, J. T., Polyviou, D., Skipp, P., Chrismas, N. A. M., Hitchcock, A., Geider, R., et al. (2015a). Quantifying integrated proteomic responses to iron stress in the globally important marine diazotroph *Trichodesmium*. *PLOS ONE* 10:e0142626. doi: 10.1371/journal.pone.0142626

Snow, J. T., Schlosser, C., Woodward, E. M. S., Mills, M. M., Achterberg, E. P., Mahaffey, C., et al. (2015b). Environmental controls on the biogeography of diazotrophy and *Trichodesmium* in the Atlantic Ocean. *Glob. Biogeochem. Cycles* 29, 865–884. doi: 10.1002/2015GB005090

Spungin, D., Pfreundt, U., Berthelot, H., Bonnet, S., AlRoumi, D., Natale, F., et al. (2016). Mechanisms of *Trichodesmium* bloom demise within the New Caledonia Lagoon during the VAHINE mesocosm experiment. *Biogeosci. Discuss.* 2016, 1–44. doi: 10.5194/bg-2015-613

Stevanovic, M. (2015). *The Putative Siderophore-Dependent Iron Transport Network in Anabaena sp. PCC* 7120. Frankfurt: Universitäts bibliothek Johann Christian Senckenberg.

Sugie, K., Nishioka, J., Kuma, K., Volkov, Y. N., and Nakatsuka, T. (2013). Availability of particulate Fe to phytoplankton in the Sea of Okhotsk. *Mar. Chem.* 152, 20–31. doi: 10.1016/j.marchem.2013.03.005

Tuit, C., Waterbury, J., and Ravizza, G. (2004). Diel variation of molybdenum and iron in marine diazotrophic cyanobacteria. *Limnol. Oceanogr.* 49, 978–990. doi: 10.4319/lo.2004.49.4.0978

van der Merwe, P., Bowie, A. R., Quéroué, F., Armand, L., Blain, S., Chever, F., et al. (2015). Sourcing the iron in the naturally fertilised bloom around the Kerguelen Plateau: particulate trace metal dynamics. *Biogeosciences* 12, 739–755. doi: 10.5194/bg-12-739-2015

Walworth, N., Pfreundt, U., Nelson, W. C., Mincer, T., Heidelberg, J. F., Fu, F., et al. (2015). *Trichodesmium* genome maintains abundant, widespread noncoding DNA in situ, despite oligotrophic lifestyle. *Proc. Natl. Acad. Sci. U.S.A.* 112, 4251–4256. doi: 10.1073/pnas.1422332112

Wang, W., and Dei, R. (2003). Bioavailability of iron complexed with organic colloids to the cyanobacteria *Synechococcus* and *Trichodesmium*. *Aquat. Microb. Ecol.* 33, 247–259. doi: 10.3354/ame033247

Wells, M. L. (1989). The availability of iron in seawater: a perspective. *Biol. Oceanogr.* 6, 463–476. doi: 10.1080/01965581.1988.10749545

Wood, P. M. (1978). Interchangeable copper and iron proteins in algal photosynthesis. Studies on plastocyanin and cytochrome c-552 in *Chlamydomonas*. *Eur. J. Biochem.* 87, 9–19. doi: 10.1111/j.1432-1033.1978.tb12346.x

Zehr, J. P., and Bombar, D. (2015). "Marine nitrogen fixation: organisms, significance, enigmas, and future directions," in *Biological Nitrogen Fixation*, ed. F. J. de Bruijn (Hoboken, NJ: John Wiley & Sons, Inc), 855–872. doi: 10.1002/9781119053095.ch84

Conflict of Interest Statement: The authors declare that the research was conducted in the absence of any commercial or financial relationships that could be construed as a potential conflict of interest.

frontiers in Marine Science

ORIGINAL RESEARCH
published: 30 January 2018
doi: 10.3389/fmars.2018.00006

Filtration via Conventional Glass Fiber Filters in $^{15}N_2$ Tracer Assays Fails to Capture All Nitrogen-Fixing Prokaryotes

Deniz Bombar, Ryan W. Paerl†, Ruth Anderson and Lasse Riemann*

Marine Biological Section, Department of Biology, University of Copenhagen, Copenhagen, Denmark

Biological dinitrogen fixation (BNF) represents a major input of reduced nitrogen (N) to the oceans. Accurate direct measurements of BNF rates are crucial for reliably determining the biogeochemical significance of diazotrophy at local and global scales. Traditionally, borosilicate glass fiber filters (GF/F, Whatman) with a nominal pore size of 0.7 μm are used to collect suspended particles by filtration after incubations with added $^{15}N_2$ tracer. We carried out BNF experiments in the Baltic Sea, Danish coastal waters, and the Pacific Ocean comparing the retentive characteristics of precombusted GF/F filters with newer Advantec glass fiber filters which have a smaller nominal pore size of 0.3 μm. Where BNF was detected, rates were nearly always higher, and sometimes even exclusively detectable, when using Advantec filters. In the majority of samples across tested habitats, significantly more cells were lost to GF/F filtrate (average = 51%, range = 10–70% of cells) than to Advantec filtrate (average = 40%, range = 10–54%). Using Illumina sequencing of nitrogenase (*nifH*) gene amplicons, we show that diazotroph communities can markedly differ between bulk water and filtrates from GF/F and Advantec filtrations, suggesting that different diazotrophs can pass through the filter types. In order to reduce the potential underestimations of BNF due to filtration loss of diazotrophs, we recommend using Advantec filters or alternatively silver membranes with 0.2 μm pore size, especially in waters expected to be inhabited by relatively small, unicellular diazotrophs.

Keywords: oceanic nitrogen fixation, diazotrophs, cyanobacteria, glass fiber filter, bias, filtration

OPEN ACCESS

Edited by:
Sophie Rabouille, UMR7093 Laboratoire d'océanographie de Villefranche (LOV), France

Reviewed by:
Ulisse Cardini, Stazione Zoologica Anton Dohrn, Italy
Antonio Bode, Instituto Español de Oceanografía (IEO), Spain

****Correspondence:***
Deniz Bombar
dbombar@bio.ku.dk

†Present Address:
Ryan W. Paerl, Marine, Earth, and Atmospheric Sciences Department, NC State University, Raleigh, NC, United States

Specialty section:
This article was submitted to Aquatic Microbiology, a section of the journal Frontiers in Marine Science

Received: *03 October 2017*
Accepted: *10 January 2018*
Published: *30 January 2018*

Citation:
Bombar D, Paerl RW, Anderson R and Riemann L (2018) Filtration via Conventional Glass Fiber Filters in $^{15}N_2$ Tracer Assays Fails to Capture All Nitrogen-Fixing Prokaryotes. Front. Mar. Sci. 5:6. doi: 10.3389/fmars.2018.00006

INTRODUCTION

Biological nitrogen (N_2) fixation (BNF) in the pelagic ocean amounts to up to 200 × 10^{12} g of nitrogen (N) globally per year, and thereby greatly influences oceanic primary production and CO_2 sequestration (Capone et al., 2005; Gruber and Galloway, 2008; Canfield et al., 2010). Cyanobacteria in the upper water column of the tropical and subtropical ocean have traditionally been considered to be the only quantitatively important N_2 fixers (diazotrophs) (Zehr, 2011). However, nitrogenase (*nifH*) gene sequencing has uncovered an almost ubiquitous distribution of diverse and presumably heterotrophic diazotrophs (Zehr et al., 1998; Farnelid et al., 2011). Notably, these organisms are even found in high-latitude, deep, cold, or coastal waters where cyanobacteria are few or absent (e.g., Fernandez et al., 2011; Blais et al., 2012; Bonnet et al., 2013) and their

lifestyles and how they impact biogeochemical element cycling seems fundamentally different from photoautotrophic diazotrophs (Rahav et al., 2013; Farnelid et al., 2014; Moisander et al., 2014; Benavides et al., 2015; Bentzon-Tilia et al., 2015a). This has inspired many investigators to hypothesize that global N inputs by BNF could potentially be much higher than previously thought. However, the ecology and actual contribution of heterotrophic diazotrophs to oceanic BNF is still largely elusive (Bombar et al., 2016).

Aside from geochemical approaches which can help to quantify BNF on the scale of ocean basins (Gruber and Sarmiento, 1997; Deutsch et al., 2007), direct rate measurements are an important and widely used tool for studying the ecology and biogeochemical impact of diazotrophs. The most commonly applied method for obtaining BNF rate measurements involves adding $^{15}N_2$ tracer gas to water samples followed by filtration of suspended plankton and measurement of ^{15}N tracer incorporation into their biomass, typically after 24 h of incubation (Montoya et al., 1996; Luo et al., 2012). However, recent studies show that slow equilibration between the added $^{15}N_2$ gas and the water sample can lead to an underestimation of rates, requiring a modified protocol in which the gas is pre-dissolved in aliquots of water (Mohr et al., 2010; Grosskopf et al., 2012). Further, some widely used commercially available $^{15}N_2$ gas stocks were shown to be contaminated with ^{15}N-labeled nitrate and ammonium, placing doubt on measurements for which the purity of the used gas stock is not explicitly confirmed (Dabundo et al., 2014). Regrettably, to date there is no clear consensus about how the $^{15}N_2$ enriched seawater should be prepared, how trace metal and other contamination can be avoided, and how incubations should best be carried out (Wilson et al., 2012; Bentzon-Tilia et al., 2015a; Klawonn et al., 2015), leaving it somewhat unclear whether rates from different studies are really comparable and whether observed magnitudes of BNF are accurate.

Clearly, an optimized and accorded protocol for how to best carry out BNF measurements is much needed. In this context, we believe that an additional potential source of error in BNF rate measurements needs to be considered, namely the traditional use of glass fiber filters (Whatman GF/F®) with a nominal pore size of 0.7 μm in post-incubation filtrations. It has long been known that significant shares of recently fixed N can be exuded from diazotroph cells as ammonium or dissolved organic nitrogen (DON), giving the obtained BNF rates the operational definition of a "net rate" (Glibert and Bronk, 1994; Mulholland et al., 2004; Berthelot et al., 2017). However, if actual diazotroph cells would also be lost to the filtrate during filtration, as suspected by other investigators (Konno et al., 2010), the resulting BNF rates would simply be operational underestimates. This kind of loss would arguably affect heterotrophic diazotrophs from the picoplankton size class (0.2–2 μm diameter) more than e.g., large *Trichodesmium* colonies, which can be up to 5 mm in length. Although investigators have tested the performance of different filters for pigment and productivity measurements (Søndergaard and Middelboe, 1993; Moran et al., 1999; Nayar and Chou, 2003 and references therein) and of GF/F filters for retention of bacterioplankton (Lee et al., 1995), there is no assessment of how specific functional groups such as different diazotroph species are retained by GF/F filters. In fall 2013 we carried out an initial test incubation in the Sargasso Sea in which we compared BNF rates obtained from filtering incubations over GF/F filters (0.7 μm pore size) with replicates filtered over different filters (Advantec® glass fiber filters, 0.3 μm pore size), with the surprising result that the "Advantec rates" were twice as high as those obtained from GF/F filters (2.95 ± 0.53 nmol N L^{-1} d^{-1} vs. 1.4 ± 0.17 nmol N L^{-1} d^{-1}, respectively; $n = 3$; Dziallas and Severin, unpublished). These results motivated the current study, in which we tested the overall retentive characteristics of these filters and whether BNF rate differences between them would be reproducible in contrasting marine environments. Further, we identified diazotrophs in bulk water and in cells passing through to the filtrates by Illumina amplicon sequencing of *nifH* genes. In the light of our results we aim to provide information and guidance on choice of filters associated with the $^{15}N_2$ tracer assay in order to obtain better measurements of BNF rates in the future.

MATERIALS AND METHODS

Sampling Overview and BNF Rate Experiments

We carried out BNF experiments with natural seawater to determine potential differences in the retentive characteristics of conventional glass fiber filters ("GF/F", 0.7 μm nominal pore size, Whatman®) and Advantec ® filters (Advantec, GF75, 25 mm diameter, Toyo Roshi Kaisha, Japan via Sterlitech Corp.) with a smaller nominal pore size (0.3 μm), and to test whether these differences in pore size would affect resulting rates of BNF. Experiments were carried out with water from three different marine sites between 2013 and 2015, in order to assess whether the retentive characteristics of the filters would differ among fundamentally different diazotroph communities (Supplemental Table S1). One station in the narrow Strait of Øresund between Denmark and Sweden (55.974 N, 12.694 E) was sampled on 28. April 2015, and experiments were carried out with water from the surface (originating from the Baltic Sea, salinity 11) as well as from 25 m depth, below the halocline (originating from Skagerrak, salinity 33). Between March and May 2015, one experiment per month was carried out with surface water from several stations along Roskilde Fjord (Denmark), which is a eutrophic estuary with a steep trophic and salinity gradient (inner buoy, salinity 14; outer buoy, salinity 20; boundary station, salinity 22; Supplemental Table S1). Previous sampling at the inner buoy showed that BNF peaked in spring and diverse heterotrophic and photoheterotrophic diazotrophs were present and active (Bentzon-Tilia et al., 2015a). Lastly, in February 2015 experiments were carried out with water from 100, 50 m, and the surface at one station off Baja California in the subtropical Pacific (23.0 N, −111.253 W).

In all experiments, BNF rates were measured using the $^{15}N_2$ tracer approach (Montoya et al., 1996). $^{15}N_2$ tracer gas was pre-dissolved in artificial seawater (Boström et al., 2007);

adjusted to local salinities), using methods modified after Mohr et al. (2010). Following sterile filtration, the artificial seawater was degassed for 1 h by heating (50°C), magnet stirring, and applying vacuum (approximately 950 mbar below atmospheric pressure). Thereafter, the water was quickly distributed bubble-free into 50 mL borosilicate serum vials, which were immediately crimp-sealed using sterile butyl rubber septa. One mL of $^{15}N_2$ tracer gas (Campro Scientific, Veenendaal, The Netherlands; 98% enrichment of ^{15}N) was then injected through the septum into each vial using a gas-tight syringe, and equilibration of the gas in the artificial seawater was achieved by shaking overnight (150 r.p.m) and subsequent storage of inverted vials at 5°C for at least 48 h. In order to avoid potential contamination with trace elements in this degassing protocol, all materials, bottles and tubings were acid-washed prior to use. At each experimental site, triplicate acid-washed and MilliQ-rinsed 1.2 L polycarbonate bottles were rinsed three times with local seawater and then filled close to capacity. We then quickly added one vial of $^{15}N_2$ enriched water before immediately closing the bottles with screw caps to obtain a theoretical initial N_2 substrate label of approximately 10 atom% ^{15}N. Bottles were incubated under simulated *in situ* conditions including flowing surface seawater for cooling and neutral density screening to approximately mimic light levels at the surface or at particular depths (i.e., 75% of sea surface irradiance for Øresund or Roskilde Fjord surface samples, 5% at 25 m in Øresund, and 75, 1, and 0% for 5, 53, and 100 m samples in the Pacific). Incubations were terminated after 24 h by gentle vacuum filtration ($\leq$ 25 cm Hg) onto 25 mm pre-combusted (450°C, 5 h) GF/F or Advantec filters (**Figure 1**). Suspended material in bulk water as well as in filtrate from both types of filters was filtered onto 0.2 μm pore size, 47 mm diameter Supor membranes (Pall Corporation) to collect biomass for DNA extraction in order to analyze diazotroph communities via *nifH* gene sequencing (see below). Further aliquots of bulk water and filtrate were also preserved for flow cytometric abundance estimations and qualitative microscopic analysis (see below).

All glass fiber filters were dried at 60°C for 12 h and packed in tin cups (IVA, Meerbusch, Germany). Filters were analyzed by isotope ratio mass spectrometry for ^{15}N and ^{14}N at the Laboratory of Applied Physical Chemistry, Gent, Belgium, including empty tin cups, blank filters (duplicates of each for every sampling campaign) and time-zero samples (no $^{15}N_2$ added) from each replicate at every station/depth, to obtain natural abundance $\delta^{15}N$ measurements of suspended particulate N. BNF rates were calculated following Montoya et al. (1996), and detectable activity was defined as when the difference between $\delta^{15}N$ in the incubated and initial samples was >3x the standard deviation among all time-zero samples at a given station/depth.

Microscopy and Flow Cytometry

For bacterial enumeration, triplicate bulk and filtrate 2 mL samples were fixed with glutaraldehyde (1% final) and stored at −80°C. After defrosting, samples were stained with SYBR green nucleic acid gel stain I (1% final concentration) and analyzed on a FACSCanto II flow cytometer (BD Biosciences, Franklin Lakes, NJ, USA) (Gasol and Del Giorgio, 2000; Supplemental Figure S1). Fluorescent beads (True count beads, BD Biosciences, Albertslund, Denmark) were used to calibrate the flow rate.

Microscopy was exclusively used for qualitative analysis of samples, i.e., to check for the presence of particles, cell aggregates, etc. in bulk samples and filtrates. Fixed subsamples (formaldehyde 1% final) from experiments were filtered onto black polycarbonate filters (0.2 μm pore size; 25 mm diameter; Whatman) and stained for 2 min with 4′,6-diamidino-2-phenylindole (DAPI; 0.01 mg ml^{-1}). Samples were examined at 1000x magnification under a Zeiss Axioskop 2 mot plus epifluorescence microscope (Carl Zeiss, Jena, Germany) using filter set U-FUW (Olympus Co., Japan).

DNA Extractions, Polymerase Chain Reaction (PCR) and *nifH* Illumina Sequencing

DNA was extracted using a phenol/chloroform protocol (Boström et al., 2004), and quantified using PicoGreen (Molecular Probes, Invitrogen, Eugene, OR, USA). *nifH* gene fragments (359 bp) were amplified by nested PCR using degenerate primers (Zehr and Mcreynolds, 1989; Zani et al., 2000). PCR reactions were prepared in a sterile workflow bench after 30 min of UV treatment, and DNA templates were added in a separate bench. PCR amplifications were carried out in 25 μL reactions using Pure Taq Ready-To-Go PCR Beads (GE Healthcare). The first round of PCR was carried out with the *nifH*3 and *nifH*4 primers (Zehr and Turner, 2001) followed by another 30-cycle-PCR in triplicate for each sample, using 1 μL PCR product from the first round as template, and custom Illumina primers consisting of gene-specific sites *nifH*1 and *nifH*2 (Zehr and Turner, 2001) dual-indexed, sample specific barcodes, and four random nucleotides at the start (Supplementary Table 2). Extracted DNA from a marine diazotroph isolate BAL286 (AY97287; Boström et al., 2007) served as positive control. All reactions were cycled at 95°C for 3 min, followed by 30 cycles of 95°C for 45 s, 54°C for 1 min, 72°C for 1:30 min, and a final elongation step of 72°C for 7 min.

Amplicons from triplicate PCR reactions from each sample were pooled, cleaned (Agencourt AMPure XP kit; Beckman Coulter, Indianapolis, USA), and quantified (PicoGreen). All samples were then pooled in equimolar amounts (approximately 10 ng DNA per sample). Negative control PCR reactions were included in the sequencing pool despite the absence of visual gel bands after amplification. Library preparation and sequencing were performed at NGI Sweden (Royal Institute of Technology) with Illumina Truseq PCR-free library preparation and the MiSeq v2 2 × 250 bp sequencing protocol. Sequences were uploaded to the Sequencing Read Archive (SRA) database on NCBI (Accession number SRP125896). Sequence reads were trimmed, merged, quality-checked (scores <20 eliminated) and demultiplexed following Qiime protocols (Caporaso et al., 2010).

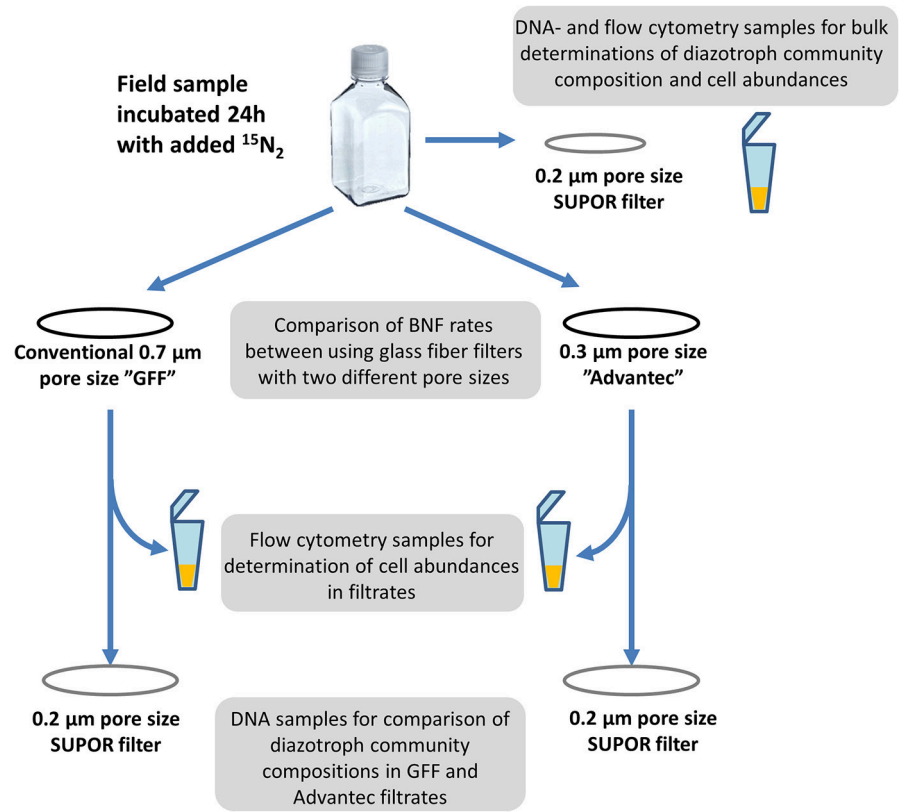

FIGURE 1 | Scheme illustrating the experimental setup for comparing GF/F and Advantec filters.

Further processing and quality control was performed using Mothur (Schloss et al., 2009), discarding reads with ambiguities and homopolymers (>8 bp). Operational taxonomic units (OTUs) were clustered at 97% nucleotide sequence similarity, and a *de novo* chimera check was performed using Uchime (Edgar et al., 2011). OTUs containing chimeras, frameshifts, and non-*nifH* sequences were removed. For non-metric multidimensional scaling (NMDS) plots, rarefied OTU tables were used by subsampling to 2,000 reads per sample, and Bray Curtis similarity matrixes were calculated and designed using PRIMER 6 (Clarke and Gorley, 2006).

Statistics

Significant differences in BNF rates and filtrate bacterial abundances between GF/F and Advantec were detected by means of *t*-tests (SigmaPlot 12.5, Systat Software Inc.). To reveal differences in *nifH* community composition among bulk and filtrate samples, Bray–Curtis similarities were calculated in PRIMER 6.1.15 based on rarefied (n = 2,000) *nifH* genes and visualized by non-metric multidimensional scaling (NMDS). Permutational multivariate analysis of variance (PERMANOVA) was carried out to test for significant differences of *nifH* communities among bulk samples and GF/F and Advantec filtrates.

RESULTS AND DISCUSSION

Different Retention Characteristics of GF/F and Advantec Filters

Recent attempts to improve the $^{15}N_2$ tracer assays for BNF measurements (Mohr et al., 2010; Dabundo et al., 2014; Klawonn et al., 2015) reemphasize that the goal of this methodology must be to obtain accurate BNF rates which are comparable between fundamentally different habitats and can be used for N budget calculations (Montoya et al., 2004; Voss et al., 2004; Capone et al., 2005; Benavides et al., 2015). Overcoming the methodological biases of $^{15}N_2$ gas dissolution and dissolved inorganic ^{15}N contamination are important steps, but they can only lead to an acceptably error-free method if other significant biases are excluded. Oceanic diazotrophs can be found in a range of sizes and exhibit different lifestyles. They encompass millimeter-sized, filamentous cyanobacteria, as well as auto- and heterotrophic prokaryotes falling into the picoplankton size class (0.2–2 µm), which includes key players such as the cyanobacterial symbiont "UCYN-A" (Farnelid et al., 2010; Thompson et al., 2012). The present study shows that glass fiber filters indeed do not catch the entire diazotroph community and therefore might commonly lead to underestimates of BNF rates. Thus, amendments to the filtration step of BNF experimental assays seem necessary.

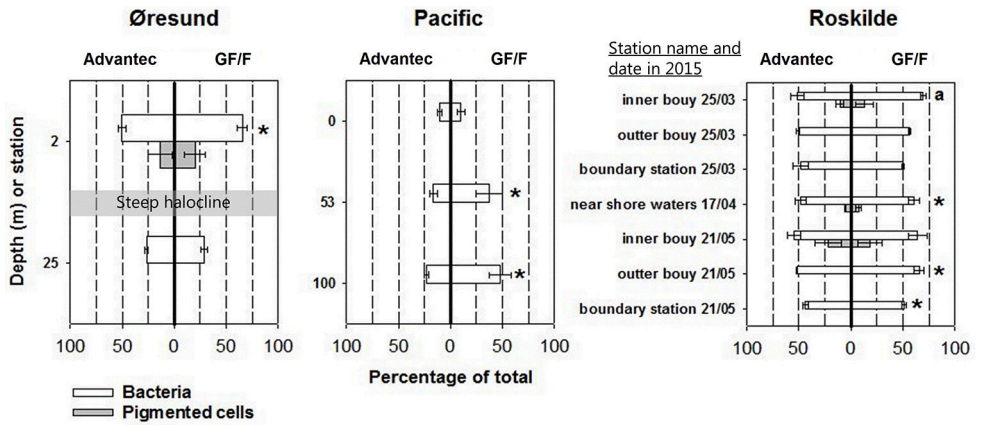

FIGURE 2 | Cell retention characteristics of Advantec and GF/F filters, illustrated as the percentages of cells found in filtrates relative to the cell abundances in bulk water samples (averages ± standard deviation, $n = 3$). The actual cell abundances can be found in Supplemental Table S1. Where gray bars are lacking, pigmented cells (which included some cells larger than the nominal pore size of the glass fiber filters) were completely retained by the filters or too low in abundance for reliable quantification. Cases where abundances were significantly different between the two filtrates are marked with asterisks (*t*-test, $p < 0.05$). In Øresund, the halocline separates surface waters with a salinity of 11 and deep waters with a salinity of 33. For the inner buoy sample on 25th March 2015 (marked with an a) statistical differences could not be calculated since only two replicates were available for flow cytometry.

Our assessment of the retentive characteristics of precombusted GF/F and Advantec filters in three different marine environments shows for both filter types that large shares of total bacteria can be lost to the filtrate (**Figure 2**). These results are similar to earlier tests of un-combusted GF/F filters (Lee et al., 1995; up to around 50% of total bacterioplankton cells lost to the filtrate). However, Advantec filters overall performed better than GF/F, as shown by significantly fewer cells passing through Advantec filters in 6 out of 12 samples across all tested habitats (**Figure 2**) and by the overall averages for all samples (for GF/F: average = 51%, range = 10–70% of cells; and for Advantec filters: average = 40%, range = 10–54%). Differences in cell retention between GF/F and Advantec filters varied across different samples, which is most clear for different depths at the Øresund and the Pacific stations. This suggests that the filtration bias varies depending on what kind of plankton/bacterial community is present, and also on whether, for example, lots of suspended debris or sediment is present. For example, microscopy showed that in the Øresund the sample from below the halocline was characterized by abundant, large particles densely colonized by bacteria, which probably explains why they were retained comparably on both filter types. At 2 m depth, such particles were scarce, and here bacterial abundances were clearly higher in the GF/F filtrate (**Figure 2**). In rare cases cells larger than the nominal pore size of glass fiber filters were found in the filtrates (**Figure 2**, Supplemental Figures S1 D–F), suggesting that they can somehow break through the pores at times. This is likely related to the matrix structure of overlapping glass fibers in these filters, which form pores of nominal size, in contrast to absolute-rated filters having pores with a defined shape and size. Interestingly, Lee et al. (1995) observed that once-retained particles can get lost to GF/F filtrate when filtering large volumes of seawater (several liters, as is rather common for studies in oligotrophic waters).Taken together, our data suggest that while both filters are suboptimal for retaining all bacteria, Advantec filters retain comparatively more cells and thus appear to be the better choice for BNF assays. Optimally, measurements of isotope signatures such as in the $^{15}N_2$ assay would be carried out by using 0.2 μm pore size silver membrane filters, but these carry a significantly increased cost considering their price (e.g., Sterlitech, approximately $6.90 per filter vs. $0.6 per filter for glass fiber filters) and the common requirement for replicate filters across multiple sampling stations, depths, or experimental time points.

Our finding that precombusted glass fiber filters fail to retain significant numbers of bacterioplankton is puzzling in the light of earlier claims of precombusted GF/F filters performing comparably as 0.2 μm pore size membrane filters in productivity and pigment measurements (Chavez et al., 1995; Nayar and Chou, 2003). While Chavez et al. (1995) focused solely on Chlorophyll *a* containing cells (prochlorophytes with 0.54–0.67 μm equivalent spherical diameter) and primary production measurements, Nayar and Chou (2003) used scanning electron microscopy and showed that the borosilicate glass microfibers get compacted during combustion, which effectively downsizes the nominal pore size. The only obvious explanation for the discrepancy to our results is that Nayar and Chou (2003) combusted their filters at 600°C for 1 h, while most studies carrying out BNF measurements (including our present one) combusted filters at 450°C for 2–12 h (e.g., Montoya et al., 1996; Capone et al., 2005; White et al., 2007; Farnelid et al., 2013; Shiozaki et al., 2017). While the lower temperature of 450°C is enough to eliminate carbon or nitrogen contamination from filters, it apparently compacts the filter fiber structure less than at 600°C. Manufacturers advise maximum temperatures of 500°C for borosilicate membranes, and Nayar and Chou (2003) observed melting of the filters when exposing them to >600°C or to longer durations of combustion. Thus, combustion like

described by Nayar and Chou (2003) can potentially further reduce the large bacterial cell loss during filtration and should be more widely adapted for measuring bacterial process rates. The current application of only 450°C together with highly variable combustion times in BNF studies adds to the uncertainty about which effective pore sizes may have actually been applied in published BNF studies.

Some investigators opt for not precombusting glass fiber filters prior to using them in BNF experiments (e.g., Fernández et al., 2010). This is due to the concern that the effective combustion temperature could vary for different filters inside the furnace (depending e.g., on how they are positioned and how close they are to the walls), and due to the belief that contamination of purchased filters is negligible and that the additional handling associated with precombustion could add further contamination. While these concerns are valid, we believe that precombustion is an essential part of the BNF protocol. In our experience, significant trace contamination of filters can exist, and thus using uncombusted filters would introduce additional uncertainty about obtained BNF rates, given the mentioned potential contamination of $^{15}N_2$ gas stocks (Dabundo et al., 2014) and the difficulties with generating contamination-free $^{15}N_2$ enriched seawater (Klawonn et al., 2015). Further, as mentioned, the effects of combustion on the filter matrix structure seem to be desirable since they increase the retention capacity of the filters (Nayar and Chou, 2003). However, a consensus protocol of preparing and carrying out BNF measurements should include reviewed instructions on how to correctly combust glass fiber filters, including recommendations on combustion times, temperatures, and positioning of the filters inside the furnace.

The Effect of Different Retention by GF/F and Advantec Filters on Obtained BNF Rates

Apart from the initial filter test in the Sargasso Sea (2.95 ± 0.53 nmol N L^{-1} d^{-1} for Advantec vs. 1.4 ± 0.17 nmol N L^{-1} d^{-1} for GF/F) all measured BNF rates in this study were below 2 nmol N L^{-1} d^{-1}, falling into the lower range of volumetric BNF measured in oceanic waters (Luo et al., 2012). At the station in the Pacific, BNF even remained undetectable. The low rates in Øresund and Roskilde (**Figure 3**) are possibly explained by the abiotic conditions encountered, including rather low temperatures measured throughout our samplings, peaking at around sampling in Roskilde Fjord. Such temperatures are below what is traditionally diazotroph growth, even for temperate cyanobacterial species like *Aphanizomenon flos aquae* or *Anabaena* spp. (Laamanen and Kuosa, 2005; Sohm et al., 2011). However, not much is known about temperature constraints on field populations of non-cyanobacterial diazotrophs. BNF rates for Roskilde Fjord were overall much lower in 2015 than in 2012 (Bentzon-Tilia et al., 2015a) although water temperatures were comparable, pointing to a high year-to-year variability. It could be speculated that our low BNF rates falsely represent uptake of $^{15}NH_4$ contaminant (Dabundo et al., 2014) by small bacteria which were subsequently retained better by Advantec filters. However, in this case it would be difficult to explain why BNF remained completely undetectable in some samples, and more importantly, our batch of $^{15}N_2$ gas from Cambridge Isotopes (lot # I-16727) was described to contain only minute levels of contaminant, theoretically triggering maximal "false" rates of ca. 0.02 nmol N L^{-1} d^{-1} (Dabundo et al., 2014). We therefore

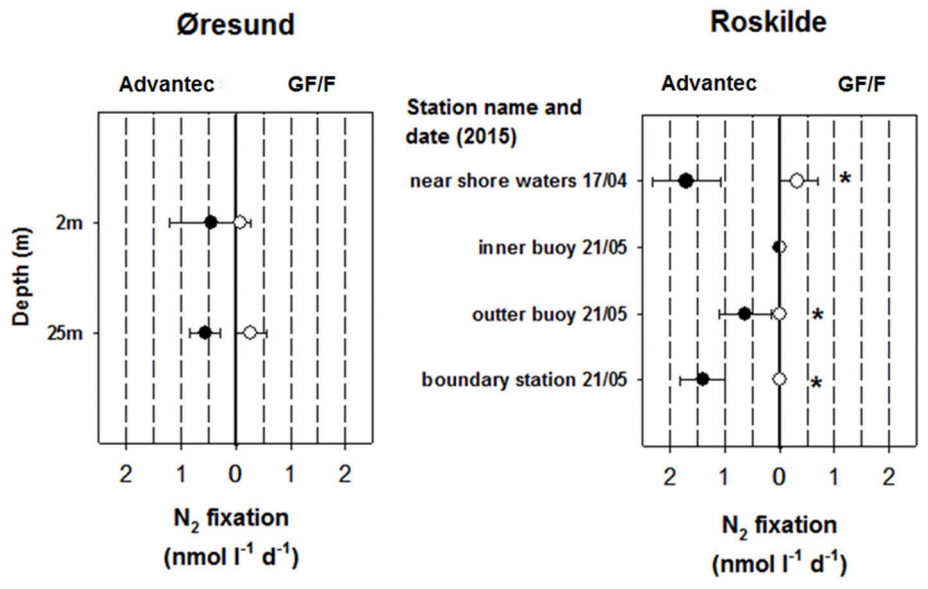

FIGURE 3 | N_2 fixation rates obtained from using Advantec or GF/F filters in Øresund and Roskilde Fjord (averages ± standard deviation, $n = 3$). N_2 fixation was undetectable in all Pacific samples and therefore a graph is not shown for that habitat. For Roskilde Fjord, N_2 fixation was not measured in March 2015. Cases where rates were significantly different between the two filter types are marked with asterisks (*t*-test, $p < 0.05$). In Øresund, the halocline separates surface waters with a salinity of 11 and deep waters with a salinity of 33.

believe that our measurements represent true diazotroph activity. diazotroph activity.

Importantly, in most cases where we detected BNF (including the initial test in the Sargasso Sea), rates were higher when using Advantec filters compared to GF/F filters, and in two cases rates remained undetectable with GF/F filters while they were detectable in Advantec replicates (Roskilde Fjord outer—and boundary station, May 2015; **Figure 3**). In all cases where BNF rates were significantly higher in Advantec replicates, we also found significantly lower bacterial abundances in Advantec filtrates (**Figure 2** vs. **Figure 3**), suggesting that cells responsible for BNF were lost via GF/F filtration but not via filtration over Advantec. Taken together, our data suggest that by using Advantec filters, detection of low BNF rates is more likely. This finding is important because BNF rates in mesopelagic waters and other "unusual" habitats are often equal to or even lower than our rates (Fernandez et al., 2011; Bonnet et al., 2013; Dekaezemacker et al., 2013; Rahav et al., 2013; Benavides et al., 2015; Löscher et al., 2016). Consequently, it would be desirable to test whether rates determined for these environments (and the biogeochemical significance derived from such rates) are underestimates due to the use of 0.7 μm pore size GF/F filters.

Diazotroph Community Composition in Bulk Samples and Filtrates of GF/F and Advantec Filters

In order to analyze and compare the presence and composition of diazotrophs in bulk and filtrate material, we attempted to PCR-amplify the *nifH* gene from a total of 62 samples (36 GF/F /Advantec filtrates, 25 bulk samples, plus one blank sample). *nifH* was successfully amplified from 58 samples, except for one bulk sample from 5 m at the Pacific station, a bulk sample from outer buoy in March 2015, and both filtrate samples at outer buoy in May 2015. The successful amplification in most filtrate samples suggests that across different habitats, glass fiber filters do not catch the entire diazotroph community.

The Illumina sequencing yielded a total of 1,489,321 reads clustering into 464 OTUs after quality control and deletion of OTUs with <100 reads across all samples or OTUs that occurred in <2 per sample ranged from 554 to 89,532, with an average of 25,678. The blank sample did not return any *nifH* sequences. Sequences accounting for at least 1% of reads in a single sample comprised 89 OTUs and were mainly affiliated with diverse Proteobacteria and a few Cyanobacteria in *nifH* cluster I, as well as putatively anaerobic prokaryotes in *nifH* cluster III (Zehr et al., 2003) (Supplemental Figure S2). As in every study sequencing *nifH* genes, some of the retrieved phylotypes potentially are contaminants, which needs to be kept in mind especially for novel sequences lacking closely related, cultured representatives. The most common OTU_1 was most closely related to *Paenibacillus wynnii* sp., a facultatively anaerobic bacterium isolated from Alexander Island, Antarctica (Rodríguez-Díaz et al., 2005). However, OTU_2 was closely related to a sequence retrieved from bottled mineral water (França et al., 2016) and was found across the different habitats, indicating that it was possibly a contaminant. In the following discussion on retentive characteristics of the filters, we therefore focus on well-studied

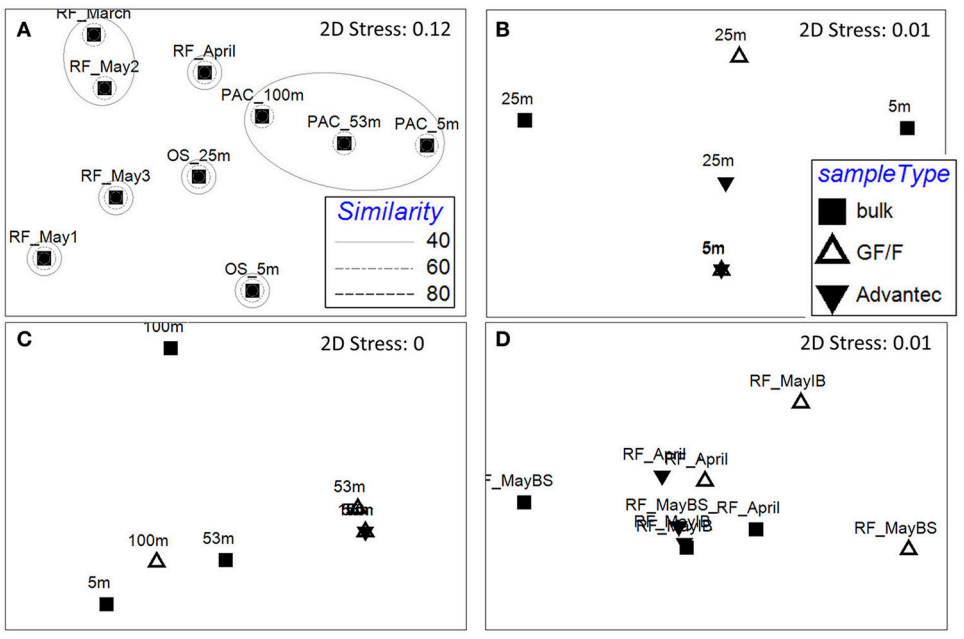

FIGURE 4 | Non-metric multidimensional scaling (NMDS) plots of the diazotroph community composition based on rarefied (n = 2,000) *nifH* genes, calculated by Bray-Curtis similarity. **(A)** Resemblance between bulk samples at the different habitats. Rings mark different similarities (%) between samples, as shown in the legend. RF: Roskilde Fjord; OS: Øresund; PAC: Pacific. **B–D**) Resemblance between bulk and filtrate samples in samples from Øresund, Pacific, and Roskilde Fjord, respectively. IB, Inner Buoy; BS, Boundary Station.

phylotypes which undoubtedly are of marine origin. Further, to reduce complexity, from here we mainly focus on bulk and filtrate samples for which BNF was measured.

The *nifH* community composition differed significantly between habitats (**Figure 4A**; PERMANOVA $p = 0.001$), offering the opportunity to test whether retentive characteristics of GF/F and Advantec filters would vary depending on the composition of diazotrophs. We mainly compare the types of diazotrophs detected in bulk and filtrate samples in a qualitative way, since Illumina sequencing of PCR amplicons does not yield truly quantitative information due to biases such as preferential amplification of some phylotypes (e.g., Turk et al., 2011). As shown in **Figures 4B–D**, *nifH* communities often differed between bulk- and filtrate samples, and between GF/F—and Advantec filtrate samples, although these differences were not significant overall (PERMANOVA, $p = 0.48$ for Øresund; $p = 0.17$ for Pacific samples, and $p = 0.26$ for Roskilde Fjord samples). While amplicon sequencing can hardly be used to infer how well the different filters retained specific diazotrophs, our data suggest that only parts of the diazotroph community potentially pass through the filters, and that there can be differences in composition between diazotrophs passing through GF/F and Advantec filters, respectively.

An important example are the few cyanobacterial OTUs found in this study (green cluster in Supplemental Figure S2), which were exclusively retrieved from bulk samples (screening all ≥1% OTUs of all 58 successfully amplified samples), except for OTU_4, which had 99% nucleotide sequence similarity to *Candidatus* Atelocyanobacterium thalassa ("UCYN-A1"). OTU_4 was only recovered in the Pacific, even though Bentzon-Tilia et al. (2015b) previously found a close relative (UCYN-A2) to be an active diazotroph in Roskilde Fjord. UCYN-A is a symbiotic unicellular cyanobacterium that lives in a fragile association with its host (Thompson et al., 2012), and this small (1–2 μm diameter) diazotroph was also clearly detected in GF/F filtrate at 100 m, although not at the shallower depths (**Figure 5**).

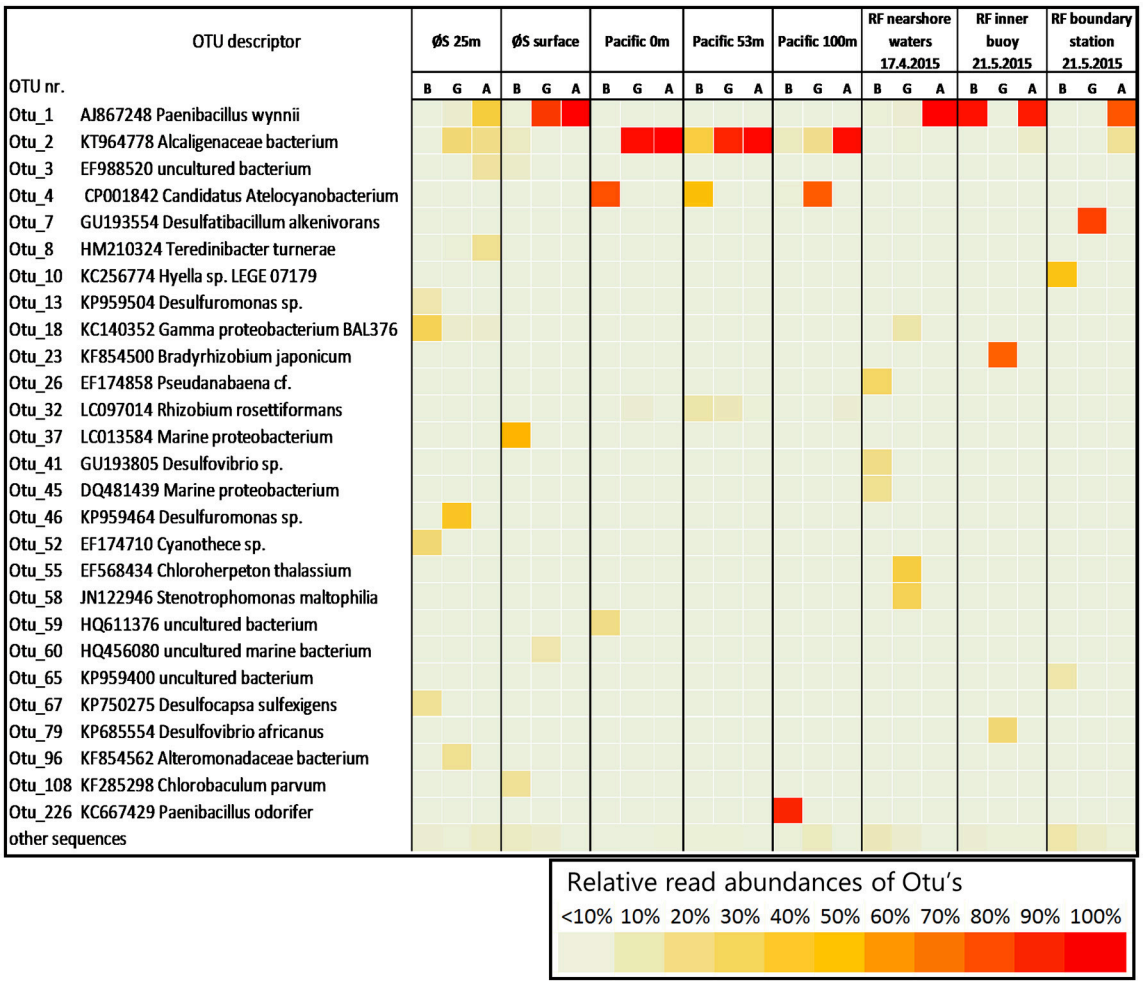

FIGURE 5 | Relative read abundances (in %) of operational taxonomic units (OTU's) in bulk water and filtrates for the 24 samples in which BNF was measured. For clarity, only OTUs accounting for ≥10% of reads in a single sample are shown. Abbreviations B, G, and A refer to bulk, GF/F, and Advantec samples, respectively. The description lists accession numbers of closest BLAST hits and, where available, organism names of closest cultured or genome-sequenced organisms.

This example documents that small, unicellular diazotroph key players can get lost to filtrate in BNF assays. In contrast, cyanobacterial OTU_10 (*Hyella* sp.) and OTU_52 (*Cyanothece* sp.) only occurred in bulk samples. This is likely explained by the morphology and size of these organisms, as *Hyella* sp. is a pseudofilamentous, slime-generating and relatively large (10s of μm long colonies) cyanobacterium (Brito et al., 2017), and *Cyanothece* sp. is a larger unicellular cyanobacterium (≥3 μm diameter) which sometimes also forms aggregates (Reddy et al., 1993). OTU_18 is a noteworthy example for a heterotrophic diazotroph found in filtrate. This phylotype is closely related to a *Pseudomonas stutzeri* (BAL376/BAL410) isolated from Baltic Sea surface waters (Farnelid et al., 2014) and is thought to be able to fix N_2 in oxygenated water by forming aggregates. These *Pseudomonas* types are likely important diazotrophs in the Baltic Sea and Danish coastal waters, and it is notable that we also detected OTU_18 in GF/F filtrate in Roskilde Fjord (**Figure 5**). Together, our results suggest that the morphology and life style of different diazotrophs influence whether they get lost to glass fiber filtrate or not.

CONCLUSIONS

The experiments carried out in this study document the significant loss of bacterial cells to filtrates of both GF/F and Advantec filters, but with the latter performing clearly better in retaining cells. While such losses have been described previously, with little or no effect on productivity or pigment measurements, we show that better retention by Advantec filters can at times result in higher BNF rates compared to GF/F filters. It is important to note that although we sampled multiple locations, our dataset is small and detected rates were rather low. We therefore explicitly encourage other investigators to test Advantec filters in $^{15}N_2$ tracer assays for other areas, including "hotspots" of diazotrophy.

Advantec filters seem generally advisable for BNF measurements, and especially in habitats expected to host small and/or heterotrophic diazotrophs fixing N_2 at low rates. Further, BNF activity of cells filtered onto GF/F is often compared with relative or absolute (qPCR determined) abundances of certain *nifH* phylotypes analyzed from nucleic acid samples filtered onto 0.2 μm pore size membrane filters. Our data shows that *nifH* containing organisms pass through the glass fiber filters, apparently including organisms with significant contributions to BNF, and thus it is advisable to use Advantec or even silver membrane filters in $^{15}N_2$ assays in order to obtain better comparable data. In general, our results highlight the importance of the filtration step in BNF measurements and suggest that choosing filters with < 0.7 μm pore size helps to gain more inclusive measurements of diazotroph activity in aquatic ecosystems.

AUTHOR CONTRIBUTIONS

DB designed and did the research, wrote the paper. RP did part of the experiments, wrote the paper. RA did the flow cytometry, wrote the paper. LR helped with designing the idea and experiments, wrote the paper.

FUNDING

This work resulted from the BONUS BLUEPRINT project supported by BONUS (Art 185), funded jointly by the EU and the Danish Agency for Science, Technology and Innovation.

ACKNOWLEDGMENTS

We thank Eero Asmala, Hans Jakobsen, and Jacob Carstensen for providing ship time and for assistance in sampling in Roskilde Fjord, as well as Francisco Chavez, Jason Smith, and the crew of the R/V Western Flyer for ship-time and assistance with experimental incubations in the Pacific. Claudia Dziallas and Ina Severin are acknowledged for providing data from the initial filter comparison in the Sargasso Sea, and Mar Benavides for proofreading the manuscript.

SUPPLEMENTARY MATERIAL

The Supplementary Material for this article can be found online at: https://www.frontiersin.org/articles/10.3389/fmars.2018.00006/full#supplementary-material

REFERENCES

Benavides, M., Moisander, P. H., Berthelot, H., Dittmar, T., Grosso, O., and Bonnet, S. (2015). Mesopelagic N_2 fixation related to organic matter composition in the solomon and Bismarck Seas (Southwest Pacific). *PLoS ONE* 10:e0143775. doi: 10.1371/journal.pone.0143775

Bentzon-Tilia, M., Severin, I., Hansen, L. H., and Riemann, L. (2015b). Genomics and ecophysiology of heterotrophic nitrogen-fixing bacteria isolated from estuarine surface water. *mBio* 6:e00929. doi: 10.1128/mBio.00929-15

Bentzon-Tilia, M., Traving, S. J., Mantikci, M., Knudsen-Leerbeck, H., Hansen, J. L. S., Markager, S., et al. (2015a). Significant N_2 fixation by heterotrophs, photoheterotrophs and heterocystous cyanobacteria in two temperate estuaries. *ISME J.* 9, 273–285. doi: 10.1038/ismej.2014.119

Berthelot, H., Benavides, M., Moisander, P. H., Grosso, O., and Bonnet, S. (2017). High-nitrogen fixation rates in the particulate and dissolved pools in the Western Tropical Pacific (Solomon and Bismarck Seas). *Geophys. Res. Lett.* 44, 8414–8423. doi: 10.1002/2017GL073856

Blais, M., Tremblay, J.-É., Jungblut, A. D., Gagnon, J., Martin, J., Thaler, M., et al. (2012). Nitrogen fixation and identification of potential diazotrophs in the Canadian Arctic. *Global Biogeochem. Cycles* 26:GB3022. doi: 10.1029/2011GB004096

Bombar, D., Paerl, R. W., and Riemann, L. (2016). Marine Non-Cyanobacterial Diazotrophs: moving beyond Molecular Detection. *Trends Microbiol.* 24, 916–927. doi: 10.1016/j.tim.2016.07.002

Bonnet, S., Dekaezemacker, J., Turk-Kubo, K. A., Moutin, T., Hamersley, R. M., Grosso, O., et al. (2013). Aphotic N2 fixation in the Eastern Tropical South Pacific Ocean. *PLoS ONE* 8:e81265. doi: 10.1371/journal.pone.0081265

Boström, K. H., Riemann, L., Kühl, M., and Hagström, Å. (2007). Isolation and gene quantification of heterotrophic N_2-fixing bacterioplankton in the Baltic Sea. *Environ. Microbiol.* 9, 152–164. doi: 10.1111/j.1462-2920.2006.01124.x

Boström, K. H., Simu, K., Hagström, Å., and Riemann, L. (2004). Optimization of DNA extraction for quantitative marine bacterioplankton community analysis. *Limnol. Oceanogr.* 2, 365–373. doi: 10.4319/lom.2004.2.365

Brito, Â., Ramos, V., Mota, R., Lima, S., Santos, A., Vieira, J., et al. (2017). Description of new genera and species of marine cyanobacteria from the Portuguese Atlantic coast. *Mol. Phylogenet. Evol.* 111, 18–34. doi: 10.1016/j.ympev.2017.03.006

Canfield, D. E., Glazer, A. N., and Falkowski, P. G. (2010). The Evolution and Future of Earth's Nitrogen Cycle. *Science* 330, 192–196. doi: 10.1126/science.1186120

Capone, D. G., Burns, J. A., Montoya, J. P., Subramaniam, A., Mahaffey, C., Gunderson, T., et al. (2005). Nitrogen fixation by *Trichodesmium* spp.: An important source of new nitrogen to the tropical and subtropical North Atlantic Ocean. *Global Biogeochem. Cycles* 19:GB2024. doi: 10.1029/2004GB002331

Caporaso, J. G., Kuczynski, J., Stombaugh, J., Bittinger, K., Bushman, F. D., Costello, E. K., et al. (2010). QIIME allows analysis of high-throughput community sequencing data. *Nat. Meth.* 7, 335–336. doi: 10.1038/nmeth.f.303

Chavez, F. P., Buck, K. R., Bidigare, R. R., Karl, D. M., Hebel, D., Latasa, M., et al. (1995). On the chlorophyll a retention properties of glass-fiber GF/F filters. *Limnol. Oceanogr.* 40, 428–433. doi: 10.4319/lo.1995.40.2.0428

Clarke, K., and Gorley, R. (2006). *PRIMER v6: User Manual/Tutorial*. Plymouth: PRIMER-E.

Dabundo, R., Lehmann, M. F., Treibergs, L., Tobias, C. R., Altabet, M. A., Moisander, P. H., et al. (2014). The Contamination of Commercial $^{15}N_2$− Gas Stocks with ^{15}N–Labeled Nitrate and Ammonium and Consequences for Nitrogen Fixation Measurements. *PLoS ONE* 9:e110335. doi: 10.1371/journal.pone.0110335

Dekaezemacker, J., Bonnet, S., Grosso, O., Moutin, T., Bressac, M., and Capone, D. (2013). Evidence of active dinitrogen fixation in surface waters of the eastern tropical South Pacific during El Ni-o and La Ni-a events and evaluation of its potential nutrient controls. *Global Biogeochem. Cycles* 27, 768–779. doi: 10.1002/gbc.20063

Deutsch, C., Sarmiento, J. L., Sigman, D. M., Gruber, N., and Dunne, J. P. (2007). Spatial coupling of nitrogen inputs and losses in the ocean. *Nature* 445, 163–167. doi: 10.1038/nature05392

Edgar, R. C., Haas, B. J., Clemente, J. C., Quince, C., and Knight, R. (2011). UCHIME improves sensitivity and speed of chimera detection. *Bioinformatics* 27, 2194–2200. doi: 10.1093/bioinformatics/btr381

Farnelid, H., Andersson, A. F., Bertilsson, S., Al-Soud, W. A., Hansen, L. H., Sørensen, S., et al. (2011). Nitrogenase gene amplicons from global marine surface waters are dominated by genes of non-cyanobacteria. *PLoS ONE* 6:e19223. doi: 10.1371/journal.pone.0019223

Farnelid, H., Bentzon-Tilia, M., Andersson, A. F., Bertilsson, S., Jost, G., Labrenz, M., et al. (2013). Active nitrogen-fixing heterotrophic bacteria at and below the chemocline of the central Baltic Sea. *ISME J.* 7, 1413–1423. doi: 10.1038/ismej.2013.26

Farnelid, H., Harder, J., Bentzon-Tilia, M., and Riemann, L. (2014). Isolation of heterotrophic diazotrophic bacteria from estuarine surface waters. *Environ. Microbiol.* 16, 3072–3082. doi: 10.1111/1462-2920.12335

Farnelid, H., Tarangkoon, W., Hansen, G., Hansen, P. J., and Riemann, L. (2010). Putative N2-fixing heterotrophic bacteria associated with dinoflagellate–Cyanobacteria consortia in the low-nitrogen Indian Ocean. *Aquat. Microb. Ecol.* 61, 105–117. doi: 10.3354/ame01440

Fernández, A., Mouri-o-Carballido, B., Bode, A., Varela, M., and Mara-ón, E. (2010). Latitudinal distribution of *Trichodesmium* spp. and N_2 fixation in the Atlantic Ocean. *Biogeosciences* 7, 3167–3176. doi: 10.5194/bg-7-3167-2010

Fernandez, C., Farías, L., and Ulloa, O. (2011). Nitrogen fixation in denitrified marine waters. *PLoS ONE* 6:e20539. doi: 10.1371/journal.pone.0020539

França, L., Albuquerque, L., Sánchez, C., Fareleira, P., and Da Costa, M. S. (2016). *Ampullimonas aquatilis* gen. nov., sp. nov. isolated from bottled mineral water. *Int. J. Syst. Evol. Microbiol.* 66, 1459–1465. doi: 10.1099/ijsem.0.000903

Gasol, J. M., and Del Giorgio, P. A. (2000). Using flow cytometry for counting natural planktonic bacteria and understanding the structure of planktonic bacterial *Communities* 64:28. doi: 10.3989/scimar.2000.64n2197

Glibert, P. M., and Bronk, D. A. (1994). Release of dissolved organic nitrogen by marine diazotrophic cyanobacteria *Trichodesmium* spp. *Appl. Environ. Microbiol.* 11, 3996–4000.

Großkopf, T., Mohr, W., Baustian, T., Schunck, H., Gill, D., Kuypers, M. M., et al. (2012). Doubling of marine dinitrogen-fixation rates based on direct measurements. *Nature* 488, 361–364. doi: 10.1038/nature11338

Gruber, N., and Galloway, J. N. (2008). An Earth-system perspective of the global nitrogen cycle. *Nature* 451, 293–296. doi: 10.1038/nature06592

Gruber, N., and Sarmiento, J. L. (1997). Global patterns of marine nitrogen fixation and denitrification. *Global Biogeochem. Cycles* 11, 235–266. doi: 10.1029/97GB00077

Klawonn, I., Lavik, G., Böning, P., Marchant, H. K., Dekaezemacker, J., Mohr, W., et al. (2015). Simple approach for the preparation of $^{15-15}N_2$-enriched water for nitrogen fixation assessments: evaluation, application and recommendations. *Front. Microbiol.* 6:769. doi: 10.3389/fmicb.2015.00769

Konno, U., Tsunogai, U., Komatsu, D. D., Daita, S., Nakagawa, F., Tsuda, A., et al. (2010). Determination of total N_2 fixation rates in the ocean taking into account both the particulate and filtrate fractions. *Biogeosciences* 7, 2369–2377. doi: 10.5194/bg-7-2369-2010

Laamanen, M., and Kuosa, H. (2005). Annual variability of biomass and heterocysts of the N_2-fixing cyanobacterium Aphanizomenon flos-aquae in the Baltic Sea with reference to *Anabaena* spp. and Nodularia spumigena. *Boreal Env. Res.* 10, 19–30.

Lee, S., Kang, Y.-C., and Fuhrman, J. A. (1995). Imperfect retention of natural bacterioplankton cells by glass fiber filters. *Mar. Ecol. Prog. Ser.* 19, 285–290. doi: 10.3354/meps119285

Löscher, C. R., Bourbonnais, A., Dekaezemacker, J., Charoenpong, C. N., Altabet, M. A., Bange, H. W., et al. (2016). N_2 fixation in eddies of the eastern tropical South Pacific Ocean. *Biogeosciences* 13, 2889–2899. doi: 10.5194/bg-13-2889-2016

Luo, Y. W., Doney, S. C., Anderson, L. A., Benavides, M., Berman-Frank, I., Bode, A., et al. (2012). Database of diazotrophs in global ocean: abundance, biomass and nitrogen fixation rates. *Earth Syst. Sci. Data* 4, 47–73. doi: 10.5194/essd-4-47-2012

Mohr, W., Grosskopf, T., Wallace, D. W. R., and Laroche, J. (2010). Methodological underestimation of oceanic nitrogen fixation rates. *PLoS ONE* 5:12583. doi: 10.1371/journal.pone.0012583

Moisander, P. H., Serros, T., Paerl, R. W., Beinart, R. A., and Zehr, J. P. (2014). Gammaproteobacterial diazotrophs and nifH gene expression in surface waters of the South Pacific Ocean. *ISME J.* 8, 1962–1973. doi: 10.1038/ismej.2014.49

Montoya, J. P., Holl, C. M., Zehr, J. P., Hansen, A., Villareal, T. A., and Capone, D. G. (2004). High rates of N_2 fixation by unicellular diazotrophs in the oligotrophic Pacific Ocean. *Nature* 430, 1027–1031. doi: 10.1038/nature02824

Montoya, J. P., Voss, M., Kahler, P., and Capone, D. G. (1996). A simple, high-precision, high-sensitivity tracer assay for N_2 fixation. *Appl. Environ. Microbiol.* 62, 986–993.

Moran, X., a,. G., Gasol, J. M., Arin, L., and Estrada, M. (1999). A comparison between glass fiber and membrane filters for the estimation of phytoplankton POC and DOC production. *Mar. Ecol. Prog. Ser.* 187, 31–41. doi: 10.3354/meps187031

Mulholland, M. R., Bronk, D., and Capone, D. G. (2004). Dinitrogen fixation and release of ammonium and dissolved organic nitrogen by Trichodesmium IMS101. *Aquat. Microb. Ecol.* 37, 85–94. doi: 10.3354/ame037085

Nayar, S., and Chou, L. M. (2003). Relative efficiencies of different filters in retaining phytoplankton for pigment and productivity studies. *Estuar. Coast. Shelf Sci.* 58, 241–248. doi: 10.1016/S0272-7714(03)00075-1

Rahav, E., Bar-Zeev, E., Ohayion, S., Elifantz, H., Belkin, N., Herut, B., et al. (2013). Dinitrogen fixation in aphotic oxygenated marine environments. *Front. Microbiol.* 4:227. doi: 10.3389/fmicb.2013.00227

Reddy, K. J., Haskell, J. B., Sherman, D. M., and Sherman, L. A. (1993). Unicellular, aerobic nitrogen-fixing cyanobacteria of the genus Cyanothece. *J. Bacteriol.* 175, 1284–1292. doi: 10.1128/jb.175.5.1284-1292.1993

Rodríguez-Díaz, M., Lebbe, L., Rodelas, B., Heyrman, J., De Vos, P., and Logan, N. A. (2005). *Paenibacillus wynnii* sp. nov., a novel species harbouring the nifH gene, isolated from Alexander Island, Antarctica. *Int. J. Syst. Evol. Microbiol.* 55, 2093–2099. doi: 10.1099/ijs.0.63395-0

Schloss, P. D., Westcott, S. L., Ryabin, T., Hall, J. R., Hartmann, M., Hollister, E. B., et al. (2009). Introducing mothur: Open-source, platform-independent, community-supported software for describing and comparing microbial communities. *Appl. Environ. Microbiol.* 75, 7537–7541. doi: 10.1128/AEM.01541-09

Shiozaki, T., Bombar, D., Riemann, L., Hashihama, F., Takeda, S., Yamaguchi, T., et al. (2017). Basin scale variability of active diazotrophs and nitrogen fixation in the North Pacific, from the tropics to the subarctic Bering Sea. *Global Biogeochem. Cycles* 31, 996–1009. doi: 10.1002/2017GB005681

Sohm, J. A., Webb, E. A., and Capone, D. G. (2011). Emerging patterns of marine nitrogen fixation. *Nat. Rev. Microbiol.* 9, 499–508. doi: 10.1038/nrmicro2594

Søndergaard, M., and Middelboe, M. (1993). Measurements of particulate organic carbon: a note on the use of glass fiber (GF/F) and Anodisc R filters. *Pol. Arch. Hydrobiol.* 127, 73–85.

Thompson, A. W., Foster, R. A., Krupke, A., Carter, B. J., Musat, N., Vaulot, D., et al. (2012). Unicellular cyanobacterium symbiotic with a single-celled eukaryotic alga. *Science* 337, 1546–1550. doi: 10.1126/science.1222700

Turk, K., Rees, A. P., Zehr, J. P., Pereira, N., Swift, P., Shelley, R., et al. (2011). Nitrogen fixation and nitrogenase (nifH) expression in tropical waters of the eastern North Atlantic. *ISME J.* 5, 1201–1212. doi: 10.1038/ismej.2010.205

Voss, M., Croot, P., Lochte, K., Mills, M., and Peeken, I. (2004). Patterns of nitrogen fixation along 10N in the tropical Atlantic. *Geophys. Res. Lett.* 31:L23S09. doi: 10.1029/2004GL020127

White, A. E., Prahl, F. G., Letelier, R. M., and Popp, B. N. (2007). Summer surface waters in the Gulf of California: prime habitat for biological N-2 fixation. *Global Biogeochem. Cycles* 21:GB2017. doi: 10.1029/2006GB002779

Wilson, S. T., Böttjer, D., Church, M. J., and Karl, D. M. (2012). Comparative assessment of nitrogen fixation methodologies, conducted in the oligotrophic North Pacific Ocean. *Appl. Environ. Microbiol.* 78, 6516–6523. doi: 10.1128/AEM.01146-12

Zani, S., Mellon, M. T., Collier, J. L., and Zehr, J. P. (2000). Expression of nifH genes in natural microbial assemblages in Lake George, NY detected with RT-PCR. *Appl. Environ. Microbiol.* 66, 3119–3124. doi: 10.1128/AEM.66.7.3119-3124.2000

Zehr, J. P. (2011). Nitrogen fixation by marine cyanobacteria. *Trends Microbiol.* 19, 162–173. doi: 10.1016/j.tim.2010.12.004

Zehr, J. P., Jenkins, B. D., Short, S. M., and Steward, G. F. (2003). Nitrogenase gene diversity and microbial community structure: a cross-system comparison. *Environ. Microbiol.* 5, 539–554. doi: 10.1046/j.1462-2920.2003.00451.x

Zehr, J. P., and Mcreynolds, L. A. (1989). Use of degenerate oligonucleotides for amplification of the nifH gene from the marine cyanobacterium *Trichodesmium thiebautii*. *Appl. Environ. Microbiol.* 55, 2522–2526.

Zehr, J. P., Mellon, M. T., and Zani, S. (1998). New nitrogen fixing microorganisms detected in oligotrophic oceans by the amplification of nitrogenase (nifH) genes. *Appl. Environ. Microbiol.* 64, 3444–3450.

Zehr, J. P., and Turner, P. J. (2001). "Nitrogen fixation: nitrogenase genes and gene expression," in *Methods in Microbiology: Marine Microbiology*, Vol. 30, ed J. H. Paul (London: Academic Press, Ltd.), 271–286.

Conflict of Interest Statement: The authors declare that the research was conducted in the absence of any commercial or financial relationships that could be construed as a potential conflict of interest.

frontiers in Marine Science

PERSPECTIVE
published: 05 February 2018
doi: 10.3389/fmars.2018.00002

A Short Comparison of Two Marine Planktonic Diazotrophic Symbioses Highlights an Un-quantified Disparity

Andrea Caputo, Marcus Stenegren, Massimo C. Pernice and Rachel A. Foster*

Department of Ecology, Environment and Plant Sciences, Stockholm University, Stockholm, Sweden

Some N_2-fixing cyanobacteria form symbiosis with diverse protists. In the plankton two groups of diazotrophic symbioses are described: (1) a collective group of diatoms which associate with heterocystous cyanobacteria (Diatom Diazotroph Associations, DDA), and (2) the microalgal prymnesiophyte *Braarudosphaera bigelowii* and its relatives which associate with the unicellular cyanobacterium *Candidatus* Atelocyanobacterium thalassa (hereafter as UCYN-A). Both symbiotic systems co-occur, and in both partnerships the symbionts function as a nitrogen (N) source. In this perspective, we provide a brief comparison between the DDAs and the prymnesiophyte-UCYN-A symbioses highlighting similarities and differences in both systems, and present a bias in the attention and current methodology that has led to an under-detection and under-estimation of the DDAs.

Keywords: cyanobacteria, diazotrophs, diatoms, symbiosis, DDA, UCYN-A, *Richelia*, *Calothrix*

OPEN ACCESS

Edited by:
Angela Landolfi,
GEOMAR Helmholtz Centre for Ocean Research Kiel (HZ), Germany

Reviewed by:
Jillian Petersen,
University of Vienna, Austria
Angelicque White,
Oregon State University, United States

****Correspondence:***
Andrea Caputo
andrea.caputo@su.se

Specialty section:
This article was submitted to Aquatic Microbiology, a section of the journal Frontiers in Marine Science

Received: *05 October 2017*
Accepted: *09 January 2018*
Published: *05 February 2018*

Citation:
Caputo A, Stenegren M, Pernice MC and Foster RA (2018) A Short Comparison of Two Marine Planktonic Diazotrophic Symbioses Highlights an Un-quantified Disparity. Front. Mar. Sci. 5:2. doi: 10.3389/fmars.2018.00002

INTRODUCTION

Some of the most inconspicuous components of the plankton are partnerships, or symbioses, between diverse unicellular eukaryotic microalgae and prokaryotic cyanobacteria. In some planktonic symbiosis, the symbionts are N_2 fixers, or diazotrophs, that reduce di-nitrogen (N_2) and provide ammonia to their respective hosts. There are two marine planktonic N_2 fixing symbiotic systems described, which can be divided by host type. The more recently discovered is a partnership between a prymnesiophyte, the microalga *Braarudosphaera bigelowii* and its relatives and several lineages of the unicellular cyanobacterium, *Candidatus* Atelocyanobacterium thalassa or more commonly called UCYN-A (Zehr et al., 2008; Tripp et al., 2010; Thompson et al., 2012). The second symbiotic system is a group referred to as diatom diazotroph associations (DDAs) (Foster and O'Mullan, 2008).

DDAs are symbioses between various diatom genera (*Rhizosolenia, Hemiaulus, Chaetoceros, Guinardia, Bacteriastrum*) and the heterocystous cyanobacteria, *Richelia intracellularis* or *Calothrix rhizosoleniae*. Each symbiotic filament is composed of several vegetative cells and a terminal heterocyst for N_2 fixation. There is an additional DDA described between the pennate diatom, *Climacodium frauenfeldianum*, and a unicellular cyanobacteria (Carpenter and Janson, 2000). For the purposes of this review, however, we limit the discussion of the DDAs to the partnerships involving heterocystous cyanobacterial symbionts.

Planktonic N_2 fixing symbioses are widespread, often co-occur and both are considered significant contributors to both the N and C cycles. The DDAs were described over a century ago, yet remain understudied, with only two dedicated reviews in the last two decades (Villareal, 1992; Foster and O'Mullan, 2008), while the prymnesiophyte-UCYN-A symbioses were recently

discovered (within a decade) and have been highlighted in several reviews (e.g., Bothe et al., 2010; Delong, 2010; Thompson and Zehr, 2013; Zehr, 2015; Farnelid et al., 2016; Zehr et al., 2016). Moreover, rarely are the two systems directly compared despite their similar nature as planktonic symbioses and function in the marine N cycle. The purpose of this short perspective is to provide a brief comparison of these two biogeochemically relevant symbioses and highlight a current disparity in attention and detection for the UCYN-A based symbiosis.

EARLY OBSERVATIONS AND FIRST GENETIC IDENTITY STUDIES

The earliest reports of DDAs came from simple microscopic observations in the late nineteenth and early twentieth centuries by Lemmermann (1905) and Ostenfeld and Schmidt (1901) when they observed and described the cyanobacterial epiphytes on *Rhizosolenia, Hemiaulus,* and *Chaetoceros* spp. diatoms. For over a century the DDAs were presumed as N_2 fixing symbiosis, since it was only recently shown that N was fixed and transferred to the hosts (Foster et al., 2011). While, the UCYN-A was initially believed as free-living and was only recently identified as a symbiont (Thompson et al., 2012). Unlike the DDAs which can be distinguished by standard epi-fluorescent microscopy, the UCYN-A symbiosis require sophisticated (e.g., competitor and dual labeled) and highly specific fluorescent *in situ* hybridization (FISH) based assays (Thompson et al., 2012; Krupke et al., 2013; Cabello et al., 2016; Cornejo-Castillo et al., 2016). However the earliest detection of UCYN-A (and DDA symbionts) were by environmental *nifH* sequence (encodes for nitrogenase enzyme complex for N_2 fixation) libraries.

In the early diversity studies using the *nifH* gene, the UCYN-A lineage and two of the three heterocystous lineages for DDAs were identified (Zehr et al., 1998, 2001; Church et al., 2005). These first sequences were referred to as: group A (hereafter UCYN-A), het-1, and het-2, however no sequence was directly linked to a particular cell or symbiosis. The het-1 and het-2 *nifH* sequences were similar to *nifH* sequences of other heterocystous cyanobacteria and therefore assumed to be derived from the symbionts of diatoms since no other heterocystous cyanobacteria were known to exist in the open ocean freely.

The identity of UYCN-A as a symbiont remained unknown for another decade, while the first two het lineages (het-1, het-2) and a third (het-3) were soon after identified as symbionts of *Rhizosolenia* spp., *Hemiaulus* spp., *Chaetoceros* spp. diatoms, respectively (Foster and Zehr, 2006). The het-3 symbiont of *Chaetoceros compressus* was isolated into culture, genome sequenced (CalSC01) and has been maintained asymbiotic since 2004 (Foster et al., 2010; Hilton et al., 2013). Currently there are six *nifH* clades designated as UCYN-A (UCYNA-1 through UCYN-A6), two clades are derived from symbiotic cells (i.e., UCYN-A1, UCYN-A2) (Thompson et al., 2014; Farnelid et al., 2016; Turk-kubo et al., 2017) and no UCYN-A cells have been isolated into culture.

SPECIFICITY, TRANSMISSION, AND MAINTENANCE

The DDAs are described as highly host specific, such that one symbiont type (e.g., het-1) associates with one host genus (*Rhizosolenia*) (Janson et al., 1999; Foster and Zehr, 2006). In fact, the specific nature in the partnerships allows the various DDAs to be quantified by quantitative PCR (qPCR) assays specific for the *nifH* sequence of the symbiont (see below). Similar high host fidelity is described in the two UCYN-A symbioses (Thompson et al., 2014; Cabello et al., 2016). The driver of specificity is unknown and unstudied in both symbiotic systems. Since both systems have evaded cultivation either entirely (e.g., UCYN-A) or for long-term (e.g., DDAs) our understanding of the life cycles and host-symbiont communication is extremely limited.

The infection and transmission (e.g., horizontal or vertical) has not been observed in either system. Earlier laboratory studies on the *Rhizosolenia-Richelia* symbioses found asynchronicity between partner growth rates and division cycles, which led to asymbiotic hosts (Villareal, 1990). Observations of asymbiotic diatom hosts and/or free-living *R. intracellularis* and *C. rhizosoleniae* are less common in the literature (Sournia, 1970; Marumo and Asaoka, 1974; Villareal, 1990; Gómez et al., 2005; White et al., 2007). Equally unknown is if another life stage persists or is required for infection in either symbioses as has been reported in terrestrial based symbioses with cyanobacteria (e.g., hormogonia) (Rasmussen, 2002). Given the rare instances of UCYN-A in asymbiotic form by CARD-FISH studies (Thompson et al., 2012; Krupke et al., 2013; Cabello et al., 2016), it is unlikely that another life stage persists for UCYN-A.

SYMBIONT LOCATION

A major finding when the draft genomes for the *Richelia* (RintHH01) and *Calothrix* (CalSC01) symbionts were reported was that the symbiont genome size and dependency was linked to location in the host diatoms (Hilton et al., 2013). A closer look at the two symbioses reveals that the housing of the symbionts are quite similar. For example, in prymnesiophyte hosts, UCYN-A have been described as internal symbionts by TEM observations of the host cytoplasm, loosely attached or in a free-floating compartment (symbiosome) (Hagino et al., 2013; Cornejo-Castillo et al., 2016). The symbionts of the DDAs vary from externally attached to a quasi-internal location residing between the host frustule and plasma membrane (Villareal, 1992). Recently using confocal microscopy we observed evidence for an internal location of *R. intracellularis* in the cytoplasm of *Hemiaulus hauckii* diatoms (Caputo et al. unpubl.). Thus the location for the symbionts in the two systems varies: external, quasi-, loosely attached, and internal.

SYMBIONT GENOME COMPARISON

Great insight into UCYN-A potential as a symbiont was revealed by sequencing and closing its genome (Zehr et al., 2008; Tripp et al., 2010). Likewise the sequencing of the draft genomes for

the DDA symbionts (RintHH01, RintHM01, CalSC01) revealed a remarkable reduction in genome size and content in the internal symbiont compared to the external symbiont (Hilton et al., 2013). There is an additional draft *Richelia* genome (RintRC01) now available (Hilton, 2014). Two UCYN-A genomes are available, one is closed, and a second is open (Zehr et al., 2008; Tripp et al., 2010; Bombar et al., 2014). We excluded the DDA symbiont RintHM01 as it was reduced and lacked genes expected for a full genome (Hilton, 2014). Here we compare all symbiont genomes by quantifying the number of genes encoding for a particular subsystem normalized by genome size (Supplementary Method).

The genome size for the symbionts are similar in that all but the external DDA (CalSC01) have been reduced compared to free-living cyanobacteria. The deleted genome content in the DDA and UCYN-A symbionts however differs and was previously highlighted (**Table 1**; Zehr et al., 2008; Tripp et al., 2010; Hilton et al., 2013). An interesting similarity, which was not reported, was a reduction in the number of genes for CO_2 uptake in the RintHH01 (internal symbiont of diatom host *H. hauckii*). In fact the decrease in genes for CO_2 uptake seems to be balanced by an increase in number of genes for N_2 fixation. Thus similar to UCYN-A1 and A2, the RintHH01 appears to be reducing its capacity for CO_2 uptake, while investing in N_2 fixation.

The number of genes encoding for K homeostasis and P uptake are similar in the DDA and the UCYN-A symbionts and perhaps related to occurrences in similarly saline and low P environments. The genomes for the UCYN-A symbionts contain more genes for N_2 fixation, vitamin synthesis, and cell division, compared to the three DDA symbionts. An increase in genes for N_2 fixation is consistent with recent studies showing a streamlined genome expression toward N_2 fixation (Cornejo-Castillo et al., 2016). The role of vitamins in the two symbiotic systems is un-studied and of interest given that at least half of the algal kingdom requires an exogenous supply of vitamin B_{12} and a large percentage of phytoplankton, including prymnesiophytes (80%) are vitamin B_1 auxotrophs (Croft et al., 2005, 2006).

Both the external (CalSC01) and quasi-internal (RintRC01) DDA symbiont draft genomes contain more genes for transport than the internal residing symbiont (RintHH01) (**Figure 1**, **Table 1**). The number of genes for transport in UCYN-A symbionts is similar to CalSC01 and is coherent with a higher investment of the genome for transport given an external location (**Table 1**). The internal DDA symbiont (RintHH01) and UCYN-A symbionts contain similar numbers of genes for stress, including genes encoding for oxidative stress.

In summary, there were more parallels in the symbiont genomes than previously highlighted. As reported earlier, the genomes of UCYN-A1 and UCYN-A2 are similar in size, content, and streamlining (Bombar et al., 2014); while the DDA symbiont draft genomes differ largely (**Figure 1**, **Table 1**), and content appears influenced by the symbiont location (Hilton et al., 2013).

METHODOLOGICAL BIASES: UN-QUANTIFIED AND UNDER-SAMPLED DISPARITIES

Prior to the global sequence surveys (see below) and still in common use today, is the use of qPCR assays to quantify the *nifH* gene for diazotrophs. The *nifH* abundances of the various DDA symbionts (het-1, het-2, and het-3) co-occur and can even outnumber UCYN-A *nifH* copy abundances, however this is rarely highlighted.

We reviewed 46 qPCR *nifH* surveys (reviewed in Farnelid et al., 2016; Stenegren et al., 2017), and found that in <30% of the studies (13 of 46 studies) all three DDA symbionts were quantified, compared to UCYN-A (96%, 44 of 46 studies) and the colonial diazotroph *Trichodesmium* (76%, 35 of 46 studies). A higher percent (ca 50%, 24 of 46 studies) quantified het-1 and to a lesser extent het-2 (ca 40%, 19 of 46 studies). Additionally, often only small subsets of the total samples were assayed. For example, 19 out of 154 samples (12%) were assayed for het-1 and het-2 in an area of the North Atlantic known for large-scale blooms of DDAs (Goebel et al., 2010). Hence it seems there is an "un-quantified disparity" against the DDA symbionts that is especially disconcerting in the context that often the global significance of an organism is associated with its abundance and distribution. Moreover, other means to collect the DDAs, e.g., gravity filtration from niskin bottles, net tows, perhaps are still a better means to quantify large and rare symbiosis.

Recent advances in sequencing platforms combined with large scale oceanic sampling surveys [e.g., global ocean survey (GOS), TARA, Malaspina] have been steadfast at revealing the rich diversity of planktonic populations in the global ocean without the need of separating populations (Caporaso et al., 2011, 2012; Werner et al., 2012; Bokulich et al., 2013). The UCYN-A based symbioses (both DNA and RNA based samples) have been reported in the TARA project and from a few select stations (Cabello et al., 2016; Cornejo-Castillo et al., 2016), while the DDAs remain un-reported. Using several genetic markers derived from the DDA symbionts (16S rRNA, *nifH*) and hosts (*rbcL*, 18S rRNA), we performed blast searches in the KEGG MGENES (www.genome.jp/mgenes/) and in the IMNGS database (https://www.imngs.org/), with a 95% identity cut off. Our searches did not generate a single hit, which was surprising, since DDAs are widespread and often bloom formers. The closest hit were at the 90% sequence identity with low coverage.

A closer look at the sampling methods employed in the global surveys identifies the use of pre-filtration steps (e.g., varying from 20 to 200 μm). The pre-filtration is necessary to avoid inclusion of larger eukaryotes (e.g., gelatinous zooplankton, larvae and eggs), which would dominate the nucleic acid composition and hence the sequence libraries. The hosts of the DDAs are large (>20 μm) and often form colonies or chains (>200 μm), thus pre-filtration would systematically exclude DDAs. The prymnesiophyte-UCYN-A symbioses are small in comparison; both hosts and symbionts are <10 μm. In fact a closer examination at the size fractionation experiments reported in Tripp et al. (2010) (Figure 4, Tripp et al., 2010), demonstrates

TABLE 1 | Summary of characters for DDA and Prymnesiophyte-UCYN-A symbioses are shown and separated by symbiont identity and common abbreviation for each symbiont is given in parenthesis (e.g. het-1)†.

R. intracellularis **(het-1)**	***R. intracellularis*** **(het-2)**	***C. rhizosoleniae*** **(het-3)**	**Character**	***A. thalassa*** **(UCYN-A1)**	***A. thalassa*** **(UCYN-A2)**
√*R. clevei* *R. styliformis*	*H. hauckii* (HH) *H. membranaceus* (HM)	*C. compressus* *Bacteriastrum*	**known host(s)**	*B. bigelowii* relative	*B. bigelowii*
80–250 μm	12–35 μm 30–70 μm	7–40 μm	**host size***	1–3 μm	4–5 μm; 7–10 μm
chains and singlet	chains and singlet	chains	**host life history**	single	single
endobiont	Presumed endobiont	external	**symbiont location**	endobiont	endobiont, symbiosome
1–32	1–2	1–4	**# symbionts/ host**	1	3–10
	5–6 μm; trichome length varies		**symbiont cell dia.**	1 μm	>1 μm
5.4	3.24 (RintHH) 2.21 (RintHM)	5.97	**Symbiont genome size (Mbp)**	1.44	1.48
39	34 (RintHH) 34 (RintHM)	39	**GC content (%)**	31	31
Draft (857)	RintHH draft (90) RintHM draft (941)	Draft (620)	**Genome status (contigs)**	Complete (1)	Draft (52)
65	56 (RintHH)	77	**Coding density (%)**	81	79
NH_4^+ transporter; NO_3 transporter and reductase; NO_2 reductase; Urea transporter and urease; GS inactivating factor	NH_4^+ transporter; NO_3 transporter and reductase; NO_2 reductase; Urea transporter and urease; GS inactivating factor; GOGAT;	Urea transporter and urease; GS inactivating factor	**reported genome deletions**	PS-II, partial or incomplete: TCA, Calvin and urea cycles; amino acids and purine synthesis	
provide N	provide N	provide N	**Symbiont function**	provide N	provide N
unknown	unknown	unknown	**Known host function**	provide C	provide C
37.0	29.9	41.5	**# Transporters/Mbp^**	41.0	41.2
3.1	6.8	4.5	**# Genes for N_2 fix/Mbp^**	11.8	9.7
27.2	29.6	22.6	**# Genes for carbon/Mbp****	19.4	20.1

† *References: Villareal, 1992; Foster and Zehr, 2006; Foster and O'Mullan, 2008; Zehr et al., 2008; Tripp et al., 2010; Thompson et al., 2012, 2014; Hagino et al., 2013; Hilton et al., 2013; Krupke et al., 2013; Bombar et al., 2014; Hilton, 2014; Cabello et al., 2016; Cornejo-Castillo et al., 2016; Martínez-Pérez et al., 2016.* √ *up to 13 species are reported for Rhizosolenia-R. intracellularis symbioses hence we report the two most common.*

**Diatom cell size are reported as apical axis length.*

***, #genes for carbon includes genes for photosystems, light-harvesting pigments and CO_2 uptake.*

^Mbp × 10^6.

that even though the UCYN-A hosts are small (e.g., 4–5 or 7–10 μm), the UCYN-A *nifH* genes were still detected in the >10 and >25 μm size fractions. Detecting UCYN-A on the larger size fractions suggests that even the UCYN-A symbioses are likely under-sampled in the global surveys. Future sampling campaigns (and interpretations of results) should consider and modify sampling to avoid biases against larger, symbiotic, and/or chains of cells.

SINGLE CELL N_2 FIXATION RATES AND SCALING UP TO THE WATER COLUMN

Measurements of N_2 fixation and transfer of fixed N from symbiont to host has been made in both symbioses using $^{15}N_2$ and nano-meter scale secondary ion-mass spectrometry (nanoSIMS) measurements (Foster et al., 2011; Thompson et al., 2012; Krupke et al., 2013, 2014; Martínez-Pérez et al., 2016). Since C fixation has only been reported in the prymnesiophyte-UCYN-A symbioses, we limit the comparison to the N_2 fixation measures. For the prymnesiophyte-UCYN-A symbiosis, a halogenated *in situ* hybridization (HISH) step is required prior to the SIMS measurements for identification of the UCYN-A symbiont, and in a more recent study, an additional probe specific for the UCYN-A hosts were used, hence a dual labeling (Martínez-Pérez et al., 2016).

A closer look at the single N_2 fixation activity by DDA and UCYN-A symbionts highlights a surprising similarity. For example, N_2 fixation for the *Hemiaulus-Richelia* DDA range between 1.15 and 50.4 fmol N $cell^{-1}$ h^{-1} (Foster et al., 2011), while recently N_2 fixation by UCYN-A1 and A2 was 0.5 and 9.16 fmol N $cell^{-1}$ h^{-1}, respectively (Martínez-Pérez et al., 2016). Both UCYN-A and the DDA symbionts function as N sources for their respective hosts. Given that *Hemiaulus* spp. hosts are larger (12–70 μm) than the prymnesiophyte hosts (1–10 μm), one expected a higher N_2 fixation in the DDAs to support the higher N demand

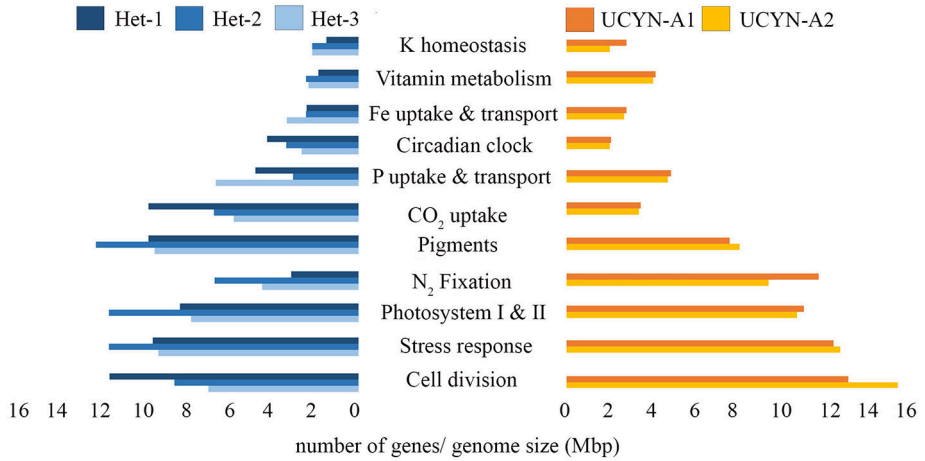

FIGURE 1 | Subsystem (genes with similar function) comparison between DDA and UCYN-A symbionts. Each bar indicates the number of genes in a particular subsystem normalized against genome size (Mbp $\times$ 10^6) for het-1 (dark blue), het-2 (lighter-blue), het-3 (lightest blue), UCYN-A1 (dark orange) and UCYN-A2 (light orange).

of the larger host diatoms. However, other factors influence N_2 fixation, e.g., host growth, light/energy availability, temperature, and iron (Villareal, 1989; Kustka et al., 2002; Berman-Frank et al., 2007).

The recent rates reported for UCYN-A1 were also 3–5 orders of magnitude higher than the rates reported earlier for UCYN-A1 (e.g., $6.35 \times 10^{-5} - 0.013 \times 10^{-2}$ fmol N cell^{-1} h^{-1}), despite similar measured enrichment values (e.g., 0.3744-0.6194 atom%^{15}N) (Krupke et al., 2013). Inherent in using the HISH-SIMS is the potential to reduce the ^{15}N fraction in the cell (e.g., up to 60%) (Musat et al., 2014). Hence it was somewhat surprising that in the recent work on UCYN-A1 that utilized a double CARD-FISH measured such a higher enrichment in ^{15}N than the earlier works that used only a single probe. The effect of double CARD-FISH on enrichment has not been tested.

One of the useful applications for the single cell rates is the ability to estimate the contribution of a particular population to bulk water activity. These types of estimates have been done for several of the open ocean diazotrophs (Foster et al., 2011, 2013; Krupke et al., 2015; Martínez-Pérez et al., 2016). For example, an estimate of 0.19 and 0.62 Tmol N yr^{-1} is provided by DDAs in the Atlantic and Pacific oceans, respectively, which is similar to 0.36–0.71 Tmol N yr^{-1} estimated for *Trichodesmium* spp. (Capone et al., 2008; Foster et al., 2011). Recently, up to 30% of N_2 fixation in the surface tropical N. Atlantic was attributed to UCYN-A symbioses, while the contribution by *Trichodesmium* in the region was far less (11%) (Martínez-Pérez et al., 2016). Hence, single cell activity measures have demonstrated that both symbioses should be included in global N models.

CONCLUSIONS

In summary, even though DDAs are one of the earliest recorded symbioses and are frequently observed at high bloom densities worldwide with high measured N_2 fixation rates leading to high export fluxes (Villareal, 1994; Carpenter et al., 1999; Foster et al., 2007, 2011; Subramaniam et al., 2008; Karl et al., 2012), the DDAs are often overlooked. The genomes for the UCYN-A lineages and one of the het symbionts (RintHH01) are uniquely streamlined and similarly optimized for a symbiotic life history. An open and interesting question is whether a similar degree of modification occurs in the respective host genomes. Both symbioses have invested in N_2 fixation in both genome content and cellular activity. Moreover, recent evidence suggests that both symbioses can have equally high N_2 fixation rates and should be recognized as major players in the N (and C) cycle. DDAs are methodologically excluded and less often assayed in qPCR *nifH* surveys leading to under-detection, while UCYN-A are often the most frequently assayed, and thus unavoidably the most detected diazotroph. In a time of incredible resources and instrumentation for detection, one must consider the "un-quantified disparity," especially if sequence abundance and information continues to be used as a comparative indices and to predict biogeochemical significance.

AUTHOR CONTRIBUTIONS

All authors contributed to the manuscript. AC, MS, and RF compiled the content of **Table 1** and MS compiled the data and generated **Figure 1**.

FUNDING

Funding was provided by the Knut and Alice Wallenberg Foundation (to RF).

ACKNOWLEDGMENTS

RF is supported by Knut and Alice Wallenberg Foundation Stiffelse. We thank the very insightful advice and suggestions from two reviewers.

REFERENCES

Berman-Frank, I., Quigg, A., Finkel, Z. V., Irwin, A. J., and Haramaty, L. (2007). Nitrogen-fixation strategies and Fe requirements in cyanobacteria. *Limnol. Oceanogr.* 52, 2260–2269. doi: 10.4319/lo.2007.52.5.2260

Bokulich, N. A., Subramanian, S., Faith, J. J., Gevers, D., Gordon, I. J., Knight, R., et al. (2013). Quality-filtering vastly improves diversity estimates from Illumina amplicon sequencing. *Nat. Methods* 10, 57–59. doi: 10.1038/nmeth.2276

Bombar, D., Heller, P., Sanchez-Baracaldo, P., Carter, B. J., and Zehr, J. P. (2014). Comparative genomics reveals surprising divergence of two closely related strains of uncultivated UCYN-A cyanobacteria. *ISME J.* 8, 2530–2542. doi: 10.1038/ismej.2014.167

Bothe, H., Tripp, H. J., and Zehr, J. P. (2010). Unicellular cyanobacteria with a new mode of life: the lack of photosynthetic oxygen evolution allows nitrogen fixation to proceed. *Arch. Microbiol.* 192, 783–790. doi: 10.1007/s00203-010-0621-5

Cabello, A. M., Cornejo-Castillo, F. M., Raho, N., Blasco, D., Vidal, M., Audic, S., et al. (2016). Global distribution and vertical patterns of a prymnesiophyte–cyanobacteria obligate symbiosis. *ISME J.* 10, 693–706. doi: 10.1038/ismej.2015.147

Capone, D. G., Bronk, D. A., Mulholland, M. R., and Carpenter, E. J. (eds.). (2008). *Nitrogen in the Marine Environment*. London: Academic Press, 1758.

Caporaso, J. G., Lauber, C. L., Walters, W. A., Berg-Lyons, D., Huntley, J., Fierer, N., et al. (2012). Ultra-high-throughput microbial community analysis on the Illumina HiSeq and MiSeq platforms. *ISME J.* 6, 1621–1624. doi: 10.1038/ismej.2012.8

Caporaso, J. G., Lauber, C. L., Walters, W. A., Berg-lyons, D., Lozupone, C. A., Turnbaugh, P. J., et al. (2011). Global patterns of 16S rRNA diversity at a depth of millions of sequences per sample. *Proc. Natl. Acad.Sci. U.S.A.* 108, 4516–4522. doi: 10.1073/pnas.1000080107

Carpenter, E. J., and Janson, S. (2000). Intracellular cyanobacterial symbionts in the marine diatom *Climacodium frauenfeldianum* (Bacillariophyceae). *J. Phycol.* 36, 540–544. doi: 10.1046/j.1529-8817.2000.99163.x

Carpenter, E. J., Montoya, J. P., Burns, J., Mulholland, M. R., Subramaniam, A., and Capone, D. G. (1999). Extensive bloom of a N_2-fixing diatom/cyanobacterial association in the tropical Atlantic Ocean. *Mar. Ecol. Prog. Ser.* 185, 273–283. doi: 10.3354/meps185273

Church, M. J., Short, C. M., Jenkins, B. D., Karl, D. M., and Zehr, J. P. (2005). Temporal patterns of nitrogenase gene (*nifH*) expression in the oligotrophic North Pacific ocean. *Appl. Environ. Microbiol.* 71, 5362–5370. doi: 10.1128/AEM.71.9.5362-5370.2005

Cornejo-Castillo, F. M., Cabello, A. M., Salazar, G., Sánchez-Baracaldo, P., Lima-mendez, G., Hingamp, P., et al. (2016). Cyanobacterial symbionts diverged in the late Cretaceous towards lineage-specific nitrogen fixation factories in single-celled phytoplankton. *Nat. Commun.* 7, 1–9. doi: 10.1038/ncomms11071

Croft, M. T., Lawrence, A. D., Raux-Deery, E., Warren, M. J., and Smith, A. G. (2005). Algae acquire vitamin B_{12} through a symbiotic relationship with bacteria. *Nature* 438, 90–93. doi: 10.1038/nature04056

Croft, M. T., Warren, M. J., and Smith, A. G. (2006). Algae need their vitamins. *Eukaryotic Cell* 5, 1175–1183. doi: 10.1128/EC.00097-06

Delong, E. F. (2010). Interesting things come in small packages. *Genome Biol.* 11:118. doi: 10.1186/gb-2010-11-5-118

Farnelid, H., Turk-Kubo, K., Muñoz-Marín, M., and Zehr, J. (2016). New insights into the ecology of the globally significant uncultured nitrogen-fixing symbiont UCYN-A. *Aquat. Microb. Ecol.* 77, 125–138. doi: 10.3354/ame01794

Foster, R. A., Goebel, N. L., and Zehr, J. P. (2010). Isolation of *Calothrix rhizosoleniae* (cyanobacteria) strain SC01 from *Chaetoceros* (Bacillariophyta) spp. diatoms of the subtropical North Pacific Ocean. *J. Phycol.* 46, 1028–1037. doi: 10.1111/j.1529-8817.2010.00885.x

Foster, R. A., Kuypers, M. M. M., Vagner, T., Paerl, R. W., Musat, N., and Zehr, J. P. (2011). Nitrogen fixation and transfer in open ocean diatom–cyanobacterial symbioses. *ISME J.* 5, 1484–1493. doi: 10.1038/ismej.2011.26

Foster, R. A., and O'Mullan, G. D. (2008). "Nitrogen-fixing and nitrifying symbioses in the marine environment," in *Nitrogen in the Marine Environment*, eds D. G. Capone, D. A. Bronk, M. R. Mulholland, and E. J. Carpenter (London: Academic Press), 1197–1218.

Foster, R. A., Subramaniam, A., Mahaffey, C., Carpenter, E. J., Capone, D. G., and Zehr, J. P. (2007). Influence of the Amazon River plume on distributions of free-living and symbiotic cyanobacteria in the western tropical north Atlantic Ocean. *Limnol. Oceanogr.* 52, 517–532. doi: 10.4319/lo.2007.52.2.0517

Foster, R. A., Sztejrenszus, S., and Kuypers, M. M. (2013). Measuring carbon and N_2 fixation in field populations of colonial and free-living unicellular cyanobacteria using nanometer-scale secondary ion mass spectrometry. *J. Phycol.* 49, 502–516. doi: 10.1111/jpy.12057

Foster, R. A., and Zehr, J. P. (2006). Characterization of diatom-cyanobacteria symbioses on the basis of *nifH*, *hetR* and 16S rRNA sequences. *Environ. Microbiol.* 8, 1913–1925. doi: 10.1111/j.1462-2920.2006.01068.x

Goebel, N. L., Turk, K. A., Achilles, K. M., Paerl, R., Hewson, I., Morrison, A. E., et al. (2010). Abundance and distribution of major groups of diazotrophic cyanobacteria and their potential contribution to N_2 fixation in the tropical Atlantic Ocean. *Environ. Microbiol.* 12, 3272–3289. doi: 10.1111/j.1462-2920.2010.02303.x

Gómez, F., Furuya, K., and Takeda, S. (2005). Distribution of the cyanobacterium *Richelia intracellularis* as an epiphyte of the diatom *Chaetoceros compressus* in the western Pacific Ocean. *J. Plankton Res.* 27, 323–330. doi: 10.1093/plankt/fbi007

Hagino, K., Onuma, R., Kawachi, M., and Horiguchi, T. (2013). Discovery of an endosymbiotic nitrogen-fixing cyanobacterium UCYN-A in *Braarudosphaera bigelowii* (Prymnesiophyceae). *PLoS ONE* 8:e81749. doi: 10.1371/journal.pone.0081749

Hilton, J. A. (2014). *Ecology and Evolution of Diatom-Associated Cyanobacteria Through Genetic Analyses*. Dissertation's thesis. Santa Cruz, CA: University of California.

Hilton, J. A., Foster, R. A., Tripp, H. J., Carter, B. J., Zehr, J. P., and Villareal, T. A. (2013). Genomic deletions disrupt nitrogen metabolism pathways of a cyanobacterial diatom symbiont. *Nat. Commun.* 4, 1–7. doi: 10.1038/ncomms2748

Janson, S., Woulters, J., Bergman, B., and Carpenter, E. (1999). Host specificity in the *Richelia*-diatom symbiosis revealed by *hetR* gene sequence analysis. *Environ. Microbiol.* 1, 431–438. doi: 10.1046/j.1462-2920.1999.00053.x

Karl, D. M., Church, M. J., Dore, J. E., Letelier, R. M., and Mahaffey, C. (2012). Predictable and efficient carbon sequestration in the North Pacific Ocean supported by symbiotic nitrogen fixation. *Proc. Natl. Acad. Sci. U.S.A.* 109, 1842–1849. doi: 10.1073/pnas.1120312109

Krupke, A., Lavik, G., Halm, H., Fuchs, B. M., Amann, R. I., and Kuypers, M. M. (2014). Distribution of a consortium between unicellular algae and the N_2 fixing cyanobacterium UCYN-A in the North Atlantic Ocean. *Environ. Microbiol.* 16, 3153–3167. doi: 10.1111/1462-2920.12431

Krupke, A., Mohr, W., Laroche, J., Fuchs, B. M., Amann, R. I., and Kuypers, M. M. (2015). The effect of nutrients on carbon and nitrogen fixation by the UCYN-A-haptophyte symbiosis. *ISME J.* 9, 1635–1647. doi: 10.1038/ismej.2014.253

Krupke, A., Musat, N., LaRoche, J., Mohr, W., Fuchs, B. M., Amann, R. I., et al. (2013). *In situ* identification and N_2 and C fixation rates of uncultivated cyanobacteria populations. *Syst. Appl. Microbiol.* 36, 259–271. doi: 10.1016/j.syapm.2013.02.002

Kustka, A., Carpenter, E. J., and Sañudo-Wilhelmy, S. A. (2002). Iron and marine nitrogen fixation: progress and future directions. *Res. Microbiol.* 153, 255–262. doi: 10.1016/S0923-2508(02)01325-6

Lemmermann, E. (1905). Die algenflora der sandwich-inseln. ergebnisse einer reise nach dem Pacific. H. Schauinsland 1896/97. *Bot. Jahrbuch Syst. Pflanzengesch. Pflanzengeogr.* 34, 607–663.

Martínez-Pérez, C., Mohr, W., Löscher, C. R., Dekaezemacker, J., Littmann, S., Yilmaz, P., et al. (2016). The small unicellular diazotrophic symbiont, UCYN-A, is a key player in the marine nitrogen cycle. *Nat. Microbiol.* 1:16163. doi: 10.1038/nmicrobiol.2016.163

Marumo, R., and Asaoka, O. (1974). Distribution of pelagic blue-green algae in the North Pacific Ocean. *J. Oceanogr. Soc. Japan* 30, 77–85. doi: 10.1007/BF02112896

Musat, N., Stryhanyuk, H., Bombach, P., Adrian, L., Audinot, J. N., and Richnow, H. H. (2014). The effect of FISH and CARD-FISH on the isotopic composition of ^{13}C- and ^{15}N-labeled *Pseudomonas putida* cells measured by nanoSIMS. *Syst. Appl. Microbiol.* 37, 267–276. doi: 10.1016/j.syapm.2014.02.002

Ostenfeld, C. H., and Schmidt, J. (1901). *Plankton fra det Rode Hav og Adenbugten (Plankton from the Red Sea and the Gulf of Aden)*. Copenhagen.

Rasmussen, U. (2002). "Cyanobacterial diversity and specificity in plant symbioses," in *Cyanobacteria in Symbiosis*, eds A. N. Rai, B. Bergman, and U. Rasmussen (Dordrecht: Kluwer Academic Press), 313–328.

Sournia, A. (1970). Les cyanophycees dans le plancton marin. *Ann. Biol.* 9, 63–76.

Stenegren, M., Caputo, A., Berg, C., Bonnet, S., and Foster, R. A. (2017). Distribution and drivers of 5 symbiotic and free-living diazotrophic cyanobacteria in the Western Tropical South Pacific. *Biogeosci. Discuss.* 2017, 1–47, doi: 10.5194/bg-2017-63

Subramaniam, A., Yager, P. L., Carpenter, E. J., Mahaffey, C., Björkman, K. M., Cooley, S., et al. (2008). Amazon river enhances diazotrophy and carbon sequestration in the tropical North Atlantic ocean. *Proc. Natl. Acad. Sci. U.S.A.* 105, 10460–10465. doi: 10.1073/pnas.0710279105

Thompson, A., Carter, B. J., Turk-Kubo, K., Malfatti, F., Azam, F., and Zehr, J. P. (2014). Genetic diversity of the unicellular nitrogen-fixing cyanobacteria UCYN-A and its prymnesiophyte host. *Environ. Microbiol.* 16, 3238–3249. doi: 10.1111/1462-2920.12490

Thompson, A. W., Foster, R. A., Krupke, A., Carter, B. J., Musat, N., Vaulot, D., et al. (2012). Unicellular cyanobacterium symbiotic with a single-celled eukaryotic alga. *Science* 337, 1546–1550. doi: 10.1126/science.1222700

Thompson, A. W., and Zehr, J. P. (2013). Cellular interactions: lessons from the nitrogen-fixing cyanobacteria. *J. Phycol.* 49, 1024–1035. doi: 10.1111/jpy.12117

Tripp, H. J., Bench, S. R., Turk, K. A., Foster, R. A., Desany, B. A., Niazi, F., et al. (2010). Metabolic streamlining in an open-ocean nitrogen-fixing cyanobacterium. *Nature* 464, 90–94. doi: 10.1038/nature08786

Turk-Kubo, K. A., Farnelid, H. M., Shilova, I. N., Henke, B., and Zehr, J. P. (2017). Distinct ecological niches of marine symbiotic N_2-fixing cyanobacterium Candidatus *Atelocyanobacterium thalassa* sublineages. *J. Phycol.* 461, 451–461. doi: 10.1111/jpy.12505

Villareal, T. A. (1989). Division cycles in the nitrogen-fixing *Rhizosolenia* (Bacillariophyceae)-*Richelia* (Nostocaceae) symbiosis. *Br. J. Phycol.* 24, 357–365. doi: 10.1080/00071618900650371

Villareal, T. A. (1990). Laboratory culture and preliminary characterization of the nitrogen-fixing *Rhizosolenia-Richelia* symbiosis. *Mar. Ecol.* 11, 117–132. doi: 10.1111/j.1439-0485.1990.tb00233.x

Villareal, T. A. (1992). "Marine nitrogen-fixing diatom-Cyanobacteria symbioses," in *Marine Pelagic Cyanobacteria: Trichodesmium and other Diazotrophs*, ed E. J. Carpenter (Dordrecht: Springer), 163–175.

Villareal, T. A. (1994). Widespread occurrence of the *Hemiaulus*-cyanobacterial symbiosis in the Southwest North Atlantic Ocean. *Bull. Mar. Sci.* 54, 1–7.

Werner, J. J., Zhou, D., Caporaso, J. G., Knight, R., and Angenent, L. T. (2012). Comparison of Illumina paired-end and single-direction sequencing for microbial 16S rRNA gene amplicon surveys. *ISME J.* 6, 1273–1276. doi: 10.1038/ismej.2011.186

White, A. E., Prahl, F. G., Letelier, R. M., and Popp, B. N. (2007). Summer surface waters in the Gulf of California: prime habitat for biological N_2-fixation. *Global Biogeochem. Cycles* 21, 1–11. doi: 10.1029/2006GB002779

Zehr, J. P. (2015). How single cells work together. *Science* 349, 1163–1164. doi: 10.1126/science.aac9752

Zehr, J. P., Bench, S. R., Carter, B. J., Hewson, I., Niazi, F., Shi, T., et al. (2008). Globally distributed uncultivated oceanic N_2-fixing cyanobacteria lack oxygenic photosystem II. *Science* 322, 1110–1112. doi: 10.1126/science.1165340

Zehr, J. P., Mellon, M. T., Zani, S., and York, N. (1998). New Nitrogen-fixing microorganisms detected in oligotrophic oceans by amplification of nitrogenase (*nifH*) genes. *Appl. Environ. Microbiol.* 64, 3444–3450.

Zehr, J. P., Shilova, I. N., Farnelid, H. M., Muñoz-marín, M. C., and Turk-Kubo, K. A. (2016). Unusual marine unicellular symbiosis with the nitrogen-fixing cyanobacterium UCYN-A. *Nat. Microbiol.* 2:16214. doi: 10.1038/nmicrobiol.2016.214

Zehr, J., Waterbury, J., and Turner, P. (2001). Unicellular cyanobacteria fix N_2 in the subtropical North Pacific Ocean. *Nature* 715, 25–28. doi: 10.1038/35088063

Conflict of Interest Statement: The authors declare that the research was conducted in the absence of any commercial or financial relationships that could be construed as a potential conflict of interest.

SUPPLEMENTARY METHOD FOR CONSTRUCTING THE SUBSYSTEMS COMPARISON (FIGURE 1)

Genomes were downloaded from the NCBI database (RintRC01 accession: PRJEB5207, RintHH01 accession: PRJEA104979, RINTHM01 accession: PRJEA104981, CalSC01 accession: PRJEB19506, UCYN-A1 ALOHA accession: PRJNA30917, UCYN-A2 SIO64986 accession: PRJNA256120) and subsequently submitted to RAST (Rapid Annotation using Subsystem Technology) for annotation. The annotated genomes where browsed for genetic pathways of interest by using key word searches. Number of genes for a particular subsystem were normalized to genome size.

frontiers in Marine Science

ORIGINAL RESEARCH
published: 22 March 2018
doi: 10.3389/fmars.2018.00089

Dissolved Organic Matter Influences N_2 Fixation in the New Caledonian Lagoon (Western Tropical South Pacific)

Mar Benavides[1,2], Chloé Martias[2], Hila Elifantz[3], Ilana Berman-Frank[3], Cécile Dupouy[2] and Sophie Bonnet[2]*

[1] Marine Biology Section, Department of Biology, University of Copenhagen, Helsingør, Denmark, [2] Aix-Marseille Université, Université de Toulon, CNRS, IRD, MIO UM 110, Marseille, France, [3] Mina and Everard Goodman Faculty of Life Sciences, Bar-Ilan University, Ramat Gan, Israel

Specialized prokaryotes performing biological dinitrogen (N_2) fixation ("diazotrophs") provide an important source of fixed nitrogen in oligotrophic marine ecosystems such as tropical and subtropical oceans. In these waters, cyanobacterial photosynthetic diazotrophs are well known to be abundant and active, yet the role and contribution of non-cyanobacterial diazotrophs are currently unclear. The latter are not photosynthetic (here called "heterotrophic") and hence require external sources of organic matter to sustain N_2 fixation. Here we added the photosynthesis inhibitor 3-(3,4-dichlorophenyl)-1,1-dimethylurea (DCMU) to estimate the N_2 fixation potential of heterotrophic diazotrophs as compared to autotrophic ones. Additionally, we explored the influence of dissolved organic matter (DOM) on these diazotrophs along a coast to open ocean gradient in the surface waters of a subtropical coral lagoon (New Caledonia). Total N_2 fixation (samples not amended with DCMU) ranged from 0.66 to 1.32 nmol N L^{-1} d^{-1}. The addition of DCMU reduced N_2 fixation by >90%, suggesting that the contribution of heterotrophic diazotrophs to overall N_2 fixation activity was minor in this environment. Higher contribution of heterotrophic diazotrophs occurred in stations closer to the shore and coincided with the decreasing lability of DOM, as shown by various colored DOM and fluorescent DOM (CDOM and FDOM) indices. We tested the response of diazotrophs (in terms of *nifH* gene expression and bulk N_2 fixation rates) upon the addition of a mix of carbohydrates ("DOC" treatment), amino acids ("DON" treatment), and phosphonates and phosphomonesters ("DOP" treatment). While *nifH* expression increased significantly in *Trichodesmium* exposed to the DOC treatment, bulk N_2 fixation rates increased significantly only in the DOP treatment. The lack of *nifH* expression by gammaproteobacteria, in any of the DOM addition treatments applied, questions the contribution of non-cyanobacterial diazotrophs to fixed nitrogen inputs in the New Caledonian lagoon. While the metabolism and ecology of heterotrophic diazotrophs is currently elusive, a deeper understanding of their ecology and relationship with DOM is needed in the light of increased DOM inputs in coastal zones due to anthropogenic pressure.

Keywords: non-cyanobacterial diazotrophs, nifH, DCMU, DOM, CDOM, FDOM

OPEN ACCESS

Edited by:
Beatriz Mouriño-Carballido, University of Vigo, Spain

Reviewed by:
Ana Fernandez-Carrera, University of Vigo, Spain
Arvind Singh, Physical Research Laboratory, India

****Correspondence:***
Mar Benavides
mar.benavides@mio.osupytheas.fr

Specialty section:
This article was submitted to Aquatic Microbiology, a section of the journal Frontiers in Marine Science

Received: *30 November 2017*
Accepted: *05 March 2018*
Published: *22 March 2018*

Citation:
Benavides M, Martias C, Elifantz H, Berman-Frank I, Dupouy C and Bonnet S (2018) Dissolved Organic Matter Influences N_2 Fixation in the New Caledonian Lagoon (Western Tropical South Pacific). Front. Mar. Sci. 5:89. doi: 10.3389/fmars.2018.00089

INTRODUCTION

Biological dinitrogen (N_2) fixation provides an important source of fixed nitrogen to fuel primary production in the oceans (Karl et al., 2002), being especially critical in areas devoid of other significant fixed nitrogen sources such as the oligotrophic subtropical gyres. N_2 fixation is performed by specialized prokaryotic microbes called "diazotrophs." These include cyanobacterial and non-cyanobacterial (bacteria and archaea) groups, that are commonly detected and quantified via the presence of the *nifH* gene, which encodes for a subunit of the nitrogenase enzyme system (Zehr, 2011). Traditionally, marine diazotrophs were hypothesized to be constrained by warm, low inorganic nitrogen waters (Sohm et al., 2011). Yet, several filamentous cyanobacteria are able to obtain energy from dissolved organic matter-DOM- (Rippka et al., 1979), and several reports have shown that the most abundant photoautotrophs in the world's oceans (*Prochlorococcus* and *Synechococcus*) harbor the genes necessary to use amino acids, peptides and sugars (Yelton et al., 2016). As evidence accumulates, it seems that the ability of using DOM as an alternative source of nutrients under limiting situations is common in various planktonic groups (Stoecker et al., 2017). Among marine diazotrophs, unicellular cyanobacteria such as *Cyanothece* have been reported to grow on glycerol (Feng et al., 2010), and filamentous diazotrophs such as *Trichodesmium* may obtain as much carbon from amino acids assimilation as from CO_2 fixation in the field (Benavides et al., 2017). Non-cyanobacterial and non-photosynthetic diazotrophs require external sources of DOM as energy sources (Riemann et al., 2010). The globally widespread non-cyanobacterial diazotroph Gamma A (Langlois et al., 2015) upregulates *nifH* gene expression upon glucose + mannitol additions (Moisander et al., 2011). Previous work has also shown that N_2 fixation activity is stimulated by DOM additions (Bonnet et al., 2013; Rahav et al., 2013, 2015), and correlates with labile DOM compounds in environments where non-cyanobacterial (non-photosynthetic) diazotrophs predominate, such as the aphotic mesopelagic layer (Benavides et al., 2015), or the surface ultraoligotrophic eastern Mediterranean Sea (Rahav et al., 2016).

N_2 fixation and diazotroph community studies have mostly focused on populations in the North Atlantic (Benavides and Voss, 2015) and North Pacific Oceans, while other areas such as the Indian and the South Atlantic and Pacific Oceans have been chronically under-sampled (Luo et al., 2012). The western tropical Southwest Pacific (WTSP) Ocean comprises warm, oligotrophic, trace metal rich waters that harbor among the high N_2 fixation rates measured at sea (>500 μmol N m^{-2} $d^{-}1$; Bonnet et al., 2017). The activity and distribution of diazotrophs in the WTSP has been related to temperature, iron and inorganic nutrient availability thresholds (e.g., Bonnet et al., 2009; Moisander et al., 2010). In austral summer conditions, the relatively warmer and productive waters like the Arafura, Timor and Solomon Seas (∼26.5–30°C) are dominated by *Trichodesmium* and UCYN-B (Messer et al., 2016), while UCYN-A remains confined to the colder and more oligotrophic Coral Sea (∼22–26.5°C; Moisander et al., 2010; Bonnet et al., 2015; Messer et al., 2016). Together with the high abundances of diazotroph phylotypes (Moisander et al., 2010; Bonnet et al., 2015), the WTSP has been recently acknowledged as a hotspot of global importance for N_2 fixation activity (Bonnet et al., 2017). Thus, understanding how environmental factors (besides temperature and inorganic nutrients) shape the distribution and activity of diazotrophs in the WTSP is of utmost importance to assess their potential to fuel primary production in these oligotrophic waters and their contribution to the oceanic nitrogen budget.

New Caledonia, situated at the eastern edge of the WTSP, is surrounded by a reef enclosing one of the largest coral lagoons in the world. Here, primary production is nitrogen-limited throughout the year (Torréton et al., 2010), prompting diazotrophic activity (Garcia et al., 2007; Biegala and Raimbault, 2008) and the presence of various cyanobacterial diazotroph phylotypes including *Trichodesmium* (often occurring as large blooms; Rodier and Le Borgne, 2008), diatom-diazotroph symbioses (DDAs) as well the unicellular cyanobacteria UCYN-A1, UCYN-A2, UCYN-B, and UCYN-C (Turk-Kubo et al., 2015). However, non-cyanobacterial diazotrophs have been far less studied, and despite representatives such as the putative gammaproteobacterium γ-24774A11 that has been detected at abundances of 10^2–10^3 *nifH* copies L^{-1} within the lagoon (Turk-Kubo et al., 2015), their contribution to N_2 fixation in this environment remains unquantified. Moreover, the importance of DOM as a source of energy and nutrition for both cyanobacterial and non-cyanobacterial diazotrophs has never been explored in this environment. In this study we assess if the inhibition of photosynthesis triggers DOM nutrition in pelagic diazotrophs, and whether the N_2 fixation activity and/or *nifH* expression of these pelagic diazotrophs is enhanced by different model DOM molecules.

MATERIALS AND METHODS

Hydrography, Oxygen, Inorganic Nutrients, Chl α and DOC Measurements

Sampling took place on 13 January 2016 approximately from 8:00 a.m. to noon at four stations along an anthropogenic pressure gradient in the New Caledonian lagoon onboard the R/V *Archamia*. Station 1 was close to the rim of the coral reef barrier and Station 4 near the harbor of the city of Nouméa (**Figure 1**, **Table 1**). This transect connects the passage of Dumbéa (the main canal for the entrance of ships into the lagoon) with the harbor. Sampling started at Station 1 at high tide and proceeded toward the coast as the tide ebbed.

At each station, temperature and salinity were measured by casting a SeaBird SB19 plus CTD probe from the surface to the bottom. Water samples for the measurement of oxygen, nutrients, chlorophyll *a* (Chl *a*) and DOC concentrations, and colored DOM (CDOM) and fluorescent DOM (FDOM) parameters (see below) were collected from the subsurface (∼3 m), using a 5 L Niskin bottle and transported to the lab for analysis in coolers equipped with icepacks within 2 h. Samples for the measurement of dissolved oxygen were taken in triplicate and analyzed ashore using an automated

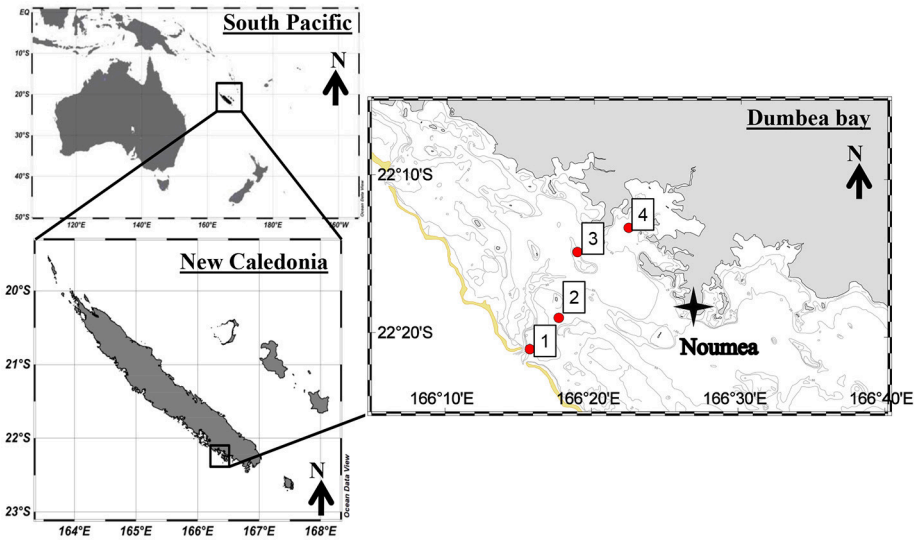

FIGURE 1 | Map of stations sampled in the New Caledonian lagoon. The yellow line represents the coral reef barrier.

titration system with a photometric endpoint (Langdon, 2010). Samples for the determination of nitrate plus nitrite (NO_x) and phosphate (PO_4^{3-}) concentrations were taken on acid-washed 20 mL polyethylene tubes, poisoned with 1% $HgCl_2$, and stored at 4°C until analysis. The samples were analyzed on a AA3 Bran+Luebbe autoanalyzer following JGOFS recommendations (JGOFS, 1994). The detection limits were 50 and 10 nM for NO_x and PO_4^{3-}, respectively. Chl *a* concentrations were estimated from seawater samples (500 mL) filtered through 25 mm GF/F filters (Whatman) and stored at −80°C until analysis, extracted in methanol on a AU Turner Designs bench fluorometer, previously calibrated with pure Chl *a* (Herbland et al., 1985). Samples for DOC were collected on triplicate precombusted (450°C, 6 h) glass ampoules and acidified to pH 2 with 50 µL of 50% phosphoric acid. The samples were analyzed by high temperature catalytic oxidation on a TOC-V analyzer (Sohrin and Sempéré, 2005).

FDOM and CDOM Analyses

Samples for the analysis of FDOM and CDOM were filtered through 0.2 µm polycarbonate filters in a custom-made filtration system pre-cleaned with 1 M HCl and Milli-Q water. Samples for FDOM analyses were stored at 4°C until analysis (within 1 month), while samples for CDOM absorption analyses were directly measured on a liquid waveguide capillary flow cell (WPI) according to the method of Kowalczuk et al. (2013). Excitation-emission matrix (EEM) spectra for analysis of FDOM were determined using a Hitachi F-7000 spectrofluorometer (Tedetti et al., 2011). FDOM components were identified by parallel factor analysis (PARAFAC), a statistical decomposition technique used to extract the most representative fluorescent components within EEMs dataset. To increase the validity of the PARAFAC analysis, data from the present experiment were pooled with 39 other samples obtained from the same waters, 3 months before and after the experiment. Indeed, to avoid systematic biases, remove signals unrelated to fluorescence and to validate the number of FDOM components, a large dataset was needed (Stedmon et al., 2003). For example, in the case where two of the components had very similar fluorescence characteristics and/or were highly correlated in their appearance among samples, the PARAFAC approach would have difficulties to discern between the two. We then determined several spectral indices: the absorption at 442 nm as a proxy of phytoplankton production and the absorption at 350 nm as an indicator of terrestrial inputs in the bay (Passow and Alldredge, 1995), a biological index (BIX) of recent autochthonous FDOM contribution (Huguet et al., 2009), a specific ultraviolet absorbance at 254 nm of DOC ($SUVA_{254}$), which is an indicator of aromatic DOM (Weishaar et al., 2003), and the ratio of spectral slopes (S_r) at 275–295 nm ($S_{275-295}$) and 350–400 nm ($S_{350-400}$) ranges, related to the molecular weight shift of DOM (Helms et al., 2008; **Table 2**).

N_2 and Carbon Fixation Rates

Seawater for the quantification of N_2 and carbon fixation rates was sampled using a Teflon pump connected to polyethylene tubing. Bulk N_2 and carbon fixation rates were measured at each transect station on triplicate 2.3 L transparent polycarbonate bottles filled to overflow and closed air-free with septum screwcaps. Once in the lab (within ∼2 h) the bottles were amended with stable isotopes to assay N_2 and carbon fixation simultaneously. Each bottle was amended with $NaH^{13}CO_3$ 99 atom% ^{13}C to a final ∼10 atom% enrichment, and 2.5 mL 98.9 atom% $^{15}N_2$ gas (both isotopes acquired from Cambridge Isotope Laboratories) injected through the septum using a gas-tight syringe (Montoya et al., 1996). Commercial $^{15}N_2$ gas stocks have been recently reported to be contaminated with varying amounts of other nitrogenated forms such as nitrous oxide and nitrite (Dabundo et al., 2014). The $^{15}N_2$ gas batch used here was

TABLE 1 | Position, core parameters, CDOM and FDOM information obtained from each transect station.

Station	Bottom depth (m)	Temperature (°C)	Salinity	Oxygen (μmol kg^{-1})	NO_x (μM)	PO_4^{3-} (μM)	Chl *a* (μg L^{-1})	DOC (μM)	a_{442} (m^{-1})	a_{350} (m^{-1})	$S_{275-295}$ (nm^{-1})	Sr	SUVA $_{254}$	BIX	Humic-like (QSU)	Tyrosine-like (QSU)	Tryptophan-like (QSU)	UCYN-A (*nifH* gene copies L^{-1})	UCYN-B (*nifH* gene copies L^{-1})	*Trichodesmium*(*nifH* gene copies L^{-1})	*γ-24774A11* (*nifH* gene copies L^{-1})
1	19	26.97	35.59	201.6 ± 2.5	0.1 ± 0.0	0.1 ± 0.0	0.22	80.3 ± 2.5	0.41	0.22	0.03	1.90	1.54	1.01	5.	26.40	0.19	$7.6 \pm 1.1 \times 10^4$	$3.2 \pm 1.3 \times 10^4$	$1.2 \pm 0.2 \times 10^6$	$1.8 \pm 0.4 \times 10^6$
2	10	27.31	35.61	200.2 ± 0.3	0.1 ± 0.0	0.1 ± 0.0	0.27	97.7 ± 0.1	0.07	0.13	0.04	2.78	1.21	1.01	4.83	9.33	0.82	$2.9 \pm 0.6 \times 10^4$	$7.8 \pm 2.5 \times 10^3$	$8.4 \pm 1.6 \times 10^4$	$7.5 \pm 3.6 \times 10^5$
3	8	28.08	35.52	197.9 ± 0.4	0.1 ± 0.0	0.1 ± 0.0	0.16	81.6 ± 3.8	0.06	0.13	0.04	3.30	1.17	1.03	4.84	5.46	n/d	n/d	n/d	$9.4 \pm 2.5 \times 10^5$	8.3×10^5
4	18	28.23	35.57	194.4 ± 0.9	0.0 ± 0.0	0.1 ± 0.0	0.28	87.9 ± 5.6	0.40	0.24	0.03	1.99	0.48	1.03	7.14	5.16	0.17	$1.6 \pm 1.5 \times 10^5$	$1.3 \pm 0.5 \times 10^4$	$2.0 \pm 0.6 \times 10^6$	n/d

Standard deviation values (± SD) are provided where available.

TABLE 2 | Spectral indices investigated in this study.

Abbreviation	Name	Formula
HIX	Humification Index	Ex: 255 nm Em: $\frac{\int 480-434}{\int 344-300}$
BIX	Biological Index	Ex: 255nm Em: $\frac{310-380}{310-430}$
$SUVA_{254}$	Specific UV Absorbance (254 nm)	$\frac{ABS\ (254)}{DOC}$
Sr	Spectral ratio	$\frac{S_{275-295}}{S_{350-400}}$

tested for contamination levels at J. Granger's lab (University of Connecticut, CT, USA), which were found to be negligible and hence did not affect our N_2 fixation rates (Benavides et al., 2015). After isotope additions, the incubation bottles were inverted 20 times, transferred to running seawater incubators covered with blue light screening reproducing the light intensity at the corresponding sampling depth, and incubated for 24 h. To test for non-cyanobacterial (non-photoautotrophic) N_2 fixation activity, a second set of incubation bottles was amended with DCMU to a final concentration of 50 μM (Rahav et al., 2015). These bottles were covered with black fabric bags to keep them in the dark at the same conditions as described above.

After incubation, the samples were filtered through precombusted GF/F filters (Whatman), and the filters were stored at −20°C until analysis. Background (time zero $\delta^{15}N$ and $\delta^{13}C$) samples were taken at every station to allow an accurate calculation of N_2 and carbon fixation rates. The samples were analyzed by continuous-flow isotope ratio mass spectrometry (IRMS) using an Integra2 Analyser (Integra CN), calibrated with International Atomic Energy Agency standards IAEA 310-A for nitrogen (47.2‰) and IAEA 303-B for carbon (466‰). The minimum quantifiable N_2 fixation rate was 0.0041 nmol N L^{-1} d^{-1}, as determined by error propagation analysis (Gradoville et al., 2017). We note that the use of the traditional $^{15}N_2$ "bubble method" (Montoya et al., 1996) instead of the "dissolved method" (Mohr et al., 2010) may have resulted in an underestimation of the actual rates (Grokopf et al., 2012), although the long incubation time (24 h) likely reduces this possibility.

DOM Addition Experiments

To test for the enhancement of N_2 fixation rates and/or *nifH* gene expression as a response to DOM enrichments, we sampled seawater in 25 extra 2.3 L polycarbonate bottles at Station 2. Five bottles were amended with a mix of carbohydrates —"DOC treatment"- (sodium pyruvate, sodium acetate and glucose), another five with a mix of amino acids —"DON treatment"- (alanine, leucine, and glutamic acid), and another five were amended with a mix of phosphomonoesters and phosphonates —"DOP treatment"- (methylphosphonic acid, 2-aminoethylphosphonic acid and fructose 1,6-biphosphate). All DOM mixtures were prepared to be equimolar in carbon (all contained 4 μM carbon; Benavides et al., 2015). Five bottles were used as a control (no DOM additions), and another five bottles were used as a "time zero" (i.e., sacrificed at the start of the experiment to know the baseline conditions). All bottles were spiked with 2.5 mL $^{15}N_2$ and incubated for 24 h as described above. At the end of the incubation period, samples for NO_x,

PO_4^{3-} and DOC analyses were taken from three bottles of each treatment (i.e., DOC, DON, DOP) as described above. The fourth and fifth bottles from each treatment were kept for RNA analyses, respectively (see below).

DNA and RNA Sampling, Extraction and qPCR Assays

Samples for DNA extractions were obtained at each transect station in 2.3 L polycarbonate bottles. Once ashore, the samples were filtered through 0.2 μm Supor filters (PALL) using a peristaltic pump. Upon filtration the filters were transferred to bead beating tubes including ∼50 μL of a mixture of 0.1 mm and 0.5 mm diameter glass beads (BioSpec Products), and stored at −80°C until analysis. DNA was extracted via the phenol-chloroform method (Massana et al., 1997). RNA samples were taken in duplicate from each treatment (see "DOM addition experiments" above), filtered through 0.2 μm Supor filters and stored in sterile bead beating tubes containing 350 μL RLT buffer (Invitrogen) and 3.5 μL ß-mercaptoethanol, and finally stored at −80°C until analysis. The RNA was extracted by TRI Reagent (Invitrogen). 1 mL of Tri reagent was added to each sample that was disrupt and homogenized by pipetting and vortexing in order to break the cells. The cell lysate was incubated at room temperature for 3 h with occasional vortexing. The samples were then centrifuge at 12,000 g for 20 min at 4°C. The supernatant was transferred to a new tube and 10% of Phase Separation Reagent, BCP (Molecular Research Center, Inc., Cincinnati, OH, USA) was added. After additional incubation (30 min) at room temperature and centrifugation (12,000 g, 15 min, 4°C) the supernatant was transferred to a new tube and a cleanup and DNase treatment was performed using the RNA Clean and Concentrator-5 kit (Zymo Research, Irvin, CA, USA). Complementary DNA (cDNA) was created using the qScript™ cDNA Synthesis Kit (Quantabio, Beverly, MA, USA) using the reverse primers of the *nifH* (nifH2 and nifH3; Zani et al., 2000). Quantitative PCR (qPCR) assays were performed on a CFX-96 Touch Real-Time PCR Detection System (Bio-Rad) using the TaqMan Fast Advanced Master Mix (Applied Biosystems) and primers for *nifH* of UCYN-A, UCYN-B, *Trichodesmium* and γ-24774A11 (here referred to as gammaproteobacteria) (Turk et al., 2011).

RESULTS

Hydrography, Nutrients and *in Situ* DOM

The temperature of surface waters increased from 26.97 to 28.23°C moving onshore from Station 1 toward Station 4, while salinity remained close to 35.6 at all stations (**Table 1**). The concentration of oxygen decreased onshore from 201 to 194 μmol kg^{-1}, while inorganic nutrient concentrations (NO_x and PO_4^{3-}) did not vary significantly along the transect, and neither did Chl *a* concentrations, with the exception of Station 3 where Chl *a* was slightly lower (**Table 1**). DOC concentrations remained between 80 and 90 μM along the transect, showing a peak of ∼98 μM at Station 2 (**Table 1**).

CDOM absorption at 442 nm and 350 nm (a_{442} and $a3_{50}$) presented lower values at station 2 and 3 as compared to the values recorded at Stations 1 and 4 (**Table 1**) which indicated a decrease in CDOM concentrations. Moreover, the spectral slope $S_{275-295}$ and the spectral ratio S_r were high with values >1 and >0.0.3 nm^{-1}, respectively, which indicated the presence of photodegraded DOM with low molecular weight. In addition, the $SUVA_{254}$ indices were <4 (this reference value is indicative of DOM with low aromaticity) with an average value of 1.09 ± 0.44. Then CDOM at 442 nm and 350 nm is strongly photodegraded with a low aromaticity. Three fluorescent DOM compounds were identified by the PARAFAC model: terrestrial humic-like (compound 1), tyrosine-like (compound 2) and tryptophan-like (compound 3; **Table 3**). Humic-like compound signatures were higher closer to the coast (Station 4) and decreased to values around ∼5 QSU at the other stations. This pattern is opposite to that of tyrosine-like compounds signals, which increased toward the barrier reef. Tryptophane-like compound concentrations did not follow any coast-open ocean pattern but presented the highest concentrations at Station 2. The BIX indices were homogenous and >1 (this value is indicative of an enrichment in DOM from bacterial origin) along the transect (**Table 1**). Overall, the optical analyses of DOM suggest that while river-derived refractory DOM was more abundant close to the coast, biological-derived labile DOM compounds were present homogeneously at all stations along the transect.

N_2 and Carbon Fixation Activity and Diazotroph Abundance

No clear spatial trends were observed in either N_2 or carbon fixation rates along the transect. N_2 fixation rates in samples not amended with DCMU ranged from 0.66 to 1.32 nmol N L^{-1} d^{-1}, with the highest rates measured at Station 3 (**Figure 2A**). Carbon fixation rates in samples without DCMU ranged from 1.50 to 2.14 μg C L^{-1} d^{-1} (**Figure 2B**). Both N_2 and carbon fixation were effectively inhibited in DCMU-amended samples (>90%; **Figures 2A,B**).

Among the diazotroph phylotypes quantified by qPCR, *Trichodesmium* and gammaproteobacteria showed the highest abundance, ranging between 8.4×10^4 and 2×10^6, and 7.5×10^5 and 1.8×10^6 *nifH* copies L^{-1}, respectively (**Table 1**). UCYN-A and UCYN-B phylotypes were one to two orders of magnitude lower, and undetectable at station 3 (**Table 1**).

N_2 Fixation, Diazotroph Abundance and Optical Response to Model DOM Compound Additions

At Station 2 we tested whether the addition of DOC, DON or DOP upregulated *nifH* expression and/or enhanced N_2 fixation rates. N_2 fixation rates were similar in the control, DOC and DON treatments (∼0.8 nmol N L^{-1} d^{-1}), yet they doubled to ∼2 nmol N L^{-1} d^{-1} when DOP was added (**Figure 3**). However, due to the variability among replicates, the enhancement of either N_2 fixation or expression of *nifH* genes was not statistically significant in any treatment (Kruskal-Wallis, $p > 0.05$).

The DOC, DON, and DOP treatments yielded slightly higher abundances of UCYN-A *nifH* transcripts compared to transcripts measured in the controls, yet similar transcript

TABLE 3 | Excitation and Emission maxima (Ex/Em) of three CDOM fluorescent components validated by PARAFAC model and identification by comparison with the literature data.

	This study			Previous study				FDOM sources
	Comp.	Ex(nm)	Em(nm)	Comp.	Ex(nm)	Em(nm)	Reference	
COMPOUND 1	Humic like	<220	454(322)	Humic-like (A)	230–260	400–480	Coble, 1996	Allochtonous: terrestrial inputs from river
				Terrestrial humic-like	<260	454	Yamashita et al., 2010	
				HumiC-like (A)	230	476	Tedetti et al., 2016	
COMPOUND 2	Tyrosine like	225(275)	304	C7	240(300)	338	Murphy et al., 2007	Autochtonous: heterotrophic bacterial degradation of DOM
				Component 8	275	304	Stedmon and Markager, 2005	
				Tyrosine-like (B)	225(275)	304	Tedetti et al., 2016	
COMPOUND 3	Tryptophane like	270(335)	340	Tryptophane (T1)	220–235	334–360	Coble, 1996	Autochtonous: coral production, heterotrophic bacterial degradation of DOM
					230(300)	352	Martias et al., 2018	

numbers were with obtained in each of the three treatments (∼5–6 × 10^3 *nifH* transcripts L^{-1}; **Figure 3**). UCYN-B did not show differential expression among treatments, while *Trichodesmium* increased by one order of magnitude when exposed to the DOC treatment (**Figure 3**). Despite being the most abundant ambient group as determined by DNA qPCR counts, gammaproteobacteria did not show detectable *nifH* gene expression in our DOM enrichment experiments (including control bottles). The prolonged incubation (24 h) in polycarbonate bottles could have affected *nifH* expression in this group (Moisander et al., 2014).

Regarding optical parameters, the DOC treatment resulted in a peak of tyrosine-like compounds concentrations (+51%) whereas no changes were recorded in humic-like and tryptophan-like compounds concentrations (**Table 4**). The effect of DON and DOP treatments on concentrations of fluorescent compounds are not shown as FDOM results were considered outliers in the validation of PARAFAC model.

DISCUSSION

Spatial Variability of N_2 Fixation Rates and Diazotrophic Phylotypes

Gammaproteobacteria and *Trichodesmium* were the most abundant diazotrophs among the four phylotypes quantified (**Table 1**). The *nifH* copies of these two phylotypes were higher than in a previous study performed in the lagoon during the austral summer. The abundances, reported by Turk-Kubo et al. in *nifH* copies, ranged from 2.8 × 10^3 to 6.4 × 10^4 (UCYN-A), 3.5 × 10^2 to 2.7 × 10^3 (UCYN-B), 3.4 × 10^2 and 1.4 × 10^5 (*Trichodesmium*), and 4 × 10^2 to 1.9 × 10^3 (gammaproteobacteria) *nifH* copies L^{-1}. Typically, the *nifH* copy numbers reported here are similar to published numbers from Berthelot et al. (2017) who reported abundances up to 1.3 × 10^3 (UCYN-A), 7.5 × 10^4 (UCYN-B), 1.6 × 10^5 (*Trichodesmium*), and 2.7 × 10^4 (gammaproteobacteria) *nifH* copies L^{-1} from the Solomon Sea.

DCMU blocks photosynthesis and thus the energy source required by autotrophic cyanobacterial diazotrophs to fix N_2. Hence, measured N_2fixation rates from DCMU-amended samples should be representative of non-cyanobacterial N_2 fixation. The lack of *nifH* expression in gammaproteobacteria in our DOM addition experiments (see below) questions whether this specific group was active. Nevertheless, other non-cyanobacterial diazotrophs such as *Bradyrhizobium* and *Mesorhizobium*, previously detected in the lagoon (Pfreundt et al., 2016), could be responsible for the measured N_2 fixation rates in DCMU-amended bottles. N_2 fixation rates in DCMU-amended incubations represented 4–7% of N_2 fixation measured without amendments. The New Caledonian lagoon is dominated by autotrophic cyanobacterial diazotrophs (Rodier and Le Borgne, 2008; Turk-Kubo et al., 2015), where non-cyanobacterial phylotypes have been reported to represent <2% of the diazotrophic community (Turk-Kubo et al., 2015; Pfreundt et al., 2016). Hence, such a low contribution to total N_2 fixation rates may not be surprising, but deserves further study in other parts of the lagoon and other times of the year. Still, N_2 fixation rates in DCMU-amended bottles ranged between 0.04 and 0.11 nmol N L^{-1} d^{-1}, which is in the range of N_2 fixation rates measured in environments where non-cyanobacterial diazotrophs prevail (Moisander et al., 2017).

It has to be noted that putative non-cyanobacterial N_2 fixation was higher at stations closer to the coast (Stations 3 and 4), which may be linked to the Dumbéa river inputs importing bioavailable CDOM at 350 nm and terrestrial humic-like DOM compounds into the bay. Spectral indices (Sr and $S_{275-295}$) revealed low molecular weight and photodegraded terrestrial CDOM/FDOM at Station 4 (the most impacted by the river), which has been seen to enhance its availability

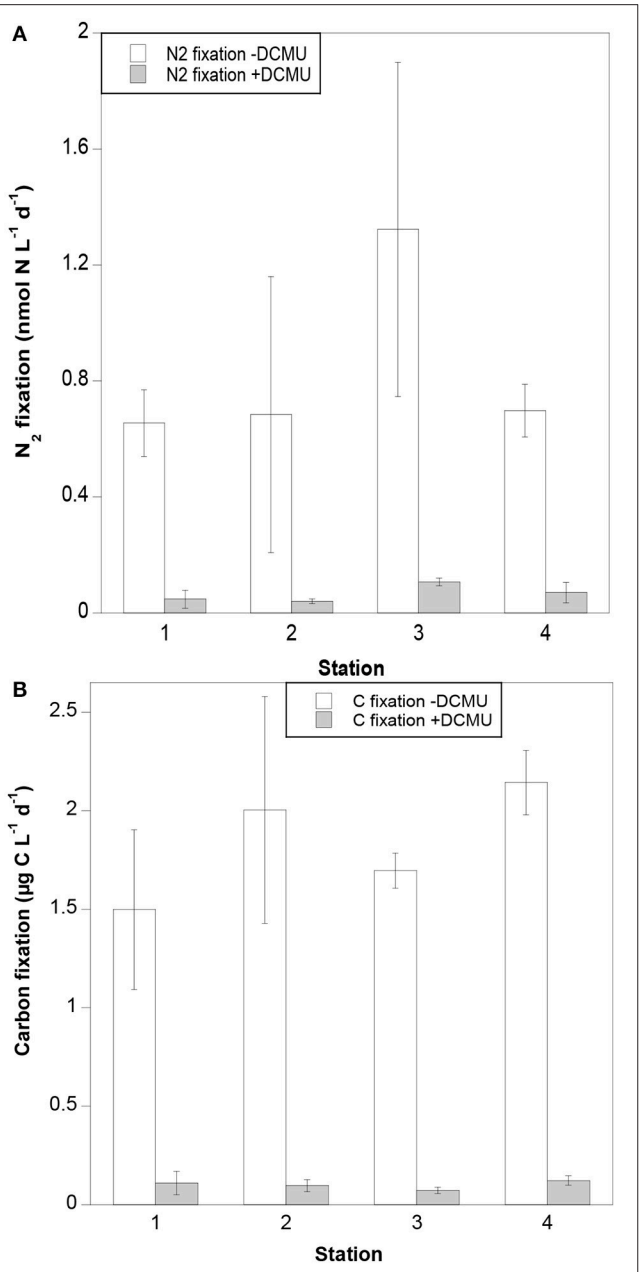

FIGURE 2 | (A) N_2 and **(B)** carbon fixation rates in DCMU and non-DCMU amended samples.

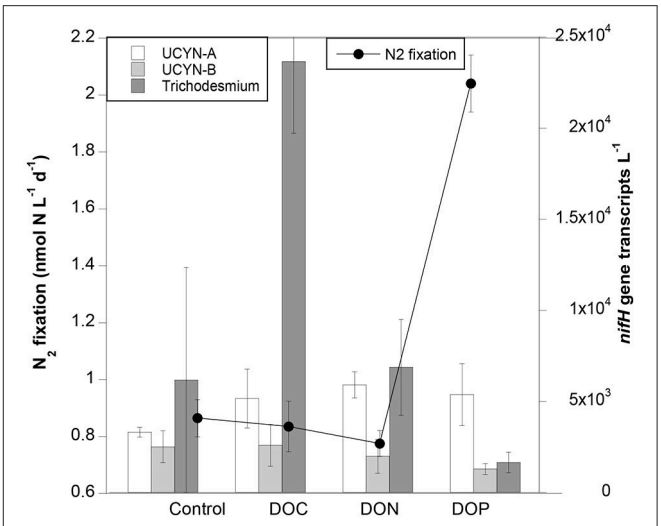

FIGURE 3 | N_2 fixation rates (line) and *nifH* gene expression (*nifH* transcripts L^{-1}; bars) in control, DOC, DON, and DOP treatments performed at Station 2. Error bars indicate the standard deviation of the mean.

to heterotrophic bacteria in oligotrophic waters (Su et al., 2017). At Station 1, DOM sources come from autochthonous phytoplankton production), which is also available for bacterial growth (based on a_{442} values >0.1 as compared to Stations 2 and 3; Steinberg et al., 2004). The observed relationship between DOM lability proxies and non-cyanobacterial N_2 fixation activity in the present study support the findings of previous studies in the WTSP and the Mediterranean Sea (Benavides et al., 2015, 2016; Rahav et al., 2016). Nevertheless, a mechanistic understanding of how non-cyanobacterial diazotrophs benefit from different DOM molecules (e.g., metabolic pathways, affinity for different substrates) is still lacking (Bombar et al., 2016).

Diazotrophic Responses to DOM Additions

The influence of the three different DOM treatments applied (DOC, DON, and DOP) differentially influenced *nifH* gene expression of different phylotypes detected, with transcript abundance increasing similarly in UCYN-A for all amendments as compared to the controls (from ~3 to 5–6 × 10^3 *nifH* transcripts L^{-1}), while no differences were observed between controls and amendments for UCYN-B transcripts (**Figure 3**). UCYN-B fixes carbon during the day and N_2 at night to avoid nitrogenase enzyme inhibition by photosynthetically derived oxygen. Thus, *nifH* expression in UCYN-B is typically higher at night (Church et al., 2005; Zehr et al., 2007). Hence, the absence of *nifH* expression in UCYN-B during the day (when our RNA samples were taken) is not surprising, even in the presence of external DOM sources. Similarly, Moisander et al. (2011) observed that *nifH* expression was not upregulated in UCYN-B when incubated with a mixture of glucose and mannitol. UCYN-A do not have a tricarboxylic acid pathway (Tripp et al., 2010), and thus require reduced organic carbon sources provided by their hosts (Thompson et al., 2012). It is therefore plausible that DOM additions in our experiments enhanced the diazotrophic activity of UCYN-A, similar to the experiments of Moisander et al. (2011), who demonstrated upregulated *nifH* gene expression in UCYN-A upon the addition of a glucose and mannitol mixture. In our experiments, however, a preference for DOC, DON or DOP was not observed and the *nifH* expression response was similar across treatments (**Figure 3**).

Active assimilation of both DOC and DON was measured in natural *Trichodesmium* colonies from the WTSP open ocean waters in similar experiments (Benavides et al., 2017). However,

TABLE 4 | NO_x, PO_4^{3-}, DOC concentrations and values of FDOM-related ratios for the different DOM additions (DOC, DON, and DOP treatments) performed at Station 2.

Treatment	NO_x (μM)	PO_4^{3-} (μM)	DOC (μM)	Humic-like (QSU)	Tyrosine-like (QSU)	Tryptophan-like (QSU)
Control	0.1 ± 0.0	0.1 ± 0.0	90.6 ± 15.5	6.54	44.79	11.71
DOC	0.2 ± 0.1	0.1 ± 0.0	98.6 ± 3.3	6.57	67.45	11.53
DON	0.2 ± 0.0	0.1 ± 0.0	104.1 ± 30.6	n/d	n/d	n/d
DOP	0.2 ± 0.0	0.3 ± 0.0	107.3 ± 7.5	n/d	n/d	n/d

Standard deviation values (± SD) are provided where available.

in that previous study only the addition of DON resulted in an increase of filament-specific N_2 fixation rates (Benavides et al., 2017). The bulk water N_2 fixation measurements presented here do not allow us to discern the contribution of each diazotroph phylotype. Nevertheless, while bulk N_2 fixation rates were highest in the DOP treatment, *nifH* gene expression by *Trichodesmium* was highest in the DOC treatment (**Figure 3**). The peak of tyrosine-like compounds coinciding with the highest *nifH* expression of *Trichodesmium* observed in the DOC treatment may be related to the production of CDOM by this cyanobacterium (Steinberg et al., 2004). Surprisingly, DOM additions did not result in any *nifH* expression in the group of non-cyanobacterial diazotrophs tested in this study. In marine waters, maximum *nifH* expression of gammaproteobacteria typically reaches $\times 10^4$ *nifH* transcripts L^{-1} (Luo et al., 2012; Langlois et al., 2015). For example, Church et al. (2005) reported an average of 4×10^2 *nifH* transcripts L^{-1} for gammaproteobacteria in a diel cycle study at station ALOHA in the North Pacific Ocean, which is in the same order of magnitude as in a study in the WTSP by Moisander et al. (2014). Nevertheless, a study including samples from a wide range of oceanographic cruises across the North and South Atlantic and Pacific Oceans reported up to $\times 10^5$ gammaproteobacterial *nifH* transcripts per liter in sunlit surface waters (Langlois et al., 2015). In offshore waters of the WTSP, the addition of glucose and mannitol upregulated *nifH* expression in gammaproteobacteria (Moisander et al., 2011).

The lack of significant responses to DOM additions in this study could reflect sufficient DOM availability (based on $Sr,S_{275-295}$ and $SUVA_{254}$ indexes) potentially provided by corals in the lagoon which are known for producing tryptophane-like compounds (available DOM sources for bacteria; Weishaar et al., 2003). However, the absence of detected gammaproteobacterial *nifH* transcripts, also in the control bottles, suggests that bottle confinement effects may have inhibited this group (Moisander et al., 2014). In addition to the diel changes in *nifH* gene expression between phylotypes (Church et al., 2005; Turk et al., 2011), it is possible that the *nifH* expression measured in our samples does not reflect the immediate response of diazotrophs to DOM additions. It must be noted that while RNA samples represent a snapshot of *nifH* expression at the time of sampling, N_2 fixation rates integrate the nitrogenase activity that has taken place over a period of 24 h. Such differences probably also account for the uncoupling observed between N_2 fixation rates and *nifH* gene expression.

N_2 Fixation Rates Enhanced by DOP Additions

Diazotrophs differ in how they access DOP. For example, *Crocosphaera watsonii* (here represented by the UCYN-B phylotype) obtains inorganic phosphorus using high affinity phosphate binding systems, and organic phosphorus sources such as phosphomonoesters utilizing alkaline phosphatases (Dyhrman and Haley, 2006). In addition to these phosphorus sources, *Trichodesmium* is also able to grow on phosphonates and use phosphite (Dyhrman et al., 2006; Polyviou et al., 2015). It is intriguing why the *nifH* gene expression of *Trichodesmium*- or of any of the other diazotroph phylotypes tested- was not enhanced when DOP was enriched, and deserves further study. However, an enhancement of N_2 fixationactivity was observed in the DOP treatment (**Figure 3**), and could be due to inorganic phosphorus limitation alleviation. Unfortunately, we do not have alkaline phosphatase activity data to confirm whether the DOP added to our incubations was ultimately transformed to inorganic phosphorus compounds, but PO_4^{3-} concentrations nearly doubled in DOP-amended samples with respect to the control (data not shown), suggesting that active alkaline phosphatases were functioning. The fact that N_2 fixation rates enhanced by DOP additions was not reflected in a significant enhancement of *nifH* expression of any of the diazotroph phylotypes tested suggests that the N_2 fixation activity measured may be provided by a diazotroph not accounted for in our *nifH* gene q-RT-PCR assays. Alternatively, transcription may be interrupted when the number of transcripts is enough to activate the nitrogenase protein, resulting in an uncoupling between expression and nitrogenase activity, as previously reported in *Trichodesmium* cultures (Levitan et al., 2010).

CONCLUSIONS

Although cyanobacterial diazotrophs predominate in the New Caledonian lagoon, here we demonstrate that non-cyanobacterial diazotrophs contribute ∼10% of total N_2 fixation rates. Comparable to previous findings (see Moisander et al., 2017) gammaproteobacteria were the most abundant based on DNA-derived qPCR *nifH* gene counts, yet we did not detect any *nifH* gene expression for this group throughout the experiments. This lack of detectable expression together with the low N_2 fixation rates measured in DCMU-treated samples questions the contribution of non-cyanobacterial diazotrophs to biologically fixed nitrogen inputs in the lagoon. Yet, the response of the

cyanobacterial diazotroph phylotypes to the amended DOM treatments suggests that mixotrophic nutrition may be important in these organisms and should be investigated further.

AUTHOR CONTRIBUTIONS

Conceived and designed the experiments: MB, CM, SB; Performed the experiments: MB, CM; Analyzed the data: MB, CM, HE; Contributed reagents, materials, analysis tools: CM, SB, HE, CD, IB-F; Wrote the paper: MB, CM, CD, HE, IB-F, SB.

FUNDING

MB was funded by the People Programme (Marie Skłodowska-Curie Actions) of the European Union's Seventh Framework Programme (FP7/2007-2013) under REA grant agreement number 625185. Funding was obtained for IB-F through a collaborative grant from Ministry of Science and Technology (MOST) Israel and the High Council for Science and Technology (HCST)-France (2013). CM and SB were funded by the Institut de Recherche pour le Développement (IRD, France).

ACKNOWLEDGMENTS

We thank the captain of R/V *Archamia* for his invaluable help at sea. We would like to thank O. Grosso for IRMS analyses. We are also grateful to P. Gérard and L. Jamet from the Laboratoire des Moyens Analytiques (LAMA) at IRD in Nouméa (New Caledonia) for oxygen, nutrient and DOC analyses.

REFERENCES

Benavides, M., Berthelot, H., Duhamel, S., Raimbault, P., and Bonnet, S. (2017). Dissolved organic matter uptake by *Trichodesmium* in the Southwest Pacific. *Sci. Rep*. 7, 1–6. doi: 10.1038/srep41315

Benavides, M., Bonnet, S., Hernández, N., Martínez-Pérez, A. M., Nieto-Cid, M., Álvarez-Salgado, X. A., et al. (2016). Basin-wide N_2 fixation in the deep waters of the Mediterranean Sea. *Glob. Biogeochem. Cycles* 30, 1–19. doi: 10.1002/2015GB005326

Benavides, M. H., Moisander, P., Berthelot, H., Dittmar, T., Grosso, O., and Bonnet, S. (2015). Mesopelagic N_2 fixation related to organic matter composition in the Solomon and Bismarck Seas (Southwest Pacific). *PLoS ONE* 10:e0143775. doi: 10.1371/journal.pone.0143775

Benavides, M., and Voss, M. (2015). Five decades of N_2 fixation research in the North Atlantic Ocean. *Front. Mar. Sci*. 2, 1–20. doi: 10.3389/fmars.2015.00040

Berthelot, H., Benavides, M., Moisander, P. H., Grosso, O., and Bonnet, S. (2017). High-nitrogen fixation rates in the particulate and dissolved pools in the Western Tropical Pacific (Solomon and Bismarck Seas). *Geophys. Res. Lett*. 44, 8414–8423. doi: 10.1002/2017GL073856

Biegala, I. C., and Raimbault, P. (2008). High abundance of diazotrophic picocyanobacteria (<3 μm) in a Southwest Pacific coral lagoon. *Aquat. Microb. Ecol*. 51, 45–53. doi: 10.3354/ame01185

Bombar, D., Paerl, R. W., and Riemann, L. (2016). Marine non-cyanobacterial diazotrophs: moving beyond molecular detection. *Trends Microbiol*. 24, 916–927. doi: 10.1016/j.tim.2016.07.002

Bonnet, S., Biegala, I. C., Dutrieux, P., Slemons, L. O., and Capone, D. G. (2009). Nitrogen fixation in the western equatorial Pacific: rates, diazotrophic cyanobacterial size class distribution, and biogeochemical significance. *Global Biogeochem. Cycles* 23, 1–13. doi: 10.1029/2008GB003439

Bonnet, S., Caffin, M., Berthelot, H., and Moutin, T. (2017). Hot spot of N_2 fixation in the western tropical South Pacific pleads for a spatial decoupling between N_2 fixation and denitrification. *Proc. Natl. Acad. Sci. U.S.A*. 114, E2800–E2801. doi: 10.1073/pnas.1619514114

Bonnet, S., Dekaezemacker, J., Turk-Kubo, K. A., Moutin, T., Hamersley, R. M., Grosso, O., et al. (2013). Aphotic N_2 fixation in the eastern tropical South Pacific Ocean. *PLoS ONE* 8:e81265. doi: 10.1371/journal.pone.0081265

Bonnet, S., Rodier, M., Turk-Kubo, K. A., Germineaud, C., Menkes, C., Ganachaud, A., et al. (2015). Contrasted geographical distribution of N_2 fixation rates and *nifH* phylotypes in the Coral and Solomon Seas (southwestern Pacific) during austral winter conditions. *Global Biogeochem. Cycles* 29, 1874–1892. doi: 10.1002/2015GB005117

Church, M. J., Short, C. M., Jenkins, B. D., Karl, D. M., and Zehr, J. P. (2005). Temporal patterns of nitrogenase gene (*nifH*) expression in the oligotrophic North Pacific Ocean. *Appl. Environ. Microbiol*. 71, 5362–5370. doi: 10.1128/AEM.71.9.5362-5370.2005

Coble, P. G. (1996). Characterization of marine and terrestrial DOM in seawater using excitation-emission matrix spectroscopy. *Mar. Chem*. 51, 325–346.

Dabundo, R., Lehmann, M. F., Treibergs, L., Tobias, C. R., Altabet, M. A., Moisander, P. H., et al. (2014). The contamination of commercial $^{15}N_2$ gas stocks with ^{15}N-labeled nitrate and ammonium and consequences for nitrogen fixation measurements. *PLoS ONE* 9:e110335. doi: 10.1371/journal.pone.0110335

Dyhrman, S. T., Chappell, P. D., Haley, S. T., Moffett, J. W., Orchard, E. D., Waterbury, J. B., et al. (2006). Phosphonate utilization by the globally important marine diazotroph *Trichodesmium*. *Nature* 439, 68–71. doi: 10.1038/nature04203

Dyhrman, S. T., and Haley, S. T. (2006). Phosphorus scavenging in the unicellular marine diazotroph *Crocosphaera watsonii*. *Appl. Environ. Microbiol*. 72, 1452–1458. doi: 10.1128/AEM.72.2.1452-1458.2006

Feng, X., Bandyopadhyay, A., Berla, B., Page, L., Wu, B., Pakrasi, H. B., et al. (2010). Mixotrophic and photoheterotrophic metabolism in *Cyanothece* sp. ATCC 51142 under continuous light. *Microbiology* 156, 2566–2574. doi: 10.1099/mic.0.038232-0

Garcia, N., Raimbault, P., and Sandroni, V. (2007). Seasonal nitrogen fixation and primary production in the Southwest Pacific: nanoplankton diazotrophy and transfer of nitrogen to picoplankton organisms. *Mar. Ecol. Prog. Ser*. 343, 25–33. doi: 10.3354/meps06882

Gradoville, M. R., Bombar, D., Crump, B. C., Letelier, R. M., Zehr, J. P., and White, A. E. (2017). Diversity and activity of nitrogen-fixing communities across ocean basins. *Limnol. Oceanogr*. 62, 1895–1909. doi: 10.1002/lno.10542

Grokopf, T., Mohr, W., Baustian, T., Schunck, H., Gill, D., Kuypers, M. M. M., et al. (2012). Doubling of marine dinitrogen-fixation rates based on direct measurements. *Nature* 488, 361–364. doi: 10.1038/nature11338

Helms, J. R., Stubbins, A., Ritchie, J. D., Minor, E. C., Kieber, D. J., and Mopper, K. (2008). Absorption spectral slopes and slope rations as indicators of molecular weight, source, and photoleaching of chromophoric dissolved organic matter. *Limnol. Oceanogr*. 53, 955–969. doi: 10.2307/40058211

Herbland, A., Le Bouteiller, A., and Raimbault, P. (1985). Size structure of phytoplankton biomass in the equatorial Atlantic Ocean. *Deep. Res*. 32, 819–836. doi: 10.1016/0198-0149(85)90118-9

Huguet, A., Vacher, L., Relexans, S., Saubusse, S., Froidefond, J. M., and Parlanti, E. (2009). Properties of fluorescent dissolved organic matter in the Gironde estuary. *Org. Geochem*. 40, 706–719. doi: 10.1016/j.orggeochem.2009.03.002

JGOFS (1994). Protocols For The Joint Global Ocean Flux Study (JGOFS) core measurements, *IOC Manuals Guid*. 29, 180.

Karl, D., Michaels, A., Bergman, B., Capone, D., Carpenter, E., Letelier, R., et al. (2002). Dinitrogen fixation in the world's oceans. *Biogeochemistry* 57/58, 47–98. doi: 10.1023/A:1015798105851

Kowalczuk, P., Tilstone, G. H., Zabłocka, M., Röttgers, R., and Thomas, R. (2013). Composition of dissolved organic matter along an Atlantic meridional transect from fluorescence spectroscopy and parallel factor analysis. *Mar. Chem*. 157, 170–184. doi: 10.1016/j.marchem.2013.10.004

Langdon, C. (2010). "Determination of dissolved oxygen in seawater by Winkler titration using the amperometric technique," in *Go-sh. Repeat Hydrogr. Man. A Collect. Expert Reports Guidel*, 18.

Langlois, R., Großkopf, T., Mills, M., Takeda, S., and LaRoche, J. (2015). Widespread distribution and expression of Gamma A (UMB), an uncultured, diazotrophic, γ-proteobacterial *nifH* phylotype. *PLoS ONE* 10:e0128912. doi: 10.1371/journal.pone.0128912

Levitan, O., Brown, C. M., Sudhaus, S., Campbell, D., LaRoche, J., and Berman-Frank, I. (2010). Regulation of nitrogen metabolism in the marine diazotroph *Trichodesmium* IMS101 under varying temperatures and atmospheric CO2concentrations. *Environ. Microbiol.* 12, 1899–1912. doi: 10.1111/j.1462-2920.2010.02195.x

Luo, Y.-W., Doney, S. C., Anderson, L. A., Benavides, M., Berman-Frank, I., Bode, A., et al. (2012). Database of diazotrophs in global ocean: abundance, biomass and nitrogen fixation rates. *Earth Syst. Sci. Data* 4, 47–73. doi: 10.5194/essd-4-47-2012

Martias, C., Tedetti, M., Lantoine, F., Jamet, L., and Dupouy, C. (2018). Characterization and sources of colored dissolved organic matter in a coral reef ecosystem subject to ultramafic erosion pressure (New Caledonia, Southwest Pacific). *Sci. Total Environ.* 616–617, 438–452. doi: 10.1016/j.scitotenv.2017.10.261

Massana, R., Murray, A. E., Preston, C. M., and DeLong, E. F. (1997). Vertical distribution and phylogenetic characterization of marine planktonic Archaea in the Santa Barbara channel. *Appl. Environ. Microbiol.* 63, 50–56.

Messer, L. F., Mahaffey, C., Robinson, C. M., Jeffries, T. C., Baker, K. G., Isaksson, J. B., et al. (2016). High levels of heterogeneity in diazotroph diversity and activity within a putative hotspot for marine nitrogen fixation. *ISME J.* 10, 1499–1513. doi: 10.1038/ismej.2015.205

Mohr, W., Großkopf, T., Wallace, D. W. R., and LaRoche, J. (2010). Methodological underestimation of oceanic nitrogen fixation rates. *PLoS ONE* 5:e0012583. doi: 10.1371/journal.pone.0012583

Moisander, P. H., Beinart, R. A., Hewson, I., White, A. E., Johnson, K. S., Carlson, C. A., et al. (2010). Unicellular cyanobacterial distributions broaden the oceanic N_2 fixation domain. *Science* 327, 1512–1514. doi: 10.1126/science.1185468

Moisander, P. H., Benavides, M., Bonnet, S., Berman-Frank, I., White, A. E., and Riemann, L. (2017). Chasing after non-cyanobacterial nitrogen fixation in marine pelagic environments. *Front. Microbiol.* 8:1736. doi: 10.3389/fmicb.2017.01736

Moisander, P. H., Serros, T., Paerl, R. W., Beinart, R. A., and Zehr, J. P. (2014). Gammaproteobacterial diazotrophs and *nifH* gene expression in surface waters of the South Pacific Ocean. *ISME J.* 8, 1962–1973. doi: 10.1038/ismej.2014.49

Moisander, P. H., Zhang, R., Boyle, E. A., Hewson, I., Montoya, J. P., and Zehr, J. P. (2011). Analogous nutrient limitations in unicellular diazotrophs and *Prochlorococcus* in the South Pacific Ocean. *ISME J.* 6, 733–744. doi: 10.1038/ismej.2011.152

Montoya, J. P., Voss, M., Kahler, P., and Capone, D. G. (1996). A simple, high-precision, high-sensitivity tracer assay for N_2 fixation. *Appl. Environ. Microbiol.* 62, 986–993.

Murphy, K. R., Stedmon, C. A., Waite, T. D., and Ruiz, G. M. (2007). Distinguishing between terrestrial and autochthonous organic matter sources in marine environments using fluorescence spectroscopy. *Mar. Chem.* 108, 40–58. doi: 10.1016/j.marchem.2007.10.003

Passow, U., and Alldredge, A. L. (1995). A dye-binding assay for the spectrophotometric measurement of transparent exopolymer particles (TEP) in the ocean. *Limnol. Oceanogr.* 40, 1326–1335. doi: 10.4319/lo.1995.40.7.1326

Pfreundt, U., Van Wambeke, F., Caffin, M., Bonnet, S., and Hess, W. R. (2016). Succession within the prokaryotic communities during the VAHINE mesocosms experiment in the New Caledonia lagoon. *Biogeosciences* 13, 2319–2337. doi: 10.5194/bg-13-2319-2016

Polyviou, D., Hitchcock, A., Baylay, A. J., Moore, C. M., and Bibby, T. S. (2015). Phosphite utilization by the globally important marine diazotroph *Trichodesmium*. *Environ. Microbiol. Rep.* 7, 824–830. doi: 10.1111/1758-2229.12308

Rahav, E., Bar-Zeev, E., Ohayon, S., Elifantz, H., Belkin, N., Herut, B., et al. (2013). Dinitrogen fixation in aphotic oxygenated marine environments. *Front. Microbiol.* 4:227. doi: 10.3389/fmicb.2013.00227

Rahav, E., Giannetto, M. J., and Bar-Zeev, E. (2016). Contribution of mono and polysaccharides to heterotrophic N_2 fixation at the eastern Mediterranean coastline. *Sci. Rep.* 6:27858. doi: 10.1038/srep27858

Rahav, E., Herut, B., Mulholland, M. R., Belkin, N., Elifantz, H., and Berman-Frank, I. (2015). Heterotrophic and autotrophic contribution to dinitrogen fixation in the Gulf of Aqaba. *Mar. Ecol. Prog. Ser.* 522, 67–77. doi: 10.3354/meps11143

Riemann, L., Farnelid, H., and Steward, G. F. (2010). Nitrogenase genes in non-cyanobacterial plankton: prevalence, diversity and regulation in marine waters. *Aquat. Microb. Ecol.* 61, 235–247. doi: 10.3354/ame01431

Rippka, R., Deruelles, J., Waterbury, J. B., Herdman, M., and Stanier, R. Y. (1979). Generic assignments, strain histories and properties of pure cultures of cyanobacteria. *Microbiology* 111, 1–61. doi: 10.1099/00221287-111-1-1

Rodier, M., and Le Borgne, R. (2008). Population dynamics and environmental conditions affecting *Trichodesmium* spp. (filamentous cyanobacteria) blooms in the south-west lagoon of New Caledonia. *J. Exp. Mar. Bio. Ecol.* 358, 20–32. doi: 10.1016/j.jembe.2008.01.016

Sohm, J. A., Webb, E. A., and Capone, D. G. (2011). Emerging patterns of marine nitrogen fixation. *Nat. Rev. Microbiol.* 9, 499–508. doi: 10.1038/nrmicro2594

Sohrin, R., and Sempéré, R. (2005). Seasonal variation in total organic carbon in the northeast Atlantic in 2000–2001. *J. Geophys. Res.* 110:C10S90. doi: 10.1029/2004JC002731

Stedmon, C. A., and Markager, S. (2005). Resolving the variability of dissolved organic matter fluorescence in a temperate estuary and its catchment using PARAFAC analysis. *Limnol. Oceanogr.* 50, 686–697. doi: 10.4319/lo.2005.50.2.0686

Stedmon, C. A., Markager, S., and Bro, R. (2003). Tracing dissolved organic matter in aquatic environments using a new approach to fluorescence spectroscopy. *Mar. Chem.* 82, 239–254. doi: 10.1016/S0304-4203(03)00072-0

Steinberg, D. K., Nelson, N. B., Carlson, C. A., and Prusak, A. C. (2004). Production of chromophoric dissolved organic matter (CDOM) in the open ocean by zooplankton and the colonial cyanobacterium *Trichodesmium* spp. *Mar. Ecol. Prog. Ser.* 267, 45–56. doi: 10.3354/meps267045

Stoecker, D. K., Hansen, P. J., Caron, D. A., and Mitra, A. (2017). Mixotrophy in the marine plankton. *Ann. Rev. Mar. Sci.* 9, 311–335. doi: 10.1146/annurev-marine-010816-060617

Su, Y., Hu, E., Feng, M., Zhang, Y., Chen, F., and Liu, Z. (2017). Comparison of bacterial growth in response to photodegraded terrestrial chromophoric dissolved organic matter in two lakes. *Sci. Total Environ.* 579, 1203–1214. doi: 10.1016/j.scitotenv.2016.11.104

Tedetti, M., Cuet, P., Guigue, C., and Goutx, M. (2011). Characterization of dissolved organic matter in a coral reef ecosystem subjected to anthropogenic pressures (La Réunion Island, Indian Ocean) using multi-dimensional fluorescence spectroscopy. *Sci. Total Environ.* 409, 2198–2210. doi: 10.1016/j.scitotenv.2011.01.058

Tedetti, M., Marie, L., Röttgers, R., Rodier, M., Van Wambeke, F., Helias, S., et al. (2016). Evolution of dissolved and particulate chromophoric materials during the VAHINE mesocosm experiment in the New Caledonian coral lagoon (south-west Pacific). *Biogeosciences* 13, 3283–3303. doi: 10.5194/bg-13-3283-2016

Thompson, A. W., Foster, R. A., Krupke, A., Carter, B. J., Musat, N., Vaulot, D., et al. (2012). Unicellular cyanobacterium symbiotic with a single-celled eukaryotic alga. *Science* 337, 1546–1550. doi: 10.1126/science.1222700

Torréton, J. P., Rochelle-Newall, E., Pringault, O., Jacquet, S., Faure, V., and Briand, E. (2010). Variability of primary and bacterial production in a coral reef lagoon (New Caledonia). *Mar. Pollut. Bull.* 61, 335–348. doi: 10.1016/j.marpolbul.2010.06.019

Tripp, H. J., Bench, S. R., Turk, K. A., Foster, R. A., Desany, B. A., Niazi, F., et al. (2010). Metabolic streamlining in an open-ocean nitrogen-fixing cyanobacterium. *Nature* 464, 90–94. doi: 10.1038/nature08786

Turk, K. A., Rees, A. P., Zehr, J. P., Pereira, N., Swift, P., Shelley, R., et al. (2011). Nitrogen fixation and nitrogenase (*nifH*) expression in tropical waters of the eastern North Atlantic. *ISME J.* 5, 1201–1212. doi: 10.1038/ismej.2010.205

Turk-Kubo, K. A., Frank, I. E., Hogan, M. E., Desnues, A., Bonnet, S., and Zehr, J. P. (2015). Diazotroph community succession during the VAHINE mesocosm experiment (New Caledonia lagoon). *Biogeosciences* 12, 7435–7452. doi: 10.5194/bg-12-7435-2015

Weishaar, J. L., Aiken, G. R., Bergamaschi, B. A., Fram, M. S., Fujii, R., and Mopper, K. (2003). Evaluation of specific ultraviolet absorbance as an indicator of the chemical composition and reactivity of dissolved organic carbon. *Environ. Sci. Technol.* 37, 4702–4708. doi: 10.1021/es030360x

Yamashita, Y., Maie, N., Briceño, H., and Jaffé, R. (2010). Optical characterization of dissolved organic matter in tropical rivers of the Guayana Shield, Venezuela. *J. Geophys. Res.* 115:G00F10. doi: 10.1029/2009JG000987

Yelton, A. P., Acinas, S. G., Sunagawa, S., Bork, P., Pedrós-Alió, C., and Chisholm, S. W. (2016). Global genetic capacity for mixotrophy in marine picocyanobacteria. *ISME J.* 10, 2946–2957. doi: 10.1038/ismej.2016.64

Zani, S., Mellon, M. T., Collier, J. L., and Zehr, J. P. (2000). Expression of *nifH* genes in natural microbial assemblages in lake george, New York, detected by reverse transcriptase PCR. *Appl. Environ. Microbiol.* 66, 3119–3124.

Zehr, J. P. (2011). Nitrogen fixation by marine cyanobacteria. *Trends Microbiol.* 19, 162–173. doi: 10.1016/j.tim.2010.12.004

Zehr, J. P., Montoya, J. P., Jenkins, B. D., Hewson, I., Mondragon, E., Short, C. M., et al. (2007). Experiments linking nitrogenase gene expression to nitrogen fixation in the North Pacific subtropical gyre. *Limnol. Oceanogr.* 52, 169–183. doi: 10.4319/lo.2007.52.1.0169

Conflict of Interest Statement: The authors declare that the research was conducted in the absence of any commercial or financial relationships that could be construed as a potential conflict of interest.

The reviewer AF-C and handling Editor declared their shared affiliation.

frontiers in Marine Science

ORIGINAL RESEARCH
published: 06 April 2018
doi: 10.3389/fmars.2018.00120

New Perspectives on Nitrogen Fixation Measurements Using $^{15}N_2$ Gas

Nicola Wannicke[1,2], Mar Benavides[3,4], Tage Dalsgaard[5,6], Joachim W. Dippner[1], Joseph P. Montoya[7] and Maren Voss[1]*

[1] Department Biological Oceanography, Leibniz Institute for Baltic Sea Research, Rostock, Germany, [2] Plasma Agriculture, Leibniz Institute for Plasma Science and Technology, Greifswald, Germany, [3] Marine Biological Section, University Copenhagen, Helsingør, Denmark, [4] Aix Marseille Univ, Université de Toulon, CNRS, IRD, MIO UM 110, Marseille, France, [5] Arctic Research Centre, Department of Bioscience, Aarhus University, Aarhus, Denmark, [6] Unisense, Aarhus, Denmark, [7] Georgia Institute of Technology, Atlanta, School of Biological Sciences, Atlanta, GA, United States

Recently, the method widely used to determine $^{15}N_2$ fixation rates in marine and freshwater environments was found to underestimate rates because the dissolution of the added $^{15}N_2$ gas bubble in seawater takes longer than theoretically calculated. As a solution to the potential underestimate of rate measurements, the usage of the enriched water method was proposed to provide constant $^{15}N_2$ enrichment. Still, the superiority of enriched water method over the previously used bubble injection remains inconclusive. To clarify this issue, we performed laboratory based experiments and implemented the results into an error analysis of $^{15}N_2$ fixation rates. Moreover, we conducted a literature search on the comparison of the two methods to calculate a mean effect size using a meta-analysis approach. Our results indicate that the error potentially introduced by an equilibrium phase of the $^{15}N_2$ gas is −72% at maximum for experiments with very short incubation times of 1 h. In contrast, the underestimation was negligible for incubations lasting 12–24 h (error is −0.2%). Our meta-analysis indicates that 84% of the measurements in the two groups will overlap and there is a 61% chance that a sample picked at random from the enriched water group will have a higher value than one picked at random from the bubble group. Overall, the underestimation of N_2 fixation rates when using the bubble method relative to the enriched water method is highly dependent on incubation time and other experimental conditions and cannot be generalized.

Keywords: $^{15}N_2$ fixation, enriched water method, bubble method, diazotrophs, meta-analysis

OPEN ACCESS

Edited by:
Sophie Rabouille, UMR7093 Laboratoire d'océanographie de Villefranche (LOV), France

Reviewed by:
Christine Ferrier-Pagès, Scientific Centre of Monaco, Monaco
Patrick Raimbault, UMR7294 Institut Méditerranéen d'océanographie (MIO), France

****Correspondence:***
Nicola Wannicke
nicola.wannicke@inp-greifswald.de

Specialty section:
This article was submitted to Aquatic Microbiology, a section of the journal Frontiers in Marine Science

Received: *20 September 2017*
Accepted: *21 March 2018*
Published: *06 April 2018*

Citation:
Wannicke N, Benavides M, Dalsgaard T, Dippner JW, Montoya JP and Voss M (2018) New Perspectives on Nitrogen Fixation Measurements Using $^{15}N_2$ Gas. Front. Mar. Sci. 5:120. doi: 10.3389/fmars.2018.00120

INTRODUCTION

Over the last few decades, the stable isotopic tracer $^{15}N_2$ was used to measure the production of diazotroph (N_2-fixer) biomass directly. This isotopic approach was first introduced by Burris and Miller (1941), but it was not until the 1990s that isotope ratio mass spectrometers (IRMS) were sensitive enough to measure low, open ocean low N_2 fixation rates. The protocol established by Montoya et al. (1996) has been widely used in the last two decades, yielding a large amount of N_2 fixation data, which are particularly abundant in the North Atlantic and North Pacific Oceans (Luo et al., 2012). Briefly, the method consists of adding a volume of $^{15}N_2$ gas into a seawater sample,

which is incubated for a given period (on deck or in situ), and finally terminated by filtration through glass fiber filters. The filters are later analyzed by IRMS to determine the amount of $^{15}N_2$ transferred from the aqueous phase to the particulate cell material. Montoya et al. (1996) introduced the calculation of the N_2 fixation rates using a mass-balance approach:

$$N_2 \text{ fixation rate } (M\,L^{-3}\,T^{-1}) = \frac{V}{2}\overline{PN} \approx \frac{V}{2} \times \left(\frac{[PN]\,0 + [PN]f}{2} \right) \quad (1)$$

With V calculated as:

$$V(T^{-}1) = \frac{1}{\Delta t} \times \frac{(A_P Nf - A_P N0)}{(A_{N_2} - A_{PN})}$$

Where M refers to mole nitrogen fixed, L to the volume (liter) and T to the incubation time. A_{PN} is the ^{15}N atom % enrichment of the particulate nitrogen (PN) pool as measured by IRMS, at the beginning (t_0) and end (t_f) of an incubation period; A_{N2} is the ^{15}N atom % enrichment of the dissolved N_2 gas in the incubated seawater; [PN] is the concentration of PN at the end of the incubation [if (PN) is stable over the incubation time; if (PN) varies significantly overtime, an average of initial and final (PN) values is recommended for calculations, see (Montoya et al., 1996)]; and Δt is the duration of the incubation. The values of all the terms in Equation (1) are measured empirically with the exception of A_{N2}. The latter term is theoretically calculated based on the volume of $^{15}N_2$ injected and the initial concentration of N_2 dissolved in seawater based on its temperature and salinity and the N_2 solubility equations of Weiss (1970) which have recently been revised by Hamme and Emerson (2004). This theoretical calculation assumes that isotopic equilibration of the $^{15}N_2$ bubble with the dissolved N_2 already present in the incubation bottle is rapid and complete relative to the incubation period. Simple mass balance tracer equations assume a constant isotope enrichment of the source pool over the duration of the incubation (Fry, 2006) an assumption violated if equilibration of $^{15}N_2$ with seawater is slow or incomplete during the experimental incubation.

Recently, Mohr et al. (2010) reported experimental evidence for a time lag in $^{15}N_2$ equilibration with the surrounding seawater of up to 24 h, depending on a number of factors such as incubation bottle size, volume of $^{15}N_2$ injected, bottle shaking, and incubation temperature. Amongst other things, an observed mismatch between $^{15}N_2$ fixation rates and biomass-specific growth rates motivated Mohr et al. (2010) to re-evaluate the $^{15}N_2$ bubble method introduced by Montoya et al. (1996). Mohr et al. (2010) proposed a new experimental procedure involving preparation of seawater enriched with $^{15}N_2$, which provides a near instantaneous enrichment of the dissolved pool of N_2 in an incubation bottle. This "enriched water" approach resulted in a 2–6 fold increase of measured N_2 fixation rates in comparison to the $^{15}N_2$ "bubble" method (Großkopf et al., 2012; Wilson et al., 2012). To the best of our knowledge, only a few comparisons of the two methods have been published up to date (11 studies) with only two studies including time series observations (Mohr et al., 2010; Klawonn et al., 2015).

There are several reasons why the bubble method may underestimate true N_2 fixation rates: (1) temperature (high temperatures inhibit dissolution of gases), (2) the volume of $^{15}N_2$ gas injected, (3) the duration of the incubation, (4) the time at which the incubation starts relative to the onset of $^{15}N_2$ fixation, and (5) possible DOM coating of the $^{15}N_2$ bubble (Mohr et al., 2010; Klawonn et al., 2015). The enriched water method on the other hand, also seems to be impacted by the mode of incubation, i.e., incubation on deck vs. an *in situ* array (Wilson et al., 2012).

Adding to these factors, Großkopf et al. (2012) reported that underestimates of N_2 fixation rate are lower when the community is dominated by colonial cyanobacteria of the genus *Trichodesmium* and higher when diazotrophs other than *Trichodesmium* predominate (e.g., symbionts, unicellular cyanobacteria, and non-cyanobacterial diazotrophs). All these factors vary widely among published works, making a global recalculation of N_2 fixation very difficult (Großkopf et al., 2012). On the other hand, a number of authors have not found significant differences between the two methods (Mulholland et al., 2012; Shiozaki et al., 2015, not published personnel communication: Berman-Frank et al., Montoya et. al., Benavides and Wannicke et al., -the latter added as unpublished data set to the meta analysis-). Moreover, using $^{15}N_2$ enriched water has a number of drawbacks, including the potential introduction of unwanted dissolved constituents (nutrients, dissolved organic matter or trace metals; Klawonn et al., 2015) and the preparation of the labeled water, which is laborious compared to the injection of a gas bubble into an incubation bottle. Degassing of seawater might also alter seawater chemistry in undesirable ways (e.g., by altering dissolved inorganic carbon concentrations or pH), and the overall extent of the degassing affects the final $^{15}N_2$ enrichment of dissolved N_2 dissolution (Klawonn et al., 2015).

The aim of this study is twofold. Firstly, we used a laboratory experiment to determine the equilibrium time of $^{15}N_2$ in Seawater from the Baltic Sea and used these numbers for an error calculation. By doing so, we tried to generate a measure for the underestimation of $^{15}N_2$ fixation rates when using the bubble method.

Secondly, we applied a meta- analytical approach to evaluate results from published papers comparing both methods. Variability and heterogeneity of published $^{15}N_2$ fixation rates were estimated for different incubation times and a mean effect size over all studies was calculated. Finally, considerations are given for the bubble method and its use in future studies.

MATERIALS AND METHODS

Laboratory Experiment and Error Calculation

Dissolution of $^{15}N_2$ in Brackish Seawater

We tested the equilibration of $^{15}N_2$ with filtered seawater empirically using both the $^{15}N_2$ bubble method (Montoya et al., 1996) and the enriched water method (Mohr et al., 2010). The seawater used in these experiments was collected from the Baltic Sea at the pier off Heiligendamm (54° 8.55′ N, 11° 50.6′ E, salinity of 14) and filtered through 0.2 µm cellulose acetate membranes (Sartorius) using a peristaltic pump. For the bubble method, filtered seawater was then transferred to 1 L

polycarbonate Nalgene®bottles fitted with septum caps, taking care to eliminate all headspace from the filled bottles. We then added 1 ml $^{15}N_2$ gas (98%, Campro Scientific lot # EB1169V) by direct injection through the septum with overpressure released via a cannula. Bottles were gently mixed for 5 min.

We followed the protocol of Mohr et al. (2010) to test the enriched water method using degassed seawater. In brief, degassed seawater was prepared using vacuum in a 1.7 × 5.5 MiniModule (3M Liqui cel) attached to a peristaltic pump (TP4000 E—Economic, Thölen, Germany 950 mbar). We assessed the efficiency of degassing by determining dissolved O_2 concentrations in the degassed water by Winkler titration until O_2 concentration were below the detection limit. Thereupon, 1.1 liter of degassed water was transferred to a Tedlar bag (Dupont, USA), flushed with helium to ensure absence of air inside the bags to which 11 mL of $^{15}N_2$ gas (98%, Campro Scientific lot # EB1169V) was added. The bag was agitated for 5 min (in which the bubble did not disappear) at room temperature. 50 mL of the enriched water was added to each 1.1L incubation bottle filled air free with Baltic Sea water.

All bottles were incubated at 15°C on a horizontal shaker (10 rpm, IKA HS 501, USA) located in a walk- in incubator. Incubations were carried out in triplicate and lasted for 24 h. Replicate sets of bottles were sampled immediately ($t = 0$ h) and at 1, 2, 4, 8, 12, and 24 h after addition of $^{15}N_2$ for analysis of the ^{15}N atom% enrichment of dissolved N_2, for which duplicate sub-samples from each bottle were transferred headspace-free into 12 mL exetainers. Crimp-sealed exetainers were stored in the dark at 4°C for up to 3 days. The ^{15}N atom % enrichment of dissolved N_2 was analyzed by measuring the abundance and concentration of masses $^{29}N_2$ and $^{30}N_2$ using a manual method similar to the automated gas chromatography-isotope ratio mass spectrometry approach described in Holtappels et al. (2011). In brief, water samples were taken from sealed exetainers with a gas tight glass syringe and a subsample was injected on-column on a 2 m stainless steel packed Porapak Q column (Supelco) with a constant flow of He carrier. Water was removed from the sample cryogenically (liquid nitrogen) and oxygen was removed by passage through a column packed with copper wire heated to 650°C. After purification, the N_2 was introduced to a mass spectrometer through an open split interface (Conflo IV, Thermo Scientific) and analyzed on a Delta V Advantage (Thermo Scientific). After every 5th sample air a standard was introduced.

We calculated dissolved $^{15}N_2$ concentrations according to Dalsgaard and Thamdrup (2002). Results of the bubble method were taken as a basis for error estimation as described below.

Error Estimate for the Bubble Method During Isotopic Equilibration

We performed an error estimation to theoretically quantify the % difference in measured $^{15}N_2$ fixation rate considering an increasing time lag (T_i) between $^{15}N_2$ tracer addition and the beginning of diazotrophic $^{15}N_2$ fixation and the duration of fixation (T_f). The error was estimated relative to instantaneous isotopic equilibration of $^{15}N_2$ gas upon bubble injection.

This estimate is relevant in case of time delay between addition of the $^{15}N_2$ tracer and the active beginning of diazotrophic $^{15}N_2$ fixation and also applies for diazotrophs fixing continuously.

Consider a seawater sample with an initial stable isotope composition of dissolved N_2, $N_i = \delta^{15}N_i$. For natural systems, this initial value will be very close to the global natural abundance of 0.366 at% ^{15}N. Into this sample, $^{15}N_2$ gas is injected and after a period of time (typically a couple of hours), the system reaches its equilibrium isotopic composition, $N_e = \delta^{15}N_{eq}$. The temporal development (**Figure 1**) of the ^{15}N enrichment in the dissolved N_2 pool is:

$$\delta^{15}\mathrm{N}\,(\mathrm{t}) = N_i + \Delta N(1 - e^{-bt}) \quad (2)$$

where $\Delta N = N_e - N_i$ is the difference between the equilibrium and initial isotopic compositions and b is an equilibration parameter with units of inverse time. The injection of $^{15}N_2$ gas has the consequence that $N_e > N_i$ and $\Delta N > 0$.

For $t \to \infty$, the equilibrium isotopic composition is reached and $N_e = N_i + \Delta N$. A general assumption of the bubble method is that fixation occurs with the dissolved N_2 pool at isotopic equilibrium. Any fixation that occurs before the system reaches equilibrium will contribute to error (underestimate) in the calculated rate, which is inversely proportional to $\delta^{15}N_2$. The simplest way to estimate the error is the integration of Equation 6 over the duration of fixation. Equation (2) can be rearranged to:

$$\delta^{15}\mathrm{N(t)} = N_e - \Delta N e^{-bt} \quad (3)$$

which allows us to separate our experimental period into phases before and after the system reaches equilibrium. Following

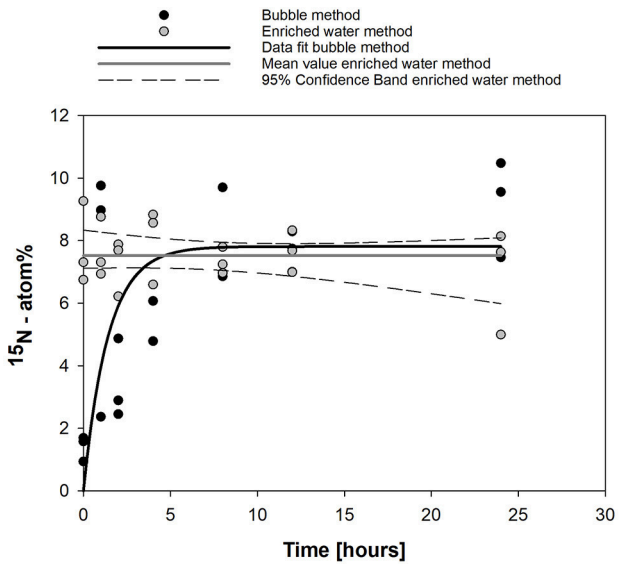

FIGURE 1 | Dissolution kinetics observed in this study for the bubble (●) and enriched water methods (⊙) over 24 h. Data fit for the bubble method (▬) was done using y = 7.81 [1–exp (−0.706 t)], ($R^2 = 0.766$, $p < 0.0001$). For the enriched water method, the mean substrate enrichment and associated 95% confidence interval are shown (▬).

addition of $^{15}N_2$ to an incubation bottle, the mean $\delta^{15}N$ of the dissolved N_2 will increase and the average enrichment of the $^{15}N_2$ pool from the start of N_2-fixation to any time, t will be:

$$\langle \delta^{15}N \rangle = \frac{1}{T_f}\left[N_e \int_{T_i}^{T_f+T_i} dt - \Delta N \int_{T_i}^{T_f+T_i} e^{-bt} dt \right] \quad (4)$$

where the phase lag T_i is the difference in time between gas injection and the start of fixation, while T_f is the duration of N_2-fixation. For $T_i = 0$, the mixing of injected gas and the start of fixation are synchronized, as in the case of a diazotroph that fixes N_2 continuously through the day. Integration of Equation (4) yields an expression for the mean $\delta^{15}N_2$ during the period of active N_2-fixation T_f:

$$\langle \delta^{15}N \rangle = N_e + \frac{\Delta N}{bT_f}\left[e^{-b(T_f+T_i)} - e^{-bT_i} \right] \quad (5)$$

In Equation (5) the mean $\delta^{15}N_2$ value can be expressed as equilibrium composition and an error, ε, which represents the underestimation of the N_2-fixation rate:

$$\langle \delta^{15}N \rangle = \delta^{15}N_{eq} - \varepsilon \quad (6)$$

and the relative percent error, R, is then simply:

$$R(\%) = 100 * \frac{\varepsilon}{\delta^{15}N_{eq}} \quad (7)$$

Fitting Equation (7) to the observations (**Figure 1**) results in Ni = 0 atom%, Ne = 7.8 atom%, Δ N = 7.8 atom%, b = 0.71 h^{-1}.

Meta-Analysis

We obtained data for meta-analysis from published and unpublished sources (Supplementary Table 1). We conducted literature searches using ISI Web of Science and by personal communication. Data selection continued until September 2016. The studies included in our assessment all included a direct comparison of the enriched water and bubble methods with common samples. In all, 13 studies met the requirements for inclusion (n = 368 observations) along with two unpublished data sets (Supplementary Table 1, Supplementary Figure 1). $^{15}N_2$ fixation rates were either provided personally by authors, retrieved from tables published in supplemental material or manually digitized from figures in the published studies using the software WebPlotDigitizer (version 3.10) (Ankit Rohatgi, http://arohatgi.info/WebPlotDigitizer/).

Before performing the meta-analysis, we determined the statistical dispersion and variability within the bubble and enriched water data sets. We calculated the mean absolute deviation (MAD) of each data set as follows:

$$\mathrm{MAD} = \frac{1}{n}\sum_{i=1}^{n} |x_i - \bar{x}| \quad (8)$$

where n is the number of observations and $\bar{x}$ is the mean of the individual observations x_i.

Meta-analysis and meta-regression were conducted with R 3.1.2 using the "metafor" package (Viechtbauer, 2010), metafor package of R [http://www.metafor-project.org/], R Development Core Team 2013). To assess the two methods, we used the logarithmically transformed response ratio (Hedges et al., 1999), lnRR, where RR is the ratio of rates (R) measured with the enriched water and bubble methods ($RR = R_{enrichedwater}:R_{bubble}$), or the effect size of individual experiments), as well as the corresponding pooled standard deviation. All lnRR values were weighted by the reciprocal of their sampling variance, followed by a random effects model to compute the overall mean effect size, which is equivalent to Cohen's d parameter (Cohen, 1977). The random effects model, based on the DerSimonian-Laird estimator (DerSimonian and Laird, 1986) calculates the between-study variance (σ^2) and weights each study by the inverse sum of the individual study variance (v_i) and the between- study variance. Mean effect sizes (i.e., Cohen's d) were statistically significant different if their 95% confidence intervals did not overlap zero.

Apart from calculating the mean effect sizes for all 13 studies and 368 observations, we also divided observations into two groups: short incubation time (0–12 h) and long incubation times (24 h). For short incubation times three data sets were available (Mohr et al., 2010; Klawonn et al., 2015; Benavides and Wannicke et al., unpubl.,). Unfortunately, the experiments of Mohr et al. (2010) and Klawonn et al. (2015) lacked replication from single time points. To be able to include this data set in our meta-analysis, we pooled values collected at t = 0 to 12 h. Results from these publications for t = 24 h had to be omitted from the meta-analysis due to lack of replication. Furthermore, we added a subgroup analysis for each meta-analysis to determine mean effect sizes excluding unpublished data sets.

To explore heterogeneity in the meta-analysis, we calculated Cochrane Q-tests for heterogeneity (Cochran, 1954). A significant Q-statistic (p-value of <0.1) indicates that there is heterogeneity within the mean effect size and a greater variance among individual effect sizes than expected by sampling error. We furthermore, examined the sensitivity of the meta-analysis by examining publication bias (the probability that statistically significant ($p < 0.05$) results are more likely to be published than non-statistically significant results) using a contour-enhanced funnel plot (Peters et al., 2008; Supplementary Figure 2). The funnel plot represents a scatter plot of the effect estimates from individual studies against the standard error of the effect estimate. Specifically, a contour-enhanced funnel plots display the area of statistical significance on a funnel plot (Peters et al., 2008) to improve the correct identification of the presence or absence of publication bias. Publication bias would be expected when the usual funnel plot is asymmetrical.

Random-effects meta-regression analysis using a linear mixed-effects model was used to evaluate the association between incubation time and the mean effect size of $^{15}N_2$ fixation.

For interpretation of the meta-analysis we converted Cohen's *d* value to Cohen's U_3 parameter (Cohen, 1977) to give a measure of the degree of separation (i.e., % non-overlap) of data produced by the bubble and enriched water methods according to:

$$U_3 = \Phi(\delta) \tag{9}$$

where Φ is the cumulative distribution function of the standard normal distribution, and δ is the population value of Cohen's *d*.

In addition, we calculated the overlapping coefficient (OVL) of data from the two methods by converting Cohen's *d* using the following formula (Reiser and Faraggi, 1999)

$$\mathrm{OVL} = 2\Phi\left(\frac{-|\delta|}{2}\right) \tag{10}$$

where Φ is the cumulative distribution function of the standard normal distribution, and δ the population Cohen's *d*.

The probability of superiority (CL) (Ruscio and Mullen, 2012) i.e., probability that a sample picked at random from the treatment group will have a higher score than a sample picked at random from the control group, was calculated the following (Ruscio, 2008)

$$\mathrm{CL} = \Phi\left(\frac{\delta}{\sqrt{2}}\right) \tag{11}$$

where Φ is the cumulative distribution function of the standard normal distribution, and δ the population Cohen's *d*.

RESULTS

Experimental Dissolution of $^{15}N_2$ in Brackish Seawater

Dissolution of $^{15}N_2$ gas according to Montoya et al. (1996) resulted in a maximum ^{15}N atom% enrichment of 9.1 % (mean value for 24 h of incubation, **Figure 1**). Fitting of data resulted in an atom% enrichment of 7.8% (solid line, **Figure 1**). The time to reach 50% of the maximum ^{15}N atom% enrichment was 1.7 h and the shift from an exponential rise in dissolved ^{15}N enrichment to a plateau with only minimal changes in ^{15}N atom% enrichment (>60% of maximum) occurred after 4 h. After 8 h, 90% of ^{15}N atom% equilibration was reached. Injection of water pre-enriched with $^{15}N_2$ gas according to Mohr et al. (2010) resulted in a stable ^{15}N atom% enrichment over 24 h with a mean value of 7.5 ± 0. 9% (**Figure 1**).

Error Estimate for the Bubble Method During Isotopic Equilibration

When using the bubble method, the rate of $^{15}N_2$ fixation will be systematically underestimated during the equilibration phase of $^{15}N_2$ gas with the dissolved pool of N_2 (**Figure 2A**). The overall magnitude of the underestimate during an incubation will depend on the length of the incubation and the timing and duration of $^{15}N_2$ fixation activity during the incubation period (**Figure 2B**), which in turn will reflect the nature (light depended or light independent) of the diazotrophic community present. The maximum error of −72% occurs when the time lag between gas injection and start of the $^{15}N_2$ fixation is zero (T_i = 0 h) and the duration of $^{15}N_2$ fixation is 1 h (T_f = 1 h, red dot in **Figure 2A**). In contrast, a 12 h period of active fixation beginning 6 h after the injection of $^{15}N_2$ gas will result in an error of −0.2% (green square in **Figure 2A**, green solid line in **Figure 2B**, T_i = 6 h and T_f = 12 h).

When organisms are able to fix N_2 continuously, the error would be −12% (blue diamond in **Figure 2A**, T_i = 0 h and T_f = 12 h) over a 12 h incubation and −6% over a 24 h incubation (T_i = 0 h and T_f = 24 h).

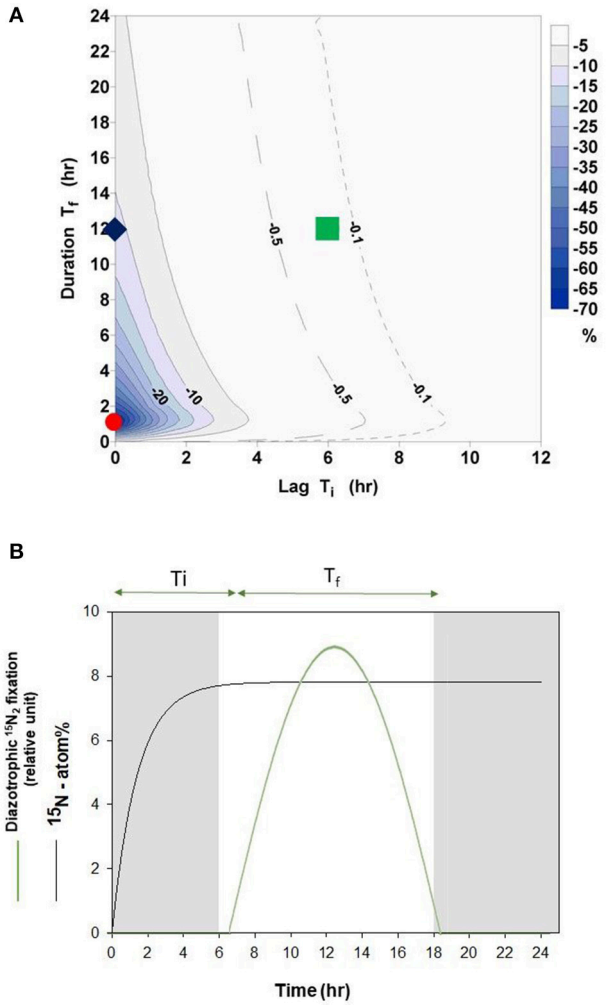

FIGURE 2 | (A) Percentage error according to Equation (7) in relation to phase lag T_i (time lag between gas injection and start of $^{15}N_2$ fixation by diazotrophs) and to T_f (length of active fixation period). The contour interval is 5%. In addition the −0.5% (dashed) and the −0.1% (dotted) line are added. Red dot = error of −72% (T_i = 0 h, T_f = 1 h), Green square = error of −0.2% (T_i = 6 h, T_f = 12 h), blue diamond = error of −12% (T_i = 0 h, T_f = 12 h). **(B)** Schematic representation of an experiment reflecting conditions of an error of −0.2% of the bubble method as presented in **(A)** (Green square). Here, active light depended $^{15}N_2$ fixation (solid green line) occurs over a 12 h period (T_f). The time lag (T_i) between $^{15}N_2$ gas injection and beginning of diazotrophic $^{15}N_2$ fixation is 6 h. Fitted data from experimental dissolution of $^{15}N_2$ is also shown (black line, see also **Figure 1**).

Meta-Analysis

Variability among the replicates of individual studies was quite large as indicated by the standard deviation for the single studies and MAD of the two methods applied (**Figure 3**). Specifically, the MAD for the enriched water method is 7 and the MAD for bubble method is 5.

To determine a mean effect size (i.e., Cohen's *d*), we firstly resolved the response ratio (lnRR) of N_2 fixation for each study (**Figure 4A**). Subsequently, we calculated the overall mean effect size across all studies which resulted in a significant Cohen's *d* of 0.406 ± 0.110, ($p < 0.001$; **Figure 4B**). The mean effect size of ∼0.4, detected in our analysis suggests that for a method comparison, 65 % of measurements from the enriched water group will be above the mean of the bubble group (Cohen's U_3, for subgroup analysis 73%) and that 84% of the measurements in the two groups will overlap (subgroup analysis 76%). In addition, there is a 61% chance that a sample picked at random from the enriched water group will have a higher value than one picked at random from the bubble group (subgroup analysis 66%).

A subgroup analysis excluding the unpublished data sets revealed a significant mean effect size of 0.631 ± 0.125 ($p < 0.001$).

We also performed a meta-regression to evaluate the influence of time on the overall mean effect size. No significant impact was detected (data not shown). Moreover, we checked for publication bias, which is expected when scatter of data in the funnel plot is asymmetric. In our analysis, assessment of the contour-enhanced funnel plot indicates an asymmetrical scatter of data and potential publication bias introduced by a lack of non-significant studies (Supplementary Figure 2).

We furthermore, did separate meta- analysis for observations with short incubation times (0–12 h) and long incubation times (24 h only, Supplementary Figures 3A,B). The overall mean effect size of the three studies with short incubation time was not significant with a Cohen's *d* of 0.057 ± 0.188, ($p > 0.1$) (Supplementary Figure 3A). Excluding the unpublished data set of Benavides and Wannicke et al., revealed a non-significant mean effect size of 0.557 ± 0.382 ($p > 0.1$). Furthermore, the meta- analysis for long incubation times of 24 h resulted in a Cohen's *d* of 0.406 ± 0.101 ($p < 0.001$) (Supplementary Figure 3B). Excluding unpublished studies resulted in a mean effect size of 0.68 ± 0.136 ($p < 0.001$).

We found no significant correlations with ocean province or temperature in exploring which factors might influence the mean effect size (data not shown).

DISCUSSION

We combined a theoretical examination of the error associated with the equilibration time of the bubble of $^{15}N_2$ gas and a meta-analysis of published and unpublished sets of N_2-fixation measurements comparing both methods. Our findings allows us to detect mean differences in rate estimates and provide critical insight into the strengths and weaknesses of the two experimental approaches.

Error Estimation of Bubble Method

Our error estimation of the bubble method during a 24 h experiment reveals a negligible error of −0.2% assuming a diazotroph community that fixes only during 12 h daytime and starting of nitrogen fixation 6 h after the injection of $^{15}N_2$ gas i.e., the addition was done 6 h before sunrise. Considering that the error introduced by using a gas-tight syringe to inject $^{15}N_2$ gas of ±1% (according to the manufacturer, Hamilton USA), the error introduced by using bubble injection is insignificant. The error introduced by using the bubble method will increase to −6% when diazotrophs fix continuously over 24 h (assuming there is no time lag between bubble injection and start of active fixation). Overall, it is important to adjust incubation times relative to the onset of active N_2 fixation (which is in turn is depended on the dominating diazotrophs present), as has been indicated before (Mohr et al., 2010; Wilson et al., 2012).

Meta-Analytical Comparison of the Enriched Water and Bubble Method

Statistical dispersion, as represented by the MAD from the mean value, appears to be higher in the data set based on the enriched water method (mean MAD of all studies 7) than in the data set of studies that used the bubble method (mean MAD of all studies 5). That is, measured N_2 fixation rates appear to be more consistent when determined using the bubble method. A larger dispersion of data in experiments using the enriched water method might be introduced in by the process of preparing the enriched water for later usage, i.e., degassing water of different volumes and varying accuracy of degassing. In addition, Wilson et al.(2012) presented evidence for a dispersion of data in experiments using the enriched water method, which was connected to abiotic factors influencing the incubation itself. They noted an interesting contrast between the two methods when comparing samples incubated at sea using either an *in situ* array or shipboard incubators. Specifically, they found that the enriched water method produced depth-integrated N_2-fixation estimates that were 30% greater when samples were incubated aboard ship in deck incubators than when incubated on an *in situ* array. In contrast, depth-integrated rates measured using the bubble method were not significantly different between incubations carried out on deck and on an *in situ* array. The 30 % difference among replicates of the enriched water method also overlaps with the divergence of the enriched water and bubble methods referred to by Mohr et al. (2010) and Wilson et al. (2012) in their methods assessments.

Our meta- analysis revealed a large congruence in the estimates of $^{15}N_2$ fixation rate produced using the two experimental methods. The 84% overlap of rate estimates make it very difficult at this stage to estimate any sort of a global factor to quantify the degree of underestimation of $^{15}N_2$ fixation rates when using the bubble method. Our literature review moreover revealed that a thorough comparison over a 24-h cycle is needed with only three studies on sort incubation times of 0–12 h. A larger comparative analysis is clearly necessary especially in view of the elevated dispersion (i.e., larger MAD)

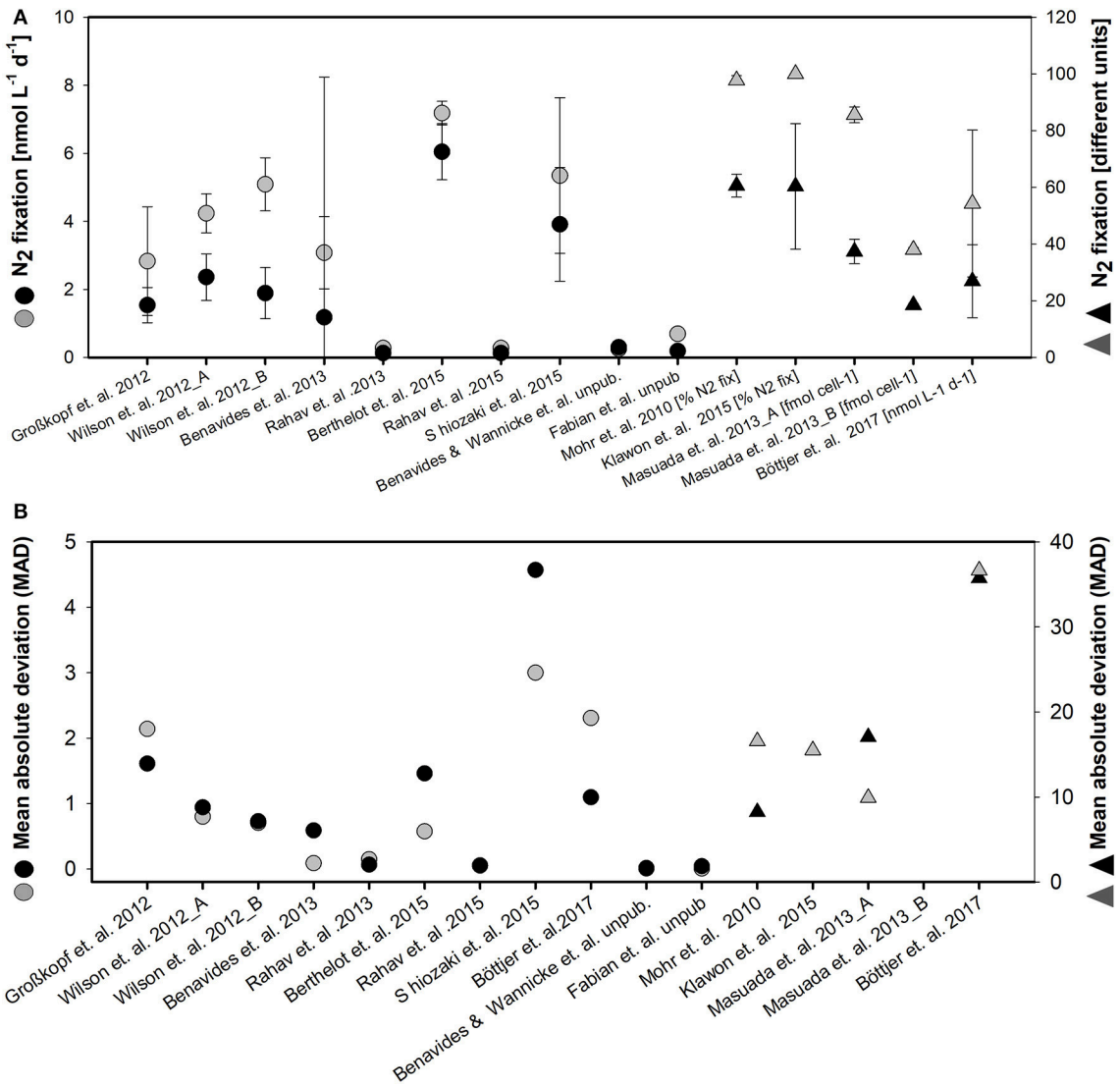

FIGURE 3 | Mean value and standard deviation for N_2 fixation (different units) **(A)** and mean absolute deviation (MAD) **(B)** for enriched water method (black symbols) and bubble method (gray symbols) of the different studies considered in the meta- analysis. Note the different scales and different units for studies indicated by the second right-handed ordinate (units are given next to the authors name in the abscissae).

of $^{15}N_2$ fixation rates measured using the enriched water method.

As Großkopf et al. (2012) have pointed out, there is an indication for a species-specific potential for underestimation of N_2 fixation rates using the bubble method, especially when buoyant diazotrophs are presented. Thus, in habitats dominated by filamentous species like *Trichodesmium* or *Nodularia,* underestimation seems to be less severe compared to habitats dominated by unicellular species (UCYN, e.g., Zehr et al., 1998), as well as non-diazotrophic *Bacteria* and *Archaea* (e.g., Riemann et al., 2010). In the latter, incubation times have to be adjusted to the equilibration time of $^{15}N_2$ when using the bubble method. Alternatively, as proposed in the sub-chapter below (see "Experimental Recommendations") the determination of the final $^{15}N_2$ (i.e., substrate) enrichment in the incubation bottle enables a concerted calculation of N_2 fixation rates.

Dealing With Unpublished Data-Sets

In our analysis, we have included two data sets that are currently unpublished (Benavides and Wannicke et al., Fabian et al., Supplementary Table 1). The literature dealing with the inclusion of unpublished data in meta-analysis clearly recommends inclusion of this sort of "gray literature" (e.g., Cook et al., 1993; McAuley et al., 2000). Exclusion from meta-analysis can lead to exaggerated overestimation of treatment effects (e.g., Cook et al., 1993; McAuley et al., 2000). This is also reflected in our analysis of funnel plot symmetry, where studies displaying no significant effect (Cohen's d of ~ 0) are under-represented and/or missing in our analysis. Overall, publication bias is the greatest

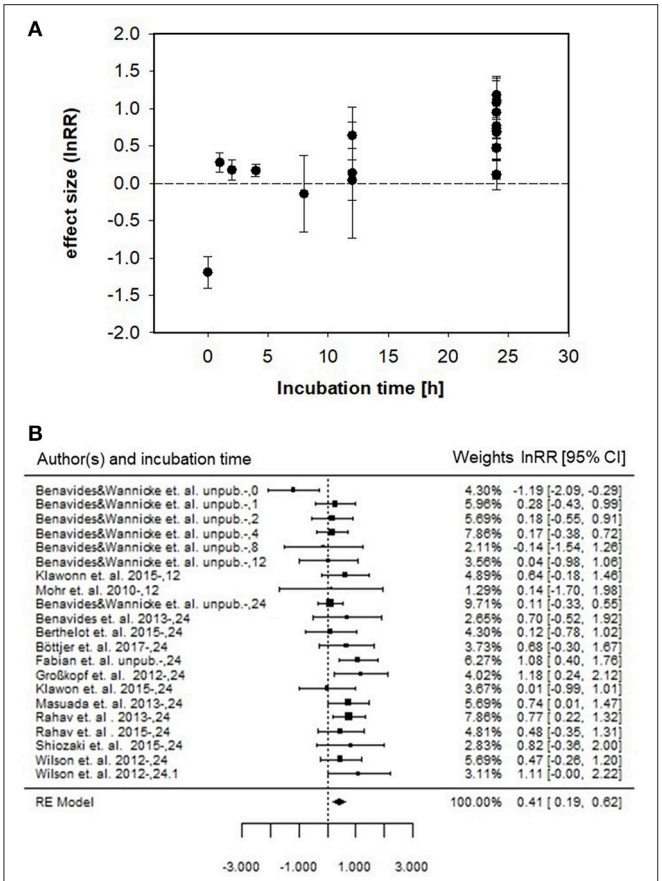

FIGURE 4 | (A) Response ratios (lnRR) of the bubble vs. dissolved enriched water method to detect $^{15}N_2$ fixation and corresponding standard error for the different studies and incubation time intervals. **(B)** Forest plot of lnRR and mean effect size (i.e. RE Model) of enriched water vs. bubble method for all incubation times. Left panel indicates authors and incubation time interval. Middle panel denotes each study represented by a filled square and horizontal line (symbol size represents corresponding weighted lnRR, line represents 95% confidence interval). Right panel provides weighted lnRR and 95% confidence interval. Studies with confidence intervals that intersect the vertical line of unity (lnRR = 0) indicate no difference between the enriched water and bubble method. Heterogeneity of the meta-analysis is indicated by $Q_M(df = 20) = 28.99$, $p = 0.0878$.

threat to the validity of meta-analysis, because combining only the identified published studies uncritically, may lead to an incorrect, unusually one sided, conclusion.

General Experimental Considerations for Future Nitrogen Fixation Measurements

A number of experimental factors have a strong influence on the precision and accuracy of the determination of N_2-fixation rates. Firstly, the sensitivity of any experiment using $^{15}N_2$ depends on the amount of tracer added to the dissolved pool of N_2. For example, addition of 1 mL of $^{15}N_2$ per liter of sample will produce an equilibrium enrichment of ∼5–10 atom% ^{15}N, depending on the size of the ambient pool of N_2. In contrast, the procedure proposed by Großkopf et al. (2012) results in an enrichment of only 2 atom%. Since N_2 availability does not limit N_2-fixation activity, greater additions may easily be realized to increase the substrate labeling, thereby increasing the sensitivity of the rate measurement. This is especially important in systems where rates are expected to be low, for example in aphotic deep waters. In general, we recommend adding sufficient $^{15}N_2$ to raise the ^{15}N content of the dissolved N_2 pool to 9–10 at% as noted by Montoya et al. (1996).

Secondly, the natural variability of $\delta^{15}N$ of the particulate nitrogen (PN) pool sets a lower limit to rate measurements. If the variability in $\delta^{15}N$ of PN is high at the start of the incubation (t_0) and the final increase in $\delta^{15}N$ values of the PN in the incubation bottles is low due to low N_2 fixation rates, then N_2-fixation activity may not be detectable. For example, Wasmund et al. (2015) have nicely explored this issue, discussing $^{15}N_2$ fixation rate measurements in the Benguela upwelling region where they compared initial (t_0) and final $\delta^{15}N$ measurements of samples incubated with $^{15}N_2$. The mean values of the two batches of filters differed only by 0.9‰, leading Wasmund et al. (2015) to conclude that $^{15}N_2$ fixation rates were too low to resolve with the tracer method. Nowadays, mass spectrometers clearly perform analytical precisions of 0.2‰ and better. Therefore, the detection limit of enriched PN is well below 4‰, as original proposed in the paper by Montoya et al. (1996).

Finally, the two experimental approaches differ fundamentally in the degree and nature of experimental manipulation of the sample. The bubble method involves minimal handling (a thourough mixing of water and gas bubble after injection has to be guaranteed, by using e.g., a continuously rotating) and perturbation of the system, but can lead to a systematic underestimate of N_2-fixation rate if a significant fraction of the overall activity during the experiment occurs during the isotopic equilibration phase. In contrast, the enriched water method requires extensive processing in advance to prepare the $^{15}N_2$-labeled water used to inject tracer into the experimental bottle as described by Klawonn et al. (2015) and Mulholland et al. (2012). Ideally, the enriched water should be obtained from the same location and depth as the experimental sample, which imposes a significant cost in time and handling while setting up the experiment, with the added risk of contamination with ammonium, DON, or other dissolved species during handling. If the enriched water is prepared in advance from artificial seawater or water obtained at a different station, it represents an addition of alien water and dissolved species and should be minimized in volume to less than a few percent of the bottle volume. The potential for contamination and the degree to which the addition of enriched water may affect estimates of N_2 fixation rates are very difficult to constrain but can clearly compromise the reliability of the final rate estimates. Another approach using the bubble addition followed by the removal of the bubble after only few hours and retrieval of a subsample for determination of $^{15}N_2$ atom% enrichment requires the tedious determination of the $^{15}N_2$ atom% enrichment for each incubation bottle (Jayakumar et al., 2017). Although this approach is easy to handle, it requires efficient handling and subsequent stable isotope analysis.

Our dissolution experiments investigating the isotopic equilibration in seawater along with the theoretical error calculation both suggest that incubation times longer than about 6 h are minimally affected by the equilibration of the added $^{15}N_2$ gas and the dissolved pool of N_2 in the experimental bottle (**Figures 3A**, **4A**). In practical terms, 24 h incubations are frequently recommended and used because these experiments integrate over a full day/night cycle.

A final recommendation to improve the accuracy of N_2 fixation measurements and potentially help resolve the source of variability among replicates is collection and preservation of a water sample from each experimental bottle for determination of the final $^{15}N_2$ (i.e., substrate) enrichment. This would improve the accuracy of the enriched water, as well as the bubble method, both of which typically rely on solubility calculations to estimate the size of the ambient pool of N_2, which in turn determines the actual $^{15}N_2$ enrichment of the dissolved pool.

AUTHOR CONTRIBUTIONS

All authors contributed to the design of the study. Laboratory and analytical work was conducted by NW, MB, JM, and TD. Data search and meta- analysis was performed by NW and MB. Error analysis was contrived by MV and JD and calculated by JD. NW wrote the initial draft of the manuscript and all authors contributed to its revision.

FUNDING

MB was supported by grant 6108-00013 from the Danish Council for independent research, and grant A1371347 from the German Academic Exchange Service. NW and MV received support from the German Ministry of Science and Technology, BIOACID grant 03F0728F. JM received support from the National Science Foundation grant NSF-OCE-1737078.

ACKNOWLEDGMENTS

We thank Dr. Sophie Rabouille for handling the editorial process and the two referees whose comments improved this manuscript.

SUPPLEMENTARY MATERIAL

The Supplementary Material for this article can be found online at: https://www.frontiersin.org/articles/10.3389/fmars.2018.00120/full#supplementary-material

REFERENCES

Burris, R. H., and Miller, C. E. (1941). Application of N 15 to the study of biological nitrogen fixation. *Science* 93, 114–115.

Cochran, W. G. (1954). The combination of estimates from different experiments. *Biometrics* 10, 101–129. doi: 10.2307/3001666

Cohen, J. (1977). *Statistical Power Analysis for the Behavioral Sciences (revised Edn)*. New York, NY: Academic Press.

Cook, D. J., Guyatt, G. H., Ryan, G., Clifton, J., Buckingham, L., Willan, A., et al. (1993). Should unpublished data be included in meta-analyses?: current convictions and controversies. *JAMA* 269, 2749–2753. doi: 10.1001/jama.1993.03500210049030

Dalsgaard, T., and Thamdrup, B. (2002). Factors controlling anaerobic ammonium oxidation with nitrite in marine sediments. *Appl. Environ. Microbiol.* 68, 3802–3808. doi: 10.1128/AEM.68.8.3802-3808.2002

DerSimonian, R., and Laird, N. (1986). Meta-analysis in clinical trials. *Control. Clin. Trials* 7, 177–188. doi: 10.1016/0197-2456(86)90046-2

Fry, B. (2006). *Stable Isotope Ecology*. New York, NY: Springer.

Großkopf, T., Mohr, W., Baustian, T., Schunck, H., Gill, D., Kuypers, M. M., et al. (2012). Doubling of marine dinitrogen-fixation rates based on direct measurements. *Nature* 488, 361–364. doi: 10.1038/nature11338

Hamme, R. C., and Emerson, S. R. (2004). The solubility of neon, nitrogen and argon in distilled water and seawater. *Deep Sea Res. Part I Oceanogr. Res. Pap.* 51, 1517–1528. doi: 10.1016/j.dsr.2004.06.009

Hedges, L. V., Gurevitch, J., and Curtis, P. S. (1999). The meta-analysis of response ratios in experimental ecology. *Ecology* 80, 1150–1156. doi: 10.1890/0012-9658(1999)080[1150:TMAORR]2.0.CO;2

Holtappels, M., Lavik, G., Jensen, M. M., and Kuypers, M. M. (2011). 15N-labeling experiments to dissect the contributions of heterotrophic denitrification and anammox to nitrogen removal in the OMZ waters of the ocean. *Methods Enzymol.* 486, 223–251. doi: 10.1016/B978-0-12-381294-0.00010-9

Jayakumar, A., Chang, B. X., Widner, B., Bernhardt, P., Mulholland, M. R., and Ward, B. B. (2017). Biological nitrogen fixation in the oxygen-minimum region of the eastern tropical North Pacific ocean. *ISME J.* 11, 2356–2367. doi: 10.1038/ismej.2017.97

Klawonn, I., Lavik, G., Böning, P., Marchant, H. K., Dekaezemacker, J., Mohr, W., et al. (2015). Simple approach for the preparation of 15– 15N2-enriched water for nitrogen fixation assessments: evaluation, application and recommendations. *Front. Microbiol.* 6:769. doi: 10.3389/fmicb.2015.00769

Luo, Y.-W., Doney, S., Anderson, L., Benavides, M., Berman-Frank, I., Bode, A., et al. (2012). Database of diazotrophs in global ocean: abundance, biomass and nitrogen fixation rates. *Earth Syst. Sci. Data* 4, 47–73. doi: 10.5194/essd-4-47-2012

McAuley, L., Tugwell, P., and Moher, D. (2000). Does the inclusion of grey literature influence estimates of intervention effectiveness reported in meta-analyses? *Lancet* 356, 1228–1231. doi: 10.1016/S0140-6736(00)02786-0

Mohr, W., Grosskopf, T., Wallace, D. W., and LaRoche, J. (2010). Methodological underestimation of oceanic nitrogen fixation rates. *PLoS ONE* 5:e12583. doi: 10.1371/journal.pone.0012583

Montoya, J. P., Voss, M., Kahler, P., and Capone, D. G. (1996). A simple, high-precision, high-sensitivity tracer assay for N (inf2) fixation. *Appl. Environ. Microbiol.* 62, 986–993.

Mulholland, M. R., Bernhardt, P. W., Blanco-Garcia, J. L., Mannino, A., Hyde, K., Mondragon, E., et al. (2012). Rates of dinitrogen fixation and the abundance of diazotrophs in North American coastal waters between Cape Hatteras and Georges Bank. *Limnol. Oceanogr.* 57, 1067–1083. doi: 10.4319/lo.2012.57.4.1067

Peters, J. L., Sutton, A. J., Jones, D. R., Abrams, K. R., and Rushton, L. (2008). Contour-enhanced meta-analysis funnel plots help distinguish publication bias from other causes of asymmetry. *J. Clin. Epidemiol.* 61, 991–996. doi: 10.1016/j.jclinepi.2007.11.010

Reiser, B., and Faraggi, D. (1999). Confidence intervals for the overlapping coefficient: the normal equal variance case. *J. R. Stat. Soc. D* 48, 413–418. doi: 10.1111/1467-9884.00199

Riemann, L., Farnelid, H., and Steward, G. F. (2010). Nitrogenase genes in non-cyanobacterial plankton: prevalence, diversity and regulation in marine waters. *Aquat. Microb. Ecol.* 61, 235–247. doi: 10.3354/ame01431

Ruscio, J. (2008). A probability-based measure of effect size: robustness to base rates and other factors. *Psychol. Methods* 13:19. doi: 10.1037/1082-989X.13.1.19

Ruscio, J., and Mullen, T. (2012). Confidence intervals for the probability of superiority effect size measure and the area under a receiver operating characteristic curve. *Multivariate Behav. Res.* 47, 201–223. doi: 10.1080/00273171.2012.658329

Shiozaki, T., Nagata, T., Ijichi, M., and Furuya, K. (2015). Nitrogen fixation and the diazotroph community in the temperate coastal region of the northwestern North Pacific. *Biogeosciences* 12, 4751–4764. doi: 10.5194/bg-12-4751-2015

Viechtbauer, W. (2010). Conducting meta-analyses in R with the metafor package. *J. Stat. Softw.* 36, 1–48. doi: 10.18637/jss.v036.i03

Wasmund, N., Struck, U., Hansen, A., Flohr, A., Nausch, G., Grüttmüller, A., et al. (2015). Missing nitrogen fixation in the Benguela region. *Deep Sea Res. I Oceanogr. Res. Pap.* 106, 30–41. doi: 10.1016/j.dsr.2015.10.007

Weiss, R. (1970). The solubility of nitrogen, oxygen and argon in water and seawater *Deep Sea Res. Oceanogr. Abstr.* 17, 721–735. doi: 10.1016/0011-7471(70)90037-9

Wilson, S. T., Böttjer, D., Church, M. J., and Karl, D. M. (2012). Comparative assessment of nitrogen fixation methodologies, conducted in the oligotrophic North Pacific Ocean. *Appl. Environ. Microbiol.* 78, 6516–6523. doi: 10.1128/AEM.01146-12

Zehr, J. P., Mellon, M. T., and Zani, S. (1998). New nitrogen-fixing microorganisms detected in oligotrophic oceans by amplification of nitrogenase (nifH) genes. *Appl. Environ. Microbiol.* 64, 3444–3450.

Conflict of Interest Statement: The authors declare that the research was conducted in the absence of any commercial or financial relationships that could be construed as a potential conflict of interest.

frontiers in Marine Science

OPINION
published: 06 April 2018
doi: 10.3389/fmars.2018.00108

Deep Into Oceanic N_2 Fixation

Mar Benavides[1,2]*, *Sophie Bonnet*[2], *Ilana Berman-Frank*[3,4] *and Lasse Riemann*[1]

[1] Marine Biology Section, Department of Biology, University of Copenhagen, Helsingør, Denmark, [2] Aix-Marseille Université, Université de Toulon, CNRS, IRD, MIO UM 110, Marseille, France, [3] Mina and Everard Goodman Faculty of Life Sciences, Bar-Ilan University, Ramat Gan, Israel, [4] Department of Marine Biology, Charney School of Marine Sciences, University of Haifa, Haifa, Israel

Keywords: nitrogen budget, mesopelagic, non-cyanobacterial diazotrophs, *nifH* gene, aphotic layer

Edited by:
Angela Landolfi, GEOMAR Helmholtz Centre for Ocean Research Kiel, Germany

Reviewed by:
Luisa I. Falcon, Universidad Nacional Autónoma de México, Mexico
Arvind Singh, Physical Research Laboratory, India

***Correspondence:**
Mar Benavides
mar.benavides@bio.ku.dk;
mar.benavides@mio.osupytheas.fr

Specialty section:
This article was submitted to Aquatic Microbiology, a section of the journal Frontiers in Marine Science

Received: *06 November 2017*
Accepted: *14 March 2018*
Published: *06 April 2018*

Citation:
Benavides M, Bonnet S, Berman-Frank I and Riemann L (2018) Deep Into Oceanic N_2 Fixation. Front. Mar. Sci. 5:108. doi: 10.3389/fmars.2018.00108

The biological fixation of dinitrogen (N_2) by marine prokaryotes called diazotrophs is the major source of nitrogen to the ocean, estimated at ∼106–120 Tg N y^{-1} (Gruber, 2004; Gruber and Galloway, 2008). This process contributes importantly to sustain primary production and maintain the global nitrogen inventory. The nitrogen reservoir is further controlled by fixed nitrogen loss processes including sediment burial, denitrification, and anammox (Falkowski, 1997), which exceed fixed nitrogen gains through N_2 fixation, leading to an imbalanced global nitrogen budget (Codispoti et al., 2001; Codispoti, 2007; Eugster and Gruber, 2012). Since the early 1970s, diazotrophic activity has been attributed to autotrophic cyanobacteria constrained to the sunlit and oligotrophic layer of the tropical and subtropical oceans (Zehr, 2011). Yet substantial evidence indicates a high diversity and wide distribution of non-cyanobacterial diazotrophs (bacteria and archaea) in the oceans (Zehr et al., 1998, 2000; Farnelid et al., 2011; Bombar et al., 2016; Moisander et al., 2017). These diazotrophs are potentially not constrained by light as are their cyanobacterial counterparts, and have been detected in wide-ranging environments such as nutrient-rich, cold, and/or dark ecosystems including coastal upwelling regions (Sohm et al., 2011), temperate coastal zones (Bentzon-Tilia et al., 2015), and the deep ocean (Hewson et al., 2007; Hamersley et al., 2011).

Stretching the environmental boundaries, beyond those traditionally thought to constrain N2 fixation, will likely impact current estimates of nitrogen input to the global ocean. Extending the latitudinal limits from the tropics and subtropics to temperate waters would already represent a considerable increase in the potentially active N_2 fixation area, but spreading this area vertically to the mesopelagic (200–1,000 m) and bathypelagic (1,000–4,000 m) ocean would be immense. Aphotic N_2 fixation rates are usually low when compared to surface activity (<1 nmol N L^{-1} d^{-1}; see **Table 1** in Moisander et al., 2017) but the volume of the deep ocean is enormous. Consequently, studies comprising both photic and aphotic N_2 fixation measurements report depth-integrated aphotic rates representing 40–95% of the whole water column activity (Bonnet et al., 2013; Rahav et al., 2013; Benavides et al., 2015). Hence, aphotic fixation can account for a significant or even predominant fraction of water column N_2 fixation.

With the mere purpose of illustrating the potential budgetary relevance of the aphotic N_2 fixation to the global fixed nitrogen input, a back-of-the-envelope calculation can be carried out. If we consider a scenario for the mesopelagic zone (where the great majority of published aphotic N_2 fixation measurements were obtained from): taking the lower-end range of aphotic N_2 fixation rates available in the literature (0.01–0.1 nmol N L^{-1} d^{-1}; **Table 1** in Moisander et al., 2017), and the estimated volume of the mesopelagic zone (2.63×10^{17} m^3; Arístegui et al., 2005), mesopelagic N_2 fixation would range between 13 and 134 Tg N y^{-1}. Fixed nitrogen inputs to the ocean include fluvial inputs, atmospheric deposition and biological N_2 fixation, which add up to 187–279 Tg N y^{-1} (**Table 1**). Combining denitrification (including sediment burial) and anammox, fixed nitrogen losses add up to 260–475 Tg N y^{-1} (**Table 1**). Adding mesopelagic N_2 fixation to fixed nitrogen inputs and subtracting losses from gains, we obtain differences ranging from a loss of 183 to a surplus of 114 Tg N y^{-1} (**Table 1**). Despite this extrapolation may be questionable given that data on aphotic N_2 fixation are so sparse that the spatial distribution of mesopelagic N_2 fixation is

TABLE 1 | Global nitrogen budgets and their variability when considering aphotic N_2 fixation.

	Codispoti et al., 2001	Galloway et al., 2004	Gruber, 2008	Jickells et al., 2017
SOURCES				
Pelagic photic N_2 fixation	117	106	120	164
River inputs (DON+PON)	76	48	80	34
Atmospheric deposition	86	33	50	39
Mesopelagic N_2 fixation	13 to 134	13 to 134	13 to 134	13 to 134
Total sources without considering aphotic N_2 fixation	279	187	250	237
Total sources considering aphotic N_2 fixation*	292 to 413	200 to 321	263 to 384	250 to 371
SINKS				
Benthic denitrification	300	206	180	
Water column denitrification	150	116	65	
Sediment burial	25	16	25	
Total sinks	475	338	270	260
Balance without considering aphotic N_2 fixation	−196	−151	−20	−23
Balance considering aphotic N_2 fixation	−183 to −62	−138 to −17	−7 to 114	−10 to 111

*All fluxes are expressed in Tg N y^{-1}. *The range of aphotic N_2 fixation rates considered is 13.45–134.45 Tg N y^{-1}, see the main text.*

unknown, it does illustrate that aphotic N_2 fixation could be important to global nitrogen budget considerations, and thus deep N_2 fixation should be further explored. Considering the stock of fixed nitrogen in the mesopelagic zone (Gruber, 2008) and the range of mesopelagic N_2 fixation rates estimated here (i.e., 13–134 Tg N y^{-1}), N_2 fixed and eventually remineralized to nitrate in the mesopelagic zone would turn over in 4 to 43 y.

The currently available dataset (Table 1 from Moisander et al., 2017, this issue) lacks robustness because (i) the number of measurements is limited and geographically sparse, and (ii) methodological difficulties are entailed in the detection of low N_2 fixation rates. While aphotic N_2 fixation has been consistently reported in several tropical and temperate waters (**Table 1**; Moisander et al., 2017, this issue), it is unknown whether it occurs homogeneously throughout the dark water column or only in micro-niches where suitable conditions are found. Such hospitable niches may comprise aggregates, or organic matter accumulation zones like ecotones, fronts or water mass boundaries (Benavides et al., 2015; Bombar et al., 2016). Only a few studies have documented *nifH* gene expression in aphotic waters (e.g., Jayakumar et al., 2012), and it is debated whether reported abundances of non-cyanobacterial diazotrophs can account for measured rates of N_2 fixation when considering published cell specific rates of cultivated strains (Turk-Kubo et al., 2014; Bentzon-Tilia et al., 2015). This introduces uncertainty to the reliability of measuring especially low N_2 fixation rates (Gradoville et al., 2017), and emphasizes the need for continued refinement of the $^{15}N_2$ incorporation method (Moisander et al., 2017).

In this context, it is pertinent to consider the methodological difficulties encompassed in the detection of low N_2 fixation rates using $^{15}N_2$ as a tracer. The precision of N_2 fixation rates may be affected by (i) a slower than theoretically assumed dissolution of the $^{15}N_2$ bubble in seawater (Mohr et al., 2010; Großkopf et al., 2012), (ii) the contamination of $^{15}N_2$ gas stocks with nitrogenous species other than N_2 (Dabundo et al., 2014), and (iii) failure to measure time zero $\delta^{15}N$ values of the particulate nitrogen pool. As any other tracer method, $^{15}N_2$-based N_2 fixation rates are subject to a number of other sources of error, including variability in incubation and/or filtration time among replicates, sample particle size and its retention in filters varying with filter pore size (Bombar et al., 2018), as well as heterogeneous distribution of particles in Niskin bottles (Suter et al., 2017). Moreover, the vast majority of $^{15}N_2$-based published N_2 fixation measurements report net rates, whereas the leakage of ^{15}N-labeled dissolved organic nitrogen and/or ammonium can be significant in certain cases (e.g., Berthelot et al., 2017).

Most of the compiled aphotic rates (Moisander et al., 2017, this issue) were measured using the bubble method (Montoya et al., 1996), and should be considered as minimum estimates, despite the fact that they were performed in cold waters (typically ∼10°C), which enhances gas dissolution and hence optimizes isotopic equilibrium in seawater samples enriched with $^{15}N_2$ gas. Moreover, the majority of the studies i) used an isotope brand that provides high purity $^{15}N_2$ gas, affecting aphotic N_2 fixation rates by <1% when ^{15}N-labeled nitrogen molecules other than N_2 are taken up (Benavides et al., 2015) and/or ii) provided time zero $\delta^{15}N$ values of the particulate nitrogen pool at each sampling depth, making their results robust (Bonnet et al., 2013; Rahav et al., 2013; Benavides et al., 2015, 2016). Finally, the variability between replicates in all terms included in the N_2 fixation calculation equation (as outlined in Montoya et al., 1996) may throw back minimum quantifiable rates values below estimated aphotic N_2 fixation rates (Gradoville et al., 2017). Propagating errors of the data (Birge, 1940), in five out of the nine aphotic N_2 fixation studies currently available, results in minimum quantifiable rates ranging from 0.01 to 2.7 nmol N L^{-1} d^{-1} (**Table S1**), suggesting

that most of the aphotic N_2 fixation rates published are significant.

The potentially high budgetary significance of aphotic N_2 fixation to the global nitrogen budget calls for further studies that will establish the geographical and temporal distribution of aphotic N_2 fixation and consolidate the volumetric rates published thus far. In future studies, we encourage researchers in the field of marine nitrogen cycling to place emphasis on documenting N_2 fixation in the aphotic ocean and identifying environmental drivers of aphotic N_2 fixation: including oxygen, dissolved organic matter availability and particle colonization (Riemann et al., 2010; Benavides et al., 2015; Bombar et al., 2016). The availability of more data is essential to facilitate modeling and assessment of the distribution and magnitude of aphotic N_2 fixation in the global ocean (i.e., association with water masses, ecotones or density fronts). Eventually, a more comprehensive understanding of the ecophysiology of aphotic N_2 fixers and their contribution to global nitrogen input, will reveal their ecological importance and may help answer such question as what are the evolutionary advantages of the energetically-expensive process of N_2 fixation in an environment rich in dissolved inorganic nitrogen, and how does it affect oceanic carbon sequestration.

AUTHOR CONTRIBUTIONS

MB gathered N_2 fixation rates and made the calculations shown in the tables. MB, IB-F, SB, and LR wrote the article.

ACKNOWLEDGMENTS

MB and LR were supported by grant 6108-00013 from the Danish Council for independent research and by the BONUS BLUEPRINT project receiving funding from BONUS (Art 185) funded jointly from the European Union's Seventh Programme for research, technological development and demonstration and from The Danish Council for Strategic Research (LR).

SUPPLEMENTARY MATERIAL

The Supplementary Material for this article can be found online at: https://www.frontiersin.org/articles/10.3389/fmars.2018.00108/full#supplementary-material

Table S1 | Error propagation analysis of aphotic N2 fixation rates from various published and unpublished studies.

REFERENCES

Arístegui, J., Agustí, S., Middelburg, J. J., and Duarte, C. M. (2005). "Respiration in the mesopelagic and bathypelagic zones of the oceans," in *Respiration in Aquatic Ecosystems*, eds P. A. Del Giorgio and P. Williams (Oxford: Oxford University Press), 182–206.

Benavides, M. H., Moisander, P., Berthelot, H., Dittmar, T., Grosso, O., and Bonnet, S. (2015). Mesopelagic N_2 fixation related to organic matter composition in the Solomon and Bismarck Seas (Southwest Pacific). *PLoS ONE* 10:e0143775. doi: 10.1371/journal.pone.0143775

Benavides, M., Bonnet, S., Hernández, N., Martínez-Pérez, A. M., Nieto-Cid, M., Álvarez-Salgado, X. A., et al. (2016). Basin-wide N_2 fixation in the deep waters of the Mediterranean Sea. *Glob. Biogeochem. Cycles* 30, 952–961. doi: 10.1002/2015GB005326

Bentzon-Tilia, M., Traving, S. J., Mantikci, M., Knudsen-Leerbeck, H., Hansen, J. L. S., Markager, S., et al. (2015). Significant N_2 fixation by heterotrophs, photoheterotrophs and heterocystous cyanobacteria in two temperate estuaries. *ISME J.* 9, 273–285. doi: 10.1038/ismej.2014.119

Berthelot, H., Benavides, M., Moisander, P. H., Grosso, O., and Bonnet, S. (2017). High-nitrogen fixation rates in the particulate and dissolved pools in the Western Tropical Pacific (Solomon and Bismarck Seas). *Geophys. Res. Lett.* 44, 8414–8423. doi: 10.1002/2017GL073856

Birge, R. T. (1940). The propagation of errors. *Am. Phys. Teacher* 7, 351–357. doi: 10.1119/1.1991484

Bombar, D., Paerl, R. W., Anderson, R., and Riemann, L. (2018). Filtration via conventional glass fiber filters in $^{15}N_2$ tracer assays fails to capture all nitrogen-fixing Prokaryotes. *Front. Mar. Sci.* 5:6. doi: 10.3389/fmars.2018.00006

Bombar, D., Paerl, R. W., and Riemann, L. (2016). Marine non-cyanobacterial diazotrophs: moving beyond molecular detection. *Trends Microbiol.* 24, 916–927. doi: 10.1016/j.tim.2016.07.002

Bonnet, S., Dekaezemacker, J., Turk-Kubo, K. A., Moutin, T., Hamersley, R. M., Grosso, O., et al. (2013). Aphotic N_2 fixation in the eastern tropical South Pacific Ocean. *PLoS ONE* 8:e81265. doi: 10.1371/journal.pone.0081265

Codispoti, L. A. (2007). An oceanic fixed nitrogen sink exceeding 400 Tg N y^{-1} vs the concept of homeostasis in the fixed-nitrogen inventory. *Biogeosciences* 4, 233–253. doi: 10.5194/bg-4-233-2007

Codispoti, L. A., Brandes, J. A., Christensen, J. P., Devol, A. H., Naqvi, S. W. A., Paerl, H. W., et al. (2001). The oceanic fixed nitrogen and nitrous oxide budgets: moving targets as we enter the anthropocene? *Sci. Mar.* 65, 85–105. doi: 10.3989/scimar.2001.65s285

Dabundo, R., Lehmann, M. F., Treibergs, L., Tobias, C. R., Altabet, M. A., Moisander, P. H., et al. (2014). The contamination of commercial $^{15}N_2$ gas stocks with ^{15}N-labeled nitrate and ammonium and consequences for nitrogen fixation measurements. *PLoS ONE* 9:e110335. doi: 10.1371/journal.pone.0110335

Eugster, O., and Gruber, N. (2012). A probabilistic estimate of global marine N-fixation and denitrification. *Global Biogeochem. Cycles* 26:4013. doi: 10.1029/2012GB004300

Falkowski, P. G. (1997). Evolution of the nitrogen cycle and its influence on the biological sequestration of CO_2 in the ocean. *Nature* 387, 272–275. doi: 10.1038/387272a0

Farnelid, H., Andersson, A. F., Bertilsson, S., Al-Soud, W. A., Hansen, L. H., Sørensen, S., et al. (2011). Nitrogenase gene amplicons from global marine surface waters are dominated by genes of non-cyanobacteria. *PLoS ONE* 6:e19223. doi: 10.1371/journal.pone.0019223

Galloway, J. N., Dentener, F. J., Capone, D. G., Boyer, E. W., Howarth, R. W., Seitzinger, S. P., et al. (2004). Nitrogen cycles: past, present, and future. *Biogeochemistry* 70, 153–226. doi: 10.1007/s10533-004-0370-0

Gradoville, M. R., Bombar, D., Crump, B. C., Letelier, R. M., Zehr, J. P., and White, A. E. (2017). Diversity and activity of nitrogen-fixing communities across ocean basins. *Limnol Oceanogr.* 62, 1895–1909. doi: 10.1002/lno.10542

Großkopf, T., Mohr, W., Baustian, T., Schunck, H., Gill, D., Kuypers, M. M. M., et al. (2012). Doubling of marine dinitrogen-fixation rates based on direct measurements. *Nature* 488, 361–364. doi: 10.1038/nature11338

Gruber, N. (2004). The dynamics of the marine nitrogen cycle and its influence on atmospheric CO_2 variations. *Ocean Carbon Cycle Clim.* 40, 97–148. doi: 10.1007/978-1-4020-2087-2_4

Gruber, N. (2008). "The Marine Nitrogen Cycle: overview and challenges," in *Nitrogen in the Marine Environment*, eds D. G. Capone, D. A. Bronk, M. R. Mulholland, and E. J. Carpenter (Academic Press), 1–50.

Gruber, N., and Galloway, J. N. (2008). An Earth-system perspective of the global nitrogen cycle. *Nature* 451, 293–296. doi: 10.1038/nature06592

Hamersley, M. R., Turk, K. A., Leinweber, A., Gruber, N., Zehr, J. P., Gunderson, T., et al. (2011). Nitrogen fixation within the water column associated with

two hypoxic basins in the Southern California Bight. *Aquat. Microb. Ecol.* 63, 193–205. doi: 10.3354/ame01494

Hewson, I., Moisander, P. H., Achilles, K. M., Carlson, C. A., Jenkins, B. D., Mondragon, E. A., et al. (2007). Characteristics of diazotrophs in surface to abyssopelagic waters of the Sargasso Sea. *Aquat. Microb. Ecol.* 46, 15–30. doi: 10.3354/ame046015

Jayakumar, A., Al-Rshaidat, M. M. D., Ward, B. B., and Mulholland, M. R. (2012). Diversity, distribution, and expression of diazotroph *nifH* genes in oxygen-deficient waters of the Arabian Sea. *FEMS Microbiol. Ecol.* 82, 597–606. doi: 10.1111/j.1574-6941.2012.01430.x

Jickells, T. D., Buitenhuis, E., Altieri, K., Baker, A. R., Capone, D., Duce, R. A., et al. (2017). A reevaluation of the magnitude and impacts of anthropogenic atmospheric nitrogen inputs on the ocean. *Glob. Biogeochem. Cycles* 31, 289–305. doi: 10.1002/2016GB005586

Moisander, P. H., Benavides, M., Bonnet, S., Berman-Frank, I., White, A. E., and Riemann, L. (2017). Chasing after non-cyanobacterial nitrogen fixation in marine pelagic environments. *Front. Microbiol.* 8:1736. doi: 10.3389/fmicb.2017.01736

Mohr, W., Großkopf, T., Wallace, D. W. R., and LaRoche, J. (2010). Methodological underestimation of oceanic nitrogen fixation rates. *PLoS ONE* 5:e12583. doi: 10.1371/journal.pone.0012583.t001

Montoya, J. P., Voss, M., Kahler, P., and Capone, D. G. (1996). A simple, high-precision, high-sensitivity tracer assay for N_2 fixation. *Appl. Environ. Microbiol.* 62, 986–993.

Rahav, E., Bar-Zeev, E., Ohayon, S., Elifantz, H., Belkin, N., Herut, B., et al. (2013). Dinitrogen fixation in aphotic oxygenated marine environments. *Front. Microbiol.* 4:227. doi: 10.3389/fmicb.2013.00227

Riemann, L., Farnelid, H., and Steward, G. F. (2010). Nitrogenase genes in non-cyanobacterial plankton: prevalence, diversity and regulation in marine waters. *Aquat. Microb. Ecol.* 61, 235–247. doi: 10.3354/ame01431

Sohm, J. A., Hilton, J. A., Noble, A. E., Zehr, J. P., Saito, M. A., and Webb, E. A. (2011). Nitrogen fixation in the South Atlantic Gyre and the Benguela Upwelling System. *Geophys. Res. Lett.* 38, 1–6. doi: 10.1029/2011GL048315

Suter, E. A., Scranton, M. I., Chow, S., Stinton, D., Medina Faull, L., and Taylor, G. T. (2017), Niskin bottle sample collection aliases microbial community composition and biogeochemical interpretation. *Limnol. Oceanogr.* 62, 606–617. doi: 10.1002/lno.10447

Turk-Kubo, K. A., Karamchandani, M., Capone, D. G., and Zehr, J. P. (2014). The paradox of marine heterotrophic nitrogen fixation: abundances of heterotrophic diazotrophs do not account for nitrogen fixation rates in the Eastern Tropical South Pacific. *Environ. Microbiol.* 16, 3095–3114. doi: 10.1111/1462-2920.12346

Zehr, J. P. (2011). Nitrogen fixation by marine cyanobacteria. *Trends Microbiol.* 19, 162–173. doi: 10.1016/j.tim.2010.12.004

Zehr, J. P., Carpenter, E., and Villareal, T. A. (2000). New perspectives on nitrogen-fixing microrganisms in tropical and subtropical oceans. *Trends Microbiol.* 8, 68–73. doi: 10.1016/S0966-842X(99)01670-4

Zehr, J. P., Mellon, M. T., and Zani, S. (1998). New nitrogen-fixing microorganisms detected in oligotrophic oceans by amplification of nitrogenase (*nifH*) genes. *Appl. Environ. Microbiol.* 64, 3444–3450.

Conflict of Interest Statement: The authors declare that the research was conducted in the absence of any commercial or financial relationships that could be construed as a potential conflict of interest.

frontiers in Microbiology

MINI REVIEW
published: 19 September 2018
doi: 10.3389/fmicb.2018.02112

Global Marine N_2 Fixation Estimates: From Observations to Models

Angela Landolfi, Paul Kähler, Wolfgang Koeve and Andreas Oschlies*

GEOMAR Helmholtz Centre for Ocean Research Kiel, Kiel, Germany

Fixed nitrogen (N) limits productivity across much of the low-latitude ocean. The magnitude of its inventory results from the balance of N input and N loss, the latter largely occurring in regionally well-defined low-oxygen waters and sediments (denitrification and anammox). The rate and distribution of N input by biotic N_2 fixation, the dominant N source, is not well known. Here we compile N_2 fixation estimates from experimental measurements, tracer-based geochemical and modeling approaches, and discuss their limitations and uncertainties. The lack of adequate experimental data coverage and the insufficient understanding of the controls of marine N_2 fixation result in high uncertainties, which make the assessment of the current N-balance a challenge. We suggest that a more comprehensive understanding of the environmental and ecological interaction of marine N_2 fixers is required to advance the field toward robust N_2 fixation rates estimates and predictions.

Keywords: marine N_2 fixation, N-cycle balance, denitrification, marine productivity, marine heterotrophic diazotrophy, nitrogen isotopes

OPEN ACCESS

Edited by:
Lasse Riemann,
University of Copenhagen, Denmark

Reviewed by:
Carolin Regina Löscher,
University of Southern Denmark, Denmark
Bess B. Ward,
Princeton University, United States

****Correspondence:***
Angela Landolfi
alandolfi@geomar.de

Specialty section:
This article was submitted to Aquatic Microbiology, a section of the journal Frontiers in Microbiology

Received: *17 May 2018*
Accepted: *20 August 2018*
Published: *19 September 2018*

Citation:
Landolfi A, Kähler P, Koeve W and Oschlies A (2018) Global Marine N_2 Fixation Estimates: From Observations to Models. Front. Microbiol. 9:2112. doi: 10.3389/fmicb.2018.02112

INTRODUCTION

Marine N_2 fixation, the largest source of fixed N to the ocean, maintains ocean fertility by compensating for N-losses via denitrification. Global warming, likely inducing ocean deoxygenation (Keeling et al., 2010), and increasing N load from the atmosphere and/or rivers, are perturbing the N cycle leading to increasing N loss via denitrification on the one hand (Codispoti et al., 2001; Codispoti, 2007) and to alterations of the niche of marine N_2 fixers on the other (Landolfi et al., 2017), with an unknown net effect on the N inventory. A prolonged mismatch between N inputs and losses would cause changes to the oceanic fixed N inventory, potentially affecting ocean productivity and ocean carbon (C) storage. Narrowing down the uncertainties in current N_2 fixation estimates is key to diagnosing any imbalance in the marine N budget and its effect on the marine C budget.

N_2 fixation can be inferred experimentally from incubation assays (Capone, 1993; Montoya et al., 1996), and from its geochemical imprint on nutrient (Gruber and Sarmiento, 1997) and stable N isotope distributions (Altabet, 2007). Geochemical estimates use the integrated N_2 fixation signature over large scales of space and time, smoothing any small-scale variability inherent in experimental N_2 fixation measurements. Traditionally, geochemical (Gruber, 2004) and experimental (Capone et al., 2005) estimates suggested highest N_2 fixation rates in the Tropical North Atlantic, remote from the region of largest pelagic N-loss in the Eastern Tropical Pacific. Although such spatial separation was difficult to reconcile with paleo-oceanographic evidence of a closely balanced N-cycle, considered to require tight stabilizing feedbacks between N-loss and N_2 fixation (Altabet, 2007), it was in line with the well-documented high energy and iron requirements of diazotrophs (Kustka et al., 2003) that would restrict them to warm and

iron-rich waters. This view has been challenged by a model-based geochemical N_2 fixation estimate suggesting prevailing control by N deficits and close spatial coupling of N_2 fixation and N loss (Deutsch et al., 2007), and by new evidence from molecular techniques demonstrating a wider diversity of N_2 fixers and N_2 fixation strategies. This includes free-living unicellular cyanobacteria (Zehr et al., 1998; Montoya et al., 2004), cyanobacterial symbionts and heterotrophic phylotypes (see Foster et al., 2011; Bombar et al., 2016; Caputo et al., 2018), covering novel habitats such as aphotic waters (Bonnet et al., 2013; Benavides et al., 2015, 2016, 2018) and oxygen deficient zones (ODZs) (Fernandez et al., 2011; Jayakumar et al., 2012; Bonnet et al., 2013; Löscher et al., 2014, 2016; Turk-Kubo et al., 2014; Knapp et al., 2016). Recently, severe problems in applying the N_2 fixation assays came to light (Mohr et al., 2010). Considering this new evidence, using a constant correction factor of historical data, a doubling of N_2 fixation has been suggested (177 ± 8 Tg N y^{-1}, Großkopf et al., 2012). Despite the pace of new discoveries, global N_2 fixation estimates remain highly uncertain (Gruber, 2016). The incomplete knowledge of the organisms involved and their physiological and ecological controls prevent any robust prediction of their distribution and activity. Here we present a brief overview of recent work covering experimental, geochemical, and model-based N_2 fixation estimates and discuss knowledge gaps. We suggest future research strategies to reduce the current uncertainty.

EXPERIMENTAL ESTIMATES

The compilation of surface marine N_2 fixation rate measurements (MARine Ecosystem DATa) by Luo et al. (2012), with more recent data from the North Pacific (Shiozaki et al., 2015a,b, 2017), western Pacific (Bonnet et al., 2009, 2015, 2017, 2018; Shiozaki et al., 2013, 2014b; Berthelot et al., 2017), eastern tropical South Pacific (Löscher et al., 2014, 2016; Knapp et al., 2016), Indian Ocean (Shiozaki et al., 2014a), and the tropical Atlantic (Großkopf et al., 2012; Singh et al., 2017), is presented in **Figure 1**. The measurements reported are mostly from bulk unfiltered upper ocean samples, including cyanobacteria and potentially other diazotrophs. Although highly variable, the highest depth-integrated N_2 fixation rates are found in the western tropical South Pacific (638 ± 1689 μmol N m^{-2} d^{-1}, 201 profiles). These are larger than the traditionally high rates in the subtropical North Atlantic (182 ± 479 μmol N m^{-2} d^{-1}, 636 profiles) and North Pacific (118 ± 101 μmol N m^{-2} d^{-1}, 272 profiles). In the phosphate-rich waters of the eastern South Pacific average N_2 fixation is 86 ± 99 μmol N m^{-2} d^{-1} (213 profiles). Low rates are found in the southern Indian Ocean (<20 μmol N m^{-2} d^{-1}, Shiozaki et al., 2014a), and in cold Bering Sea waters (10 μmol N m^{-2} d^{-1}, Shiozaki et al., 2017). Based on the MAREDAT database, Luo et al. (2012) estimated a global N_2 fixation rate of 137 ± 9.2 Tg N y^{-1} (**Table 1**). Global extrapolations are difficult as observations remain sparse and highly variable in space and time (**Figure 1**). Only few ocean regions have sufficient data coverage to assess spatial, seasonal, or inter-annual variability (SD, **Figure 1B**). The large standard deviation in the western tropical South Pacific suggests a large spatio-temporal variability. The North Atlantic variability appears related to the strong spatial and temporal gradients of physical forcing and associated environmental factors (e.g., Mouriño-Carballido et al., 2011; Landolfi et al., 2016). The variability in the North Pacific is mostly associated with seasonal changes (Böttjer et al., 2016) and variable mesoscale activity (e.g., Church et al., 2009).

Experimental measurements have technical drawbacks. The acetylene reduction assay (Capone, 1993), a proxy measurement of both incorporated and exuded (gross) fixed N_2, measures the rate of ethylene production from added acetylene. Microbial activity repression (Fulweiler et al., 2015), low sensitivity and highly variable conversion factors for C_2H_4:N_2 (Wilson et al., 2012), limit the robustness of this technique. The more widely (∼75% of the measurements) applied method involves adding $^{15}N_2$ gas to a water sample and measuring the net incorporation of $^{15}N_2$ into plankton biomass after filtration (Montoya et al., 1996). This method may result in significant underestimation of N_2 fixation rates if the added $^{15}N_2$ gas is not equilibrated before the start of the incubation (Mohr et al., 2010; Wilson et al., 2012; Wannicke et al., 2018). The degree of underestimation is variable and dependent on the experimental conditions (incubation time, size of bottle, shaking vigor), making the correction of historical data with a constant factor arbitrary. The $^{15}N_2$ gas stock contamination by $^{15}NH_4^+$ or $^{15}NO_x$, may result in N_2 fixation overestimate (Dabundo et al., 2014). Fixation rates may be underestimated if small cells (<2 μm) are lost during filtration, particularly affecting rates where small diazotrophs may dominate the N_2-fixing community (Bombar et al., 2018). Robust quantification of low rates is currently limited by the low sensitivity and high potential errors of present methods (Gradoville et al., 2017; Moisander et al., 2017). Inadequate consideration of experimental biases must be warned against. Community efforts are being made toward a consensus on methods and protocols refinement[1] for yielding more accurate and comparable fixation rates.

GEOCHEMICAL ESTIMATES

Geochemical estimates of N_2 fixation have been inferred from excess NO_3 with respect to the Redfield-equivalent PO_4 (the N* method), constructed from the high-quality global nutrient surveys (e.g., JGOFS/WOCE; Conkright et al., 2002), combined with information on ocean ventilation ages derived from measurements of abiotic transient tracers such as chlorofluorocarbons (CFCs). This method rests on the assumption that nutrients' departure from the global average ratio of NO_3:PO_4 = 16:1 (RR, the Redfield ratio) is due to N_2 fixation adding (N:P > RR), and denitrification removing (N:P < RR), nitrogen. This approach has been used to compute North Atlantic N_2 fixation rates (Michaels et al., 1996; Gruber and Sarmiento, 1997; Hansell et al., 2004, 2007; Kähler et al., 2010), and derive a global estimate of

[1] https://www.us-ocb.org/n-fixation-working-group/

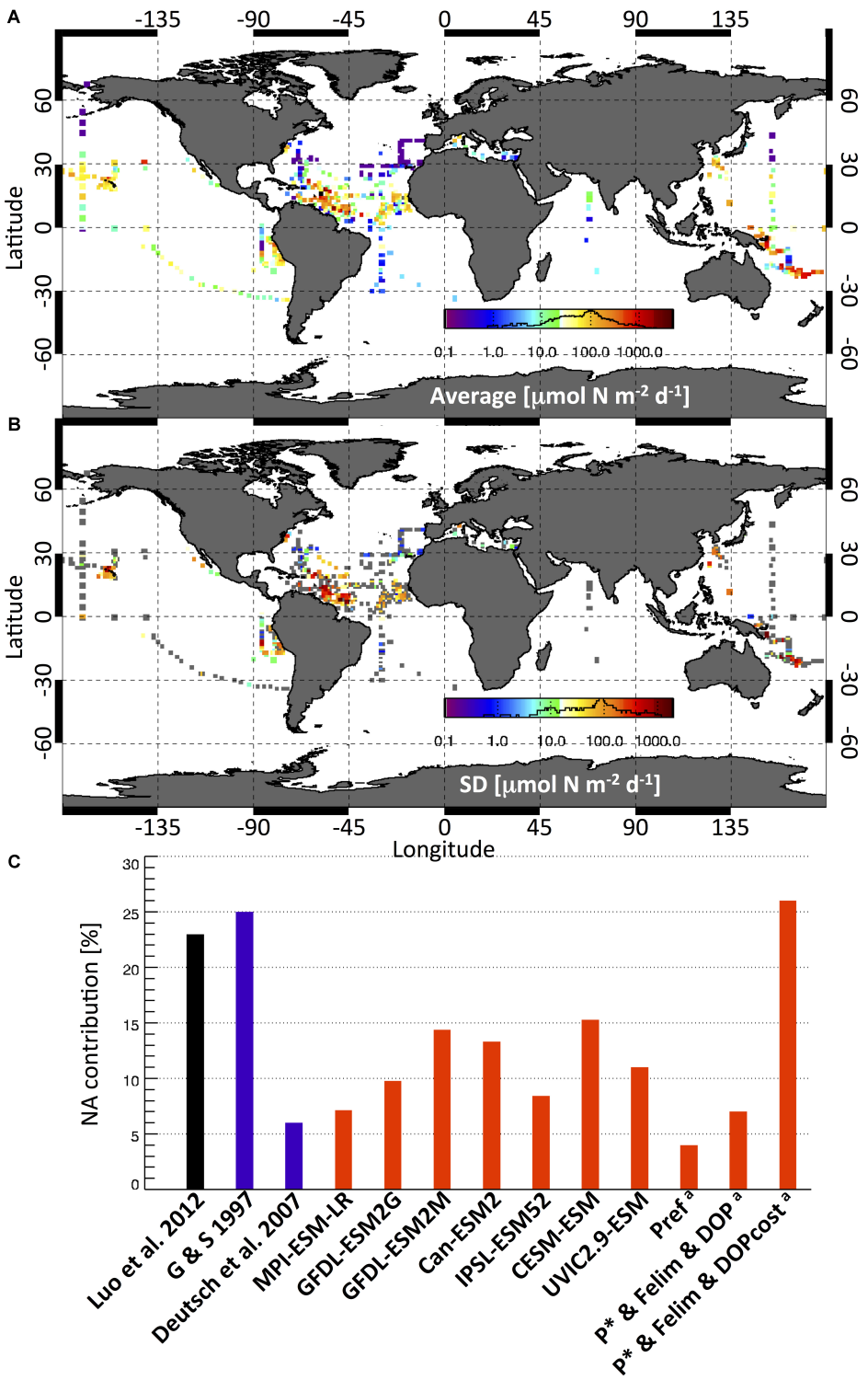

FIGURE 1 | 1 × 1 degree grid **(A)** average and **(B)** standard deviation (SD) of depth integrated N_2 fixation rate (μmol N m^{-2} d^{-1}) experimental measurements from the MAREDAT database (Luo et al., 2012) and 800 additional data points (see text for details). Gray squares in SD plot indicate one-only data point. Data distribution histogram is shown in the color bar. **(C)** Experimental (black)-, geochemical (blue)-, and model (red) -based estimated contribution (%) of the North Atlantic to global N_2 fixation rates. Models include those of the Coupled Model Intercomparison Project (CMIP5, see **Table 1**), a model with additional energetic costs of DOP uptake (UVIC2.9-ESM, Landolfi et al., 2017) and [a]model experiments of Landolfi et al. (2015) accounting for preferential phosphorus remineralization (PREF), P* and iron limitation and DOP uptake without (P* and Fe and DOP), and with additional energetic and also N costs (P* and Fe and DOPcost).

TABLE 1 | Experimental, geochemical, and ESM-based (1996–2005 average) regional and global annual N_2 fixation estimates (Tg N y^{-1}).

Source	Pacific Tg N y^{-1}	Indian Tg N y^{-1}	Atlantic Tg N y^{-1}	Global Tg N y^{-1}
Luo et al., 2012	102 ± 20	–	34 ± 7	137 ± 9
Gruber and Sarmiento, l997			28	110 ± 40
Deutsch et al., 2007[1]	95	22	20	137
CMIP5-MPI-ESM-LR[a]	132	32	38	213
CMIP5-GFDL-ESM2G[b]	106	28	36	181
CMIP5-GFDL-ESM2M[b]	75	30	40	154
CMIP5-CanESM2[c]	72	28	28	130
CMIP5-IPSL-CM52-LR[2,d]	54	14	16	89
CMIP5-CESM[e]	72	48	46	173
ESM-UVIC2.9[f]	73	31	24	128

[1]Estimate from the Standard model that includes DOP, which is 5% higher than P*-only estimate. Coupled Model Intercomparison Project (CMIP5) model output has been retrieved from https://esgf-node.llnl.gov/projects/cmip5/. [2]Estimated from model C:N = 122:16. References a–f below list the model descriptions of the respective biogeochemical modules. [a]Ilyina et al., 2013; [b]Dunne et al., 2013; [c]Zahariev et al., 2008; [d]Aumont et al., 2015; [e]Moore et al., 2013; and [f]Landolfi et al., 2017.*

110 ± 40 Tg N y^{-1} (Gruber and Sarmiento, 1997; **Table 1**). While this method has the advantage of integrating over large scales of space and time and implicitly includes potential contributions of non-cyanobacterial N_2 fixation, several potential shortcomings have been discussed: Impacts of non-Redfield remineralization of organic matter were addressed in Landolfi et al. (2008), where we extended the inorganic N* concept to total nitrogen excess, TN_{xs}, to include organic nutrients. We found that for the subtropical North Atlantic, N_2 fixation rates estimated via TN_{xs} were approximately twice as high as those estimated by the N* method, but cautioned that other processes such as atmospheric N deposition (Zamora et al., 2010) and non-Redfield uptake of nutrients by phytoplankton (Mills and Arrigo, 2010; Weber and Deutsch, 2012), can also affect regional patterns of oceanic N* and TN_{xs} and thereby influence N_2 fixation rate estimates. These caveats also apply to the P_t* method introduced by Deutsch et al. (2007) that estimates N_2 fixation from the consumption of P_t*, which is defined as total excess P relative to the Redfield N equivalent. In contrast to the classical N* tracer, but similar to TN_{xs}, P_t* also accounts for organic nutrients. Deutsch et al. (2007) estimated a global N_2 fixation rate of 137 Tg N y^{-1} (i.e., about 25% higher than the N*-based estimate), with a very large contribution from surface waters in close proximity to the largest ODZ in the eastern South Pacific and only a small contribution from the P_t*-poor North Atlantic (**Table 1**). The P_t*-based estimate contrasts with the prevailing view of elevated N_2 fixation rates in the North Atlantic, as indicated both from N* and experimental evidence (**Figure 1**). Besides the above mentioned non-Redfield processes other than N_2 fixation errors in the rate estimates also arise from the assumed ocean circulation that generally is not fully consistent with the observed nutrient fields to which it is applied. While current-generation global circulation models represent global-scale patterns reasonably well, they have particular deficiencies in reproducing low-oxygen regions (Cabré et al., 2015) and tracer distributions in the tropical regions (Dietze and Löptien, 2013). The refinement of global ocean GCMs is an on-going process. However, improvements to the geochemical methods may be limited given that the available nutrient distributions represent composites of data from decad of observations from a turbulent ocean, for which no underlying "mean" circulation may exist. Errors may also stem from uncertainties in tracer-derived water ages and age-based rate estimates: The differential effects of mixing on water age versus nutrient tracers may lead to errors in tracer-based N_2 fixation estimates (Koeve and Kähler, 2016).

MODEL-BASED ESTIMATES

Global N_2 fixation estimates have been derived from models using both implicit (diagnostic) and explicit (prognostic) N_2 fixation parameterizations. Implicit N_2 fixation parameterizations used in some IPCC-type earth-system-models (ESM) are based on restoring-type approaches that simulate N_2 fixation by restoring upper-ocean nutrient ratios toward Redfield NO_3:PO_4 stoichiometry (MPI-ESM, Ilyina et al., 2013). This implies that N_2 fixation is mainly restricted to areas with observed low NO_3:PO_4 ratios. Other models restrict N_2 fixation to N limited areas, but account also for light and temperature dependence (Can ESM, Zahariev et al., 2008) and phosphate and iron limitation (IPSL-PISCES, Aumont et al., 2015). These methods implicitly assume a constant standing stock of diazotrophs and thereby require fewer assumptions on not well-known ecophysiological processes and parameters compared to models that explicitly model the dynamics of diazotrophs. Explicit parameterizations of N_2 fixation are mostly based on the assumption that diazotrophs are slow-growing photosynthetic organisms that can fix N_2. This simple mechanistic approach results in diazotrophs being outcompeted by the faster growing ordinary phytoplankton in N-replete regions, yielding a control by excess PO_4, or P*, in early on simple box-models (Tyrrell, 1999). Controls by other environmental factors such as temperature, light, iron (CESM, Moore et al., 2013) and also specific trade-offs (e.g., DOP-uptake, Landolfi et al., 2015) or nitrate and oxygen inhibition (GFDL-TOPAZ, Dunne et al., 2013) have been implemented in more complex functional-types ecosystem-ocean circulation models, modulating the rates and regional patterns of fixation. Some studies also parameterize different groups of diazotrophs, in particular Trichodesmium-type, unicellular cyanobacteria, and diatom-cyanobacterial associations (Monteiro et al., 2010). There is a significant spread in global and regional N_2 fixation estimates by ESMs (**Table 1**). This arises from differences in model parameterizations and parameter values, and the different underlying circulation fields. In restoring approaches, N_2 fixation is strongly associated with regions of NO_3 deficits, or high P*, from denitrification in low-oxygen waters (Ilyina et al., 2013). This tight coupling is relaxed in parameterizations with temperature-dependent and Fe-limited growth rates, and also with NO_3 uptake by diazotrophs (Moore et al., 2013; Landolfi et al., 2017) or NO_3 inhibition of N_2 fixation (Zahariev et al., 2008; Dunne et al., 2013; Aumont et al., 2015), which all tend to

reduce the simulated rates of N_2 fixation in NO_3-replete regions (e.g., Eastern Tropical South Pacific upwelling) and enhance them toward warm, dusty and P-rich waters in line with the traditional paradigm (Redfield et al., 1963; Falkowski, 1997). Most models do not reproduce the observed high fixation rates in the oligotrophic, dusty, North Atlantic due to the modeled low supply of P* in this region. This implies that unaccounted factors may also be important in controlling marine diazotrophs and require to go beyond the traditional paradigm. In a recent model study, we found that preferential phosphorus remineralization, dissolved organic phosphors uptake (DOP), or Fe-limited growth, were all not able to significantly enhance P* supply and expand the diazotrophs' niche in this region. Only accounting for the elevated N-cost of dissolved organic P scavenging allowed the success of diazotrophs in the N-rich P-poor North Atlantic (Landolfi et al., 2015; **Figure 1C**). This theory, however, awaits experimental testing. Current global models do not account for non-cyanobacterial N_2 fixation, which requires a more in-depth understanding of the relevant players, their ecophysiology and their environmental controls.

IMPLICATIONS FOR THE N BUDGET

As N_2 fixation and denitrification may be uncoupled, the oceanic N inventory is susceptible to imbalances. Despite the relatively short residence time of oceanic N of less than 3000 years (e.g., Somes et al., 2013), the geological isotopic record suggests a close-to-balanced budget over the past 3000 years (Altabet, 2007). This indicates the existence of negative feedbacks that stabilize the marine N reservoir. The nature, intensities and timescales of these feedbacks are still debated. Their effect on time scales shorter than those associated with the global ocean overturning circulation is assumed to require a spatial proximity of regions of N_2 fixation and N removal, such that any N deficit generated by denitrification in ODZs is rapidly compensated for by N_2 fixation (Deutsch et al., 2007). However, because denitrification consumes more N than is fixed per mole of organic P, a too tight spatial coupling would lead to net N removal (Landolfi et al., 2013). Thus any N deficit may need to be transported and compensated for far away from ODZ-influenced regions, suggesting that longer (ocean-circulation) timescales may be required to counteract any N imbalance (Landolfi et al., 2013; Somes et al., 2016).

Some studies suggested that N loss by denitrification may exceed, by more than 100 Tg N y^{-1}, the inputs of N from N_2 fixation, atmospheric and riverine supply, as a result of anthropogenic perturbations (Codispoti et al., 2001; Codispoti, 2007). While the recent revised estimates of N_2 fixation (**Table 1**), atmospheric and river N supply (39 and 34 Tg N y^{-1}, respectively, Jickellset al., 2017), and denitrification (120–240 Tg N y^{-1}, DeVries et al., 2013) may suggest a reduced imbalance to less than 100 Tg N y^{-1}, the annual rate and distribution at which N enters the ocean is still highly uncertain, making current and future N inventory projections speculative. The persistence of a 50–100 Tg N y^{-1} imbalance for 100 years would cause the N inventory to decline by 0.75–1.5% (N inventory of 6.6 10^5 Tg N, Gruber and Galloway, 2008) possibly weakening the biological carbon pump.

Quantification of non-cyanobacterial N_2 fixation is currently hampered by the lack of reliable data (Moisander et al., 2017; Benavides et al., 2018) and knowledge of their metabolisms and environmental controls (Riemann et al., 2010; Bombar et al., 2016). However, biogeochemical observations can provide strong constraints on the potential magnitude of this process, which should leave its imprint on the spatial and vertical cumulative distributions of nutrients and the $\delta^{15}NO_3$ signature in the ocean. Although thermodynamically favorable ($\Delta G < 0$), the reduction of N_2 to NH_3 requires a large input of energy, from light or organic matter degradation, to proceed at measurable rates (Postgate, 1982) and maintain a low-oxygen cellular environment for the functioning of the enzyme complex nitrogenase. In ODZs the energy requirements may be reduced and iron limitation, a further constraint in oxic surface waters, may be relaxed. Here fixing N_2 might be energetically advantageous compared with NO_3-uptake (Großkopf and LaRoche, 2012). However, the low energetic efficiency of the anaerobic metabolism may quantitatively constrain the rates of non-cyanobacterial N_2 fixation, which may result in invisible ("cryptic") nutrient and isotopic tracer-distributions patterns as denitrification and anammox may override its signature. Further investigations should asses the contribution of this process.

Our current understanding of stabilizing N-inventory feedbacks stands on the regulatory-competition between N_2 fixers and non-fixing phytoplankton (Redfield, 1963; Gruber, 2004). N_2 fixers fertilize the ocean with N until fixed N levels are, relative to P, high enough for their competitive exclusion. The potential for N inputs via non-cyanobacterial N_2 fixation independent of N deficits would fail this regulatory mechanism. Overall, the detailed mechanisms by which N_2 fixation responds to N losses are not well understood to have high confidence of marine nutrient cycles future predictions. In this context, the extent to which the North Atlantic stands out as a region of high N_2 fixation may be a pivotal question. Answering it will help to better understand how tight the feedback is between N_2 fixation and N loss processes.

SYNTHESIS AND OUTLOOK

All approaches to constrain global rates of N_2 fixation (experimental, geochemical, and model-based estimates) have their own uncertainties and biases. Albeit the recent progress we still lack a comprehensive knowledge of the relevant environmental and ecological interactions, which prevent us from making robust N_2 fixation rates estimates and predictions. To reduce the current level of uncertainty an improved understanding of the players, their ecological interactions, and the factors that control N_2 fixation in the ocean must be drawn from a collective research effort. This requires to take novel approaches that go beyond assuming simple correlations/sensitivities, but rather consider a combination of environmental factors and emerging ecological interactions, both in the field and in the laboratory. To this end, identifying essential

traits and ecological interactions experimentally, and develop mechanistic based models, may help us decipher the complexity of marine N_2 fixation and allow robust fixation estimates. As of now, the large uncertainties in existing N_2 fixation estimates and in the underlying feedbacks with N loss processes rule out reliable predictions. This task needs a fresh turn.

AUTHOR CONTRIBUTIONS

AL designed and wrote the paper. All authors contributed to the writing of the paper.

FUNDING

This work was supported by the Deutsche Forschungsgemeinschaft (DFG) project SFB754.

ACKNOWLEDGMENTS

We would like to thank S. Bonnet, C. Löscher, T. Shiozaki, and A. Singh for providing their N_2 fixation measurements. We acknowledge the Coupled Model Intercomparison Project (CMIP) for providing accessible model output (http://pcmdi9.llnl.gov). We acknowledge the World Climate Research Program's Working Group on Coupled Modeling, which is responsible for CMIP, and we thank the climate modeling groups (listed in **Table 1**) for producing and making available their model output. For CMIP the United States Department of Energy's Program for Climate Model Diagnosis and Intercomparison provides coordinating support and led development of software infrastructure in partnership with the Global Organization for Earth System Science Portals. Many thanks to G. Volpe for his helpful input. Data to reproduce **Figure 1** is available on https://data.geomar.de.

REFERENCES

Altabet, M. A. (2007). Constraints on oceanic N balance/imbalance from sedimentary 15N records. *Biogeoscience* 4, 75–86. doi: 10.5194/bg-4-75-2007

Aumont, O., Ethé, C., Tagliabue, A., Bopp, L., and Gehlen, M. (2015). PISCES-v2: An ocean biogeochemical model for carbon and ecosystem studies. *Geosci. Model Dev.* 8, 2465–2513. doi: 10.5194/gmd-8-2465-2015

Benavides, M., Bonnet, S., Berman-Frank, I., and Riemann, L. (2018). Deep into oceanic N_2 fixation. *Front. Mar. Sci.* 5:108. doi: 10.3389/fmars.2018.00108

Benavides, M., Bonnet, S., Hernández, N., Martínez-Pérez, A. M., Nieto-Cid, M., Álvarez-Salgado, X. A., et al. (2016). Basin-wide N_2 fixation in the deep waters of the Mediterranean Sea. *Glob. Biogeochem. Cycles* 30, 1–19. doi: 10.1002/2015GB005326

Benavides, M. H., Moisander, P., Berthelot, H., Dittmar, T., Grosso, O., and Bonnet, S. (2015). Mesopelagic N_2 fixation related to organic matter composition in the Solomon and Bismarck Seas (Southwest pacific). *PLoS One* 10:e0143775. doi: 10.1371/journal.pone.0143775

Berthelot, H., Benavides, M., Moisander, P. H., Grosso, O., and Bonnet S. (2017). High-nitrogen fixation rates in the particulate and dissolved pools in the Western Tropical Pacific (Solomon and Bismarck Seas). *Geophys. Res. Lett.* 44, 8414–8423. doi: 10.1002/2017GL073856

Bombar, D., Paerl, R. W., Anderson, R., and Riemann, L. (2018). Filtration via conventional glass fiber filters in $^{15}N_2$ tracer assays fails to capture all nitrogen-fixing prokaryotes. *Front. Mar. Sci.* 5:6. doi: 10.3389/fmars.2018.00006

Bombar, D., Paerl, R. W., and Riemann, L. (2016). Marine non-cyanobacterial diazotrophs: moving beyond molecular detection. *Trends Microbiol.* 24, 916–927. doi: 10.1016/j.tim.2016.07.002

Bonnet, S., and Biegala, I. C., Dutrieux, P., Slemons, L. O., and. Capone, D. G. (2009), Nitrogen fixation in the western equatorial Pacific: rates, diazotrophic cyanobacterial size class distribution, and biogeochemical significance. *Global Biogeochem. Cycles* 23:GB3012. doi: 10.1029/2008GB003439

Bonnet, S., Caffin, M., Berthelot, H., and Moutin, T. (2017). Hot spot of N_2 fixation in the western tropical South Pacific pleads for a spatial decoupling between N_2 fixation and denitrification. *Proc. Natl. Acad. Sci. U.S.A.* 114, E2800–E2801. doi: 10.1073/pnas.1619514114

Bonnet, S., Dekaezemacker, J., Turk-Kubo, K. A., Moutin, T., Hamersley, R. M., Grosso, O., et al. (2013). Aphotic N_2 fixation in the eastern tropical South Pacific Ocean. *PLoS One* 8:e81265. doi: 10.1371/journal.pone.0081265

Bonnet, S., Rodier, M., Turk-Kubo, K. A., Germineaud, C., Menkes, C., Ganachaud, A., et al. (2015). Contrasted geographical distribution of N_2 fixation rates and nifH phylotypes in the Coral and Solomon Seas (southwestern Pacific) during austral winter conditions. *Global Biogeochem. Cycles* 29, 1874–1892. doi: 10.1002/2015GB005117

Bonnet, S., Caffin, M., Berthelot, H., Grosso, O., Benavides, M., Helias-Nunige, S., et al. (2018). In depth characterization of diazotroph activity across the western tropical south pacific hot spot of N_2 fixation (OUTPACE cruise). *Biogeosciences* 15, 4215–4232. doi: 10.5194/bg-15-4215-2018

Böttjer, D., Dore, Karl, J. E., D. M. Letelier, R. M., Mahaffey, C., Wilson, S. T., Zehr, J., et al. (2016). Temporal variability of nitrogen fixation and particulate nitrogen export at Station ALOHA. *Limnol. Oceanogr.* 62, 200–216. doi: 10.1002/lno.10386

Cabré, A., Marinov, I., Bernardello, R., and Bianchi, D. (2015). Oxygen minimum zones in the tropical Pacific across CMIP5 models: mean state differences and climate change trends. *Biogeosciences* 12, 5429–5454. doi: 10.5194/bg-12-5429-2015

Capone, D. G. (1993). "Determination of nitrogenase activity in aquatic samples using the acetylene reduction procedure," in *Handbook of Methods in Aquatic Microbial Ecology*, eds P. F. Kemp, B. F. Sherr, E. B. Sherr, and J. J. Cole (Boca Raton, FL: Lewis Publishers), 62–631.

Capone, D. G., Burns, J. A., Montoya, J. P., Subramaniam, A., Mahaffey, C., Gunderson, T., et al. (2005). Nitrogen fixation by *Trichodesmium* spp.: an important source of new nitrogen to the tropical and subtropical North Atlantic Ocean. *Global Biogeochem. Cycles* 19:GB2024. doi: 10.1029/2004GB002331

Caputo, A., Stenegren, M., Pernice, M. C., and Foster, R. A. (2018). A short comparison of two marine planktonic diazotrophic symbioses highlights an un-quantified disparity. *Front. Mar. Sci.* 5:2. doi: 10.3389/fmars.2018.00002

Church, M. J., Mahaffey, C., Letelier, R. M., Lukas, R., Zehr, J. P., and Karl, D. M. (2009). Physical forcing of nitrogen fixation and diazotroph community structure in the North Pacific Subtropical Gyre. *Glob. Biogeochem. Cycles* 23:GB2020. doi: 10.1029/2008GB003418

Codispoti, L. (2007). An oceanic fixed nitrogen sink exceeding 400 Tg N a21 vs the concept of homeostasis in the fixednitrogen inventory. *Biogeoscience* 4, 233–253. doi: 10.5194/bg-4-233-2007

Codispoti, L. A., Brandes, J. A., Christensen, J. P., Devol, A. H., Naqvi, S. W. A., Paerl, H. W., et al. (2001). The oceanic fixed nitrogen and nitrous oxide budgets: moving targets as we enter the anthropocene? *Sci. Mar.* 65, 85–105. doi: 10.3989/scimar.2001.65s285

Conkright, M. E., Locarnini, R. A., Garcia, H. E., O'Brien, T. D., Boyer, T. P., Stephens, C., et al. (2002), *World Ocean Atlas 2001: Objective Analyses, Data Statistics, and Figures [CD-ROM Documentation*]. Silver Spring, MD: National Oceanographic Data Center, 1–17.

Dabundo, R., Lehmann, M. F., Treibergs, L., Tobias, C. R., Altabet, M. A., Moisander, P. H., et al. (2014). The contamination of commercial $^{15}N_2$ gas stocks with 15N-labeled nitrate and ammonium and consequences for

nitrogen fixation measurements. *PLoS One* 9:e110335. doi: 10.1371/journal.pone.0110335

Deutsch, C., Sarmiento, J. L., Sigman, D. M., Gruber, N., and Dunne J. P. (2007). Spatial coupling of nitrogen inputs and losses in the ocean. *Nature* 445, 163–167. doi: 10.1038/nature05392

DeVries, T., Deutsch, C., Rafter, P. A., and Primeau, F. (2013). Marine denitrification rates determined from a global 3-D inverse model. *Biogeosciences* 10, 2481–2496. doi: 10.5194/bg-10-2481-2013

Dietze, H., and Löptien, U. (2013). Revisiting "Nutrient Trapping" in global coupled biogeochemical Ocean Circulation Models. *Global Biogeochem. Cycles* 27, 265–284. doi: 10.1002/gbc.20029

Dunne, J. P., John, J. G., Shevliakova, E., Stouffer, R. J., Krasting, J. P., Malyshev, S. L., et al. (2013). GFDL's ESM2 global coupled climate-carbon earth system models. Part II: carbon system formulation and baseline simulation characteristics. *J. Climate.* 26, 2247–2267. doi: 10.1175/jcli-d-12-00150.1

Falkowski, P. G. (1997). Evolution of the nitrogen cycle and its influence on the biological sequestration of CO2 in the ocean. *Nature* 387, 272–275. doi: 10.1038/387272a0

Fernandez, C., Farías, L., and Ulloa, O. (2011). Nitrogen fixation in denitrified marine waters. *PLoS One* 6:e20539. doi: 10.1371/journal.pone.0020539

Foster, R. A., Kuypers, M. M. M., Vagner, T., Paerl, R. W., Musat, N., and Zehr, J. P. (2011). Nitrogen fixation and transfer in open ocean diatom – Cyanobacterial symbioses. *ISME J.* 5, 1484–1493. doi: 10.1038/ismej.2011.26

Fulweiler, R. W., Heiss, E. M., Rogener, M. K., Newell, S. E., LeCleir, G. R., Kortebein, S. M., et al. (2015). Examining the impact of acetylene on N-fixation and the active sediment microbial community. *Front. Microbiol.* 6:418. doi: 10.3389/fmicb.2015.00418

Gradoville, M. R., Bombar, D., Crump, B. C., Letelier, R. M., Zehr, J. P., and White, A. E. (2017). Diversity and activity of nitrogen-fixing communities across ocean basins. *Limnol. Oceanogr.* 62, 1895–1909. doi: 10.1002/lno.10542

Großkopf, T., and LaRoche, J. (2012). Direct and indirect costs of dinitrogen fixation in crocosphaera watsonii WH8501 and possible implications for the nitrogen cycle. *Front. Microbiol.* 3:236. doi: 10.3389/fmicb.2012.00236

Großkopf, T., Mohr, W., Baustian, T., Schunck, H., Gill, D., Kuypers, M. M. M., et al. (2012). Doubling of marine dinitrogen-fixation rates based on direct measurements. *Nature* 488, 361–364. doi: 10.1038/nature11338

Gruber, N. (2004). "The dynamics of the marine nitrogen cycle and its influence on atmospheric CO_2 variations," in *The Ocean Carbon Cycle and Climate, NATO ASI Series,* eds M. Follows and T. Oguz (Dordrecht: Kluwer Academic), 97–148.

Gruber, N. (2016). Elusive marine nitrogen fixation. *Proc. Natl. Acad. Sci. U.S.A.* 113, 4246–4248. doi: 10.1073/pnas.1603646113

Gruber, N., and Galloway, J. N. (2008). An earth-system perspective of the global nitrogen cycle. *Nature* 451, 293–296. doi: 10.1038/nature06592

Gruber, N., and Sarmiento, J. L. (1997). Global patterns of marine nitrogen fixation and denitrification. *Global Biogeochem. Cycles* 11, 235–266. doi: 10.1029/97GB00077

Hansell, D. A., Bates, N. R., and Olson, D. B. (2004). Excess nitrate and nitrogen fixation in the North Atlantic Ocean. *Mar. Chem.* 84, 243–265. doi: 10.1016/j.marchem.2003.08.004

Hansell, D. A., Olson, D. B., Dentener, F., and Zamora, L. M. (2007). Assessment of excess nitrate development in the subtropical North Atlantic. *Mar. Chem.* 106, 562–579. doi: 10.1016/j.marchem.20070605

Ilyina, T., Six, K. D., Segschneider, J., Maier-Reimer, E., Li, H. M., and Nunez-Riboni, I. (2013). Global ocean biogeochemistry model HAMOCC: model architecture and performance as component of the MPI-Earth system model in different CMIP5 experimental realizations. *J. Adv. Model. Earth Sys.* 5, 287–315. doi: 10.1029/2012ms000178

Jayakumar, A., Al-Rshaidat, M., Ward, B. B., and Mulholland, M. R. (2012). Diversity, distribution, and expression of diazotroph nifH genes in oxygen-deficient waters of the Arabian Sea. *FEMS Microbiol. Ecol.* 82, 597–606. doi: 10.1111/j.1574-6941.2012.01430.x

Jickells, T. D., Buitenhuis, E., Altieri, K., Baker, A. R., Capone, D., Duce, R. A., et al. (2017). A reevaluation of the magnitude and impacts of anthropogenic atmospheric nitrogen inputs on the ocean. *Global Biogeochem. Cycles* 31, 289–305. doi: 10.1002/2016GB005586

Kähler, P., Oschlies, A., Dietze, H., and Koeve, W. (2010). Oxygen, carbon, and nutrients in the oligotrophic eastern subtropical North Atlantic. *Biogeoscience* 7, 1143–1156. doi: 10.5194/bg-7-1143-2010

Keeling, R. F., Körtzinger, A., and Gruber, N. (2010). Ocean deoxygenation in a warming world. *Annu. Rev. Mar. Sci.* 2, 199–229. doi: 10.1146/annurev.marine.010908.163855

Knapp, A. N., Casciotti, L., Berelson, W. M., Prokopenko, M. G., and Capone, D. G. (2016). Low rates of nitrogen fixation in eastern tropical South Pacific surface waters. *Proc. Natl. Acad. Sci. U.S.A.* 113, 4398–4403. doi: 10.1073/pnas.1515641113

Koeve, W., and Kähler, P. (2016). Oxygen utilization rate (OUR) underestimates ocean respiration: a model study. *Global Biogeochem. Cycles* 30, 1166–1182. doi: 10.1002/2015GB005354

Kustka, A., Sanudo-Wilhelmy, S., Carpenter, E. J., Capone, D. G., and Raven, A. (2003). A revised estimate of the iron use efficiency of nitrogen fixation, with special reference to the marine cyanobacterium *Trichodesmium* spp. (Cyanophyta). *J. Phycol.* 39, 12–25. doi: 10.1046/j.1529-8817.2003.01156.x

Landolfi, A., Dietze, H., Koeve, W., and Oschlies, A. (2013). Overlooked runaway feedback in the marine nitrogen cycle: the vicious cycle. *Biogeoscience* 10, 1351–1363. doi: 10.5194/bg-10-1351-2013

Landolfi, A., Dietze, H., and Volpe, G. (2016). Longitudinal variability of organic nutrients in the North Atlantic subtropical gyre. *Deep Sea Res. Part I* 111, 50–60. doi: 10.1016/j.dsr.2015.11.009

Landolfi, A., Koeve, W., Dietze, H., Kähler, P., and Oschlies, A. (2015). A new perspective on environmental controls of marine nitrogen fixation. *Geoph. Res. Lett.* 42, 4482–4489. doi: 10.1002/2015GL063756

Landolfi, A., Oschlies, A., and Sanders R. (2008), Organic nutrients and excess nitrogen in the North Atlantic subtropical gyre. *Biogeoscience* 5, 1199–1213. doi: 10.5194/bg-5-1199-2008

Landolfi, A., Somes, C. J., Koeve, W., Zamora, L. M., and Oschlies, A. (2017). Oceanic nitrogen cycling and N_2O flux perturbations in the Anthropocene. *Global Biogeochem. Cycles* 31, 1236–1255. doi: 10.1002/2017GB005633

Löscher, C. R., Bourbonnais, A., Dekaezemacker, J., Charoenpong, C. N., Altabet, M. A., Bange, H. W., et al. (2016). N_2 fixation in eddies of the eastern tropical South Pacific Ocean. *Biogeosciences* 13, 2889–2899. doi: 10.5194/bg-13-2889-2016

Löscher, C. R., Großkopf, T., Desai, F. D., Gill, D., Schunck, H., Croot, P. L., et al. (2014). Facets of diazotrophy in the oxygen minimum zone waters off Peru. *ISME J.* 8, 2180–2192. doi: 10.1038/ismej.2014.71

Luo, Y.-W., Doney, S. C., Anderson, L. A., Benavides, M., Berman-Frank, I., Bode, A., et al. (2012). Database of diazotrophs in global ocean: abundance, biomass and nitrogen fixation rates. *Earth Syst. Sci. Data* 4, 47–73. doi: 10.5194/essd-4-47-2012

Michaels, A. F., Olson, D., Sarmiento, J. L., Ammerman, J. W., Fanning, K., Jahnke, R., et al. (1996). Inputs, losses and transformations of nitrogen and phosphorus in the pelagic North Atlantic Ocean. *Biogeochemistry* 35, 181–226. doi: 10.1007/BF02179827

Mills, M. M., and Arrigo, K. R. (2010). Magnitude of oceanic nitrogen fixation influenced by the nutrient uptake ratio of phytoplankton. *Nat. Geosci.* 1, 439–443. doi: 10.1038/ngeo856

Mohr, W., Großkopf, T., Wallace, D. W., R., and Laroche J. (2010). Methodological underestimation of oceanic nitrogen fixation rates. *PLoS One* 5:e0012583. doi: 10.1371/journal.pone.0012583

Moisander, P. H., Benavides, M., Bonnet, S., Berman-Frank, I., White, A. E., and Riemann, L. (2017). Chasing after non-cyanobacterial nitrogen fixation in marine pelagic environments. *Front. Microbiol.* 8:1736. doi: 10.3389/fmicb.2017.01736

Monteiro, F., Follows, M. J., and Dutkiewicz, S. (2010). Distribution of diverse nitrogen fixers in the global ocean. *Global Biogeochem. Cycles* 24:GB3017. doi: 10.1029/2009GB003731

Montoya, J. P., Holl, C. M., Zehr, J. P., Hansen, A., Villareal, T. A., and Capone, D. G. (2004). High rates of N_2 fixation by unicellular diazotrophs in the oligotrophic Pacific Ocean. *Nature* 430, 1027–1032. doi: 10.1038/nature02824

Montoya, J. P., Voss, M., Kähler, P., and Capone, D. G. (1996). A simple, high-precision, high-sensitivity tracer assay for N_2 fixation. *Appl. Environ. Microbiol.* 62, 986–993.

Moore, J. K., Lindsay, K., Doney, S. C., Long, M. C., and Misumi, K. (2013). Marine ecosystem dynamics and biogeochemical cycling in the community Earth system model [CESM1(BGC)]: comparison of the 1990s with the 2090s under the RCP4.5 and RCP8.5 scenarios. *J. Clim.* 26, 9291–9312. doi: 10.1175/JCLI-D-12-00566.1

Mouriño-Carballido, B., Graña, R., Fernández, A., Bode, A., Varela, M., Domínguez, J. F., et al. (2011). Importance of N_2 fixation vs. nitrate eddy diffusion along a latitudinal transect in the Atlantic Ocean. *Limnol. Oceanogr.* 56, 999–1007. doi: 10.4319/lo.2011.56.3.0999

Postgate, J. R. (1982). *The Fundamentals of Nitrogen Fixation*. Cambridge: Cambridge University Press.

Redfield, A. C., Ketchum, B. H., Richards, F. A. (1963). "The influence of organisms on the composition of sea-water," in *The Composition of Seawater: Comparative and Descriptive Oceanography. The Sea: Ideas and Observations on Progress in the Study of the Seas*, Vol. 2, ed. M. N. Hill (Hoboken, NJ: Wiley-Interscience), 26–77.

Riemann, L., Farnelid, H., and Steward, G. F. (2010). Nitrogenase genes in non-cyanobacterial plankton: prevalence, diversity and regulation in marine waters. *Aquat. Microb. Ecol.* 61, 235–247. doi: 10.3354/ame01431

Shiozaki, T., Bombar, D., Riemann, L., Hashihama, F., Takeda, S., Yamaguchi, T., et al. (2017). Basin scale variability of active diazotrophs and nitrogen fixation in the North Pacific, from the tropics to the subarctic Bering Sea. *Global Biogeochem. Cycles* 31, 996–1009. doi: 10.1002/2017GB005681

Shiozaki, T., Ijichi, M., Kodama, T., Takeda, S., and Furuya. K. (2014a). Heterotrophic bacteria are major nitrogen fixers in the euphotic zone of the Indian Ocean. *Global Biogeochem. Cycles* 28, 1096–1110. doi: 10.1002/2014GB004886

Shiozaki, T., Kodama, T., and Furuya K. (2014b). Large-scale impact of the island mass effect through nitrogen fixation in the western South Pacific Ocean. *Geophys. Res. Lett.* 41, 2907–2913. doi: 10.1002/2014GL059835

Shiozaki, T., Kodama, T., Kitajima, S., Sato, M., and Furuya, K. (2013). Advective transport of diazotrophs and importance of their nitrogen fixation on new and primary production in the western Pacific warm pool. *Limnol. Oceanogr.* 58, 49–60. doi: 10.4319/lo.2013.58.1.0049

Shiozaki, T., Nagata, T., Ijichi, M., and Furuya, K. (2015a). Nitrogen fixation and the diazotroph community in the temperate coastal region of the northwestern North Pacific. *Biogeoscience* 12, 4751–4764. doi: 10.5194/bg-12-4751-2015

Shiozaki, T., Takeda, S., Itoh, S., Kodama, T., Liu, X., Hashihama, F., et al. (2015b). Why is Trichodesmium abundant in the Kuroshio? *Biogeoscience* 12, 6931–6943. doi: 10.5194/bg-12-6931-2015

Singh, A., Bach, L. T., Fischer, T., Hauss, H., Kiko, R., Paul, A. J., et al. (2017). Niche construction by non-diazotrophs for N_2 fixers in the eastern tropical North Atlantic Ocean. *Geophys. Res. Lett.* 44, 6904–6913. doi: 10.1002/2017GL074218

Somes, C. J., Landolfi, A., Koeve, W., and Oschlies, A. (2016). Limited impact of atmospheric nitrogen deposition on marine productivity due to biogeochemical feedbacks in a global ocean model. *Geophys. Res. Lett.* 43, 4500–4509. doi: 10.1002/2016GL068335

Somes, C. J., Oschlies, A., and Schmittner, A. (2013). Isotopic constraints on the pre-industrial oceanic nitrogen budget. *Biogeosciences* 10, 5889–5910. doi: 10.5194/bg-10-5889-2013

Turk-Kubo, K. A., Karamchandani, M., Capone, D. G., and Zehr, J. P. (2014). The paradox of marine heterotrophic nitrogen fixation: abundances of heterotrophic diazotrophs do not account for nitrogen fixation rates in the Eastern Tropical South Pacific. *Environ. Microbiol.* 16, 3095–3114. doi: 10.1111/1462-2920.12346

Tyrrell, T. (1999). The relative influences of nitrogen and phosphorus on oceanic primary production. *Nature* 400, 525–553. doi: 10.1038/22941

Wannicke, N., Benavides, M., Dalsgaard, T., Dippner, J. W., Montoya, J. P., and Voss, M. (2018). New perspectives on nitrogen fixation measurements using $^{15}N_2$ Gas. *Front. Mar. Sci.* 5:120. doi: 10.3389/fmars.2018.00120

Weber, T., and Deutsch, C. (2012). Oceanic nitrogen reservoir regulated by plankton diversity and ocean circulation. *Nature* 489, 419–422. doi: 10.1038/nature11357

Wilson, S. T., Böttjer, D., Church, M. J., and Karl, D. M. (2012). Comparative assessment of nitrogen fixation methodologies, conducted in the oligotrophic North Pacific Ocean. *Appl. Environ. Microbiol.* 78, 6516–6523. doi: 10.1128/AEM.01146-12

Zahariev, K., Christian, J. R., and Denman, K. L. (2008). Preindustrial, historical, and fertilization simulations using a global ocean carbon model with new parameterizations of iron limitation, calcification, and N_2 fixation. *Progr. Oceanogr.* 77, 56–82. doi: 10.1016/j.pocean.2008.01.007

Zamora, L. M., Landolfi, A., Oschlies, A., Hansell, D. A., Dietze, H., and Dentener, F. (2010). Atmospheric deposition of nutrients and excess N formation in the North Atlantic. *Biogeosciences* 7, 777–793. doi: 10.5194/bg-7-777-2010

Zehr, J. P., Mellon, T., and Zani. S. (1998). New nitrogen-fixing microorganisms detected in oligotrophic oceans by amplification of nitrogenase (nifH) genes. *Appl. Environ. Microbiol.* 64, 3444–3450.

Conflict of Interest Statement: The authors declare that the research was conducted in the absence of any commercial or financial relationships that could be construed as a potential conflict of interest.

frontiers in Microbiology

ORIGINAL RESEARCH
published: 19 August 2020
doi: 10.3389/fmicb.2020.02010

Nitrogen Flow in Diazotrophic Cyanobacterium *Aphanizomenon flos-aquae* Is Altered by Cyanophage Infection

Jolita Kuznecova[1†], Sigitas Šulčius[1†], Angela Vogts[2], Maren Voss[2], Klaus Jürgens[2] and Eugenijus Šimoliūnas[3]*

[1] Laboratory of Algology and Microbial Ecology, Nature Research Centre, Vilnius, Lithuania, [2] Section Biological Oceanography, Leibniz Institute for Baltic Sea Research, Warnemünde, Germany, [3] Department of Molecular Microbiology and Biotechnology, Life Sciences Center, Vilnius University, Vilnius, Lithuania

Viruses can significantly influence cyanobacteria population dynamics and activity, and through this the biogeochemical cycling of major nutrients. However, surprisingly little attention has been given to understand how viral infections alter the ability of diazotrophic cyanobacteria for atmospheric nitrogen fixation and its release to the environment. This study addressed the importance of cyanophages for net $^{15}N_2$ assimilation rate, expression of nitrogenase reductase gene (*nifH*) and changes in nitrogen enrichment ($^{15}N/^{14}N$) in the diazotrophic cyanobacterium *Aphanizomenon flos-aquae* during infection by the cyanophage vB_AphaS-CL131. We found that while the growth of *A. flos-aquae* was inhibited by cyanophage addition (decreased from 0.02 h^{-1} to 0.002 h^{-1}), there were no significant differences in nitrogen fixation rates (control: 22.7×10^{-7} nmol N heterocyte^{-1}; infected: 23.9×10^{-7} nmol N heterocyte^{-1}) and *nifH* expression level (control: 0.6–1.6 transcripts heterocyte^{-1}; infected: 0.7–1.1 transcripts heterocyte^{-1}) between the infected and control *A. flos-aquae* cultures. This implies that cyanophage genome replication and progeny production within the vegetative cells does not interfere with the N_2 fixation reactions in the heterocytes of these cyanobacteria. However, higher ^{15}N enrichment at the poles of heterocytes of the infected *A. flos-aquae*, revealed by NanoSIMS analysis indicates the accumulation of fixed nitrogen in response to cyanophage addition. This suggests reduced nitrogen transport to vegetative cells and the alterations in the flow of fixed nitrogen within the filaments. In addition, we found that cyanophage lysis resulted in a substantial release of ammonium into culture medium. Cyanophage infection seems to substantially redirect N flow from cyanobacterial biomass to the production of N storage compounds and N release.

Keywords: ^{15}N, *Aphanizomenon flos-aquae*, Baltic Sea, diazotrophy, nitrogen fixation, nanoSIMS, vB_AphaS-CL131, virus-host interactions

OPEN ACCESS

Edited by:
Sophie Rabouille, UMR 7621 Laboratoire d'Océanographie Microbienne (LOMIC), France

Reviewed by:
Mikkel Bentzon-Tilia, Technical University of Denmark, Denmark
Iris Maldener, University of Tübingen, Germany

****Correspondence:***
Sigitas Šulčius
sigitas.sulcius@gamtc.lt;
sigitas.sulcius@gmail.com

† These authors have contributed equally to this work

Specialty section:
This article was submitted to Aquatic Microbiology, a section of the journal Frontiers in Microbiology

Received: *02 April 2020*
Accepted: *29 July 2020*
Published: *19 August 2020*

Citation:
Kuznecova J, Šulčius S, Vogts A, Voss M, Jürgens K and Šimoliūnas E (2020) Nitrogen Flow in Diazotrophic Cyanobacterium Aphanizomenon flos-aquae Is Altered by Cyanophage Infection. Front. Microbiol. 11:2010. doi: 10.3389/fmicb.2020.02010

INTRODUCTION

Biological nitrogen (N_2) fixation (conversion of dissolved N_2 gas into ammonia by microorganisms) is an important process of the global biogeochemical cycles, considerably replenishing N losses to denitrification and anaerobic ammonium oxidation (Deutsch et al., 2007), and therefore sustaining carbon export and sequestration in the ecosystem

(Karl et al., 2012). Nitrogen fixing microorganisms (diazotrophs) provide bioavailable nitrogen to the system in the form of ammonia and dissolved organic nitrogen that fuels primary and secondary production and, thus significantly contribute to the ecosystem functioning. Since cyanobacteria dominate epipelagic N_2 fixation in both marine and freshwater environments, it is of great importance to understand factors controlling nitrogen fixation and release in these microorganisms (Benavides and Voss, 2015; Savchuk, 2018). It has been shown that both abiotic (e.g., nutrients, temperature, and mixing) and biotic (e.g., grazing) factors can influence diazotrophic activity and nitrogen distribution within the food web (reviewed in Benavides and Voss, 2015; Kuypers et al., 2018; Pajares and Ramos, 2019). However, the role of virus-host interactions in N_2 assimilation in diazotrophic cyanobacteria and the effect of infection and lysis on the fate of fixed N_2 is poorly described, representing a major knowledge gap in our understanding of the global nitrogen cycling.

It was suggested that viruses have the potential to impact nutrient cycling at scales from single cells to whole ecosystems (Brussaard et al., 2008; Shelford et al., 2012; Zimmerman et al., 2020). For example, it was shown that viral infection leads to the decreased carbon to nitrogen ratio (Ankrah et al., 2014), consequently resulting in stoichiometric imbalance of the infected cell and, thus, potential changes in its nutritional value. Recent studies of marine non-diazotrophic cyanobacteria *Synechococcus* demonstrated that viruses employ host nutrient uptake machinery to acquire extracellular nitrogen (in the form of nitrates) from the surrounding environment, which is then incorporated into newly synthesized viral particles (Pasulka et al., 2018; Waldbauer et al., 2019). In addition, viral genes encoding for proteins involved in nitrogen uptake (homolog of *amt*; Monier et al., 2017) or ammonium oxidation (homologs of *amoC* and *amoA*; Ahlgren et al., 2019) was found in viral metagenomes and culture isolates. Experiments demonstrated that these genes (e.g., *amt*) are expressed during infection and even enhance ammonium uptake rates by the infected cells (Monier et al., 2017). Moreover, as the infection proceeds viruses can switch from using host biomass-derived nitrogen to the extracellularly derived nitrogen sources to meet their N demand required for effective replication (Waldbauer et al., 2019). Lysis of the infected cells and release of dissolved organic and inorganic nitrogen (viral shunt; Wilhelm and Suttle, 1999) were shown to induce structural and functional changes in co-occurring microbial communities and promoted pelagic production due to increased remineralization of the released nutrients (Shelford et al., 2012). These examples suggest that viral infection and lysis can directly modulate N transformations in the ecosystems. From the perspective of atmospheric nitrogen dynamics in diazotrophic cyanobacteria, one thus could hypothesize that infection by viruses can induce alterations in (i) nitrogen assimilation (N_2 fixation) and (ii) release (ammonium) rates, due to, for example, metabolic reprogramming of the host cells (Doron et al., 2016) as well as (iii) redistribution of N within the infected cells by redirecting intracellular nutrient pool toward production of new virions (Ankrah et al., 2014).

The *Aphanizomenon flos-aquae* is a bloom-forming heterocytous cyanobacterium, distributed worldwide in fresh and brackish water ecosystems (Cirés and Ballot, 2016). *A. flos-aquae* substantially contributes to the nitrogen pool in the Baltic Sea and fixes up to 75% of total fixed nitrogen in this ecosystem of which up to 50% are released (Ploug et al., 2010; Klawonn et al., 2016). *A. flos-aquae* and other filamentous cyanobacteria in the Baltic Sea fuel a microbial food web which is efficiently grazed by zooplankton in particular during the late phase of a bloom (Wannicke et al., 2013; Woodland et al., 2013; Karlson et al., 2015; Adam et al., 2016). Cyanophages were shown to significantly reduce population size of *A. flos-aquae* in laboratory incubations (Šulčius et al., 2015a). In addition, cyanophage infection can substantially alter the population structure of *A. flos-aquae* via reduction of the filament size and due to caused changes in ratio between vegetative cells, heterocytes and akinetes, since the latter two types of *A. flos-aquae* cells were shown to be insensitive to cyanophage additions (Šulčius et al., 2015a, 2017). Thus, this raises an intriguing question whether and to what extent cyanobacterial viruses (cyanophages) influences N_2 fixation and nitrogen transformation processes in these cyanobacteria, and, in particular, whether viral infections alter the level of gene expression (e.g., *nifH*) and net incorporation of N_2 into cyanobacterial biomass. In addition, there is a paucity of knowledge regarding how infection affects nitrogen flow within the filaments of the infected cyanobacteria. The lack of this information hampers our understanding of how virus-bacterium interactions influence biological nitrogen fixation process in the Baltic Sea and other aquatic ecosystems in which *A. flos-aquae* occurs at the high densities.

To advance our understanding of the effect of cyanophage infection on diazotrophic activity, we infected a culture of *A. flos-aquae* with the virulent cyanophage vB_AphaS-CL131 (hereafter CL 131; Šulčius et al., 2015a) in a short-term (36 h; within one infection cycle of CL 131) laboratory incubation experiment. We then followed changes in nitrogen fixation rates using a $^{15}N_2$ stable isotope tracer addition (Montoya et al., 1996) and the transcript abundance of *nifH*, a marker gene for N_2 fixation (Raymond et al., 2004), in infected *A. flos-aquae* cultures and compared these expression levels and fixation rates to those of uninfected controls. In addition, we used high-resolution nanometer-scale secondary ion mass spectrometry (nanoSIMS) of *A. flos-aquae* to evaluate the cellular distributions of ^{15}N enrichments during infection as a proxy for nitrogen assimilation and flow among the cells within the filament.

RESULTS

Dynamics of *A. flos-aquae* and Cyanophage vB_AphaS-CL131

In the control treatment without virus addition, the abundance of *A. flos-aquae* cells increased by 62.6% at the end of the experiment compared to its initial counts and changed from 2.5×10^5 cells mL^{-1} ($\pm 0.7 \times 10^3$ cells mL^{-1}) to 4.0×10^5 cells mL^{-1} ($\pm 1.1 \times 10^4$ cells mL^{-1}). No significant changes in *A. flos-aquae* abundance over the period of 36 h was

observed in the infected culture (**Figure 1**), which indicated the suppression of *A. flos-aquae* population growth. The apparent growth rate of *A. flos-aquae* in the control culture was about 0.02 h^{-1} ($\pm$0.0008 h^{-1}) and significantly ($\sim$10-fold; *t*-test, $t = 8.90$, $p < 0.0$, $df = 12$) exceeded that of the infected culture [0.002 h^{-1} ($\pm$0.0009 h^{-1})].

Changes in cyanophage CL 131 abundances were assessed by enumerating gene copy numbers of the structural gene gp046 in cell-free filtrate (**Figure 1**). Six hours after cyanophage addition, the number of CL 131 cyanophages decreased to $\sim$73% of its initial numbers, indicating that about 1/4 of all cyanophages in the stock adsorbed to its host cells. The CL 131 density then significantly (Tukey HSD $p < 0.00$) increased 24 h after cyanophage addition (2.4×10^6 gp046 gene copies $mL^{-1} \pm 9.2 \times 10^4$ gp046 gene copies mL^{-1}) and reached its peak in abundance at about 30 h post inoculation (4.5×10^6 gp046 gene copies $mL^{-1} \pm 1.0 \times 10^5$ gp046 gene copies mL^{-1}; **Figure 1**).

Nitrogen Fixation and Gene Expression

The net $^{15}N_2$ fixation rates by *A. flos-aquae* cumulated over the course of incubation experiment in both treatments (**Figure 2A**), and eventually reached 22.7×10^{-7} nmol N heterocyte^{-1} ($\pm 3.3 \times 10^{-7}$ nmol N heterocyte^{-1}) and 23.9×10^{-7} nmol N heterocyte^{-1} ($\pm 7.3 \times 10^{-7}$ nmol N heterocyte^{-1}) in the control and infected culture, respectively. No statistically significant differences in N_2 fixation rates were found between the infected and control treatments (RM ANOVA $F = 2.25$, $p = 0.14$, $df = 1$) over the course of the incubation experiment. These observations were consistent with changes in the number of *nifH* transcripts (**Figure 2B**), where no differences between the two treatments were detected (RM ANOVA $F = 4.22$, $p = 0.06$, $df = 1$), except for 12 h post inoculation. The number of *nifH* transcripts varied from 0.6 ($\pm$0.2) to 1.6 ($\pm$0.1) transcripts per heterocyte and from 0.7 ($\pm$0.2) to 1.1 ($\pm$0.2) transcripts per heterocyte in the control and infected cultures, respectively.

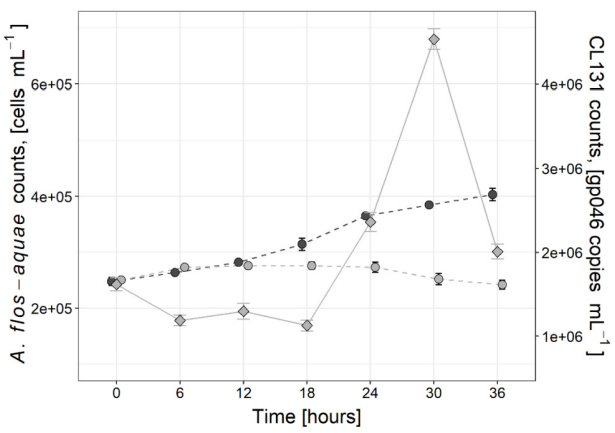

FIGURE 1 | Changes in *Aphanizomenon flos-aquae* strain 2012/KM1/D3 cell abundance (circles) in the control (dark gray) and infected (light gray) treatments as well as dynamics of cyanophage vB_AphaS-CL131 gp046 gene copy numbers (diamonds) during the course of incubation experiment. Symbols indicate the mean values, and the error bar shows the standard deviation of three technical replicates.

Nitrogen Enrichments in *A. flos-aquae* Filaments

The ^{15}N enrichment was assessed using nanoSIMS analysis in both *A. flos-aquae* heterocytes and vegetative cells. Significantly increased (*t*-test, $t = 6.92$, $p = 0.01$, $df = 19$) ^{15}N enrichment was detected in the heterocytes of the infected *A. flos-aquae* culture (**Figures 3A**, **4A**), indicating accumulation of the newly fixed N_2 within those cells. The local ^{15}N enrichment at the poles of the heterocytes of the infected *A. flos-aquae* filaments were also significantly higher (*t*-test, $t = 5.08$, $p = 0.03$, $df = 34$) compared to the control cultures (**Figures 3B**, **4B**). No statistically significant differences (*t*-test, $t = 0.22$, $p = 0.82$, $df = 98$) in whole-cell ^{15}N enrichment in vegetative *A. flos-aquae* cells were found between the two treatments (**Figure 3C**), although the variation width in the infected cells was higher compared to the control. The nanoSIMS data showed that significant local ^{15}N enrichments in vegetative cells were distributed randomly and occurred at a very low abundance (data not shown), having no impact on the average cell isotopic signal.

Changes in Nutrient Concentration

Statistically significant (RM ANOVA $F = 28.42$, $p = 0.01$, $df = 1$) increase in ammonium concentration was observed in the medium of the infected culture compared to non-infected controls at 36 h (**Figure 5A**). The concentration of ammonium in the infected treatment changed from 0.90 μmol L^{-1} ($\pm$0.09 μmol L^{-1}) at the beginning to 1.53 μmol L^{-1} ($\pm$0.22 μmol L^{-1}) at the end of the experiment whereas in the controls it decreased from 0.72 μmol L^{-1} ($\pm$0.52 μmol L^{-1}) to 0.58 μmol L^{-1} ($\pm$0.22 μmol L^{-1}). Both curves had minimum concentrations between 12 and 24 h. The concentration of other inorganic nitrogen forms (nitrate and nitrite) remained below or just above the detection limit (0.2 μmol L^{-1} for nitrate, 0.05 μmol L^{-1} for nitrite) during the experiment and did not show any clear pattern (data not shown). The measured concentration of phosphates varied from 88.0 to 91.2 μmol L^{-1} and from 89.5 to 93.8 μmol L^{-1} in control and infected treatments, respectively (**Figure 5B**).

DISCUSSION

Understanding the factors controlling biological N_2 fixation is important to fully comprehend the flow of energy and matter in the ecosystem. In this study, we analyzed the effect of cyanophage infection on nitrogen fixation and flow in diazotrophic cyanobacterium *A. flos-aquae*. We demonstrated that viral infection and diazotrophic activity in these filamentous cyanobacteria do not interfere with one another, indicating low degree of virus-mediated metabolic remodeling of *A. flos-aquae* heterocytes. Our results also suggest that CL 131 cyanophages contribute to nitrogen dynamics by (i) inducing alterations in nitrogen distribution within the infected *A. flos-aquae* filaments and (ii) through ammonium release by lysis.

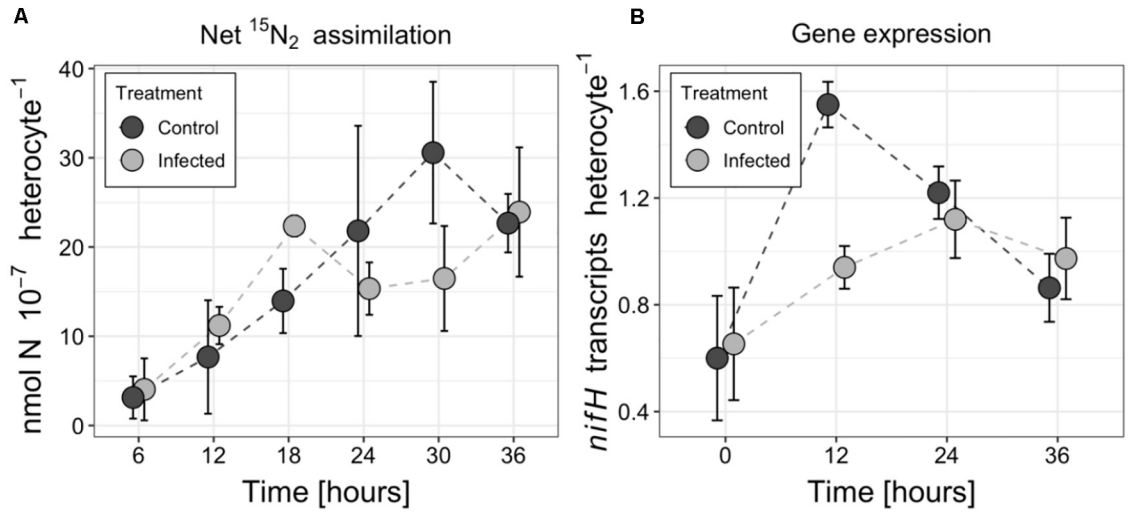

FIGURE 2 | Changes in nitrogen fixation **(A)** and *nifH* transcript abundance **(B)** in the control and infected cultures of the *Aphanizomenon flos-aquae* strain 2012/KM1/D3. Symbols indicate the mean values, and the error bar shows the standard deviation of three technical replicates.

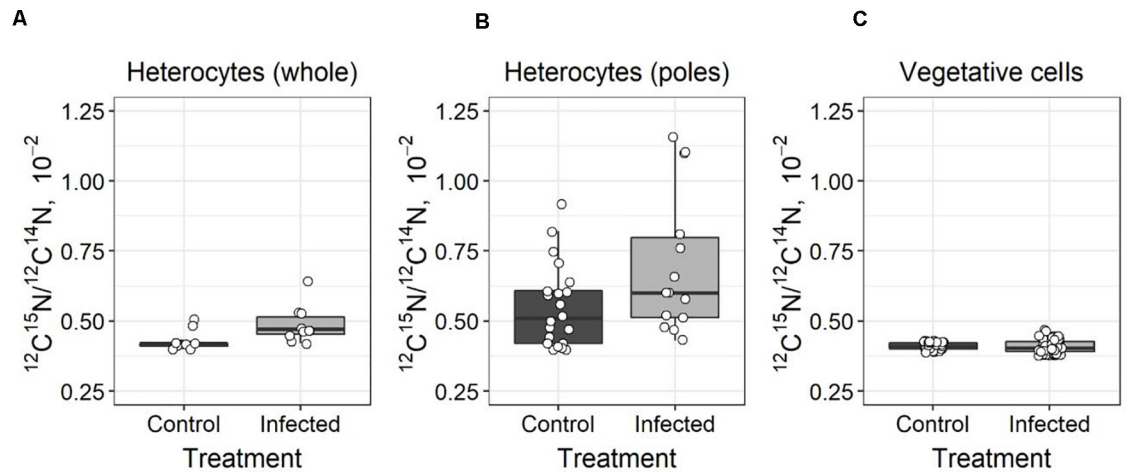

FIGURE 3 | Differences in ^{15}N enrichment in *Aphanizomenon flos-aquae* strain 2012/KM1/D3 heterocytes (whole cell–**A**, poles–**B**) and vegetative cells **(C)** indicated as $^{12}C^{15}N/^{12}C^{14}N$ ratio (calculated from nanoSIMS analysis). The solid line within the box marks the mean, the boundaries of the box represent the standard error, and the whiskers above and below the box show the standard deviation from the mean. White circles represent the data value of each measured heterocyte **(A,B)** or vegetative cell **(C)**.

The infection cycle of CL 131 progressed similarly to previously observed infection dynamics for this cyanophage (Šulčius et al., 2015a) as well as to that described for other cyanophages infecting filamentous cyanobacteria (Wang and Chen, 2008; Gao et al., 2009; Dwivedi et al., 2013; Watkins et al., 2014; Coloma et al., 2017; Šulčius et al., 2018). A significant increase in CL 131 abundance was detected 24–30 h after cyanophage addition (**Figure 1**), indicating lysis of *A. flos-aquae* cells and completion of the first infection cycle (Šulčius et al., 2015a). Changes in CL 131 abundance from T0 to T6 (**Figure 1**) imply slow CL 131 adsorption as only approximately 27% of the cyanophages were found associated with *A. flos-aquae* cells. Nevertheless, the calculated ratio of the adsorbed phages to each cyanobacterial cell was ∼1.7, suggesting that most of the cells were still infected. However, due to unsynchronized cell growth and division rates in filamentous cyanobacteria (Sakr et al., 2006), which likely occurs as a result of variation in metabolic and physiological state of each individual cell within the filaments, the increased variation in the latent period of the cyanophages and therefore differences in lysis timing may occur (Parada et al., 2006; Hyman and Abedon, 2009). Although both relatively low adsorption rates and unsynchronized cell lysis were also found for other virus and filamentous cyanobacteria host systems, eventually (e.g., after prolonged period of time and several

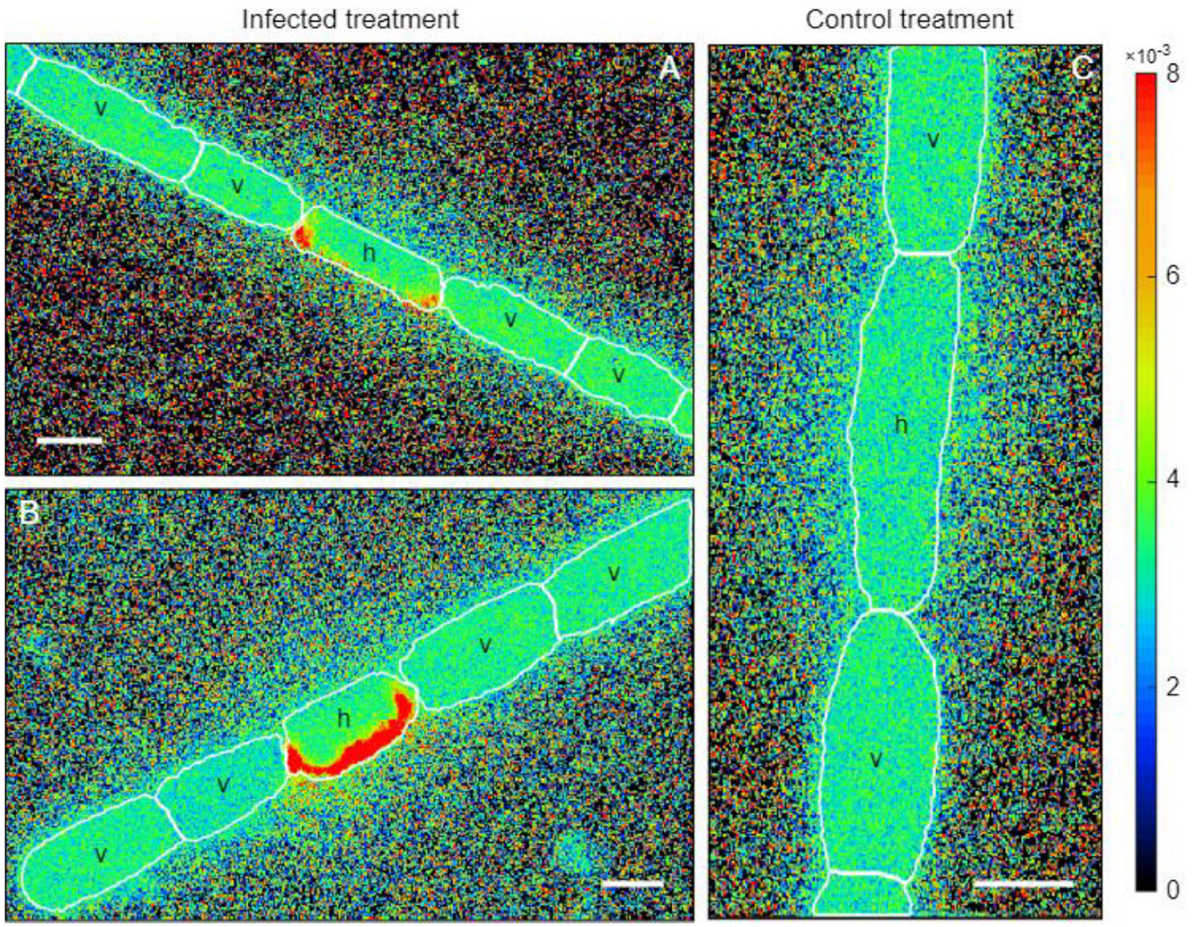

FIGURE 4 | Nanometer-scale secondary ion mass spectrometry (nanoSIMS) micrographs of *Aphanizomenon flos-aquae* strain 2012/KM1/D3 heterocytes (h) and adjacent vegetative cells (v) in the infected **(A,B)** and control **(C)** treatments. The cellular nitrogen distribution is indicated as $^{12}C^{15}N/^{12}C^{14}N$ ratio.

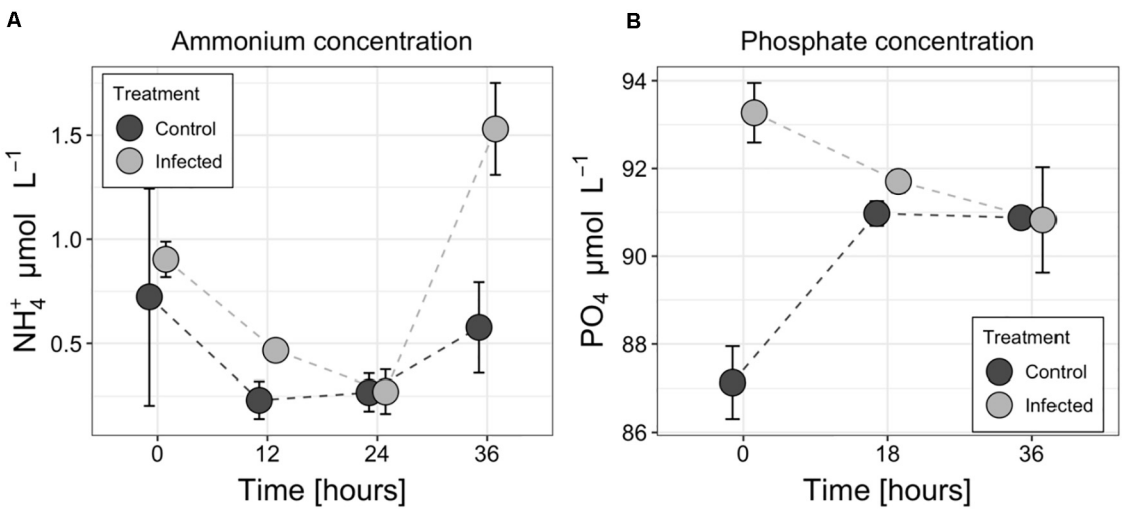

FIGURE 5 | Changes in ammonium **(A)** and phosphate **(B)** concentrations in the medium of the control and infected cultures of the *Aphanizomenon flos-aquae* strain 2012/KM1/D3. Symbols indicate the mean values, and the error bar shows the standard deviation of three technical replicates.

infection cycles) most of the cells are lysed (Hewson et al., 2004; Gao et al., 2009; Šulčius et al., 2015a, 2018; Coloma et al., 2017). This further suggests that under conditions of massive infection and lysis such as for example during the blooms of filamentous cyanobacteria (Gons et al., 2002), a substantial amount of fixed N_2 might be redirected toward the microbial loop.

Nitrogen Fixation During Cyanophage Infection

To meet their N demand required for the efficient replication of viral nucleic acids and proteins within the infected cells, viruses are known to employ at least three different mechanisms for N acquisition: recycling of intracellular N sources (Ankrah et al., 2014), acquisition of extracellular nitrogen using host cell nitrogen uptake machinery (Waldbauer et al., 2019) and expression of host-derived viral genes involved in nitrogen metabolism (Yoshida et al., 2008; Monier et al., 2017). Noting that cyanophage CL 131 do not encode any known proteins involved in N metabolism (e.g., phycobilisomes degradation enzymes or N transporters; Šulčius et al., 2019), our findings suggest that cyanophage CL 131 replication strongly relies on the pre-existing intracellular nitrogen pool in *A. flos-aquae* cells. The major ecological implication, therefore, is that production rate (including latent period and burst size) of cyanophage CL 131 is more likely to be limited by the physiological state of *A. flos-aquae* and the ability of cyanophage to efficiently catabolize host intracellular compounds rather than by virus-mediated metabolic reprogramming of the host cells. This observation represents a relatively less common mode of the phage-host interactions that differ from other laboratory virus-host systems, including marine cyanobacteria, algae, and heterotrophic bacteria, in which viral replication significantly interfere with carbon and nitrogen cycling within the infected cells (reviewed in Zimmerman et al., 2020). Negligible effect of cyanophage infection on host metabolic activity was also observed for freshwater bloom-forming cyanobacteria *Microcystis aeruginosa* (Morimoto et al., 2018). The authors hypothesized that the lack of significant metabolic reprogramming of the infected cells might be associated with cyanophage avoidance strategy to prevent the activation of host defense systems, while material necessary for cyanophage DNA replication and protein synthesis can be derived from the host nucleotide and amino acid precursor pools (Morimoto et al., 2018).

The spatial separation of nitrogen fixation in heterocytes and cyanophage replication within the vegetative cells might explain the lack of interference between these two processes. Although N_2 fixation and growth are usually tightly connected under relatively stable growth conditions (Muñoz-García and Ares, 2016), uncoupling between nitrogen and carbon metabolism may occur under environmental stress. Since heterocytes are capable of independent production of the reducing equivalents and ATP for the nitrogenase reactions in photosystem I (Magnuson and Cardona, 2016), nitrogen fixation can be maintained when growth conditions change. Thus, from the perspective of virus-mediated metabolic reprogramming of the infected cell, a process which essentially is a redirection of the energy supply from cellular reactions to the synthesis of viral particles (Puxty et al., 2015; Rosenwasser et al., 2016), the energy demanding process of N_2 fixation taking place in physically separated and relatively energetically independent heterocyte, should not influence or restrict virus replication. This is because the required energy for virus replication within the vegetative cells is provided by other reactions such as for example pentose phosphate pathway (Thompson et al., 2011). Thus, such energetic "independence" of heterocytes and/or inability of a virus to access the ATP produced within the heterocytes makes possible that diazotrophic activity of the infected filaments is maintained, especially over the relatively short period of time, such as the time needed for cyanophage replication and assembly. Similar to our observations, studies with zooplankton predation (including *Daphnia*, *Diaptomus,* and *Bosmina*), which is another major biotic factor of cyanobacteria mortality, indicated that grazing on the vegetative cells of the filamentous cyanobacteria do not exert any effect on heterocyte activity and rates of nitrogen fixation (Shtina and Nekrasova, 1971; Chan et al., 2004), suggesting that heterocytes remain metabolically active even when vegetative cells are dying.

The importance of diazotrophically fixed nitrogen in the aquatic food web is strongly associated with its transformation within the cell (e.g., cellular stoichiometry and nutritional value) and a subsequent release into environment (e.g., in either dissolved or particulate form). In case of active virus-mediated metabolic reprogramming, as studies with marine heterotrophic bacteria and algae would suggest (reviewed in Zimmerman et al., 2020), the intracellular nitrogen resources should be effectively redirected from the production of cellular compounds toward new phage particles resulting in significant changes in cellular stoichiometry (nutritional value of the cell is changed; Ankrah et al., 2014; Monier et al., 2017). Alternatively, however, the metabolism of the assimilated nitrogen, including both synthesis and degradation of host proteins and various metabolites, might remain significantly unchanged during cyanophage infection (Morimoto et al., 2018), in turn, possibly having no impact on intracellular nutrient ratios (nutritional value of the cell does not change). Our observations, however, suggest another rather subtle effect of cyanophages on the N flow, when newly fixed nitrogen is neither incorporated into viral particles nor it accumulates into cyanobacteria biomass. Instead it remains in the heterocytes, changing N flow within the infected filaments and delaying any of its further transformations.

Re-distribution of Fixed Nitrogen Within the Infected Filaments

In diazotrophic cyanobacteria, newly fixed N_2 is either (i) transferred to the vegetative cells where it is used for cellular growth (biomass accumulation), (ii) released as ammonium (cellular exudation) to the surrounding environment, or (iii) under unfavorable growth conditions is converted into N storage compounds. These processes and thus the flow of nitrogen is actively regulated in cyanobacteria to maintain the beneficial interactions with other microorganisms and in response to environmental conditions to ensure cellular growth and survival

(Flores and Herrero, 2005; Foster et al., 2011; Zehr and Kudela, 2011). Viral infection of the host cells has the potential to modulate the nitrogen metabolism and alter the flow of N within the infected cells (Brussaard et al., 2008; Ankrah et al., 2014). Both growth inhibition (**Figure 1**) and the lack of changes in N_2 fixation activity (**Figure 2**) in the infected *A. flos-aquae* might suggest that newly fixed nitrogen is used for the production of cyanophage progeny rather than for incorporation into cyanobacterial biomass. In this case, and assuming that viruses are enriched in N compared to their hosts (Jover et al., 2014; Pasulka et al., 2018), increased local ^{15}N enrichments relative to the control *A. flos-aquae* filaments can be expected in the cytoplasmic regions where the assembly of the newly produced cyanophage virions within the infected vegetative cell occurs. These regions can be clearly seen in the thin sections of the infected *A. flos-aquae* cells (for details see Šulčius et al., 2015a). Recent study has demonstrated the ability of nanoSIMS to resolve ^{15}N enrichments in each individual viral particle (Pasulka et al., 2018). Thus, to test our hypothesis, we analyzed cellular distribution of ^{15}N enrichments in vegetative cells of the infected and control cultures. The nanoSIMS analysis revealed no differences in both local (data not shown) and total (**Figure 3C**) ^{15}N enrichments between infected and control vegetative *A. flos-aquae* cells, suggesting that only limited (if any) amount of newly fixed N_2 is incorporated into cyanophage progeny. Also, this suggest that cyanophage infection does not result in the relative accumulation of nitrogen within infected cells as it was shown for some marine bacteria and algae virus-host systems (Ankrah et al., 2014; Monier et al., 2017).

In this study, we found different ^{15}N enrichments in the heterocytes of the infected cultures compared to the uninfected controls (**Figure 3A**). The observed ^{15}N enrichment in the heterocytes was also localized at its poles (at both ends close to the heterocyte neck; **Figure 3B**). The reason for this localization is not fully understood at this time but one possible explanation is nitrogen conversion into N storage compounds. It has been shown that heterocyte ends are the sites of accumulation of cyanophycin (Sherman et al., 2000) a polymer composed of aspartate and arginine that serves as a nitrogen reservoir (Flores et al., 2019). Cyanophycin granules were previously detected in the heterocytes of the field isolates of *A. flos-aquae*, yet at the relatively low concentrations, suggesting that fixed N was rapidly transported to the adjacent cells during population growth (Ploug et al., 2010). However, increased production of cyanophycin may occur under stress or growth-limiting conditions (Obst and Steinbüchel, 2006), including during the inhibition of host protein synthesis that is known to occur during viral infection (Rosenwasser et al., 2016). The accumulation of fixed N_2 in the form of cyanophycin would be consistent with the observed ^{15}N enrichments at heterocyte poles (**Figure 3B**) and growth inhibition of vegetative cells of *A. flos-aquae* by cyanophage CL 131 infection in our experiment (**Figure 1**). Consequently, it may further suggest that GS/GOGAT pathway, linking carbon and nitrogen metabolism in the filaments, may also be affected by the cyanophage infection. For example, one could expect that incorporation of fixed nitrogen into aspartate and arginine would also reduce the formation and transport of 2-oxoglutarate (2OG) and glutamine (Gln) into the vegetative cells. This in turn might result in downregulation of *NtcA* genes, global nitrogen regulators essential for regulation of the expression of numerous other important genes involved in maintenance of *A. flos-aquae* metabolism and physiology. Whether the above discussed phenomenon (cyanophycin accumulation in heterocytes and reduced supply of Gln and 2OG to vegetative cells) represents a case of coordinated cellular response to cyanophage infection remains unknown and further studies are needed to test this hypothesis. Nevertheless, the ecological implications could be that diazotrophically fixed nitrogen is neither accumulated into cyanobacteria biomass nor it is incorporated into newly synthesized phage particles. The nanoSIMS results suggest that the transport of newly fixed N_2 from the heterocytes to the infected vegetative cells is suspended. The subsequent transformations of N_2 is delayed and newly fixed N_2 may not be released.

Nitrogen Release by Cyanophage Infection and Lysis

Biological nitrogen fixation and its subsequent release is one of the largest sources of nitrogen enabling microbial community to alleviate general summer nitrogen limitation in many aquatic ecosystems (Vahtera et al., 2007; Degerholm et al., 2008; Wannicke et al., 2013; Karlson et al., 2015). Diazotrophically derived nitrogen can be released and transferred to co-occurring microbes either through the exudation of dissolved nitrogen products from cyanobacterial cells (mostly in the form of ammonium; Adam et al., 2016), zooplankton grazing (e.g., sloppy feeding and excretion of N compounds within the fecal pellets; Hasegawa et al., 2001), decay of the senescent cells (e.g., at the end of the vegetation period; Engström-Öst et al., 2013), viral lysis (Coloma et al., 2017) or combination of these processes. Although the type of material released by all of these processes includes a spectrum of compounds ranging from highly labile to recalcitrant, the stoichiometric composition and bioavailability of the released material is thought to be different (Suttle, 2007). It is generally believed that cellular exudation and lysis-mediated release of organic and inorganic molecules is more readily accessible to pelagic bacteria compared to zooplankton fecal pellets or decaying cells (Adam et al., 2016). Therefore, our observations revealing threefold higher ammonium concentration in the cell-free filtrates of the infected *A. flos-aquae* culture at the end of the incubation experiment (**Figure 5A**), would, therefore, tentatively suggest that cyanophage lysis can not only redirect the flow of nitrogen from cellular biomass (which otherwise would be grazed or decayed) toward higher N release, but also significantly increase N bioavailability in the system. It is worth to note that since the flow of newly fixed nitrogen is significantly reduced or inhibited in the infected filaments (as discussed above; **Figures 3**, **4**), the released nitrogen should have probably been fixed and transferred to vegetative cyanobacterial cell before the cyanophage infection. Nevertheless, ammonium release would enhance N remineralization by uninfected bacteria and algae,

having a net stimulatory effect on the growth of co-occurring microbial assemblages as it was experimentally shown for filamentous diazotrophic cyanobacterium *Nodularia spumigena* (Cairns et al., 2016) and natural phytoplankton community (Shelford et al., 2012). The extent of this effect, however, would depend on the host species (in our case *A. flos-aquae*), composition of the co-occurring community and the ability of each individual microbial species to assimilate lysis-released compounds.

On the other hand, it is also possible that infection and lysis of the vegetative cells would reduce or even prevent the supply of glutamate produced by GOGAT (glutamine oxoglutarate aminotransferase) in vegetative cells, which is used as a substrate by the glutamine synthetase (GS) in the heterocytes to produce Gln, a process during which fixed nitrogen is incorporated into amino acids. Therefore, one could hypothesize that ammonium produced in the un-infected and metabolically active heterocytes, and no longer being transferred (as Gln) to the adjacent lysed vegetative cells, is released into surrounding environment. Thus, future studies should include measurements of the GS/GOGAT activity to better understand nitrogen release from heterocytes during and after cyanophage infection.

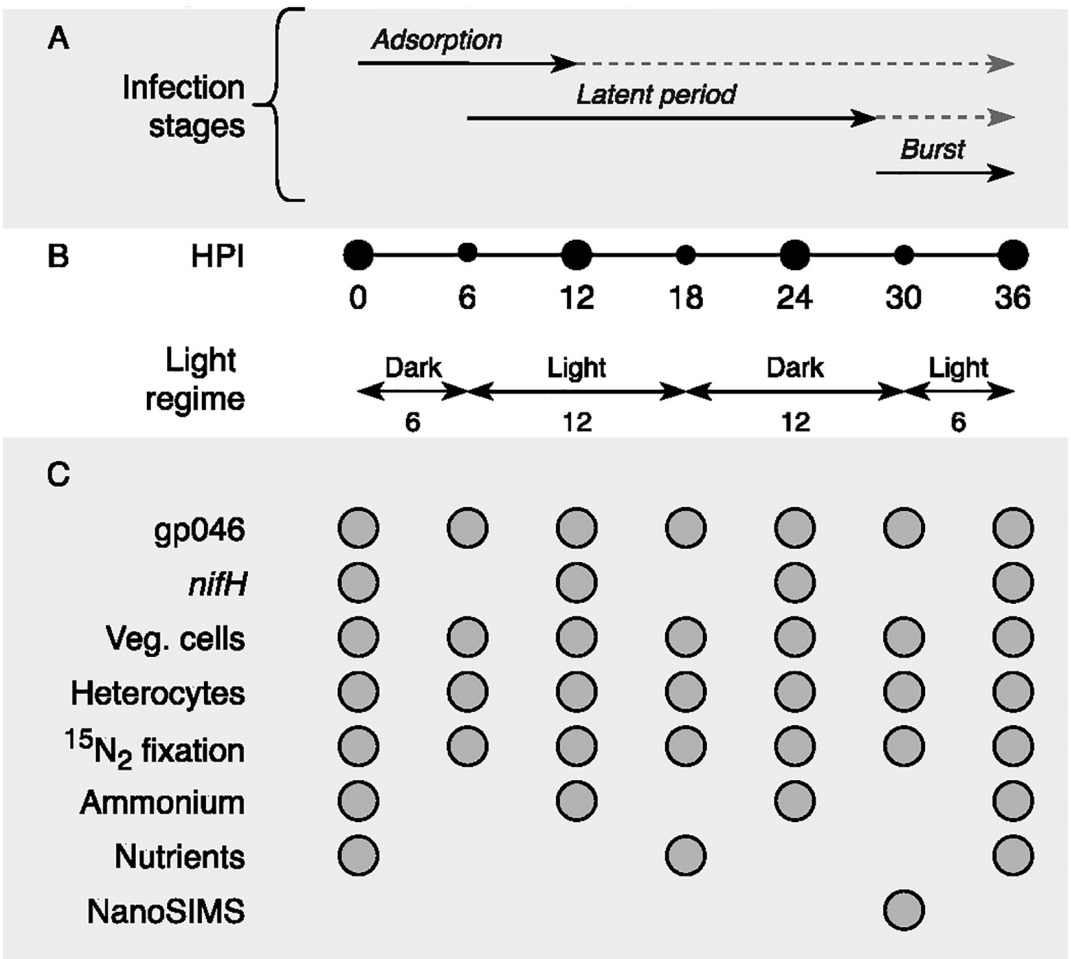

FIGURE 6 | Schematic representation of **(A)** cyanophage vB_AphaS-CL131 infection stages (adsorption, latent period, and burst; modified from Šulčius et al., 2015a), **(B)** sampling points (black circles) in the context of light regime (hours), and **(C)** list of measurements taken during the course of the incubation experiment. HPI, hours post inoculation; Veg. cells, vegetative cells.

TABLE 1 | Primer sets used for droplet digital PCR analysis of *nifH* gene expression (*nifH*), DNA contamination in RNA samples (16S) and cyanophage CL131 abundance (gp046).

Target gene	Forward primer (5′ to 3′)	Reverse primer (5′ to 3′)	Product length, bp	References
nifH	GATAGCTTTCTACGGCAAGGGC	GGTAGAGTCAGCTTTAGGATCG	124	This study
16S	GTGCCAGCMGCCGCGGTAA	GGACTACHVGGGTWTCTAAT	255	Caporaso et al., 2011
gp046	CACAACTCATTGCTGGTGGC	GGTTGGTGGTTCATAGGGCT	143	This study

Finally, no accompanied changes in phosphate concentration was found between the control and infected treatments at the lysis onset (36 h; **Figure 5B**), suggesting that viral lysis in addition to the induced alterations in the ammonium concentration (**Figure 5A**) and possibly in the prevailing N form in the environment, also have implications for the overall nutrient stoichiometry in aquatic ecosystems (Suttle, 2007). The observed differences in phosphate concentration between the infected and control cultures at T0 (**Figure 5B**) cannot be explained by any differences in the experimental setup, but would, however, have no substantial effect neither on *A. flos-aquae* growth nor for cyanophage infection process during the period of incubation experiment as the total P concentration far exceeded (>3-fold) the limit proposed to inhibit *A. flos-aquae* development (De Nobel et al., 1997; Takano and Hino, 2000; Vahtera et al., 2007).

CONCLUSION

Determining the fate of diazotrophically derived nitrogen in the infected cells is important not only for the better assessment of the role of viruses in the nutrient flows and functioning of the microbial food web, but also for the development of more efficient ecosystem management plans. In this study, we described the effect of cyanophage infection on diazotrophic activity and N flow in the ecologically relevant heterocytous cyanobacterium *A. flos-aquae*. Although this represents a single case based on using the same initial culture and therefore may obscure the inference about the variance of the observed effect of infection in natural *A. flos-aquae* population consisting of various genotypes with different sensitivity to cyanophages, the random biological variation of *A. flos-aquae* filaments and individual cells, emerging due to its multicellular nature, asymmetric division and unsynchronized growth in our incubations might well reflect the general patterns of *A. flos-aquae* physiological state and fitness in aquatic environments, at least for the fraction of infection sensitive sub-population. Nevertheless, we demonstrated that infection with the cyanophage CL 131 does not inhibit the expression of *nifH* genes or the rate of net N_2 assimilation (**Figure 2**); thus, the metabolism and activity of heterocytes remained unchanged. However, these observations may hinder the actual effect of viral infections on nitrogen dynamics and metabolism within host cells. The increased total (whole heterocytes; **Figure 3A**) and local (at the heterocyte poles; **Figure 3B**) ^{15}N enrichment in the heterocytes of the infected *A. flos-aquae* culture indicates that the flow of fixed N_2 within the filament might be altered as a result of viral infection. Whether and how these changes influence the stoichiometry and amino acid profiles of the infected vegetative cells of *A. flos-aquae* or, for example, the recovery of the resistant *A. flos-aquae* subpopulation remain to be elucidated. Finally, nitrogen that has been fixed before the infection of vegetative cyanobacterial cells takes place is released as ammonium (**Figure 5A**) or dissolved organic nitrogen upon cell lysis and would probably also change the flow of fixed N_2 within the microbial food web (Shelford et al., 2012). We, thus, suggest that cyanophage infection redirect the pathway of fixed N_2 from *A. flos-aquae* biomass (**Figure 1**) toward production of N storage compounds (**Figure 3B**) and enhanced N release (**Figure 5A**).

MATERIALS AND METHODS

Experimental Organisms and Culture Conditions

The clonal cyanobacterium *A. flos-aquae* strain 2012/KM1/D3 was isolated from surface water collected from the Curonian Lagoon (N 55°30′, E 21°15′) in the south-eastern part of the Baltic Sea (Šulčius et al., 2015a) Unialgal yet non-axenic *A. flos-aquae* culture was grown in modified (pH 7.8–8.0) AF-6 medium (Watanabe et al., 2000) without the addition of a nitrogen source (AF-$6N_0$) under a 14/10-h light-dark cycle with a light intensity of 30 $\mu mol\ m^{-2}\ s^{-1}$ and at a constant 20°C temperature.

Cyanophage vB_AphaS-CL131 was isolated from the Curonian Lagoon (Lithuania) using *A. flos-aquae* strain 2012/KM1/D3 as a host organism (Šulčius et al., 2015b). CL 131 is a large (capsid size of ∼97 nm, tail length – ∼361 nm, genome size – ∼113 kb) virulent siphovirus with an infection cycle of ∼36 h (Šulčius et al., 2015b, 2019). Prior the experiment, CL 131 was propagated using exponential growth phase *A. flos-aquae* culture under the same conditions as those described above. Cyanophage inoculum for incubation experiment was prepared from *A. flos-aquae* lysates purified using cesium chloride ($CsCl_2$) density gradient centrifugation (Šulčius et al., 2015b).

Incubation Experiment and Sampling Scheme

We limited our experiment to one infection cycle of the cyanophage CL 131 (Šulčius et al., 2015b) to emphasize the effect of cyanophage infection on N_2 fixation and *nifH* gene expression in *A. flos-aquae* rather than the combined effect of infection and cell lysis. More specifically, we tried to prevent the potential effect of organic and inorganic nitrogen, which may be released into the medium due to cell lysis, on *A. flos-aquae* N metabolism. It has been suggested that these filamentous cyanobacteria may exhibit a preferential uptake of nitrates, nitrites, and ammonium instead of $^{15}N_2$ (Layzell et al., 1985). The duration of the *A. flos-aquae* infection was determined in our previous studies and shown to be ∼36 h (Šulčius et al., 2015b). This period of time includes CL 131 adsorption, replication and burst (Šulčius et al., 2015b; **Figure 6**). In addition, the apparent growth rate of *A. flos-aquae* ($0.24\ d^{-1}$, corresponding to population doubling time of 2.89 days) was measured before the experiment to ensure that experiment will be performed within the same *A. flos-aquae* generation.

For incubation experiment, the early exponential growth phase cyanobacterial culture at the density of $\sim 2.5 \times 10^5$ cells mL^{-1} was mixed with purified cyanophage CL 131 suspension at the density of $\sim 1.6 \times 10^6$ phages mL^{-1}, giving the ratio of phages added to each cyanobacterial cell of ∼6.5. The control treatment was amended with filter-sterilized AF-$6N_0$ medium instead of cyanophage suspension. Both (infected and control) treatments were then subdivided into three technical replicates in glass septum bottles and were mixed by inverting

them every 6 h. Nitrogen ($^{15}N_2$) gas (99.2 atom% ^{15}N; Campro Scientific) was directly added as a bubble into incubation bottles (final concentration 0.2% v/v) of either infected or control cultures following descriptions in Montoya et al. (1996).

Samples for CL 131 and *A. flos-aquae* abundance and $^{15}N_2$ fixation activity measurements were taken every 6 h. Samples for *nifH* gene expression and ammonium concentration measurements were taken every 12 h of the incubation experiment (**Figure 6**).

RNA Extraction and cDNA Synthesis

Samples for RNA extraction were collected by filtering 24 mL of culture suspension onto Whatman polycarbonate filters (0.2 μm pore size, 47 mm diameter), flash frozen in liquid nitrogen and stored at −80°C until analysis. Total RNA was extracted following descriptions in Weinbauer et al. (2002) with modifications as in Glaubitz et al. (2009). The cell wall was mechanically disrupted using silanized glass beads (2–3 mm) in acidic extraction buffer [450 μL; 50 mM sodium acetate, 10 mM EDTA, 2% SDS (w/v), pH 4.2] mixed with equal volume of acidic phenol-chloroform (8:1, pH 4.2) suspension. Samples were homogenized and centrifuged for 5 min at 16,000 × g at 4°C. The aqueous phase containing RNA was transferred into new tube, washed twice with chloroform-isoamyl alcohol (24:1) and precipitated for 30 min at −80°C with isopropanol containing 3 M sodium acetate (0.1 volume) and 1.3 μL glycogen. The precipitated RNA was pelleted by centrifugation (60 min) and purified by washing twice with pre-cooled ethanol (70%, v/v). RNA was recovered from dry pellets by elution in nuclease-free DEPC-treated water and treated with DNase I (Turbo DNA-Free kit, Thermo Fisher Scientific) to remove the remaining DNA.

RNA samples were checked for DNA contamination using PCR and universal bacterial 16S rDNA gene primers (Com1/Com2; **Table 1**). RNA concentration and purity was assessed spectrophotometrically using the 2100 Electrophoresis Bioanalyzer (Agilent Technologies) and RNA 6000 Pico Kit (Agilent Technologies) following manufacturer's recommendations. RNA was reverse transcribed into complementary DNA (cDNA) using MultiScribe Reverse Transcriptase (Thermo Fisher Scientific) following the manufacturer's protocol. A PCR control without a reverse transcriptase and with a reaction mixture lacking template RNA were used to test the specificity of cDNA synthesis.

Primer Design and Validation

Specific primer pairs (**Table 1**) targeting *A. flos-aquae nifH* gene (Accession No. NZ_JSDP01000132.1) were designed with Primer3web software (v4.1.0; Untergasser et al., 2012). Primers specificity to ensure that they amplified only the target genetic locus were tested via conventional PCR using *A. flos-aquae* DNA (data not shown).

The CL 131-specific primers (**Table 1**) targeting so-far unique cyanophage structural gene (gp046; Accession No. ATW59314.1; Šulčius et al., 2019) were designed to give 143 bp amplicon with Primer3web software (v4.1.0; Untergasser et al., 2012) and tested for specificity with conventional PCR using cyanophage DNA and metagenomic analysis (for more details see Šulčius et al., 2019).

Droplet Digital PCR

Droplet digital PCR (ddPCR) was performed using QX200™ Droplet Digital PCR System (Bio-Rad Laboratories, Inc., Hercules, CA, United States). ddPCR reaction mixtures were prepared following manufacturer's protocol. Each reaction mixture contained 1 ng of cDNA or 1 μL of particle-free filtrate (for CL 131 gp046 analysis). DEPC water and *A. flos-aquae* DNA was used instead of cDNA or particle-free filtrate as negative and positive controls, respectively. ddPCR reaction mixtures were loaded into Bio-Rad 8-chanell disposable droplet generator cartridge containing 70 μL of droplet generation oil in each well. Droplets were generated using QX200 droplet generator, transferred into a 96-well PCR plate, heat-sealed with a foil seal and amplified in a two (for *nifH*) or three-step (for *gp046*) PCR using conventional thermal cycler. PCR cycling conditions included an initial 5 min denaturing step at 95°C followed by 40 cycles of denaturation at 98°C for 30 s, annealing and elongation at 60°C for 60 s (for nifH) or 60°C for 90 s (for gp046), and a final signal stabilization step at 90°C for 5 min. After PCR, droplets were counted using QX200 droplet reader and analyzed with QuantaSoft software. Positive droplets, containing amplification products, were discriminated from negative droplets by setting the fluorescence threshold at the lowest point of the positive control droplet cluster and at the highest point of the negative control droplet cluster. The *nifH* transcript abundance was normalized for heterocyte abundance by dividing the number of *nifH* transcripts by the number of heterocytes recorded at each sampling point.

Measurements of Nitrogen Fixation Rates

At each sampling point (**Figure 6**), 24 mL of culture suspension was filtered onto pre-combusted (450°C for 4.5 h) Whatman GF/F filters and stored at −20°C until further processing. Prior the measurements GF/F filters were dried at 60°C overnight and pelletized into tin cups, which then were analyzed with Thermo Flash 2000 elemental analyzer coupled to an DeltaV isotopic ratio mass spectrometer (Thermo Fisher Scientific). The rates of nitrogen fixation were calculated following descriptions given in Montoya et al. (1996) and normalized for heterocyte abundance.

Microscopy Analysis

Samples (1 mL) for determination of *A. flos-aquae* cell density were preserved with formalin solution (final concentration of ∼1%) and kept in the dark at +4°C until further analysis. Vegetative cells and heterocytes of *A. flos-aquae* were enumerated at each sampling point under a light microscope (Nikon Eclipse C_i H550S) using the Nageotte counting chamber and examining no less than 600 units. The *A. flos-aquae* population growth rates were calculated by fitting linear regressions to the natural log of cell abundance versus incubation time and calculating the regression slope.

Nutrient Analysis

Samples (15 mL) for the analysis of dissolved inorganic nutrients [ammonium, nitrates and nitrites (NO_X) and phosphates] were pre-filtered through Whatman PC filters (0.2 μm pore diameter) and measured spectrophotometrically according to Hansen and Koroleff (1999) using an automated constant flow analyzer Seal Analytical QuAAtro (for nitrates, nitrites and phosphates) or spectrophotometer Shimadzu, UV-1202 UV-Vis (for ammonium) with the detection limits of 0.2 μM L^{-1} for nitrate, 0.05 μM L^{-1} for nitrite, 0.1 μM L^{-1} for phosphate and 0.05 μM L^{-1} for ammonium.

Nanoscale Secondary Ion Mass Spectrometry (NanoSIMS) Analysis

Subsamples (120 mL) for nanoSIMS analysis were taken at the lysis onset (30 h; **Figure 6**) and were additionally supplemented with 1 mL of $^{15}N_2$ gas (99.2 atom% ^{15}N; Campro Scientific) to increase net nitrogen dissolution to compensate for short incubation time. Subsamples were incubated for 6 h under the same conditions as described above and fixed with 37% formaldehyde (final concentration 2%). Culture suspension was serially diluted and filtered onto 0.2 μm Millipore polycarbonate filters (Billerica, MA, United States). The samples were coated with ca. 30 nm gold with a Cressington 108auto sputter coater (Watford, United Kingdom). SIMS imaging was performed using a NanoSIMS 50 L instrument (Cameca, France) at the Leibniz-Institute for Baltic Sea Research Warnemünde (IOW). A $^{133}Cs^+$ primary ion beam was used to erode and ionize atoms of the sample. Among the received secondary ions, images of $^{12}C^-$, $^{13}C^-$, $^{12}C^{14}N^-$, $^{12}C^{15}N^-$ were recorded simultaneously for areas of interest using mass detectors equipped with electron multipliers (Hamamatsu). The mass resolving power was adjusted to be sufficient to suppress interferences at all masses allowing, e.g., the separation of $^{13}C^-$ from interfering ions such as $^{12}C^1H^-$. Prior to the analysis, sample areas of 40 × 40 μm were sputtered for 4:30 min with 600 pA to erode the gold, clean the surface, reach the steady state of secondary ion formation and penetrate into the cell. The primary ion beam current during the analysis was 3 pA; the scanning parameters were 512 × 512 pixels for areas of 35 × 35 μm, with a dwell time of 250 μs per pixel. Sixty planes were analyzed.

Samples were analyzed with the Look@NanoSIMS software (Gregor and Maršálek, 2004). The planes were checked for inconsistencies, drift corrected based on the $^{12}C^{14}N^-$ signals and accumulated. Regions of interest (ROIs) for the calculation of ratios were drawn according to the cell outlines of the $^{12}C^{14}N^-$ signals. The ROI outlines were crosschecked and corrected with the cell appearances of $^{12}C^{15}N^-$ signals to include the areas with high enrichments. In parallel ROIs on the filter surface were defined for quality control of the measurement and correction of instrumental offset. For each ROI a $^{12}C^{15}N^-/^{12}C^{14}N^-$ ratio was calculated. The $^{12}C^{15}N^-/^{12}C^{14}N^-$ ratio of the averaged filter areas was used to calculate a correction value to reach nominal values (0.0036734) for the areas outside the cells. The cell values were corrected with this value. Thus, if enrichment material, e.g., from lysed cells, settled on the filter, the received values might underestimate the activity of the cells.

For two randomly selected spots additional implantation and analysis was performed to penetrate deeper in the cell. The results did not change in deeper cell parts but we must admit, that no cell was consumed in total by the analysis. Parallel to $^{12}C^{15}N^-/^{12}C^{14}N^-$ ratios also the $^{13}C^-/^{12}C^-$ ratios were analyzed routinely. No enrichments occurred there. This points to the fact, that the observed enrichments are no methodical artifact by e.g., topography.

Statistical Analysis

Differences in *nifH* transcript abundance and nitrogen fixation rates were compared between treatments over the time course of the experiment using a repeated-measures ANOVA (RM-ANOVA). Variables were tested for normality and homogeneity of variance using the Shapiro–Wilk and Levene's test, respectively, and log10-transformed if needed to meet the assumption of normality. Additionally, independent samples t-test assuming equal variances was applied to find out whether ^{15}N enrichments, *A. flos-aquae* growth rate and nutrient concentrations differed from the control or from each other on specific sampling points (both within and between the treatments). All statistical analyses were performed using RStudio (v. 1.2.5001) with R version 3.6.1, and with a p-value < 0.05 considered as significant.

DATA AVAILABILITY STATEMENT

The raw data supporting the conclusions of this article will be made available by the authors, without undue reservation.

AUTHOR CONTRIBUTIONS

SŠ and JK conceived the study and analyzed the data. JK performed the experiments, collected and processed the samples, and conducted laboratory measurements. AV performed nanoSIMS and analyzed the data. EŠ designed PCR primers for *nifH* gene in *A. flos-aquae*. SŠ wrote the manuscript. All authors contributed to manuscript editing.

FUNDING

This work was supported by the Research Council of Lithuania (grant number S-MIP-17-28) to SŠ and by the Nature Research Centre through the open access to the research infrastructure of the Nature Research Centre under Lithuanian open access network initiative. JK was supported by Deutsche Bundesstiftung Umwelt (DBU) scholarship (No. 30018/772). MV received support through the Human Frontiers Science Program (RGP0020/2016). The NanoSIMS at the Leibnitz-Institute for Baltic Sea Research in Warnemünde (IOW) was funded by the German Federal Ministry of Education and Research (BMBF), grant identifier 03F0626A. This work is in partial

fulfillment of the requirements for a Ph.D. degree from the University of Vilnius to JK.

ACKNOWLEDGMENTS

We are grateful to Christian Meeske and Christian Stolle for their advice and support with gene expression analysis and Jūratė Kasperovičienė for enumeration of *A. flos-aquae* cells. We also thank Iris Liskow and Christian Burmeister for assisting with nutrients and stable isotope analysis. The help of Nadia Samira Ahlers during incubation experiment is also appreciated. Annett Grüttmüller is acknowledged for NanoSIMS routine operation. We are grateful to editor and reviewers for helping us to improve earlier version of the manuscript.

REFERENCES

Adam, B., Klawonn, I., Svedén, J. B., Bergkvist, J., Nahar, N., Walve, J., et al. (2016). N2-fixation, ammonium release and N-transfer to the microbial and classical food web within a plankton community. *ISME J.* 10, 450–459. doi: 10.1038/ismej.2015.126

Ahlgren, N. A., Fuchsman, C. A., Rocap, G., and Fuhrman, J. A. (2019). Discovery of several novel, widespread, and ecologically distinct marine Thaumarchaeota viruses that encode amoC nitrification genes. *ISME J.* 13, 618–631. doi: 10.1038/s41396-018-0289-4

Ankrah, N. Y. D., May, A. L., Middleton, J. L., Jones, D. R., Hadden, M. K., Gooding, J. R., et al. (2014). Phage infection of an environmentally relevant marine bacterium alters host metabolism and lysate composition. *ISME J.* 8, 1089–1100. doi: 10.1038/ismej.2013.216

Benavides, M., and Voss, M. (2015). Five decades of N2 fixation research in the North Atlantic Ocean. *Front. Mar. Sci.* 2:40. doi: 10.3389/fmars.2015.00040

Brussaard, C. P. D., Wilhelm, S. W., Thingstad, F., Weinbauer, M. G., Bratbak, G., Heldal, M., et al. (2008). Global-scale processes with a nanoscale drive: the role of marine viruses. *ISME J.* 2, 575–578. doi: 10.1038/ismej.2008.31

Cairns, J., Coloma, S. S., Sivonen, K., and Hiltunen, T. (2016). Evolving interactions between diazotrophic cyanobacterium and phage mediate nitrogen release and host competitive ability. *R. Soc. Open Sci.* 3:160839. doi: 10.1098/rsos.160839

Caporaso, J. G., Lauber, C. L., Walters, W. A., Berg-Lyons, D., Lozupone, C. A., Turnbaugh, P. J., et al. (2011). Global patterns of 16S rRNA diversity at a depth of millions of sequences per sample. *Proc. Natl. Acad. Sci. U.S.A.* 108, 4516–4522. doi: 10.1073/pnas.1000080107

Chan, F., Pace, M. L., Howarth, R. W., and Marino, R. M. (2004). Bloom formation in heterocystic nitrogen-fixing cyanobacteria: the dependence on colony size and zooplankton grazing. *Limnol. Oceanogr.* 49, 2171–2178. doi: 10.4319/lo.2004.49.6.2171

Cirés, S., and Ballot, A. (2016). A review of the phylogeny, ecology and toxin production of bloom-forming *Aphanizomenon* spp. and related species within the Nostocales (cyanobacteria). *Harmful Algae* 54, 21–43. doi: 10.1016/j.hal.2015.09.007

Coloma, S. E., Dienstbier, A., Bamford, D. H., Sivonen, K., Roine, E., and Hiltunen, T. (2017). Newly isolated Nodularia phage influences cyanobacterial community dynamics. *Environ. Microbiol.* 19, 273–286. doi: 10.1111/1462-2920.13601

De Nobel, W. T., Huisman, J., Snoep, J. L., and Mur, L. R. (1997). Competition for phosphorus between the nitrogen-fixing cyanobacteria Anabaena and Aphanizomenon. *FEMS Microbiol. Ecol.* 24, 259–267. doi: 10.1016/s0168-6496(97)00067-6

Degerholm, J., Gundersen, K., Bergman, B., and Söderbäck, E. (2008). Seasonal significance of N2 fixation in coastal and offshore waters of the northwestern Baltic Sea. *Mar. Ecol. Prog. Ser.* 360, 73–84. doi: 10.3354/meps07379

Deutsch, C., Sarmiento, J. L., Sigman, D. M., Gruber, N., and Dunne, J. P. (2007). Spatial coupling of nitrogen inputs and losses in the ocean. *Nature* 445, 163–167. doi: 10.1038/nature05392

Doron, S., Fedida, A., Hernández-Prieto, M. A., Sabehi, G., Karunker, I., Stazic, D., et al. (2016). Transcriptome dynamics of a broad host-range cyanophage and its hosts. *ISME J.* 10, 1437–1455. doi: 10.1038/ismej.2015.210

Dwivedi, B., Xue, B., Lundin, D., Edwards, R. A., and Breitbart, M. (2013). A bioinformatic analysis of ribonucleotide reductase genes in phage genomes and metagenomes. *BMC Evol. Biol.* 13:33. doi: 10.1186/1471-2148-13-33

Engström-Öst, J., Autio, R., Setälä, O., Sopanen, S., and Suikkanen, S. (2013). Plankton community dynamics during decay of a cyanobacteria bloom: a mesocosm experiment. *Hydrobiologia* 701, 25–35. doi: 10.1007/s10750-012-1247-1

Flores, E., Arévalo, S., and Burnat, M. (2019). Cyanophycin and arginine metabolism in cyanobacteria. *Algal Res.* 42:101577. doi: 10.1016/j.algal.2019.101577

Flores, E., and Herrero, A. (2005). Nitrogen assimilation and nitrogen control in cyanobacteria. *Biochem. Soc. Trans.* 33, 164–167. doi: 10.1042/BST0330164

Foster, R. A., Kuypers, M. M. M., Vagner, T., Paerl, R. W., Musat, N., and Zehr, J. P. (2011). Nitrogen fixation and transfer in open ocean diatom–cyanobacterial symbioses. *ISME J.* 5, 1484–1493. doi: 10.1038/ismej.2011.26

Gao, E.-B., Yuan, X.-P., Li, R.-H., and Zhang, Q.-Y. (2009). Isolation of a novel cyanophage infectious to the filamentous cyanobacterium *Planktothrix agardhii* (Cyanophyceae) from Lake Donghu, China. *Aquat. Microb. Ecol.* 54, 163–170. doi: 10.3354/ame01266

Glaubitz, S., Lueders, T., Abraham, W. R., Jost, G., Jürgens, K., and Labrenz, M. (2009). ^{13}C-isotope analyses reveal that chemolithoautotrophic *Gamma-* and *Epsilonproteobacteria* feed a microbial food web in a pelagic redoxcline of the central Baltic Sea. *Environ. Microbiol.* 11, 326–337. doi: 10.1111/j.1462-2920.2008.01770.x

Gons, H. J., Ebert, J., Hoogveld, H. L., Van den Hove, L., Pel, R., Takkenberg, W., et al. (2002). Observations on cyanobacterial population collapse in eutrophic lake water. *Anton. Leeuw. J. Microbiol.* 81, 319–326. doi: 10.1023/a:1020595408169

Gregor, J., and Maršálek, B. (2004). Freshwater phytoplankton quantification by chlorophyll *a*: a comparative study of *in vitro*, *in vivo* and *in situ* methods. *Water Res.* 38, 517–522. doi: 10.1016/j.watres.2003.10.033

Hansen, H. P., and Koroleff, E. (1999). "Determination of nutrients," in *Methods of Seawater Analysis*, eds K. Grasshoff, K. Kremling, and M. Ehrhardt (Weinheim: Wiley-VCH), 159–228.

Hasegawa, T., Koike, I., and Mukai, H. (2001). Fate of food nitrogen in marine copepods. *Mar. Ecol. Prog. Ser.* 210, 167–174. doi: 10.3354/meps210167

Hewson, I., Govil, S. R., Capone, D. G., Carpenter, E. J., and Fuhrman, J. A. (2004). Evidence of *Trichodesmium* viral lysis and potential significance for biogeochemical cycling in the oligotrophic ocean. *Aquat. Microb. Ecol.* 36, 1–8. doi: 10.3354/ame036001

Hyman, P., and Abedon, S. T. (2009). "Practical methods for determining phage growth parameters," in *Bacteriophages: Methods and Protocols*, eds M. R. J. Clokie and A. M. Kropinski (Totowa, NJ: Humana Press), 175–202. doi: 10.1007/978-1-60327-164-6_18

Jover, L. F., Effler, T. C., Buchan, A., Wilhelm, S. W., and Weitz, J. S. (2014). The elemental composition of virus particles: implications for marine biogeochemical cycles. *Nat. Rev. Microbiol.* 12, 519–528. doi: 10.1038/nrmicro3289

Karl, D. M., Church, M. J., Dore, J. E., Letelier, R. M., and Mahaffey, C. (2012). Predictable and efficient carbon sequestration in the North Pacific Ocean supported by symbiotic nitrogen fixation. *Proc. Natl. Acad. Sci. U.S.A.* 109, 1842–1849. doi: 10.1073/pnas.1120312109

Karlson, A. M. L., Duberg, J., Motwani, N. H., Hogfors, H., Klawonn, I., Ploug, H., et al. (2015). Nitrogen fixation by cyanobacteria stimulates production in Baltic food webs. *Ambio* 44, 413–426. doi: 10.1007/s13280-015-0660-x

Klawonn, I., Nahar, N., Walve, J., Andersson, B., Olofsson, M., Svedén, J. B., et al. (2016). Cell-specific nitrogen- and carbon-fixation of cyanobacteria in a temperate marine system (Baltic Sea). *Environ. Microbiol.* 18, 4596–4609. doi: 10.1111/1462-2920.13557

Kuypers, M. M. M., Marchant, H. K., and Kartal, B. (2018). The microbial nitrogen-cycling network. *Nat. Rev. Microbiol.* 16, 263–276. doi: 10.1038/nrmicro.2018.9

Layzell, D. B., Turpin, D. H., and Elrifi, I. R. (1985). Effect of N source on the steady state growth and N assimilation of P-limited Anabaena flos-aquae. *Plant Physiol.* 78, 739–745. doi: 10.1104/pp.78.4.739

Magnuson, A., and Cardona, T. (2016). Thylakoid membrane function in heterocysts. *Biochim. Biophys. Acta* 1857, 309–319. doi: 10.1016/j.bbabio.2015.10.016

Monier, A., Chambouvet, A., Milner, D. S., Attah, V., Terrado, R., Lovejoy, C., et al. (2017). Host-derived viral transporter protein for nitrogen uptake in infected marine phytoplankton. *Proc. Natl. Acad. Sci. U.S.A.* 114, E7489–E7498. doi: 10.1073/pnas.1708097114

Montoya, J. P., Voss, M., Kahler, P., and Capone, D. G. (1996). A simple, high-precision, high-sensitivity tracer assay for N2 fixation. *Appl. Environ. Microbiol.* 62, 986–993. doi: 10.1128/aem.62.3.986-993.1996

Morimoto, D., Kimura, S., Sako, Y., and Yoshida, T. (2018). Transcriptome analysis of a bloom-forming cyanobacterium Microcystis aeruginosa during Ma-LMM01 phage infection. *Front. Microbiol.* 9:2. doi: 10.3389/fmicb.2018.00002

Muñoz-García, J., and Ares, S. (2016). Formation and maintenance of nitrogen-fixing cell patterns in filamentous cyanobacteria. *Proc. Natl. Acad. Sci. U.S.A.* 113, 6218–6223. doi: 10.1073/pnas.1524383113

Obst, M., and Steinbüchel, A. (2006). "Cyanophycin – an ideal bacterial nitrogen storage material with unique chemical properties," in *Inclusions in Prokaryotes*, ed. J. M. Shively (Berlin: Springer), 167–193. doi: 10.1007/7171_007

Pajares, S., and Ramos, R. (2019). Processes and microorganisms involved in the marine nitrogen cycle: knowledge and gaps. *Front. Mar. Sci.* 6:739. doi: 10.3389/fmars.2019.00739

Parada, V., Herndl, G. J., and Weinbauer, M. G. (2006). Viral burst size of heterotrophic prokaryotes in aquatic systems. *J. Mar. Biol. Assoc. U.K.* 86, 613–621. doi: 10.1017/S002531540601352X

Pasulka, A. L., Thamatrakoln, K., Kopf, S. H., Guan, Y., Poulos, B., Moradian, A., et al. (2018). Interrogating marine virus-host interactions and elemental transfer with BONCAT and nanoSIMS-based methods. *Environ. Microbiol.* 20, 671–692. doi: 10.1111/1462-2920.13996

Ploug, H., Musat, N., Adam, B., Moraru, C. L., Lavik, G., Vagner, T., et al. (2010). Carbon and nitrogen fluxes associated with the cyanobacterium *Aphanizomenon* sp. in the Baltic Sea. *ISME J.* 4, 1215–1223. doi: 10.1038/ismej.2010.53

Puxty, R. J., Millard, A. D., Evans, D. J., and Scanlan, D. J. (2015). Shedding new light on viral photosynthesis. *Photosynth. Res.* 126, 71–97. doi: 10.1007/s11120-014-0057-x

Raymond, J., Siefert, J. L., Staples, C. R., and Blankenship, R. E. (2004). The natural history of nitrogen fixation. *Mol. Biol. Evol.* 21, 541–554. doi: 10.1093/molbev/msh047

Rosenwasser, S., Ziv, C., van Creveld, S. G., and Vardi, A. (2016). Virocell metabolism: metabolic innovations during host-virus interactions in the ocean. *Trends Microbiol.* 24, 821–832. doi: 10.1016/j.tim.2016.06.006

Sakr, S., Thyssen, M., Denis, M., and Zhang, C. (2006). Relationship among several key cell cycle events in the developmental cyanobacterium *Anabaena* sp. strain PCC 7120. *J. Bacteriol.* 188, 5958–5965. doi: 10.1128/JB.00524-06

Savchuk, O. P. (2018). Large-scale nutrient dynamics in the Baltic Sea, 1970–2016. *Front. Mar. Sci.* 5:95. doi: 10.3389/fmars.2018.00095

Shelford, E. J., Middelboe, M., Møller, E. F., and Suttle, C. A. (2012). Virus-driven nitrogen cycling enhances phytoplankton growth. *Aquat. Microb. Ecol.* 66, 41–46. doi: 10.3354/ame01553

Sherman, D. M., Tucker, D., and Sherman, L. A. (2000). Heterocyst development and localization of cyanophycin in N2-fixing cultures of *Anabaena* sp. PCC7120 (Cyanobacteria). *J. Phycol.* 36, 932–941. doi: 10.1046/j.1529-8817.2000.99132.x

Shtina, E. A., and Nekrasova, K. A. (1971). "The direct and indirect contribution of soil algae to the primary production of biocenoses," in *Organismes du sol et Production Primaire, Annales de Zoologie-Ecologie Animale*, eds J. d'Aguilar, C. Athias-Henriet, A. Bessard, M. B. Bouche, and M. Pussard (Dijon: Elsevier), 37–45.

Šulčius, S., Alzbutas, G., Kvederavičiūtė, K., Koreivienė, J., Zakrys, L., Lubys, A., et al. (2015b). Draft genome sequence of the cyanobacterium *Aphanizomenon flos-aquae* strain 2012/KM1/D3, isolated from the Curonian Lagoon (Baltic Sea). *Genome Announc.* 3:e01392-14. doi: 10.1128/genomeA.01392-14

Šulčius, S., Mazur-Marzec, H., Vitonytė, I., Kvederavičiūtė, K., Kuznecova, J., Šimoliūnas, E., et al. (2018). Insights into cyanophage-mediated dynamics of nodularin and other non-ribosomal peptides in Nodularia spumigena. *Harmful Algae* 78, 69–74. doi: 10.1016/j.hal.2018.07.004

Šulčius, S., Šimoliūnas, E., Alzbutas, G., Gasiūnas, G., Jauniškis, V., Kuznecova, J., et al. (2019). Genomic characterization of cyanophage vB_AphaS-CL131 infecting filamentous diazotrophic cyanobacterium Aphanizomenon flos-aquae reveals novel insights into virus-bacterium interactions. *Appl. Environ. Microbiol.* 85:e1311-18. doi: 10.1128/AEM.01311-18

Šulčius, S., Šimoliūnas, E., Staniulis, J., Koreivienė, J., Baltrušis, P., Meškys, R., et al. (2015a). Characterization of a lytic cyanophage that infects the bloom-forming cyanobacterium Aphanizomenon flos-aquae. *FEMS Microbiol. Ecol.* 91, 1–7. doi: 10.1093/femsec/fiu012

Šulčius, S., Slavuckytė, K., and Paškauskas, R. (2017). The predation paradox: synergistic and antagonistic interactions between grazing by crustacean predator and infection by cyanophages promotes bloom formation in filamentous cyanobacteria. *Limnol. Oceanogr.* 62, 2189–2199. doi: 10.1002/lno.10559

Suttle, C. A. (2007). Marine viruses - major players in the global ecosystem. *Nat. Rev. Microbiol.* 5, 801–812. doi: 10.1038/nrmicro1750

Takano, K., and Hino, S. (2000). Effect of temperature and soluble reactive phosphorus on abundance of Aphanizomenon flos-aquae (Cyanophyceae). *Phycol. Res.* 48, 9–13. doi: 10.1046/j.1440-1835.2000.00180.x

Thompson, L. R., Zeng, Q., Kelly, L., Huang, K. H., Singer, A. U., Stubbe, J., et al. (2011). Phage auxiliary metabolic genes and the redirection of cyanobacterial host carbon metabolism. *Proc. Natl. Acad. Sci. U.S.A.* 108, E757–E764. doi: 10.1073/pnas.1102164108

Untergasser, A., Cutcutache, I., Koressaar, T., Ye, J., Faircloth, B. C., Remm, M., et al. (2012). Primer3 – new capabilities and interfaces. *Nucleic Acids Res.* 40:e115. doi: 10.1093/nar/gks596

Vahtera, E., Laamanen, M., and Rintala, J. M. (2007). Use of different phosphorus sources by the bloom-forming cyanobacteria Aphanizomenon flos-aquae and Nodularia spumigena. *Aquat. Microb. Ecol.* 46, 225–237. doi: 10.3354/ame046225

Waldbauer, J. R., Coleman, M. L., Rizzo, A. I., Campbell, K. L., Lotus, J., and Zhang, L. (2019). Nitrogen sourcing during viral infection of marine cyanobacteria. *Proc. Natl. Acad. Sci. U.S.A.* 116, 15590–15595. doi: 10.1073/pnas.1901856116

Wang, K., and Chen, F. (2008). Prevalence of highly host−specific cyanophages in the estuarine environment. *Environ. Microbiol.* 10, 300–312. doi: 10.1111/j.1462-2920.2007.01452.x

Wannicke, N., Korth, F., Liskow, I., and Voss, M. (2013). Incorporation of diazotrophic fixed N2 by mesozooplankton — Case studies in the southern Baltic Sea. *J. Mar. Syst.* 117–118, 1–13. doi: 10.1016/j.jmarsys.2013.03.005

Watanabe, M. M., Kawachi, M., Hiroki, M., and Kasai, F. (Eds.) (2000). *NIES Collection List of Strains*, 6th Edn. Tsukuba: National Institute for Environmental Studies.

Watkins, S. C., Smith, J. R., Hayes, P. K., and Watts, J. E. M. (2014). Characterisation of host growth after infection with a broad-range freshwater cyanopodophage. *PLoS One* 9:e87339. doi: 10.1371/journal.pone.0087339

Weinbauer, M. G., Fritz, I., Wenderoth, D. F., and Höfle, M. G. (2002). Simultaneous extraction from bacterioplankton of total RNA and DNA suitable for quantitative structure and function analyses. *Appl. Environ. Microbiol.* 68, 1082–1087. doi: 10.1128/aem.68.3.1082-1087.2002

Wilhelm, S. W., and Suttle, C. A. (1999). Viruses and nutrient cycles in the sea. *Bioscience* 49, 781–788. doi: 10.2307/1313569

Woodland, R. J., Holland, D. P., Beardall, J., Smith, J., Scicluna, T., and Cook, P. L. M. (2013). Assimilation of diazotrophic nitrogen into pelagic food webs. *PLoS One* 8:e67588. doi: 10.1371/journal.pone.0067588

Yoshida, T., Nagasaki, K., Takashima, Y., Shirai, Y., Tomaru, Y., Takao, Y., et al. (2008). Ma-LMM01 infecting toxic Microcystis aeruginosa illuminates diverse cyanophage genome strategies. *J. Bacteriol.* 190, 1762–1772. doi: 10.1128/JB.01534-07

Zehr, J. P., and Kudela, R. M. (2011). Nitrogen cycle of the open ocean: from genes to ecosystems. *Ann. Rev. Mar. Sci.* 3, 197–225. doi: 10.1146/annurev-marine-120709-142819

Zimmerman, A. E., Howard-Varona, C., Needham, D. M., John, S. G., Worden, A. Z., Sullivan, M. B., et al. (2020). Metabolic and biogeochemical consequences of viral infection in aquatic ecosystems. *Nat. Rev. Microbiol.* 18, 21–34. doi: 10.1038/s41579-019-0270-x

Conflict of Interest: The authors declare that the research was conducted in the absence of any commercial or financial relationships that could be construed as a potential conflict of interest.

Advantages of publishing in Frontiers

OPEN ACCESS
Articles are free to read for greatest visibility and readership

FAST PUBLICATION
Around 90 days from submission to decision

HIGH QUALITY PEER-REVIEW
Rigorous, collaborative, and constructive peer-review

TRANSPARENT PEER-REVIEW
Editors and reviewers acknowledged by name on published articles

Frontiers
Avenue du Tribunal-Fédéral 34
1005 Lausanne | Switzerland

Visit us: www.frontiersin.org
Contact us: frontiersin.org/about/contact

REPRODUCIBILITY OF RESEARCH
Support open data and methods to enhance research reproducibility

DIGITAL PUBLISHING
Articles designed for optimal readership across devices

FOLLOW US
@frontiersin

IMPACT METRICS
Advanced article metrics track visibility across digital media

EXTENSIVE PROMOTION
Marketing and promotion of impactful research

LOOP RESEARCH NETWORK
Our network increases your article's readership